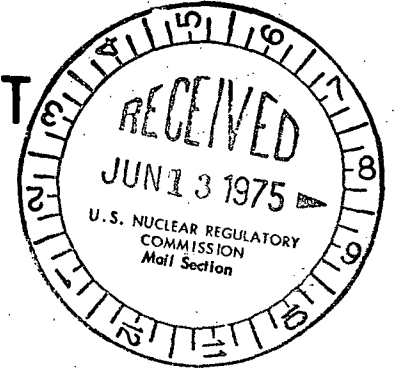


**CLINCH RIVER
BREEDER REACTOR PROJECT**

50-537

**PRELIMINARY
SAFETY ANALYSIS
REPORT**



VOLUME 4

PROJECT MANAGEMENT CORPORATION

6428

TABLE OF CONTENTS

<u>Section</u>		<u>Page</u>
1.0	<u>INTRODUCTION AND GENERAL DESCRIPTION OF THE PLANT</u>	1.1-1
1.1	<u>INTRODUCTION</u>	1.1-1
1.1.1	General Information	1.1-2
1.1.2	Overview of Safety Design Approach	1.1-3
1.1.3	Applicability of Regulatory Guides	1.1-5
1.2	<u>GENERAL PLANT DESCRIPTION</u>	1.2-1
1.2.1	Site	1.2-1
1.2.2	Engineered Safety Features	1.2-2
1.2.3	Reactor, Heat Transport and Related Systems	1.2-2
1.2.4	Steam Generator - Turbine and Related Systems	1.2-3
1.2.5	Offsite and Onsite Power	1.2-5
1.2.6	Instrumentation, Control and Protection	1.2-6
1.2.7	Auxiliary Systems	1.2-7
1.2.8	Refueling System	1.2-8
1.2.9	Radwaste Disposal System	1.2-9
1.2.10	Reactor Confinement/Containment System	1.2-9
1.2.11	Major Structures	1.2-10
1.3	<u>COMPARISON TABLES</u>	1.3-1
1.3.1	Comparisons with Similar Designs	1.3-1
1.3.2	Detailed Comparison with Fast Flux Test Facility	1.3-2
1.4	<u>IDENTIFICATION OF PROJECT PARTICIPANTS</u>	1.4-1
1.4.1	Functions, Responsibilities and Authorities of Project Participants	1.4-2
1.4.2	Description of Organizations	1.4-3
1.4.3	Interrelationships with Contractors and Suppliers	1.4-21a
1.4.4	General Qualification Requirement of CRBRP Project Participants	1.4-22
1.5	<u>REQUIREMENTS FOR FURTHER TECHNICAL INFORMATION</u>	1.5-1
1.5.1	Information Concerning the Adequacy of a New Design	1.5-2
1.5.2	Information Concerning Margin of Conservatism of Proven Design	1.5-28
1.5.3	References	1.5-47

TABLE OF CONTENTS (Cont'd.)

<u>Section</u>		<u>Page</u>
1.6	<u>MATERIAL INCORPORATED BY REFERENCE</u>	1.6-1
1.6.1	Introduction	1.6-1
1.6.2	References	1.6-1
	Appendix 1-A Flow Diagram Symbols	1.A-1
2.0	<u>SITE CHARACTERISTICS</u>	2.1-1
2.1	<u>GEOGRAPHY AND DEMOGRAPHY</u>	2.1-1
2.1.1	Site Location and Layout	2.1-1
2.1.2	Site Description	2.1-2
2.1.3	Population and Population Distribution	2.1-4
2.1.4	Uses of Adjacent Lands and Waters	2.1-8
2.2	<u>NEARBY INDUSTRIAL, TRANSPORTATION AND MILITARY FACILITIES</u>	2.2-1
2.2.1	Locations, Routes, and Descriptions	2.2-1
2.2.2	Evaluations	2.2-3
2.2.3	New Facility/Land Use Requirements	2.2-4c
2.3	<u>METEOROLOGY</u>	2.3-1
2.3.1	Regional Climatology	2.3-1
2.3.2	Local Meteorology	2.3-4
2.3.3	On-site Meteorological Monitoring Program	2.3-9
2.3.4	Short-Term (Accident) Diffusion Estimates	2.3-9
2.3.5	Long-Term (Average) Diffusion Estimates	2.3-13
2.4	<u>HYDROLOGIC ENGINEERING</u>	2.4-1
2.4.1	Hydrologic Description	2.4-1
2.4.2	Floods	2.4-6
2.4.3	Probable Maximum Flood (PMF) on Streams and Rivers	2.4-10
2.4.4	Potential Dam Failures (Seismically and Otherwise Induced)	2.4-21
2.4.7	Ice Flooding	2.4-31
2.4.8	Cooling Water Canals and Reservoirs	2.4-31a
2.4.9	Channel Diversions	2.4-32
2.4.10	Flooding Protection Requirements	2.4-32
2.4.11	Low Water Considerations	2.4-33
2.4.12	Environmental Acceptance of Effluents	2.4-42
2.4.13	Groundwater	2.4-44
2.4.14	Technical Specification and Emergency Operation Requirement	2.4-55

TABLE OF CONTENTS (Cont'd.)

<u>Section</u>		<u>Page</u>
2.5	<u>GEOLOGY AND SEISMOLOGY</u>	2.5-1
2.5.1	Basic Geologic and Seismic Information	2.5-1
2.5.2	Vibratory Ground Motion	2.5-20
2.5.3	Surface Faulting	2.5-27
2.5.4	Stability of Subsurface Materials	2.5-32
2.5.5	Slope Stability	2.5-48a
	Appendix 2-A Field Investigative Procedures	2A-1
	Appendix 2-B Laboratory Test Procedures	2B-1
	Appendix 2-C Report of Test Grouting Program	2C-1
	Appendix 2-D Report of Engineering Properties for Crushed Stone Materials from Commercial Suppliers	2D-1
	Appendix 2-E Extracts from U.S. Atomic Energy Commission AEC Manual	2E-1
	Supplement 1 to Chapter 2 Deleted	
	Supplement 2 to Chapter 2 Question and Responses Related to Chapter Two Information and Critical For NRC Docketing of CRBRP Environmental Report	1
3.0	<u>DESIGN CRITERIA - STRUCTURES, COMPONENTS EQUIPMENT AND SYSTEMS</u>	3.1-1
3.1	<u>CONFORMANCE WITH GENERAL DESIGN CRITERIA</u>	3.1-1
3.1.1	Introduction and Scope	3.1-1
3.1.2	Definitions and Explanations	3.1-2
3.1.3	Conformance with CRBRP General Design Criteria	3.1-8
3.2	<u>CLASSIFICATIONS OF STRUCTURES, SYSTEMS, AND COMPONENTS</u>	3.2-1
3.2.1	Seismic Classifications	3.2-1
3.2.2	Safety Classifications	3.2-2
3.3	<u>WIND AND TORNADO LOADINGS</u>	3.3-1
3.3.1	Wind Loadings	3.3-1
3.3.2	Tornado Loadings	3.3-2
3.4	<u>WATER LEVEL (FLOOD) DESIGN</u>	3.4-1
3.4.1	Flood Protection	3.4-1
3.4.2	Analysis Procedures	3.4-1a

TABLE OF CONTENTS (Cont'd.)

<u>Section</u>		<u>Page</u>
3.5	<u>MISSILE PROTECTION</u>	3.5-1
3.5.1	Missile Barrier and Loadings	3.5-4
3.5.2	Missile Selection	3.5-4a
3.5.3	Selected Missiles	3.5-7
3.5.4	Barrier Design Procedures	3.5-10
3.5.5	Missile Barrier Features	3.5-13c
3.6	<u>PROTECTION AGAINST DYNAMIC EFFECTS ASSOCIATED WITH THE POSTULATED RUPTURE OF PIPING</u>	3.6-1
3.6.1	Systems In Which Pipe Breaks are Postulated	3.6-1
3.6.2	Pipe Break Criteria	3.6-2
3.6.3	Design Loading Combinations	3.6-2
3.6.4	Dynamic Analysis	3.6-3
3.6.5	Protective Measures	3.6-8
3.7	<u>SEISMIC DESIGN</u>	3.7-1
3.7.1	Seismic Input	3.7-1
3.7.2	Seismic System Analysis	3.7-4a
3.7.3	Seismic Subsystem Analysis	3.7-11
3.7.4	Seismic Instrumentation Program	3.7-16
3.7.5	Seismic Design Control	3.7-20
	Appendix to Section 3.7 Seismic Design Criteria	3.7-A.1
3.8	<u>DESIGN OF CATEGORY I STRUCTURES</u>	3.8-1
3.8.1	Concrete Containment (Not Applicable)	3.8-1
3.8.2	Steel Containment System	3.8-1
3.8.3	Concrete and Structural Steel Internal Structures of Steel Containment	3.8-8
3.8.4	Other Seismic Category I Structures	3.8-22a
3.8.5	Foundation and Concrete Supports	3.8-35
	Appendix 3.8A Buckling Stress Criteria	3.8A-1
	Appendix 3.8-B Cell Liner Design Criteria	3.8-B.1
	Appendix 3.8-C Catch Pan and Fire Suppression Deck Design Criteria	3.8-C.1
3.9	<u>MECHANICAL SYSTEMS AND COMPONENTS</u>	3.9-1
3.9.1	Dynamic System Analysis and Testing	3.9-1
3.9.2	ASME Code Class 2 and 3 Components	3.9-3a
3.9.3	Components Not Covered by ASME Code	3.9-5
3.10	<u>SEISMIC DESIGN OF CATEGORY I INSTRUMENTATION AND ELECTRICAL EQUIPMENT</u>	3.10-1
3.10.1	Seismic Design Criteria	3.10-1

TABLE OF CONTENTS (Cont'd.)

<u>Section</u>		<u>Page</u>
3.10.2	Analysis, Testing Procedures and Restraint Measures	3.10-3
3.11	<u>ENVIRONMENTAL DESIGN OF MECHANICAL AND ELECTRICAL EQUIPMENT</u>	3.11-1
3.11.1	Equipment Identification	3.11-1
3.11.2	Qualification Test and Analysis	3.11-1
3.11.3	Qualification Test Results	3.11-1
3.11.4	Loss of Ventilation	3.11-2
3.11.5	Special Considerations	3.11-2
3A.0	<u>SUPPLEMENTARY INFORMATION ON SEISMIC CATEGORY I STRUCTURES</u>	3A.1-1
3A.1	Inner Cell System	3A.1-1
3A.2	Head Access Area	3A.2-1
3A.3	Control Building	3A.3-1
3A.4	Reactor Service Building (RSB)	3A.4-1
3A.5	Steam Generator Building	3A.5-1
3A.6	Diesel Generator Building	3A.6-1
3A.7	Deleted	
3A.8	Cell Liner Systems	3A.8-1
4.0	<u>REACTOR</u>	4.1-1
4.1	<u>SUMMARY DESCRIPTION</u>	4.1-1
4.1.1	Lower Internals	4.1-1
4.1.2	Upper Internals	4.1-3
4.1.3	Core Restraint	4.1-4
4.1.4	Fuel Blanket and Removable Radial Shield Regions	4.1-4
4.1.5	Design and Performance Characteristics	4.1-9
4.1.6	Loading Conditions and Analysis Techniques	4.1-9
4.1.7	Computer Codes	4.1-10
4.2	<u>MECHANICAL DESIGN</u>	4.2-1
4.2.1	Fuel and Blanket Design	4.2-1
4.2.2	Reactor Vessels Internals	4.2-118
4.2.3	Reactivity Control Systems	4.2-228
4.3	<u>NUCLEAR DESIGN</u>	4.3-1
4.3.1	Design Bases	4.3-1
4.3.2	Description	4.3-3
4.3.3	Analytical Methods	4.3-69
4.3.4	Changes	

TABLE OF CONTENTS (Cont'd.)

<u>Section</u>		<u>Page</u>
4.4	<u>THERMAL AND HYDRAULIC DESIGN</u>	4.4-1
4.4.1	Design Bases	4.4-1
4.4.2	Description	4.4-4
4.4.3	Evaluation	4.4-45
4.4.4	Testing and Verification	4.4-75
4.4.5	Core Instrumentation	4.4-80
5.0	<u>HEAT TRANSPORT AND CONNECTED SYSTEMS</u>	5.1-1
5.1	<u>SUMMARY DESCRIPTION</u>	5.1-1a
5.1.1	Reactor Vessel, Closure Head, and Guard Vessel	5.1-1a
5.1.2	Primary Heat Transport System	5.1-2
5.1.3	Intermediate Heat Transport System	5.1-5
5.1.4	Steam Generator System	5.1-7
5.1.5	Residual Heat Removal System	5.1-8
5.1.6	Auxiliary Liquid Metal System	5.1-9
5.1.7	Features for Heat Transport System Safety	5.1-10
5.1.8	Physical Arrangement	5.1-11
5.2	<u>REACTOR VESSEL, CLOSURE HEAD, AND GUARD VESSEL</u>	5.2-1
5.2.1	Design Basis	5.2-1
5.2.2	Design Parameters	5.2-4b
5.2.3	Special Processes for Fabrication and Inspection	5.2-7
5.2.4	Features for Improved Reliability	5.2-8
5.2.5	Quality Assurance Surveillance	5.2-10d
5.2.6	Materials and Inspections	5.2-11
5.2.7	Packing, Packaging, and Storage	5.2-11a
	Appendix 5.2.A Modifications to the High Temperature Design Rules for Austenitic Stainless Steel	5.2A-1
5.3	<u>PRIMARY HEAT TRANSPORT SYSTEM (PHTS)</u>	5.3-1
5.3.1	Design Bases	5.3-1
5.3.2	Design Description	5.3-9
5.3.3	Design Evaluation	5.3-33
5.3.4	Tests and Inspections	5.3-72
5.4	<u>INTERMEDIATE HEAT TRANSPORT SYSTEM (IHTS)</u>	5.4-1
5.4.1	Design Basis	5.4-1
5.4.2	Design Description	5.4-6
5.4.3	Design Evaluation	5.4-12

TABLE OF CONTENTS (Cont'd.)

<u>Section</u>		<u>Page</u>
5.5	<u>STEAM GENERATOR SYSTEM (SGS)</u>	5.5-1
5.5.1	Design Bases	5.5-1
5.5.2	Design Description	5.5-5
5.5.3	Design Evaluation	5.5-17
5.6	<u>RESIDUAL HEAT REMOVAL SYSTEMS</u>	5.6-1
5.6.1	Steam Generator Auxiliary Heat Removal System (SGAHRs)	5.6-1b
5.6.2	Direct Heat Removal Service (DHRS)	5.6-20
5.7	<u>OVERALL HEAT TRANSPORT SYSTEM EVALUATION</u>	5.7-1
5.7.1	Startup and Shutdown	5.7-1
5.7.2	Load Following Characteristics	5.7-2
5.7.3	Transient Effects	5.7-2a
5.7.4	Evaluation of Thermal Hydraulic Characteristics and Plant Design Heat Transport System Design Transient Summary	5.7-6
6.0	<u>ENGINEERED SAFETY FEATURES</u>	6.1-1
6.1	<u>GENERAL</u>	6.1-1
6.2	<u>CONTAINMENT SYSTEMS</u>	6.2-1
6.2.1	Confinement/Containment Functional Design	6.2-1
6.2.2	Containment Heat Removal	6.2-9
6.2.3	Containment Air Purification and Cleanup System	6.2-9
6.2.4	Containment Isolation Systems	6.2-10
6.2.5	Annulus Filtration System	6.2-14
6.2.6	Reactor Service Building (RSB) Filtration System	6.2-16
6.2.7	Steam Generator Building Aerosol Release Mitigation System Functional Design	6.2-17
6.3	<u>HABITABILITY SYSTEMS</u>	6.3-1
6.3.1	Habitability System Functional Design	6.3-1
6.4	<u>CELL LINER SYSTEM</u>	6.4-1
6.4.1	Design Base	6.4-1
6.4.2	System Design	6.4-1
6.4.3	Design Evaluation	6.4-1
6.4.4	Tests and Inspections	6.4-1
6.4.5	Instrumentation Requirements	6.4-1

TABLE OF CONTENTS (Cont'd.)

<u>Section</u>		<u>Page</u>
6.5	<u>CATCH PAN</u>	6.5-1
6.5.1	Design Base	6.5-1
6.5.2	System Design Description and Evaluation	6.5-1
6.5.3	Tests and Inspections	6.5-1
6.5.4	Instrumentation Requirements	6.5-1
7.0	<u>INSTRUMENTATION AND CONTROLS</u>	7.1-1
7.1	<u>INTRODUCTION</u>	7.1-1
7.1.1	Identification of Safety Related Instrumentation and Control Systems	7.1-1
7.1.2	Identification of Safety Criteria	7.1-1
7.2	<u>REACTOR SHUTDOWN SYSTEM</u>	7.2-1
7.2.1	Description	7.2-1
7.2.2	Analysis	7.2-13
7.3	<u>ENGINEERED SAFETY FEATURE INSTRUMENTATION AND CONTROL</u>	7.3-1
7.3.1	Containment Isolation System	7.3-1
7.3.2	Analysis	7.3-3
7.4	<u>INSTRUMENTATION AND CONTROL SYSTEMS REQUIRED FOR SAFE SHUTDOWN</u>	7.4-1
7.4.1	Steam Generator Auxiliary Heat Removal Instrumentation and Control Systems	7.4-1
7.4.2	Outlet Steam Isolation Instrumentation and Control System	7.4-6
7.4.3	Remote Shutdown System	7.4-8a
7.5	<u>INSTRUMENTATION AND MONITORING SYSTEM</u>	7.5-1
7.5.1	Flux Monitoring System	7.5-1
7.5.2	Heat Transport Instrumentation System	7.5-5
7.5.3	Reactor and Vessel Instrumentation	7.5-13
7.5.4	Fuel Failure Monitoring System	7.5-14
7.5.5	Leak Detection Systems	7.5-18
7.5.6	Sodium-Water Reaction Pressure Relief System (SWRPRS) Instrumentation and Controls	7.5-30
7.5.7	Containment Hydrogen Monitoring	7.5-33b
7.5.8	Containment Vessel Temperature Monitoring	7.5-33b
7.5.9	Containment Pressure Monitoring	7.5-33b
7.5.10	Containment Atmosphere Temperature	7.5-33c
7.5.11	Post Accident Monitoring	7.5-33c

TABLE OF CONTENTS (Cont'd.)

<u>Section</u>		<u>Page</u>
7.6	<u>OTHER INSTRUMENTATION AND CONTROL SYSTEMS REQUIRED FOR SAFETY</u>	7.6-1
7.6.1	Plant Service Water and Chilled Water Instrumentation and Control Systems	7.6-1
7.6.2	Deleted	
7.6.3	Direct Heat Removal Service (DHRS) Instrumentation and Control System	7.6-3
7.6.4	Heating, Ventilating, and Air Conditioning Instrumentation and Control System	7.6-3e
7.6.5	SGB Flooding Protection Subsystem	7.6-3f
7.7	<u>INSTRUMENTATION AND CONTROL SYSTEMS NOT REQUIRED FOR SAFETY</u>	7.7-1
7.7.1	Plant Control System Description	7.7-1
7.7.2	Design Analysis	7.7-16
7.8	<u>PLANT DATA HANDLING AND DISPLAY SYSTEM</u>	7.8-1
7.8.1	Design Description	7.8-1
7.8.2	Design Analysis	7.8-2
7.9	<u>OPERATING CONTROL STATIONS</u>	7.9-1
7.9.1	Design Basis	7.9-1
7.9.2	Control Room	7.9-1
7.9.3	Local Control Stations	7.9-6
7.9.4	Communications	7.9-6
7.9.5	Design Evaluation	7.9-6
8.0	<u>ELECTRIC POWER</u>	8.1-1
8.1	<u>INTRODUCTION</u>	8.1-1
8.1.1	Utility Grid and Interconnections	8.1-1
8.1.2	Plant Electrical Power System	8.1-1
8.1.3	Criteria and Standards	8.1-3
8.2	<u>OFFSITE POWER SYSTEM</u>	8.2-1
8.2.1	Description	8.2-1
8.2.2	Analysis	8.2-4
8.3	<u>ON-SITE POWER SYSTEMS</u>	8.3-1
8.3.1	AC Power Systems	8.3-1
8.3.2	DC Power System	8.3-44

TABLE OF CONTENTS (Cont'd.)

<u>Section</u>		<u>Page</u>
9.0	<u>AUXILIARY SYSTEMS</u>	9.1-1
9.1	<u>FUEL STORAGE AND HANDLING</u>	9.1-1
9.1.1	New Fuel Storage	9.1-3
9.1.2	Spent Fuel Storage	9.1-5
9.1.3	Spent Fuel Cooling and Cleanup System	9.1-20
9.1.4	Fuel Handling System	9.1-33
9.2	<u>NUCLEAR ISLAND GENERAL PURPOSE MAINTENANCE SYSTEM</u>	9.2-1
9.2.1	Design Basis	9.2-1
9.2.2	System Description	9.2-1
9.2.3	Safety Evaluation	9.2-3
9.2-4	Tests and Inspections	9.2-3
9.2-5	Instrumentation Applications	9.2-4
9.3	<u>AUXILIARY LIQUID METAL SYSTEM</u>	9.3-1
9.3.1	Sodium and NaK Receiving System	9.3-1a
9.3.2	Primary Na Storage and Processing	9.3-2
9.3.3	EVS Sodium Processing	9.3-9a
9.3.4	Primary Cold Trap NaK Cooling System	9.3-10
9.3.5	Intermediate Na Processing System	9.3-12
9.4	<u>PIPING AND EQUIPMENT ELECTRICAL HEATING</u>	9.4-1
9.4.1	Design Bases	9.4-1
9.4.2	Systems Description	9.4-2
9.4.3	Safety Evaluation	9.4-3
9.4.4	Tests and Inspections	9.4-3b
9.4.5	Instrumentation Application	9.4-3b
9.5	<u>INERT GAS RECEIVING AND PROCESSING SYSTEM</u>	9.5-1
9.5.1	Argon Distribution Subsystem	9.5-2
9.5.2	Nitrogen Distribution System	9.5-6
9.5.3	Safety Evaluation	9.5-10
9.5.4	Tests and Inspections	9.5-12
9.5.5	Instrumentation Requirements	9.5-12
9.6	<u>HEATING, VENTILATING AND AIR CONDITIONING SYSTEM</u>	9.6-1
9.6.1	Control Building HVAC System	9.6-1
9.6.2	Reactor Containment Building	9.6-12
9.6.3	Reactor Service Building HVAC System	9.6-25
9.6.4	Turbine Generator Building HVAC System	9.6-37
9.6.5	Diesel Generator Building HVAC System	9.6-40
9.6.6	Steam Generator Building HVAC System	9.6-45

TABLE OF CONTENTS (Cont'd.)

<u>Section</u>		<u>Page</u>
9.7	<u>CHILLED WATER SYSTEMS</u>	9.7-1
9.7.1	Normal Chilled Water System	9.7-1
9.7.2	Emergency Chilled Water System	9.7-4
9.7.3	Prevention of Sodium or NaK/Water Interactions	9.7-9
9.7.4	Secondary Coolant Loops (SCL)	9.7-12
9.8	<u>IMPURITY MONITORING AND ANALYSIS SYSTEM</u>	9.8-1
9.8.1	Design Basis	9.8-1
9.8.2	Design Description	9.8-2
9.8.3	Design Evaluation	9.8-5
9.8.4	Tests and Inspection	9.8-7
9.8.5	Instrumentation Requirements	9.8-8
9.9	<u>SERVICE WATER SYSTEMS</u>	9.9-1
9.9.1	Normal Plant Service Water System	9.9-1
9.9.2	Emergency Plant Service Water System	9.9-2
9.9.3	Secondary Service Closed Cooling Water System	9.9-4
9.9.5	River Water Service	9.9-11
9.10	<u>COMPRESSED GAS SYSTEM</u>	9.10-1
9.10.1	Service Air and Instrument Air Systems	9.10-1
9.10.2	Hydrogen System	9.10-3a
9.10.3	Carbon Dioxide System	9.10-4
9.11	<u>COMMUNICATIONS SYSTEM</u>	9.11-1
9.11.1	Design Bases	9.11-1
9.11.2	Description	9.11-3
9.12	<u>LIGHTING SYSTEMS</u>	9.12-1
9.12.1	Normal Lighting System	9.12-1
9.12.2	Standby Lighting Systems	9.12-2
9.12.3	Emergency Lighting System	9.12-3
9.12.4	Design Evaluation	9.12-4
9.13	<u>PLANT FIRE PROTECTION SYSTEM</u>	9.13-1
9.13.1	Non-Sodium Fire Protection System	9.13-1
9.13.2	Sodium Fire Protection System (SFPS)	9.13-13
9.13A	Overall Fire Protection Requirements -- CRBRP Design Compared with APCSB 9.5-1 & ASB 9.5-1	9.13A-1
9.14	<u>DIESEL GENERATOR AUXILIARY SYSTEM</u>	9.14-1
9.14.1	Fuel Oil Storage and Transfer System	9.14-1

TABLE OF CONTENTS (Cont'd.)

<u>Section</u>		<u>Page</u>
9.14.2	Cooling Water System	9.14-2
9.14.3	Starting Air Systems	9.14-4
9.14.4	Lubrication System	9.14-5
9.15	<u>EQUIPMENT AND FLOOR DRAINAGE SYSTEM</u>	9.15-1
9.15.1	Design Bases	9.15-1
9.15.2	System Description	9.15-1
9.15.3	Safety Evaluation	9.15-2
9.15.4	Tests and Inspections	9.15-2
9.15.5	Instrumentation Application	9.15-2
9.16	<u>RECIRCULATION GAS COOLING SYSTEM</u>	9.16-1
9.16.1	Design Basis	9.16-1
9.16.2	System Description	9.16-1
9.16.3	Safety Evaluation	9.16-6
9.16.4	Tests and Inspection	9.16-7
9.16.5	Instrumentation and Control	9.16-7
10.0	<u>STEAM AND POWER CONVERSION SYSTEM</u>	10.1-1
10.1	<u>SUMMARY DESCRIPTION</u>	10.1-1
10.2	<u>TURBINE GENERATOR</u>	10.2-1
10.2.1	Design Bases	10.2-1
10.2.2	Description	10.2-1a
10.2.3	Turbine Missiles	10.2-5
10.2.4	Evaluation	10.2-9
10.3	<u>MAIN STEAM SUPPLY SYSTEM</u>	10.3-1
10.3.1	Design Bases	10.3-1
10.3.2	Description	10.3-1
10.3.3	Evaluation	10.3-2
10.3.4	Inspection and Testing Requirements	10.3-2
10.3.5	Water Chemistry	10.3-3
10.4	<u>OTHER FEATURES OF STEAM AND POWER CONVERSION SYSTEM</u>	10.4-1
10.4.1	Condenser	10.4-1
10.4.2	Condenser Air Removal System	10.4-2
10.4.3	Turbine Gland Sealing System	10.4.3
10.4.4	Turbine Bypass System	10.4-4
10.4.5	Circulating Water System	10.4-5
10.4.6	Condensate Cleanup System	10.4-7

TABLE OF CONTENTS (Cont'd.)

<u>Section</u>		<u>Page</u>
10.4.7	Condensate and Feedwater Systems	10.4-9
10.4.8	Steam Generator Blowdown System	10.4-14
11.0	<u>RADIOACTIVE WASTE MANAGEMENT</u>	11.1-1
11.1	<u>SOURCE TERMS</u>	11.1-1
11.1.1	Modes of Radioactive Waste Production	11.1-1
11.1.2	Activation Product Source Strength Models	11.1-2
11.1.3	Fission Product and Plutonium Release Models	11.1-5
11.1.4	Tritium Production Sources	11.1-7
11.1.5	Summary of Design Bases for Deposition of Radioactivity in Primary Sodium on Reactor and Primary Heat Transfer Surfaces and Within Reactor Auxiliary Systems	11.1-7
11.1.6	Leakage Rates	11.1-10
11.2	<u>LIQUID WASTE SYSTEM</u>	11.2-1
11.2.1	Design Objectives	11.2-1
11.2.2	System Description	11.2-2
11.2.3	System Design	11.2-4
11.2.4	Operating Procedures and Performance Tests	11.2-5
11.2.5	Estimated Releases	11.2-6
11.2.6	Release Points	11.2-6
11.2.7	Dilution Factors	11.2-7
11.2.8	Estimated Doses	11.2-8
	Appendix 11.2A Dose Models: Liquid Effluents	11.2A-1
11.3	<u>GASEOUS WASTE SYSTEM</u>	11.3-1
11.3.1	Design Base	11.3-1
11.3.2	System Description	11.3-1
11.3.3	System Design	11.3-10
11.3.4	Operating Procedures and Performance Tests	11.3-11a
11.3.5	Estimated Releases	11.3-14
11.3.6	Release Points	11.3-15
11.3.7	Dilution Factors	11.3-17
11.3.8	Dose Estimates	11.3-17
	Appendix 11.3A Dose Models: Gaseous Effluents	11.3A-1
11.4	<u>PROCESS AND EFFLUENT RADIOLOGICAL MONITORING SYSTEM</u>	11.4-1
11.4.1	Design Objectives	11.4-1
11.4.2	Continuous Monitoring/Sampling	11.4-2
11.4.3	Sampling	11.4-3

TABLE OF CONTENTS (Cont'd.)

<u>Section</u>		<u>Page</u>
11.5	<u>SOLID WASTE SYSTEM</u>	11.5-1
11.5.1	Design Objectives	11.5-1
11.5.2	System Inputs	11.5-1
11.5.3	Equipment Description	11.5-1
11.5.4	Expected Volumes	11.5-3
11.5.5	Packaging	11.5-4
11.5.6	Storage Facilities	11.5-4
11.5.7	Shipment	11.5-4
11.6	<u>OFFSITE RADIOLOGICAL MONITORING PROGRAM</u>	11.6-1
11.6.1	Expected Background	11.6-1
11.6.2	Critical Pathways to Man	11.6-2
11.6.3	Sampling Media, Locations and Frequencies	11.6-4
11.6.4	Analytical Sensitivity	11.6-4
11.6.5	Data Analysis and Presentation	11.6-4
11.6.6	Program Statistical Sensitivity	11.6-5
12.0	<u>RADIATION PROTECTION</u>	12.1-1
12.1	<u>SHIELDING</u>	12.1-1
12.1.1	Design Objectives	12.1-1
12.1.2	Design Description	12.1-3
12.1.3	Source Terms	12.1-13
12.1.4	Area Radiation Monitoring	12.1-23
12.1.5	Estimates of Exposure	12.1-24
	Appendix to Section 12.1	12.1A-1
12.2	<u>VENTILATION</u>	12.2-1
12.2.1	Design Objectives	12.2-1
12.2.2	Design Description	12.2-1
12.2.3	Source Terms	12.2-3
12.2.4	Airborne Radioactivity Monitoring	12.2-3
12.2.5	Inhalation Doses	12.2-5
12.3	<u>HEALTH PHYSICS PROGRAM</u>	12.3-1
12.3.1	Program Objectives	12.3-1
12.3.2	Facilities and Equipment	12.3-3
12.3.3	Personnel Dosimetry	12.3-6
12.3.4	Estimated Occupancy Times	12.3-7
	Appendix 12A - Information Related to ALARA for Occupational Radiation Exposures	12A-1

TABLE OF CONTENTS (Cont'd.)

<u>Section</u>		<u>Page</u>
13.0	<u>CONDUCT OF OPERATIONS</u>	13.1-1
13.1	<u>ORGANIZATIONAL STRUCTURE OF THE APPLICANT</u>	13.1-1
13.1.1	Project Organization	13.1-1
13.1.2	Operating Organization	13.1-5
13.1.3	Qualification Requirements for Nuclear Plant Personnel	13.1-12
13.2	<u>TRAINING PROGRAM</u>	13.2-1
13.2.1	Program Description	13.2-1
13.2.2	Retraining Program	13.2-6
13.2.3	Replacement Training	13.2-6
13.2.4	Records	13.2-6
13.3	<u>EMERGENCY PLANNING</u>	13.3-1
13.3.1	General	13.3-1
13.3.2	Emergency Organization	13.3-2
13.3.3	Coordination with Offsite Groups	13.3-5
13.3.4	Emergency Action Levels	13.3-6
13.3.5	Protective Measures	13.3-7
13.3.6	Review and Updating	13.3-7
13.3.7	Medical Support	13.3-7
13.3.8	Exercises and Drills	13.3-8
13.3.9	Training	13.3-8
13.3.10	Recovery and Reentry	13.3-9
13.3.11	Implementation	13.3-9
	Appendix 13.3A	13.3A-1
13.4	<u>REVIEW AND AUDIT</u>	13.4-1
13.4.1	Review and Audit - Construction	13.4-1
13.4.2	Review and Audit - Test and Operation	13.4-1
13.5	<u>PLANT PROCEDURES</u>	13.5-1
13.5.1	General	13.5-1
13.5.2	Normal Operating Instructions	13.5-1
13.5.3	Abnormal Operating Instructions	13.5-2
13.5.4	Emergency Operating Instructions	13.5-2
13.5.5	Maintenance Instructions	13.5-3

Amend. 68
May 1982

TABLE OF CONTENTS (Cont'd.)

<u>Section</u>		<u>Page</u>
13.5.6	Surveillance Instructions	13.5-4
13.5.7	Technical Instructions	13.5-4
13.5.8	Sections Instruction Letters	13.5-4
13.5.9	Site Emergency Plans	13.5-4
13.5.10	Radiation Control Instructions	13.5-4
13.6	<u>PLANT RECORDS</u>	13.6-1
13.6.1	Plant History	13.6-1
13.6.2	Operating Records	13.6-1
13.6.3	Event Records	13.6-1
13.7	<u>RADIOLOGICAL SECURITY</u>	13.7-1
13.7.1	Organization and Personnel	13.7-1
13.7.2	Plant Design	13.7-3
13.7.3	Security Plan	13.7-6
14.0	<u>INITIAL TESTS AND OPERATION</u>	14.1-1
14.1	<u>DESCRIPTION OF TEST PROGRAMS</u>	14.1-1
14.1.1	Preoperational Test Programs	14.1-2
14.1.2	Startup Test Program	14.1-2
14.1.3	Administration of Test Program	14.1-3
14.1.4	Test Objectives of First-of-a-Kind Principal Design Features	14.1-6
14.2	<u>AUGMENTATION OF OPERATOR'S STAFF FOR INITIAL TESTS AND OPERATION</u>	14.2-1
15.0	<u>ACCIDENT ANALYSES</u>	15.1-1
15.1	<u>INTRODUCTION</u>	15.1-1
15.1.1	Design Approach to Safety	15.1-1
15.1.2	Requirements and Criteria for Assessment of Fuel and Blanket Rod Transient Performance	15.1-50
15.1.3	Control Rod Shutdown Rate and Plant Protection System Trip Settings	15.1-93
15.1.4	Effect of Design Changes on Analyses of Accident Events	15.1-105
15.2	<u>REACTIVITY INSERTION DESIGN EVENTS - INTRODUCTION</u>	15.2-1
15.2.1	Anticipated Events	15.2-5
15.2.2	Unlikely Events	15.2-34
15.2.3	Extremely Unlikely Events	15.2-51

TABLE OF CONTENTS (Cont'd.)

<u>Section</u>		<u>Page</u>
15.3	<u>UNDERCOOLING DESIGN EVENTS - INTRODUCTION</u>	15.3-1
15.3.1	Anticipated Events	15.3-6
15.3.2	Unlikely Events	15.3-29
15.3.3	Extremely Unlikely Events	15.3-38
15.4	<u>LOCAL FAILURE EVENTS - INTRODUCTION</u>	15.4-1
15.4.1	Fuel Assembly	15.4-2
15.4.2	Control Assemblies	15.4-42
15.4.3	Radial Blanket Assembly	15.4-51
15.5	<u>FUEL HANDLING AND STORAGE EVENTS - INTRODUCTION</u>	15.5-1
15.5.1	Anticipated Events (None)	15.5-4
15.5.2	Unlikely Events	15.5-4
15.5.3	Extremely Unlikely Events	15.5-23
15.6	<u>SODIUM SPILLS - INTRODUCTION</u>	15.6-1
15.6.1	Extremely Unlikely Events	15.6-4
15.7	<u>OTHER EVENTS - INTRODUCTION</u>	15.7-1
15.7.1	Anticipated Events	15.7-3
15.7.2	Unlikely Events	15.7-9
15.7.3	Extremely Unlikely Events	15.7-18
15.A	Appendix 15.A - Radiological Source Term for Assessment of Site Suitability	15.A-1
16.0	<u>TECHNICAL SPECIFICATIONS</u>	16.1-1
16.1	<u>DEFINITIONS</u>	16.1-1
16.1.1	Reactor Operating Condition	16.1-1
16.1.2	Reactor Core	16.1-2
16.1.3	Plant Protection System Instrumentation	16.1-3
16.1.4	Safety Limit	16.1-5
16.1.5	Limiting Safety System Setting (LSSS)	16.1-5
16.1.6	Limiting Conditions for Operation (LCO)	16.1-6
16.1.7	Surveillance Requirements	16.1-6
16.1.8	Containment Integrity	16.1-6
16.1.9	Abnormal Occurrence	16.1-6

TABLE OF CONTENTS (Cont'd.)

<u>Section</u>		<u>Page</u>
16.2	<u>SAFETY LIMITS AND LIMITING SAFETY SYSTEM SETTINGS</u>	16.2-1
16.2.1	Safety Limit, Reactor Core	16.2-1
16.2.2	Limiting Safety System Settings	16.2-1
16.3	<u>LIMITING CONDITIONS FOR OPERATION</u>	16.3-1
16.3.1	Reactor Operating Conditions	16.3-1
16.3.2	Primary Heat Transport System (PHTS)	16.3-2
16.3.3	Intermediate Heat Transport Coolant System	16.3-6
16.3.4	Steam Generation System (SGS)	16.3-7
16.3.5	Auxiliary Liquid Metal System	16.3-12
16.3.6	Inert Gas System Cover Gas Purification System	16.3-13
16.3.7	Auxiliary Cooling System	16.3-14
16.3.8	Containment Integrity	16.3-21
16.3.9	Auxiliary Electrical System	16.3-21
16.3.10	Refueling	16.3-24
16.3.11	Effluent Release	16.3-27
16.3.12	Reactivity and Control Rod Limits	16.3-31
16.3.13	Plant Protection System	16.3-34
16.4	<u>SURVEILLANCE REQUIREMENTS</u>	16.4-1
16.4.1	Operational Safety Review	16.4-1
16.4.2	Reactor Coolant System Surveillance	16.4-1
16.4.3	Containment Tests	16.4-3
16.4.4	HVAC and Radioactive Effluents	16.4-6
16.4.5	Emergency Power System Periodic Tests	16.4-10
16.4.6	Inert Gas System	16.4-13
16.4.7	Reactivity Anomalies	16.4-13
16.4.8	Pressure and Leakage Rate Test of RAPS Cold Box Cell	16.4-15
16.4.9	Pressure and Leakage Rate Test of RAPS Noble Gas Storage Vessel Cell	16.4-15a
16.5	<u>DESIGN FEATURES</u>	16.5-1
16.5.1	Site	16.5-1
16.5.2	Confinement/Containment	16.5-1
16.5.3	Reactor	16.5-2
16.5.4	Heat Transport System	16.5-5
16.5.5	Fuel Storage	16.5-7
16.6	<u>ADMINISTRATIVE CONTROLS</u>	16.6-1
16.6.1	Organization	16.6-1
16.6.2	Review and Audit	16.6-1
16.6.3	Instructions	16.6-4
16.6.4	Actions to be Taken In the Event of Reportable Occurrence In Plant Operation	16.6-6

TABLE OF CONTENTS (Cont'd.)

<u>Section</u>		<u>Page</u>
16.6.5	Action to be Taken in the Event a Safety Limit Is Exceeded	16.6-6
16.6.6	Station Operating Records	16.6-6
16.6.7	Reporting Requirements	16.6-7
16.6.8	Minimum Staffing	16.6-8
17.0	<u>QUALITY ASSURANCE - INTRODUCTION</u>	17.0-1
17.0.1	Scope	17.0-1
17.0.2	Quality Philosophy	17.0-1
17.0.3	Participants	17.0-2
17.0.4	Project Phase Approach	17.0-3
17.0.5	Applicability	17.0-3
17.1	<u>QUALITY ASSURANCE DURING DESIGN AND CONSTRUCTION</u>	17.1-1
17.1.1	Organization	17.1-1
17.1.2	Quality Assurance Program	17.1-2
17.1.3	References Referred to in the Text	17.1-6
17.1.4	Acronyms Used in Chapter 17 Text and Appendices	17.1-6a

TABLE OF CONTENTS (Cont'd.)

<u>Section</u>		<u>Page</u>
Appendix 17A	A Description of the Owner Quality Assurance Program	17A-1
Appendix 17B	A Description of the Fuel Supplier Quality Assurance Program	17B-1
Appendix 17C	A Description of the Balance of Plant Supply Quality Assurance Program	17C-1
Appendix 17D	A Description of the ARD Lead Reactor Manufacturer Quality Assurance Program	17D-1
Appendix 17E	A Description of the Architect-Engineer Quality Assurance Program	17E-1
Appendix 17F	A Description of the Constructor Quality Assurance Program	17F-1
Appendix 17G	RDT Standard F2-2, 1973, Quality Assurance Program Requirements	17G-1
Appendix 17H	A Description of the ARD Reactor Manufacturer Quality Assurance Program	17H-1
Appendix 17I	A Description of the GE-ARSD-RM Quality Assurance Program	17I-1
Appendix 17J	A Description of the ESG-RM Quality Assurance Program	17J-1
Appendix A	Computer Codes	A-1
Appendix B	General Plant Transient Data	B-1
Appendix C	Safety Related Reliability Program	C.1-1
Appendix D	Deleted	
Appendix E	Deleted	
Appendix F	Deleted	
Appendix G	Plan for Inservice and Preservice Inspections	G-1
Appendix H	Post TMI Requirements	H-1

3.9 MECHANICAL SYSTEMS AND COMPONENTS

3.9.1 Dynamic System Analysis and Testing

The startup functional testing which will include vibration, thermal expansion, and dynamic effects (operational transients) on specified high and moderate energy piping, and the associated supports and restraints. The test program, to be supplied by the FSAR, will include:

- (1) A list of systems to be monitored.
- (2) A listing of flow modes and transients.
- (3) A list of selected locations in the piping systems where visual inspections and measurements (as needed) will be performed.
- (4) A list of snubbers on systems that will be measured for snubber travel from cold to hot positions.
- (5) A description of the thermal motion monitoring program.
- (6) A description of actions necessary to correct vibration that is beyond the acceptance levels.

3.9.1.1 Vibration Operational Test Program

The preoperational vibrational and dynamic effects testing program that is to be conducted during startup functional testing for safety-related piping classified as Code Class 1, 2 and 3 and for piping and component supports will be described fully in the FSAR. The purpose of these tests will be to confirm that the piping, components, and supports have been designed to withstand the dynamic loadings from operational transient conditions that will be encountered during service, as required by the ASME Code. In general terms, the preoperational vibrational test program to confirm the adequacy of the designs will consist of the following:

- a. A listing of systems to be monitored.
- b. A listing of the different flow modes such as pump trips, valve closures, etc. to which the piping will be subjected during the test.
- c. A list of selected locations in the piping system where visual inspections and measurements will be performed to assure that the deflections are within the design limits.
- d. A list of snubbers that will be measured for travel from cold to hot positions.
- e. A description of the thermal motion monitoring program.
- f. If vibration is noted beyond the acceptance levels set by the criteria of (c) above, corrective restraints will be designed, incorporated in the piping system analysis, and installed. Another test will then be performed to determine that the vibrations have been reduced to an acceptable level.

3.9.1.2 Dynamic Testing Procedures

The seismic qualification program which will be employed to qualify all safety-related equipment will be described fully in the FSAR. The purpose of this program will be to confirm the ability of all seismic Category I mechanical equipment to function as needed during and after an earthquake of magnitude up to and including the SSE. In general terms, the seismic qualification program will take into account the following:

- a. Analysis without testing will be acceptable if structural integrity alone can assure the design-intended function. When a complete seismic test is impractical, a combination of test and analysis will be acceptable.
- b. Mechanical equipment will be tested in the operational condition (if possible or necessary). Loadings simulating those of plant normal operation, such as thermal and flow-induced loadings, if any, will be concurrently superimposed upon the seismic loading. Operability will be verified during and after the test.
- c. For the analysis or qualification, the characteristics of the seismic input motion will be specified by one or more of the following:
 - (1) Sine Beats
 - (2) Response spectrum
 - (3) Time history

Such characteristics, as derived from the structure or system seismic, will be representative of the seismic input motion at the equipment mounting.

- d. The test input motion will be characterized in the same manner as the seismic input motion, and the conservatism in amplitude and frequency content will be demonstrated.
- e. When single frequency sine beat resonant testing is performed for qualification testing, additional testing will also be performed with multi-frequency motion such that the TRS (Test Response Spectrum) envelops the RRS (Required Response Spectrum).
- f. Dynamic coupling between the equipment and related systems, if any, such as connected piping and other mechanical components, will be considered.
- g. Any test fixture used will meet the following requirements:
 - (1) Simulate the actual service mounting
 - (2) Cause no extraneous dynamic coupling to the test item
- h. The in situ application of vibratory loadings on a complex active device for operability testing will be used if it is shown that a meaningful test can be made in this way.

- i. The test program may be based upon selectively testing a representative number of mechanical components according to type, load level, size, etc., on a prototype basis.
- j. Analyses or tests will be performed for all support of mechanical equipment to assure their structural capability to withstand seismic excitation.
- k. Supports that are to be tested, will be tested with equipment installed or with an equivalent mass that simulates the equipment dynamic coupling to the support. If the equipment is installed in a nonoperating condition for the support test, the response at the equipment mounting location will be characterized in the manner as stated in (c) above. In such a case, the equipment will be tested separately for operability and the actual input to the equipment will be more conservative in amplitude and frequency than the monitored response.
- l. The requirements of (c), (d), (e), (f) and (h), above, will be applied when tests are conducted on equipment supports.

3.9.1.3 Dynamic System Analysis Methods for Reactor Internals

3.9.1.3.1 Summary of Overall Flow Induced Vibration Assessment Program for CRBRP

A comprehensive vibration assessment program to assure that excessive flow induced vibratory motion of reactor internals does not exist, is part of the CRBRP program. The program, schematically illustrated in Figure 3.9-4, assures the structural integrity of reactor internals. The program accomplishes this objective by means of the following key actions:

1. Design to avoid flow induced vibration.
2. Evaluate susceptibility of each component to flow induced vibration.
3. Analyze to provide a model evaluation of each component.
4. Test both scale model and full system simulations.
5. Factor FFTF operational measurements and experience, as well as relation between FFTF scale model testing and in-reactor data, into CRBRP evaluations.
6. Monitor upper Internals structure vibrational response during pre-operational testing to supplement and confirm vibration results from the model test program.

The program integrates the input from these sources to assure that excessive flow induced vibratory motion of reactor internals does not occur.

The overall program has been formulated to meet the intent of NRC Regulatory Guide 1.20. The program relies on highly instrumented model tests to assure that flow induced vibration problems will not exist in the reactor. This

approach is an extension of the vibration assessment program developed for FFTF. It utilizes the experience gained from FFTF model testing, where models were used to assess the potential for flow induced vibration, with the objective of developing correlations which will predict CRBRP prototypic motions using scale model test data. Where scale model tests may not be adequate, such as for long, slender members with flow thru clearances, full scale tests are performed.

Details of the program's key features are provided in the following sections.

3.9.1.3.1.1 Design

CRBRP components are designed to avoid excessive flow induced vibration. Heavy structures are utilized, where possible, to withstand vibratory forces. Generally, structures and components are designed to have natural frequencies as high as practical to avoid coincidence with known forcing mechanisms. Mechanical stresses that are caused by flow induced vibrations that are unavoidable must meet the fatigue requirements of the ASME Boiler and Pressure Vessel, Section III, and Code Case N-47. When combined with the effects of other operating conditions, maximum displacements will be limited, as required, to assure proper functioning of the components.

3.9.1.3.1.2 Component Evaluation

A general survey of all CRBRP reactor internals was made. In this survey the following considerations were given to each component:

- o Type of possible component excitation, vortex shedding, turbulence, pump pulsation, jet impingement, jet reaction, gap modulation or other fluid elastic mechanisms.
- o Importance index - based on the relative importance of the component and type of excitation.
- o Investigative priority - priority is based on degree of concern and whether the component can be evaluated by state-of-the-art methods.

Table 3.9-9 summarizes this survey and provides the methods selected to address the question of flow induced vibration.

3.9.1.3.1.3 Analysis

Existing analysis methods (ANSYS, etc) are used to compute the natural frequencies and mode shapes. Component response is calculated, assuming a fluid forcing mechanism, and the resulting stress or component motion evaluated. Presently, one of the most effective means of designing against the occurrence of severe flow induced vibration problems is to separate structural natural frequencies from expected excitation frequencies; generally, natural frequencies of interfacing components are separated.

By utilizing existing flow induced vibration analysis and information, the free and forced response of the CRBRP structures are investigated. The prediction of flow induced vibration response is limited to the state-of-the-

art in describing the fluid to forcing function associated with fluid excitation mechanisms and damping. Many excitation mechanisms could be responsible for CRBRP component vibration. Some examples are cross-flow vortex shedding, parallel flow boundary layers, fluid borne noise, wakes from adjacent components and fluid elastic coupling between adjacent components. Although all of these mechanisms are of concern, generally characterization is possible for only the first two mechanisms when each is assumed to act alone. Even then the forcing functions are based on assumption. Therefore, experimental evaluation of components using scale models is relied upon. The results from the experimental portion of the program will be factored into the analysis and final assessment of the component acceptability regarding flow induced vibration.

3.9.1.3.1.4 Testing

For many regions of the reactor, the complex interaction of the flow field with the reactor structures precludes the utilization of analytical methods for evaluation of component flow induced vibration. For this reason a comprehensive series of system tests, both scale model and full scale, have been planned for CRBRP. These tests reproduce flow fields closely matching those which will exist in the actual reactor. The planning of the experimental programs was carried out in consultation with recognized personnel in the field of flow induced vibration from the Argonne National Laboratory, Hanford Engineering Development Laboratory and the Westinghouse Research Laboratories. In addition, during performance of the program, the test methods, similarity requirements, test results, etc. are continually reviewed by these personnel as well as by personnel from other organizations knowledgeable in flow induced vibration. Every effort is made to ensure that the results obtained from the model studies are correct and directly applicable to CRBRP.

The major models used in the experimental portion of the CRBRP comprehensive vibration assessment program consist of the following:

- a. Inlet Plenum Feature Model
- b. Bench Test Models
- c. Selected Full Scale Models
- d. Integral Reactor Feature Model (IRFM)

A description of these various models follows. Since the IRFM test program is the most significant part of the total test program this test is discussed in detail in later sections. Results from the various model tests are provided in Section 3.9.1.3.2.

a. Inlet Plenum Feature Model (IPFM)

The IPFM models all hydrodynamically wetted surfaces in a full 360 degree (0.248 scale) sector of the inlet plenum and lower internal components. This test, initiated in 1974, was completed in 1976. Seven of the 61 lower inlet modules (LIM) were dynamically simulated with accelerometers mounted on four of these seven modules to monitor their vibrational response. The LIMs which were dynamically simulated (i.e., equal Strouhal number) are those located nearest to the reactor vessel inlet nozzles, because they are subjected to the highest cross-flow velocity and thus most susceptible to vibration. Results from the IPFM test series are summarized in Section 3.9.1.3.2.

b. Bench Tests

Based on component evaluations, an experimental program to evaluate the flow induced vibration characteristics of selected regions of the Upper Internals Structure was established. Testing was performed by Argonne National Laboratory in a 1/3 scale facility which structurally and hydraulically simulated the instrumentation post and a chimney with a lower shroud tube.

Results of these bench tests are given in Section 3.9.1.3.2.

c. Full Scale Model Testing

It was anticipated that during the performance of the experimental program, the need for additional, selected full scale model tests might be identified. For example, it became necessary to conduct selected full scale tests on portions of the UIS where similarity criteria or Reynolds number similarity could not be satisfied by scale model testing. These full scale tests include the gap modulation flow induced vibration test of the control rod upper to lower shroud tube slip joint, the UIS chimney vibro impact test, and the IVTM port plug gap modulation flow induced vibration test.

In addition to these full scale tests, a special test is being conducted on the IVTM Port Plug in conjunction with the gap modulation flow induced vibration test. During the test it is planned to assess the susceptibility of the IVTM Port Plug to self-excited vibration. If the levels do not increase, it will be a positive indication that the potential for self-excited vibration does not exist.

Finally, full scale testing of a prototype Primary Control Rod System - a Primary Control Rod Drive Mechanism, Primary Control Rod Driveline, and Primary Control Assembly in sodium at 400°F - has been performed. The Primary Control Drive (PCRD) was instrumented with three pairs of accelerometers to measure its flow induced vibration response. Emphasis on the PCRD was at the dashpot/cup area. The PCA was instrumented with four accelerometers which were positioned at two elevations on the outer

duct of the assembly. The in sodium tests were conducted in an aligned and misaligned configuration, the test variables for a given configuration being rod withdrawal height and prototypic sodium flow through the PCA and the shroud tube enveloping the driveline. Results of this testing are given in Section 3.9.1.3.2.

d. Integral Reactor Flow Model (IRFM)

The outlet plenum region of the reactor contains components which could potentially have flow induced vibration problems. Therefore planning for a 1/4 scale flow and vibration system model of this region was initiated in 1975. The objectives of the IRFM test program are as follows:

1. Measurement of the velocity pattern in the outlet plenum and in the vicinity of major outlet plenum structures to provide input for the prediction of flow induced vibration.
2. Evaluation of flow induced vibration characteristics of selected outlet plenum structures.
3. Evaluation of flow induced vibration characteristics of the primary and secondary control rod drivelines.

It was decided that to satisfy these objectives the model test program would be conducted in two phases since the design of all outlet plenum components was not finalized. For the initial phase of IRFM testing, Phase I, approximately 100 accelerometers were located on critical regions of the outlet plenum components as shown in Figure 3.9-5. The location of this instrumentation is based on modal analyses of these components. Table 3.9-10 summarizes the instrumentation planned for the Phase II vibration tests in IRFM.

In order to satisfy the objectives of the test program the following tests were performed during Phase I:

1. Velocity Test (outlet plenum for both three-loop and two-loop operation, Inter-chimney region, chimney, core assemblies - upper Internals).
2. Flow Induced Vibrations (preliminary evaluation of current designs).

A flow step summary of the flow induced vibration test is provided in Table 3.9-6. As the table shows, vibration data was obtained on the model for the full range of anticipated flow including the refueling mode. In addition to the flow induced vibration data, experimental modal analysis (shaker tests) of the UIS and outlet plenum Internals was conducted for two conditions: (1) the model dry in air and (2) no flow but model vessel full of water. For the Phase II testing, the flow induced vibration test sequence will be repeated. The shaker tests will also be repeated for the final designs.

Model Description

The IRFM is an approximately 0.248 scale model of the wetted surfaces in the CRBRP reactor outlet plenum. It is a 360° model, including three outlet nozzles as in the CRBRP reactor, and is capable of two or three loop operation. The vessel support is not prototypic, but it provides sufficient frequency separation between support, vessel and components.

Both hydraulic and vibrational testing are performed in IRFM. However, since flow induced vibrations are of concern for only certain outlet plenum structures, only those structures will reflect hydraulic and structural simulation. Table 3.9-8 is provided to define the components which require one or both types of simulation.

In the design of the IRFM, provision was made for simulating the height variation of the reactor assembly exit nozzles. Provisions were also made for simulating misalignment between the UIS and the core. Two height and two radial alignment variations have been tested. Also, the refueling position mode, in which the upper Internals structure is raised 9-1/2" and decoupled from the lower Internals, has been tested.

For the Phase I series of tests the following components were modeled in IRFM:

- o Upper Internals Structure
- o Instrumentation Post
- o Instrumentation Conduit
- o Liquid Level Monitor
- o IVTM Port Plug
- o Ex-vessel Transfer Machine Guide Tube
- o Upper Control Rod Shroud Tube
- o Control Rod Driveline

The second phase of IRFM testing structurally simulates the final, released designs of outlet plenum hardware. Phase II model simulations provide data on prototypically modeled components prior to reactor operation and will be used to predict prototypic vibration of outlet plenum components. To date the IRFM has been modified to include the thermal liner, the outlet nozzle liner, a redesigned Liquid Level Monitor Port Plug (LLMPP), and a dynamic simulation of the vortex suppressor plate. For the final series of IRFM Phase II tests, the simulation of the UIS is being modified to include dynamic simulation of the following: two chimneys, the thermal liner plates in the mixing chamber, and the UIS jacking mechanism method of UIS column support.

In addition, it is planned to locate four biaxial accelerometers on the UIS model to monitor its gross motion during a simulation of the reactor's preoperational test program. The accelerometers are located on the model in the identical positions of the plant accelerometers. By correlating the data from these two sets of accelerometers, predictions on the motion of the prototype unit can be made from data obtained from the highly instrumented IRFM model.

Vibration Modeling Considerations

The similitude requirements for valid flow induced vibration model testing are generally well known (see Refs. 1 and 2).

Similitude ratios which are pertinent to flow induced vibration modeling are summarized below. Subscripts m and p refer to model and prototype, respectively.

$(Re)_m / (Re)_p$, where Re is the Reynolds number (DU/γ),

S_m / S_p , where S is the Strouhal number (fD/U),

$(\rho_s/\rho)_m / (\rho_s/\rho)_p$, where ρ_s is the structure material density and ρ is the fluid density, and

(δ_m/δ_p) , where δ is the log decrement.

For a given structure in incompressible flow, and ignoring (a) externally driven boundary motions, (b) externally generated forces (such as pump pulsations), (c) surface wave effects (Froude number), and (d) surface tension effects (Weber number) the dependent parameters of interest are a function of four main independent parameters.

$$y/D = \phi \left[\frac{f_n D}{u}, \frac{\rho_s}{\rho}, \frac{Du}{\nu}, \delta \right]$$

where y = vibration amplitude

D = characteristic length (diameter)

f_n = natural frequency

U = flow velocity

ρ_s = density of structure

ρ = density of fluid

ν = kinematic viscosity

δ = mechanical damping, log decrement

An equivalent set of parameters is:

$$y/D = \phi \left[\frac{K}{u^2 D}, \frac{\rho_s}{\rho}, \frac{Du}{\nu}, \frac{C}{\rho u D^2} \right]$$

where K = spring rate, lb/in

C = mechanical damping constant, lb-sec/in

For geometrically similar structures, the scaling law between model and prototype using subscripts m and p respectively, is

$$\left(\frac{Y}{D}\right)_p = \left(\frac{Y}{D}\right)_m$$

This relationship will hold when the four similitude parameters are the same in model and prototype.

Table 3.9-7 shows the flow vibration parameters and associated ratios for the model and prototype.

In the following paragraphs, the similitude ratios are discussed as they pertain to the IRFM simulation. The model fluid will be water at 100°F and the prototype fluid is sodium at 950°F. The structural material is stainless steel.

Reduced Frequency and Density

Using stainless steel and a model temperature of 100°F will result in component stiffnesses which are approximately 24% greater than properly scaled values.

Because the stiffness is about 24% higher, the vibration natural frequencies will be about 11.4% higher as a result. To obtain the same values of reduced frequencies $f_n D/U$ in the model as in the prototype, the model flow velocities must be 11.4% higher than the prototype flow velocities. The structural mass will be properly scaled, but the fluid densities will not.

Under these conditions, the fluid elastic parameter $K/\rho U^2 D$ will be .83 times the prototype value, which is conservative.

Reynolds Number

A modeling scale $D_{\text{model}}/D_{\text{prototype}} = 0.248$ has been chosen. A flow velocity ratio $U_{\text{model}}/U_{\text{prototype}} = 1.1$ was chosen, corresponding to an operation condition giving the same reduced frequency of structural vibration, $f_n D/U$, in model and prototype. Under these conditions the ratio of Reynolds numbers ($Re = Du/\nu$) will be:

$$Re_{\text{model}}/Re_{\text{prototype}} = 0.1$$

Reynolds number will not be duplicated in the model. This is not considered to be significant except possibly in a limited flow/vibration regime. This is further discussed below.

Circular cylinders in steady cross flow exhibit regular vortex shedding with well defined shedding frequency in the Reynolds number regime $80 \leq Re \leq 3.5 \times 10^5$ (subcritical) and $Re \geq 3.5 \times 10^6$ (transcritical), where $Re = DU/\nu$ is based on the cylinder diameter D and cross flow velocity U . For $500 \leq Re \leq 3.5 \times 10^5$ the shedding frequency f_s is given with fairly good accuracy by $f_s = .2 U/D$ Hz*, whereas for $Re \geq 3.5 \times 10^6$, $f_s = .27 U/D$. In the subcritical and transcritical regimes, coincidence between vortex shedding frequency f_s and structural vibration natural frequency f_n , can give rise to large alternating forces and large lateral vibration amplitudes. In the supercritical regime, $3.5 \times 10^5 \leq Re \leq 3.5 \times 10^6$, any shedding is irregular and the resulting vibration excitation forces are random. Therefore in the supercritical region there is no possibility of driving frequency coincidence with the structural vibration natural frequency.

On account of the foregoing considerations, it is important to identify the Reynolds number regimes of cross flow past cylindrical structural components of CRBRP prototype and flow vibration models.

Values of Reynolds numbers in the model and in the prototype, determined for the aforementioned assumed conditions are given in Figure 3.9-3 as functions of the product (prototype cross flow velocity) \times (prototype cylindrical-component diameter). Also indicated in Figure 3.9-3 are the limits defining the supercritical regime of random excitation. It can be seen that the model will be conservative for subcritical flows but non-conservative for transcritical flows. That is, there is a DU regime ($11 \text{ in-ft/sec} \leq DU \leq 107 \text{ in-ft/sec}$) where vortex shedding frequency coincidence that might take place in the model would not take place in the prototype; and there is another DU regime ($116 \text{ in-ft/sec} \leq DU \leq 1200 \text{ in-ft/sec}$) where vortex shedding frequency coincidence that might take place in the prototype would not occur in the model. CRBRP model vibration test results must be viewed with this point in mind. The mismatch in Reynolds numbers emphasizes the need for analytically examining upper internal components for susceptibility to vortex shedding excitation.

*In the formulas for shedding frequency, the units of U and D are such that U/D has units of sec^{-1} .

Density Ratios

The value of density ratios, $(\rho_s/\rho)_m (\rho_s/\rho)_p$, from Table 3.9-7 is 0.851. The hydraulic modeling in IRFM is designed to reproduce the flow fields and thus the fluid forcing functions which will occur in the actual reactor. The difference in density ratio between model and prototype results in model structures having a lower natural frequency than comparable prototype structures when the effects of the virtual mass of the fluid in the model are considered. By applying equivalent fluid forcing functions on the model and prototype, the onset of unstable vibrations, if present, will occur in the model before the prototype. The increased density of the test fluid also provides a slightly higher driving energy in the model as opposed to the prototype. Both effects are small but make the model testing conservative.

Vibration Displacements

With respect to the modeling based on the requirements that the ratio of model-to-prototype Strouhal number be unity, the previously cited regimes of DU will establish the scalability of model results. In those regimes where the model is conservative, the effect of density ratio damping should be further conservatism. Then the ratio $(y/D)_m = (y/D)_p$ is considered conservative. The model results obtained in the non-conservative regime and the regime wherein $S_m/S_p \neq 1$ are not directly scalable to the prototype, and the results must be further analyzed based upon the test circumstances to establish applicability.

Model to Prototype Scaling Ratios

Based upon the values of Table 3.9-7 and the geometric scaling ratio of 0.248, the following are model-to-prototype ratios of measured parameters:

$$\begin{aligned}f_m/f_p &= 4.432 \text{ (frequency)} \\ \Delta_m/\Delta_p &= 0.248 \text{ (displacement)} \\ F_m/F_p &= 0.076 \text{ (force)} \\ \ddot{x}_m/\ddot{x}_p &= 4.871 \text{ (acceleration)}\end{aligned}$$

To aid concentration of the testing on areas of significance, guidelines have been established for vibration levels requiring detailed measurements and assessment. If the vibration measurement for a component show either acceleration levels greater than 0.3g's, occurrence of impacting or a flow rate dependent resonance, the component data is assessed for potential design impact with additional measurements performed if necessary to obtain conclusive data. If neither of these effects occur, the component does not require further vibration assessment.

3.9.1.3.2 Test Results

A. IPFM

Data from the IPFM tests show the maximum prototypic vibrational amplitude of a LIM is 0.2 mils. This value is very low and is structurally acceptable. The tests have also shown that dynamic coupling between the Core Support Structure and the LIMs is negligible.

B. Bench Model Tests

Test results from the 1/3 ANL scale model of an instrumentation post indicate vibrational response is extremely small, less than 0.4 mils in bending. Testing of an outer chimney (chimney located above a blanket region) showed small vibration amplitudes and only slight rattling between the chimney and its support. Testing of a central chimney with a shroud tube (chimney located above an active region of the core) indicated similar results.

C. Full Scale Model Testing

- o The upper to lower shroud tube slip joint test have been successfully completed with no excitation mechanism discovered for simulated prototypic leakage conditions.
- o The UIS chimney vibro-impact test has been completed and the data is being evaluated. Preliminary evaluation of test data indicates that no gross motion of the chimney occurs at flow rates up to 95% of design flow rate. At 95% of design flow rate, signals from displacement transducers indicated fluctuations. It does not appear however that impacting is occurring at the 95% flow condition. Additional data evaluation is being performed and the model will be visually inspected for signs of impacting at disassembly.

Primary Control Rod System Tests

- o Low energy level flow induced vibration occurred across a broad frequency spectrum.

- o Acceleration levels increased according to the square of flow velocity without indicating any resonant peaks or instabilities.
- o Vibration behavior of the system was not significantly affected by either rod withdrawal height or misalignment.
- o Low level flow induced impacting did occur in both the dashpot and control assembly areas. The acceleration magnitude and rate of impacting also increased approximately as the square of the flow rate.

D. IRFM Phase I

Test results of the Phase I tests can be summarized as follows:

- o The measured responses of instrumented components were generally small and proportional to the flow rate over the flow regime tested.
- o There were no observed unstable dependencies upon flow rate nor abnormally high fluid excited forced components.
- o There were no observed occurrences of vortex shedding synchronous with component resonant frequency over the full flow range tested.
- o The vibrational characteristics of the UIS and instrumented outlet plenum components were essentially independent of core configuration, loop mode operation, and UIS/core alignment.
- o Impacting was observed on the following components, with the location of impacting coinciding with assembly gaps incorporated in the prototype design and scaled in IRFM;

UIS Keys/Core Former Ring

At 110% flow a maximum impacting of approximately 2.1 g's peak-to-peak was measured on an accelerometer mounted on the model core former ring radially outward from the keyways. The cyclic rate of this impact was less than 1 cycle/sec. The corresponding g value in the plant is 0.43 g's.

UIS Upper Shroud Tube/Lower Shroud Tube

At 110% flow a maximum impacting of up to 3.5 g's p-p at a cyclic rate of 4 to 5 impacts/sec was detected. These measurements were recorded from a shroud tube containing a control rod driveline. Another shroud tube without a CRDL exhibited impacting level of 3 g's p-p with a cyclic rate of 2 impacts/sec. These g levels when scaled to the reactor are 0.71 and 0.62 respectively. Based on these results, a full scale model test of the upper to lower shroud tube joint was performed for the final design configuration. As noted in C above, no vibrational problems were found.

Chimney/Spider/Lower Shroud Tube

This region was not directly instrumented for Phase I but responses on neighboring accelerometers indicate impacting was probable. The results of the full scale chimney test are described in C above.

UIS Column/Closure Head

Indications of impacting were detected with maximum levels of response less than 1 g p-p and a cyclic rate less than 1 impact/sec. The corresponding g value for the plant is 0.21 g's.

Control Rod Driveline

The control rod driveline response was acceptable at 100% and higher fluid velocities. Impacting at the dashpot/piston interface was infrequent.

E. IREM Phase II

Results from the completed portions of the Phase II testing are as follows:

- o The measured response of the Phase II components was generally small.
- o The thermal liner, outlet nozzle liner, and the Liquid Level Monitor Port Plug measured responses exhibited no unstable, flow rate dependency nor excessively high fluid excited response over the entire range of flow rates tested. Suppressor plate measured response was generally consistent and small over the range of test flow rates. The measured displacement amplitudes were less than 0.5 mils rms (model scale) at the maximum observed response levels.

- o The gross motion of the UIS during simulated refueling conditions (UIS raised to remove keys from the core former structure) was generally of low amplitude and erratic. The dominant measured lateral frequency was 12 Hz with calculated displacements on the order of 0.1 to 0.2 mils rms (model). Infrequent large amplitude responses were recorded. The maximum peak model displacement at the lower end of the UIS during these large amplitude responses was 16 mils. The motion was very sporadic and random occurring once every two to five seconds on the average.

3.9.1.3.3 Application of FFTF Experience to CRBRP

The CRBRP reactor intervals vibration program is similar to the FFTF vibration program and was formulated to maximize use of FFTF experience. Both programs utilize a combination of analysis, scale model tests, feature tests and selected in-reactor vibration monitors. The FFTF Hydraulic Core Mockup (HCM), a 0.285 scale model, was designed to simulate the vibrational and hydraulic characteristics of the reactor system just as IRFM does for the CRBR. Vibration measurements were obtained in the HCM and found to result in acceptable vibration levels.

FFTF in-reactor vibration monitoring of selected components was performed during pre-operational acceptance testing for confirmation of the scale model test conclusions. Pre-operational, non-nuclear, in-reactor vibration tests included accelerometer instrumentation in the Instrument Tree Guide Tubes (IGTs) and the Vibration Open Test Assembly (VOTA). Upon completion of the non-nuclear acceptance tests, IGT accelerometers were replaced with normal plant instrumentation for nuclear operation while the VOTA instrumentation was retained. Although the HCM and FFTF tests do not have identical instrumentation locations to permit direct one-to-one comparison, the FFTF data permits conclusions on the following points: 1) Overall vibration conclusions from both FFTF and HCM; and 2) Comparisons of HCM scale model test results with FFTF measurements for similar, although not identical, locations.

The overall conclusions from the HCM and FFTF tests are:

- o Overall test results from HCM and FFTF were similar and in fair agreement with respect to frequency and rms for similar instrumented components.
- o No gross vibrational problems such as significant impacting were observed in either HCM or FFTF.

- o The measured responses were stable and a function of increasing flow rate.
- o There is no incidence of synchronous vortex shedding at component natural frequencies.

FFTF In-reactor vibration measurements were obtained from two Instrument Tree Instrument Guide Tubes (IGTs) representing the shortest and longest IGTs. Accelerometers were mounted on a flow and temperature removable instrumentation assembly inserted in the IGTs. The HCM IGT accelerometers were mounted externally on the IGTs. However, the HCM IGTs were not prototypic of the final FFTF design. Figure 3.9-7 compares the first mode rms displacements for the two shortest HCM IGTs with the shortest FFTF IGT. The HCM rms displacement prediction compares well with the FFTF results and are conservative. The HCM frequency prediction is quite good and consistent with the slight length differences. For the longer HCM IGTs and the longest FFTF IGT, the frequency and flow dependence are similar in trend with the HCM rms displacement predictions being non-conservatively smaller (approx. 7 mils max.) than FFTF (approx. 30 mils max.). The non-prototypicality of the HCM IGTs is expected to be more influential for the long IGTs and could be the cause of the non-conservative HCM results in this case.

The FFTF Vibration Open Test Assembly (VOTA) was designed primarily as a vibration sensor and is a 40 foot assembly spring loaded into a core assembly receptacle. The HCM Closed Loop In-Reactor Assembly (CLIRA) is similar to the FFTF VOTA. The HCM CLIRA accelerometer measurements were scaled to FFTF and modified for differences in accelerometer locations based on analytical mode shapes for fully constrained and partially constrained support conditions. The Isothermal VOTA tests showed a first mode response of 4 Hz indicating partial constraint. Figure 3.9-8 compares the FFTF VOTA Isothermal results with the projected HCM results for partial constraint. The agreement is quite good. During FFTF power ascent, the VOTA first mode shifts from 4 to 10 Hz due to increased core clamping. The VOTA results for this condition compared to the HCM CLIRA projections for full constraint show that the HCM results are conservative (approx. 3 mils rms displacement compared to 1 mil for VOTA).

The FFTF vibration comparisons confirm that the HCM scaling parameters (similar to IRFM vibration model parameters given in Section 3.9.1.3.1.4) generally result in the expected conservative predictions for the reactor internals. The agreement between FFTF and HCM results is quite good for both overall vibration conclusions and for comparable vibration magnitudes.

3.9.1.3.4 Overall Test Conclusions

The good agreement between FFTF and HCM test results support the validity of well designed scale model testing for predicting reactor internals vibration response. Acceptable comparisons between FFTF and HCM were obtained for vibration displacements, flow dependence and frequencies with both tests showing low vibration levels for FFTF.

The CRBR reactor internals scale model and full scale test results completed to date show no indication of any significant vibration problems. No unstable dependence upon flow rate nor highly fluid excited forced components have been observed. Vibrationally induced impacting at gaps has been shown to result in low g level impacts judged to be below material damage thresholds. Although some testing remains to be completed for final design configurations, the differences between the preliminary and final test configurations are not likely to cause a major change in the vibrational responses for the outlet plenum components. Where the acceptability of scale model testing might be questionable such as for flow thru small clearances (UIS shroud tube gap, IVTM port plug, primary control rod driveline), full scale tests were performed to further assess vibration potentials.

In general, the test configurations were constructed to maximize the gaps between components. In the CRBR, misalignments from normal manufacturing tolerances (UIS chimneys, shroud tubes and IVTM port plug for example) and thermal gradients (UIS mixing chamber liner plates and the horizontal baffle for example) tend to close gaps and minimize vibration potentials.

Both the FFTF and CRBR pre-reactor operation test programs have shown no significant vibrational problems for the reactor internals. The CRBR plan for in-reactor confirmation of the test results is similar to the FFTF in-reactor program of using in-reactor vibration monitoring of selected components to confirm the pre-reactor operation test and analysis results.

The FFTF VOTA accelerometers in the core regions exhibited excessively large reciprocal of frequency (1/f) noise characteristics starting at very low power levels (<1%). Accelerometers above the core had minor low frequency degradation as a result of elevated temperature exposure (<1000°F). The mechanisms for these effects are not fully understood at this time. FFTF utilized piezoelectric, lithium niobate crystal accelerometers for the in-reactor tests which are the same accelerometers planned for CRBR in-reactor testing. Based on these FFTF results, the accuracy of CRBR measurements under reactor power conditions cannot be determined.

3.9.1.3.5 CRBRP In-Reactor Vibration Monitoring for Reactor Internals

The results of the test and analysis program completed to date have shown the adequacy of the reactor internals for flow induced vibration considerations. To supplement this comprehensive vibration assessment program and to provide confirmation of scale model test results, vibration monitoring of the UIS is planned for CRBRP. While the test results indicate acceptable vibration levels for all reactor internals, the principal area of concern from an inadequacy of the pre-reactor operation test program would be gross vibratory motion of the UIS. Conceptually, gross vibratory motion of the UIS could cause impacting of the keys to the core former structure keyways with resulting fatigue failures at the keys or other gap elements. Based on the vibration test results, other areas of the reactor internals are even less sensitive to vibration than the gross UIS motion.

Four biaxial accelerometers will be located on the UIS as shown in Figure 3.9-6. As can be seen from the accelerometers' orientation, lateral, vertical and torional motions of the UIS or impacting at the UIS keys can be monitored with the accelerometers.

Accelerometer measurements will be recorded and evaluated at varying flow rates during pre-operational testing. Acceptable accelerometer performance at temperatures above about 600°F and at reactor power conditions cannot be assured. If the accelerometers remain operational with acceptable accuracy, data will be obtained and evaluated during the initial power ascent.

Phase II of the IRFM scale model tests has four accelerometers in the UIS at the same location as the CRBRP UIS. These IRFM accelerometers will be correlated with other extensive instrumentation on the IRFM UIS to provide a reference data base for interpretation of the CRBRP UIS accelerometer measurements. Identification of the peaks and frequencies in the IRFM tests will provide guidance for assessment of the CRBRP measurements.

Vibration data from the final series of IRFM tests will be evaluated to demonstrate component acceptability and to develop acceptance criteria for the CRBRP internals vibration tests. Components with significant vibration in the IRFM tests will be evaluated to show stress, fatigue and wear acceptability including allowances for test uncertainties. These analyses will be used to develop acceptance criteria for the plant tests to assure that UIS structural and functional requirements are satisfied. The UIS measurements will be compared to the acceptance criteria and to the IRFM data. Major differences between the IRFM and plant data will be assessed to assure that the differences are not an indication of an unexpected, significant vibration problem. Acceptance criteria for the UIS accelerometer measurements will be provided in the FSAR.

3.9.1.3.6 Application of Regulatory Guide 1.20

The following comments address application of Regulatory guide 1.20 to CRBRP.

Regulatory Position C.1: Classification of Reactor Internals

The classification provided in this regulatory position will be followed by the CRBRP Project to categorize the reactor internals. It is anticipated that most of the CRBRP internals will be in the category of "Prototype."

Regulatory Position C.2: Vibration Assessment Program for Prototype Internals

Item C.2.1 (Vibration Analysis Program), is applicable to CRBRP. The scope of the analysis for the CRBRP is described in Section 3.9.1.3.1 and Chapter 4 of the PSAR.

Item C.2.2 (Vibration Measurement Program) is applicable to CRBRP. The test operating conditions will be provided when the preoperational and initial startup test details are established.

The provisions as given in Item C.2.3 (Inspection Program) were developed primarily for LWRs. Due to the limitation of the state-of-the-art of inspectability of LMFBRs, the requirements set forth in Item C.2.3 are considered largely not applicable to the CRBRP.

The intent of Item C.2.4 (Documentation of Results) will be met, as applicable, in the context of the program described above.

Item C.2.5 (Schedule) is provided herein. Sub-item 1 requesting classification of the reactor internals is fulfilled by the above "Prototype" designation. Sub-item 2 for a commitment on the scope of the vibration assessment program is fulfilled by Section 3.9.1.3. Sub-items 3 (description of the vibration measurement phase) and 4 (summary of the vibration analysis program) will be provided in the FSAR as a further development of the information given in Section 3.9.1.3. Sub-item 5 requests preliminary and final reports within 60 and 180 days, respectively, of the completion of CRBRP vibration testing. CRBRP reports will be provided consistent with these requested periods.

Regulatory Position C.3: Vibration Assessment Program for Non-Prototype Reactor Internals

Presently, no CRBRP reactor internals are expected to be classified as "Non-Prototype." Therefore, no assessment with regard to the applicability of this regulatory position is attempted at this time.

3.9.1.4 Correlation of Test and Analytical Results (To be Supplied in the FSAR)

3.9.1.5 Analysis Methods Under Accident Loadings

Detailed information on the analysis methods for the reactor components and the reactor coolant system under accident loadings will be provided in the FSAR, including a summary of the results of the analyses and the associated loading combinations. An over-view of the procedures to be employed is summarized in the following. Structures and components of physically connected systems will either be idealized as a single mathematical model or subdivided into smaller separate mathematical models depending upon the significance of the associated coupling effects. In all cases, the dynamic coupling effects will be included in the analysis. In most cases, the structures and components will be modeled as multi-degree of freedom spring-mass-dashpot systems.

Where the complexity of the system and components so requires, finite element codes will be used for adequate representation of the structural system. Significant non-linearities, such as gaps or clearances between components will be considered and included in the mathematical model. A nonlinear time history analysis which considers the impact forces generated at the gap locations will be used. Translational and rotational degrees of freedom will be considered at the mass points, as well as rocking at foundations or points of support. Nonsymmetrical features of geometry, mass and stiffness will be modeled to include their torsional effects in the analysis. Hydrodynamic effects resulting from confined fluid subjected to vibratory motion will be considered in the mathematical model where applicable. Soil-structure interaction parameters will be included in the model of the structures.

Where appropriate, the mathematical model of a large system may be subdivided into two or more subsystems. The uncoupling of the mathematical models can be justified if the mass and stiffness of the supporting and supported subsystems are such that they do not appreciably affect the dynamic response of each other, or if the mathematical models can be suitably modified to account for the interaction effects at the interfaces. The justifications for mathematical models uncoupling will be documented with the design analysis. Decoupling criteria are given in Appendix 3.7-A.

The seismic forcing functions will be in the form of response spectra and/or motion time histories at the support point of the system or subsystem being analyzed. Other forcing functions will be provided later.

Dynamic analyses will be made using a modal analysis, plus either response spectrum analysis, or integration of the uncoupled modal equations, or by direct integration of the coupled differential equations of motion. In addition, other dynamic analysis methods exist (such as Laplace and Fourier transforms, and power spectral density analysis) and may be used, but the Westinghouse computer program and machine capability conveniently perform the above analyses on a production basis.

See Section 3.7 for a detailed description of the seismic analysis methods. Briefly, a dynamic analysis consists of mathematical modeling of a structure or component, determining the equations of motion of the system, and solving the equations of motion for the forcing functions considering the system boundary conditions.

In general, a computer program will be used for performing the dynamic analyses. Exceptions may exist where a limited amount of complexity and/or number of degrees of freedom exists, and a hand solution can be made. The mathematical model, boundary conditions, and forcing functions are input to the program and deflections, stresses, etc., are output from the program.

Loadings involving operating loads in conjunction with Seismic Loads for ASME III Code components are combined in the manner described in Appendix 3.7-A.

In the design of the ASME III Code components, the absolute or linear summation (ABS) method is in general used when combining the stresses due to plant transients or accident loads and the loads caused by natural phenomena such as OBE or SSE. The square root of the sum of the squares (SRSS) method is used where appropriate such as in the calculation or combination of the seismic loads as described in Section 3.7.2.1.2 and Attachment A to Appendix 3.7-A of this PSAR.

3.9.1.6 Analytical Methods for ASME Code Class 1 Components and Component Supports*

The design transients for these components are described in Appendix B of this PSAR. The analytical methods and stress limits will be discussed in the FSAR. The evaluation of ASME Code Class 1 components will comply with the requirements of the ASME Boiler and Pressure Vessel Code Section III, Subsection NB, supplemented by the following:

(1) Low Temperature Components (below 800°F) for austenitic steels and below 720°F for ferritic steels):

RDT Standard E15-2NB-T, October 1975.

NUREG-0800, Section 3.9.3, ASME Code Class 1, 2, and 3 components, component supports, and core support structures.

(2) Elevated Temperature Components:

(a) Interpretations of the ASME Boiler and Pressure Vessel Code Case 1592, "Class 1 Components in Elevated Temperature Service Section III".**

(b) RDT Standard F9-4T, "Requirements for Design of Nuclear System Components at elevated Temperatures" Jan. 1976.

(c) RDT Standard E15-2NB-T, October 1975.

(d) NUREG-0800, Section 3.9.3.

The inelastic and limit analysis methods having the stress and deformation (limits) established by the ASME Code, Section III, and Code Case 1592 (elevated temperature design) for normal, upset and emergency conditions may be used with the dynamic analysis. For these cases, the limits are sufficiently low to assure that the dynamic elastic system analysis is not invalidated.

For the case of elevated temperature components designed in accordance with Code Case 1592, conservative deformation (or strain) limits have been formulated to help ensure the applicability of the other rules of the Code Case; i.e. the strain limits in Code Case 1592 are set conservatively low such that they effectively ensure that small deformation theory is applicable for most structural analyses of elevated temperature components. The small deformation assumptions, which have been the cornerstone for analyses of structures at low temperatures, are retained by the majority of current computer structural models being used for elevated temperature analysis.

**There are no deviations at present. All supplemental criteria will be fully identified and justified in the FSAR.

*The code editions and addenda are those shown in Table 3.2-5 for the appropriate components

The elevated temperature Code Case places the following limits on the maximum accumulated inelastic strain for parent material (Section T-1310 of Case 1592):

1. Strains averaged through the thickness, 1%
2. Strains at the surface due to an equivalent linear distribution of strain through the thickness, 2%

These limits are consistent with the NRC Standard Review Plan, Section 3.9.1, which states that small deformation methods of analysis typically tend to have acceptable effective strain limits in the range of 0.5 to 1.5 percent.

For components designed in accordance with the low temperature rules of Section III of the ASME Code, the $3 S_m$ limit on primary-plus-secondary stress ensure the applicability of small deformation theory: i.e., the $3 S_m$ limit ensures shakedown and precludes ratchetting.

For faulted conditions, the plastic and limit analysis stress and deformation limits are specified in Appendix F of the ASME Code, Section III. These limits are established in terms of an equivalent adopted elastic limit which can be used with a dynamic elastic system analysis. Particular cases of concern will be checked by use of simulated inelastic internal properties in the elastic system analysis.

At the component level, use of plastic or inelastic stress analysis or application of inelastic stress and deformation limits may be used with the elastically calculated dynamic external loads provided that shakedown occurs (as opposed to continuing deformation) or deformations do not exceed specified limits. Otherwise, readjustment to the elastic system analysis will be required. A list of components for which inelastic analysis has been performed or is planned is shown in Table 3.9-11.

Complete system inelastic methods of flexibility analysis combined with inelastic stress techniques may be used if there is justification.

Design loading combinations to be used for ASME Section III Class 1 components are those as given in Appendix 3.7-A with the additional combinations given below.

Normal and Emergency Conditions: Dead + Live + Operating
+ Thermal + Transients

The complete set of load combinations for ASME Code Class 1, 2, and 3 components is summarized in Tables 3.9-5a and 5b. Active components will be qualified for operability on a component by component basis in accordance with Reference 12, PSAR Section 1.6.

ASME Class 1 Component Supports will be designed and analyzed to the rules and requirements of ASME Section III Subsection NF. The methods for analysis and associated allowable limits that are used in the evaluation of plate and shell type and linear supports for faulted conditions are those defined in ASME Code, Section III, Appendix F.

The load combinations for ASME Class 1 Component Supports are given in Table 3.9-5a and 5b for normal, upset, emergency and faulted plant conditions. The stress limits to be used in the design of the Class 1 supports for the various service loadings are provided in Table 3.9-5c.

Component supports may be designed using the following three design procedures: (1) Design by Analysis, (2) Experimental Stress Analysis, and (3) Load Rating. Plate and shell type supports shall be designed and analyzed in accordance with the rules of paragraph NF-3220 of Subsection NF. Elastic analysis based on maximum stress theory in accordance with the rules of NF-3230 and Appendix XVII-2000 (Section III) shall be used for the design of linear type supports. For component support configurations where compressive stresses occur, the critical buckling stress shall be taken into account. To avoid column buckling in compression members, local instability associated with compression in flexural members and web/flange buckling in plate members, the allowable stress shall be limited to one-half of the critical buckling stress for plate and shell type supports and to two-thirds of the critical buckling stress for linear type supports. The calculation of the critical buckling stress shall account for the member slenderness ratio, width-to-thickness ratio of member flange, depth-to-thickness ratio of the member web and laterally unsupported length. Dynamic buckling as well as static buckling shall be considered when calculating critical buckling stress. The critical buckling is defined as the CRC curve (Column Research Council).

The design of bolts for ASME Class 1 Component Supports for normal and upset plant conditions will be in accordance with paragraph NF-3280 of ASME Section III, Subsection NF. For emergency and faulted plant conditions, bolts will be treated as linear supports, and the methods for analysis and associated allowable limits are those defined in paragraph NF-3230, Subsection NF and paragraph F-1370, Appendix F of ASME Code, Section III, respectively.

The stress limits for the Emergency Conditions may be increased by one-third over the values for the normal/upset conditions. For the Faulted Conditions, the allowable stresses obtained for the normal conditions may be increased by a factor of 1.2 (S_y/F_t). In no case shall the allowables for the Emergency/Faulted Conditions exceed the yield strength of the material at temperature.

Additional Material Design Considerations

- o The ASME Code, Winter 1982 Addenda, reduced fatigue design curves for austenitic materials cycled beyond 10^6 cycles will be evaluated.
- o The design curves being developed by ASME Code Committees, Winter 1982, regarding the 2-1/4 Cr - 1 Mo elevated temperature fatigue design will be evaluated.
- o Wherever the simplified elastic-plastic method of the ASME Code has been used, an evaluation of a conservative or actual plastic strain concentration and the resulting fatigue design life will be performed.

3.9.2 ASME Code Class 2 and 3 Components and Component Supports*

3.9.2.1 Component Operating Conditions and Design Loading Combinations

Design pressure, temperature, and other loading conditions that provide the design basis for fluid system Code Class 2 and 3 components are described in Appendix B of this PSAR and referenced in the sections that describe the system functional requirements.

3.9.2.2 Design Loading Combinations

Design loading combinations for ASME Code Class 2 and 3 components, and piping, are given in Appendix 3.7-A which are the same as for Class 1 components. Corresponding stress and pressure limits for each case are specified in Section 3.9.2.3.

For ASME-III Class 2 and 3 components which are not sodium-containing and high temperature, the CRBRP will fully conform with the requirements of ASME-III Code. The load combinations given in Tables 3.9-5a and 5b will be utilized.

ASME Class 2 and 3 Component Supports will be designed and analyzed to the rules and requirements of ASME Section III Subsection NF. The design and analysis of Class 2 and 3 component supports shall be as discussed in Section 3.9.1.6 for Class 1 supports.

The load combinations for ASME Class 2 and 3 Component Supports are given in Table 3.9-5a and 5b for normal, upset, emergency and faulted plant conditions. The stress limits to be used in the design of the Class 2/3 supports are provided in Table 3.9-5d.

The design of bolts for ASME Class 2 and 3 Component Supports for normal and upset plant conditions will be in accordance with paragraph NF-3280 of ASME Section III Subsection NF. For emergency and faulted plant conditions, bolts will be treated as linear supports, and the methods for analysis and associated allowable limits are those defined in paragraph NF-3230, Subsection NF of ASME Section III. In no case shall the allowables for the Emergency/Faulted conditions exceed the yield strength of the material at temperature.

*The code editions and addenda are those shown in Table 3.2-5 for the appropriate components.

3.9.2.3 Design Stress and Pressure Limits

Design stress and pressure limits for each component operating condition are presented in Tables 3.9-3 and 3.9-4, respectively. The components covered by these tables are ASME Class 2 and 3 vessels, pumps, and valves. Design stress and pressure limits for Code Class 2 and 3 piping are indicated in Table 3.9-5. The limits established for nonactive components and piping are intended to assure the structural integrity under all postulated service conditions. As discussed in Section 3.9.1.6 for ASME Class 1 components, some Class 2 or 3 components may require inelastic analysis. A list of components for which inelastic analysis has been performed or is planned is shown in Table 3.9-11.

The design limits for Code Class 2 and 3 Active components are discussed in Reference 12, PSAR Section 1.6.

3.9.2.4 Analytical and Empirical Methods for Design of Pumps and Valves

Code Class 2 and 3 pumps and valves will be designed in accordance with the requirements for ASME-III Subsections NC and ND. The components functional capabilities during transients or events considered in the respective operating conditions are assured by the low stress limits selected and described in Sections 3.9.2.2 and 3.9.2.3.

3.9.2.5 Design and Installation Criteria: Pressure-Relieving Devices

Pressure-relieving devices for the over-pressure protection of Code Class 2 and 3 fluid system components will be designed to comply with the requirements of ASME-III, Articles NC-7000 and ND-7000 of Subsections NC and ND, respectively.

Although both apply only to open discharge systems with limited discharge pipes, the basic intent of Regulatory Guide 1.67 and the recommendations of Code Case 1569 will be followed in the installation of the pressure relieving devices. A dynamic hydraulic/structural analysis will be performed to determine the load due to the fluid's reaction force from the opening and subsequent venting of the relief device.

For the design and installation of discharge piping supports, the rules of ASME-III Subsection NF will be used. Supports will be provided as near to the device as possible to minimize the load at the branch connection of the device inlet piping and main flow piping during discharge.

The following loads will be considered in the analysis of the pressure relief/safety valve station to determine the maximum stress:

- a. Loads due to the dynamic and steady-state effects of the discharging fluid;
- b. Loads due to the dynamic effects of the disk assembly of the device upon initial lift and reseating during safety and power relief operations;
- c. Loads due to the thermal expansion of the device and its associated piping; and
- d. Loads due to the dynamic effects of the device and its associated piping during a seismic event.

The combination, as applicable, of the above loads resulting in the highest stress will be determined. At each location in the loop, the sequence of valve openings which will result in the maximum instantaneous stress will be analyzed. The design stress limits for Code Class 2 and 3 valves shall be those provided in Table 3.9-3.

Details on design, installation, and pressure settings will be provided.

3.9.2.6 Component and Piping Supports

Class 2 and Class 3 components and piping systems will be supported at specific locations for deadweight conditions and will be restrained at specific locations against seismic disturbances. The supports to be used in the CRBRP will be designed to meet the requirements of the ASME Code, Section III, Subsection NF for Class 2 and 3 supports. The design and structural integrity of the supports will be evaluated to ensure adequate margins of safety under all applicable combinations of loading. The assessments will address the three types of supports: plate and shell, linear and component standard types.

Although classified as component standard supports, snubbers will receive special consideration due to their unique function. Snubbers provide no load path or force transmission during normal plant operations, but function as rigid supports when subjected to dynamic transient or seismic loads.

Components and piping systems which utilize snubbers as vibration and/or seismic restraints will be analyzed using mathematical representations of the snubbers to predict the piping or component dynamic response, and to ascertain the interaction effects of the snubbers with the piping and components to which they are attached. The representation of the snubbers, for piping and component dynamic analysis, models the effective stiffness and mass of the support train including that of the snubber, clamp or attaching device and supporting structure. Other characteristics of the snubber devices such as damping and free play have been considered in developing the snubber models. If snubbers are installed in locations different than those considered in the design analysis, the differences will be fully evaluated and documented in the as-built stress reports before pre-operational testing begins.

The general functional requirements, the operating environment and the applicable codes and standards are specified for the Class 2 and 3 snubbers. Special controls and requirements are provided to ensure that snubber operability and structural integrity will be maintained during the CRBRP lifetime. These include the following:

- a) The manufacturer will perform rigorous acceptance testing for each snubber from the production line and the results shall demonstrate conformance with requirements. Acceptance tests to be performed will include dimensional and visual examination, breakaway load/drag load, dead band, and acceleration limit tests.

- b) Qualification testing on each snubber design and rating to be used in the CRBRP piping and component support systems. Qualification tests to be performed will include dynamic, low temperature, high humidity, corrosion, sand and dust, irradiation, low level vibration, faulted load, sodium aerosol and sodium jet impingement (if applicable).
- c) Use of corrosion resistant materials for construction of those parts where corrosion could impair performance. The designs will include special features to prevent galling of any mating moving parts.
- d) Use of minimum/maximum motion indicators to verify snubber operability.
- e) Rigorous handling and installation procedures will be utilized to ensure that the quality of the installed equipment is not degraded.

The operability of the piping and component snubbers will be monitored during pre-operational testing and will receive pre-service inspection prior to ascent to power. Visual observation of piping systems and measurements of thermal movements during pre-operational tests will verify that snubbers are operable (not locked up) and in their correct positions.

The operability of the snubbers will be confirmed during plant operation by Inservice Inspections performed in accordance with Appendix G.

All safety-related piping and components which utilize snubbers in their support systems will be identified and tabulated in the FSAR.

3.9.3 Components Not Covered by ASME Code (See Appendix 3.7-A)

3.9.3.1 Reactor System Components

3.9.3.1.1 Core Components

Details of the design procedures, design criteria, and/or applicable codes and standards are provided in Section 4.2.1.

3.9.3.1.2 Control Rod System

The analytical procedures and the design criteria are provided in Section 4.2.3.

The seismic impact analysis is presented in Section 3.7.3.15.3. See also Sections 3.7.3.15.1 and 3.7.3.15.2 for the reactor system seismic analysis, and Section 4.2.3 for the seismic scram analysis.

3.9.3.2 Other Mechanical Components

In Chapters 4.0 and 5.0, other safety related mechanical components not covered by the ASME Boiler and Pressure Vessel Code are identified, including design criteria and applicable code/standards.

References to Section 3.9

- 1) BNWL-575, "Applications of Geometric Models for the FFTF Hydraulic Core Mockup," D. S. Trent, November 1967.
- 2) Franklin Institute Research Laboratories Report, F-B2437, "Study of the Feasibility of Modeling Vibration," George P. Wachtell, November 22, 1965.
- 3) Report, ANL-CT-75-37, "An Evaluation of Flow Induced Vibration Prediction Techniques for In-Reactor Components," dated May 1975.
- 4) Report, ANL-CT-76-31, "Comparison of Analytical Predictions With HCM Results for FFTF Reactor Flow Induced Vibrations and Summary of Prediction Methods," dated April 1976.

30

43

Tables 3.9-1, 3.9-2 and 3.9-2A
have been intentionally deleted.

46

Amend. 46
Aug. 1978

3.9-6 (next page is 3.9-8)

TABLE 3.9-3

STRESS LIMITS FOR ASME CLASS 2 AND 3*
COMPONENTS AND THEIR SUPPORTS

CONDITIONS	PUMPS		VALVES		VESSELS ATMOSPHERIC STORAGE TANKS AND 0-15 PSIG STORAGE TANKS ¹	PLATE AND SHELL SUPPORTS FOR CATEGORY I ACTIVE COMPONENTS ³
NORMAL		ASME-III		ASME-III ANSI B16.5	ASME III	ASME III
UPSET		$\sigma_m \leq 1.10S$ $\sigma_x + \sigma_b \leq 1.65S$		$\sigma_m \leq 1.10S$ $\sigma_x + \sigma_b \leq 1.65S$	$\sigma_m \leq 1.10S$ $\sigma_x + \sigma_b \leq 1.65S$	$\sigma_1 \leq S$ $\sigma_1 + \sigma_2 \leq 1.5S$
EMERGENCY		$\sigma_m \leq 1.5S$ $\sigma_x + \sigma_b \leq 1.8S$		$\sigma_m \leq 1.5S$ $\sigma_x + \sigma_b \leq 1.8S$	$\sigma_m \leq 1.5S$ $\sigma_x + \sigma_b \leq 1.8S$	$\sigma_1 \leq 1.4$ $\sigma_1 + \sigma_2 \leq 1.6$
FAULTED		$\sigma_m \leq 2.0S$ $\sigma_x + \sigma_b \leq 2.4S$		$\sigma_m \leq 2.0S$ $\sigma_x + \sigma_b \leq 2.4S$	$\sigma_m \leq 2.0S$ $\sigma_x + \sigma_b \leq 2.4S$	$\sigma_1 \leq 1.8S$ $\sigma_1 + \sigma_2 \leq 2.1S$

WHERE $\sigma_x = \sigma_m$ OR σ_L

- 1 Excluding the NC/ND-3200 alternate.
- 2 The quantities σ_m , σ_b , σ_1 , σ_2 are defined in Code Cases 1607-1, 1635-1 and 1636-1.
- 3 For linear-type supports, the stress limits for Normal and Upset are as specified in ASME III. For Emergency and Faulted, the stress limits are increased by one-third over those values, based on ASME Code Subsection NF3231.1.

*Based on the following code cases:

- CODE CASE
- 1607-1 . . . Stress Criteria for Section III Class 2 and 3 Vessels Designed to NC/ND-3300 excluding the NC-3200 Alternate, approved 11/4/74.
 - 1635-1 . . . Stress Criteria for Section III Class 2 and 3 Valves subjected to Upset Emergency and Faulted Operating Conditions, approved 8/12/74.
 - 1636-1 . . . Stress Criteria for Section III Class 2 and 3 Pumps subjected to Upset Emergency and Faulted Operating Conditions, approved 8/12/74.

3.9-8

44

13

29

25

Amend. 44
April 1978

This page intentionally left blank.

Table 3.9-4

PRESSURE LIMITS FOR ASME CLASS 2 AND 3 COMPONENTS

CONDITIONS	P_{MAX}^1 , PUMPS AND VALVES
NORMAL	1.0
UPSET	1.1
EMERGENCY	1.2
FAULTED	1.5

44

NOTE 1: The maximum pressure shall not exceed the tabulated factor listed under P_{MAX} times the design pressure or the rated pressure at the applicable operating temperature.

17

TABLE 3.9-5

STRESS LIMITS FOR ASME CLASS 2 AND 3 PIPING

CONDITIONS	ASME III EQUATIONS ¹				
	PRESSURE LIMITS	STRESS LIMITS			
	4	8	9	10	11
DESIGN	P	$S_L \leq S_h$	$S_{OL} \leq 1.2 S_h$		
NORMAL ²		$S_L \leq S_h$		$S_E \leq S_A$	$S_{TE} \leq (S_h + S_A)$
UPSET ³		$S_L \leq S_h$	$S_{OL} \leq 1.2 S_h$	$S_E \leq S_A$	$S_{TE} \leq (S_h + S_A)$
EMERGENCY			$S_{OL} \leq 1.8 S_h$		
FAULTED	$2P^4$		$S_{OL} \leq 2.4 S_h^4$		

¹ ASME III equations and terms are defined in NC or ND sections 3641.1 and 3652 for Class 2 and 3 piping, respectively.

² Use design pressure and normal operating temperature.

³ Use maximum pressure occurring during upset conditions.

⁴ ASME Code Case 1606 faulted stress and pressure limits.

47 | 3 9-9h

Amend. 47
Nov. 1978

Table 3.9-5a

Load Combinations for Seismic Category I
Vessels, Piping and Non-Active Pumps and Valves and
Associated Component Supports (Class 1, 2 and 3)

<u>System Operating Condition</u>	<u>Load Combination</u>	<u>ASME Service Stress Limits</u>
Normal	Dead + Live + Operating + Thermal + Transients	Normal (or Level A)
Upset	Dead + Live + Operating + Thermal + Transients ⁽¹⁾ + OBE	Upset (or Level B)
Emergency	Dead + Live + Operating + Thermal + Transients + DSL ⁽²⁾	Emergency (or Level C)
Faulted	(a) Dead + Live + Operating + Thermal + Transients ⁽³⁾ + DSL ⁽³⁾ + SSE	Faulted (or Level D)
	(b) Dead + Live + Operating + Thermal + Transients ⁽⁴⁾ + SSE	Faulted (or Level D)
	(c) Dead + Live + Operating + Thermal + Transients	Faulted (or Level D)

(1) Includes worst normal operation transient with four OBEs and worst upset operation transient with one OBE, independently.

(2) Includes only those dynamic system loadings associated with sodium water reactions.

(3) Dynamic system loadings and transients associated with ex-containment IHTS design basis leaks and water/steam pipe rupture events.

(4) Includes only normal operating transients.

Table 3.9-5b

Load Combinations for Seismic Category I
Active Pumps and Valves and Associated Component
Supports (Class 1, 2 and 3)

<u>System Operating Condition</u>	<u>Load Combination</u>	<u>ASME Service Stress Limits</u>
Normal	Dead + Live + Operating Thermal + Transients	Normal (or Level A)
Upset	Dead + Live + Operating Thermal + Transients ⁽¹⁾ + OBE	Upset (or Level B)
Emergency	Dead + Live + Operating Thermal + Transients +DSL ⁽⁴⁾	Upset (or Level B) Upset (or Level B)
Faulted	(a) Dead + Live + Operating Thermal + Transients ⁽²⁾ + DSL ⁽²⁾ + SSE	Upset (or Level B)
	(b) Dead + Live + Operating Thermal + Transients ⁽³⁾ + SSE	Upset (or Level B)
	(c) Dead + Live + Operating Thermal + Transients	Upset (or Level B)

- (1) Includes worst normal operation transient with four OBEs and worst upset operation transient with one OBE, independently.
- (2) Dynamic system loadings and transients associated with ex-containment IHTS design basis leaks and water/steam pipe rupture events.
- (3) Includes worst nominal operation transient with the SSE.
- (4) Includes only those dynamic system loadings associated with sodium water reactions.

Table 3.9-5c

Stress Criteria for All ASME Code Class 1
Component Supports of Plate and Shell Type

<u>Condition</u>	<u>Stress Limits</u> (1) (2)
Design	$P_m \leq S_m$ $P_m + P_b \leq 1.5 S_m$
Normal/Upset (or Level A/B)	$P_m \leq S_m$ $P_m + P_b \leq 1.5 S_m$ $P_e \leq 3 S_m$ $P_m + P_b + P_e \leq 3 S_m$
Emergency (or Level C)	$P_m \leq 1.2 S_m$ $P_m + P_b \leq \begin{matrix} 1.8 S_m \\ 0.8 C_L \end{matrix}$
Faulted (or Level D)	$P_m \leq \begin{matrix} 1.5 S_m \\ 1.2 S_y \end{matrix}$ $P_m + P_b \leq \begin{matrix} 2.25 S_m \\ 1.8 S_y \end{matrix}$

Notes:

- (1) Terminology is as defined in the ASME Code, Subsection NF.
- (2) For linear supports the stress limits given in NF-3231 of Subsection NF and Appendix XVII of Section III may be used.

Table 3.9-5d

Stress Criteria for ASME Code Class 2/3
Component Supports

<u>Condition</u>	<u>Stress Limits</u> (1) (2)
Design	$\sigma_1 \leq S$ $\sigma_1 + \sigma_2 \leq 1.5S$
Normal/Upset	$\sigma_1 \leq S$ $\sigma_1 + \sigma_2 \leq 1.5S$
Emergency	1.2 x Normal Condition Limits
Faulted	1.5 x Normal Condition Limits

Notes:

- (1) Terminology is as defined in ASME Code, Subsection NF.
- (2) For linear supports use same limits as for Class 1.

TABLE 3.9-6
FLOW STEP SUMMARY

Test or Test Condition	Flow Rate of Fluid Condition								
	Shaker Test		Water (% of CRBRP Rated Velocity)+						
	Still		10	33	66	100	110	120*	**
<u>Three Loop Operation</u>	Air	Water							
Velocity Test									X
<u>Vibrations</u>									
a) Operating Mode	X	X	X	X	X	X	X	X	X
b) Refueling Mode***	X	X	X						
<u>Two Loop Operation</u>									
Velocity Test						X			X
Flow Vibrations							X	X	X

* Operating at this flow depends on proximity to vibration limit

** To be determined, vibration limit or test facility limit

+ For two loop operation, rated flow is approximately 2/3 three loop operation value.

*** Approximately 11 in. gap between top of reactor assemblies and the upper internals structure for the refueling mode.

NOTE: All components will be monitored and only those shown most responsive will be recorded and analyzed.

30

19

TABLE 3.9-7

Flow Vibration Parameters - CRBRP Model and Prototype

Conditions:

Same structural material in model and prototype (stainless steel)

Model Fluid = water at 100°F

Prototype fluid = liquid sodium at 995°F

Parameter	Model	Prototype	Ratio
Young's Modulus of Elastic, E (psi)	28.2x10 ⁶	22.7x10 ⁶	$\frac{E_m}{E_p} = 1.242$
Fluid Density, ρ (lbs/cu in.)	0.0359	0.0297	$\frac{\rho_m}{\rho_p} = 1.206$
Material Density, ρ_s (lbs/cu in.)	0.290	0.282	$\frac{(\rho_s)_m}{(\rho_s)_p} = 1.028$
ρ_s/ρ	8.078	9.495	$\frac{(\rho_s/\rho)_m}{(\rho_s/\rho)_p} = 0.851$
Poisson's Ratio, μ	0.282	0.301	$\frac{\mu_m}{\mu_p} = 0.937$
Kinematic Viscosity, ν	9.0x10 ⁻⁶	3.05x10 ⁻⁶	$\frac{\nu_m}{\nu_p} = 2.951$

30

TABLE 3.9-8
 Outlet Plenum Components Modeled
 In IRFM Test

Component	Hydraulic Simulation	Structural Simulation	FIV Instrumentation
<u>UIS Structure</u>			
Support Columns	Yes	Yes	Yes
Chimneys	Yes	2 (Ph. II)	Yes
Support Plates	Yes	Yes	Yes
Instrument Post	Yes	3	Yes
UIS Lower Shield Plate	Yes	Yes	Yes
<u>Control Rod System</u>			
Control Rod Driveline	1	1	Yes
Shroud	Yes	3 (Ph. I/1 (Ph. II)	Yes
Guide Tube	Yes	3	Yes
Shroud/Guide Gap	2	2	
<u>Instrumentation</u>			
LLM	2 Yes	2 1	Yes Yes
<u>Vessel</u>			
Thermal Liner	Yes	Yes	Yes
Thermal Baffle	Yes	No	No
In-Vessel Storage	1	No	No
Suppressor Plate	Yes	Yes	Yes
Outlet Nozzle Liner	Yes	Yes	Yes
<u>Reactor</u>			
Fuel, Blanket and Radial Shield Assembly	Yes*	Yes**	Yes**
Control Assembly	Yes*	Yes	No
Core Barrel	Yes	No	No
Core Barrel UIS Keys	Yes	Yes	Yes
<u>Miscellaneous</u>			
EVTM Guide Tube	Yes	Yes	Yes
IVTM Port Plug	Yes	Yes	Yes

* Flow Distribution and Assembly Exit Geometry need only be simulated for fuel, blanket and control assemblies. For radial shield assemblies, only outlet flow distribution will be simulated.

**Testing Involving Core Dynamic Simulation may be performed at ANL rather than in the IRFM.

Table 3.9-9
FLOW VIBRATION OF CRBP INTERNALS
General Survey

Reactor Internals Components	Type of Excitation	IMPORTANCE INDEX			METHODS SELECTED for RESOLUTION			
		High	Medium	Low	Analysis	IRFM Testing	Full Scale Test	Bench Test
1. Entire Upper Internals Structure (cross motion)	Vortex Shedding Jet Impingement Jet Reaction Turbulence Pump Pulsations		X X	X X	X X	X X X X		
2. UIS Guide Tubes for Control Rods	Vortex Shedding Turbulence Pump Pulsations Gap Modulation	X X		X X	X X X	X X X	X	
3. UIS Chimneys	Vortex Shedding Turbulence Pump Pulsations Jet Reaction	X		X X X	X X X	X X X	X X	X X
4. UIS Support Columns	Vortex Shedding Turbulence Pump Pulsations	X		X X	X X X	X X X		
5. UIS Instrumentation Leads	Vortex Shedding Turbulence Pump Pulsations	X X		X	X X X	X X X		
6. UIS Support Plates and Plate Liner	Vortex Shedding Turbulence Pump Pulsations			X X X		X X X		
7. UIS Instrumentation Posts	Vortex Shedding Turbulence Jet Impingement	X	X X			X X X		X X X
8. UIS Cylindrical Liners Sleeve	Vortex Shedding Turbulence "Base Motion"			X X X				X X X
9. UIS IVTH Port Plug	Vortex Shedding Turbulence Pump Pulsations Gap Modulation	X X		X X	X X X	X X X	X	
10. Control Rod Drivelines	Vortex Shedding Turbulence Gap Modulation	X X			X X	X X	X X	
11. Core Support Structure Core Barrel	Turbulence Pump Pulsations			X X	X X			
12. Core Support Structure Module Liners	Vortex Shedding Turbulence Pump Pulsation			X X X	X X X	X X X		
13. Horizontal Baffle	Vortex Shedding Turbulence Pump Pulsation			X X X	X X X			
14. EVTH Guide Tube	Vortex Shedding Turbulence Pump Pulsation	X		X X	X X	X		
15. Suppressor Plate Supporting Hangers	Vortex Shedding Turbulence Pump Pulsation	X		X X	X X	X X		
16. Suppressor Plate Segments	Vortex Shedding Turbulence Pump Pulsation			X X X	X X X	X X X		
17. Liquid Level Monitor (LLM) Tubes and Support Members	Vortex Shedding Turbulence Pump Pulsation	X		X X	X X	X X		
18. Vessel Thermal Liner	Turbulence Pump Pulsation			X X	X X	X X		
19. Outlet Nozzle Liner	Turbulence Pump Pulsation Jet Reaction			X X X	X X X	X X X		

Table 3.9-10

IRFM PHASE 2E VIBRATION TEST INSTRUMENTATION SUMMARY

Component	Concern	Data Required	Instrumentation Quantity			Instrumentation Location			Comments
			Displacement	Accelerometers	Strain	Displacement	Accelerometers	Strain	
1) UIS Keys (0° & 120° & 240°)	Impact - Wear Stress	Displacement - Acceleration - Force	6	6	8	R-T	R-T	See Comments	Strain gages appropri- ately located and cali- brated - need 4/Key
2) IVTM Port Plug	Impact - Wear	Displacement - Acceleration - Force	3	11		R-T and 0°, 180°, 300°	R-T 0°, 90°		Two strings of four accelero- meters along length
3) UIS Chim- ney	Excitation due UIS motion, Structural	Acceleration, Displacement	8	8		R-T Top, Bottom Sup- port	R-T Midspan, Top		Two struct- urally simu- lated chim- neys
4) UIS Col- umn	Mode shape	Strain		8					Two strings of four accelerom- eters along length See Note 1
5) UIS Col- umn to Bearing	Impact and Bearing Load	Displacement Force	2		4				Force trans- ducers at top of bearing race on one column) See Note 1
6) UIS Col- umn to Structure	Impact - Force	Force			3				Force trans- ducers on structure perpendic- ular to pin axis See Note 1

3.9-10

Amend. 69
July 1982

7) Column to Vibration UIS CRCM Plug	Acceleration		2	R-T	
8) UIS Upper Impact - /Lower Vibration Shroud	Acceleration - Displacement - Mode Shape	2	10	R-T	R-T
9) Instru- Post	Vibration	Acceleration	4		R-T Tip
10) UIS Top Plate	Vibration	Acceleration	1		V Center
11) Bottom Plate	Vibration	Acceleration	1		V Center
12) UIS Thermal Liners	Vibration	Acceleration			
13) Prototype Instrumentation	Acceleration		4		

Two strings of four accelerometers along length 0, 90° shroud to include instrumented drive line and dash pot to monitor their response to shroud excitation

A study is required to establish the modeling for this component

Biaxial accelerometers located same as shown on UIS drawing.

Note 1: This instrumentation to be aligned with same axis.

3.9-11

Amend. 69
July 1982

Table 3.9-11
Components for Which Inelastic Structural Analysis Is Required

Reactor System

- Reactor Vessel
- Closure Head (reflector and suppressor plate assemblies only)
- Liquid Level Monitor
- Primary Control Assembly
- Primary Control Rod Drive Line
- Upper Internal Structure (Including IVTM Port Plug and Rotating Guide Tube)
- Lower Internal Structures (Core Support Structure, Core Barrel, Horizontal Baffle Assembly and Upper Core Former)

Heat Transport System

- PHTS and IHTS hot leg piping
- PHTS and IHTS pumps
- Intermediate Heat Exchanger
- Cold Leg Check Valve
- All guard vessels
- IHTS transition joints
- IHTS Expansion Tank
- Steam Generators (rupture disks, tube sheets, inlet nozzles and support rings)
- Small Sodium Thermal Transient Valves

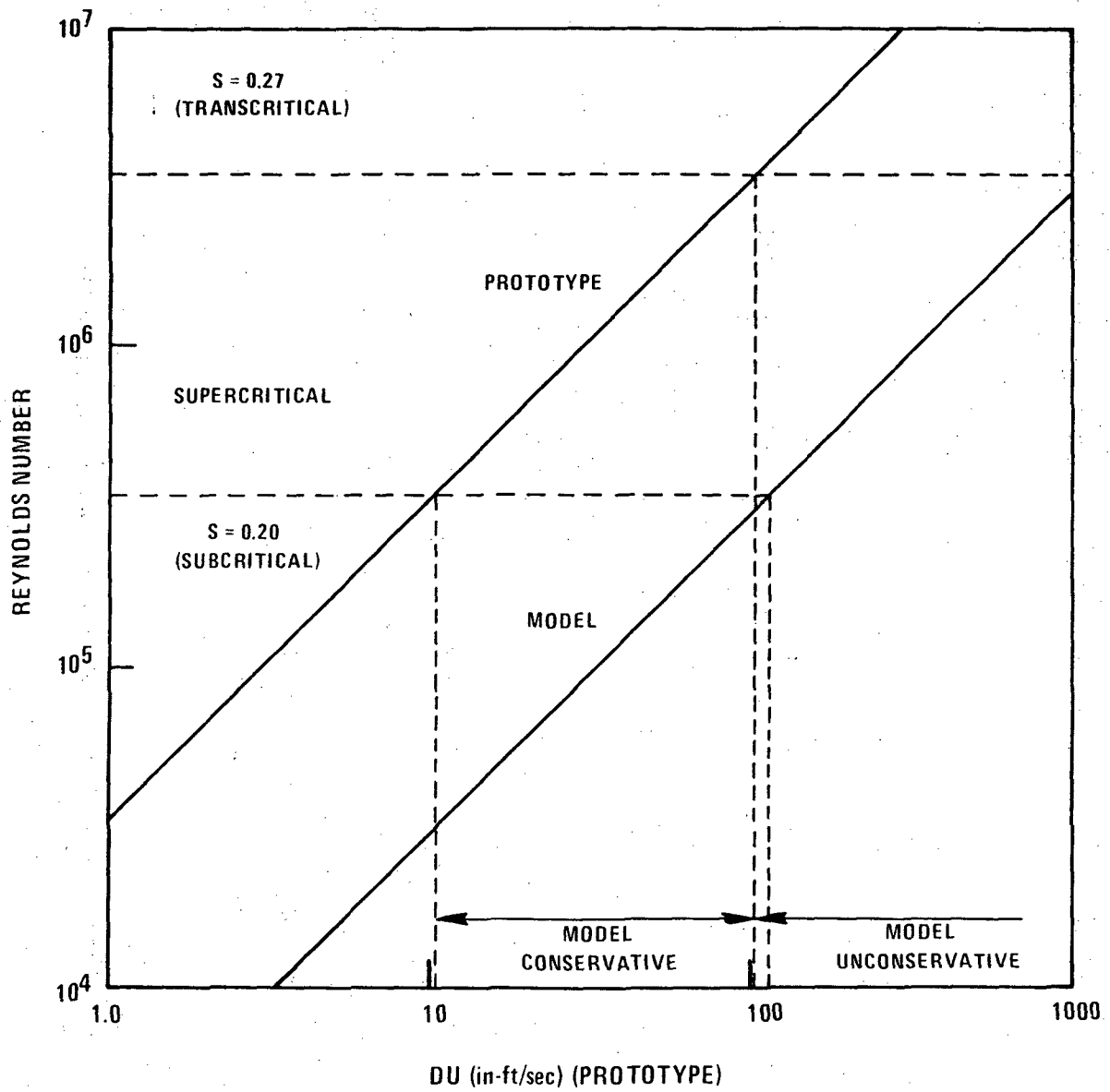


Figure 3.9-3. Reynolds Number for Prototype

9038-1

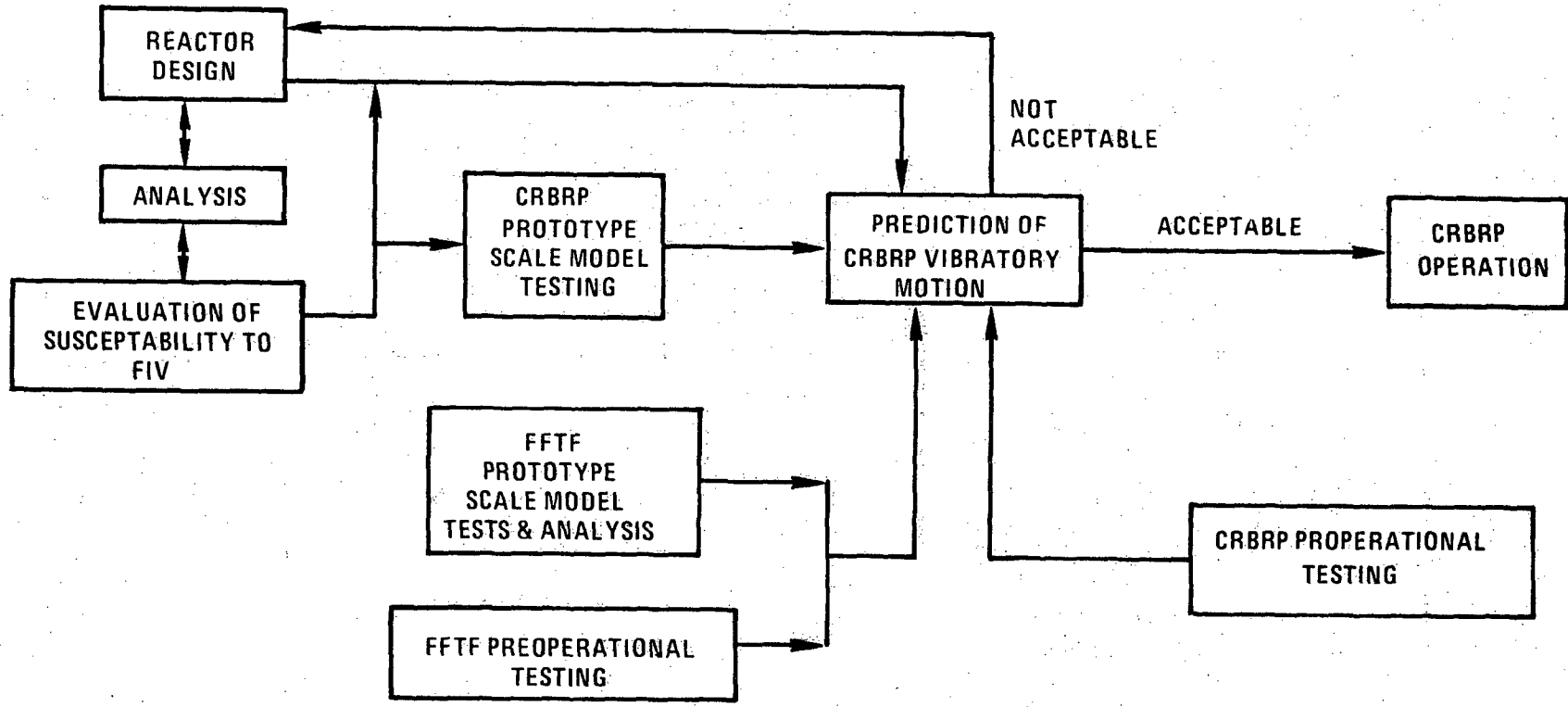


Figure 3.9-4 Reactor Internals Flow Induced Vibration Program

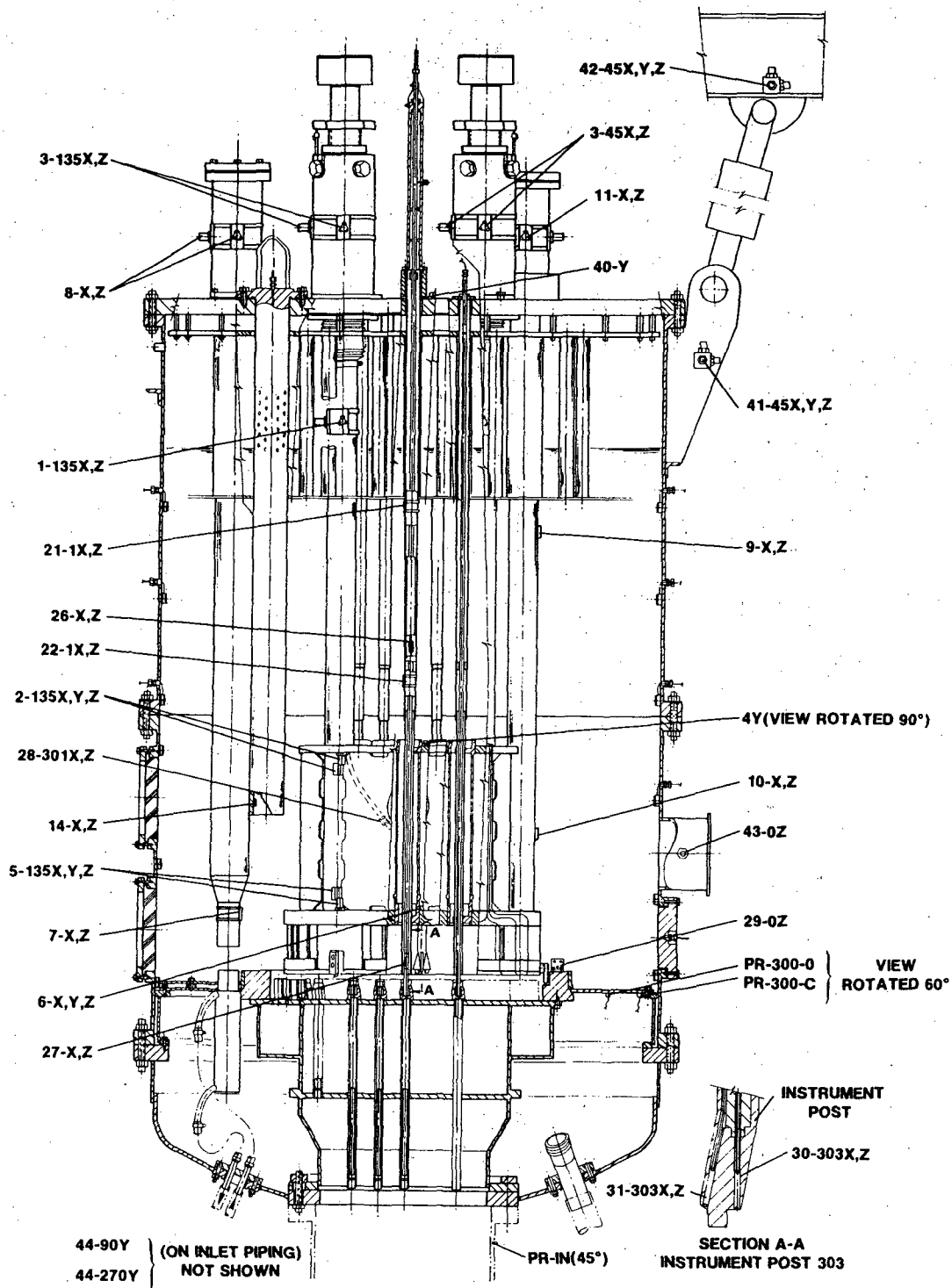
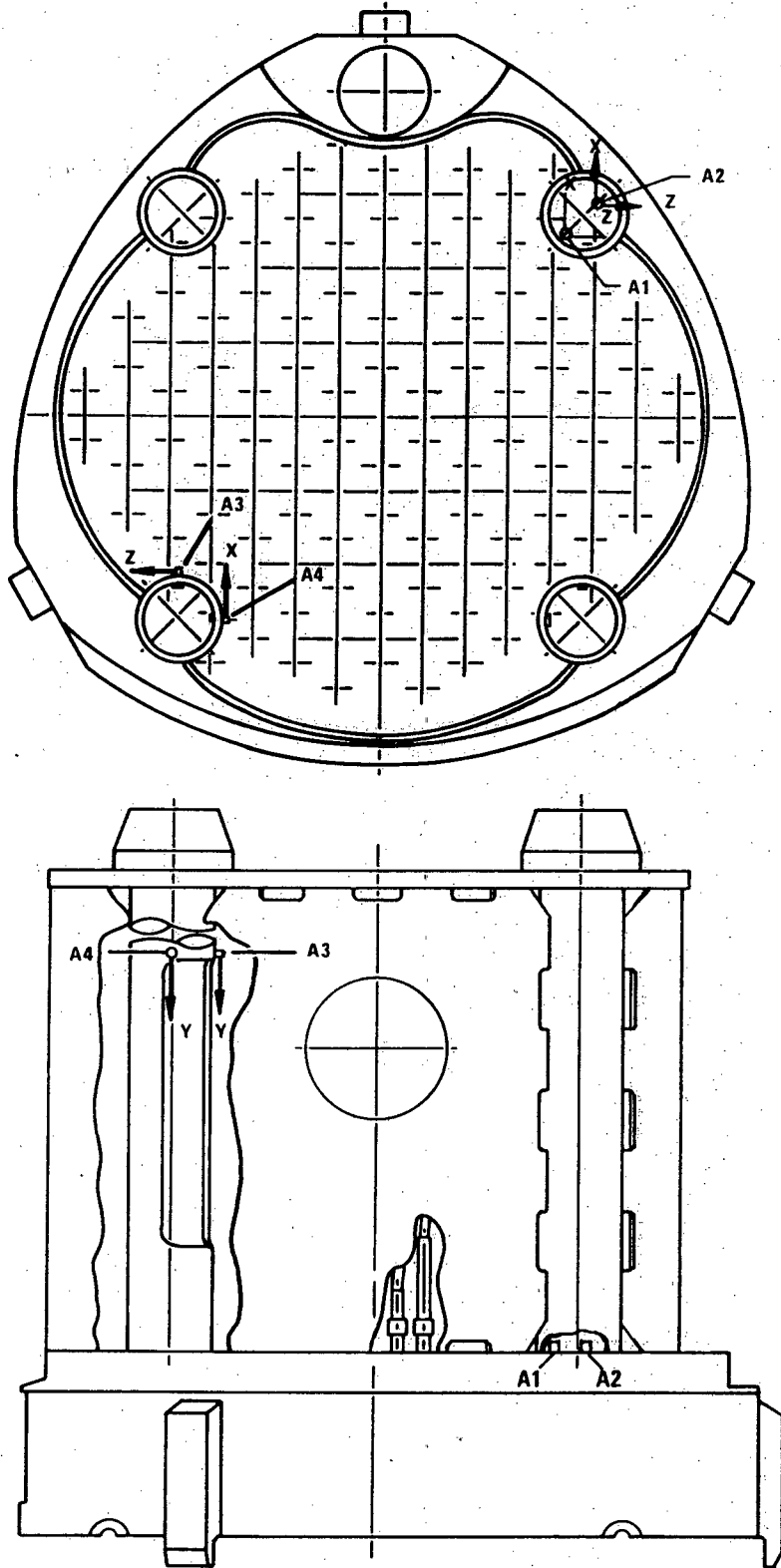


Figure 3.9-5 Integral Reactor Flow Model and Instrumentation



NOTE: A1 TO A4 ACCELEROMETERS (BIAXIAL)

9088-1 Figure 3.9-6 Location of Accelerometers on Upper Internal's Structure

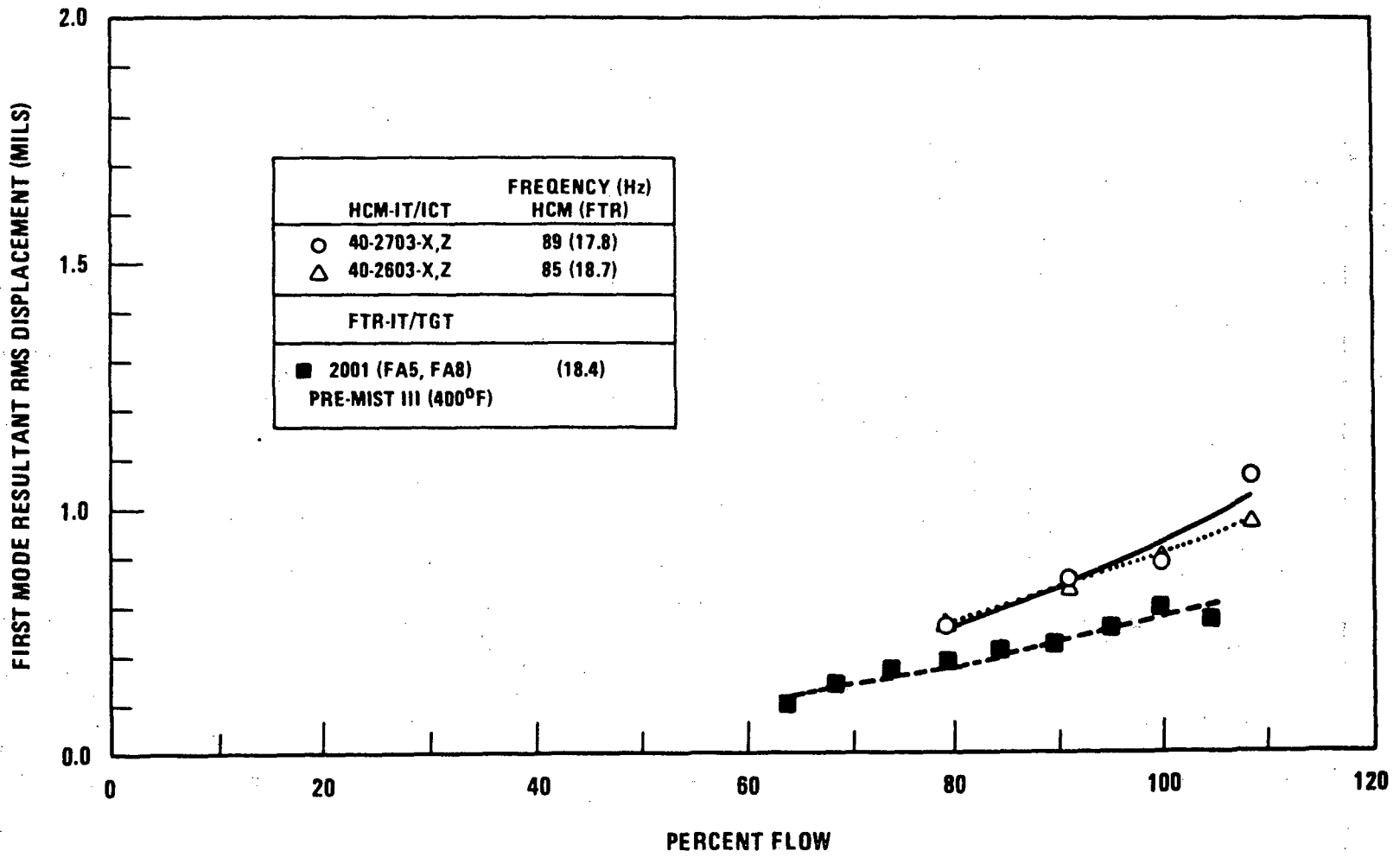


Figure 3.9-7. HCM/FTR Instrument Tree (Short) Instrument Guide Tube Response

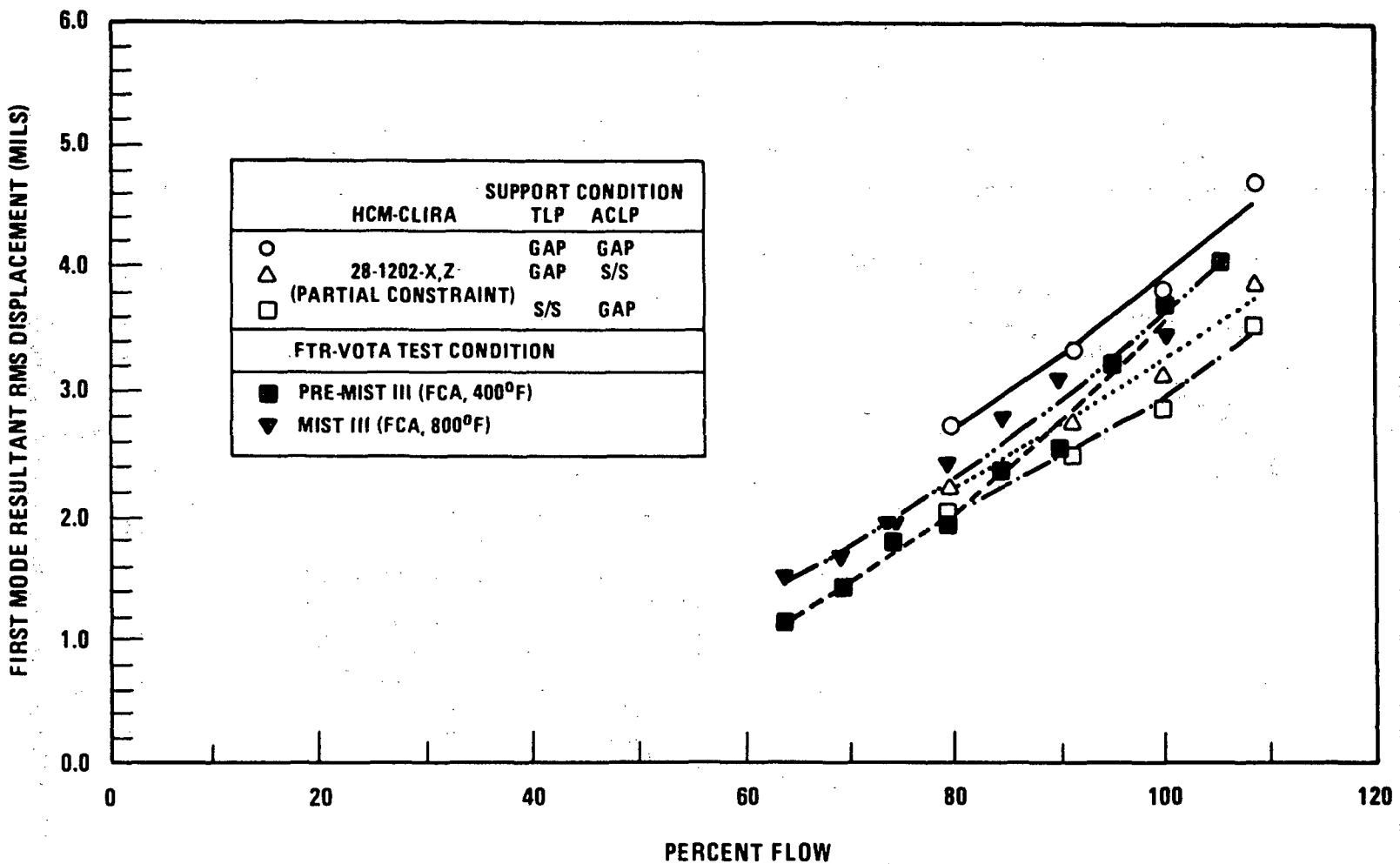


Figure 3.9-8. FTR-VOTA Stalk (Isothermal Flow) Response Vs. Projected HCM-CLIRA Response with Partial Constraint

3.10 SEISMIC DESIGN OF CATEGORY I INSTRUMENTATION AND ELECTRICAL EQUIPMENT

3.10.1 Seismic Design Criteria

61 The Category I instrumentation and electrical equipment will be designed against failure to perform their intended functions during and after an earthquake of the intensity of the Safe Shutdown Earthquake (SSE) during normal and accident conditions. The seismic qualification program for Class 1E equipment is described in Reference 13 of PSAR Section 1.6, "CRBRP Requirements for the Qualification of Class 1E Equipment." The structural requirements for foundations and supports will be in accordance with Section 3.8.

In addition, the Plant Protective System (PPS) actuation system and its controlled devices will be designed to have the capability to initiate a protective action during the SSE.

In addition to the general criteria as stated above, the standby power supply system and Category I instrumentation and electrical equipment necessary for safe shutdown will be designed to withstand seismic disturbances of the intensity of the SSE during post accident operation.

3 Category I instrumentation and electrical equipment and components will be designed to ensure the functional integrity of the equipment under the specified operating conditions. This equipment will require a detailed investigation to demonstrate its ability to withstand seismic forces while performing its intended function without leading to fuel damage or unacceptable release of radiation.

53 IEEE Standard 344-1975, "IEEE Recommended Practices for Seismic Qualification of Class 1E Equipment for Nuclear Power Generating Stations", supplemented by
46 Regulatory Guide 1.100, Rev. 1 will be used as the basis for all seismic
46 qualification of Class 1E equipment. The qualification tests will be based on either single frequency sine beat testing at resonance or multiple frequency testing. Single frequency sine beat testing at resonance constitutes severe testing under the most unfavorable conditions where a measured equipment natural frequency has been conservatively assumed to coincide with a building or supporting system natural frequency. Thus, uncertainties in the analytical
46 determination of building natural frequencies will be conservatively accounted and the maximum peak response acceleration on the appropriate response spectrum is conservatively assumed to occur at the equipment's natural frequency. However, when single frequency sine beat testing is used for qualification, additional testing with multiple frequency motion is performed
46 to comply with the general requirements of IEEE Std. 344-1975, unless they are fully satisfied by the sine beat testing alone. (See Appendix 3.7-A).

The factor of 1.5 in Section 6.6.2.1 of IEEE-344-1975 will not be used in either the sine beat or the multi-frequency testing. The peak sine beat acceleration and the maximum acceleration of the multi-frequency motion input to the shake table will be at least equal to the ZPA (Zero Period Acceleration) on the appropriate response spectrum.

The static coefficient analysis in IEEE-344-1975 Section 5.3 would be used for simple systems for which it has been demonstrated that this simplified analysis provides adequate conservatism. This type of analysis, which uses the maximum peak response acceleration on the response spectrum regardless of frequency, plus an additional factor of 1.5, is generally very conservative. However, IEEE 344-1975 is used as the criteria for testing and not for analysis.

Sine sweep testing is not used for equipment seismic qualification. This type of testing would be used to locate the equipment's natural frequencies for resonant sine beat qualification testing as discussed above.

The means by which a manufacturer can qualify the equipment include analysis or testing the equipment under simulated seismic conditions or qualification by combined test and analysis. The seismic specification will be provided to the manufacturer with appropriate response-spectrum curves at the floor elevations and instructions on their use.

The general approach employed in the dynamic analysis of Category I equipment and component design will be based on the response spectrum technique where applicable.

At each level of the structure where Class IE equipment are located, horizontal spectra for each of the two major areas of the structure and a vertical response spectrum will be developed.

For certain Category I complex equipment for which analytic modeling is not feasible, the equipment supplier will be required to perform dynamic testing using methods described in IEEE Standard 344-1975.

The above procedures are applicable to the analysis of seismic design adequacy of Class IE equipment, including supports such as cable tray supports, batteries and racks, instruments and racks, control consoles, medium voltage switchgears, unit sub-stations, motor control centers and motors.

Suppliers of such equipment will be required to submit test data and/or calculations to substantiate that their components and systems will not suffer loss of function before, during, or after seismic loading due to the SSE.

All cable tray supports are designed by the response spectrum method. Analysis and seismic restraint measures for tray supports are based on combined limiting values for static load, space length and computed seismic response.

The following basis will be used in the seismic analysis of typical cable tray supports:

- a. All Class IE cable tray supports will be designed to meet the requirement by dynamic analysis using the appropriate seismic response spectra.
- b. The support system will be designed to exclude all natural frequencies in a band covering the peak or peaks of response-spectrum curve.
- c. Maximum stress will be limited to 90 percent of minimum yield to compensate for effects of higher modes and minor inaccuracies in method of analysis.

The design of typical instrument racks and supports for the instrument tubing is based on the attainment of a fundamental natural frequency of more than 20 Hz so that the floor seismic input will be transmitted through the support without amplification.

The equipment will be analyzed as an assembly that simulates the intended service mounting, thereby accounting for possible amplification of the seismic input by the equipment support.

Seismic documentation submitted by the vendor will be reviewed by the design engineering group to ensure that the support system has been considered.

Where it is necessary to test individual devices (e.g., relays or instruments) separate from the panel on which they are mounted, the acceleration of the panel at the device locations will be checked to ensure a level less than that at which the devices are qualified.

59 | The structures that will be seismically qualified as Seismic Category I are listed in Section 3.2, Table 3.2-1. The Class 1E equipment is listed in Table 3.2-3. | 1

3.10.2 Analysis, Testing Procedures and Restraint Measures

59 | The seismic qualification of safety related instrumentation will be performed and documented as specified in Reference 13 of PSAR Section 1.6. | 1

Category I electric equipment such as battery racks, instrument racks, and control consoles located in Category I structures will be supported and restrained to resist uplift or overturning resulting from seismic forces.

61 | TABLE 3.10-1 HAS BEEN DELETED

TABLE 3.10-1 (CONTINUED)

LIST OF CLASS IE ELECTRICAL POWER SYSTEM EQUIPMENT

<u>Equipment</u>	<u>Number in Plant</u>	<u>Location</u>	<u>Expected Method of Seismic Qualifications</u>
125 V DC Battery Distribution Boards	3	CB	The battery distribution boards will be seismically qualified by testing*
<u>Standby AC Power Supply System</u>			
Diesel Generators	2	DGB	The Diesel Generators will be seismically qualified by Dynamic Analysis.
Diesel Control Panels	2	DGB	The control panels will be seismically qualified by testing*
<u>Electrical Penetrations</u>			
(Details to be provided in the FSAR)		RCB	

*Test reports of prototype or previously built equipment proven to be of similar construction and/or dynamic analysis based on previously qualified equipment will be acceptable.

Notes: Motors on Class I driven equipment are included with the driven component listed in Table 3.2-2

SGB - Steam Generator Building CB - Control Building
 RSB - Reactor Service Building
 DGB - Diesel Generator Building
 RCB - Reactor Containment Building

3.10-5

3.11 ENVIRONMENTAL DESIGN OF MECHANICAL AND ELECTRICAL EQUIPMENT

3.11.1 Equipment Identification

The safety-related systems which are required to function during and following an accident are identified in Section 3.2. Worst case environmental conditions including temperature, pressure, humidity, sodium aerosol and radiation exposure which result from a postulated design basis accident have been defined for each location. The accident environments and the appropriate time of operation applicable to safety-related mechanical equipment will be incorporated into the Equipment Specifications. Reference 13, PSAR Section 1.6, describes the environmental qualification basis for 1E electrical equipment and the program that will be followed to assure the basis is satisfied. The objective of this qualification basis and this qualification program is to conform to IEEE Standard 323-1974, "IEEE Standard for Qualifying Class 1E Equipment for Nuclear Power Generating Stations," and NUREG-0588, Rev. 1, "Interim Staff Position on Environmental Qualification of Safety-Related Electrical Equipment." Differences in CRBRP Reactor Technology and Plant Configuration exist and result in deviations from the specific LWR requirements delineated in NUREG-0588 for electrical equipment. These differences are: the use of liquid metal sodium for the reactor coolant and the resulting sodium combustion product aerosol environmental parameter; a low pressure coolant system with no mechanism for a highly pressurized containment; the absence of steam, containment spray and the mechanism for water flooding within the containment; environmental separation of the upper containment from the lower containment; and placement of redundant heat transport loops in separate cells resulting in independent loop environmental conditions. (Environments in one loop do not propagate to the cells of another loop.)

NUREG-0588 specifies the worst radiation environment as an instantaneous release from the fuel to the atmosphere of 100 percent of the noble gases, 50 percent of the iodines, and 1 percent of the remaining fission products. As specified in NUREG-0588, CRBRP uses the normally expected radiation environment over the equipment qualified life plus that associated with the most severe design basis accident during or following which that equipment must remain functional. The worst case radiation DBAs are the sodium tank failure during maintenance, the cover gas release, and the application of Site Suitability Source Term (SSST). For the Containment Isolation System, CRBRP uses the source term defined in NUREG-0588 modified to include 1 percent plutonium for qualifying Class 1E required to mitigate the consequences of any SSST radiation environment. In NUREG-0588, minimum qualification time of 1 hour is specified. CRBRP requires that equipment be qualified for the environment in which it must perform its safety function for the time duration specified for the safety response plus time margin per IEEE Std. 323-1974. CRBRP is in general compliance with the 1 hour time margin requirement; however, CRBRP expects that specific exceptions to the 1-hour time margin will be necessary. Each exception will be justified on a case by case basis. Failure of any equipment after its qualification (whether longer or shorter than 1 hour) will not result in unsafe plant conditions.

3.11.2 Qualification Tests and Analyses

The CRBRP has a program for environmental qualification of Safety-Related Electrical Equipment which is consistent with the objectives and requirements delineated in NUREG-0588, Rev. 1, "Interim Staff Position on Environmental Qualification of Safety-Related Electrical Equipment," except as noted above.

This program is described in Reference (13) of PSAR Section 1.6, "CRBRP Requirements for Environmental Qualification of Class 1E Equipment." This document establishes the qualification program which will be conducted to qualify Class 1E equipment located in different areas of the CRBRP and sets forth the documentation to be completed for qualification. The entire program is designed to conform to the IEEE Standard 323-1974 as endorsed by NUREG-0588.

For safety-related mechanical equipment, the capability of the equipment to perform its safety function will be demonstrated by design, analysis, testing, prior operating experience, or a combination of these. When it is determined that design and/or analysis is not adequate, environmental testing will be performed. In addition, the safety-related mechanical equipment designs will be reviewed to ensure material compatibility with the accident environments and the maintenance and testing required to ensure operability throughout the lifetime of the plant will be defined.

The analysis and/or test program will include aging of all age sensitive components of mechanical equipment for the normal as well as accident environments.

3.11.3 Qualification Test Results

The results of the electrical equipment qualification tests will be documented as specified in Reference 13 of the PSAR Section 1.6 and summarized, as appropriate, in the FSAR. The mechanical equipment qualification results will be contained with the Equipment Specification data package.

3.11.4 Loss of Ventilation

All plant locations containing safety related control and electrical equipment, that need a controlled environment to maintain the required operability, are to be provided with redundant air conditioning and/or ventilation facilities for the needed environmental control. Analytical information on the various local environmental conditions in the plant is given in the corresponding sections in Chapters 2, 3, 6, 9 and 15.

As described in Section 3.11.1 above, the safety-related equipment is designed to operate successfully at environmental extremes.

3.11.5 Special Considerations

Enclosures containing safety related equipment will be designed to withstand the effects of normal, emergency and faulted conditions expected on the system. The effects of sodium spillage or fire will be protected against by placing redundant safety related equipment in separate compartments or rooms or by enclosing the safety related equipment in nonabsorptive, noncombustible, explosion proof casings. Applicable code requirements including those of the National Electric Code will be satisfied, as appropriate.

CHAPTER 3A SUPPLEMENTARY INFORMATION ON SEISMIC CATEGORY I STRUCTURES

TABLE OF CONTENTS

		<u>Page No.</u>
3A	<u>SUPPLEMENTARY INFORMATION ON SEISMIC CATEGORY I STRUCTURES</u>	
3A.1	Inner Cell System	3A.1-1
3A.1.1	Functional Design	3A.1-1
3A.1.2	Design Bases	3A.1-2
3A.1.3	Design Description	3A.1-3
3A.1.4	Design Evaluation	3A.1-3b
3A.1.4.1	Structures	3A.1-3b
3A.1.4.2	Inerted Cell Atmosphere Control System	3A.1-4
3A.1.5	Testing and Inspection	3A.1-5
3A.1.6	Instrumentation Requirement	3A.1-5
3A.1.7	Materials	3A.1-5
3A.1.8	Inner Barrier	3A.1-5a
3A.2	Head Access Area	3A.2-1
3A.2.1	Head Access Area Functional Design	3A.2-1
3A.2.1.1	Design Bases	3A.2-1
3A.2.1.2	Design Description	3A.2-1
3A.2.1.3	Design Evaluation	3A.2-3
3A.2.1.4	Testing and Inspection	3A.2-3
3A.2.2	Head Access Area Heat Removal System	3A.2-3
3A.3	Control Building	3A.3-1
3A.3.1	Design Bases	3A.3-1
3A.3.2	Design Description	3A.3-1
3A.3.3	Design Evaluation	3A.3-2
3A.3.4	Testing and Inspection	3A.3-2

TABLE OF CONTENTS (Continued)

		<u>Page No.</u>
3A.3.5	Instrumentation Requirements	3A.3-2
3A.4	Reactor Service Building (RSB)	3A.4-1
3A.4.1	Design Bases	3A.4-1
3A.4.2	Design Description	3A.4-1
3A.4.2.1	Reactor Services Building	3A.4-1
3A.4.2.2	Auxiliary Coolant Fluid	3A.4-3
39 3A.4.2.3	Deleted	3A.4-3
3A.4.2.4	Heating and Ventilation	3A.4-3
3A.4.2.5	Sodium Fire Protection	3A.4-3
3A.4.2.6	Recirculating Gas Cooling	3A.4-3
3A.4.2.7	Reactor Refueling	3A.4-4
3A.4.2.8	Nuclear Island General Purpose Maintenance Equipment	3A.4-4
3A.4.2.9	Auxiliary Liquid Metal	3A.4-5
3A.4.2.10	Inert Gas Receiving and Processing	3A.4-5
3A.4.2.11	Impurity Monitoring and Analysis	3A.4-5
3A.4.2.12	Fuel Failure Monitoring	3A.4-5
3A.4.3	Design Evaluation	3A.4-5
3A.4.4	Tests and Inspection	3A.4-6
3A.4.5	Instrumentation Requirements	3A.4-6
3A.5	Steam Generator Building	3A.5-1
3A.5.1	Design Bases	3A.5-1
3A.5.2	Design Description	3A.5-1
3A.5.2.1	Heat Transport and Steam Generator System	3A.5-3
3A.5.2.2	Steam Generator Auxiliary Heat Removal System	3A.5-3

TABLE OF CONTENTS (Continued)

		<u>Page No.</u>
3A.5.2.3	Heating and Ventilating	3A.5-3
3A.5.2.4	Fire Protection	3A.5-3
3A.5.2.5	Maintenance	3A.5-3
3A.5.3	Design Evaluation	3A.5-3
3A.5.4	Tests and Inspections	3A.5-4
3A.5.5	Instrumentation Requirements	3A.5-5
3A.6	Diesel Generator Building	3A.6-1
3A.6.1	Design Bases	3A.6-1
3A.6.2	System Design Description	3A.6-1
3A.6.3	Design Evaluation	3A.6-2
3A.6.4	Testing and Inspection	3A.6-3
3A.7	Deleted	3A.7-1
3A.8	Cell Liner Systems	3A.8-1
3A.8.1	Design Bases	3A.8-1
3A.8.2	Design Description	3A.8-1
3A.8.3	Design Evaluation	3A.8-3
3A.8.3.1	Sodium Spill Evaluation	3A.8-3
3A.8.3.2	Brittle Failure Potential of the Liner in Irradiated Areas	3A.8-3

44 | 33

37

TABLE OF CONTENTS (Continued)

		<u>Page No.</u>
3A.8.3.3	Liner Analysis	3A.8-4
3A.8.4	Testing and Inspection	3A.8-8
3A.8.4.1	Planned Testing Programs	3A.8-8
3A.9	Catch Pan System	3A.9-1
3A.9.1	Design Description	3A.9-1
3A.9.2	Design Evaluation	3A.9-3
3A.9.3	Testing	3A.9-4

LIST OF TABLES

		<u>Page No.</u>
47/	3A.1-1 Deleted	3A.1-6
	3A.1-2 Acceptance Ranges for Impurities and Pressures in Cell Atmospheres During Normal Operation	3A.1-8
	3A.1-3 Description of Inner Cells	3A.1-9
	3A.4-1 Systems Located in RSB	3A.4-7
	3A.4-2 Supporting Systems Located in RSB	3A.4-8
	3A.5-1 Systems Located in SGB	3A.5-6
	3A.5-2 Supporting Systems Located in SGB	3A.5-7
	3A.6-1 Systems Located in DGB	3A.6-4
	3A.6-2 Supporting Systems Located in DGB	3A.6-5

LIST OF FIGURES

		<u>Page No.</u>
3A.2-1	Head Access Area Plan View	3A.2-4
3A.2-2	Elevation View of Head Access Area	3A.2-5
3A.8-1	Analysis of Liner With Stud-Type Anchors	3A.8-10
3A.8-2	Analysis of Liner With Stud-Type Anchors	3A.8-11
3A.8-3	Wall - Floor Liner Corner	3A.8-12
3A.8-4	Floor & Wall Detail	3A.8-13
3A.8-5	Wall-Wall Detail	3A.8-14
3A.8-6	Typical Cell Liner Isometric-Corner Detail	3A.8-15
3A.9-1	Catch Pan with Fire Suppression Deck	3A.9-5

3A.0 SUPPLEMENTARY INFORMATION ON SEISMIC CATEGORY I STRUCTURES

This chapter provides additional information on Seismic Category I structures discussed in Sections 3.8.3 and 3.8.4 of Chapter 3.0. The following is a listing of these structures.

Inner Cell System
Head Access Area (HAA)
Control Building (CB)
Reactor Service Building (RSB)
Steam Generator Building (SGB)
Diesel Generator Building (DGB)

44 | 32 |

3A.1 INNER CELL SYSTEM

3A.1.1 Functional Design

The inner cell system comprises individual cells housing the reactor, the three sodium heat transport loops, sodium cold traps, sodium storage tank and reactor overflow vessel. These inner cells will have a nitrogen inerted atmosphere with a very low (see Table 3A.1-3) and controlled oxygen content.

The functional design of the inner cell system in the CRBRP is:

- (1) To maintain an inerted atmosphere in the inner cells such that the consequence of any potential spill of primary sodium inside these cells will be mitigated and contained; and
- (2) To provide a suitable structural configuration such that any potential detrimental sodium/construction material reaction due to any sodium spill will be precluded; and
- (3) To maintain the structural integrity of the inner cell system following any of the design basis accidents.

69

To fulfill these functional requirements, the inner cell system is designed to have a nominal leak tightness for the purpose of maintaining the purity of the inerted atmosphere in the inner cells during normal plant operation. For the safety analyses of all the postulated sodium spill accidents, no credit is taken of this nominal leaktightness. In fact, no credit for any cell leaktightness is taken for any in-containment cells in the accident analyses.

This same basis is used in all the analyses of the postulated accidents inside the containment, including: the containment design basis accident (described in detail in Section 6.2), and other postulated major sodium spill accidents (described in detail in Section 15.6).

All these cells have Engineered Safety Feature (ESF) steel liners and have the structural capability to accommodate hot sodium spills (see Section 3A.8). The inner cell system is designed to maintain the structural integrity following any of the postulated accidents and prevent sodium concrete reaction under DBA sodium/NaK spill conditions.

In the CRBRP, in addition to the inner cells inside containment, there are inerted cells inside the RSB (see PSAR Section 3A.4). These inerted cells have the similar functional design requirements as described above for the inner cells, although the accidents postulated for the design evaluations are of course different.

The above is based upon preliminary accident analysis as provided in Section 15.7 of this PSAR.

3A.1.2 Design Bases

The design basis accidents used for evaluation of the functional capability of the inner cell system have been identified in Section 3A.1.1 above. The inner cell system is required to have the following functional capability during normal plant operation or accident conditions as described below.

- 1) Cells which contain primary sodium will have a nitrogen inerted atmosphere to mitigate the effects of sodium spills.
- 2) Cells which contain primary sodium will have a steel liner to conserve nitrogen.
- 3) Those cells with large sodium inventories (the Reactor Cavity, PHTS Cells, and the Overflow & Primary Sodium Storage Tank Cell) will have steel liners capable of retaining a large sodium spill where a potential sodium spill could accumulate.
- 4) Each inerted cell will be structurally capable of withstanding the postulated accident conditions resulting from sodium and NaK spills. The preliminary design conditions of the inner cells are presented in Table 3.8-2. These accident considerations are further discussed in Section 15.6.
- 5) Each inerted cell will be designed for an anticipated leak rate of 0.36% vol/day at 2.5 inches of water.

For a discussion of design bases see Section 3.8-B.3.

Functional Bases For Containment Barrier Cells

The only inner cell specifically designed to act as a containment barrier against the accidental release of radioactivity is the RAPS Surge and Delay Tank Cell, located in the Reactor Service Building.

The functional design basis for controlled leakage from the RAPS Surge and Delay Tank Cell has been established to assure limiting the integrated 2-hour, site boundary dose and the integrated accident duration dose at the low population zone (B + γ) to a value below 10% of 10CFR100 following the postulated rupture of the RAPS Surge Tank. A detailed description of this postulated event and the associated radiological analyses are presented in Section 15.7.2.4.

Specific accident conditions and assumptions relating to this evaluation are as follows:

1. The RAPS Surge Tank is pressurized to its design pressure, 135 psig. Pressurization occurs in such a manner as to maximize the radioactive gas inventory in the Tank (See item 2, below). It is then assumed that the Tank ruptures and instantly releases its contents and mixes the contents with the cell atmosphere. Concurrent with the postulated rupture, it is assumed that a weather front occurs which lowers the barometric pressure by 0.5 psi for the duration of the accident.
2. The radioactive source term for this event is maximized by assuming that the reactor has been operating sufficiently long with gaseous fission products from 1% failed fuel that steady-state conditions exist. Additionally, it is assumed that outflow from the tank is cut off and that the normal radioactive gas in-flow continues until the tank is pressurized to its design pressure. Energy release to the cell is maximized by assuming instantaneous tank rupture and an adiabatic cell, i.e., all the fission product gases decay heat raise the cell gas temperature; no credit is taken for steel structures within the cell.
3. No credit is taken for the contribution of design features (such as building retention) other than the limited cell leakage in limiting the maximum value of radioactivity or energy released to the cell.
4. The only mechanism affecting post-accident cell pressure reduction employed in establishing the functional design basis is the limited leakage from the cell. The Cell Atmosphere Processing System is available to purge the radioactive gas from the RAPS Surge Tank Cell and this reduces cell pressure but credit for this mechanism is neglected for establishing the functional design basis.

5. The consistent application of conservative assumptions with respect to the radioactive term, the energy release to the cell, and the mitigating contribution of other design features, insures that the functional design basis for the RAPS Surge and Delay Tank Cell provides adequate conservation.

3A.1.3 Design Description

44 There are 13 independent inner cells in the RCB having
47 44 inert atmospheres cooled by the Recirculating Gas Cooling System.
The Recirculating Gas Cooling System is described in detail in
39 Section 9.16. Table 3A.1-3 lists these inner cells indicating the
equipment contained in each and the atmosphere cooled. The inner
cell arrangements and equipment layouts are shown in the RCB General
Arrangement drawings in Section 1.2.

44 The steel-lined reinforced concrete walls completely
enclosing each inner cell insure cell structural integrity under
dynamic effects associated with pipe breaks or equipment failure
resulting in the generation of missiles. The pressure boundaries
44 of the inner cells are designed for the pressures listed in Table
3A.1-3. Should dynamic effects following component failure result
44 in a sodium leak or spill, the steel liners are designed to contain
the sodium and prevent degradation of the concrete, while the inert
atmosphere provided by the Inert Gas Receiving and Processing System
protects against sodium fires. Design and analysis procedures for
37 the inner cell concrete structures are described in Section 3.8.3.4,
and for the cell liners in Paragraph 3.5 of the Appendix 3.8-B.

47

3A.1.4 Design Evaluation

3A.1.4.1 Structures

Structural design information of the inner cell system is provided in Section 3.8.

47

44

3A.1.4.2 Inerted Cell Atmosphere Control System

The function of the atmosphere control system for the inerted cells is to maintain control of the composition and the pressure of the cell atmosphere. All of the systems involved in the control of cell atmospheres are made of highly reliable, commercially available components. The control logic used is similar to that employed in the control of cell atmospheres in other reactors, in numerous hot cell and glove box applications and in certain industrial facilities and is therefore state-of-the-art so that no development work is required to assure proper performance.

47

These cells require a control and monitoring system to ensure that:

- a) The oxygen and water contents of the inerted cells are sufficiently low to mitigate the consequences of a major sodium spill and fire. (See Section 15.6 for an analysis of these accidents.)
- b) The oxygen content of the inerted cells is sufficiently high to prevent nitriding of high temperature piping.
- c) The radioactive gas content of the inerted cells is sufficiently low to permit detection of system leaks, and to ensure that cell atmosphere leakage into corridors in the RCB and RSB will not result in radioactivity concentrations in excess of 10CFR20 limits.
- d) Cell pressures can be controlled within acceptable limits.

All cell purge gas that contains radioactivity will be processed by CAPS. The CAPS system and its processing ability are discussed in detail in Section 11.3. Table 3A.1-2 shows the acceptable ranges for impurities and pressures in the RCB cells based upon these requirements.

Based upon preliminary design analysis, post-accident heat removal or atmosphere control is not required.

Amend. 47
Nov. 1978

3A.1.5 Testing and Inspection

37 Cell integrity will be assured during construction by the requirements and procedures as described in PSAR Appendix 3.8-B.

37 For inerted cells, the atmosphere control system may provide for detection of any excessive leakage during plant operation whether leakage is cell-to-cell or cell-to-upper-containment.

37 The inerted cells are designed to operate at slightly negative pressure. The cell atmosphere control system may provide for the detection of cell-in-leakage which could cause the oxygen level to exceed 2% (See Section 16.3.6.3). Should the 2% oxygen limit be exceeded, the cell or plant will be shut down and the leakage corrected. Currently the Cell Atmosphere Processing System is sized to process 100 SCFM.

The liner seam, penetration and attachment welds will be installed in accordance with the requirements of Section 3.8-B.

37 3A.1.6 Instrumentation Requirements

There are no instrumentation requirements identified with the inner cells directly, but rather with the supporting systems. These are discussed in Chapter 9.0.

3A.1.7 Materials

The cell structure will be of reinforced concrete.

37 Cell liner materials are described in Appendix 3.8-B to Section 3.8.

Materials used for construction of cells and associated fixtures or appurtenances, besides concrete, are identified as follows:

Cell Liners and Liner Support System	Carbon Steel
Piping	Carbon Steel & Stainless Steel
Pipe Insulation and Canning Material	Note 1
Pipe Supports and Auxiliary Steel	Carbon Steel
Conduit	Carbon Steel
Embedments	Carbon Steel
Penetration Seals	
Piping	Welded
Hatches and Doors	Silastic Rubber Compression
	Gaskets*
Electrical	TBD

*Some hatches, such as the piping cell hatches (Cells 101C, D, and E) may be seal-welded.

Note 1: Material requirements for piping insulation and piping are applicable to the components and piping in the inner cells. These are discussed in Chapter 9 for individual systems.

47 |

Table 3A.1-1 is intentionally deleted.

TABLE 3A.1-1 (Continued)

Bldg. Loc.	Served System (Nitrogen)	Cell Numbers	Heat Load per Subsystem 000 (Btu/hr)	Gas Flow per Subsystem 000 (scfm)	System Gas Pressure		System Gas Temperatures		Liquid Temperature		Liquid Supply Pressure psig
					Operate in.-H ₂ O	Emergency psig	To Cell F	From Cell F	To Cooler °F	From Cooler °F	
RCB	Primary Na Make-up Pump	104	*	*	+6	12	60	120	42	65	100
	Piping, Valves, Freeze vent & Gamma Heat	104									
	Overflow heat exchanger & Support	107									
	System 81 Piping & Valves	107									
	System 85 Piping & Valves	107									
RSB	EVST		492	*	+6	12	60	120	42	65	100
	EVST Tank Insulation	327									
	Pipe Insulation	327									
	Upper Periphery	327									
RSB	FHC (Argon)		588	*	+6	12	60	120	42	65	100
	Spent Fuel Storage Tank & Gamma Heat	341									
	New Fuel Flow Test	341									
	Motors, Manipulators, Cranes, Misc. Elec. Equip. Lighting	341									

3A.1-7a
44

Amend. 44
April 1978

43

TABLE 3A.1-1 (Continued)

Bldg. Loc.	Served System (Nitrogen)	Cell Numbers	Heat Load per Subsystem 000 (Btu/hr)	Gas Flow per Subsystem 000 (scfm)	System Gas Pressure		System Gas Temperatures		Liquid Temperature		Liquid Supply Pressure psig
					Operate in. -H ₂ O	Emergency psig	To Cell F	From Cell F	To Cooler °F	From Cooler °F	
RSB	EVS Pump Loop 2	360	399	*	±6	12	60	120	42	65	100
	EVS Na Cooler, Piping & Freeze Vents	360									
	EVS SSP, Piping & Valves	386									
	EVS PTI, Piping, Valves & Freeze Vents FHC Service Pump	387 3518									
RSB	EVS Pump Loop 1	357	667	*	±6	12	60	120	42	65	100
	EVS Cold Trap, Piping & Freeze Vents	361									
	EVS Na Cooler, Piping Valves & Freeze Vents	357									
RSB	EVS Loop 3	331	170	2.4	± 6		60	120	45	65	100

*These values shall be provided at a future date.

3A.1-7b

43

45

44

Amend. 45
July 1978

43

3

TABLE 3A.1-2
ACCEPTANCE RANGES FOR IMPURITIES AND PRESSURES IN
CELL ATMOSPHERES DURING NORMAL OPERATION

	Inerted RCB Cells	Inerted RSB Cells	RAPS and CAPS Cold Box Cells	Fuel Handling Cell	
Oxygen					
(Volume %)	0.5 - 2.0*	0.5-2.0*	20	0.005 ± 0.0025	1
Water Vapor					
(Volume ppm)	<8000	<8000	<14,600	50 ± 25	1, 23
Radioactivity					
(μCi/cc)	<0.001	<0.001	<0.008	0.001	1
Cell Pressure**					
(in H ₂ O)	-10 to +10	-10 to +10	-10 to +10	-10 to +3	

* Tentative Values

** Control range; the operation specification may require control within the quoted range.

47

1 23

TABLE 3A.1-3
INNER CELL DESIGNATION LIST
REACTOR CONTAINMENT BUILDING

Sheet 1 of 3

CELL (1) NO.	TITLE	FLOOR ELEVATION	RADIATION OPERATION	ZONE (2) SHUTDOWN	STRUCT. DESIGN PRESS. PSIG	UPSET DESIGN (4) TEMP. (°F)	OPERATING TEMP. (°F)	NORMAL (3) ATMOS.	EQUIPMENT CONTAINED
101A	Reactor Cavity **	740'	V	V	35	150	120	N	Reactor Vessel, Guard Vessel
101C	Flowmeter Cell (PHTS Loop #1)	786'-3"	V	V	35	150	120	N	PHTS Piping Perma- nent Magnet Flowmeter
101D	Flowmeter Cell (PHTS Loop #2)	786'-3"	V	V	35	150	120	N	PHTS Piping Perma- nent Magnet Flowmeter
101E	Flowmeter Cell (PHTS Loop #3)	786'-3"	V	V	35	150	120	N	PHTS Piping Perma- nent Magnet Flowmeter
102A	Overflow and Primary Na Storage Tank Cell	733'-0"	V	IV	12	150	120	N	Primary Na Storage Vessel, Reactor Overflow Vessel, Na Drain Tank
102B	System 81 Reactor Cavity Piping Penetra- tion Area	782'-0"	V	IV	12	150	120	N	System 81 Pri. Na Overflow and Make- up lines from Reactor Vessel
103	Primary Na Make-up Pump Cell	733'-0"	V	IV	12	150	120	N	Primary Na EM Makeup Pump

3A.1-9

Amend. 75
Feb. 1983

TABLE 3A.1-3 (Continued)

CELL (1) NO.	TITLE	FLOOR ELEVATION	RADIATION OPERATION	ZONE (2) SHUTDOWN	STRUCT. DESIGN PRESS. PSIG	UPSET DESIGN (4) TEMP. (OF)	OPERATING TEMP. (OF)	NORMAL (3) ATMOS.	EQUIPMENT CONTAINED
104	Primary Na Makeup & Future Pump Cell	733'-0"	V	IV	15	150	120	N	Primary Na EM Make-up Pump
107A	Primary Na Makeup Pump Valve Gallery	733'-0"	V	V	15	150	120	N	Primary Na EM Make-up Piping & Valves
107B	Aux. LM Pipeway and Valve Gallery	733'-0"	V	V	15	150	120	N	Direct Heat Removal Service DHRs Cooler Sodium Piping & Valves
121	PHTS Loop #1 Cell **	752'-8"	V	V	30	150	120	N	Primary Na Pump & Guard Vessel, Intermediate Heat Exchanger & Guard Vessel, Cold Leg Check Valve, PHTS and IHTS Hot Leg & Cold Leg Sodium Piping
122	PHTS Loop #2 Cell **	752'-8"	V	V	30	150	120	N	"
123	PHTS Loop #3 Cell **	752'-8"	V	V	30	150	120	N	"
131	NaK Cooling Equip. Cell	769'-0"	III	III	12	150	120	N	NaK Storage Tank, NaK EM Pump, NaK Cooler
132	NaK Sampling Cell	769'-0"	V	V	12	150	120	N	Multipurpose Sample (MPS), MPS Valve Cabinet, Master Slave Manipulator, Sodium Piping, Radiation Shielding Window, Sodium Transfer Tunnel

3A.1-9a

Amend. 75
Feb. 1983

TABLE 3A.1-3 (Continued)

Sheet 3 of 3

CELL (1) NO.	TITLE	FLOOR ELEVATION	RADIATION OPERATION	ZONE (2) SHUTDOWN	STRUCT. DESIGN PRESS. PSIG	UPSET DESIGN (4) TEMP. (°F)	OPERATING TEMP. (°F)	NORMAL (3) ATMOS.	EQUIPMENT CONTAINED
141	PTI Cell	783'-9"	V	V	12	150	120	N	Plugging Temp. Indicator (PTI), PTI Valve Cabinet
143	PTI Cell	792'-0"	V	V	12	150	120	N	"
157A	Pri. Na Cold Trap Cell (A)	793'-0"	V	V	12	150	120	N	Pri. Na Cold Traps
157B	Pri. Na Cold Trap Cell (B)	792'-9"	V	V	12	150	120	N	Pri. Na Cold Traps
157D	Cold Trap Valve Gallery (A)	792'-9"	V	IV	12	150	120	N	Cold Traps Piping & Valves
157E	Cold Trap Valve Gallery (B)	792'-9"	V	IV	12	150	120	N	Cold Traps Piping & Valves

- NOTES:
- 1) Alphabetical designations following cell nos. indicate sub-cells sharing a common atmosphere.
 - 2) For definition of Radiation Zones see Table 12.1-1
 - 3) N = Nitrogen
 - 4) Liner Design Temperature

** These cells shall have a design capability of surviving a one time high temperature sodium spill of 1050°F.

3A.1-9b

Amend. 75
Feb. 1983

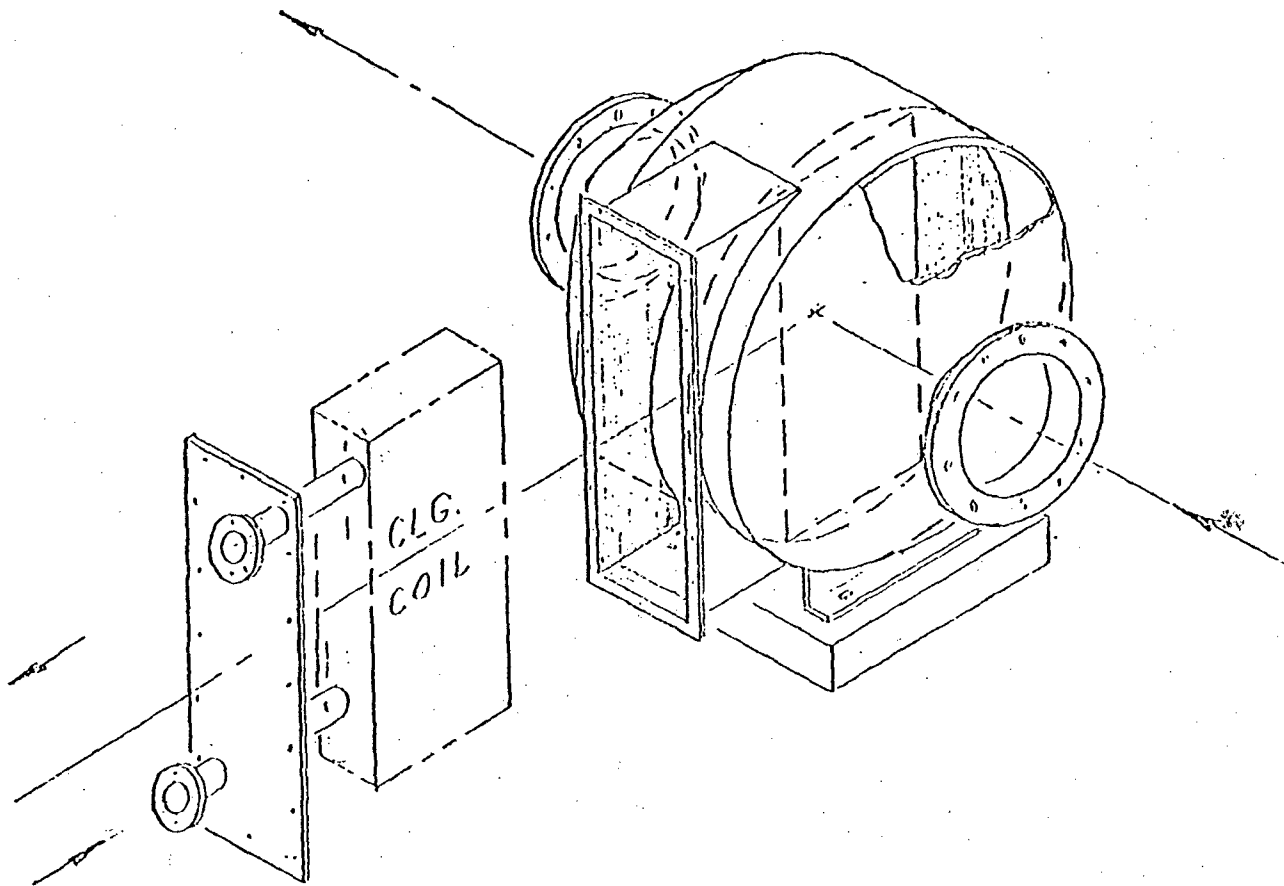


Figure 3A.1-1 COOLER ASSEMBLY

Amend. 44
April 1978

3A.1-11

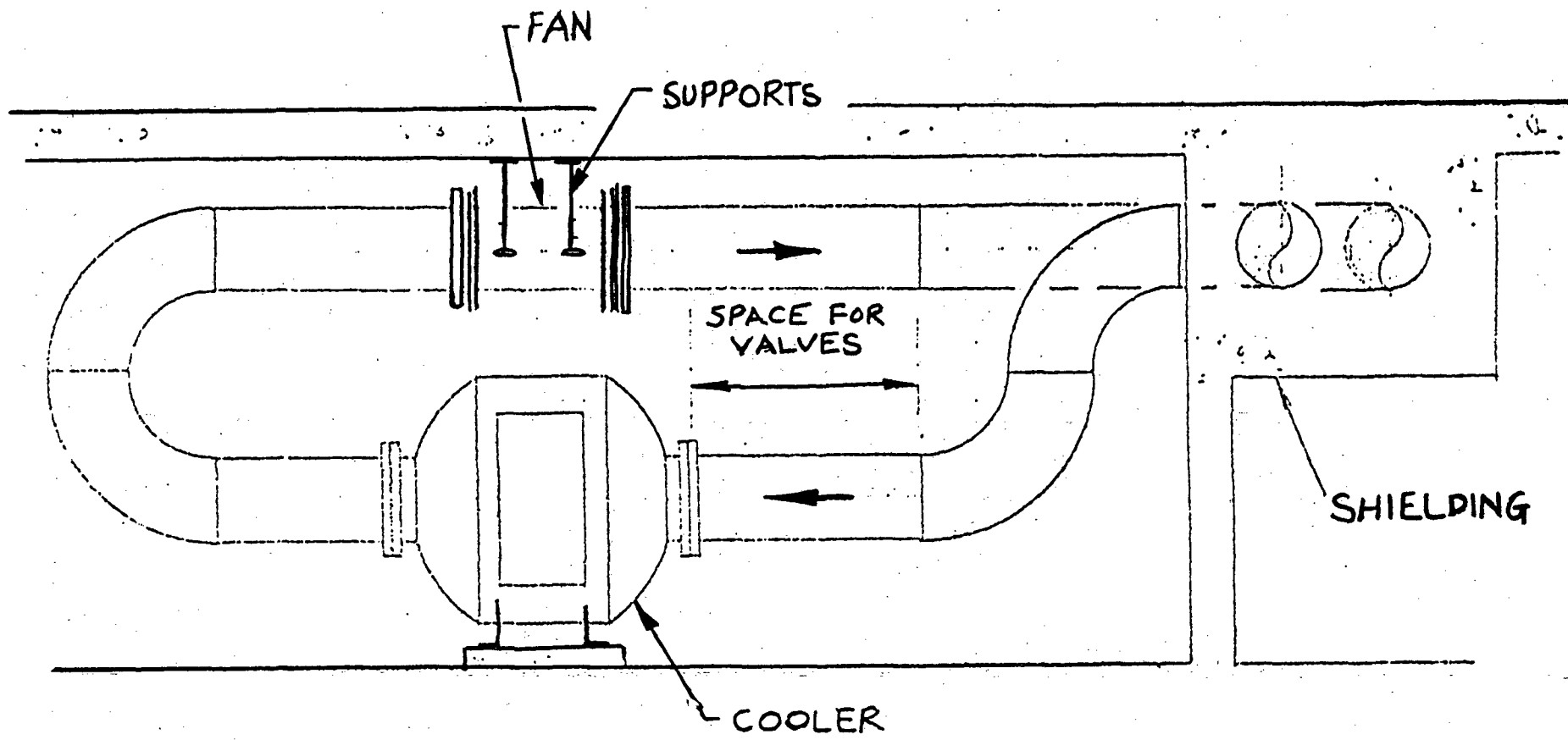


Figure 3A.1-2 TYPICAL COOLER & FAN ARRANGEMENT

Amend. 44
April 1978

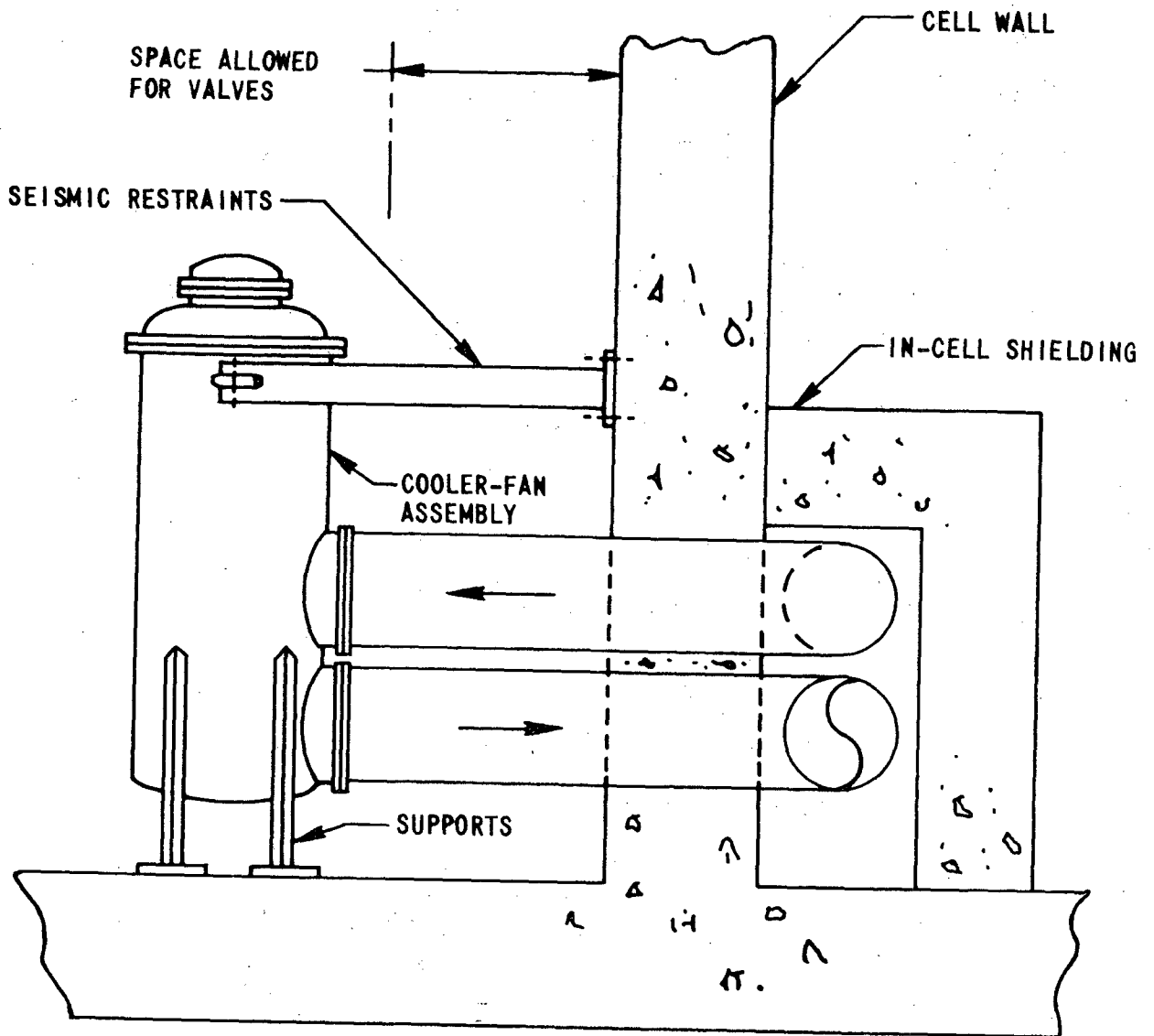


Figure 3A.1-3. Vertical Cooler-Fan Installation

6676-3

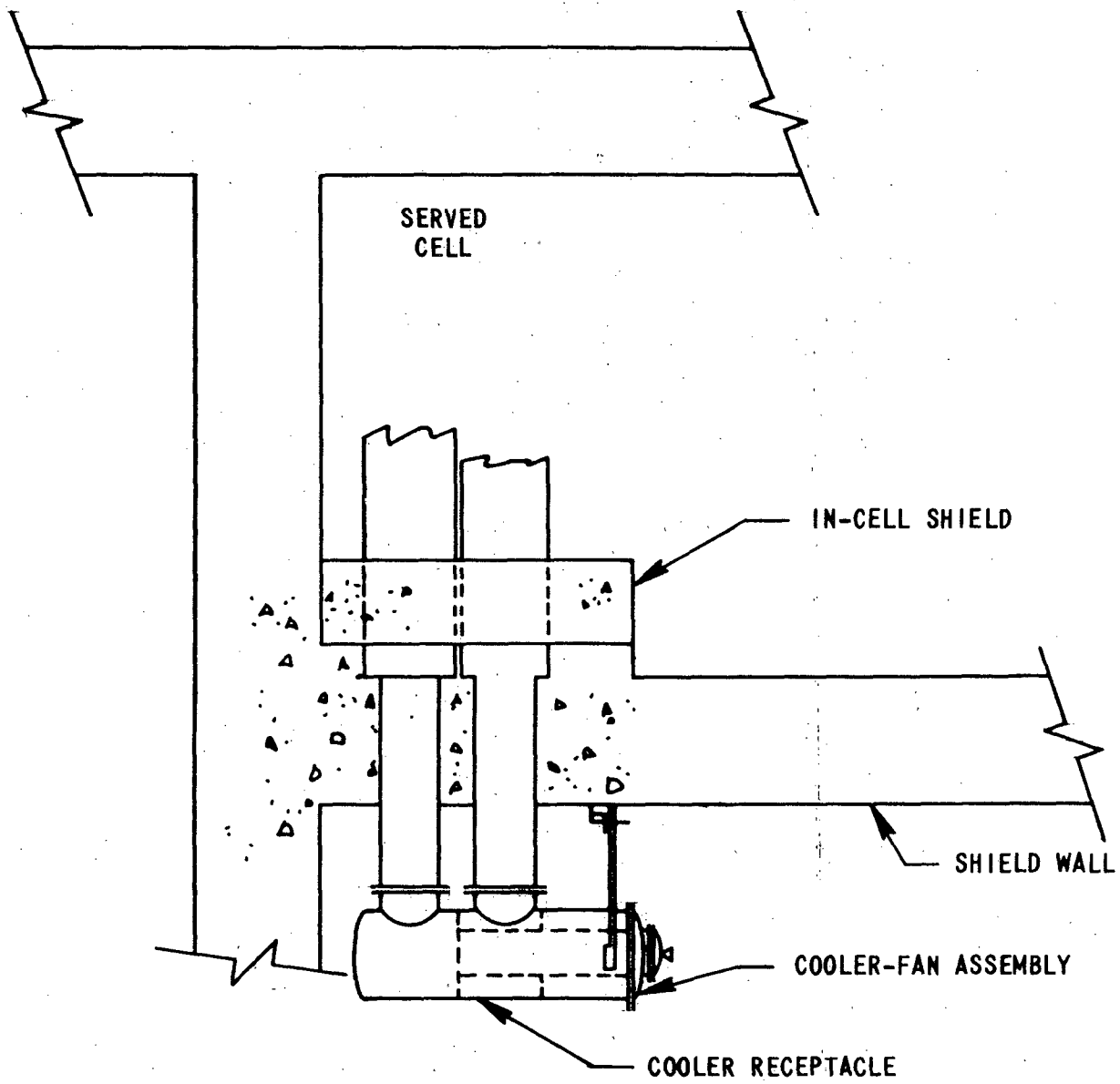


Figure 3A.1-4. Horizontal Cooler-Fan Installation

6676-4

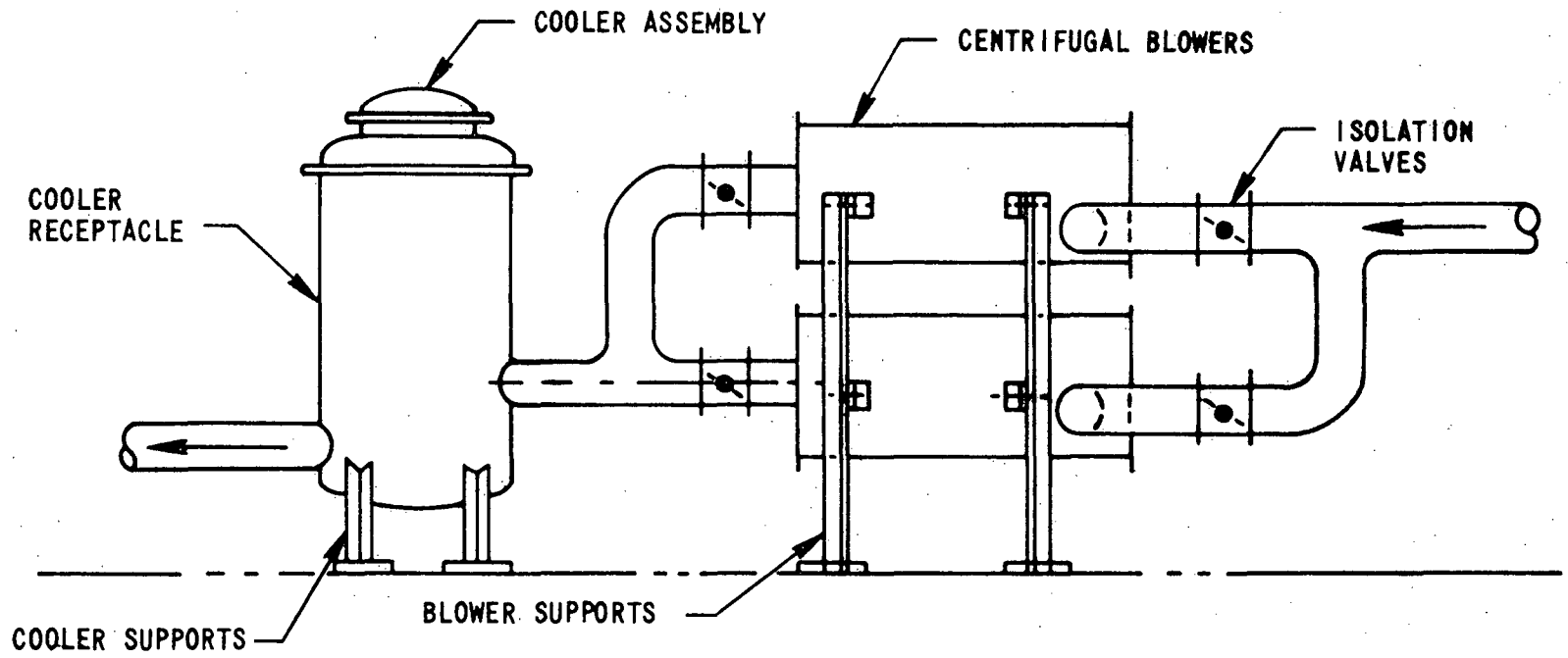


Figure 3A.1-5. High Pressure Cooler and Blower Installation

3A.2 HEAD ACCESS AREA

3A.2.1 Head Access Area Functional Design

The Head Access Area (HAA) provides electrical and gas services, access platforms and the environment necessary for reactor operation, refueling, inspection, surveillance and maintenance.

3A.2.1.1 Design Bases

The HAA air temperature must be compatible with instrumentation, equipment, seals and personnel access. The temperature of all routinely accessible surfaces of HAA equipment will be limited to 125°F maximum for metallic surfaces and 140°F for insulated surfaces. Stairways, ladders, walkways, and platforms will be designed to OSHA standards. The radiation dose rate will be limited to values as defined in Section 12.1.

3A.2.1.2 Design Description

The HAA is open to reactor containment at the operating floor elevation (816'). The general arrangement is shown on Figure 3A.2-1. The HAA is 44 feet square and 14 feet deep (below operating floor level). The top surface of the reactor head and the HAA floor are at the same elevation (802').

Electrical services enter the HAA by way of wall penetrations leading into terminal boxes and/or conduit. Electrical cables are routed via wireway and conduit (separated according to signal type) to the equipment on the reactor closure head. During refueling the service bridges are swung aside and the cable transfer machine provides the services needed on the rotating plugs.

Gas services enter the HAA via pipes through the south and east walls. Gas services to the rotating plugs are also provided through the service bridges and cable transfer machines.

Major items within the HAA include:

Small Rotating Plug/Riser Assembly

In-Vessel Transfer Machine (IVTM) Port Nozzle
IVTM Port Adapter (Preparation for Refueling)
IVTM (Refueling)

Intermediate Rotating Plug/Riser Assembly

Primary Control Rod Drive Mechanisms (PCRDs)
Secondary Control Rod Drive Mechanisms (SCRDs)
Shield & Seismic Support (S&SS)
Liquid Level Monitors (2)
Upper Internals Structure (UIS) Columns (4)
UIS Jacking Mechanisms (UISJMs) (4)
IRP Platforms and Ladders
IRP Cable Transfer Machine & Cooling Duct
SRP Drive Unit & Lock

Large Rotating Plug/Riser Assembly

Fuel Transfer Port and Lower Adapter
FTP Upper Adapter & Floor Valve (Refueling)
Liquid Level Monitors (2)
LRP Platform & Ladders
Cable Transfer Machine and Cooling Ducts
IRP Drive Unit & Lock

Off Head Items

Reactor Vessel Support Ring & Cavity Seal
Head Heating System Cabinets
LRP Drive Units (2) and Lock
HAA Electrical Equipment & Wiring
Radiation Monitors (4)
FLux Monitor Preamplifiers
Remote Data Acquisition Terminal
HAA Service Bridges and Reference Units
HAA PCRD Cooling Pipes
HAA Cooling Ducts
HAA Gas Service Equipment
Seismic Recorders
North & South Service Platforms & Stairs
HAA Plug Drive Control Box
EVTM Cavity Beams & Columns

3A.2.1.3 Design Evaluation

A Head Access Area which provides ready access to operating personnel enhances both the safety and availability of the plant by permitting surveillance and inspection of the many systems and component in this area during operation. This will provide a good basis for decisions that must be made during operation.

Radioactivity in the Head Access Area will be monitored to detect leakage of gas from any of the seals in the head. Detectors will be located in the head access area. The HAA air will be recirculated once every two minutes. This will reduce the chance of any local buildup of leaking gas. The relatively low cover gas pressure (10 inches of water) and the use of double seals with buffer gas between will minimize leakage and dilute any cover gas which may leak into the HAA.

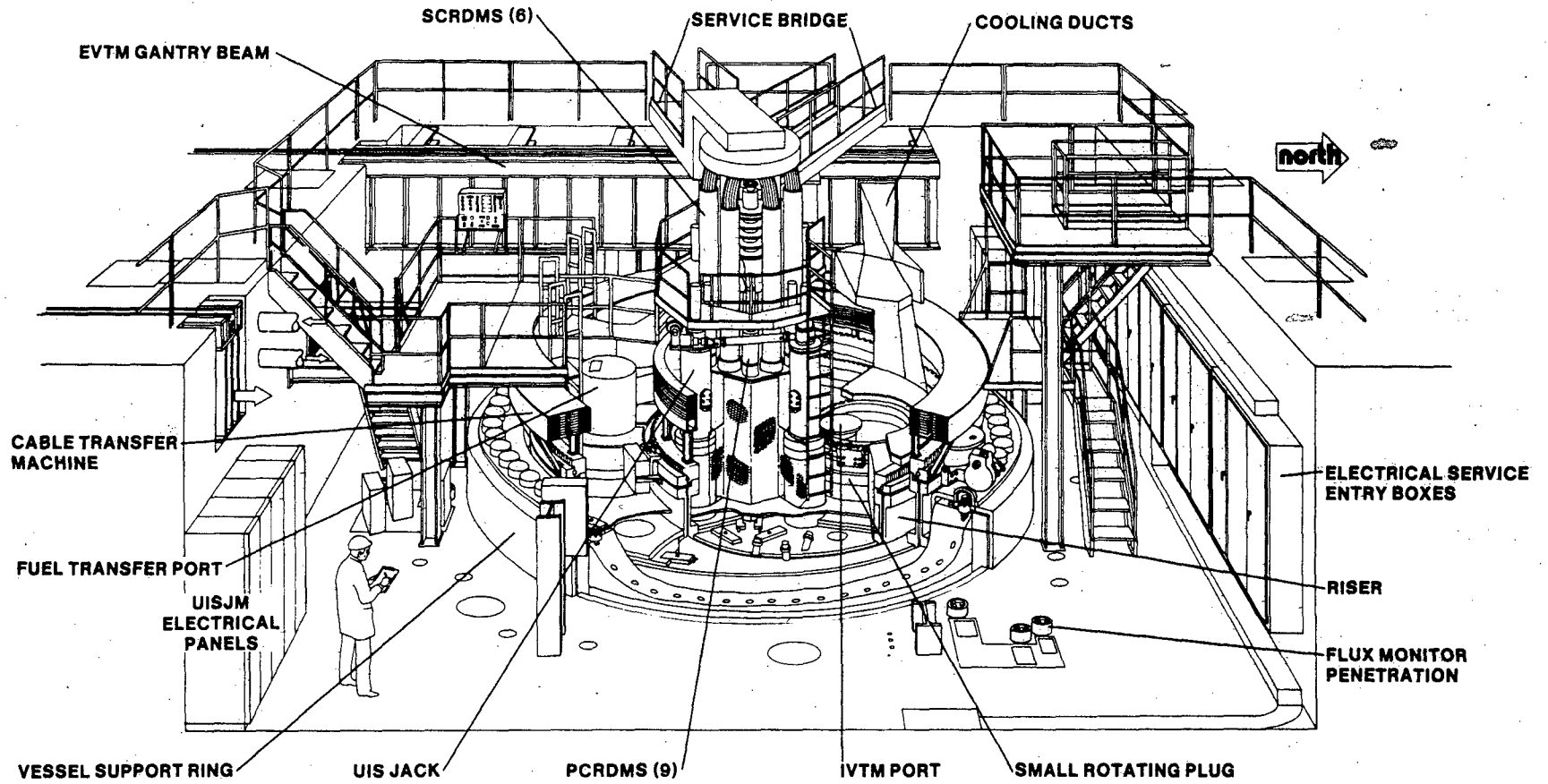
3A.2.1.4 Testing and Inspection

There are no testing and in-service inspection requirements for the Head Access Area.

3A.2.2 Head Access Area Heat Removal System

HAA heat loads include heat from the reactor vessel support ledge, HAA floor, closure head and heaters, and miscellaneous electrical equipment. Cooling is provided by an independent air conditioning system located in an adjacent cell. The cool pool/focused flow ducting system directs cooling air to critical regions on the closure head. Warmed air returns to the air conditioning system via a grille located in the south wall of the HAA.

Loss of the heat removal system would result in a natural convective air flow that would transfer heat to the reactor containment building atmosphere. In the worse case (loss of off-site power and loss of power to the HAA cooling system) the RCB atmosphere is expected to rise to a maximum of 120°F from its normal temperature of 80 to 85°F resulting in a temperature rise within the head access area which will not exceed 40°F. Equipment in the HAA will remain functional at an RCB atmospheric temperature of 120°F.



3A.2-4

Amend. 62
Nov. 1981

Figure 3A.2-1. CRBRP Head Access Area

3A.3.1 Design Bases

The design bases accident used in determining the design requirements for the Control Building (CB) and in particular the control room and its Habitability System are discussed in detail in Chapter 6, Section 6.3.

3A.3.2 Design Description

The structural aspects of the Control Building are described in Section 3.8.4. The Control Building houses the main control room which contains both the NSSS controls and the balance of plant controls, the life supporting heating and ventilating systems for the main Control Room, the cable spreading room, safety related a.c. and d.c. power supply, control rod drive mechanism switchgear, primary and intermediate pump speed controllers and the NSSS switchgear. The Control Building will be designed to allow access and occupancy during and following any postulated accident. The building is a tornado hardened, seismic Category 1 structure consistent with the requirements to protect the control and safety related systems.

The plant will be controlled from the main control room during normal operation and emergency conditions. Capability to shut down the plant and maintain it in a safe condition is provided even if loss of control room access is postulated.

The Control Building houses all or portions of the systems listed below:

Control Building Contents

- Building Electrical Power System
- Heating, Ventilating, Cooling and Air-Conditioning System
- Plant Fire Protection System
- Plant Annunciator System
- Piping & Equipment Electrical Heating Control System
- Balance of Plant Instrumentation & Control System
- Plant Control System
- Data Handling & Display System
- Radiation Monitoring System
- Plant Protection System

To permit operating personnel access during and after postulated accident conditions, a life support heating and ventilating system provides a safe and conditioned air supply to meet the continuous occupancy requirement. This system includes suitable radiation monitors which initiate closure of outside air makeup in the event this becomes necessary.

To meet the intent of Criterion 19, Appendix A, 10CFR50 shield design bases is such that the whole body dose for operating personnel will not exceed 5 rem for the duration of any design basis accident.

Design evaluations in this respect are provided in Sections 6.3.1.3 and 12.1.2.

Evaluation of the structural design is given in Section 3.8.4.

3A.3.4 Testing and Inspection

Tests and inspections conducted on the Control Room Habitability System are mainly concerned with the HVAC System capability to keep a positive pressure within the main control room, and the operation of the airborne hazards monitors. Discussions are provided in Section 6.3.1.4.

There are no testing and in-service surveillance requirements for the structures.

3A.3.5 Instrumentation Requirements

Instrumentation requirements for the Control Building are closely associated with the Control Room Habitability System. This is described in Section 6.3.1.5.

3A.4 REACTOR SERVICE BUILDING (RSB)

3A.4.1 Design Bases

The Reactor Service Building (RSB) design is based on:

- 61 | 1) Providing housing and structural support for portions of the Auxiliary, Liquid Metal Reactor Refueling, and Maintenance Systems. Table 3A.4-1 lists the functional systems located in the RSB. Table 3A.4-2 lists the supporting systems located in the RSB.
- 39 | 2) Providing protection against seismic and tornado events, and some degree of confinement for several systems that contain radioactive materials and spent reactor fuel.
- 29 | 3) Serving as an intermediate transfer and storage facility for new and spent fuel, other components, equipment, and materials entering and leaving the Reactor Containment Building (RCB).
- 4) Providing radiation protection, primarily in the form of concrete shielding, to meet the radiation shielding-zoning criteria presented in Table 12.1-1.
- 5) Allowing installation, removal, repair, maintenance, and re-installation of equipment and components housed therein.
- 29 | 6) Providing safe entrance and egress for operating and maintenance personnel who perform work in the RSB.
- 7) Providing environmental control (heating and ventilating, inerted cell, etc.) for various functional systems.
- 8) Providing sealing protection against ground water and flood water conditions.
- 9) Providing security to safeguard fuel per 10CFR73.

3A.4.2 Design Description

3A.4.2.1 Reactor Service Building

Following is a brief description of the RSB and certain systems located therein. Table 3A.4-1 lists all the systems the RSB and the appropriate PSAR references for detailed information of these systems. Additional information is provided in Section 3.8.4.1.1. General Arrangement Drawings are provided in Section 1.2.

The RSB is a reinforced concrete, and with the exception of the radwaste area is designed as a Seismic Category I, tornado hardened structure above and below grade level at El. 815 ft. The RSB structure, in addition, houses an airlock, cranes, a freight elevator, and a railroad track that allows railroad cars to be brought directly into the building.

The airlock, 13'4" in internal diameter, is provided between the RSB and the RCB. The elevation of the airlock is adjusted to provide a 8-ft. wide by 8-ft. high passage between the operating floor of the RSB (El. 816 ft.) and the RCB. The minimum clear space between the doors of the airlock is 20 ft.

A 125 ton capacity bridge crane is provided in the RSB. The hook on the crane will have a clearance of 42 ft. above the operating floor.

A hardened railroad door 18'0" x 22'0" is provided between the RSB and the Radwaste Building (RWB). This door is designed to withstand tornado generated missiles.

Personnel access and egress is provided in the RSB structure from all levels, via four staircases and one elevator. The elevator and one of the staircases are located in the southwest corner, the other three staircases are located in the northwest, southwest and northeast corners, respectively, as shown in the general arrangement drawings in Section 1.2. Corridors are extensively provided throughout the building for rapid egress.

Leakage of radioactive gas from the various systems within the RSB will be restricted by utilizing commercially available seals to limit, under normal operating conditions, the dose rate within the RSB due to radioactive gas leakage below 10% of the zoning criteria, as established in Table 12.1-1.

Additionally the RSB internal pressure is maintained at negative 1/4" W.G. to restrict the release of radioactive contaminants to the atmosphere.

The foundation for the west end of the Radwaste Area is at grade elevation and is founded on compacted structural backfill. The Radwaste Area structure is designed to meet the requirements of the Standard Building Code. In addition the structure below grade as well as the Solid Radwaste Area above grade are designed as reinforced concrete structure.

The upper part of Radwaste Area, the steel framed structure is designed to ensure that the adjacent seismic Category I structure of Reactor Service Area is not damaged nor its safety functions compromised during an SSE.

The RSB has been designed as Seismic Category I consistent with its safety function. The sections in this report dealing with the various systems located in the RSB (see Table 3A.4-1) present their individual seismic category requirements.

The RSB contains several inerted cells. These cells perform similar functions as those for the inerted cells in the Reactor Containment Building (see PSAR Section 3A.1). Table 3A.4-3 lists the inerted cells in the RSB.

3A.4.2.2 Auxiliary Coolant Systems

39 | 61 | The decay heat generated in the EVST sodium is removed by a Na-NaK heat exchanger. The NaK, in turn, releases its heat through an air blast heat exchanger. These heat exchangers, Na-NaK are located at elevation 765'0" of the RSB. A complete, redundant system of heat exchangers is present, as a standby in the event of a failure. The redundant systems and their accompanying lines are routed independently of each other by physical barrier separation. The FHC is cooled by the Recirculating Gas Cooling System, which, in turn, gives up its heat in gas-Dowtherm J heat exchangers. The Dowtherm J gives up this heat to a Chilled Water System Dowtherm to water heat exchanger. 61 | Section 9.7 provides more details on this system.

3A.4.2.3 Deleted

39 | 3A.4.2.4 Heating and Ventilation

61 | The Heating and Ventilation System provides for air-conditioning and ventilating the plant atmosphere. Section 9.6 and 12.2 provides more details on this system.

3A.4.2.5 Sodium Fire Protection

38 | The Sodium Fire Protection System provides the means of detecting, alarming, containing, and controlling sodium and/or NaK fires. Details of the SFPS are described in Section 9.13.

3A.4.2.6 Recirculating Gas Cooling

The Recirculating Gas Cooling System provides cooling of the inerted cells and is described in detail in Section 9.16.

47 |

47

3A.4.2.7 Reactor Refueling

44 The Reactor Refueling System performs all handling operations on core assemblies destined for the reactor, from the new fuel shipping and receiving to the installation of the spent fuel shipping cask into the railroad flat car. Its functions are performed in the RSB and RCB. Section 9.1 provides details of this system.

61

The three major areas occupied by this system within the RSB Reactor Service area are as follows:

- 1) Ex-Vessel Storage Tank - The EVST, located below the operating floor, will receive, hold and cool all core assemblies discharged from the reactor vessel prior to shipment offsite.
- 2) Fuel Handling Cell - The FHC is a subfloor hot cell which can hold up to three core assemblies for inspections, measurements and transfer to spent the fuel shipping casks for offsite shipment.
- 3) Two New Fuel Unloading Stations - Each station will contain one new fuel assembly in a new fuel shipping container.

20

44

3A.4.2.8 Nuclear Island General Purpose Maintenance Equipment

59

The Nuclear Island General Purpose Maintenance Equipment System provides the capability for maintenance of the Nuclear Steam Supply System (NSSS). These maintenance operations are accomplished within the Reactor Containment Building, The Reactor Service Building, and the Steam Generator Building. The system provides general purpose equipment and procedures for removal and replacement of radioactive and/or sodium service components of the Fuel Handling System, Heat Transport System, Auxillary Systems, and Reactor Systems. Capability is also provided for sodium removal and decontamination. The system also provides the general purpose equipment used for the removal, repair, maintenance, and reinstallation of equipment and components housed within the nuclear island.

3A.4.2.9 Auxiliary Liquid Metal

46 | The Auxiliary Liquid Metal System provides the facilities for purification and cooling of the sodium in the ex-vessel storage tank (EVST). The EVST sodium storage is provided by the Primary Sodium Storage and Processing System of the Auxiliary Liquid Metal System. This is discussed in greater detail in Section 9.1, 9.3.

The maximum activity in the EVST sodium (i.e., after 30 years of plant operation and with no EVST cold trapping) is given in Table 12.1-23.

3A.4.2.10 Inert Gas Receiving and Processing

Sections 9.5 and 11.3 present details of this system. The radioactive inventory, by isotope, present in the various cells within the RSB are given in Table 12.1-12 through 12.1-18.

3A.4.2.11 Impurity Monitoring and Analysis

46 | The Impurity Monitoring and Analysis System provides for the sampling monitoring, and analysis of sodium and cover gas impurities in the CRBRP systems. The system provides the following areas of impurity monitoring and sampling:

- 1) EVS cover gas sampling
- 2) Primary cover gas sampling
- 46 | 3) EVS sodium sampling

Section 9.8 presents more details of this system.

3A.4.2.12 Fuel Failure Monitoring

Section 7.5.4 presents details of this system. The isotopic gas activity in the sampling trap cell (gas tag analysis) and the cover gas monitor cell are presented in Table 12.1-20.

3A.4.3 Design Evaluation

61 | The RSB is designed to house the various systems listed in Table 3A.4-1. Each of the systems containing radioactive fluids or components will be housed in separate cells, that are provided with walls of adequate thickness. These walls, in addition to providing radiation protection to operating personnel, will act as a confinement barrier. Accidents considered by the individual systems housed in the RSB are presented in Chapter 15.

3A.4.4 Tests and Inspection

A CRBRP Quality Assurance Program is established to assure that critical structures are built in accordance with specifications. This program is described in Chapter 17.

Principal Materials Used in the RSB - Concrete, reinforcing steel, steel liner plates, and structural steel - are manufactured in accordance with nationally recognized standards. User installation tests and inspections are detailed in construction specifications.

Conventional methods will be used to inspect the cell liners. These methods may include:

- 1) Visual inspection of welds
- 2) Dye penetrant
- 3) Vacuum box

Tests and inspection will be performed during construction of the RSB structure, to verify conformance with construction specifications and applicable parts of building codes.

The tests and inspection of systems within the RSB are discussed in detail in those sections of this report pertaining to the individual systems housed by the RSB (see Table 3A.4-1).

3A.4.5 Instrumentation Requirements

The RSB will be sufficiently instrumented to provide for the safety of both operating personnel and the general public. This instrumentation will include such items as neutron counters for EVST and the FHC area, radiation detectors in all accessible areas, exhaust monitors for the H&V System, etc. The specific instrumentation requirements for the various systems in the RSB will be the joint responsibility of the functional system and its corresponding instrumentation system. These pairs of systems, together with a brief discussion of their instrumentation requirements, are given in other sections of this PSAR (see Table 3A.4-1). The responsibility of providing general radiation monitoring (i.e., not within the jurisdiction of any functional system) will be the Radiation Monitoring System. Section 12.2.4 of this PSAR presents the requirement for radiation monitoring in the RSB.

TABLE 3A.4-1

MAJOR SYSTEMS LOCATED IN RSB

29 |

15 |

39 |

47 |

29 |

<u>System Name</u>	<u>PSAR Reference</u>
Chilled Water (Normal & Emergency)	9.7
Heating and Ventilating	12.2
Sodium Fire Protection	9.13.2
Recirculating Gas Cooling	9.16
Reactor Refueling	9.1, 7.6
Maintenance (NSSS)	9.2
Auxiliary Liquid Metal	9.3
Inert Gas Receiving and Processing	9.5, 11.3
Impurity Monitoring and Analysis	9.8
Fuel Failure Monitoring	7.5.4
Radiation Monitoring	12.2.4
Non Sodium Fire Protection	9.13.1

3A.4-7

Amend. 47
NOV. 1978

TABLE 3A.4-2

SUPPORTING SYSTEMS LOCATED IN THE RSB

<u>System Name</u>	<u>Service and Function</u>
Building Electrical Power	Electrical power for outlets, equipment, and emergency power
Communication	Communication within the RSB and to outside areas
Lighting System	Provide space and special lighting
Reactor Containment	Provide equipment air lock and maintenance cask door that opens into the RSB
Plant Annunciator System	Provide annunciators within appropriate areas of the RSB
Piping and Equipment Electric Heating and Control	Provide trace heating on selected piping in the RSB
Radiation Monitoring	Provide radiation monitoring throughout RSB
Plant Protection	Provide plant protection systems and devices to prevent unauthorized entry into the RSB and fuel storage vault
Containment Cleanup System	Provide cleanup operations for the RCB Annulus Atmosphere during a TMDBB event.

61

TABLE SR.4-3
INERTED CELL DESIGNATION LIST
REACTOR SERVICE BUILDING

CELL NO.	TITLE	FLOOR ELEVATION	RADIATION OPERATION	ZONE(1) SHUTDOWN	STRUCTURAL DESIGN PRESS. (PSIG)	UPSET DES. TEMP. (°F) (3)	NORMAL ATMOS. (2)	EQUIPMENT CONTAINED
331	EVST Thirld Loop IHX Cell	798'-6"	IV	III	12	150	N	EVST Backup Na Cooler
331A	EVST Thirld Loop Pipeway	798'-6"	IV	III	12	150	N	Piping
337	EVST Cell	759'-4"	V	IV	12	150	N	Ex-Vessel Storage Tank
341	Fuel Handling Cell	781'-0"	V	III	12	150	A	FHC Equipment
351C	Pipeway	770'-0"	IV	III	12	150	N	Piping
351D	Pipeway	770'-0"	IV	III	12	150	N	Piping
351A	Main EVS Cooling Sys. Pipeway	775'-0"	IV	III	12	150	N	Piping
351B	Main EVS Cooling Sys. Pipeway	775'-0"	IV	III	12	150	N	Piping
357	EVS Cooling Loop B Cell	779'-0"	IV	III	12	150	N	EVST Na Cooler Pump
357A	Cooling Loop B Pipeway	798'-6"	IV	III	12	150	N	Piping
357B	Cooling Loop B Pipeway	798'-6"	IV	III	12	150	N	Piping
360	EVS Cooling Loop A Cell	779'-0"	IV	III	12	150	N	EVST Na Cooler & Pump
360A	EVS Cooling Loop A Pipeway	798'-6"	IV	III	12	150	N	Piping
361	EVS Na Cold Trap Cell	779'-0"	IV	IV	12	150	N	EVS Cold Trap & Economizer
386	EVS SSP Cell	779'-0"	IV	III	12	150	N	Ex-Vessel Na SMPLG Pkg.
387	PTI Cell	765'-0"	IV	III	12	150	N	PTI

Notes: (1) For definition of Radiation Zones see Table 12.3-1.
 (2) N = Nitrogen A = Argon
 (3) Liner Design Temperature

3A.4-9

Amend. 77
May 1983

3A.5 STEAM GENERATOR BUILDING

3A.5.1 Design Basis

The Steam Generator Building (SGB) design is based on:

- 61 | 1) Providing housing and structural support for portions of the Intermediate Heat Transport System, Steam Generation and Steam Generator Auxiliary Heat Removal System and Maintenance Systems. Table 3A.5-1 lists the functional systems located in the SGB. Table 3A.5-2 lists the supporting systems located in the SGB.
- 2) Providing protection against seismic and tornado events.
- 3) Allowing removal, repair, maintenance and re-installation of equipment and components housed therein.
- 4) Providing environmental control (heating and ventilating) for the various functional systems.
- 5) Providing sealing protection against ground water and flood water conditions.
- 6) Providing safe entrance and egress for operating and maintenance personnel who perform work in the SGB.

3A.5.2 Design Description

Following is a brief description of the Steam Generator Building. Table 3A.5-1 lists all the systems inside the SGB and the appropriate PSAR references for detailed information of these systems. General Arrangement Drawings are provided in Section 1.2.

- 45 | 61 | The Steam Generator Building is a Seismic Category I, tornado hardened reinforced concrete structure with an attached Seismic Category I unhardened structure for equipment maintenance and repair. The building is functionally subdivided into four bays which house the major equipment noted below:

Intermediate Bay

- 61 | Ex-Containment,
Primary Sodium Storage Vessel
Intermediate Sodium Piping
15 | Cable Distribution
Chilled Water Systems

Steam Generator Bay

Intermediate Sodium Dump Tanks
Evaporators
Superheaters
Intermediate Sodium Pump
Intermediate Cold Traps
Intermediate Sodium Expansion Tanks
Reactor Products Separation Tanks

Auxiliary Bay

Instrumentation and Control Panels
Auxiliary Heat Removal System
Steam Generator Recirculation Pump
Steam Drum

Maintenance Bay

Intermediate Sodium Removal System and Cleaning Cell
Maintenance Platforms for Steam Generator, Superheater and IHTS Pump
Railroad Siding

The Intermediate Bay, Steam Generator Bay and the Auxiliary Bay are tornado-hardened Seismic Category I structures and will be reinforced concrete enclosures with reinforced concrete slabs on structural steel framing. The Maintenance Bay housing noncritical components and systems will not be a tornado-hardened structure but will have a Seismic Category I steel framework. The metal wall siding and metal roof decking will be designed in accordance with standard practice for industrial buildings. Interior structures will consist of structural framing, floor grating or concrete decks. Structural steel will receive a fire protection cover in accordance with the requirements of the Standard Building Code.

Postulated accidents as discussed in Chapter 15 do not impose a leak rate capability on the SGB (except the primary sodium storage cell in the Intermediate Bay) or require more than a 3 psi differential pressure capability as stipulated by the tornado considerations.

A brief description of the structural design features of the building is given in Section 3.8.4. A detailed description of the Heating, Ventilation, Cooling and Air-Conditioning System serving the building is given in Section 9.6.

Design characteristics of the SGB to mitigate the effects of seismic and tornado events and steam line ruptures, resulting loads and the building structural design criteria are described in Chapter 3. General Arrangement Drawings are provided in Section 1.2.

3A.5.2.1 Heat Transport and Steam Generator Systems

61 | The SGB houses the three intermediate heat transport loops. Each loop transports heat from the respective IHX to the steam generator system and returns the cooled sodium back to the IHX. All piping and components are Seismically supported and housed in Seismic Category 1, tornado hardened structures. The steam generator system consists of 2 evaporators and 1 superheater per loop with their associated steam drum and recirculation system. Section 5.5 provides more details of this system.

3A.5.2.2 Steam Generator Auxiliary Heat Removal System SGAHRS

61 | The SGAHRS is a safety related system which provides safe shutdown of the reactor for both short and long periods of time should the normal steam dump to the condenser be inoperative. This system is housed entirely within the Auxiliary Bay. Section 5.6 provides more detailed description of this system.

3A.5.2.3 Heating and Ventilating

61 | The Heating, Ventilating and Air Conditioning System provides for air-conditioning of the atmosphere within the SGB. Sections 9.6 and 12.2 presents more details of this system.

3A.5.2.4 Fire Protection

35 | The Sodium Fire Protection System provides the means of detecting, containing, alarming and controlling sodium fires. Details of the SFPS are described in Section 9.13.

3A.5.2.5 Maintenance

61 | A maintenance bay is provided adjacent to the steam generator cell. This structure provides housing for maintenance stands for both an intermediate sodium pump and an evaporator/superheater module. Additional description is provided in Section 9.2.

3A.5.3 Design Evaluation

61 | Sodium fires within the Steam Generator Building represent an additional loading in the building as discussed in Section 3.8.4. The sodium fire accident sequences and resulting loadings on the Steam Generator Building are provided in Section 15.6.

Each of three intermediate sodium loops and its associated steam generator system are physically separated in independent cells to prevent an accident in one loop from causing failures in any of the other loops. The extent of the isolation is described below.

- o Separate primary sodium loops contained within separate cells in the RCB.
- o Separate intermediate sodium loops contained within separate cells in the intermediate bay.
- o Separate steam generator systems and their associated portions of SGAHRS contained within separate cells in the steam generator building.

Reinforced concrete walls provide loop separation in all buildings and steel catch pans will be provided to retain sodium at locations of potential spillage. Each cell containing a portion of a loop is independently controlled to permit loop-to-loop isolation. Piping systems do not interconnect in the intermediate system loops, except for small vent and drain lines which can be closed off by valves to permit loop-to-loop isolation. Drains from cells containing portions of a loop will be isolated by suitable valving. Electrical, instrument and control cabling will be routed separately to each loop so that cabling for one loop does not pass through a cell containing another loop. The same applies to piping and ventilation ducting. Where unavoidable, piping and duct penetrations between cells containing loops, will be provided with protective missile sleeves or similar protective measures.

Separation of the loops in the auxiliary bay is provided to prevent propagation of an accident into an adjacent cell. Reinforced concrete walls and barrier doors provide this protection. The arrangement and orientation of components (e.g., piping, valves, rotating machinery) is such that the protection of vital equipment in adjacent cells from equipment generated missiles is provided.

In cases where piping systems do interconnect the steam generating system loops, (i.e. main steam lines, normal and auxiliary feed water lines) automatic isolation is provided to prevent propagation of a fault from one loop system to another. The auxiliary feed water system is designed so that no single active failure following the initiating event can prevent auxiliary feed water from reaching the operating steam generator loops.

This separation is necessary to ensure the operability of the SGAHRS System after an accident occurs in one loop.

3A.5.4 Tests and Inspections

A CRBRP Quality Assurance Program is established to assure that critical structures are built in accordance with specifications. This program is described in Chapter 17.

Principal Materials Used in the SGB - Concrete, reinforcing steel, steel liner plates, and structural steel - are manufactured in accordance with nationally recognized standards. User installation tests and inspections are detailed in construction specifications.

Tests and inspection will be performed during construction of the SGB structure, to verify conformance with construction specifications and applicable parts of building codes.

The tests and inspection of systems within the SGB are discussed in detail in those sections of this report pertaining to the individual systems housed by the SGB (See table 3A.5-1).

3A.5.5 Instrumentation Requirements

The specific instrumentation requirements for the various systems in the SGB are discussed in Chapter 7.0. These systems, together with a brief discussion of their instrumentation requirements, are given in other sections of this PSAR (See Table 3A.5-1).

TABLE 3A.5-1

SYSTEMS LOCATED IN SGB

<u>System</u>	<u>PSAR Reference</u>
Heating & Ventilating	9.6 & 12.2
Plant Fire Protection	9.14
Maintenance System	9.2
Reactor Heat Transport System	5.0
Steam Generator System	5.5
Steam Generator Auxiliary Heat Removal System	5.6
Inert Gas Receiving & Processing	9.5
Radiation Monitoring	12.1.4 & 12.2.4
Normal Chilled Water	9.7.1
Emergency Chilled Water	9.7.2

TABLE 3A.5-2

SUPPORTING SYSTEMS LOCATED IN THE
STEAM GENERATOR BUILDING

System

Building Electrical Power

Communications

Lighting System

Compressed Gas System

Plant Annunciator System

Plant Protection

Plant Fire Protection

3A.6 DIESEL GENERATOR BUILDING

3A.6.1 Design Bases

15 | The Diesel Generator Building is immediately adjacent to the Control Building. It contains safety related emergency electrical power supply equipment to supply emergency shutdown power in the event of loss of all offsite AC power.

The Diesel Generator Building design is based upon:

- 61 |
- 1) Providing housing and support for portions of the functional systems listed in Table 3A.6-1. Table 3A.6-2 lists the supporting systems in the DGB.
 - 2) Providing protection against seismic and tornado events for those systems in the DGB.
 - 3) Allowing removal, repair, maintenance and re-installation of equipment and components housed therein.
 - 4) Providing safe entrance and egress for operating and maintenance personnel, who perform work in the DGB.
 - 5) Providing environmental control (heating and ventilating) for various functional systems.
 - 6) Providing sealing protection against ground water and flood water conditions.

3A.6.2 System Design Description

61 | The Diesel Generator Building is a tornado hardened, seismic Category I structure. The two diesel generators are supported at grade elevation, and are separated from each other by a wall designed to withstand the impact of any missile generated by a diesel-generator casualty. Building materials and adequate wall thicknesses provide the required fire barriers; doorways are provided with the required fire rated doors. Openings in exterior walls and roof are missile protected with barrier walls or a Penthouse. The building is also protected against floods. (See Section 3.4)

61 | The Diesel Generator Building HVAC system provides the required ventilation to maintain adequate temperatures under normal and emergency conditions for the various areas in the building. The description of the Diesel Generator Building HVAC System is presented in Section 9.6.

An equipment removal hatch is provided in the building for the purposes of installation, maintenance, and removal of equipment located on the elevations below grade.

61 Complete separation is maintained between the redundant diesel-generators with their respective auxiliary support systems to ensure that a malfunction or failure of an active or passive component will not impair the capability of at least one diesel-generator to supply power for a safe plant shutdown. The diesel-generator auxiliary support systems, which include fuel oil, lube oil, starting air, and cooling water systems, are classified moderate energy systems and, as such, are subject to through-the-wall pipe leakage cracks with possible subsequent flooding. Each diesel-generator cell is designed to prevent propagation of flooding to the other diesel-generator cell.

61 53 A set of M. V. switchgear buses, unit substations, and motor control centers are located in the Diesel Generator Building. These electrical components are separated by a wall to prevent a casualty to one cell from propagating to the other redundant cell.

61 15 The Diesel Generator Building is protected by the seismically supported Non-Sodium Fire Protection System. The appropriate fire extinguishing systems will be provided throughout the building to minimize the adverse effects of fires to safety related systems.

3A.6.3 Design Evaluation

The Diesel Generator Building has the following features that collectively provide the capability needed to satisfy CRBRP General Design Criteria 2, 3, and 4 as described in Section 3.1.

- 1) The building is designed to withstand natural phenomena such as earthquakes, tornadoes, tornado-generated missiles, and floods as described in Sections 3.8, 3.3 and 3.4, respectively.
- 2) The building and the systems contained are protected against fire using detection equipment and the appropriate fire extinguishing devices as described in Section 9.13.1.
- 3) All systems inside the Diesel Generator Building, important to safety, are redundant and are separated and protected so that the failure of one system will not cause the failure of the redundant system.

3A.6.4 Testing and Inspection

Pre-operational and periodic tests and inspections will be performed for the HVAC systems and Fire Protection Systems in the Diesel Generator Building to assure the adequate and reliable performance of these systems as described in Sections 9.6.5 and 9.13.1.

Testing and inspection of the systems contained in the building will be performed as described in Sections 8.3, 9.7.4, 9.9.1.4, and 9.9.2.4.

A CRBRP Quality Assurance Program is established to assure that critical structures are built in accordance with specifications. This program is described in Chapter 17.

- 61| Principal materials used in the DGB - concrete, reinforcing steel and structural steel - are manufactured in accordance with nationally recognized standards. User installation tests and inspections are detailed in construction specifications.

Tests and inspection will be performed during construction of the DGB structure, to verify conformance with construction specifications and applicable parts of building codes.

- 61| The tests and inspection of systems within the DGB are discussed in detail in those sections of this report pertaining to the individual systems housed by the DGB (See Table 3A.6-1).

TABLE 3A.6-1

SYSTEMS LOCATED IN THE DGB

	<u>System</u>	<u>PSAR Reference</u>
	Building Electrical Power Systems	8.0
15	Plant Protection System	7.0
17	Service Water System	9.0
61	Heating and Ventilating	9.6

TABLE 3A.6-2

SUPPORTING SYSTEMS LOCATED IN THE DGB

Communications

Lighting

Plant Fire Protection

Plant Protection

Radiation Monitoring

3A.7 Deleted

45 32

3A.7-2

Amend. 45
July 1978

3A.8 Cell Liner Systems

Cell liners are located in Na and NaK cells in order to maintain the inert atmosphere (Nitrogen) under normal operating conditions, to facilitate decontamination and decrease downtime following an accidental sodium spill, to provide an Engineered Safety Feature (ESF) sodium/NaK barrier to prevent sodium concrete reactions, and to protect the structural integrity of the cell for the preservation of the capital investment.

3A.8.1 Design Bases

See Section 3 of Appendix B to Section 3.8 for a discussion of cell liner requirements.

3A.8.2 Design Description

The CRBRP cell liner system utilizes a steel plate liner, including edge embedments, to restrain the thermal inplane expansion - contraction forces, and stud anchors (in walls and ceilings) and structural sections (in floors) to provide out of plane restraints to minimize the effects of bending caused by behind the liner pressure or by the buckling of the plate. Additional features of the cell liner design include an integral insulation panel to protect the structure from severe thermal loading, and an integral vent system, to relieve the behind the liner steam buildup under sodium spill accident conditions. The cell liner system consists of the following typical wall and ceiling panel elements:

1. Carbon steel liner plate - to provide a leaktight sodium spill boundary
2. Insulating Concrete panel - to protect the structural concrete from the elevated temperatures resulting from the "Na" spill
3. Nelson Steel Anchors (wall/ceilings) or Embedded Structural Sections (Floor) Welded to Liner Plate - to minimize the out of plane bending of the cell liner plate
4. Continuous Air Gap Between Insulating Concrete and Liner Plate - to vent and relieve the buildup of gas (steam) pressure behind the liner due to the heating of the insulating and structural concrete

The typical wall and ceiling panels are prefabricated in large modular-panel sections. This will minimize the amount of field welding required. The studs anchors extend deep enough into the concrete structure so that the integrity of the wall/ceiling liner system is maintained and the full strength of the stud anchor is developed. At the corners the liner plates are attached to steel sections embedded in the structural concrete in order to prevent the in plane thermal expansion of the liner plate and the excessive strains in the anchors that would result.

45 | The typical floor liner is a carbon steel plate welded to rolled
45 | steel sections which are embedded in the concrete slab such that approx-
37 | imately half their depth projects above the top of the floor slab. The
59 | 45 | floor liner will be supported on embedded steel sections. The space
37 | between the floor slab and the liner is filled with a precast insulating
45 | concrete panel. The function of the floor insulation is to:

- a) Provide an insulating barrier between the steel floor liner plate and the structural concrete such that the temperature of the concrete floor slab will not exceed the limits specified in Section 3.1.7 of Appendix 3.8-B.
- b) Provide a vent path for the gasses generated beneath the floor liner as a result of a sodium spill.
- c) Limit the deformations of the floor liner plates under a positive pressure differential by transmission of the internal cell pressure through the insulation to the structural slab.

37

59| The insulating concrete floor panel is assumed to provide no lateral support to the embedded steel sections. The size and spacing of the embedded rolled steel sections are designed such that stresses and strains in the beam web and the liner plate fall within the limits specified in Table 3.8-1 of Appendix 3.8-B.

37

45 | 37 | A liner vent system will be installed to limit the pressure behind the liner generated by the heatup of structural concrete during a sodium spill. The liners will be designed to withstand the pressure under the maximum liner temperature.

60 | 59 | The steam generated below the floor liner by the heat up of the structural and insulating concretes will be vented through the air gaps provided as shown in Figure 3A.8-4 and through holes in the webs of the floor liner embedment beams to collective points along the periphery of the cell. The steam generated below the reactor cavity floor liner is vented independently of the cell walls due to the need for compartmentalization of the cell liner vent system to satisfy TMBDB requirements (Reference 10b, PSAR Section 1.6). Each zone in the reactor cavity is vented independently and is separated by a baffle plate for the adjacent zone. In areas other than the reactor cavity, the steam from the floors will be released with the steam from the walls and ceilings into the liner vent system piping. Effects on stiffness caused by liner corrosion will be accounted for in the liner plate/anchors analysis. Equipment supported on the floor liner will be provided with special supports to transmit the loads directly to the structural slab. During construction and maintenance the floor liner will be protected from loading as specified in Section 3.1.1 of Appendix 3.8-B. Diagrams of the cell liner configurations are shown in Figures 3A.8-4, 3A.8-5 and 3A.8-6.

47 | 48 | 48 | 59 | The vent path for the cell liner wall and ceiling system is provided by a 1/4" continuous air gap as shown in Figures 3A.8-4 and 3A.8-5. The air gap is prefabricated with the modular cell liner panel. The air gap between the insulating concrete and the cell liner plate will be inspected before installation. The continuity of the air gap is maintained during construction and the life of the plant by a) sealing the joints between adjacent insulating concrete panels during construction to prevent the entrance of the structural concrete; b) the bearing and/or bond strength of the insulating concrete panel to the cell liner plate at the stud anchors to prevent the closure of the air gap during construction and installation; c) the preoperational testing of the cell liner vent system. Local plugging of the air gap is precluded since the air gap is continuous over the entire surface area of the lined cell. Therefore, there are no effects on the liner or liner anchors due to pressure buildup.

37

37

Liners will not ordinarily be exposed to sodium. The structural concrete will be protected by an insulating concrete between the steel liner and the structural concrete. During accident conditions, some spalling of this non-structural concrete insulation may occur. However, this is considered acceptable since liner failure due to spalling of the insulating concrete is prevented by embedding liner anchors into the structural concrete.

59 | The inner cells are constructed reinforced concrete with steel liners designed to maintain the atmospheric leak tightness requirement of section 3.1.1.1 of Appendix 3.8-B during normal operating conditions. Piping penetrations entering inerted cells are designed to prevent leakage, and are sealed by any of the following methods, depending upon individual design requirements:

- 59 | a) packing between pipe and a pipe sleeve which is welded to the cell liner using full penetration welds.
- 59 | b) flued head or flexible bellows attachments welded to pipe and pipe sleeve with sleeve seal welded to cell liner using full penetration welds.
- 59 | c) pipe embedded in concrete and seal welded directly to cell liner with full penetration welds.

Penetrations between Inerted cells having a common atmosphere may also consist of an open pipe sleeve which is welded to the cell liner at each face with full penetration welds.

3A.8.3 Design Evaluation

The piping integrity investigation analysis of crack growth due to all design duty cycle events indicated negligible crack growth. Based upon this evaluation, it is concluded that no leaks will occur under operation in accordance with the piping design specifications.

The sodium and NaK components and piping in the CRBRP nuclear steam supply system and auxiliary systems are all designed to prevent leakage. The liners in cells which contain sodium or NaK should therefore not be exposed to any conditions more severe than those corresponding to normal plant operation. However, accidental sodium leaks or spills cannot be precluded and therefore must be considered in the design of the liners.

To accommodate the effects of accidental sodium leaks or spills, the cell liners will be designed for a design basis sodium spill. Based on the operating experience of existing sodium facilities and previous assessments of sodium spills, the amount and/or leakage rate of an accidental sodium spill into a cell are minor. Leaks which could develop from flaws, fatigue, creep, etc. are expected to be much less than the Design Basis Leak as discussed in Reference 2 of Section 1.6.

3A.8.3.1 Sodium Spill Evaluation

The evaluation of the consequence of sodium spills is provided in PSAR Section 15.6. Cells other than those analyzed in PSAR Section 15.6 are analyzed in a similar fashion. The cells will be designed to accommodate the peak pressure from these spills. For the cells that are specified as a 15 psig cell, the worst case maximum peak pressure is calculated to be 13 psig. For the cells with a 12 psig design pressure the peak cell pressures are in the range of 2-6 psig. The method and criteria for evaluation of the cell liners are discussed in Section 3.8-B.

3A.8.3.2 Brittle Failure Potential of the Liner in Irradiated Areas

The increase in ductile-brittle transition temperature due to neutron damage is estimated to be less than 10^oF for the reactor cavity liner. This is based on damage function analysis, which indicates that the damage level for the neutron spectrum in the reactor cavity will be approximately 100 times lower than that for LWR reactor vessels.

For the neutron embrittlement evaluation of the cell liner plate, the methods and limits established by USNRC Regulatory guide 1.99, "Effects of Residual Elements on predicted Radiation Damage to Reactor Vessel Materials" will be used. The only area of the plant exposed to neutron fluence is the reactor

cavity. By considering the worst case exposure condition for the reactor cavity cell liner where the maximum fluence is $7.8 \times 10^{18} \text{n/cm}^2$, ($E > 0.1 \text{ MeV}$) and $6.1 \times 10^{13} \text{n/cm}^2$ ($E < 1.0 \text{ MeV}$), the maximum adjustment of Nil-ductility temperature (NDT) is 10°F and does not require trace element control. This indicates that the liner steel is not effected by neutron embrittlement nor does gamma radiation result in steel degradation.

59

3A.8.3.3 Liner Analysis

.1 General

The liner system is described in Section 3A.8.2. The Design Requirements, Load Categories, Load Combinations, Stress and Strain allowables and Design Analysis procedures are given in paragraphs 3.1 through 3.5 of PSAR Appendix 3.8-B. Attachment D to Appendix 3.8-B gives the bases for the strain criteria and strain limits adopted for the Postulated Large Liquid Metal Spill (PLLMS) Loads.

The spacing and size of the Nelson stud anchors in the wall and ceiling panels and of the floor anchors are designed such that the stresses and strains fall within the limits specified in Table 3.8-B-1 of Appendix 3.8-B.

The anchors will resist the shear forces induced when unbalanced forces exist between sections of the liner and axial forces caused by the maximum specified pressure (5 psig) acting on the backside of the liner under the PLLMS loads. Since there is a 1/4 inch gap between the cell liner and the insulating concrete, some axial loads in the anchors will be caused by the cell's internal pressure.

The insulating concrete does not act integrally with the structural concrete and a bond breaker will be provided on the surface separating the two materials to reduce shear transfer. The insulating concrete is not considered a main structural element; its main function is to provide a thermal shield to prevent degradation of the structural concrete under the elevated temperatures of the PLLMS conditions. The adequacy of the insulation thickness has been demonstrated by a preliminary finite element thermal analysis using the computer program ANSYS. The temperatures calculated at the face of the structural concrete did not exceed the limits established in Section 3.1.7 of Appendix 3.8-B. Local hotspots due to heat transfer into the structural concrete through the studs may occur. These effects will be evaluated by both analytical and testing methods.

Spalling or degradation of the insulating concrete under the PLLMS Loads will not cause a failure of the liners or liner anchor system. The anchors will be embedded in the structural concrete to ensure adequate restraint and the design is such that even if no lateral support to the anchors is provided by the insulating concrete, the specified anchor strain limits will not be exceeded.

Liner failure due to behind the liner steam pressure is prevented by the provision of a venting system on the backside of the liner where necessary, to reduce steam pressure generated from heatup of the insulating material and structural concrete during a sodium spill. The 5 psig cell liner vent system pressure developed behind the cell liner plate is addressed in the analysis of the liner system. Two cases of pressure differential across the liner are considered. The first case considers the 5 psig vent pressure behind the liner combined with the peak internal cell accident pressure; the second case a 0 psig vent pressure combined with the peak internal cell accident pressure. These two cases provide conservative bounding conditions for the pressure differential across the cell liner under Design Basis Accident conditions.

Specific vent paths behind the liner will be provided where analysis and/or testing indicates they are required. Steam produced would be vented to the non-inerted areas

Specific vent paths behind the liner will be provided where analysis and/or testing indicates they are required. Steam produced would be vented to the non-inerted areas within the RCB or RSB consistent with the location of the sodium spill. Preliminary analysis under Postulated Large Liquid Metal Spill (PLLMS) conditions indicates that this venting scheme will not require the containment to be purged. A more detailed analysis will be performed to verify these preliminary indications. Since any steam produced during a sodium spill would be vented to the non-inerted areas, hydrogen evolution due to sodium/water reactions would occur only following a liner failure. Failed liner testing is planned and the amount of hydrogen evolved during these tests will be monitored. Even in the unlikely event of the liner failure, purging of containment is not expected to be required. The liner system will be designed to withstand a backside pressure of 5 psig.

Due to the magnitude of the compressive thermal forces caused by the restraining actions of the concrete structure, buckling of the liner plates is anticipated. Buckling in itself will not produce failure since the thermal deformations are self limiting. However, due to the reduced load carrying capacity of a buckled panel, unbalanced lateral forces can be induced at the anchor. The liner-anchor system will be designed such that under the unbalanced lateral forces due to opanel buckling, the strains will not exceed the allowable limits. Buckling of panels will improve the stress-strain conditions at the corner anchors since the unbalanced lateral forces will be reduced.

The dead and live loads, seismic loads, operating pressure and thermal loads, etc., will affect the cell liners through the interaction of the liner-anchor system with the structural concrete. Since the structural concrete is by far more rigid than the liner, the deformations of the concrete under these loads and the restraint it provides to the liner will determine the stress-strain condition of the liner-anchor system for these loads. For these conditions other than sodium spills, the stress levels in the cell liners are expected to be below the yield strength of the material. The maximum normal operating temperature (peak) will not exceed 130°F and no significant stresses and strains will be imposed on the liners under these conditions.

The cell liners shall be designed to have the capacity to sustain non-mechanistic thermal cycling during the lifetime of the plant (15 cycles from 130°F to 220°F, 14 cycles from 130°F to 210°F, 3 cycles from 130°F to 150°F and 1 cycle from 130° to 260°F) which is within the ASME Code limitations such that the cyclic fatigue should not be a problem. Based on Section NE-3222.4d of Section III, Division 1 of the ASME B&PV Code, for the specified temperature ranges and number of cycles, no fatigue analysis is required.

.2 Analysis

Calculations have been conducted to investigate the adequacy of the liner-anchor system under the PLLMS Condition. They consist of elasto-plastic analyses using the computer program ANSYS. The strain values obtained from the finite element analyses under sodium spill conditions are compared against

the allowable strains at the exposure temperature. The allowable PLLMS strains are determined using Table 3.8-B-1 and the materials test data presented in 3A.8.4. Table 3A.8-1 summarize the allowable strains under load combination D (PLLMS spill).

An analysis conducted at ORNL (Ref. 1) considered a wall liner panel, 15 inches square. It was assumed that the corners, where the stud anchors are located, were rigidly supported, which is justified when there are no unbalanced lateral forces acting on the anchors. The analysis considered transient conditions immediately after the sodium spill, an isothermal condition under a steady state of 1000°F and a cooldown to an isothermal condition of 150°F. The maximum calculated strain was 1.7%.

To investigate the cell wall liner-anchor system, a finite element analysis of a typical cell liner panel having a 1/8" bow at the middle of the panel was performed. A typical 75" x 75" portion of the wall liner having a line of symmetry along the edges and 1/8" bow at the center span was considered to determine the effect of an unbalanced lateral force on the stud anchors. By using symmetry, the model was reduced to a one eighth segment (Figures 3A.8-1 and 3A.8-2). The liner studs were modeled at 15" on center. The insulating concrete was assumed to provide full lateral support to the studs. A behind the liner pressure of 5 psi was included.

The cell liner (plate) temperature was raised prototypically from 700°F to 1000°F and the allowed to cool down gradually to 200°F. The cell liner strains and displacements were observed at different stages. At 1000°F the maximum strains in the bowed panel were 2.31% while the maximum strains in the unbowed "Typical panel" were 1.5%. The result of these calculations show the maximum effective strain in the liner system well below the allowable limits presented in Table 3A.8-1.

Another analysis included a bi-planar corner (wall to floor). The mathematical model is shown in Figure 3A.8-3. A 15 inch wide strip (equal to the spacing of the stud anchors) was considered. Two models were used: in one the insulating concrete layer was assumed to provide the full lateral support to the stud anchors; in the second it was assumed that the insulating concrete layer provided no lateral support. In both models it was assumed that the insulating gravel under the floor liner provided no lateral support to the floor anchors. A 5 psi pressure was applied on the back face of the liners (to simulate strain pressure buildup) and a uniform temperature of 1000°F in both liner and anchors. The results give a maximum effective strain of 2.3% in the liner plate and 1.7% in the anchors. There is no substantial difference between the results of the two models. Since the strains obtained are much below the allowables specified in Table 3.8A-1 of Appendix 3.8A, liner integrity is maintained. The effect of the Appendix 3.8B corrosion allowance of 1/16 inch was investigated using the same mathematical model described above. A strain response was obtained after reducing the thickness of the cell liner plates (both wall and floor) by 1/16 inch to account for the effect of corrosion while keeping the remaining parameters the same. The results obtained were of the same order of magnitude as was obtained from the same model without corrosion.

59 | This result was anticipated since the major components of the strain
induced in the liners are membrane strains. Accordingly it has been
concluded that the effect of a maximum 1/16" corrosion over a thirty
year plant life will not compromise liner integrity.

45 | A finite element analysis was performed to determine the
response of the cell liner wall/ceiling system in the close proximity of
a large diameter penetration. The cell liner panel, penetration sleeve,
and collar plate were evaluated under the PLLMS condition to verify the
integrity of the cell liner system under sodium spill conditions.

The large diameter pipe penetration sleeve detail used in
this analysis utilized a thickened plate collar welded to the penetration
sleeve and the cell liner, for resisting the thermal expansion choking
forces developed by the fixed cell liner plate at the penetration opening.
The collar plate is anchored directly into the structural concrete.

The penetration analyzed consisted of a 24 inch diameter schedule
80 pipe sleeve reinforced with a circular stiffening collar with gusset
plates spaced at 45° around the penetration. A cross-section of these
elements is presented in Figure 3A.8-7. The penetration assembly was
located in a wall/ceiling liner area having the standard cell liner
configuration (Figure 3A.8-4).

The analysis performed considered temperatures ranging from
normal operating to 850°F. An elastoplastic computer analysis
was performed using one eighth symmetry as shown in Figure 3A.8-8.
The analysis considered the insulating concrete not available to support
the cell liner stud anchor laterally, but available to support the liner
plate in the event of local closure of the air gap at the penetration/liner
interface.

At 850°F the maximum membrane strain of 2.02% was calculated
at the liner interface with the penetration collar. The combined membrane
plus bending strain at the same location was 2.14%. The maximum membrane
stud strain adjacent to the penetration was 1.7% with membrane plus bending
strain of 2.6%. These strains compare favorably with the allowable values
of 7.6% membrane and 10.2% membrane plus bending strain at 850°F as presented
in Table 3A.8-1.

59 | A thermal analysis was performed to determine the consequences
of thermal shock if any on the 3/8" wall liner plate resulting from a
design basis sodium spill accident. A finite element model was utilized
which considered the sodium film coefficient, 3/8 inch liner plate, 1/4
inch air gap, 3-7/8 inch insulating concrete and 35 inch structural
concrete. The analysis assumed a one dimensional heat flow. The temperature
distribution through the thickness of the liner plate and the corresponding
time were required for the evaluation of thermal shock.

Using an initial sodium temperature 1000⁰F at time t=0 hours and a final sodium temperature of 100⁰F at time t=60 hours, the temperature distribution through the thickness of the plate and the concrete were obtained from the finite element computer solution. It was observed that the max. temperature difference through the 3/8 inch thickness of the liner was 95.5⁰F at 3.12 seconds and that the difference was gradually decreasing. This resultant temperature difference is insufficient to cause any thermal shock. Moreover, during the heat up and cool down phase of the analysis, the liner was subjected to yielding and high strain as demonstrated in previous analyses. Accordingly, thermal shock is not considered to be a problem in the analysis of the liner. Similar results were also obtained in the case of a thermal shock analysis performed on a floor liner.

45

The stud anchor yield force, displacement capacity and ultimate force and displacement capacity have been evaluated based on manufacturers test data.

59

The final analysis considered load categories including thermal shock, thermal transients, and the heat-up and cool-down of the liner under the sodium spill accident; hot spots; the effects of variations in the steel properties and thicknesses; the effect of the 1/16 inch corrosion allowance, etc.

37

The postulated breaks of sodium lines may generate hot sodium sprays on the liner. The effects of the hot spot on the liner including the dynamic effects, if any, of the jet impact will be considered.

59

3A.8.4 TESTING AND INSPECTION

3A.8.4.1 Development Testing Programs

45 | A series of development testing programs have been developed to support the cell liner design. These programs provide materials data to support the objective of designing the cell liners to accommodate large sodium spills without failure, demonstrate through qualification testing that integrity of the liner is maintained under sodium spill conditions, and provide test materials data on sodium-concrete reactions to assess the consequences of cell liner failure.

Five individual testing programs have been completed or are ongoing in support of the cell liner design. These development programs are:

- (a) Comprehensive Testing Program for Concrete at Elevated Temperatures
- (b) Sodium-Concrete Reaction Tests
- (c) Sodium Spill Design Qualification Tests
- (d) Cell Penetration Sealant Tests
- (e) Base Material Tests for Liner Steels

The tests included in the development programs listed above are modeled to minimize the difference between small scale tests results and the actual mass concrete response at elevated temperatures. The development programs indicated above are directed toward the goal of designing and testing a cell liner system which will not fail, even
59 | under the unlikely event of a large sodium spill.

Comprehensive Testing Program for Concrete at Elevated Temperatures

45 | This ongoing experimental program will define the variation with temperature of various physical and thermal properties of prototypic CRBRP limestone aggregate concrete and lightweight insulating concrete. The properties include, but are not limited to, compressive strength, modulus of elasticity, shear strength, bond strength, thermal conductivity, specific heat, and coefficient of thermal expansion. The series of
37 | experiments will be carried out at various temperatures including those representative of accident conditions.

The results of this testing program can be directly applied to the analysis of the building structures supporting the cell liners. The testing program is nearing completion and the results will be included in an ORNL/CRBRP report following completion.

Since the biaxial and triaxial testing of concrete at elevated temperatures will yield a greater compressive strength than uniaxial testing due to the influence of the lateral confining stress, the concrete tests performed on specimens in the uniaxial state of stress will yield a more conservative value of strength. Therefore the consequences of biaxial and triaxial loading can be disregarded.

Sodium-Concrete Reaction Tests

The objective of this ongoing program is to determine the rate and extent of penetration due to sodium-concrete reaction. The effect of reaction product accumulation and gas release on the sodium-concrete reaction rates will be determined to allow upgrading of analytical capability. Additionally, intentionally defected liner tests will be performed to assess the response of the liner to a sodium-concrete reaction. Results of these tests will be documented as they become available.

The dimensions of the test articles have been selected to ensure that results representative of the actual mass concrete structure can be obtained.

Sodium Spill Design Qualification Tests

A large scale model of a CRBRP cell liner has been performance tested to demonstrate the ability of the cell liner system to maintain liner integrity, mitigate consequences of a large sodium spill, and prevent sodium-concrete reactions. A total of 3500 pounds of liquid sodium at 1100°F was spilled against a CRBRP cell liner wall forming a 50 inch deep sodium pool above the CRBRP liner floor in the test article. The sodium pool was then heated, using electric heaters, to temperatures ranging between 1460°F and 1580°F and maintained until six days after the spill. The 1100°F sodium spill simulated a Design Basis Accident sodium spill event and the subsequent heat up to approximately 1600°F simulated the fission decay heat of a sodium pool under TMDBB Accident conditions.

The test data and post test examination revealed no failures or liner defects and minimal deformation of the liner system under the DBA and TMDBB spill conditions. The results of this testing program are included in the HEDL final report (Reference 5).

Cell Penetration Sealant Tests

The objective of this program was to determine the effects of temperature, sodium and radiation on various candidate sealant materials for cell penetrations. This series of experiments enables selection of the most suitable sealant material for use in the CRBRP. Following selections of the prime sealant material, prototypic electrical cable penetration assembly performance testing were conducted. The results of this testing program were published in Reference (4).

Base Material Tests for Liner Steels

The objective of this completed testing program was to determine the response of the cell liner plate material (SA-516 Grade 55) and its associated weldment material to elevated temperatures up to 7100°F. The base liner steel will be tested for residual tensile strength (including stress-strain response), stress-rupture (Creep) and thermal expansion. The weldment material was tested for residual tensile strength (including stress-strain response) and stress-rupture (Creep). Both longitudinal and transverse welds were investigated. The results of the base liner steel and weldment material tests have been published in Reference 6.

The material properties information at elevated temperatures which was obtained in this program has been used in the design and analysis of the cell liner system.

59

References:

1. McAfee, W.J., Sartory, W.K., "Evaluation of the Structural Integrity of LMFBR cell liners - Results of Preliminary Investigations", ORNL-TM-5145, January, 1976.
2. Chapman, R.H., ORNL-TM-4714, "A State of the Art Review of Equipment Cell Liners for LMFBR's", February, 1975.
3. Sartory, W.K., McAfee, W.J., ORNL-TM-5145, "Evaluation of the Structural Integrity of LMFBR Equipment Cell Liner - Results of Preliminary Investigation", February, 1976.
4. Humphrey, L.H., Horton, P.H., AI-DOE-13227 "Selection of a Sodium and Radiation Resistant Sealant for LMFBR Equipment Cell Penetrations", January 31, 1978.
5. Wireman, R., Simmons, L., Muhlestein, I., HEDL TME 79-35, "Large Scale Liner Sodium Spill Test (LT-1)", December, 1980.
6. Cowgill, M.G., WARD-D-0252, "Base Material Tests for Cell Liner Steels", February, 1980.

TABLE 3A.8-1
 STRAIN ALLOWABLES FOR
 POSTULATED LARGE LIQUID METAL SPILL (PLLMS) CONDITIONS
 LOAD COMBINATION D

Temperature °F	Membrane Strain 0.50 ϵ_{μ} in/in	Membrane + Bending Strain 0.67 ϵ_{μ} in/in
75	0.0955	0.1280
600	0.1185	0.1588
800	0.0815	0.1092
850	0.0759	0.1017
900	0.0703	0.0942
1000	0.0590	0.0791

Where:

ϵ_{μ} = Uniform elongation or the strain at ultimate load as obtained from the elevated temperature testing of SA 516 Grade 55. Liner Steel.

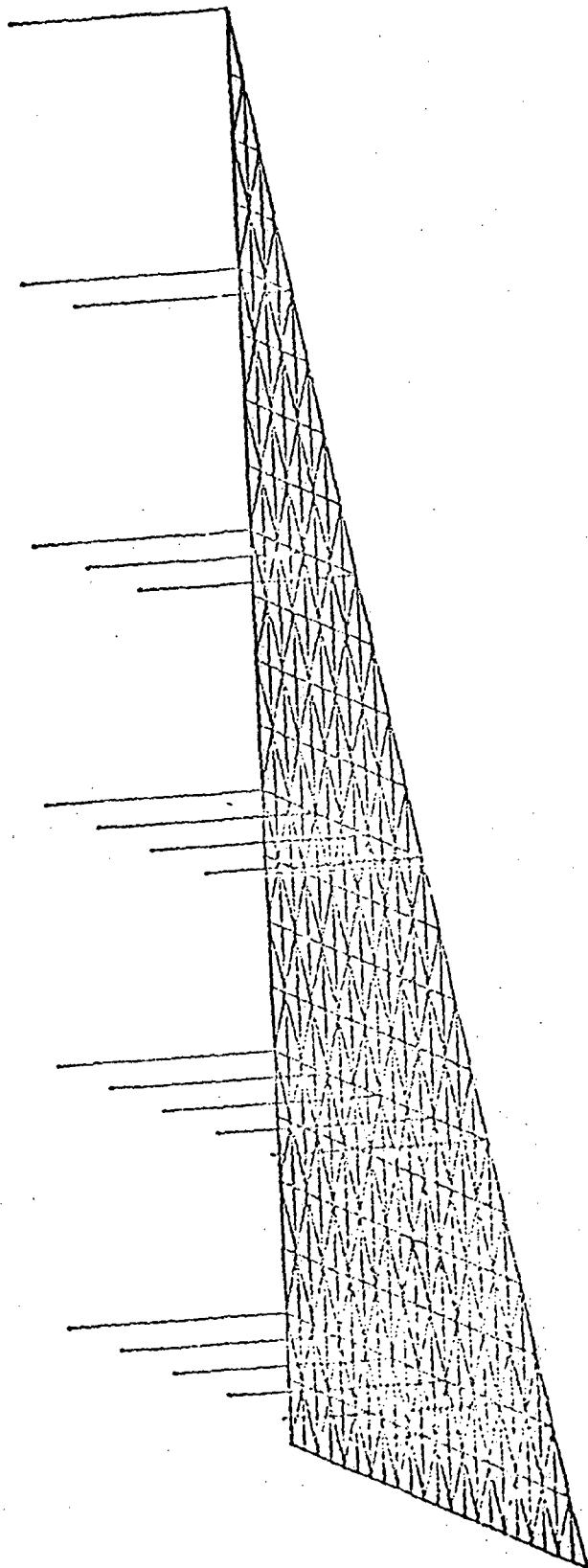
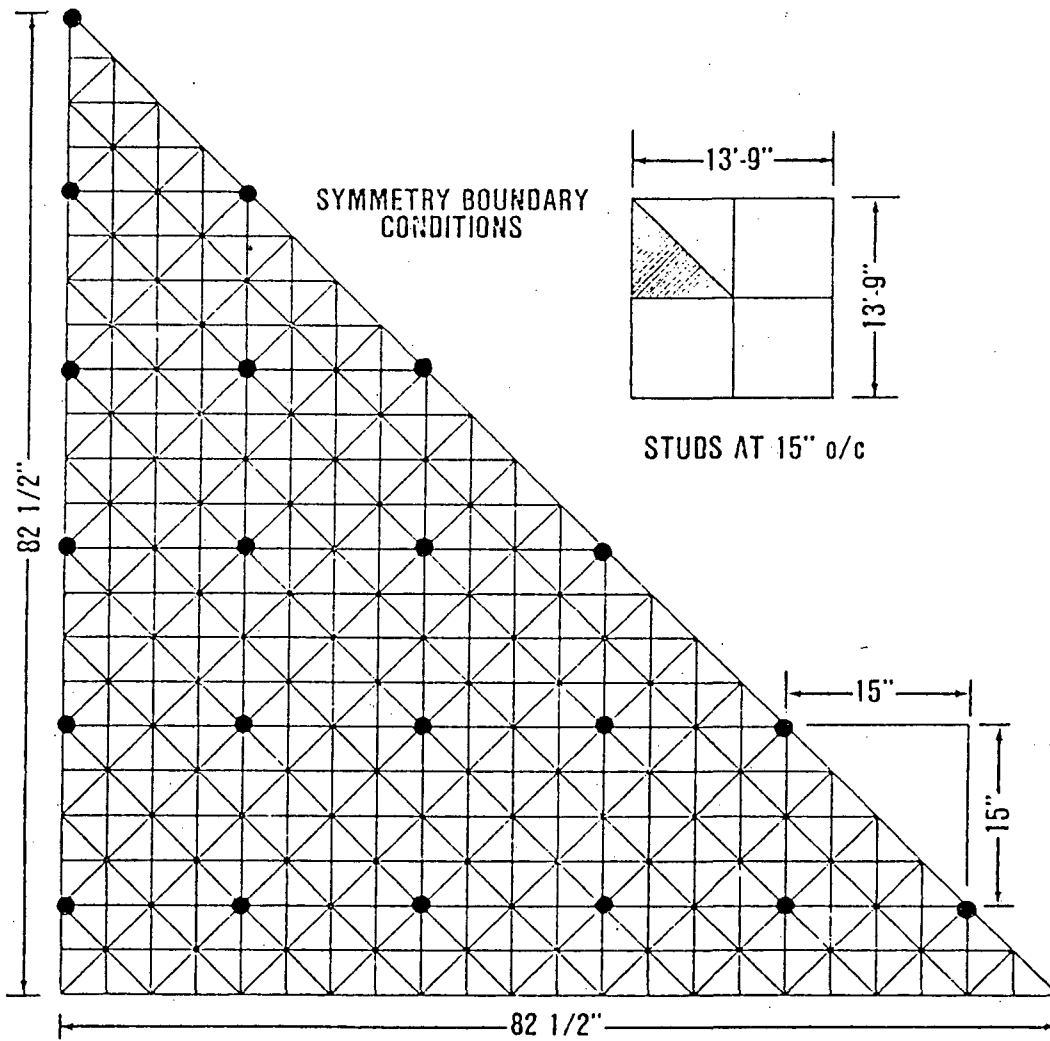


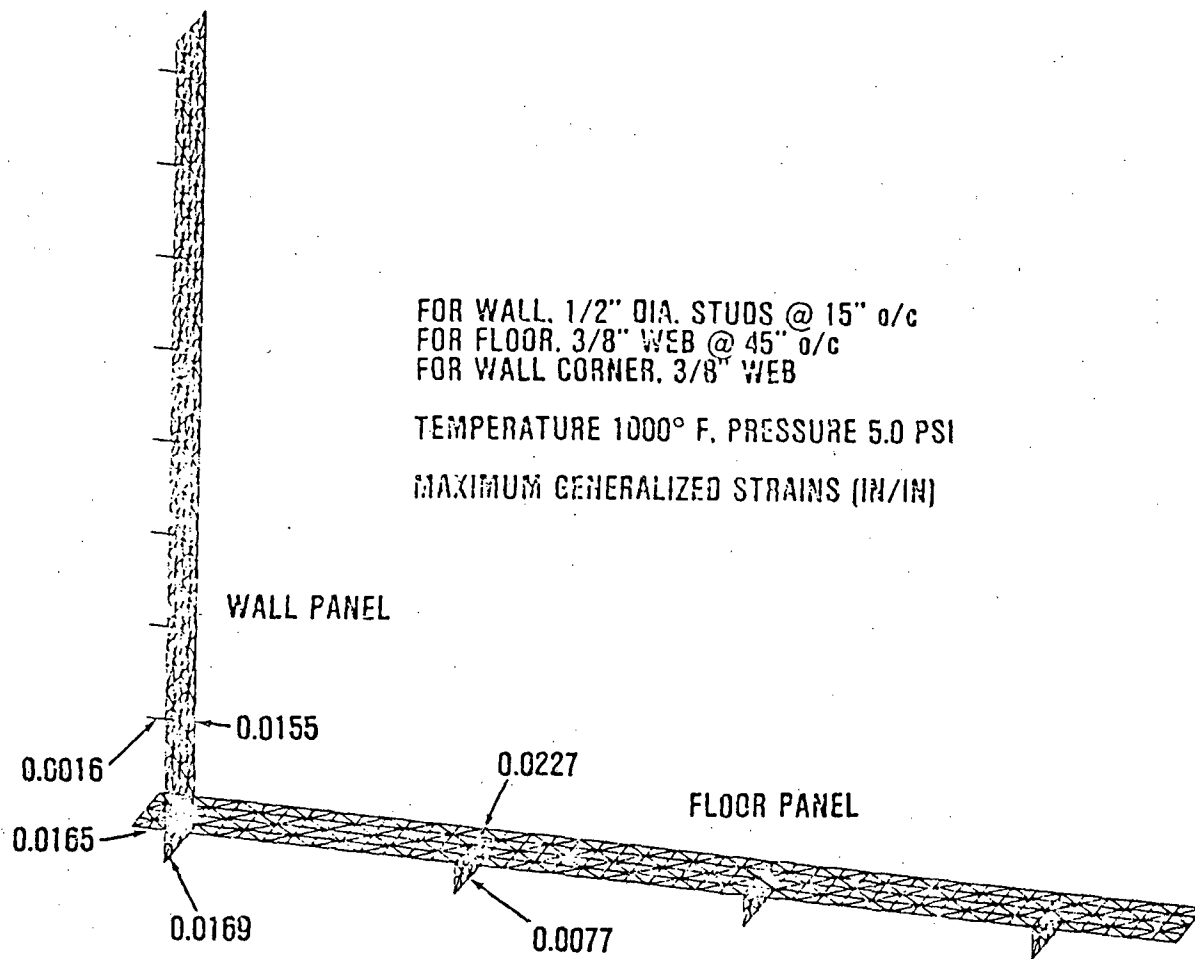
Figure 3A.8-1 ANALYSIS OF LINER WITH STUD-TYPE ANCHORS



CRBRP: ANALYSIS OF LINER WITH STUD-TYPE ANCHORS

FIGURE 3A.8-2

Amend. 59
Dec. 1980

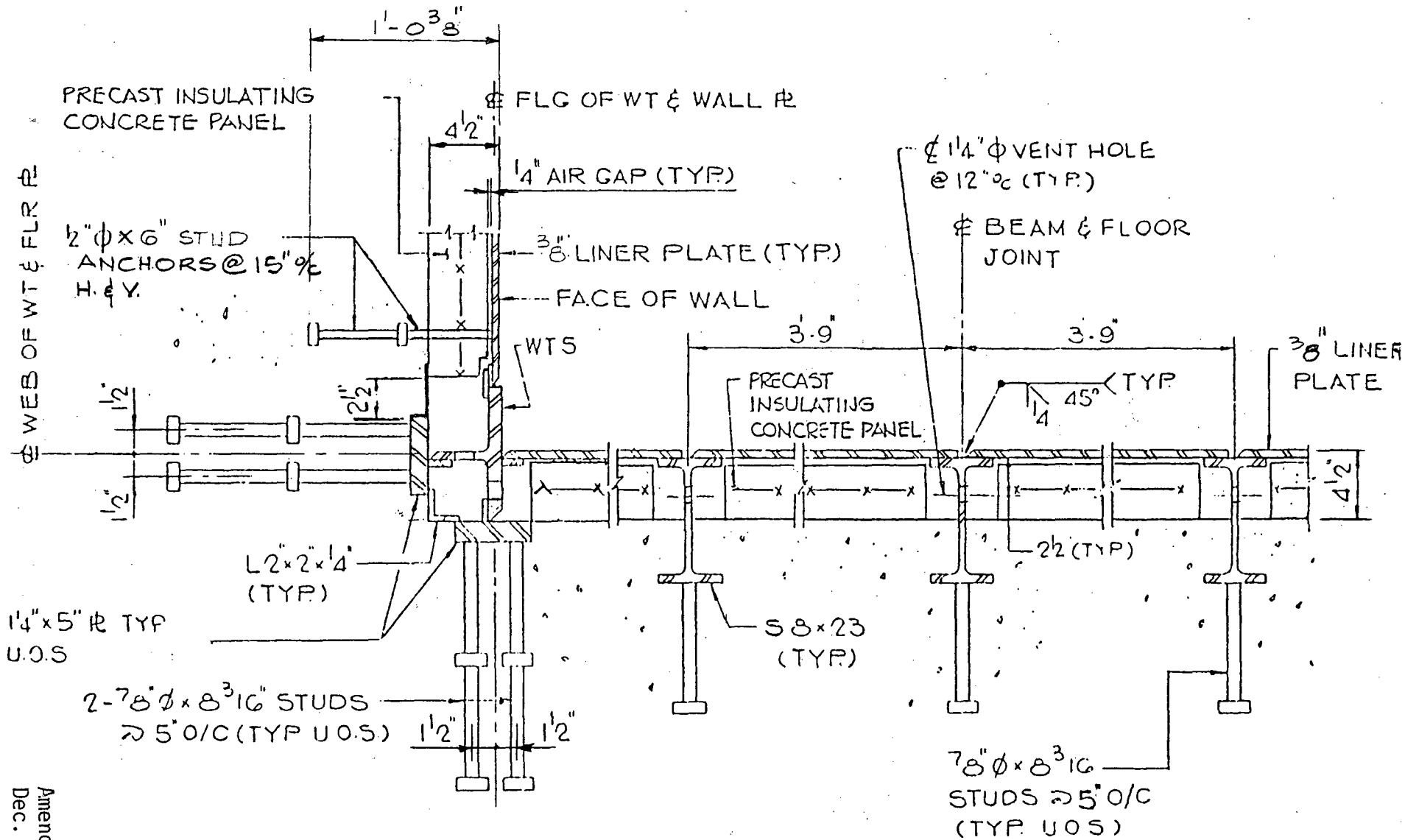


WALL-FLOOR LINER CORNER

FIGURE 3A.8-3

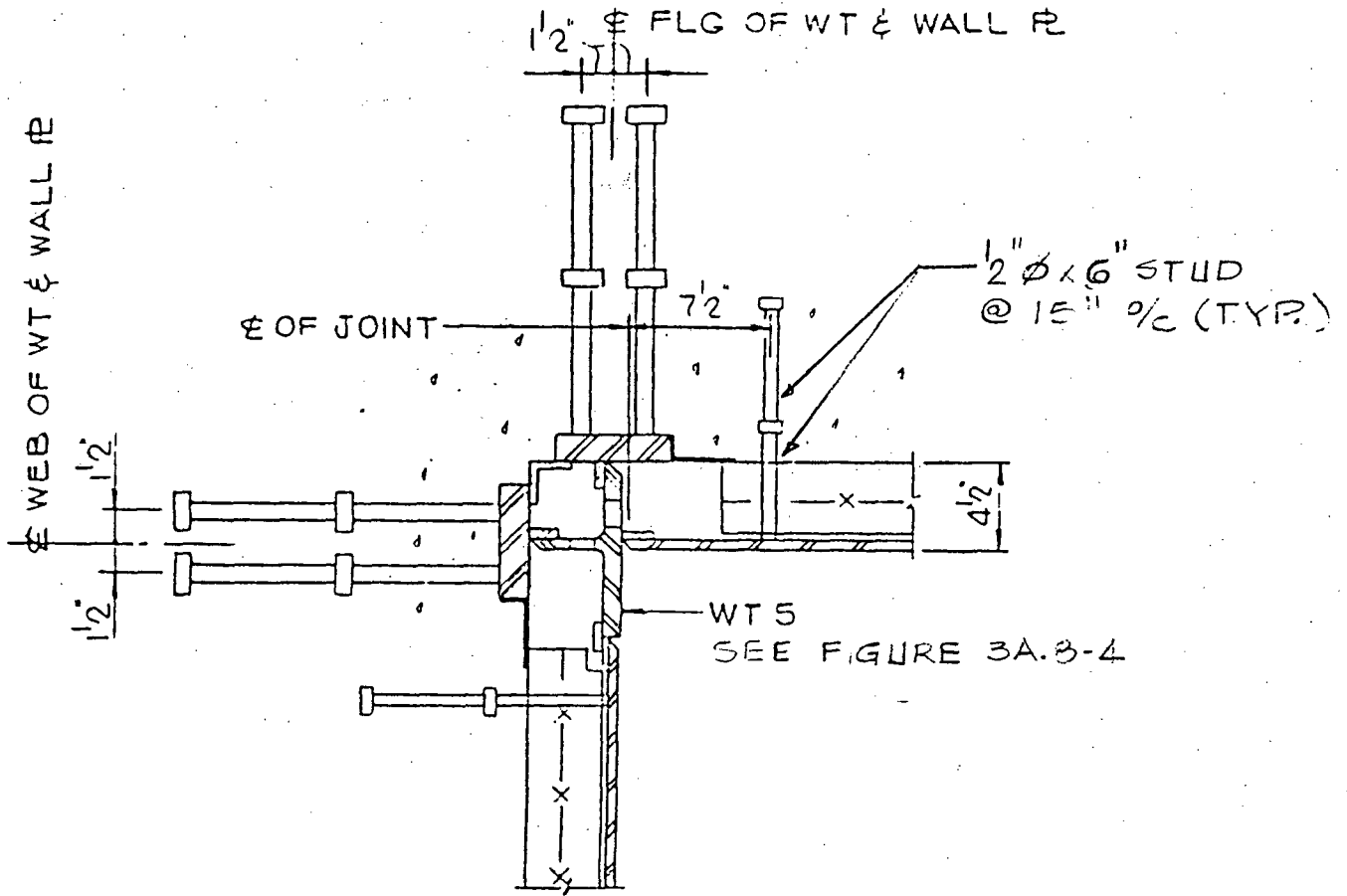
Amend. 59
 Dec. 1980

3A.8-13



Amend. 59
Dec. 1980

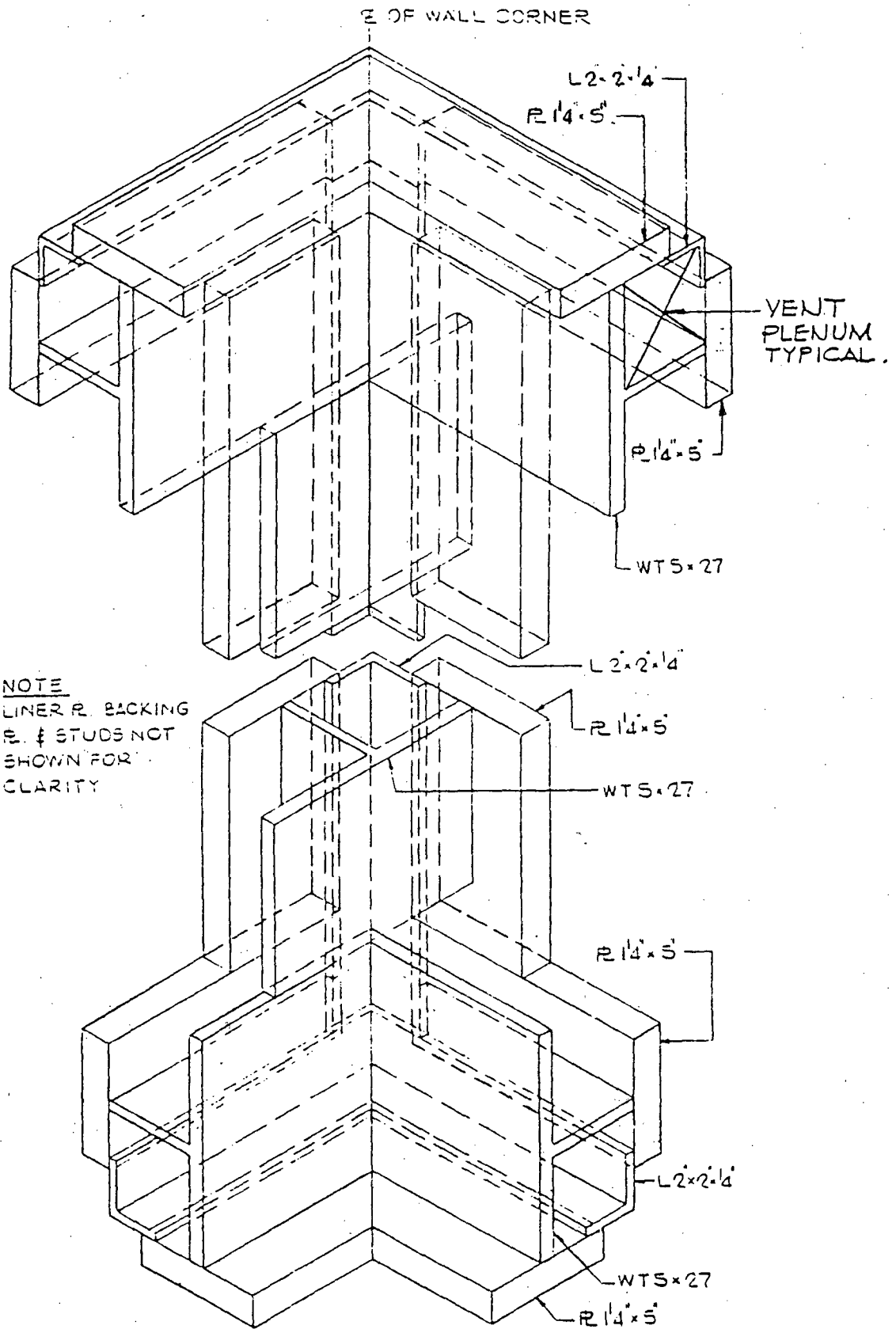
FLOOR & WALL DETAIL
FIGURE 3A.8-4



TYPICAL INSIDE WALL CORNER DETAIL

FIGURE 3A.8-5

Amend. 59
Dec. 1980

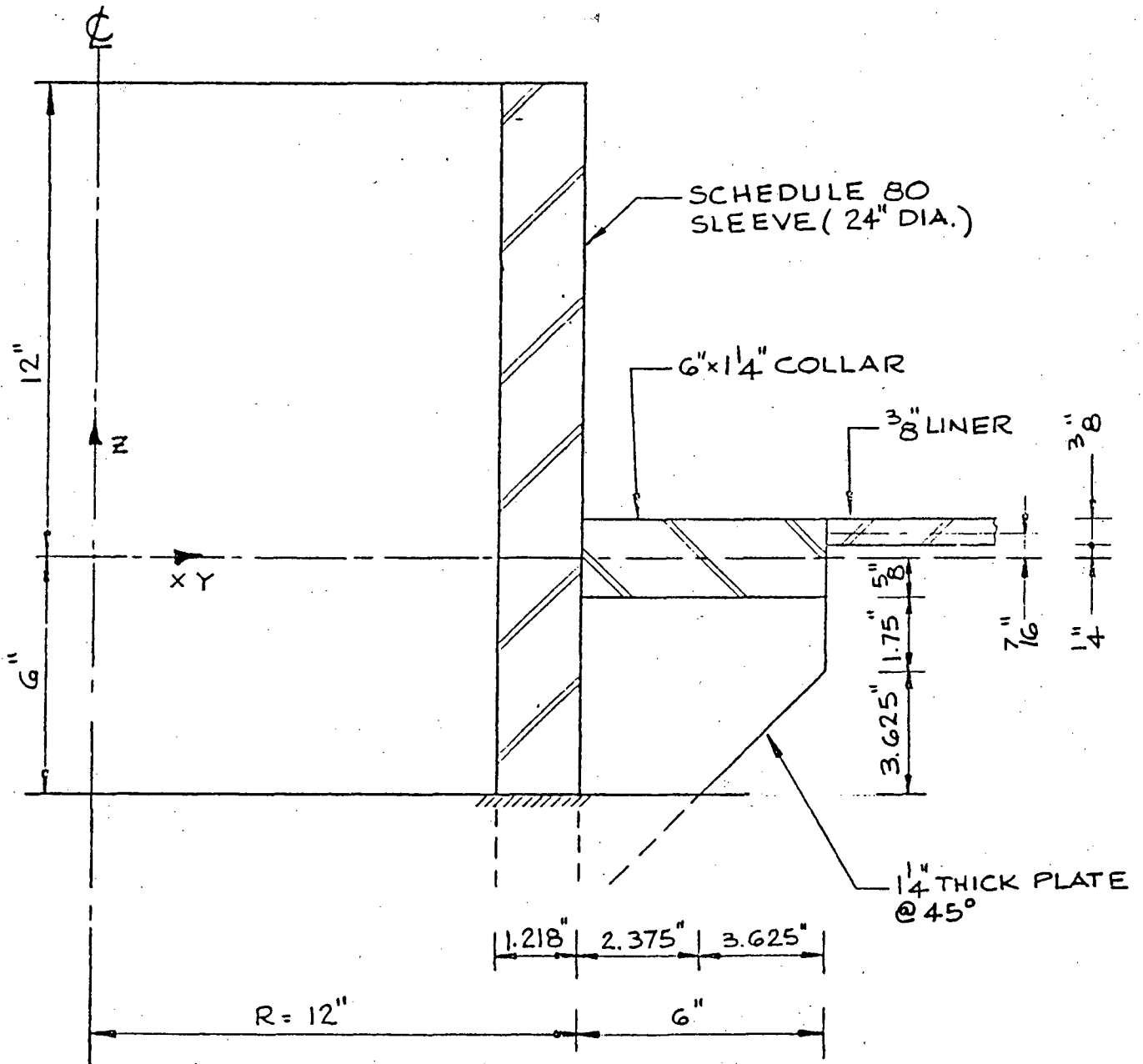


ISOMETRIC OF CORNER ANCHORAGE

Amend. 59
Dec. 1980

FIGURE 3A.8-6

3A.8-15



Section Of Wall Liner Penetration

Figure 3A.8-7

Amend. 59
Dec. 1980

3A.9 Catchpan System

The catch pan system is part of the Sodium Fire Protection System (SFPS) which provides a passive fire suppression system for sodium fires in air filled cells. The overall Sodium Fire Protection System is described in Section 9.13.2.2.

The catch pan - fire suppression system is an Engineered Safety Feature located in non-radioactive Na and NaK cells. Its purpose is to prevent sodium-concrete reactions between the liquid metal pool and concrete following an accidental spill, to reduce pool burning, to limit the temperature imposed on the structural concrete, and to limit the amount of sodium aerosols generated during a sodium-NaK spill accident.

3A.9.1 Design Description

3A.9.1.1 Catch Pan Types

There are two basic types of catch pans located in the air filled cells:

- 1) Catch Pans with Fire Suppression Deck - This catch pan type is located in sodium-NaK cells where the consequences of unmitigated sodium-NaK burning would have a significant impact on the structures or safety related systems. In these areas the liquid metal forms a pool in the catch pan below a fire suppression deck. The fire suppression deck is designed to limit the oxygen supply available to the liquid metal pool for the continued burning of the liquid metal. In this manner the consequences of a postulated liquid metal spill are mitigated.
- 2) Open Catch Pans - This catch pan type is located in sodium-NaK cells where the volume of the liquid metal spill is small and full burning of the liquid metal will not have significant effects on the structures or safety related equipment. The sodium is collected in open catch pans to prevent sodium-concrete reactions with the liquid metal pool.

Open catch pans are also used in cells with substantial sodium leak volumes. In these cells, a pool is not allowed to form. The sodium collects in an open catch pan and drains, by gravity, through drain pipes or large openings in the catch pan into a catch pan cell equipped with a fire suppression deck. The flow can be lateral or vertical.

One exception is Cell 211A which drains into Cell 211 which does not have a fire suppression deck. Both cells have a common atmosphere and contain the Ex-Containment Primary Sodium Storage Tanks and associated piping. These cells are inerted prior to the introduction of sodium.

Further descriptions and catch pan arrangements are presented in PSAR Section 9.13.2.2. Figures 9.13-3 and 9.13-4 present typical arrangements of the two catch pan types described above.

Catch pans are located in the non-radioactive Na/NaK cells of the Steam Generator and Reactor Service Buildings. Table 9.13-10 of Section 9.13 lists the RSB and SGB cells having each type of catch pan. The configuration of these cells is shown in PSAR Section 1.2.

3A.9.1.2 Structural Features

3A.9.1.2.1 Catch Pan with Fire Suppression Deck

The components of a Catch Pan with Fire Suppression Deck are shown on Figure 3A.9-1 and consist of the following:

- 1) Catch Pan
- 2) Fire Suppression Deck and Structural Support Beams and Columns
- 3) Fire Suppression Deck Drains
- 4) Fire Suppression Deck Vents
- 5) Insulation
- 6) Catch Pan Lip Plate

3A.9.1.2.1.1 Catch Pan - The Catch Pan consists of 3/8 inch thick carbon steel plate constructed using full penetration welds and forming a leak tight boundary to catch and contain a potential sodium-NaK spill.

In general, the catch pan is "floating", i.e., it is allowed free thermal expansion to minimize thermal stresses. Gaps are provided between the concrete structures and the catch pan side walls to permit the thermal expansion of the catch pan. Around embedments, penetrations, fire suppression deck support columns or other elements attached directly to the concrete structure, a vertical sidewall catch pan plate is provided to permit the free floating catch pan to expand or translate relative to the fixed embedment location without imposing additional load on the catch pan (Figure 3A.9-1).

3A.9.1.2.1.2 Fire Suppression Deck and Structural Supports - The Fire Suppression System consists of standard metal deck panels, 4-1/2 inches deep, supported on steel framing composed of wide flange beams. The steel framing is supported above the catch pan plate by stub columns with base plates anchored directly to the concrete floor slab. At the perimeter of the catch pan cell, the support beams are attached to steel brackets anchored to the concrete walls. The deck and beam structural connections are designed to allow for thermal expansion thereby minimizing thermal stresses.

A steel grating is located above the fire suppression deck and provided as a walkway for maintenance access. The steel grating is not a part of the catch pan system and does not have a fire suppression function. It is supported by the fire suppression deck support framing.

3A.9.1.2.1.3 Fire Suppression Deck Drains - As liquid sodium spills onto the fire suppression deck it flows through small diameter drain pipes in the fire suppression deck and into the catch pan. These carbon steel drain pipes are welded to the deck and extended downward to a point 1/2 inch nominal above the catch pan. The drain pipes are spaced to form a uniform array over the catch pan. As the liquid sodium drains into the catch pans, the level of Na in the drain pipe rises, thus limiting the effective surface burning area of the resulting liquid metal pool to the cross sectional area of the drain pipes.

Burning is terminated when following the Na spill the drain pipes become plugged with combustion products and air is prevented from reaching the liquid metal surface within the pipes.

3A.9.1.2.1.4 Fire Suppression Deck Vent Pipes - Vent pipes are also welded to the fire suppression deck. They are provided to vent hot gases from the region below the deck to the cell atmosphere to prevent the buildup of pressure below the fire suppression deck.

3A.9.1.2.1.5 Insulation - Insulation is provided under the catch pan floor and alongside the catch pan walls to protect the reinforced concrete structure from excessive temperature.

Below the catch pan a granular insulation material (MgO) is used in varying thickness to limit the floor slab concrete temperature and to provide a vent path for the water vapor released by the heating of the structural concrete. A blanket type insulation (aluminum silicate or the equivalent) is attached to the reinforced concrete walls behind the side wall of the catch pan. A gap between the insulation and the catch pan side wall permits the free thermal expansion of the catch pan.

3A.9.1.2.1.6 Catch Pan Lip Plate - To prevent liquid sodium from falling into the gap between the building concrete walls and the catch pan side walls, a continuous steel lip plate is provided along the perimeter of the catch pan. The steel lip plate is welded to a plate embedded in the concrete wall and covers the gap between concrete and steel walls. Lip plates are also provided to cover gaps between catch pan and embedments or penetrations anchored in the concrete floor slab.

3A.9.1.2.2 Open Catch Pans - The open catch pans are similar to the catch pans described in Section 3A.9.1.2.1 except that they do not utilize a fire suppression deck. Open catch pans utilize insulation under the catch pan floor but not along the side walls. There is no substantial buildup of liquid metal in open catch pans since they are used where either the volume of the spill is small or the liquid sodium can be conducted through drains into catch pans equipped with a fire suppression deck. In open catch pans with drains, the catch pan floor is sloped toward the drains to facilitate draining. A minimum slope of 1/8 to 1/4 inch per foot is used except for cells 244, 245 and 246 where the slope is 1/10"/foot. The open catch pan drains in most cells are vertical. However horizontal drains (scuppers) are used in regions where vertical draining is not possible due to the arrangement of the catch pan cells. In a limited number of cells located above cells equipped with fire suppression decks, the sodium flows to the catch pan below through large lined openings passing through the floor slab. Some open catch pans are equipped with a grating to facilitate access for equipment maintenance.

3A.9.2 Design Evaluation

3A.9.2.1 Sodium Spill Evaluation

An evaluation of the consequences of a sodium/NaK spill is provided in PSAR Section 15.6.1.5. The methods and criteria used for the evaluation of the catch pan system are discussed in PSAR Appendix 3.8-C.

3A.9.2.2 Catch Pan System Analysis and Design

The catch pan system is described in Section 3A.9.1 and 9.13.2.2. The Design Requirements, Load Categories, Load Combinations, Stress and Strain Allowables, and Design Analysis procedures are given in PSAR Appendix 3.8-C. Attachment D to Appendix 3.8-C gives the basis for the strain criteria and strain limits adopted for the cell liner system and utilized for the catch pan system under sodium spill accident conditions.

The catch pan plate has been designed for the loads and temperatures specified in Section 3.8-C, Attachment A. The catch pan is designed as a free floating basin to collect DBA sodium/NaK spills. The catch pan is free to expand under the thermal loading of a DBA sodium spill thus minimizing the induced thermal stresses. The major stresses in the catch pan are generated by the hydrostatic pressure of the sodium/NaK pool including the dynamic effects during an earthquake. The hydrostatic seismic effects were calculated using Housner's theory (TID-7024; Nuclear Reactors and Earthquakes by T. H. Thomas et al. USAEC., August 1963). The reduced strength of the catch pan plate due to sodium spill temperature conditions has been included based on Reference (6) of Section 3A.8.

The fire suppression deck and fire suppression deck framing support structure have been designed based upon typical panels and using beam theory. Seismic effects were considered based upon the applicable floor response spectra by using the appropriate seismic accelerations. The reduction in steel strength with temperature was considered in determining the allowable stresses.

The catch pan is supported on granular insulation.

The primary function of the insulation is to provide a thermal barrier to prevent the degradation of the structural concrete slab supporting the catch pan under DBA sodium spill conditions. The insulation also provides a uniform support for the catch pan plate while providing a vent path, through the voids in the granular matrix, for the release of water vapor generated during the heatup of the structural concrete.

Insulation is also provided, in some cases, along the perimeter of the catch pan to provide a thermal barrier to protect the structural concrete near the sodium pool. The insulation is attached to the structural concrete and separated from the catch pan plate by an air gap to permit the unrestrained growth of the floating catch pan.

3A.9.3 Testing

For testing program see PSAR Section 1.5.2.8.

3A.9-5

Amend. 74
Dec. 1982

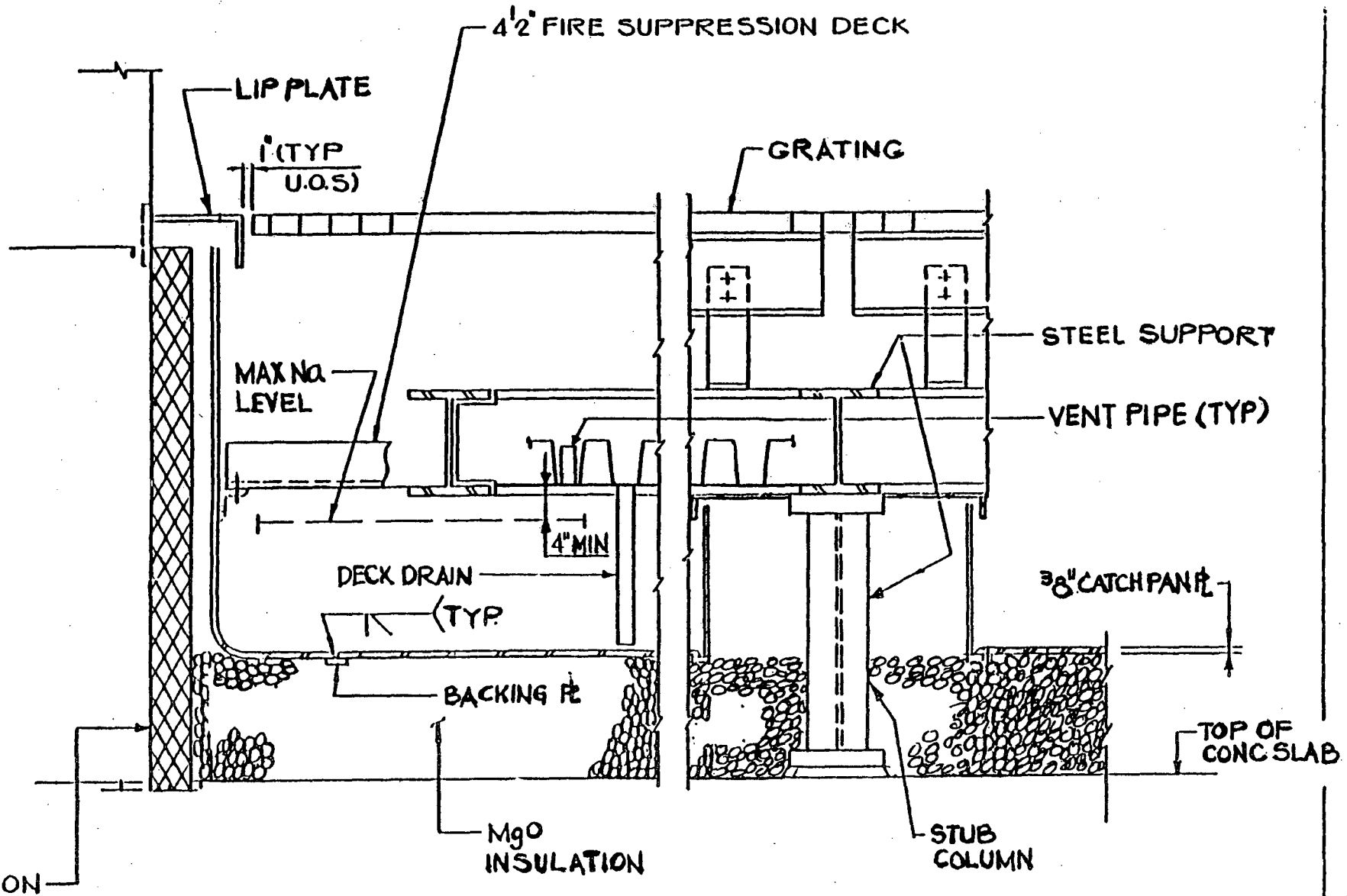


FIGURE 3A.9-1

CATCH PAN WITH FIRE SUPPRESSION DECK

**CLINCH RIVER
BREEDER REACTOR PROJECT**

**PRELIMINARY
SAFETY ANALYSIS
REPORT**

**CHAPTER 4
REACTOR**

PROJECT MANAGEMENT CORPORATION

CHAPTER 4.0 - REACTOR
TABLE OF CONTENTS

		<u>Page No.</u>
4.1	<u>SUMMARY DESCRIPTION</u>	4.1-1
4.1.1	Lower Internals	4.1-3
4.1.2	Upper Internals	4.1-3
4.1.3	Core Restraint	4.1-4
4.1.4	Fuel, Blanket and Removable Radial Shield Regions	4.1-4
4.1.4.1	Fuel and Axial Blankets	4.1-4
4.1.4.2	Inner and Radial Blanket	4.1-6
4.1.4.3	Removable Radial Shield	4.1-7
4.1.4.4	Control	4.1-7
4.1.5	Design and Performance Characteristics	4.1-9
4.1.6	Loading Conditions and Analysis Techniques	4.1-9
4.1.7	Computer Codes	4.1-10
4.2	<u>MECHANICAL DESIGN</u>	
4.2.1	Fuel and Blanket Design	4.2-1
4.2.1.1	Design Bases	4.2-1
4.2.1.1.1	Functional Requirements	4.2-1
4.2.1.1.2	Operational and Design Requirements	4.2-2
4.2.1.1.2.1	Operating Conditions	4.2-2
4.2.1.1.2.2	Design Requirements	4.2-5
4.2.1.1.2.2.1	Fuel and Blanket Assembly Structural Component Design Criteria	4.2-15
4.2.1.1.2.2.2	Removable Radial Shield Assembly Structural Component Design Criteria	4.2-17

TABLE OF CONTENTS Continued

		<u>Page No.</u>	
	4.2.1.1.2.3	Requirements for Design Features	4.2-17
	4.2.1.1.3	Environmental and Material Considerations	4.2-18
	4.2.1.1.3.1	Irradiation Induced Creep and Swelling	4.2-19
	4.2.1.1.3.2	Creep Rupture Properties and Thermal Creep	4.2-19
	4.2.1.1.3.3	Tensile Properties	4.2-20
	4.2.1.1.3.4	Cladding Wastage	4.2-20
	4.2.1.1.3.5	Effects of Fuel and Cladding Swelling	4.2-23
	4.2.1.1.3.6	Environmental Effects—Blanket Assemblies	4.2-26
	4.2.1.1.3.7	Fission Product Redistribution	4.2-26
	4.2.1.1.3.8	Performance of Defected Fuel and Blanket Rods	4.2-27
	4.2.1.1.3.9	Fission Gas Release	4.2-35
	4.2.1.1.4	Surveillance and Post Irradiation Examination of Fuel and Blanket Assemblies	4.2-37
	4.2.1.1.4.1	General Surveillance and Examination Plan—Fuel Assemblies	4.2-38
	4.2.1.1.4.2	General Surveillance and Examination Plan—Blanket Assemblies	4.2-39
	4.2.1.1.4.3	Typical Examination Requirements—Fuel and Blanket Assemblies	4.2-40
	4.2.1.1.4.4	Evaluation of Results—Fuel and Blanket Assemblies	4.2-41
	4.2.1.2	Design Description	4.2-41
	4.2.1.2.1	Core Design and Operation	4.2-41
51	4.2.1.2.2	Fuel Assemblies	4.2-42

TABLE OF CONTENTS Continued

		<u>Page No.</u>
	4.2.1.2.3 Radial Blanket Assembly	4.2-50
	4.2.1.2.4 Inner Blanket Assembly Design	4.2-51
	4.2.1.2.5 Discrimination System for Correct Loading Assurance	4.2-52
	4.2.1.3 Design Evaluation	4.2-54
	4.2.1.3.1 Fuel and Blanket Rods	4.2-58
	4.2.1.3.1.1 Fuel and Blanket Rod Damage Mechanisms	4.2-59
54	4.2.1.3.1.2 Rod Performance Analysis Results	4.2-73
	4.2.1.3.1.2.1 Cladding CDF	4.2-73
	4.2.1.3.1.2.2 Cladding Ductility Limited Strain	4.2-77
	4.2.1.3.1.2.3 Wire Wrap Loads	4.2-79
	4.2.1.3.1.2.4 Fatigue Effects in Fuel Rods	4.2-82
	4.2.1.3.1.2.5 Load Follow Capability	4.2-83
	4.2.1.3.2 Fuel and Blanket Assembly Structural Evaluation	4.2-84
	4.2.1.3.2.1 Duct Dilation	4.2-84
	4.2.1.3.2.2 Rod Bundle-Duct Interaction	4.2-85
	4.2.1.3.2.3 Stress Analysis of Core Assembly Structural Components	4.2-87
	4.2.1.3.2.3.1 Loads Specification	4.2-88
	4.2.1.3.2.3.2 Selection of Data Location	4.2-88
	4.2.1.3.2.3.3 Loads and Environments for Core Assembly Components	4.2-89
51	4.2.1.3.2.3.4 Materials Property Considerations	4.2-91

TABLE OF CONTENTS Continued

	<u>Page No.</u>
4.2.1.3.2.3.5 Analysis Methods	4.2-93
4.2.1.3.2.3.6 Design Margins	4.2-95
4.2.1.4 Irradiation Experience	4.2-95
4.2.1.4.1 Fuel Rods	4.2-95
4.2.1.4.2 Blanket Rods	4.2-108
4.2.1.5 Testing and Inspection Plans	4.2-109
4.2.1.5.1 Fuel Assembly Design Verification Tests	4.2-109
4.2.1.5.2 Fuel Assembly Fabrication and Site Examination Quality Assurance Provisions	4.2-112
4.2.1.5.3 Blanket Assembly Planned Design Verification Tests	4.2-113
4.2.1.5.4 Blanket Assembly Examination Quality Assurance Provisions	4.2-114
4.2.1.6 Alternatives and Fallback Positions	4.2-115
4.2.2 Reactor Vessel Internals	4.2-118
4.2.2.1 Design Bases	4.2-118
4.2.2.1.1 Functional Requirements	4.2-118
4.2.2.1.1.1 Core Support Structure	4.2-118
4.2.2.1.1.2 Lower Inlet Modules (LIM)	4.2-119
4.2.2.1.1.3 Bypass Flow Modules	4.2-120
4.2.2.1.1.4 Fixed Radial Shielding	4.2-121
4.2.2.1.1.5 Fuel Transfer and Storage Assembly	4.2-122
4.2.2.1.1.6 Horizontal Baffle	4.2-123
51 4.2.2.1.1.7 Upper Internals Structure (UIS)	4.2-124

TABLE OF CONTENTS Continued

		<u>Page No.</u>
	4.2.2.1.1.8 Core Restraint System	4.2-125
	4.2.2.1.1.9 Removable Radial Shielding (RRS)	4.2-127
	4.2.2.1.1.10 Core Former Structure (CFS)	4.2-127a
	4.2.2.1.1.11 Maintainability	4.2-128
	4.2.2.1.1.12 Surveillance	4.2-128
58	4.2.2.1.1.13 Margin Beyond the Design Base Considerations	4.2-128
	4.2.2.1.2 Bases for Functional Requirements	4.2-128
	4.2.2.1.2.1 Core Support Structure	4.2-128
	4.2.2.1.2.2 Lower Inlet Modules	4.2-131
	4.2.2.1.2.3 Bypass Flow Module	4.2-134
	4.2.2.1.2.4 Fixed Radial Shielding	4.2-137
	4.2.2.1.2.5 Fuel Transfer and Storage Assembly	4.2-138
	4.2.2.1.2.6 Horizontal Baffle	4.2-139
	4.2.2.1.2.7 Upper Internals Structure	4.2-141
	4.2.2.1.2.8 Core Restraint System	4.2-146
	4.2.2.1.2.9 Removable Radial Shielding (RRS)	4.2-151
	4.2.2.1.2.10 Core Former Structure (CFS)	4.2-153
58	4.2.2.1.3 Design Loading	4.2-153a
	4.2.2.1.3.1 Core Support Structure	4.2-154
	4.2.2.1.3.2 Upper Internals Structure (UIS)	4.2-157
	4.2.2.2 Design Description	4.2-161
	4.2.2.2.1 Reactor Internals Structures	4.2-161
	4.2.2.2.1.1 Lower Internals Structure	4.2-162
51	4.2.2.2.1.2 Lower Inlet Module	4.2-165

TABLE OF CONTENTS Continued

		<u>Page No.</u>
	4.2.2.2.1.3 Bypass Flow Module	4.2-166
	4.2.2.2.1.4 Fixed Radial Shield	4.2-167
59 58	4.2.2.2.1.5 Fuel Transfer and Storage Assembly	4.2-168
	4.2.2.2.1.6 Horizontal Baffle	4.2-168
	4.2.2.2.1.7 Upper Internal Structure	4.2-170
	4.2.2.2.1.8 Core Restraint System	4.2-174
	4.2.2.2.1.9 Removable Radial Shield	4.2-175
	4.2.2.2.1.10 Core Former Structure	4.2-175
	4.2.2.2.1.11 Maintainability	4.2-175
59 58	4.2.2.2.1.12 Surveillance	4.2-175
	4.2.2.3 Design Criteria	4.2-175a
	4.2.2.3.1 Lower Internals Structure (LIS)	4.2-176
	4.2.2.3.1.1 Core Support Structure (CSS)	4.2-176
	4.2.2.3.1.2 Lower Inlet Module (LIM), Bypass Flow Module (BPFM), and Core Former Structure (CFS)	4.2-176
	4.2.2.3.1.3 Horizontal Baffle (HB), Fuel Transfer and Storage Assembly (FT & SA), and Fixed Radial Shield (FRS)	4.2-176
	4.2.2.3.2 Upper Internals Structure (UIS)	4.2-177
	4.2.2.3.2.1 Class 1 Appurtenances	4.2-177
	4.2.2.3.2.2 Internal Structure	4.2-177
59	4.2.2.3.2.3 Modifications to the High Temperature Design Rules for Austenitic Stainless Steel	4.2-178
51	4.2.2.3.3 Additional Material Properties	4.2-181
	4.2.2.3.3.1 Inconel 718 Fatigue Properties	4.2-181
	4.2.2.3.3.2 Environmental Effects on Material Properties	4.2-182

TABLE OF CONTENTS Continued

	<u>Page No.</u>
4.2.2.3.3.2.1 Sodium Effects	4.2-182
4.2.2.3.3.2.2 Irradiation Effects	4.2-191
4.2.2.3.3.3 Friction, Wear, and Self Welding Considerations	4.2-191
4.2.2.4 Evaluation	4.2-193
59 4.2.2.4.1 Lower Internals Structure	4.2-193
4.2.2.4.1.1 Analysis of Core Support Structure (CSS)	4.2-194
4.2.2.4.1.2 Analysis of Lower Inlet Module (LIM)	4.2-206
4.2.2.4.1.3 Analysis of Bypass Flow Modules (BPFM)	4.2-207
4.2.2.4.1.4 Analysis of the Fixed Radial Shield (FRS)	4.2-210
4.2.2.4.1.5 Analysis of the Fuel Transfer and Storage Assembly (FT&SA)	4.2-210
51 4.2.2.4.1.6 Analysis of the Horizontal Baffle (HB)	4.2-210
4.2.2.4.1.7 Analysis of the Core Former Structure (CFS)	4.2-210
4.2.2.4.2 Upper Internals Structure	4.2-210
4.2.2.4.2.1 Components Analysed	4.2-210
4.2.2.4.2.2 Material Properties	4.2-211
4.2.2.4.2.3 Structural Design Criteria	4.2-213
4.2.2.4.2.4 Mechanical Loads	4.2-214
4.2.2.4.2.5 Thermal Environment	4.2-215
4.2.2.4.2.6 Methods of Analysis	4.2-216
4.2.2.4.2.7 Structural Analysis	4.2-216
4.2.2.4.3 Core Restraint System Evaluation	4.2-221
4.2.2.4.3.1 Summary of Results	4.2-221
59 51 4.2.2.4.3.2 Material Properties	4.2-221

TABLE OF CONTENTS Continued

		<u>Page No.</u>
	4.2.2.4.3.3 Analysis of Assembly Bowing and Duct Dilation	4.2-222
59	4.2.2.4.4 Removable Radial Shielding (RRS)	4.2-227
	4.2.2.5 Welding and Seizing of Reactor Internal Parts	4.2-228
	4.2.3 Reactivity Control Systems	4.2-228
	4.2.3.1 Design Basis	4.2-230
	4.2.3.1.1 General Safety Design Criteria	4.2-230
	4.2.3.1.2 Control Rod System Clearances	4.2-231
	4.2.3.1.3 Mechanical Insertion Requirements	4.2-231
	4.2.3.1.4 Positioning Requirements	4.2-241
	4.2.3.1.5 Structural Requirements	4.2-242
	4.2.3.1.6 Environmental Requirements	4.2-247
	4.2.3.1.6.1 Nuclear Environment	4.2-248
	4.2.3.1.6.2 Control Rod Systems Duty Cycle	4.2-249
	4.2.3.1.6.3 Thermal and Hydraulic Environment	4.2-249
	4.2.3.1.7 Material Selection and Radiation Damage	4.2-250
	4.2.3.2 Description and Drawings	4.2-255
	4.2.3.2.1 Primary Control Rod System	4.2-256
	4.2.3.2.1.1 Primary Control Rod Drive Mechanisms	4.2-256
	4.2.3.2.1.2 Primary Control Rod Driveline	4.2-260
	4.2.3.2.1.3 Primary Control Assemblies	4.2-261
	4.2.3.2.2 Secondary Control Rod System	4.2-264
51	4.2.3.2.2.1 Secondary Control Rod Mechanism	4.2-266

TABLE OF CONTENTS Continued

	<u>Page No.</u>
4.2.3.2.2.2 Secondary Control Rod Driveline	4.2-268
4.2.3.2.2.3 Secondary Control Assembly	4.2-269
4.2.3.3 System Evaluation	4.2-270
4.2.3.3.1 Primary System Evaluation	4.2-270
4.2.3.3.1.1 Alignment Analysis	4.2-271
4.2.3.3.1.2 Control Assembly Bowing Analysis	4.2-274
4.2.3.3.1.3 Scram Analysis	4.2-278
4.2.3.3.1.4 Seismic Scram Analysis	4.2-279
4.2.3.3.1.5 Control Assembly Analysis	4.2-280
4.2.3.3.1.6 PCRDM and PCRD Structural Analysis	4.2-283
4.2.3.3.1.7 Overall System Performance Evaluation	4.2-283
4.2.3.3.1.8 Previous Experience and Development Work	4.2-288
4.2.3.3.2 Secondary System Evaluation	4.2-289
4.2.3.3.2.1 Tolerance Analysis	4.2-289
4.2.3.3.2.2 Scram Analysis	4.2-290
4.2.3.3.2.3 Control Assembly Analyses	4.2-292
4.2.3.3.2.4 Overall System Performance Evaluation	4.2-296
4.2.3.3.2.5 Previous Experience and/or Development Work with Similar Systems and Materials	4.2-302
4.2.3.4 Testing and Inspection Plan	4.2-303
4.2.3.4.1 Performance Test Program	4.2-304
4.2.3.4.1.1 Primary Control Rod System	4.2-304
4.2.3.4.1.2 Secondary Control Rod System	4.2-305

51

TABLE OF CONTENTS Continued

	<u>Page No.</u>	
4.2.3.4.2	Plant Tests	4.2-306
4.2.3.4.3	Surveillance	4.2-307
4.2.3.4.4	Acceptance Tests	4.2-308
4.2.3.4.5	Post-Irradiation Examinations	4.2-310
4.2.3.5	Instrumentation	4.2-311
4.2.3.5.1	Primary Control Rod System Instrumentation	4.2-311
4.2.3.5.1.1	Absolute Control Rod Position Indication System	4.2-311
4.2.3.5.1.2	Relative Control Rod Position Indication System	4.2-311
4.2.3.5.1.3	CRDM Pressure Switch	4.2-312
4.2.3.5.1.4	CRDM Stator Thermocouples	4.2-313
4.2.3.5.2	Secondary Control Rod System Instrumentation	4.2-313
4.2.3.5.2.1	Leadscrew Encoder Position Indication System	4.2-313
4.2.3.5.2.2	Proximity Switch Position Indication System	4.2-313
4.2.3.5.2.3	Scram Latch Indication System	4.2-313
4.2.3.5.2.4	SCRDM Pressure and Leakage Monitoring	4.2-314
4.2.3.5.2.5	SCRDM Thermocouples	4.2-314
4.2.3.5.2.6	Acoustic Monitor	4.2-314
4.3	<u>NUCLEAR DESIGN</u>	
4.3.1	Design Bases	4.3-1
4.3.1.1	Core Design Lifetime and Fuel Burnup	4.3-1
4.3.1.2	Reactivity Control	4.3-1

TABLE OF CONTENTS Continued

		<u>Page No.</u>
4.3.1.3	Power Oscillations	4.3-2
4.3.1.4	Reactivity Coefficients	4.3-2
4.3.1.5	Fuel Management and Power Distributions	4.3-2
4.3.1.6	Excess Reactivity	4.3-2
4.3.1.7	Fuel Buildup in Fertile Material	4.3-2
4.3.1.8	Shim Control	4.3-2
4.3.1.9	Annual Refueling	4.3-2
4.3.1.10	Reactivity Insertion Rates	4.3-3
4.3.2	Description	4.3-3
4.3.2.1	Nuclear Design Description	4.3-3
4.3.2.1.1	Fuel Enrichments and Loadings	4.3-3
4.3.2.1.2	Fuel and Blanket Management	4.3-5
4.3.2.1.3	Delayed Neutron Fraction and Neutron Lifetime	4.3-6
4.3.2.1.4	Multi-Group Nuclear Cross Section Data	4.3-7
4.3.2.1.5	Source Range Flux Monitoring System	4.3-7
4.3.2.2	Power Distribution	4.3-18
4.3.2.2.1	Calculational Method	4.3-18
4.3.2.2.2	Core Layout	4.3-18
4.3.2.2.3	Region Power Fractions	4.3-19
4.3.2.2.4	Normalized Radial Power Shape	4.3-19
4.3.2.2.5	Axial Blanket (Extension) Power	4.3-20
51 4.3.2.2.6	Radial Blanket Power History	4.3-20

TABLE OF CONTENTS Continued

		<u>Page No.</u>
4.3.2.2.7	Normalized Axial Power Shape	4.3-20
4.3.2.2.8	Synthesis of Power Distribution Throughout the Core	4.3-21
4.3.2.2.9	Power Uncertainty Evaluation	4.3-22
4.3.2.2.9A	Core Fuel Assembly Power Uncertainties	4.3-23
4.3.2.2.9B	Inner Blanket Assembly Power Uncertainties	4.3-27
4.3.2.2.9C	Radial Blanket Assembly Power Uncertainties	4.3-29
4.3.2.2.10	Peak Linear Power	4.3-31
4.3.2.2.11	Burnup	4.3-32
4.3.2.3	Reactivity Coefficients	4.3-34
4.3.2.3.1	Doppler Constants	4.3-34
4.3.2.3.2	Sodium Void Worth	4.3-37
4.3.2.3.3	Sodium Density Reactivity Coefficient	4.3-38
4.3.2.3.4	Expansion and Bowing Reactivity Coefficients	4.3-39
4.3.2.3.5	Power and Startup Coefficients and Temperature Defect	4.3-43
4.3.2.4	Control Requirements	4.3-46
4.3.2.5	Control Rod Patterns	4.3-51
4.3.2.6	Control Rod Worths	4.3-53
4.3.2.6.1	Calculational Methods	4.3-53
4.3.2.6.2	Control Rod Worth Bias Uncertainty	4.3-53a
4.3.2.6.3	Control Rod Interactions	4.3-55
4.3.2.6.4	Stuck Rod	4.3-55
4.3.2.6.5	Minimum Shutdown Capacity	4.3-56
4.3.2.6.6	Integral Worth Curve	4.3-57
4.3.2.6.7	Primary Control Rod Withdrawal Histories	4.3-57

4.3.2.6.8	Minimum worth Available for Scram	4.3-58
4.3.2.6.9	Minimum Zero Power Subcriticality with 15 Control Rods Inserted	4.3-58
4.3.2.6.10	Maximum Ramp Reactivity	4.3-59
4.3.2.7	Criticality of Fuel Assemblies	4.3-59
4.3.2.7.1	Reactor Eigenvalue Prediction	4.3-59
4.3.2.7.2	Minimum Critical Configuration	4.3-60
4.3.2.8	Reactor Stability	4.3-61

TABLE OF CONTENTS Continued

		<u>Page No.</u>
4.3.2.8.1	Linear Stability Analysis	4.3-62
4.3.2.8.2	General Stability Analysis	4.3-66
4.3.2.9	Vessel Irradiation	4.3-68
4.3.3	Analytical Methods	4.3-69
4.3.3.1	Analytical Approach	4.3-69
4.3.3.2	Neutron Cross Section Data	4.3-71
4.3.3.3	Critical Experiments in Support of CRBRP	4.3-72
4.3.3.4	ZPPR Assembly 2 and ZPR-6 Assembly 7	4.3-72
4.3.3.5	ZPPR Assembly 3	4.3-73
4.3.3.6	ZPPR-3 Modified Phase 3 Sodium Void Benchmark	4.3-74
4.3.3.7	ZPPR-4 (Pre-Engineering Mockup Critical for Homogeneous CRBRP)	4.3-75
4.3.3.8	ZPPR-5 (HCDA Engineering Mockup Critical for Homogeneous CRBR)	4.3-77
4.3.3.9	ZPPR-7 (Pre-Engineering Mockup Critical for Heterogeneous Core)	4.3-77
4.3.3.10	Computer Code Abstracts	4.3-83
4.3.4	Changes	4.3-83
4.4	<u>THERMAL AND HYDRAULIC DESIGN</u>	
4.4.1	Design Bases	4.4-1
4.4.2	Description	4.4-4
4.4.2.1	Summary Comparison	4.4-4
4.4.2.2	Fuel Rod Temperature	4.4-5
4.4.2.3	Flux Tilt Considerations	4.4-6
51 4.4.2.4	Reactor Coolant Flow Distribution	4.4-7

TABLE OF CONTENTS Continued

		<u>Page No.</u>
4.4.2.4.1	Reactor Component Flow Path Description	4.4-7
4.4.2.5	Fuel and Blanket Assemblies Orificing	4.4-10
4.4.2.5.1	Orificing Philosophy, Approach and Constraints	4.4-10
4.4.2.5.2	Calculation of Equivalent Limiting Temperatures	4.4-12
4.4.2.5.3	Results	4.4-15
4.4.2.6	Reactor Coolant Flow Distribution at Low Reactor Flows	4.4-17
4.4.2.7	Reactor Pressure Drops and Hydraulic Loads	4.4-19
4.4.2.7.1	Introduction	4.4-19
4.4.2.7.2	Core Assemblies Pressure Drop Correlations	4.4-20
4.4.2.7.3	Reactor Internals Pressure Drop	4.4-24
4.4.2.7.4	Results	4.4-24
4.4.1.7.5	Hydraulic Loads and Hydraulic Balance	4.4-25
4.4.2.8	Correlations and Physical Properties	4.4-26
4.4.2.8.1	Sodium Properties	4.4-26
4.4.2.8.2	Film Heat Transfer Coefficient	4.4-26
4.4.2.8.3	Cladding Thermal Conductivity	4.4-27
4.4.2.8.4	Cladding Linear Thermal Expansion Coefficient	4.4-27
4.4.2.8.5	Fuel and Blanket Assemblies Fuel-Cladding Gap Conductance	4.4-27
4.4.2.8.6	Control Rod Gap Conductance	4.4-29
4.4.2.8.7	Fuel Thermal Conductivity	4.4-32
51 4.4.2.8.8	B ₄ C Thermal Conductivity	4.4-34

TABLE OF CONTENTS Continued

		<u>Page No.</u>
	4.4.2.8.9 B ₄ C Linear Thermal Expansion Coefficient	4.4-35
	4.4.2.8.10 B ₄ C Density	4.4-35
	4.4.2.8.11 Fuel Theoretical Density	4.4-35
	4.4.2.8.12 Fuel Melting Temperature	4.4-35
	4.4.2.8.13 B ₄ C Melting Temperature	4.4-37
	4.4.2.8.14 Fuel Linear Power-To-Melt	4.4-38
	4.4.2.8.15 Fuel Restructuring Parameters	4.4-39
	4.4.2.8.16 Fission Gas Release and Fission Gas Yield	4.4-39
	4.4.2.9 Thermal Effects of Operational Transients	4.4-42
	4.4.2.10 Plant Configuration Data	4.4-44
52	4.4.3 Evaluation	4.4-45
	4.4.3.1 Reactor Hydraulics	4.4-45
	4.4.3.2 Uncertainties Analysis	4.4-46
	4.4.3.2.1 Introduction	4.4-46
	4.4.3.2.2 Power-To-Melt Uncertainties	4.4-52
	4.4.3.2.3 Nuclear Uncertainties	4.4-53
	4.4.3.2.4 Plenum Pressure Uncertainties	4.4-55
	4.4.3.3 Steady State Performance Predictions	4.4-57
	4.4.3.3.1 Plant Conditions	4.4-57
	4.4.3.3.2 Linear Power	4.4-59
	4.4.3.3.3 Assemblies Mixed Mean Temperatures	4.4-59
	4.4.3.3.4 Rod Lifetime Cladding Temperature/Pressure Histories	4.4-61
51	4.4.3.3.5 Core Assemblies Duct Temperatures	4.4-62

TABLE OF CONTENTS Continued

	<u>Page No.</u>	
4.4.3.3.6	Power-To-Melt Analysis	4.4-63
4.4.3.3.7	Control Assemblies Thermal-Hydraulic Performance	4.4-65
4.4.3.3.8	RRS Thermal-Hydraulic Analysis	4.4-66
4.4.3.4	Analytical Techniques	4.4-67
4.4.3.4.1	Fuel and Blanket Assemblies	4.4-67
4.4.3.4.2	Primary Control Assemblies	4.4-72
4.4.3.4.3	Secondary Control Assemblies	4.4-74
4.4.3.5	Hydraulic Instability Analysis	4.4-74
4.4.3.6	Temperature Transient Effects Analysis	4.4-74
4.4.3.7	Potentially Damaging Temperature Effects During Transients	4.4-75
4.4.3.8	Thermal Description of the Direct Heat Removal Service (DHRS)	4.4-75
4.4.4	Testing and Verification	4.4-75
4.4.4.1	Feature Model Test	4.4-76
4.4.4.2	Reactor Assemblies T&H Testing	4.4-78
4.4.5	Core Instrumentation	4.4-80
4.4.5.1	Design Bases	4.4-80
4.4.5.2	Design Description	4.4-80
4.4.5.3	Design Evaluation of Reactor Control Thermocouples	4.4-80a

Table No.

LIST OF TABLES

4.1-1	Reactor System Design Performance Parameters	4.1-11
4.2-A	Design Procedure for Steady-State Creep Analysis	4.2-331
4.2-B	Comparison of Design Lifetime Predicted by Strain Criteria with Actual Lifetime	4.2-332
4.2-C	316 Stainless Steel Fretting and Wear Data in Sodium	4.2-333

LIST OF TABLES Continued

		<u>Page No.</u>
4.2-D	Over-Temperature Transient Experiments	4.2-334
4.2-E	Rapid Reactivity Insertion Experiments	4.2-335
4.2-1	Densities of Compounds In the U-Na-O System	4.2-336
4.2-2	Calculated and Experimental Isothermal Oxygen Contents Fuel and Sodium for Fuel Sodium Reaction	4.2-337
4.2-3	Typical Surveillance Examination Plan	4.2-338
4.2-4	Comparison of CRBRP and FFTF Fuel Assembly Details	4.2-339
4.2-5	Nominal Radial Blanket Assembly Design Parameters	4.2-343
4.2-5A	General Plan for Verification of Fuel Design Analysis and Criteria	4.2-345
4.2-6	Deleted	
4.2-7	CRBR Core Assembly Structural Inelastic Criteria and Limits	4.2-347
4.2-8A	Summary of Design Loading Conditions for Fuel Assembly Structural Analysis	4.2-348
4.2-8B	Design Seismic and Core Restraint Loads of the Fuel Assembly ACLP	4.2-349
4.2-8C	Seismic Loads In Vertical Direction	4.2-350
4.2-9	Testing for Load Follow	4.2-351
4.2-9A	Typical Neutron Environment in the CRBRP Shield Assemblies	6.2-351a
4.2-9B	Shield Assembly Inelastic Strain Criteria	6.2-351b
4.2-10	Steady-State CDF Value for the Hot Rod of Blanket Assembly 201 of the First Core	4.2-352
4.2-11	Worst Fuel Assembly Hot Rod Steady-State Ductility Limited Strains at Hot Spot	4.2-353

LIST OF TABLES Continued

		<u>Page No.</u>
4.2-11A	Characterized Cladding Breach Summary	4.2-354
4.2-12	Summary of Design Loading Conditions for Blanket Assembly Structural Analysis	4.2-355
4.2-13	Design Seismic and Core Restraint Loads at the Blanket Assembly ACLP	4.2-356
4.2-14	EOL Steady-State Cladding Strains Due to FCMI and Plenum Pressure	4.2-357
4.2-15	CRBR First Core Wire-Wrap Performance Summary	4.2-358
4.2-16	Fuel Assembly Bounding Margin of Safety Summary	4.2-359
4.2-17	Blanket Assembly Bounding Margin of Safety Summary	4.2-360
4.2-18	Assessment of Applicability of FFTF Design Verification Tests	4.2-361
4.2-19	Planned CRBRP Fuel Assembly Design Verification Tests	4.2-363
4.2-20	Planned CRBRP Blanket Design Verification Tests	4.2-364
4.2-21	Design Temperatures vs Predicted Steady-State Temperatures for Permanent Reactor Internals Components	4.2-365
4.2-22	Deleted	4.2-366
4.2-23	Core Support Structure Stress and Fatigue Damage Summary for Normal and Upset Conditions	4.2-367
4.2-24	Deleted	4.2-368
4.2-25	Deleted	4.2-369
4.2-26	Deleted	4.2-370
4.2-27	Deleted	4.2-371
4.2-28	Deleted	4.2-372

TABLE OF CONTENTS Continued

	<u>Page No.</u>
4.2.3.2.2.2 Secondary Control Rod Driveline	4.2-268
4.2.3.2.2.3 Secondary Control Assembly	4.2-269
4.2.3.3 System Evaluation	4.2-270
4.2.3.3.1 Primary System Evaluation	4.2-270
4.2.3.3.1.1 Alignment Analysis	4.2-271
4.2.3.3.1.2 Control Assembly Bowing Analysis	4.2-274
4.2.3.3.1.3 Scram Analysis	4.2-278
4.2.3.3.1.4 Seismic Scram Analysis	4.2-279
4.2.3.3.1.5 Control Assembly Analysis	4.2-280
4.2.3.3.1.6 PCRDM and PCRD Structural Analysis	4.2-283
4.2.3.3.1.7 Overall System Performance Evaluation	4.2-283
4.2.3.3.1.8 Previous Experience and Development Work	4.2-288
4.2.3.3.2 Secondary System Evaluation	4.2-289
4.2.3.3.2.1 Tolerance Analysis	4.2-289
4.2.3.3.2.2 Scram Analysis	4.2-290
4.2.3.3.2.3 Control Assembly Analyses	4.2-292
4.2.3.3.2.4 Overall System Performance Evaluation	4.2-296
4.2.3.3.2.5 Previous Experience and/or Development Work with Similar Systems and Materials	4.2-302
4.2.3.4 Testing and Inspection Plan	4.2-303
4.2.3.4.1 Performance Test Program	4.2-304
4.2.3.4.1.1 Primary Control Rod System	4.2-304
4.2.3.4.1.2 Secondary Control Rod System	4.2-305

TABLE OF CONTENTS Continued

	<u>Page No.</u>	
4.2.3.4.2	Plant Tests	4.2-306
4.2.3.4.3	Surveillance	4.2-307
4.2.3.4.4	Acceptance Tests	4.2-308
4.2.3.4.5	Post-Irradiation Examinations	4.2-310
4.2.3.5	Instrumentation	4.2-311
4.2.3.5.1	Primary Control Rod System Instrumentation	4.2-311
4.2.3.5.1.1	Absolute Control Rod Position Indication System	4.2-311
4.2.3.5.1.2	Relative Control Rod Position Indication System	4.2-311
4.2.3.5.1.3	CRDM Pressure Switch	4.2-312
4.2.3.5.1.4	CRDM Stator Thermocouples	4.2-313
4.2.3.5.2	Secondary Control Rod System Instrumentation	4.2-313
4.2.3.5.2.1	Leadscrew Encoder Position Indication System	4.2-313
4.2.3.5.2.2	Proximity Switch Position Indication System	4.2-313
4.2.3.5.2.3	Scram Latch Indication System	4.2-313
4.2.3.5.2.4	SCRDM Pressure Switches	4.2-314
4.2.3.5.2.5	SCRDM Thermocouples	4.2-314
4.2.3.5.2.6	Acoustic Monitor	4.2-314
4.3	<u>NUCLEAR DESIGN</u>	
4.3.1	Design Bases	4.3-1
4.3.1.1	Core Design Lifetime and Fuel Burnup	4.3-1
4.3.1.2	Reactivity Control	4.3-1

TABLE OF CONTENTS Continued

		<u>Page No.</u>
4.3.1.3	Power Oscillations	4.3-2
4.3.1.4	Reactivity Coefficients	4.3-2
4.3.1.5	Fuel Management and Power Distributions	4.3-2
4.3.1.6	Excess Reactivity	4.3-2
4.3.1.7	Fuel Buildup in Fertile Material	4.3-2
4.3.1.8	Shim Control	4.3-2
4.3.1.9	Annual Refueling	4.3-2
4.3.1.10	Reactivity Insertion Rates	4.3-3
4.3.2	Description	4.3-3
4.3.2.1	Nuclear Design Description	4.3-3
4.3.2.1.1	Fuel Enrichments and Loadings	4.3-3
4.3.2.1.2	Fuel and Blanket Management	4.3-5
4.3.2.1.3	Delayed Neutron Fraction and Neutron Lifetime	4.3-6
4.3.2.1.4	Multi-Group Nuclear Cross Section Data	4.3-7
4.3.2.1.5	Source Range Flux Monitoring System	4.3-7
4.3.2.2	Power Distribution	4.3-18
4.3.2.2.1	Calculational Method	4.3-18
4.3.2.2.2	Core Layout	4.3-18
4.3.2.2.3	Region Power Fractions	4.3-19
4.3.2.2.4	Normalized Radial Power Shape	4.3-19
4.3.2.2.5	Axial Blanket (Extension) Power	4.3-20
51 4.3.2.2.6	Radial Blanket Power History	4.3-20

TABLE OF CONTENTS Continued

		<u>Page No.</u>
4.3.2.2.7	Normalized Axial Power Shape	4.3-20
4.3.2.2.8	Synthesis of Power Distribution Throughout the Core	4.3-21
4.3.2.2.9	Power Uncertainty Evaluation	4.3-22
4.3.2.2.9A	Core Fuel Assembly Power Uncertainties	4.3-23
4.3.2.2.9B	Inner Blanket Assembly Power Uncertainties	4.3-27
4.3.2.2.9C	Radial Blanket Assembly Power Uncertainty	4.3-29
4.3.2.2.10	Peak Linear Power	4.3-31
4.3.2.2.11	Burnup	4.3-32
4.3.2.3	Reactivity Coefficients	4.3-34
4.3.2.3.1	Doppler Constants	4.3-34
4.3.2.3.2	Sodium Void Worth	4.3-37
4.3.2.3.3	Sodium Density Reactivity Coefficient	4.3-38
4.3.2.3.4	Expansion and Bowing Reactivity Coefficients	4.3-39
4.3.2.3.5	Power and Startup Coefficients and Temperature Defect	4.3-43
4.3.2.4	Control Requirements	4.3-46
4.3.2.5	Control Rod Patterns	4.3-51
4.3.2.6	Control Rod Worths	4.3-53
4.3.2.7	Criticality of Fuel Assemblies	4.3-59
4.3.2.7.1	Reactor Eigenvalue Prediction	4.3-59
4.3.2.7.2	Minimum Critical Configuration	4.3-60
51 4.3.2.8	Reactor Stability	4.3-61

TABLE OF CONTENTS Continued

		<u>Page No.</u>
4.3.2.8.1	Linear Stability Analysis	4.3-62
4.3.2.8.2	General Stability Analysis	4.3-66
4.3.2.9	Vessel Irradiation	4.3-68
4.3.3	Analytical Methods	4.3-69
4.3.3.1	Analytical Approach	4.3-69
4.3.3.2	Neutron Cross Section Data	4.3-71
4.3.3.3	Critical Experiments in Support of CRBRP	4.3-72
4.3.3.4	ZPPR Assembly 2 and ZPR-6 Assembly 7	4.3-72
4.3.3.5	ZPPR Assembly 3	4.3-73
4.3.3.6	ZPPR-3 Modified Phase 3 Sodium Void Benchmark	4.3-74
4.3.3.7	ZPPR-4 (Pre-Engineering Mockup Critical for Homogeneous CRBRP)	4.3-75
4.3.3.8	ZPPR-5 (HCDA Engineering Mockup Critical for Homogeneous CRBR)	4.3-77
4.3.3.9	ZPPR-7 (Pre-Engineering Mockup Critical for Heterogeneous Core)	4.3-77
4.3.3.10	Computer Code Abstracts	4.3-83
4.3.4	Changes	4.3-83
4.4	<u>THERMAL AND HYDRAULIC DESIGN</u>	
4.4.1	Design Bases	4.4-1
4.4.2	Description	4.4-4
4.4.2.1	Summary Comparison	4.4-4
4.4.2.2	Fuel Rod Temperature	4.4-5
4.4.2.3	Flux Tilt Considerations	4.4-6
51 4.4.2.4	Reactor Coolant Flow Distribution	4.4-7

TABLE OF CONTENTS Continued

		<u>Page No.</u>
4.4.2.4.1	Reactor Component Flow Path Description	4.4-7
4.4.2.5	Fuel and Blanket Assemblies Orificing	4.4-10
4.4.2.5.1	Orificing Philosophy, Approach and Constraints	4.4-10
4.4.2.5.2	Calculation of Equivalent Limiting Temperatures	4.4-12
4.4.2.5.3	Results	4.4-15
4.4.2.6	Reactor Coolant Flow Distribution at Low Reactor Flows	4.4-17
4.4.2.7	Reactor Pressure Drops and Hydraulic Loads	4.4-19
4.4.2.7.1	Introduction	4.4-19
4.4.2.7.2	Core Assemblies Pressure Drop Correlations	4.4-20
4.4.2.7.3	Reactor Internals Pressure Drop	4.4-24
4.4.2.7.4	Results	4.4-24
4.4.1.7.5	Hydraulic Loads and Hydraulic Balance	4.4-25
4.4.2.8	Correlations and Physical Properties	4.4-26
4.4.2.8.1	Sodium Properties	4.4-26
4.4.2.8.2	Film Heat Transfer Coefficient	4.4-26
4.4.2.8.3	Cladding Thermal Conductivity	4.4-27
4.4.2.8.4	Cladding Linear Thermal Expansion Coefficient	4.4-27
4.4.2.8.5	Fuel and Blanket Assemblies Fuel-Cladding Gap Conductance	4.4-27
4.4.2.8.6	Control Rod Gap Conductance	4.4-29
4.4.2.8.7	Fuel Thermal Conductivity	4.4-32
51 4.4.2.8.8	B ₄ C Thermal Conductivity	4.4-34

TABLE OF CONTENTS Continued

		<u>Page No.</u>
	4.4.2.8.9 B ₄ C Linear Thermal Expansion Coefficient	4.4-35
	4.4.2.8.10 B ₄ C Density	4.4-35
	4.4.2.8.11 Fuel Theoretical Density	4.4-35
	4.4.2.8.12 Fuel Melting Temperature	4.4-35
	4.4.2.8.13 B ₄ C Melting Temperature	4.4-37
	4.4.2.8.14 Fuel Linear Power-To-Melt	4.4-38
	4.4.2.8.15 Fuel Restructuring Parameters	4.4-39
	4.4.2.8.16 Fission Gas Release and Fission Gas Yield	4.4-39
	4.4.2.9 Thermal Effects of Operational Transients	4.4-42
	4.4.2.10 Plant Configuration Data	4.4-44
52	4.4.3 Evaluation	4.4-45
	4.4.3.1 Reactor Hydraulics	4.4-45
	4.4.3.2 Uncertainties Analysis	4.4-46
	4.4.3.2.1 Introduction	4.4-46
	4.4.3.2.2 Power-To-Melt Uncertainties	4.4-52
	4.4.3.2.3 Nuclear Uncertainties	4.4-53
	4.4.3.2.4 Plenum Pressure Uncertainties	4.4-55
	4.4.3.3 Steady State Performance Predictions	4.4-57
	4.4.3.3.1 Plant Conditions	4.4-57
	4.4.3.3.2 Linear Power	4.4-59
	4.4.3.3.3 Assemblies Mixed Mean Temperatures	4.4-59
	4.4.3.3.4 Rod Lifetime Cladding Temperature/Pressure Histories	4.4-61
51	4.4.3.3.5 Core Assemblies Duct Temperatures	4.4-62

TABLE OF CONTENTS Continued

		<u>Page No.</u>
	4.4.3.3.6 Power-To-Melt Analysis	4.4-63
	4.4.3.3.7 Control Assemblies Thermal-Hydraulic Performance	4.4-65
58	4.4.3.3.8 RRS Thermal-Hydraulic Analysis	4.4-66
	4.4.3.4 Analytical Techniques	4.4-67
	4.4.3.4.1 Fuel and Blanket Assemblies	4.4-67
	4.4.3.4.2 Primary Control Assemblies	4.4-72
	4.4.3.5 Hydraulic Instability Analysis	4.4-74
	4.4.3.6 Temperature Transient Effects Analysis	4.4-74
	4.4.3.7 Potentially Damaging Temperature Effects During Transients	4.4-75
52	4.4.3.8 Thermal Description of the Direct Heat Removal Service (DHRS)	4.4-75
	4.4.4 Testing and Verification	4.4-75
	4.4.4.1 Feature Model Test	4.4-76
	4.4.4.2 Reactor Assemblies T&H Testing	4.4-78
	4.4.5 Core Instrumentation	4.4-80
	4.4.5.1 Design Bases	4.4-80
	4.4.5.2 Design Description	4.4-80
54	4.4.5.3 Design Evaluation of Reactor Control Thermocouples	4.4-80a

Table No.

LIST OF TABLES

	4.1-1 Reactor System Design Performance Parameters	4.1-11
	4.2-A Design Procedure for Steady State Creep Analysis	4.2-331
	4.2-B Comparison of Design Lifetime Predicted by Strain Criteria with Actual Lifetime	4.2-332
51	4.2-C 316 Stainless Steel Fretting and Wear Data in Sodium	4.2-333

LIST OF TABLES Continued

		<u>Page No.</u>
4.2-D	Over-Temperature Transient Experiments	4.2-334
4.2-E	Rapid Reactivity Insertion Experiments	4.2-335
4.2-1	Densities of Compounds in the U-Na-O System	4.2-336
4.2-2	Calculated and Experimental Isothermal Oxygen Contents Fuel and Sodium for Fuel Sodium Reaction	4.2-337
4.2-3	Typical Surveillance Examination Plan	4.2-338
4.2-4	Comparison of CRBRP and FFTF Fuel Assembly Details	4.2-339
4.2-5	Nominal Radial Blanket Assembly Design Parameters	4.2-343
4.2-5A	General Plan for Verification of Fuel Design Analysis and Criteria	4.2-345
4.2-6	Deleted	
4.2-7	CRBR Core Assembly Structural Inelastic Criteria and Limits	4.2-347
4.2-8A	Summary of Design Loading Conditions for Fuel Assembly Structural Analysis	4.2-348
4.2-8B	Design Seismic and Core Restraint Loads of the Fuel Assembly ACLP	4.2-349
4.2-8C	Seismic Loads in Vertical Direction	4.2-350
4.2-9	Testing for Load Follow	4.2-351
4.2-10	Steady State CDF Value for the Hot Rod of Blanket Assembly 201 of the First Core	4.2-352
4.2-11	Worst Fuel Assembly Hot Rod Steady State Ductility Limited Strains at Hot Spot	4.2-353

51

LIST OF TABLES Continued

		<u>Page No.</u>
	4.2-11A Characterized Cladding Breach Summary	4.2-354
	4.2-12 Summary of Design Loading Conditions for Blanket Assembly Structural Analysis	4.2-355
	4.2-13 Design Seismic and Core Restraint Loads at the Blanket Assembly ACLP	4.2-356
	4.2-14 EOL Steady State Cladding Strains Due to FCMI and Plenum Pressure	4.2-357
	4.2-15 CRBR First Core Wire Wrap Performance Summary	4.2-358
	4.2-16 Fuel Assembly Bounding Margin of Safety Summary	4.2-359
	4.2-17 Blanket Assembly Bounding Margin of Safety Summary	4.2-360
	4.2-18 Assessment of Applicability of FFTF Design Verification Tests	4.2-361
	4.2-19 Planned CRBRP Fuel Assembly Design Verification Tests	4.2-363
52	4.2-20 Planned CRBRP Blanket Design Verification Tests	4.2-364
	4.2-21 Deleted	4.2-365
	4.2-22 Deleted	4.2-366
	4.2-23 Core Support Structure Stress and Fatigue Damage Summary for Normal and Upset Conditions	4.2-367
	4.2-24 Deleted	4.2-368
	4.2-25 Deleted	4.2-369
	4.2-26 Deleted	4.2-370
	4.2-27 Deleted	4.2-371
59 51	4.2-28 Deleted	4.2-372

LIST OF TABLES Continued

		<u>Page No.</u>
	4.2-29 Deleted	4.2-373
59	4.2-29A BPFM Stress Summary (OBE)	4.2-374
	4.2-29B Deleted	4.2-375
51	4.2-29C Deleted	4.2-376
	4.2-29D Evaluation Summary of the Load Controlled Stresses (For FRS)	4.2-376a
	4.2-29E Results of Load-Controlled Analysis: Lower Support Block	4.2-376b
59	4.2-29F Results of Load-Controlled Analysis: Horizontal Baffle Plate	4.2-376c
	4.2-30 Effect of (C+N) Level on Tensile Properties of Type 304 Stainless Steel	4.2-377
	4.2-31 Effect of (C+N) Level on Tensile Properties of Type 316 Stainless Steel	4.2-378
	4.2-31A Summary of Friction Results for Irradiated Duct Load Pad Material	4.2-379
53	4.2-31B Summary Table of Friction in Sodium	4.2-379a
	4.2-32 Deleted	
	4.2-33 Deleted	
	4.2-34 Results of Dilation Analysis (Mid-Flat Dilation)	4.2-381
	4.2-35 Primary and Secondary Shutdown System Damage Severity Limits	4.2-382
	4.2-36 Control Rod Systems Clearance Requirements	4.2-383
	4.2-36A Friction Coefficients	4.2-387
	4.2-36B Average Friction Coefficients from W-ARD Test Data	4.2-388
59	4.2-36C Summary of Average Friction Coefficients	4.2-391
51		

LIST OF TABLES Continued

		<u>Page No.</u>
4.2-36D	FFTF Prototype Control Rod Systems Tests	4.2-393
4.2-36E	Maximum Effective Coefficient of Friction Data	4.2-394
4.2-37	Control Rod Drive System Maximum Loading Conditions	4.2-395
4.2-37A	Control Assembly - Absorber Pin Structural Criteria	4.2-396
4.2-37B	Control Assembly - Balance of Assembly Structural Criteria	4.2-397
4.2-38	Control Rod Systems Service Life	4.2-399
4.2-39	Nuclear Environment	4.2-400
4.2-40	Grouping of Plant Duty Cycle Events into CRD Umbrella Transients	4.2-401

51

LIST OF TABLES Continued

		<u>Page No.</u>
4.2-41	Comparison of Primary and Secondary Control Rod Systems	4.2-404
4.2-42	Secondary Control Assembly Dimensions	4.2-406
4.2-42A	Primary Control Assembly Dimensions	4.2-407
4.2-43	Primary Control Rod System Lateral Misalignment Forces	4.2-408
4.2-43A	Effects of Worst Case Misalignment Assumption	4.2-409
4.2-44	PCRS Cycle Dependent Withdrawal Positions	4.2-410
4.2-45	Deleted	
4.2-46	Preliminary Performance Parameters for PCA Absorber Pins	4.2-412
4.2-46A	Currently Committed B ₄ C Tests Supporting CRBRP Control Assembly Design	4.2-413
4.2-47	CRDM Design Loading Preliminary Analysis Summary	4.2-414
4.2-48	Comparison Analysis-HEDL Experiments for FFTF Control Assembly	4.2-416
4.2-49	Secondary Control Assembly Operating Parameters (THDV)	4.2-417
4.2-50	AI Frictional Data	4.2-418
4.2-51	Self-Welding Test Results After 3 and 6 Months at 1050°F in Flowing Sodium	4.2-419
4.2-52	References Supporting CRBRP Fuel Rod Loading	4.2-420
4.2-53	Reactor Internals Irradiation Environment and Design Criteria	4.2-421
4.2-54	Post-Irradiation Tensile Properties of Annealed Type 304 Stainless Steel	4.2-423
4.2-55	Post-Irradiation Tensile Properties of Annealed Type 316 Stainless Steel	4.2-429
4.2-56	Tensile Properties of Irradiated Inconel 718	4.2-433

LIST OF TABLES Continued

		<u>Page No.</u>
4.2-57	Irradiated Weld Material Tensile Properties	4.2-435
4.2-58	Deleted	
4.2-59	CRBRP Design Basis Transients to be Enveloped In Fuel Rod Transient Tests	4.2-439
4.2-60	Deleted	
4.2-61	Deleted	
4.2-62	National Reference Fuel Steady-State Program Activities Summary	4.2-441
4.2-63	Deleted	
4.2-64	Design Considerations for Self-Welding and Seizing of Rotating or Moving Parts	4.2-445
4.2-65	CRBRP Fuel Assembly Development Planning	4.2-448
4.2-66	Preliminary Cladding Fatigue Estimate	4.2-458
4.2-67	Design Parameters for 61 Pin Tests	4.2-459
4.2-68	Reactor Internals Thermal Striping Potential, and Striping Factors	4.2-459a
4.2-69	Allowable Striping Metal Temperature Range for 304 and 316 SS Including Mean Strain Effects (<1100°F)	4.2-459c
4.3-1	Reactor Description	4.3-90
4.3-2	Fuel Isotopic Composition	4.3-96
4.3-3	Start-of-Cycle Excess Reactivity Requirement	4.3-97
4.3-4	Heavy Metal Mass (KG) Inventory in the CRBRP	4.3-98
4.3-5	CRBRP Fuel Management Scheme	4.3-104
4.3-6	Delayed Neutron Constants for CRBRP	4.3-105
4.3-7	Fuel and Inner Blanket Power Fraction Summary	4.3-106
4.3-8	Axial Blanket, Axial Extension Power Normalization Factors	4.3-107
4.3-9	Radial Blanket Assembly Power Summary	4.3-108

LIST OF TABLES Continued

		<u>Page No.</u>
4.3-10	Radial Blanket Peak Rod Power Summary	4.3-109
4.3-11	Radial Blanket Power and Burnup History Highest Power Assembly (#1)	4.3-110
4.3-12	Axial Peak-To-Average Power Factors, $F_{\frac{N}{Z}}$	4.3-111
4.3-13	CRBRP Power Distribution Uncertainty (%) Fuel Assemblies	4.3-112
4.3-14	CRBRP Inner Blanket Power Distribution Uncertainty (%)	4.3-113
4.3-15	CRBRP Radial Blanket Power Distribution Uncertainty (%)	4.3-114
4.3-16	CRBRP Doppler Constants	4.3-115
4.3-17	CRBRP Voided Doppler Constants	4.3-116
4.3-18	Nodal Doppler Constants	4.3-117
4.3-19	Temperature Dependence of Doppler Constant	4.3-118
4.3-20	CRBRP Regionwise Sodium Void Reactivity	4.3-119
4.3-21	CRBRP Sodium Density Reactivity Coefficient	4.3-120
4.3-22	CRBRP Axial Expansion Coefficient by Assembly Row	4.3-121
4.3-23	CRBRP Uniform Radial Expansion Coefficients	4.3-122
4.3-24	Radial Motion Reactivity Coefficients (Beginning of Cycle One-Hot Standby)	4.3-123
4.3-25	Radial Motion Reactivity Coefficients (End of Cycle Two-All Rods Out)	4.3-124
4.3-26	CRBRP Inherent Feedback Reactivity (\$) Startup From Hot-Standby Conditions to 40% Power/40% Flow	4.3-125
4.3-27	CRBRP Temperature Defect Components	4.3-126
51 4.3-28	CRBRP Temperature Defect Summary	4.3-127

LIST OF TABLES Continued

		<u>Page No.</u>
	4.3-29 CRBRP Primary Control System Requirements and Minimum Control Worths (% ΔK)	4.3-128
	4.3-30 CRBRP Secondary Control System Requirements and Minimum Control Worths (% ΔK)	4.3-129
	4.3-31 CRBRP Summary of Control Rod Interaction Effects	4.3-132
	4.3-32 Minimum Shutdown Margins (% ΔK) for CRBRP Primary and Secondary Control System	4.3-133
	4.3-33 ZPPR Critical Eigenvalue (K_{eff}) Predicted by CRBRP Design Method and Data	4.3-134
59	4.3-34 Maximum Parameter Values During a Reactor Inherent Response Transient at a Reactor Startup Operating Point (9% Power, 40% Flow)	4.3-135
	4.3-35 Ex-Core Neutron Flux at Beginning of Cycle Three	4.3-136
	4.3-36 Group Structure of 30, 21, and 9 Group Sets	4.3-137
52	4.3-37 Comparisons of W-ARD Calculations with Pin and Plate Measurements	4.3-138
	4.3-38 ZPPR-4 Critical Eigenvalue Predicted with CRBRP Design Method and Data	4.3-139
	4.3-39 ZPPR-4 Reaction Rate Summary	4.3-140
	4.3-40 ZPPR-4 Control Rod Worths	4.3-141
	4.3-41 ZPPR-7 & 8 Critical Eigenvalue Predicted with CRBRP Design Method and Data	4.3-142
	4.3-42 ZPPR-7 Reaction Rate Summary	4.3-143
	4.3-43 ZPPR-7 Control Rod Worth Calculation-To-Experiment Ratios	4.3-144
51	4.3-44 Comparison of Nuclear Parameters for CRBRP and FFTF	4.3-145

Amend. 59
Dec. 1980

LIST OF TABLES Continued

		<u>Page No.</u>
4.3-45	Comparison of Reactivity Coefficients for CRBRP and FFTF	4.3-149
4.4-1	CRBRP Core Loading During Cycles 1 Through 5	4.4-87
4.4-2	Summary of Strain Equivalent Limiting Temperature Calculations for Second Core Fuel Assemblies	4.4-88
4.4-3	Coolant Limiting Temperatures for Telt Calculations	4.4-89
4.4-4	Core Orificing Zones Flow Allocation	4.4-90
4.4-5	Fuel Assembly Component Pressure Drop Data Linear Regression Analysis	4.4-91
4.4-6	Fuel Assembly Component Hydraulic Correlations	4.4-92
4.4-7	Blanket Assemblies Component Hydraulic Correlations	4.4-93
4.4-8	Bases for Reactor Internals Pressure Drops	4.4-94
52 4.4-9	Detailed Pressure Drop Breakdown and Plant THDV Conditions (41.446×10^6 lb/hr) and Maximum Uncertainties	4.4-95
4.4-10	Melting Temperatures for Unirradiated Mixed Urania -Plutonia	4.4-96
4.4-11	Effects of Burnup on Melting Point of Mixed Urania -Plutonia	4.4-97
4.4-12	Principal Parameters of EBR-II Irradiated Pins Used to Calibrate Fission Gas Release Model	4.4-98
4.4-13	Principal Parameters of EBR-II Irradiated High-Burnup Pins Used to Verify Fission Gas Release Model	4.4-99
51 4.4-14	Principal Parameters of EBR-II Irradiated Pins at High Cladding Temperature Used to Verify Fission Gas Release Model	4.4-100

LIST OF TABLES Continued

	<u>Page No.</u>
4.4-15	ENDF/B-IV Fission Yields (Gaseous Xe + Kr) 4.4-101
4.4-16	Event Classification and Cladding Damage Severity Limit 4.4-102
4.4-17	Summary of Preliminary Design Criteria 4.4-103
4.4-18.A	CRBR Fuel Assemblies Rod Temperature Engineering Uncertainty Factors 4.4-104
4.4-18.B	CRBR Fuel Assemblies Rod Temperature Nuclear Uncertainty Factors With and Without Control Assembly Influence 4.4-105
4.4-19.A	CRBR Fuel Assemblies Mixed Mean Exit Temperature Engineering Uncertainty Factors 4.4-106
4.4-19.B	CRBR Fuel Assemblies Mixed Mean Exit Temperature Nuclear Uncertainty Factors 4.4-107
4.4-20.A	CRBR Fuel Assemblies Plenum Pressure Engineering Uncertainty Factors 4.4-108
4.4-20.B	CRBR Fuel Assemblies Plenum Pressure Nuclear Uncertainty Factors With and Without Control Assembly Influence 4.4-109
4.4-21.A	CRBR Inner/Radial Blanket Assemblies Rod Temperature Engineering Uncertainty Factors 4.4-110
4.4-21.B	CRBR Inner/Radial Blanket Assemblies Rod Temperature Nuclear Uncertainty Factors 4.4-111
4.4-22.A	CRBR Inner/Radial Blanket Assemblies Mixed Mean Exit Temperature Engineering Uncertainty Factors 4.4-112
4.4-22.B	CRBR Inner/Radial Blanket Assemblies Mixed Mean Exit Temperature Nuclear Uncertainty Factors 4.4-113
4.4-23.A	CRBR Inner/Radial Blanket Assemblies Plenum Pressure Engineering Uncertainty Factors 4.4-114
4.4-23.B	CRBR Inner/Radial Blanket Assemblies Plenum Pressure Nuclear Uncertainty Factors 4.4-115
4.4-24	CRBRP Primary Control Assemblies Pin Temperatures Hot Channel/Spot Factors 4.4-116

LIST OF TABLES Continued

		<u>Page No.</u>
4.4-25	CRBRP Primary Control Assemblies Mixed Mean Exit Temperature Hot Channel Factors	4.4-117
4.4-26	CRBRP Primary Control Assemblies Plenum Pressure Hot Channel Factors	4.4-118
4.4-27	CRBRP Secondary Control Assemblies Pin Temperatures Hot Channel/Spot Factors	4.4-119
4.4-28	CRBR Expected Operating Conditions During Plant Lifetime	4.4-120
4.4-29	Plant Expected Conditions and Associated Uncertainties Considered on CRBRP Core Thermo-Fluids Analysis	4.4-121
4.4-30	Center Temperature and Power-To-Melt of Incipient Melt Sections as Computed by Life-3	4.4-122
4.4-31	Comparison of 3 Minimum Power-To-Melt to Power at 15% Overpower	4.4-123
4.4-32a	Primary Control Assembly Operating Parameters	4.4-124
4.4-32b	Secondary Control Assembly Operating Parameters	4.4-124a
4.4-33	Summary of Flotation Evaluation	4.4-125
4.4-34	RRSA Power and Flow Uncertainty Factors	4.4-126
4.4-35	Lifetime Variation of Nominal Mixed Mean Temperature of Selected Assemblies and Average Temperature Used for Reactor Control	4.4-126a
4.4-36	Experimental Data References for Flow Distribution Calculations at Low Flow (Section 4.4.2.6)	4.4-126b

LIST OF FIGURES

<u>Figure No.</u>		
4.2-1	Creep-Rupture Data for 20% C.W. 316 Stainless Steel Tubes	4.2-460
4.2-1A	Stress Biaxiality Rupture Strain Factor	4.2-461
4.2-1B	Effect of Degradation on Damage Accumulation	4.2-462
4.2-2	Creep Rupture Data for 20% C.W. 316 S.S. Irradiated to 3×10^{22} nvt at $525 \pm 25^\circ\text{C}$	4.2-463

LIST OF FIGURES Continued

		<u>Page No.</u>
4.2-2A	Bilinear Stress-Strain Relationship for Cladding Strain Criterion	4.2-463a
4.2-2B	Comparison of Assumed Values to Experimental Ultimate Stress for Dynamic Cladding Loading	4.2-463b
4.2-3	Design Basis Stress Free Swelling Equation for 20% C.W. Type 316 Stainless Steel	4.2-464
4.2-4	Design Basis Stress Enhanced Swelling and Irradiation Creep for 20% C.W. Type 316 Stainless Steel	4.2-465
4.2-5	Isothermal Section of the Na-U-O Phase Diagram at About 800°C	4.2-467
4.2-6	Oxygen Potentials for UO_{2+x} System	4.2-468
4.2-7	Oxygen Potentials for (U, Pu) O_{2+x} as a Function of Metal Valence and Temperature	4.2-469
4.2-8	Variation of O/M With Burnup $(U_{0.75}Pu_{0.25})O_{2x}$	4.2-470
4.2-9	Maximum Swelling Observed as a Function of the Oxygen Available for Reaction	4.2-471
4.2-9A	Conditions Partitioning the CS_2UO_4 and CS_2MoO_4 Reactions in CRBRP	4.2-472
4.2-9B	As-Fabricated Smeared Density and O/M Ratio for UO_2 Pellets Required to Preclude Severe Mechanical Interaction With Cladding	4.2-473
4.2-10A	Core Layout	4.2-474
4.2-10B	Assembly Numbering Scheme	4.2-475
4.2-11	Fuel Assembly Schematic	4.2-476
4.2-11A	Fuel Assembly Holddown System	4.2-477
4.2-12	Fuel Rod Assembly	4.2-478
4.2-12A	Determination of Wire Wrap Diameter	4.2-479
4.2-13	Blanket Rod Assembly Schematic	4.2-480
4.2-14	Radial Blanket Assembly Schematic	4.2-481

LIST OF FIGURES Continued

		<u>Page No.</u>
4.2-15	Fuel and Inner Blanket Assembly Discriminator Diameters	4.2-482
4.2-16	Startup Procedures	4.2-483
4.2-17A	F/A 10 Hot Rod Total Cladding Design Pressure vs. Time, First Core	4.2-484
4.2-17B	F/A 14 Hot Rod Total Cladding Design Pressure vs. Time, First Core	4.2-485
4.2-17C	IB/A 67 Hot Rod Total Cladding Design Pressure	4.2-486
4.2-17D	RB/A 201 Hot Rod Total Cladding Design Pressure	4.2-487
4.2-18	Cumulative Mechanical Damage Function Due to Steady-State Operation Top of the Fuel Stack in Hot Pin in a Typical Fuel Rod	4.2-488
4.2-19	Umbrella Transients for Fuel Rod Cladding Upset Event for Example Calculation	4.2-489
4.2-20	Umbrella Transient for Fuel Rod Cladding Emergency Event for Example Calculation	4.2-490
4.2-21	Loss of Flow Transient Limit Curve for Example Fuel Rod CDF Analysis Problem	4.2-491
4.2-22	Transient Limit Curve for Fast Reactivity Insertion Emergency Events: Fuel Cladding Contact Pressure and Inner Wall Temperature to Cause Failure During Transient Example Fuel Rod CDF Analysis Problem	4.2-492
4.2-23	Cumulative Mechanical Damage Function Due to Steady-State Operation, Upset Events and a Natural Circulation Emergency Event, Example Fuel Rod CDF Analysis Problem	4.2-493
4.2-24	Comparison of FCMI for Various Startup Procedures	4.2-494
4.2-24E	Enveloping Transient Fuel Rod Temperature Due to U-2b Event	4.2-495
4.2-24F	Fuel Rod Enveloping Emergency Undercooling Transient Temperature History	4.2-496

LIST OF FIGURES Continued

		<u>Page No.</u>
4.2-24G	Variation of Maximum Cladding Temperatures of Inner Blanket Assembly for U-2b Transient	4.2-497
4.2-24H	Variation of Maximum Cladding/Coolant Temperatures of Inner Blanket Assembly for E-16 Transient	4.2-498
4.2-24I	Variation of Maximum Cladding Temperatures of Radial Blanket Assembly for U-2b Transient	4.2-499
4.2-24J	Variation of Maximum Cladding/Coolant Temperatures of Radial Blanket Assembly for E-16 Transient	4.2-500
4.2-25	Steady State CDF at End-of-Life for Hot Rod in Each Fuel Assembly	4.2-501
53 4.2-26	Deleted	4.2-502
4.2-26A	Transient Limit Curve for Fuel Assembly 14 Hot Rod, Hot Spot Location	4.2-503
4.2-26B	Transient Limit Curve for F/A 14 Hot Rod, X/L = 0.75	4.2-504
4.2-27	End-of-Life CDF at the Hot Spot of Each Blanket Assembly Hot Rod-Steady State Plenum Gas Pressure Loads Only	4.2-505
4.2-28A	Blanket Assembly 67 Transient Limit Evaluation	4.2-506
4.2-28B	Radial Blanket Assembly 201 Transient Limit Evaluation	4.2-507
4.2-29	Model for Duct Swelling Calculation	4.2-508
4.2-30	Deflected Shape of the Duct after Irradiation Creep and Swelling	4.2-509
4.2-31A	Maximum Duct Radial Dilatation Across Flats Versus Axial Location at End-of-Life, For F/A 45	4.2-510
51 4.2-31B	Duct Dilatation vs. Axial Height for IB/A 67 and RB/A 201	4.2-511

LIST OF FIGURES Continued

		<u>Page No.</u>
4.2-32	Maximum Fuel Rod Bundle-Duct Diametral Clearance and Interference vs Time - F/A 45, First Core	4.2-512
4.2-33	Maximum CRBR Blanket Assembly Bundle-Duct Interference and Clearance vs Time	4.2-513
4.2-33A	Designation Scheme for Seismic and Core Restraint Loads	4.2-514
4.2-33B	F/A Shield Block Thermal/Mechanical Model Dimensional Extents and Finite Element Detail	4.2-515
4.2-34	LMFBR Fuel Development Steady-State Irradiation Testing Program	4.2-516
4.2-35	Number of Fuel Rods Exceeding FFTF/CRBRP Goal Burnup	4.2-517
4.2-35a	Design Fallback Positions	4.2-518
4.2-36	Reactor Elevation	4.2-519
4.2-37	304 Stainless Steel Core Support Structure	4.2-520
4.2-38	Core Module Liner	4.2-521
4.2-39	Core Support Structure Secondary Plenum Concept	4.2-522
4.2-40	Elevation of Typical Lower Inlet Module	4.2-523
4.2-41	Inlet Module Core Map Showing the Orificing Plan for the Compactor Assemblies	4.2-524
4.2-41A	Bypass Flow Module Assembly	4.2-525
4.2-41B	Bypass Flow Module Section View	4.2-526
4.2-42	The Fixed Radial Shielding	4.2-527
4.2-43	Removable Radial Shield Assembly	4.2-528
4.2-43A	Loading Histogram used in Inelastic Analysis of RRS ACLP	4.2-528a

LIST OF FIGURES Continued

		<u>Page No.</u>
4.2-44	Horizontal Baffle	4.2-529
4.2-45	Elevation of the UIS in the CRBRP	4.2-530
4.2-45A	Instrumentation Post (Bench Assembly)	4.2-531
4.2-45B	Method of Positioning Control Rod Shroud Tube	4.2-532
4.2-45C	Instrumentation Post Installation	4.2-533
4.2-45D	Instrumentation Post Installation	4.2-534
4.2-46	Core Former Structure	4.2-535
4.2-47	Limited Free Bow Core Restraint Concept	4.2-536
4.2-47A	Creep-Fatigue Damage Envelope	4.2-536a
4.2-48	Design Fatigue Curve for Nickel-Chromium Alloy 718	4.2-537
4.2-48A	Corrosion Rate of Types 304 and 316 Stainless Steel in Flowing Sodium	4.2-538
4.2-48B	Corrosion Rate of Inconel 718 in Sodium	4.2-539
4.2-48C	Design Factor for Estimating the Decrease in Rupture Strength of Type 316 Stainless Steel from Surface Interactions with Sodium	4.2-540
4.2-48D	Deleted	
4.2-48E	Deleted	
4.2-48F	Deleted	
4.2-48G	Calculation of Stress-Strain Curves for Type 304 and 316 Stainless Steel	4.2-544
4.2-48H	Deleted	
4.2-48I	Effect of Carbon and Nitrogen Concentration on the Fatigue Strength of Type 316 Stainless Steel at Room Temperature	4.2-546
4.2-48J	Deleted	

LIST OF FIGURES Continued

		<u>Page No.</u>
4.2-48K	Effect of Carbon Concentration on the Fatigue Strength of Type 316 Stainless Steel at 1200°F	4.2-548
4.2-48L	Decrease in Yield Strength of Type 316 SS as a Function of Decrease in (C + N) Concentration	4.2-548a
4.2-48M	Decrease in Tensile Strength of Type 316 SS as a Function of Decrease in (C + N) Concentration	4.2-548b
4.2-49	Design Fatigue Strength (10^8 Cycles or More) for Alloy 718	4.2-549
4.2-50	Core Support Structure (CSS)	4.2-550
4.2-51	Core Support Structure Axisymmetric Thermal Stress Model	4.2-551
4.2-52	Identifying Cut Numbers In Sector of the Lower Support Structure Central Region	4.2-552
4.2-53	LIM Liner Finite Element Stress Model with Key Structural Evaluation Sections	4.2-553
4.2-54	Core Support Structure Seismic and Deadweight Model	4.2-554
4.2-55	Deleted	4.2-555
4.2-56	Deleted	4.2-556
4.2-57	Deleted	4.2-557
4.2-58	Deleted	4.2-558
4.2-59	Deleted	4.2-559
4.2-60	Deleted	4.2-560
4.2-61	Deleted	4.2-561
4.2-62	Deleted	4.2-562

LIST OF FIGURES Continued

		<u>Page No.</u>
4.2-63	Deleted	4.2-563
4.2-63A	One-Eighth BPFM 3-D Finite Element Thermal Molded Geometry	4.2-564
4.2-63B	BPFM Critical Sections in the One-Eight BPFM 3-D Finite Element Stress Module	4.2-565
4.2-64	Deleted	
4.2-65	Deleted	
4.2-66	Deleted	
4.2-67	Deleted	4.2-567

LIST OF FIGURES Continued

Page No.

53	4.2-68	Deleted	
	4.2-69	Deleted	
	4.2-70	Deleted	
	4.2-71	Deleted	
	4.2-72	Deleted	
	4.2-73	Deleted	
	4.2-74	Deleted	
	4.2-75	FRS Computer Model W/8 Node Isoparametric Elements	4.2-574a
	4.2-76	Finite Element Model of FT and SA Assembly	4.2-574b
	4.2-77	Heat Transfer Coefficient Regions for the CFS	4.2-574c
	4.2-78 thru 4.2-83	Deleted	
	4.2-84	CRBRP Core Restraint System	4.2-576
	4.2-85	Schematic View of Reactor Core Showing Sector of Core Simulated in NUBOW-3D Model	4.2-577
	4.2-86	Deleted	
59	4.2-87	Deleted	
	4.2-87A	Illustration of Effects of Core Thermal and Flux Gradients in Radial Blanket Rod	4.2-580
	4.2-88	On-Power Bow Shapes at SOC1	4.2-581
	4.2-89	On-Power Bow Shapes at EOC2	4.2-582
	4.2-90	On-Power Forces and Displacement at the Above Core Load Plane at Start of Cycle 1	4.2-583
	4.2-91	Deleted	

LIST OF FIGURES Continued

		<u>Page No.</u>
59	4.2-92 Deleted	4.2-585
	4.2-92A Bowing Displacements and Reactivity Change Versus Power to Flow Ratio	4.2-586
	4.2-92B Bowing Reactivity vs. Power-to-Flow Ratio at 40% Flow at Various Times in Fuel Assembly Life	4.2-587
59	4.2-92C Bowing Reactivity Versus Power-to-Flow Ratio	4.2-587a
	4.2-93 PCRS Scram Insertion Requirements for the Heterogeneous Core	4.2-588
	4.2-93A Calculated Axial Profile of B_4C Captures in the Secondary Control Assembly	4.2-589
	4.2-94 Secondary Control Rod System Minimum SCRAM Insertion Requirements	4.2-590
	4.2-95A Control Rod System Operating Misalignment Envelope	4.2-591
	4.2-95B Control Rod System Refueling Misalignment Envelope	4.2-592
	4.2-96 Control Rod Driveline 30 Year Histogram	4.2-593
	4.2-97 Reactor Steady State Thermal Environment	4.2-594
	4.2-97A Exposure Time Required to Cause Room Temperature Toughness to Fall Below 15 Ft. Lbs.	4.2-595
	4.2-97B Exposure Time Required to Deplete Room Temperature Toughness by One Half	4.2-596
	4.2-98 Control Rod Systems - Reactor Elevation	4.2-597
	4.2-99 Deleted	
	4.2-100 Primary Mechanical Sub-System	4.2-599
	4.2-101 Primary Control Rod Drive Mechanism (PCRD) Upper CRDM Assembly and Extension Nozzle	4.2-600
51	4.2-102 Lower CRDM Assembly Extension Nozzle and Upper Shroud Tube	4.2-601

LIST OF FIGURES Continued

		<u>Page No.</u>
	4.2-103 Lower CRD Assembly, Extension Nozzle and Lower Shroud Tube	4.2-602
	4.2-104 Primary Control Assembly (PCA)	4.2-603
	4.2-105 Secondary Control Rod System Schematic	4.2-604
	4.2-106 Secondary Control Assembly (SCA)	4.2-605
	4.2-107 Secondary Control Rod Driveline (SCRD)	4.2-606
	4.2-108 Secondary Control Rod Drive Mechanism (SCRDM)	4.2-607
	4.2-109 Lateral Misalignment Load Model	4.2-608
	4.2-110 Predicted Inner/Outer Duce Bow-PCA	4.2-609
	4.2-110A PCA Clearance (Lateral Displacement Due to Thermal and Radiation Bowing Row 7 Corner for 1 Cycle)	4.2-610
	4.2-111 Primary Control Assembly Duct Bowing Configuration	4.2-611
	4.2-111A Pellet Swelling and Clad Gap	4.2-612
	4.2-111B Primary Control Rod Axial Burnup Profile	4.2-613
	4.2-112 Primary Control Rod System Scram Insertion Distance vs. Time	4.2-614
	4.2-113 Comparison Analysis Tests for FFTF Control Assembly (Misaligned Conditions)	4.2-615
	4.2-114 Preliminary PCRS Scram Insertion Performance (Non-Seismic)	4.2-616
	4.2-115 Deleted	
	4.2-116 Deleted	4.2-618
53	4.2-117 Deleted	4.2-619
	4.2-118 Typical PCRS Total Contact Forces vs. Time During SSE	4.2-620
	4.2-119 Heterogeneous Core PCRS SSE Seismic Scram Predicted Performance	4.2-621
51	4.2-120 Absorber Assembly Scram Impact Dynamic Model	4.2-622

LIST OF FIGURES Continued

		<u>Page No.</u>
4.2-120A	CRDM Primary Pressure Boundary Seals	4.2-623
4.2-121	SCRS Rod Displacement vs. Time	4.2-624
4.2-122	Deleted	
4.2-123	Deleted	
4.2-124	Deleted	
4.2-125	Collet Type Latch	4.2-628
4.2-126	Total Actuation Force vs. Friction Coefficient	4.2-629
4.2-127	Deleted	
4.2-128	Typical Sequence for Reference Fuel Transient Testing	4.2-631
4.2-129	Porosity/Fuel Rod Ring Histories for Experimental and CRBR Fuel Assemblies	4.2-632
4.3-1	Clinch River Breeder Reactor Core Layout	4.3-150
4.3-2	Power Distribution Computational Method	4.3-151
4.3-3	CRBRP Assembly Numbering Scheme	4.3-152
4.3-4	Peak and Average Radial Power Factors BOC1	4.3-153
4.3-5	Peak and Average Radial Power Factors EOC1	4.3-154
4.3-6	Peak and Average Radial Power Factors BOC2	4.3-155
4.3-7	Peak and Average Radial Power Factors EOC2	4.3-156
4.3-8	Peak and Average Radial Power Factors BOC3	4.3-157
4.3-9	Peak and Average Radial Power Factors EOC3	4.3-158
4.3-10	Peak and Average Radial Power Factors BOC4	4.3-159
4.3-11	Peak and Average Radial Power Factors EOC4	4.3-160
4.3-12	Peak and Average Radial Power Factors BOC5	4.3-161

LIST OF FIGURES Continued

		<u>Page No.</u>
	4.3-13 Peak and Average Radial Power Factors EOC5	4.3-162
	4.3-14 Peak and Average Radial Power Factors BOC6	4.3-163
	4.3-15 Peak and Average Radial Power Factors EOC6	4.3-164
52	4.3-16 Normalized Axial Power Distribution Clean Fuel Zones (Power Normalized To 1.0 Over 92.04 cm Core Height)	4.3-165
	4.3-17 Normalized Axial Power Distribution Fuel Zones With Control Rod Influence (Power Normalized to 1.0 Over 92.04 cm Fuel Height)	4.3-166
	4.3-18 Normalized Axial Power Distribution Inner Blanket Rows 2,4 (Power Normalized to 1.0 Over 92.04 cm Central Region)	4.3-167
	4.3-19 Normalized Axial Power Distribution Inner Blanket Rows 6,8 (Power Normalized to 1.0 Over 92.04 cm Central Region)	4.3-168
	4.3-20 Normalized Axial Power Distribution Radial Blanket (Power Normalized to 1.0 Over 92.04 cm Central Region)	4.3-169
	4.3-21 Normalized Axial Power Distribution, Axial Blankets (Typical)	4.3-170
	4.3-22 Peak Linear Power Distribution (KW/FT)	4.3-171
	4.3-23 Peak and Average Rod Burnup (MWD/KG) Cycles 1-2	4.3-172
	4.3-24 Peak and Average Rod Burnup (MWD/KG) Cycles 3-4	4.3-173
	4.3-25 Peak and Average Rod Burnup (MWD/KG) Cycles 5-6	4.3-174
	4.3-26 Flow Chart for Doppler Calculations	4.3-175
	4.3-27a CRBRP Doppler Constant by Assembly-Beginning of Cycle One	4.3-176
51	4.3-27b CRBRP Doppler Constant by Assembly - End-of-Cycle Four	4.3-177

LIST OF FIGURES Continued

		<u>Page No.</u>
4.3-28	Flow Chart for Sodium Voiding Reactivity Worth Calculations	4.3-178
4.3-29a	CRBRP Sodium Void Worth by Assembly - Beginning-of-Cycle One	4.3-179
4.3-29b	CRBRP Sodium Void Worth by Assembly - End-of-Cycle Four	4.3-180
4.3-30	Radial Row Numbering Scheme for CRBRP Bowing Model	4.3-181
4.3-31	Control Worth Computational Sequence	4.3-182
4.3-32	Control Rod Interaction Effects as a Function of Depth of Insertion of the Row 7 Corner PCA Bank at Beginning of Life	4.3-183
4.3-33	Control Rod Integral Worth	4.3-184
4.3-34	Control Rod Bank Withdrawal History - Cycle 1,2	4.3-185
4.3-35	Control Rod Bank Withdrawal History - Cycle 3,4	4.3-186
4.3-36	Deleted	
4.3-37	Deleted	
4.3-38	Deleted	
4.3-39	Deleted	
4.3-40	Criticality of Fuel Assemblies (Immersed in Sodium and in Air)	4.3-188
4.3-41	Schematic of Feedback Effects	4.3-189
4.3-42	Transfer Functions for Various Feedback Reactivities	4.3-190
4.3-43	Transfer Functions for Various Feedback Reactivities	4.3-191
4.3-44	Transfer Functions for Various Feedback Reactivities	4.3-192

LIST OF FIGURES Continued

		<u>Page No.</u>
59	4.3-45 Deleted	4.3-193
	4.3-46 Reactor Power Response to Inherent Reactivity Feedback Following a 2¢ Step Insertion	4.3-194
59	4.3-47 Base Core Maximum Fuel Temperature Response To Inherent Reactivity Feedbacks Following a 2¢ Step Insertion	4.3-195
59	4.3-48 Base Core Maximum Cladding Temperature Response to Inherent Reactivity Feedbacks Following a 2¢ Step Insertion	4.3-196
59	4.3-49 Base Case Maximum Coolant Temperature Response to Inherent Reactivity Feedbacks Following a 2¢ Step Insertion	4.3-197
	4.3-50 Assembly Average (36 Inch) Total Flux (10^{15} n/cm ² sec) and Fast Flux Fraction at the Beginning of Cycle One	4.3-198
	4.3-51 Assembly Average (36 Inch) Total Flux (10^{15} n/cm ² sec) and Fast Flux Fraction at the End of Cycle Four	4.3-199
	4.3-52 Axial Distribution of the Total Flux in Clean Fuel at the SOCl and EOC4	4.3-200
	4.3-53 Axial Distribution of the Fast Flux Fraction in Clean Fuel at the SOCl and EOC4	4.3-201
	4.3-54 Calculational Scheme for Analysis of CRBRP	4.3-202
	4.3-55 Calculational Scheme for Evaluation of ZPPR Critical Experiments	4.3-203
	4.3-56 Pin Zones and Central Plate and Pin Cells for ZPPR-2	4.3-204
	4.3-57 Core Layout for ZPPR-3, Phases 1B, 2 and 3	4.3-205
	4.3-58 Reference 632 Drawer Sodium Void Configuration for the Modified Phase 3 Core of ZPPR Assembly 3	4.3-206

51

LIST OF FIGURES Continued

		<u>Page No.</u>
4.3-59	ZPPR-3, Modified Core, Two-Dimensional (R,Z) Calculation Model	4.3-207
4.3-60	Measured Sodium Void Reactivity Effect in ZPPR-3 Modified Phase 3 as a Function of the Void Radius	4.3-208
4.3-61	Sodium Void Worths in ZPPR-3, Phase 3	4.3-209
4.3-62	Sodium Void Worths in ZPPR-3, Phase 3 Modified Core	4.3-210
4.3-63	ZPPR Assembly 4 Phase 1 Reference Configuration	4.3-211
4.3-64	ZPPR-7&8 Heterogeneous Core Layout	4.3-212
4.3-65	ZPPR-7 Phase B Midplane Calculated-To-Experimental Ratios for ^{239}Pu (n,f)	4.3-213
4.3-66	ZPPR-7 Phase C Midplane Calculated-To-Experimental Ratios for ^{239}Pu (n,f)	4.3-214
4.4-1	Typical Axial Temperature Profile in CRBRP Fuel Rod	4.4-127
4.4-2	CRBRP Flows and Hydraulic Loads	4.4-128
4.4-3	Inlet Module Map, Showing Orificing Requirements of Reactor Assemblies	4.4-129
4.4-4	Modular CSS Assembly: Flow Paths	4.4-130
4.4-5	Elevation of Typical Lower Inlet Module	4.4-131
4.4-6	Lower Core Support Plate Low Pressure Manifold System	4.4-132
4.4-7	Radial Shield Orificing Flow Path	4.4-133
4.4-8	Upper Internals Structure Concept Feature	4.4-134
4.4-9	CRBRP Core 60° Symmetry Sector and Assemblies Numbering Scheme	4.4-135
4.4-10	Typical DELT Determination for First Core Fuel Assemblies	4.4-136

LIST OF FIGURES Continued

		<u>Page No.</u>
	4.4-11 Typical DELT Determination for First Core Inner Blanket Assemblies	4.4-137
	4.4-12 Typical DELT Determination for Second Core Fuel Assemblies	4.4-138
	4.4-13 Typical DELT Determination for Second Core Inner Blanket Assemblies	4.4-139
	4.4-14 Typical DELT Determination for Radial Blanket Assemblies	4.4-140
	4.4-15 Individual Assemblies Limiting Temperatures at First Core	4.4-141
	4.4-16 Individual Assemblies Limiting Temperatures at Second Core	4.4-142
	4.4-17 Individual Assemblies Minimum Flow Rates at First and Second Core Necessary to Satisfy the Constraints	4.4-143
	4.4-18 Core Orificing Scheme	4.4-144
	4.4-19 DELETED	4.4-145
	4.4-20 DELETED	
	4.4-21 DELETED	
	4.4-22 DELETED	
54	4.4-23 DELETED	
51	4.4-24 Typical CRBR Fuel Assembly Orifice Stack Cavitation Data	4.4-150

LIST OF FIGURES Continued

	<u>Page No.</u>
4.4-25 Fuel Assembly Inlet Nozzle-Orifice-Shield- Pressure Drop for Orifice Hole Velocity Limit of 40 Ft./Sec.	4.4-151
4.4-26 Map of CRBRP Lower Inlet Modules (1/3 Symmetry Sector)	4.4-152
4.4-27 Phase Diagram for UO_2 - PuO_2	4.4-153
4.4-28 Effect of Burnup on Melting Point of $(U,Pu)O_{2-x}$	4.4-154
4.4-29 Power-To-Melt/Cold Gap Size Relationship from P-19 Data and Uncertainty Band	4.4-155
4.4-30 Comparison of Measured and Predicted Fission Gas Release	4.4-156
4.4-31 Graphical Illustration of Semi-Static Method	4.4-157
4.4-32 Core Assemblies Linear Power Ratings @ BOC1	4.4-158
4.4-33 Core Assemblies Linear Power Ratings @ EOC4	4.4-159
4.4-34 Core Assemblies Mixed Mean Outlet Temperature at BOC1	4.4-160
4.4-35 Core Assemblies Mixed Mean Outlet Temperature at EOC4	4.4-161
4.4-36 Lifetime Cladding Temperature/Pressure History in Fuel Assembly #10, First Core, Orifing Zone 1	4.4-162
4.4-37 Lifetime Cladding Temperature/Pressure History in Fuel Assembly #101, Second Core, Orifing Zone 1	4.4-163
4.4-38 Lifetime Cladding Temperature/Pressure History in Fuel Assembly #2, Second Core, Orifing Zone 3	4.4-164
4.4-39 Lifetime Cladding Temperature/Pressure History in in Fuel Assembly #52, First Core, Orifing Zone 4	4.4-165
4.4-40 Lifetime Cladding Temperature/Pressure History in Assembly #98, First Core, Orifing Zone 6, Row 6 Alternating Position	4.4-166

LIST OF FIGURES Continued

		<u>Page No.</u>
4.4-41	Lifetime Cladding Temperature/Pressure History in Assembly#62 Second Core, Orificing Zone 6, Row 6 Alternating Position	4.4-167
4.4-42	Lifetime Cladding Temperature/Pressure History in Inner Blanket Assembly #99, Second Core, Orificing Zone 7	4.4-168
4.4-43	Lifetime Cladding Temperature/Pressure History in Radial Blanket Assembly #201, Orificing Zone 9	4.4-169
4.4-44	Lifetime Cladding Temperature/Pressure History in Radial Blanket Assembly #212, Orificing Zone 12	4.4-170
4.4-45	Envelope of Assemblies Maximum Cladding ID Temperature at Plant Expected Conditions During the First Core and Time of Occurrence	4.4-171
4.4-46	Envelope of Assemblies Maximum Cladding ID Temperature at Plant Expected Conditions During the Second Core and Time of Occurrence	4.4-172
4.4-47	Core Wide Duct Midwall Temperatures at 60" Elevation, BOC1, Under Nominal Conditions	4.4-173
4.4-48	Core Wide Duct Midwall Temperatures at 112" Elevation, BOC1, Under Nominal Conditions	4.4-174
4.4-49	Core Wide Duct Midwall Temperatures at 60" Elevation, EOC4, Under Nominal Conditions	4.4-175
4.4-50	Core Wide Duct Midwall Temperatures at 112" Elevation, EOC4, Under Nominal Conditions	4.4-176
4.4-51	Comparison of Assemblies Mixed Mean Exit Temperatures Under Adiabatic Conditions and Including Inter-Assembly Heat Transfer Effects at BOC1	4.4-177
4.4-52	Comparison of Assemblies Mixed Mean Exit Temperature Under Adiabatic Conditions and Including Inter-Assembly Heat Transfer Effects at EOC4	4.4-178
4.4-53	Power History (Programmed Startup) Used in Fuel Assemblies Power-To-Melt Analyses	4.4-179

LIST OF FIGURES Continued

		<u>Page No.</u>
4.4-54	Typical 10.5-Inch Withdrawn C/R Absorber Axial Temperatures	4.4-180
4.4-55	Typical 36-Inch Withdrawal C/R Absorber Axial Temperatures	4.4-181
4.4-55a	Typical Fully Withdrawn Secondary Control Rod Absorber Axial Temperatures Under THDV Conditions at 115% Overpower	4.4-181a
4.4-56	Two Zone Orificing Scheme of Removable Radial Shield Assemblies	4.4-182
4.4-57	Removable Radial Shield Duct Midwall Temperatures at Core Midplane (+2 RRS Uncertainties)	4.4-183
4.4-58	Removable Radial Shield Duct Midwall Temperatures at Above Core Load Pad (+2 RRS Uncertainties)	4.4-184
4.4-59	Removable Radial Shield Duct Midwall Temperature at Top Core Load Pad (2+ RRS Uncertainties)	4.4-185
4.4-60	Removable Radial Shield Duct Midwall Temperatures at Core Midplane (-2 RRS Uncertainties)	4.4-186
4.4-61	Removable Radial Shield Duct Midwall Temperatures at Above Core Load Pad (-2 RRS Uncertainties)	4.4-187
4.4-62	Removable Radial Shield Duct Midwall Temperatures at Top Core Load Pad (-2 RRS Uncertainties)	4.4-188
4.4-63	Fuel and Blanket Assemblies Thermal-Hydraulic Analysis Flow Diagram	4.4-189
4.4-64	Control Assembly and Absorber Pin Thermal-Hydraulic Analysis Flow Diagram	4.4-190
4.4-64a	Secondary Control Assembly and Absorber Pin Thermal-Hydraulic Analysis Flow Diagram	4.4-190a
4.4-65	CRBRP Heterogeneous Core Exit Thermocouples Coverage	4.4-191
4.4-66	Typical Inter-Assembly Flow Redistribution for Peak Fuel, Inner Blanket and Radial Blanket Assemblies During Natural Circulation Transient	4.4-192
4.4-67	Typical Inter-Assembly Flow Redistribution for Several Core Orificing Zones During Natural Circulation Transient	4.4-193

4.4-68
54

Typical Effect of Uncertainties and Inter-/Intra-
Assembly Flow/Heat Redistribution on F/A Peak
Coolant Temperatures During Natural Convection
Cooling

4.4-194

LIST OF REFERENCES

51	4.1	None
	4.2	4.2-315 thru 330
	4.3	4.3-87 thru 89
	4.4	4.4-81 thru 86

CHAPTER 4.0 REACTOR

4.1 SUMMARY DESCRIPTION

The Clinch River Breeder Reactor Plant (CRBRP) uses a mixed (Pu-U) oxide fueled, sodium cooled fast reactor having a total thermal output of 975 Mwt. A schematic of the reactor is shown in Figure 4.2-36. The reactor vessel, the closure head, the inlet nozzles and the core barrel are identified in this figure. The core support plate and the support cone form the principal pressure boundary inside the vessel. The fuel, control, blanket and removable shield assemblies are supported by the core support plate which also supports a fixed radial shield. Each of these reactor assemblies has two load pad areas which match the elevation of the core former rings. The rings are supported by the core barrel which is welded to the core support plate.

The upper internals structure, located above the core, is supported from the intermediate rotating plug of the vessel closure and keyed to the upper core former ring permitting vertical motion while restraining lateral and rotational motion. The structure laterally stabilizes primary and secondary control rod shroud tubes. In case of a loss of hydraulic balance, the upper internals structure acts as a secondary holddown device. The four support columns of the upper internal structure have jacks for lifting the upper internals structure with its keys clear of the core former ring and reactor assemblies for refueling. The in-vessel transfer machine rotates with the upper internals structure for removing and replacing of reactor assemblies at refueling.

A vortex suppressor plate is provided just below the sodium pool surface to minimize gas entrainment in the sodium exiting from the outlet plenum. Fuel transfer and contingency storage positions are provided in the annulus formed between the core barrel and the reactor vessel thermal liner.

The active length of the core is 36 inches and the equivalent diameter is 79.5 inches. The fuel region consists of a single enrichment zone with a total fissile plutonium loading of ~ 1500 Kg. The reactor control systems include 9 primary and 6 secondary control rods. The two systems are independent and diverse. Both the systems are capable of shutting down the reactor from full power to hot standby conditions. The core mid-plane details are shown schematically in Figure 4.3-1.

4.1.1 Lower Internals

The lower internals structure positions and restrains the reactor assemblies. The main components of the structure are: the core support structure composed of the core support plate and core barrel, horizontal baffle, core former structure fixed radial shield, lower inlet modules, bypass flow modules and fuel transfer and storage assembly. These components are shown in Figure 4.2-36. Most of these components are also shown in Figure 4.2-37.

58
51

The core support cone, a component of the reactor vessel, is an inverted truncated conical shell that connects the thick circular perforated core support plate with the reactor vessel wall. These two welded-in components (plate and cone) form the upper boundary for the reactor vessel inlet high pressure plenum.

The core barrel is a thick wall right circular cylinder that extends upward from the outer edge of the core support plate to the top plane of the reactor assembly outlet nozzles.

The horizontal baffle forms the upper boundary of the annular region between the core barrel and the reactor vessel and separates sodium in the outlet plenum region from bypass flow sodium below the baffle. It limits leakage to the outlet plenum and heat flow to the bypass sodium to provide for cooling components within the annulus and the reactor vessel above the baffle while minimizing flow which bypasses the core.

Supported inside the core barrel is the core former structure composed of upper and lower core former rings. These rings are contoured inside to the outline formed by the outer surfaces of the upper and lower load pads of the outer row radial shield assemblies. A small gap is provided in the cold condition between the rings and shield assemblies to allow a small amount of free bow at power operation. This gap facilitates replacement of reactor assemblies at refueling.

Fitted to the inside of the core barrel is fixed radial radiation shielding for protecting the barrel from structural damage from neutron fluence.

There are 61 lower inlet modules for the core. A lower inlet module is shown in Figure 4.2-40. The lower inlet modules are inserted into lined holes in the core support plate. Each lower inlet module holds and distributes sodium coolant flow to the inlet nozzles of seven reactor assemblies. The bypass flow modules also receive low pressure coolant from the lower inlet modules and distributes the coolant to the removable radial shield assemblies.

The core lattice of equilateral triangular pitch is established by the core support plate and the lower inlet modules. The inlet nozzles of the reactor assemblies are held on this lattice by their respective modules which allow some on-plant rotation of the nozzles as part of the core restraint system. Lateral above-core restraint of the reactor assemblies is provided by the core former rings of the core former structure, reference Figure 4.2-47, which are located at the upper and lower hard-faced pad elevations of the reactor assemblies. These rings act on the outer row radial shield assemblies and contribute to the stable control of reactivity as the reactor power and coolant temperature are changed. In addition, they provide the lateral support required to withstand seismic events.

58]

The fuel, control and blanket assemblies are held down against the upward flowing sodium by a hydraulic balance arrangement and their own weight. The hydraulic balance is accomplished by differential coolant pressure zones in the inlet modules and the inlet nozzles of the assemblies, reference Figure 4.2-40. Backup mechanical holddown for all reactor assemblies is provided by the upper internal structure as discussed below.

4.1.2 Upper Internals

The upper internals structure, reference Figure 4.2-45, stabilizes the control rod drivelines, supports in-vessel instrumentation and provides mechanical backup holddown for the reactor assemblies. Shroud and flow conduits in this structure are designed to mitigate transient temperature effects on the structure from the reactor core effluent. The principal components of the structure are: the four support columns, two transverse interconnected plates, four interconnecting shear webs, flow chimneys, shroud tubes, and instrumentation posts.

The support columns extend down from above the intermediate rotating plug of the reactor vessel upper closure head assembly. Connected to the upper end of each column is a jacking mechanism. Together, the jacking mechanisms are used at shutdown to raise and lower the upper internal structure to allow clearance for operation of the fuel handling machines of the Reactor Refueling System and for rotation of the intermediate plug.

The upper and lower support plates are integral with the four columns and the interconnecting curved plates which form a shear web. This welded assembly provides the structural strength required in the upper internal structure for withstanding seismic events. Three radial key extensions from the peripheral shroud structure below the lower transverse plate engage the lower internals structure for providing alignment and seismic support of the upper internal structure.

The instrumentation posts extend from the lower support plate over the outlet nozzles of the fuel and blanket assemblies. The chimneys pass through the transverse plates and conduct the hot reactor core effluent into the upper region of the reactor vessel outlet plenum. Each chimney collects outlet flow from a number of reactor assemblies.

51

Reactor system thermocouples of the Reactor and Vessel Instrumentation System are mounted on the upper internals structure for measuring fuel and blanket outlet and outlet plenum sodium temperatures. The leads for these thermocouples are routed up and out of the reactor vessel inside the support columns.

4.1.3 Core Restraint

A passive core restraint system is provided in the design which involves all of the fuel, control, blanket and removable radial shield assemblies, core support, lower inlet modules, bypass flow modules, upper internals structures and the upper and lower core former rings of the core former structure. The two core former rings girth the outside contours formed by the upper and lower load pads on the outer row removable radial shield assemblies.

Outward actions by the fuel, control, blanket and removable radial shield assemblies are limited at the core former rings which are placed at the same elevations as the hard faced load pads on the outside ducts of the reactor assemblies. Interactions between the reactor assemblies and the core former rings are limited to these pads since they are raised above the outer surfaces of the assembly ducts.

Since the core restraint system involves all of the reactor assemblies and the upper and lower internals structures, additional core restraint features which apply to individual components are discussed in the component description subsections which follow.

4.1.4 Fuel, Blanket and Removable Radial Shield Regions

The components in the core region include the 156 fuel assemblies, the 76 inner blanket assemblies dispersed heterogeneously throughout the central regions of the core, the 6 assemblies which are alternately fuel or inner blanket, the 126 radial blanket assemblies surrounding the fuel, the 9 primary system control assemblies, and the six secondary system control assemblies. Also discussed in the control subsection below are the control rod drivelines and control rod drive mechanisms. The axial blanket regions are formed in the fuel assemblies above and below the fuel.

The 312 radial shield assemblies that are located in the radial rows outside the radial blanket rows comprise the removable radial shield region.

4.1.4.1 Fuel and Axial Blankets

Each fuel assembly consists of 217 fuel rods, an outer duct, inlet and outlet nozzles, and a lower shield piece. The outer duct is a hexagonal tube that forms a discrete coolant flow path for each assembly. A total of 156 + 6 (See Section 4.1.4) fuel assemblies are installed in the core.

Each fuel rod contains a stack of (Pu+U)₂O₂ pellets which form the 36-inch active core region, and 14-inch long stacks of depleted UO₂ pellets that form the upper and lower axial blanket regions. The fuel rods are spaced from each other by spiral wire wraps that allow space for and promote mixing and cross flow of the coolant flow.

A plenum is provided in each fuel rod above the upper axial blanket for collecting the fission gases released from the pellets during power operation. This plenum is non-vented and is sized to allow the design fuel burnup to be reached without the buildup of excessive internal gas pressure. Additional information on fission gas buildup is provided in Section 4.2.1.1.3.9. A small capsule of tag gas that is unique to each fuel assembly is included in the rod. After sealing the rod in low pressure helium, this capsule is ruptured. The tag gas provides the basic means for detection and location of assemblies containing leaking fuel rods. (See Section 7.5.4.2.3.)

The inlet nozzle is a cylindrical, hollow extension at the bottom of the fuel assembly. It contains radial slots which admit reactor coolant flow from the inlet module into which it is nested. Mechanical/hydraulic features of the nozzle that complement those of the lower inlet module contribute to the balance of axial hydraulic forces so that the lifting action of the sodium flow is eliminated.

The outlet nozzle is a hexagonal hollow extension at the upper end of the fuel assembly. It releases the sodium coolant to the outlet module of the upper internals structure above. This nozzle also serves as the handling portion of the assembly and is contoured to mate with the grapples of the fuel handling machines.

A shield-orifice assembly is located in the lower portion of each fuel assembly. The shield piece of the assembly has vertical flow holes but still provides the radiation protection required for assuring the design lifetime of the inlet modules and core support plate. The orifices, located just below the shield piece, control the flow of coolant to the fuel assembly.

51 Pads are located on the outside faces of the fuel assemblies at two elevations above the fuel region. Similar pads are located on the outsides of all other reactor assemblies. The above core load pads (ACLPs) are raised or thickened portions of the duct walls protruding slightly beyond the dimensions of the nominal duct cross section, forming a continuous flat load-bearing surface across the complete width of the hexagonal duct sides. The flat surfaces of the hexagonal outlet nozzle serve as the top load pads. The above core load pad height will be approximately 4 inches. The load pads will be hard surfaced with chrome-carbide. Figure 4.2-11 provides a schematic indication of the location of the load pads on the fuel assembly, and Figure 4.2-36 illustrates the core former rings which are at the matching load pad elevations. The purpose of the pads is to limit interactions between reactor assemblies to these elevations so that the desired bowed configuration of the fuel assemblies is achieved. As power is increased, the fuel assemblies, under the restraints imposed at the pads and in the inlet nozzles, bow increasingly into an "S" configuration. This shape generally results in a net outward bowing of the active region of the fuel assemblies which contributes a negative reactivity effect.

Several other important features are included in the fuel assembly designs. The fuel region of the core is divided into six coolant flow zones for flattening the temperature profile. The flow allocation to the orificed core assemblies is such as to satisfy design and operational constraints as discussed in Section 4.4.2.5. Discrimination posts at the bottom and identification notches near the top of each fuel assembly preclude placement of a fuel assembly in a lattice position where it would be under cooled. Camming surfaces on the outside of each assembly promote self-alignment upon insertion into the reactor assembly group.

The residence time for the fuel in the first core of the CRBRP is expected to be at least two calendar years (328 equivalent full power days), corresponding to 74,000 MWD/T burnup in the peak fuel pellet. The structural analyses given in Section 4.2 reflects this expectation. Similarly, the maximum residence time of inner blanket assemblies in the reactor is two years, whereas the radial blanket assemblies reside in the reactor for 4 or 5 years, respectively, in the first and second blanket rows.

4.1.4.2 Inner and Radial Blanket

The inner and radial blanket provides most of the fertile material for breeding fissile plutonium. The 76 + 6 inner and 126 radial blanket assemblies are constructed similar to the fuel assemblies but contain fewer and larger diameter rods. They have the same length and outside shape as the fuel assemblies.

Each blanket assembly consists of 61 rods, an outer duct, inlet and outlet nozzles, and a lower shield piece. The outer hexagonal duct forms a discrete reactor coolant flow path for the assembly.

Each blanket rod contains a stack of depleted UO_2 pellets of overall height that matches that of the fuel plus the upper and lower axial blankets. The stack height is centered on the core midplane. Space is provided above the stack for collecting fission gases.

As in the fuel assemblies, the blanket rods are spiral wire wrapped to allow space for and promote mixing and cross flow of the coolant flow; each rod contains a tag gas that is unique to the particular assembly.

The blanket assemblies are classified according to their location in the core; inner blanket assemblies are located among the fuel assemblies in the interior region of the core, while radial blanket assemblies are located in two rows around the core periphery (see Figure 4.2-10A). Except for inlet nozzles and flow orificing, the radial and inner blanket assemblies are identical.

Three flow zones are provided for the inner blanket assemblies. A discrimination system similar to that for the fuel assemblies is provided to prevent inner blanket assembly insertion into an incorrect position. As described in Section 4.3, three or six fuel and inner blanket assemblies exchange positions in alternating reactor cycles. All radial blanket assemblies are identical; orificing for these assemblies is provided in the lower inlet modules.

4.1.4.3 Removable Radial Shield

Radial shielding is provided in approximately four radial rows outside the radial blanket regions to protect the core former rings and the core barrel from excessive radiation damage. The shielding in this region consists of radial shield assemblies which have the same outside shape and length as the fuel assemblies and can be moved in and out of the reactor vessel by the fuel handling machines.

Each radial shield assembly consists of a thin-wall hexagonal tube or duct to contain the shield material. The thin wall of the duct provides the required coolant baffling and is the primary structural member in the assembly. The assembly is reinforced at the load pads to absorb seismic loads. Thermal stresses induced by transients are minimized by the thin wall. The design allows placement of the shielding material as a bundle of solid shield rods only at those elevations where it is required. Coolant is distributed through the interstices of the solid shield rods.

The inlet and outlet nozzles of each assembly are included in structural extensions at the bottom and top ends of the duct tube, respectively. Their constructions are similar to those of the fuel assemblies described above.

4.1.4.4 Control

The net reactivity and the power level of the reactor core is controlled by two independent control rod systems, the primary and secondary. The primary control system is used in the normal operating mode while the secondary system is used only in shutdown of the reactor. Each system is capable of shutting down the reactor in either the normal or scram mode with the other system inoperable.

Sufficiently different design features are included in designs for the two systems to assure functional diversity and preclude common mode failures.

51

The principal components for each system are the control assemblies, the control rod drive lines (CRDs) and the control rod drive mechanisms (CRDMs).

The primary control system includes 9 each of control assemblies, CRDs and CRDMs while the secondary system includes six each of these components. All control assemblies occupy core lattice positions.

The control rod assemblies of both systems consist of pins with boron carbide (B_4C) pellets sealed inside tubes or cladding in a manner similar to that of the fuel rods. These pins are spaced with wire wraps on their outsides and held within a duct which slides within an outer duct. Gas plenums are provided in each pin above and below the pellets for collecting the helium gas released from the B^{10} (n,α) reaction.

The outer duct of each control assembly has inlet and outlet nozzle extensions which provide an outside shape and overall length for the assembly that is nearly identical to that of the fuel assemblies. Each control assembly can be moved in and out of the reactor by the fuel handling machines.

The control rods in both systems are connected to their respective CRDMs by the long tubular CRDs to which they are coupled. The CRDMs are electro-mechanical devices that are located outside the reactor vessel on top of the intermediate rotating plug of the upper vessel closure assembly. The primary and the secondary mechanisms are internally pressurized with inert gas. Both mechanisms are sealed from the reactor vessel cover gas by bellows seals.

In the primary control system, the control rods contain 37 pins that are held within the control assemblies in hexagonal inner ducts. The control rods are vertically positioned in their respective core lattice positions by the CRDMs.

The secondary control rods each contain 31 pins surrounded by a circular wrapper tube. The lower end of the control rod is guided by the circular piston assembly within a cylindrical guide tube; the upper end is guided within the hexagonal duct by a circular wear ring moduled at the top end of the damper assembly. These rods are withdrawn from the core within their respective assemblies during normal reactor power operation.

Both the primary and secondary CRDMs have sufficient stroke to drive the rods fully into the core to the point where the neutron absorber bundles are centered on the core midplane. It is not possible for the bundles to go below this point due to mechanical stops within the drives and control assemblies.

The nozzles, shielding, orifices, and discrimination features of the control assemblies are similar to those of the fuel assembly described previously and, therefore will not be further described in this summary.

4.1.5 Design and Performance Characteristics

The reactor design is based upon the design parameters presented in Table 4.1-1. Non-replaceable components are being designed with the capability to accommodate the stretch power conditions as mentioned in Section 1.1.

The reactor core has been designed to have a sufficiently negative reactivity feedback coefficient. Redundancies and safeguards have been designed into the reactor to assure a high degree of reliability. Redundant flow paths are included in the inlet modules, support plate and reactor assembly nozzles to preclude flow blockage. Strainer holes are incorporated in the inlet module stems to prevent particulate matter having dimensions greater than $\frac{1}{4}$ inch from entering the fuel and blanket assemblies. Anti-blockage features are provided on the outside of the inlet module liners to prevent plate or can-type flow blockages of the inlet modules.

The spiral wire wraps on the outside of the fuel and blanket rods and the neutron absorber pins promote sodium coolant mixing and hence more uniform cladding and duct wall temperatures. The fuel and blanket assemblies are enclosed in separate ducts to limit the potential for propagation of local fuel failures and to promote safety in fuel handling.

Operational and shutdown control reliability of a high degree is assured by redundancies and design diversities in the two control systems. Each system is capable of shutting down the reactor independently of the other system with the highest worth rod in the operable system stuck. Scram release for the primary control rod system is located in the mechanism and releases the driveline and control assembly with spring assisted scram insertion. Scram release for the secondary control rod system is achieved by release of a pneumatically activated latch located within the control assembly. A hydraulic scram assist is provided for the secondary control rod.

Flux detectors are located outside the reactor vessel for continuous monitoring of the neutron flux level of the reactor core. Thermocouples are placed in selected fuel and blanket assembly outlet and outlet plenum positions for surveillance of reactor thermal performance.

4.1.6 Loading Conditions and Analysis Techniques

The Reactor System is being designed to withstand the various loadings which result from the CRBRP Design Duty Cycle events. The duty cycle events are specified in Appendix B. This specification covers the event categories of Normal, Upset, Emergency and Faulted Conditions of Section III of the ASME Boiler and Pressure Vessel Code. RDT C16-1T, "Supplementary Criteria and Requirements for RDT Reactor Plant Protection Systems", December, 1969, is also being applied in the design of the reactor in accordance with the equivalent descriptions that are summarized in Table 15.1.2-1.

The analysis of the Reactor System performance under the various loading conditions is being carried out by the extensive use of well established and accepted computer codes. Analytical models are being established for the reactor to determine neutronic, thermal-hydraulic and structural parameters for the reference design and will be continued in the design evolution leading to the final reactor design. Detailed and interrelated allowances for the changes with time in the properties of the materials subjected to high-energy radiation and high temperatures are being carefully considered and accommodated in the design. Radiation shielding is being strategically located in the design with the aid of analysis to assure that the design lifetimes of all materials and components are achieved and radiation streaming is controlled. Comprehensive tests are planned and are being implemented to assure the validity of the reactor design and the analysis upon which it is based (Sections 1.5, 4.2.1.3, 4.2.2.4, 4.2.3.4 and 4.4.4).

4.1.7 Computer Codes

The computer codes that are being used in the neutronic, thermal-hydraulic and structural analysis for the Reactor System and its components are included in Appendix A.

4.1.8 Additional Items to be Addressed in the FSAR

- 1) An evaluation of the fatigue damage in the CDF and DLS models will be included in the final design or justification for its omission will be provided in the FSAR.
- 2) Failed fuel, blanket or control assemblies will be removed at the first shutdown after the failure occurs (i.e. not necessarily the End-of-Cycle).

Upon the detection of a breached fuel or blanket pin, as indicated by fission gas, the assembly will be removed from the reactor at the first plant shutdown. Upon the detection of sodium-fuel contact, as indicated by a generally increasing delayed neutron signal, the reactor will be brought to a controlled shutdown and the assembly removed from the reactor.

- 3) The fuel and blanket fuel design methodology will be verified against steady state and transient data and will be documented in the FSAR. Issues related to the "fuel adjacency effect" and fluence dependency of material properties will be explicitly addressed.
- 4) The fuel and blanket fuel design methodology will be verified against steady state and transient data and will be documented in the FSAR. Issues related to the "fuel adjacency effect" and fluence dependency of material properties will be explicitly addressed.
- 5) Prior to the FSAR submittal, the project will develop and submit quantitative limits to assure a core coolable geometry. The following potential mechanisms for compromising core coolable geometry will be addressed:

Fuel melting and explosion
Cladding melting and deformation
Coolant boiling and dryout.

- 6) The project will review the extent to which thermal uncertainties were included in the duct analyses to confirm adequacy of the analysis. FSAR core seismic analyses will include bundle-to-duct interaction evaluations.
- 7) The conservativeness of the umbrella events with respect to the temperature and loading potential of the fuel and blanket design events will be described further in the FSAR.
- 8) Prior to the FSAR submittal, the project will develop and submit quantitative limits to assure core coolable geometry. The following potential mechanisms for compromising core coolable geometry will be addressed:

Fuel melting and explosion
Cladding melting and deformation
Coolant boiling and dryout.

- 9) Final design documentation for the fuel and blanket design methodology will address the procedures for determining load and temperature history, will address the adequacy of confidence limits used for mechanical properties and will show that the statistical methods utilized are appropriate.
- 10) The adequacy of methods used to determine the core power distribution will be verified with ZPPR EMC data for the FSAR.
- 11) ZPPR EMC experimental data specific for Doppler constants have been performed and will be evaluated for the FSAR.
- 12) Nuclear codes and design procedures used for reactivity coefficient and control rod worth predictions, and verification of their adequacy based on experimental data, will be documented for the FSAR.
- 13) The project will examine FFTF stability tests and analyses to confirm that no power oscillations exist and will so document this in the FSAR.
- 14) Fuel densification effects will be addressed in the FSAR.

- 15) The Project will provide in the FSAR, revised, self-consistent sets of hot channel factors for the core assemblies. Confidence levels of the hot channel factors will be established where appropriate. The effects of the non-linear application of the hot channel factors will be investigated; Monte Carlo analyses will be performed for representative core assemblies to substantiate the conservatism of the adopted factors and methodology.
- 16) The Project will consider the FFTF observed increased reactor/primary loop Delta P in the CRBRP final design and will provide documentation in the FSAR.
- 17) The Project will incorporate results of the DEA-2 power-to-melt test into the final design methodology and will provide documentation in the FSAR.
- 18) Prior to the FSAR submittal, the Project will develop and submit quantitative limits to assure core coolable geometry. The following potential mechanisms for compromising core coolable geometry will be addressed:

Fuel melting and explusion
Cladding melting and deformation
Coolant boiling and dryout.
- 19) The nuclear impact of space-time kinetics will be accounted for and will be addressed in the FSAR for appropriate transient analyses.
- 20) The applicant will include in the FSAR, the response of the reactor to the SCRS for extremely unlikely events.
- 21) The FSAR will reflect that the Secondary Control Rod system will shutdown the reactor for all design basis events (anticipated operational occurrences) and will maintain a core coolable geometry assuming the total failure of the Primary Control Rod System and one stuck Secondary Rod. This includes Chapter 15 accident analyses.
- 22) The FSAR will include the End-of-Life criteria for the Drive Mechanism Drivelines and Control Assemblies, and a limited scoping analysis for failures resulting in exceeding these End-of-Life criteria (both for the Primary and Secondary Systems).
- 23) The FSAR will reflect the results of an analysis of the effects of increased primary system delta Ps (as observed in FFTF) on the flotation of the Primary Control Assembly. The Project will also reanalyze Primary Control Rod floatation using a 5% pump overspeed condition.

TABLE 4.1-1

REACTOR SYSTEM DESIGN PERFORMANCE PARAMETERS

Parameter	Value
Total Reactor power, MWt	975
Plant Capacity Factor (Availability factor x load factor) Ultimate/First Cycle, %	75/35
Range of Operation, (% Rated Thermal Power) (3 Loop Operation)	40 to 100
Total Coolant Flow Rate (Design Range), 10^6 lb/hr	41.5 to 47.7
51 Maximum Nozzle-to-Nozzle Pressure Drop (At 41.5×10^6 lb/hr, Thermal Hydraulic Design Value), psi	123
Reactor Inlet Temperature, (Thermal/Hydraulic Design Value) $^{\circ}$ F	730
51 Reactor Bulk Coolant Temperature Difference (Thermal Hydraulic Design Value) $^{\circ}$ F	265
Reactor Mixed Mean Outlet Temperature (Thermal/Hydraulic Design Value), $^{\circ}$ F	995
Average Breeding Ratio (Initial Cycle)*	1.29
51 Total Fissile Pu Inventory, Kg (for beginning of life)	1502
Fuel Burnup, Capability Objective, MWd/MT Initial Core, Peak	80,000
Nuclear Power Peaking Factors	
Initial Core, Axial, Beginning-of-Cycle	1.28
Initial Core, Radial, Beginning-of-Cycle	1.18
51 Maximum Neutron Flux, Total, $n/cm^2/sec$	5.5×10^{15}
Cycle Lengths Initial Cycle (full power days)	128
51 Second Cycle (full power days)	200
Later Cycles (full power days)	275
Pressure Drop, psi	
Across Core Support Structure (Design)	170
Through Reactor Vessel (Maximum Anticipated)	123

16 | *The breeding ratio is the ratio of the production of fissile plutonium (Pu-239+Pu-241) to the destruction of fissile material (U-235 Pu-239+Pu-241). In this definition, Pu-240, Pu-242 and the mass of U-235 up to the weight fraction found in depleted uranium (0.2%) is not considered as fissile material.

4.2 MECHANICAL DESIGN

4.2.1 Fuel and Blanket Design

4.2.1.1 Design Bases

The fuel and blanket assemblies shall be designed to satisfy the general performance and safety criteria presented in Section 3.1 by performing their respective functions in a safe and reliable manner over their design lives. The functional requirements, design and operational requirements, environmental and material considerations, and surveillance and examination requirements to achieve this objective are delineated in the following subsections.

4.2.1.1.1 Functional Requirements

The primary functions of the fuel assembly are:

1. Provide, protect and position the nuclear fuel of the fast breeder reactor core type to produce heat for the Reactor Heat Transport System.
2. Provide neutrons for breeding plutonium in the fuel and blanket assemblies.
3. Breed plutonium in the upper and lower axial blankets.

The primary functions of the blanket assemblies are:

1. Provide, protect and position the fertile material in and around the core for conversion to plutonium.
2. Produce heat for the Primary Heat Transport System.

Both assemblies shall also be designed to:

1. Provide a compact structural unit that can be moved in and out of the reactor by the refueling machines.
2. Provide a controlled path for the primary sodium coolant of the Reactor Heat Transport System.
3. Provide shielding to protect the core support structure from excessive radiation.
4. Interact with the other core assemblies, core restraint system and lower internals structure to assure safe and predictable reactor core geometry.

4.2.1.1.2 Operational and Design Requirements

4.2.1.1.2.1 Operating Conditions

The initial core fuel and inner blanket assemblies for CRBRP have a maximum required residence time of 328 full power days corresponding to the first two cycles of operation. (This results in a peak fuel pellet burn-up of less than 80000 MWD/T in the peak power fuel assembly.) The initial core radial blanket assemblies have an 878 day (cycle 1-4) lifetime in the inner row, and an 1153 day (cycle 1-5) lifetime in the outer row. First-core physics data and thermal hydraulic data (Sections 4.3 and 4.4) are generally used as the basis for the PSAR design analyses. For certain specific analyses, simplified enveloping environments are used to reduce the complexity of the calculations.

It is primarily the initial core data needs that are being supported by the LMFBR fuel technology programs. The scope and schedule of the steady state fuel irradiation program, transient fuel irradiation program and reference cladding and duct irradiated materials program are provided in the references 164, 168, and the Reference Cladding and Duct Test Plan (provided to NRC 6/7/76) respectively. When the data from these programs supporting later cycle operation are available it will be incorporated into the CRBRP FSAR.

During actual reactor operation, the long term damage accumulated by the fuel and blanket assembly components is expected to correspond to the damage which would be calculated using time averaged nominal temperatures.

54|52| However, in assessing the effects of steady state operation and anticipated faults (normal and upset conditions), fuel and blanket assembly component temperatures shall be based upon maximum expected plant operating conditions and upper 2σ level semistatistical hot channel factors. At this level, there is a 97.5% probability that the corresponding temperatures will not be exceeded. This is conservative since the calculated damage accumulation generally increases with temperature (for example, see Figure 4.2-18, described in Section 4.2.1.1.2.2 below). For the single unlikely and extremely unlikely faults (emergency and faulted conditions), and upper limit on plant conditions (T&H design values) and the 3σ uncertainty level shall be utilized. At this level, the probability of exceeding the calculated temperature is approximately 0.1%. Because of the life limiting nature and safety consequences of these types of events coupled with their low probability of occurrence, this extreme degree of conservatism is felt to be warranted at this time.

51 During the life of the fuel and blanket assemblies they will be subjected to non-operational shipping and handling loads. The fuel assembly shipping loads shall be based on 6g axial and 2g lateral accelerations. These limits were selected as the basis for FFTF fuel assembly design; subsequent shipping tests have shown that the expected values are much lower than this.

The description and results of the tests which measured fuel assembly shipping and handling loads are given in Reference 70. In these tests, shock and vibration measurements were made on the fuel assembly shipping container (a wooden box) and on the floor of the vehicle trailer in which the assembly was being transported.

The fuel assembly utilized in this test (the CCTL Mark II assembly) is similar to the CRBRP fuel assembly in cross sectional configurations and the fuel rod spacer and support methods. Other differences and similarities between the CRBRP fuel assembly and the Mark II assembly are:

1. The CRBRP fuel rods are 21.0 inches longer;
2. The overall CRBRP assembly length is the same;
3. The CRBRP assembly weight is 128 pounds greater.

Based on preliminary design requirements, it is anticipated that the CRBRP fuel shipping container will provide even better shock protection than the box utilized in the tests.

The referenced tests demonstrate:

1. It is possible to transport a LMFBR fuel assembly with maximum shipping loads to the fuel assembly container far less than those specified, and
2. The shipping and handling loads experienced by the Mark II assembly during the test caused no discernable change to the fuel assembly (Reference 71).

The CCTL Mark II fuel assembly and the CRBRP fuel assembly are sufficiently similar that these conclusions apply to the CRBRP fuel assembly shipping and handling loads as well.

The maximum shipping load for the blanket assemblies shall be 6g axial and 6g lateral accelerations to facilitate shipment in commercial containers. During in-reactor refueling operations, the maximum fuel and blanket assembly drop heights are less than 1.5 inches when the assemblies are correctly located. An incorrectly located assembly cannot be released by the IVTM. These design limits are based upon the refueling grapple release mechanism, the assembly outlet nozzle configuration, and the discriminator post geometry.

The normal, upset, emergency and faulted operational conditions of the CRBRP Design Duty Cycle (Appendix B) shall be utilized in evaluating the fuel and blanket assembly performance potential and safety aspects. The number of events given in Appendix B for the 30 year reactor life shall be uniformly applied until the number of events reaches an amount proportional to the respective assembly design life. The design duty cycle conservatively identifies the undercooling, seismic, and reactivity insertion events appropriate for CRBRP operation. The appropriate accident conditions of Section 15.4 shall also be considered on an individual event basis.

During the above operational and accident conditions, it is expected that the fuel and blanket assembly fuel rods would be subjected to a combination of the following loading mechanisms:

1. Fuel and cladding loading due to differential growth between these components shall be considered. Sources of differential growth are fuel and cladding irradiation induced swelling and creep, thermal expansion and creep, elastic and plastic strain. As described below, cladding deformation may be restricted by the spacer system.
2. Gas released from the fuel during burnup with additional release and fuel expansion during overpower transients will produce cladding pressure loadings in the sealed fuel and blanket rods.
3. During steady state operation, secondary stresses will be generated due to radial, axial and circumferential thermal and flux gradients in the cladding material. These stresses are generated primarily by variations in local swelling rate; however, they are relaxed by fuel rod bowing and irradiation creep. During transient events, thermal stresses due to unequal heating or cooling rates may be generated. At shutdown, part load, and refueling conditions, residual stresses associated with the above relaxation mechanisms will be present.
4. Interaction forces between the rod cladding and the wire wrap will be generated by differential axial and radial growth of the two components. Furthermore, differential growth between the fuel rod bundle and assembly duct will transmit compressive cladding forces back through the wire wrap.
5. Fuel and blanket rod flow induced vibration will produce cyclic cladding and wire wrap stresses. Low-cycle fatigue stresses may also be generated during certain transients, seismic events, and non-operational shock loadings.
6. Accident loadings such as fission gas jet impingement or sodium-fuel interaction for rods are described and evaluated in Section 15.4. Characteristics of fuel-coolant interaction are described in subsection 4.2.1.1.3.

As shown in Table 4.2-52 and the exemplary references cited therein, the above loading conditions are supported by FFTF fuel assembly design evaluation and EBR-II reactor operating experience and information from the U.S. and foreign LMFBR programs. Therefore, as a minimum, these loadings shall be required for evaluation of the design adequacy of the fuel and blanket assembly fuel rods. Although not expected at this time, additional loading mechanisms could be discovered during future irradiation testing and/or technology programs (see Subsection 4.2.1.5). The impact of any such additional loadings on design adequacy shall also be evaluated. Reference 60 is provided to identify loading mechanisms only and is not intended as a reference on actual loads. Further information is given in the response to Question 241.68.

In addition to items 3 to 6 above which produce interacting forces with the assembly structure, the following events shall be considered for evaluation of the fuel and blanket assembly structures. Again, these are based upon a review similar to that performed for the rods.

1. Restraint of assembly bowing (due to differential growth rates across the assembly) and interaction with other core assemblies and the core support structure, including seismic loading, through the core restraint system.
2. Forces induced by sodium flow and the corresponding pressure drop through the assembly. This would include axial lift forces counterbalanced by assembly weight and hydraulic holddown and pressure differences across the duct wall, inlet and outlet nozzles.
3. Secondary stresses due to the steady state and transient temperature gradients through the component thickness. Irradiation induced stresses in the duct are included in the core restraint loading mechanisms.
4. Maximum push, pull and lateral loading applied through the refueling equipment.

As in the case of the fuel rods, these loadings shall be the current minimum basis required for evaluation.

4.2.1.1.2.2 Design Requirements

For the CRBRP fuel and blanket assembly fuel rod operating conditions and loading mechanisms identified in subsection 4.2.1.1, the following criteria shall be satisfied on a conservative basis, i.e., assumption of the maximum expected loading conditions and environment and the appropriate material properties of subsection 4.2.1.1.3. These criteria were selected so that the fuel rods will satisfy their functional requirements and performance objectives in a safe and reliable manner based upon current LMFBR technology. Further information on the bases of these design requirements are given later in this Section. The same limits apply to the wire wrap.

52 | It should be noted that the following design requirements are preliminary estimates based upon available LMFBR technology. These estimates are currently being evaluated through extensive LMFBR Base Technology and FFTF development programs which are summarized in subsections 4.2.1.4 and 4.2.1.5 respectively. As data from these programs becomes available, the following design requirements may change or the magnitudes of limits associated with these requirements could change. Ultimately, there may be a single criterion developed for the FSAR based on the best correlation with the experimental data. The true measure of performance potential will be determined by the results from FFTF and CRBRP surveillance and post-irradiation testing.

51

Amend. 52
Oct. 1979

1. During steady state operation, the primary and secondary thermal creep strain in the circumferential (hoop) direction shall be less than 0.2% for a 2 to 1 stress biaxiality ratio. This criteria applies primarily to fuel rod cladding and with appropriate stress biaxiality corrections for other rod components.

This strain limit was selected for the design of fuel rods in FFTF in 1970. They were based on available strain-rupture data for 20% cold worked and irradiated Type 316 Stainless Steel cladding material with a 0.230 inch outside diameter and 15 mil wall thickness. The alloy composition of the material tested was prototypic (see Reference 74). Templug information indicated an irradiation temperature of $525 \pm 25^\circ\text{C}$, but structural studies on other material irradiated in the experiment suggest the temperature could have been as high as 700°C . All post-irradiation testing was done at $550 \pm 1^\circ\text{C}$. The cladding was tested using internally pressurized tube segments with hoop and axial stresses (2 to 1 biaxiality ratio) calculated consistent with the thin-walled approximations of the design procedure. The true circumferential (hoop) strain which must be uniform through the cladding thickness, was calculated based upon diameter measurements at four circumferential locations using the expression:

$$\epsilon = \ln(d_i/d_o)$$

Where, d_o = original mean diameter after irradiation, but before testing, and

d_i = mean diameter after irradiation and testing.

Therefore, any deformation occurring in the reactor, which would be expected to be insignificant for the low levels of irradiation, would be obviated by utilizing d_o in the ratio rather than the as-fabricated diameter. For the maximum measured strain of 2.5%, the true circumferential strain is approximated by $(d_i - d_o)/d_o$ within an accuracy of 1.2%. Figure 4.2-1 shows diametral rupture strains plotted as a function of rupture time. The figure includes the original data obtained from material irradiated at about 1000°F in the Dounreay Fast Reactor (DFR) to a total fluence of 3×10^{22} n/cm² or $\sim 2.6 \times 10^{22}$ n/cm² for $E > 0.1$ Mev. The dashed curve shows an extrapolation of the data to a fuel rod lifetime of approximately 10000 hr. At this maximum time, the diametral creep rupture strain would be 0.7 percent. Based on this 0.7 percent limit, a value of 0.2 percent hoop strain was selected to cover steady state operation.

Within any reactor (DFR, EBR-II or CRBRP) thermal creep can only be distinguished from irradiation creep if one form of creep is essentially nonexistent. This could occur in a high temperature very low flux environment, where thermal creep predominates, or in a low temperature high flux environment where irradiation creep predominates. With regard to the data of Figure 4.2-1, the creep strain shown is only the amount of thermal creep measured during post irradiation testing. More details are provided in the following paragraphs.

Since the reporting of the above DFR information in 1968, more biaxial rupture strain data has been obtained for prototypic FTR cladding from EBR-II irradiations. These data in Figure 4.2-1 show that the long term creep rupture points in general still indicate that steady state strains of up to at least 0.3% could be attained at maximum fuel burn-up without failure and indicate a safe margin against failure for the design limit of 0.2% hoop strain.

A preliminary indication that the 0.2% thermal creep strain limit in conjunction with the strain calculation procedure described in Section 4.2.1.1 and summarized in Table 4.2-A, is conservative relative to life-time prediction is given in Reference 75. This reference used a procedure similar to that of Table 4.2-A to calculate the design life-time of 20% cold worked 316 stainless steel clad fuel rods irradiated in EBR-II over a temperature and burnup range encompassing CRBRP operation. The prototypicality of the design and operating conditions of the EBR-II experimental fuel pins is demonstrated in Table 2 of Reference 75. The major differences in the procedure used for experimental verification and the design procedure of Table 4.2-A are:

Nominal, rather than hotspot temperatures were utilized, strain due to radial temperature gradient was neglected, and no fuel loading was considered.

Even with these assumptions, the procedure and the corresponding strain limit, were shown to be conservative as summarized in Table 4.2-B. In the last two cases where the post irradiation examination is incomplete, preliminary evidence suggests that cladding fretting and wear may have been significantly in excess of the design wastage allowance. This was because these EBR-II experimental assemblies had bundle to duct porosities well in excess of the current design given in Section 4.2.1.2.2.

52 |

To determine the primary and secondary thermal creep strain limit for other stress biaxiality ratios, the curves on Figure 4.2-1A are being utilized for preliminary design. Only the largest component of strain, hoop or axial, is considered. For a given stress biaxiality ratio, the strain correction factor for the largest strain component is read from Figure 4.2-1A. This factor is then multiplied times the 0.2% strain limit to obtain the limit for the maximum strain component for the given biaxiality ratio. For example, for a rod component in pure axial tension, the axial strain component is the largest. For this stress biaxiality ratio (0/1), the strain correction factor is ~ 3.0 . Thus, the limit for the primary and secondary thermal creep strain in the axial direction for this component is $3.0 \times 0.2\%$ or 0.6%.

The curves in Figure 4.2-1A are discussed in Reference 95.

For a thin, internally pressurized cylinder, the circumferential to axial stress ratio is 2 to 1. See, for example, Reference 96.

51 |

For the purpose of fuel rod performance analysis, the calculated cladding strain is not directly related to the measured cladding strain at any given time. Instead, for a given set of environmental conditions, the cladding strain is calculated as a function of time to determine the time required for the cladding to reach the appropriate strain limit. This time is considered to be the maximum fuel rod design lifetime as determined by the strain criteria for the given conditions. To verify this performance evaluation method, calculated fuel rod lifetimes have been compared to the actual lifetimes of fuel rods exposed to a particular environment. These comparisons have indicated this technique for calculating fuel rod cladding lifetimes to be conservative.

The radial blanket rod cladding experiences a lower stress level over a longer period of time, resulting in a lower creep rate than in the fuel rod cladding. Figure 4.2-2 which was used in selecting strain limits shows the diametral strain at failure as the function of the average deformation rate. The deformation rate of radial blanket fuel rods is only 20% of the deformation rate of the core fuel rod. Assuming that the core fuel rods will fail with 0.7% diametral strain then Figure 4.2-2 shows the radial blanket with a 20% lower strain rate will fail with 1/2 this strain of 0.35%. The maximum allowable steady state ductility limited strain is set at 0.1% for the radial blanket rods. For the inner blanket rods a 0.2% strain limit is utilized since the inner blanket rod lifetime does not exceed that of the fuel rods.

To maintain fuel rod cladding integrity during the faster acting transients the design limit discussed below must also be satisfied. This design limit is that the total thermal creep strain and plastic strain accumulated during steady state operation, all operational (upset) events and the worst minor incident (emergency event) shall be less than 0.3% at a 2-to-1 stress biaxiality ratio. Plastic strain accumulation shall be calculated using the bilinear stress strain curve approximation shown in Figure 4.2-2A. This figure shows simplified (bi-linear) stress strain curves for three temperatures. The permanent strain at the beginning of the transient (ϵ_p) has resulted from steady state creep plus any additional creep strain which has resulted from previous operational transients. The total strain (ϵ_T) at the beginning of the transient is the sum of this permanent strain and the elastic strain (ϵ_E) associated with the operating condition at the beginning of the transient. The design strain limit (ϵ^*) determines the shape of the curve between the yield stress (σ_y) and the ultimate stress (σ_u) for any temperature. This method assures that failure is predicted whenever the ultimate stress is exceeded independent of the accumulated creep strain. The ultimate strength of the material is an important parameter in the above application of the strain criteria. The stress-strain curves used for the analysis are those for unirradiated solution treated Type 316 stainless steel. Confidence that the ultimate strength for irradiated cold worked Type 316 stainless steel will be greater than these values is supported by comparing the assumed values with recently published irradiated data from Reference 183. Figure 4.2-2B shows the experimental data for typical transient strain rates (as calculated with the above bi-linear model) and the values assumed in the analysis. As can be seen, by comparing the experimental data and the values assumed for the analysis, conservatism is built into the analyses with respect to the ultimate strength of the

actual coldworked cladding. In keeping with the lower design limit for radial blanket rod steady state cladding strain, the design basis strain limit for radial blanket rod steady state and transient operation shall be 0.2%. Again, the fuel rod design limit (0.3%) is applied to the inner blanket rods since their lifetime does not exceed the fuel rod lifetime.

2. During steady state operation, the power (and corresponding fuel temperature) in the peak power fuel and blanket assembly rod shall be less than the minimum value for incipient fuel melting with a 15% overpower margin. The purpose of this requirement is to provide some margin between the normal operating power level required to produce incipient fuel melting. This is not meant to imply that incipient fuel melting is, in itself, detrimental. Rather, by providing such a margin, the task of terminating severe transients, in which gross fuel melting can be important, becomes easier.

One of the design guidelines to assure conservative design of the CRBR core and operational margins is no inception of fuel melting under steady state operation up to 115% of rated power. Consequently, the Plant Protection System and the Control System limits are established to assure that the above criterion is not violated. In fact, the CRBRP power can increase by a minimum of 7% and a maximum of 15% over the rated level (975 Mwt) without causing reactor trip. At 115% power level, the reactor will be tripped over a high flux signal. Therefore, fuel temperatures and linear power ratings have been calculated under the maximum possible overpower conditions to assure that the no-melting criterion was satisfied.

3. Ductility limited strain components include only thermal creep strain (covered in item 1) and plastic strain. Therefore, to maintain a total ductility limited strain of less than 0.2% consistent with item 1, no plastic strain is allowed during steady state operation. The design limit for steady state operation is that the primary equivalent stress must remain below the proportional elastic limit or alternatively 90 percent of the yield strength.

Irradiation induced creep and swelling are currently believed to be superplastic phenomenon and thus not ductility limited. Although LWR experience with Zircaloy-2 cladding indicated that irradiation creep strains on the order of 10% were achievable without failure, it had been postulated that there might be a limit on either total cladding strain (as measured by profilometry) or on inelastic strain which is total strain less one-third the volumetric change due to swelling (as measured by immersion density). However, as of this time no unique limit or sets of limits can be identified for total strain, swelling induced strain or inelastic strain which is primarily irradiation induced creep. Table 4.2-11A summarizes the failures of EBR-II irradiated fuel pins clad with 300 series austenitic stainless steel which have been characterized. These failures are described in Section V.E of Reference 101 and Reference 158. Table 4.2-11A shows a wide variation in both total and inelastic strain at breach, probably due to the lack of consistent breach causes. Furthermore, Figure V.E.2 (for PNL 5-1) of Reference 101 and Figures 7, 8, 9, and 10 (EBR-II Driver Fuel) of Reference 158 clearly show that cladding breach did not occur at the axial locations with either maximum total strain or maximum inelastic strain. Finally, recent results from the Reference Cladding and Duct Irradiated Materials Program, Task A, Mechanical Properties, reported in Reference 159, support the design position that prior irradiation creep is superplastic and thus not damaging. Simulated transient testing was completed at 1500 F on 10 specimens from X-157B and X-157C, which had been irradiated at 700 to 1000 F under 0 to 60,000 psi stress to fluences of 1.1×10^{23} n/cm². The failure strengths during the postirradiation transients for the unstressed specimens were not significantly different than those of the stressed specimens which had accumulated up to 1% irradiation creep strain.

4. While irradiation induced fuel rod and wire wrap deformation is not ductility limited, it is deformation limited by the following restriction. Flow channel closure due to fuel rod bowing and differential radial growth of the fuel rod, wire wrap and duct shall be limited by the flow area reduction used to derive the thermal hot spot factors of Section 4.4. This requirement is necessary to preclude locally damaging hot spots in excess of those considered in the design basis of subsection 4.2.1.1.2.

The hot spot factor referred to here is the statistical factor on coolant subchannel flow area where a subchannel is the region between 3 adjacent fuel rods. Therefore, the effect at 3σ confidence of the statistical combination of fuel rod bowing, nominal geometry variations and differential radial growth variations along the length of the subchannel shall not produce a variation in the hot subchannel coolant temperature rise at the core outlet greater than the value accounted for in the hot channel factor.

It would be inappropriate to provide only a maximum value of irradiation induced deformation which would account for the full hot spot uncertainty. The coolant temperature at the core outlet is the result of integrating all geometric and thermal variation over the lower length of the rod bundle in both the hot channel and in neighboring channels. Therefore, the irradiation induced deformation must be evaluated with all other geometric and thermal variations considered.

Fuel rod bowing in combination with irradiation induced deformation and other geometric and thermal variations such as manufacturing tolerances shall be evaluated against this limit.

5. To insure structural integrity up through an unlikely fault the cumulative mechanical damage function (CDF) for the fuel and blanket rod cladding shall be limited by

$$\Delta L_1 + \sum_{j=2}^M \left[\sum_{i=1}^N \Delta L_{j,i} \right] + \Delta L_E + \Sigma_2 < 1 \quad (1)$$

where

ΔL_1 = CDF increment due to steady state operation,

$M-1$ = number of different types of upset events,

N_j = number of occurrences of the j^{th} type upset event,

$\Delta L_{j,i}$ = CDF increment due to the i^{th} occurrence of the j^{th} type event,

Σ_2 = total uncertainty in the CDF,

ΔL_E = CDF increment due to the single unlikely fault

As shown, the CDF considers normal steady state operation, the expected number and types of upset events and the life limiting emergency transient. A description of the CDF procedure is given in Reference 58.

An example CDF analysis is illustrated in Figures 4.2-18 through 4.2-23. For this example analysis, a fuel rod was subjected to a hypothetical steady state environment, and a transient duty cycle which included the transient cladding temperature histories shown in Figures 4.2-19 and 4.2-20.

The CDF due to the steady-state environment and the combined upset events, which essentially give no additional damage at the three levels of uncertainty, are shown in Figure 4.2-18 for the example problem. At the design level, excluding any emergency events, the expected failure would occur at 540 full power days. However, at the lesser levels of uncertainty an 800 day lifetime is achievable.

This example cladding CDF evaluation assumes the upset transients are applied at equal time intervals throughout cladding life, with the emergency event applied at end-of-life. Cladding temperature increases during all transients were set equal to the maximum beginning-of-life values. Degradation of the cladding materials properties due to the environment at the time of transient occurrence was included in all CDF calculations.

The transient limit curves (TLC's) for the case in question are shown in Figures 4.2-21 and 4.2-22. The TLC's in Figure 4.2-21 are for any undercooling emergency event within the indicated time envelope of Figure 4.2-20, i.e., a 25 second transient followed by a 2 minute coastdown to equilibrium. The curves show, at the three levels of uncertainty, the time dependent peak cladding temperature expected to cause failure during undercooling event.

The family of TLC's shown in Figure 4.2-22 are for any rapid reactivity insertion ≤ 1 second in duration. These curves show, at the maximum level of uncertainty, the combinations of peak cladding temperature and fuel-cladding contact pressure expected to cause failure.

The general time dependence of the TLC's results from the combined effects of the following continuing phenomena:

- (a) the build-up of fission gas,
- (b) the degradation of mechanical properties caused by interstitial loss,
- (c) the effective clad thinning caused by the growth of the depleted substrate (ferrite layer) and the fuel-clad reaction zone,
- (d) the degradation of mechanical properties due to prior mechanical history including that from steady-state operation and the umbrella upset events.

(e) the steady-state temperature change due to burn-up and control rod movement with residual time.

It must be emphasized that the above TLC's are restricted to:

- (a) the fuel rod steady state environment assumed in this example problem;
- (b) the classification of the upset events in the derivation;
- (c) the time envelope considered.

The generality of the TLC's notwithstanding, a specific emergency event was analyzed via direct application of equation (11.B1) in Reference 58. In this case the limiting emergency event was taken to be that given in Figure 4.2-20 (notably, this is the identical time envelope used for the TLC's).

Importantly, the analysis of this particular event is not meant to imply that it is the most limiting in its category; rather, the intention is to provide a benchmark solution to which other emergency events may be compared, in the future, vis-a-vis the TLC's.

The example combined CDF's from steady-state operation, from the upset events and from the above emergency event are shown in Figure 4.2-23. As shown, the umbrella emergency event would cause failure, at the design level, at 485 full power days*, this includes 26 slow reactivity insertions and 18 undercooling (upset) events.

For nominal material properties, a 700 day lifetime is readily achievable. Thus, as measured in operating time, the total uncertainty for this event exceeds 200 full power days. This uncertainty is the effective design margin associated with this particular analysis (i.e., 28%) and is indicative of the design margins typically obtained through the CDF procedure.

It is emphasized that this CDF analysis is an example for illustrative purposes only; the CDF analysis of the CRBRP fuel rods is presented in Section 4.2.1.3.1.2.1.

*At this time the peak clad temperature at the end of the transient period is 1505°F. Thus, the above expected failure time would have been obtained directly from the TLC in Figure 4.2-21.

In the classical sense, the safety factor is a number greater than unity, which is divided into a material property (e.g., ultimate strength) to obtain a design limit below which a particular design is expected to operate. For example, for a stress limit based on the ultimate strength, we may specify.

$$\sigma_{dl} \leq \frac{\sigma_{ult}}{S.F.} \quad (3)$$

where σ_{dl} is the design limit for the operating stress for a specific environment, S.F. is the safety factor, and, for this example, σ_{ult} is the material ultimate strength. Assuming the design loads are accurately and/or conservatively known, this safety factor is a measure of the uncertainty in the values of the materials properties used in the design limit calculation, i.e., the safety factor approaches unity as the confidence in the materials property values increases. Equation (3) may also be written

$$F(\sigma) = \frac{(S.F.)\sigma_{dl}}{\sigma_{ult}} \leq 1.0 \quad (4)$$

In general, if the part in question is subjected to a time varying environment, $F(\sigma)$ will also be a function of time. Note that in this case, the factor of safety is contained in the expression for $F(\sigma)$ rather than in the 1.0. Thus, if for some reason the factor of safety were to change, we would not change the 1.0, but would rather change the value of $F(\sigma)$ calculated for a given time.

Equation (4) is analogous to the CDF limit in Equation (1). However, unlike the simple example of equation (4):

- a. The CDF is a complex function of several material properties, and
- b. The CDF does not utilize the classical safety factor concept, i.e., a single valued, simple factor applied to the various materials properties. Instead, the CDF procedure calculates statistically the time varying worst expected values of the pertinent materials properties at a given level of confidence, and uses these worst expected materials properties to calculate a maximum expected CDF at that level of confidence as a function of time.

The relationship between the classical safety factor and the statistical confidence limits used in the CDF is difficult to define explicitly because the concepts are mathematically completely different. Roughly speaking, the ratio of a CDF value calculated with worst expected materials properties to the same CDF calculated with nominal materials properties is analogous to a safety factor which would be applied to the nominal CDF. However, this ratio is time varying, and is not used directly in fuel rod performance analysis. If desired, such "safety factors" can be calculated from Figure 4.2-18. In this Figure, the ratio of the upper curve CDF values to the middle curve values represent a time varying safety factor based on materials properties alone. The ratio of the upper curve CDF values to the lower (solid line) curve values represent a time varying factor of safety which includes uncertainties in the applied loads as well as material properties. The uncertainties in the applied loads are considered separately from the CDF analysis (see Section 4.4). A definitive discussion of the techniques used in the CDF procedure to calculate statistically these worst expected values is given in Appendix E of Reference 58.

6. As of this time, the cumulative damage analysis technique does not consider fatigue effects. For cyclic fatigue due to transient and seismic events, vibration, handling and part load operations the criteria will be of the form:

$$\text{CDF} + \sum \frac{n_i}{N_i} \leq 1.0 \quad (2)$$

where

CDF is the cumulative damage function of item

n_i is the number of events at a given stress or strain range,

N_i is the allowable number of events at the corresponding stress or strain range,

i is the index on the different types of events expected over the design life.

If necessary, the appropriate fatigue component will be added to the CDF.

7. As a design guideline, the maximum cladding midwall temperature during an emergency event shall be less than 1600°F for any extended period of time (on the order of minutes) (the term "design guideline" is defined in the response to NRC Question 241.85). The rationale for this guideline is the lack of long term tensile and creep rupture data beyond 1600°F. Transients of short duration (on the order of seconds) and in excess of 1600°F, are felt to be within the extrapolation capability of the CDF analysis, since recent data on irradiated prototypic cladding indicate short term failure at temperatures much higher than 1600°F.
8. For faulted conditions, the required coolable geometry is achieved by maintaining the sodium temperature below its boiling point, saturation temperature at the existing pressure. As described in subsection 15.1.2.2 this criterion is a necessary and sufficient condition to preclude cladding melting.

The analysis results of Section 4.2.1.3.1.2 showed that no coolant boiling occurred for the worst umbrella transient conditions in the fuel assembly.

The cladding stress, strain, and deflection limits given in the fuel rod design criteria elsewhere in this Section are design limits chosen to preclude failure. If these limits are exceeded, cladding failure and/or coolant boiling does not necessarily occur. The conditions in the fuel assembly corresponding to a specific transient event must be calculated to determine if coolable geometry (i.e., no coolant boiling) is maintained during that event.

4.2.1.1.2.2.1 Fuel and Blanket Assembly Structural Component Design Criteria

For the CRBRP fuel and blanket assembly structural components and the operating conditions and loading mechanisms identified in subsection 4.2.1.1.2.1, the criteria listed in Table 4.2-7 shall be satisfied on a conservative basis, i.e., assumption of the maximum expected loading conditions and environment and where appropriate, worst case material properties. These criteria were selected so that the assembly structural components (excluding the previously covered fuel rods) will satisfy their functional requirements and performance objectives in a safe and reliable manner. As for the fuel rods, the design requirements of Table 4.2-7 are preliminary estimates based upon available LMFBR technology and are subject to change as results from the LMFBR Base Technology and FFTF development programs become available.

The CRBRP structural criteria require special consideration of nuclear fluence effects at elevated temperatures in a liquid sodium environment. The proposed Structural Design Criteria for Breeder Reactor Core Components provide guidelines to cover the combined effects of irradiation at elevated temperature, but recognize that specific structural criteria in terms of deformation limits which assure the functional requirements of a core component

can only be specified on a case-by-case basis. The CRBRP structural criteria and limits were therefore formulated in accordance with the general rules and guidance provided in the RDT Draft for Breeder Reactor Core Components, (Reference 174) but were modified to include additional safeguards and to more properly reflect the fuel and blanket assembly functional requirements as identified in the Equipment Specification.

In accordance with the RDT draft rules and guidelines, the CRBRP fuel and blanket assemblies are considered Class B Breeder Reactor core components which require a high level of assured structural integrity in protecting against crack initiation, elastic/plastic/creep instability, and excessive deformation so as to satisfy reliability and functional requirements during Normal, Upset, Emergency and Faulted conditions specified for the reactor core. A summary of the failure modes protected against by the CRBRP core component criteria are as follows:

- Crack initiation caused by ductile rupture from combined short and long term loading,
- Crack initiation caused by creep-fatigue interaction under combined short and long term loading,
- Elastic/plastic/creep instability causing gross distortion or incremental collapse under short and long term loading, and
- Loss of reliability and function due to excessive deformations under short and long term loading.

The fundamental difference between RDT draft rules for Breeder Reactor Core Components and the CRBRP structural design criteria is that crack initiation and elastic/plastic/creep instability failure modes are only of significance if the loss of function expressed in terms of excessive deformation limits are not exceeded. Alternately, crack initiation and elastic/plastic/creep instability failure modes which occur at deformations which exceed the deformation limits necessary to assure function for the specific core assembly region evaluated are not relevant. Accordingly, the CRBRP inelastic structural criteria were formulated on the basis of assuring that crack initiation and elastic/plastic/creep instability failure modes would not occur before deformation associated with functional limits are exceeded. The protection against elastic/plastic/creep instability failure modes prior to exceeding deformation limits was assured by requiring large deformation non-linear analysis for core assembly regions subjected to mechanical loads which are energy unbounded and load controlled. Conversely, for core assembly regions with thermal loads which are energy bounded and deformation controlled, non-linear small deformation analysis is required. In this arrangement, the structural integrity of the CRBRP core assembly regions reduces to assuring that crack initiation failure modes would not occur before limits on excessive deformation failure modes were exceeded.

The detailed formulation of the design criteria of Table 4.2-7 and the conditions for which they are applicable, are given in the CRBRP fuel assembly stress report, Reference 171.

4.2.1.1.2.2.2 Removable Radial Shield Assembly (RRS) Structural Component Design Criteria

The design criteria were selected so that the RRS structural components will satisfy their functional requirements described in Section 4.2.2.1.1.9 at the following operating and loading conditions over their design life within the constraints of the damage severity limits of Table 15.1.2-1.

(A) Operating and Loading Conditions

1. Thermal-Hydraulic:

Steady-state and transient conditions shall be considered.

The umbrella transients for the shield assembly include normal, upset, emergency and faulted categories. An appropriate number of events will be determined for hottest shield assemblies based upon the design replacement schedule, since some of the shield assemblies will have less than a 30 year life.

2. Mechanical Loads

For determining loading sources to be considered in the structural evaluation of shield assembly duct structures; core restraint, seismic, thermal and miscellaneous effects are considered.

These loadings represent a generalization of all the currently postulated loading mechanisms applicable to CRBRP core assembly duct structures. While some of these loadings may be negligible or inapplicable to the shield assemblies, they nevertheless form the minimum basis for the conservative evaluation of the design adequacy of the shield assembly duct structures. The determination of structural loads shall utilize the environmental conditions in accordance with the requirements of Table 15.1.2-1.

3. Nuclear Environment

Table 4.2-9A summarizes the range of environment of the shield assemblies.

(B) Structural Design Criteria

The shield assembly is not currently covered directly by an existing structural design code. The shield assembly structural design criteria are basically similar to those in 4.2.1.1.2.2.1 for fuel and blanket assemblies. The following subsections describe specific requirements which are used for the design of the RRS.

1. General Criteria for All Shield Assembly Structures

The general structural criteria which are used in the shield assembly structural evaluation are defined in Table 4.2-9B. The shield assembly structural components shall be designed so that deformation due to mechanical loading, thermal expansion, and neutron irradiation induced swelling and creep does not produce gross interference with adjacent components such that the equipment functional requirements of 4.2.2.1.1.9 cannot be satisfied. The effect of loss of carbon, nitrogen, and alloying elements shall be considered when determining the strength of the material.

2. Component Structural Design Criteria

Shield Assembly Inlet Hardware:

In the inlet hardware (nozzle, transition, orifice, rod support), where maximum temperatures do not exceed 800°F, the base metal is ductile and the time dependent thermal creep is expected to be negligible. Time independent ductile failure modes covered by the applicable ASME Boiler and Pressure Vessel Code are used as the basis for structural design requirements.

Consequences of shield assembly inlet hardware loss of structural integrity are significantly less severe than those for pressure boundaries and permanent components. Therefore, the emergency stress limits for shield assembly inlet hardware are higher than those given by the ASME B&PV code⁽¹⁾, but the maximum stress intensity shall not exceed the minimum ultimate tensile strength.

Shield Assembly Outlet Hardware:

The material is expected to be ductile and thermal creep may be significant. Both the time-independent and time-dependent ductile failure modes covered by the applicable ASME B&PV code, code cases and RDT standards are used as the basis for the structural design requirements.

The time independent stress limits for normal and upset condition specified by the ASME B&PV Code are used directly for outlet nozzle design.

Thermal fatigue failure and creep related failures (creep rupture, excessive strain, creep fatigue) are prevented by imposing the appropriate design limits in Table 4.2-9B.

3. Shield Assembly Duct

Where a minimum uniform elongation greater than 3% cannot be demonstrated, brittle fracture is considered as a potential failure mode and specific

⁽¹⁾The ASME B&PV Code is applicable to pressure boundaries and permanent components. The shield assemblies are not pressure boundaries and are removable.

analytical methods to be used in fracture mechanics evaluations are developed.

4. Design Limits for Inelastic Analysis

Because of the inherent simplifications in elastic and simplified inelastic analyses which are offset by additional conservatism in the corresponding limits, inelastic analysis methods may be used in lieu of the elastic analysis methods. The structural criteria are given in Table 4.2-9B.

5. Special Weld Requirements

Since all of the joining is accomplished by mechanically pinning the components and seal welding, there are no structural weldments in the shield assembly.

4.2.1.1.2.3 Requirements for Design Features

In addition to the preceding operational requirements, specific design features shall be incorporated into the fuel and blanket assembly designs to preclude the accident conditions discussed in Chapter 15.4 and any detrimental effects which could adversely affect the attainable design life.

1. Sufficient constraint shall be applied to the fuel and blanket rods to minimize fretting and wear at the support points.
2. The fuel and blanket assembly materials shall be compatible with adjoining materials and environmental conditions during their design lifetime. Where potential for excessive galling or self-welding exists, mating components shall be hard coated.
3. The relative location of the pellet column with the fuel and blanket rods shall be maintained during shipment to prevent damaging reactivity fluctuations during start-up by utilizing a properly designed axial spring support system.
4. The assembly axial support system shall maintain fuel and blanket assembly axial positions under all steady-state and transient operating conditions while providing for differential thermal expansion of the internal structures and the irradiation induced expansion of the assemblies. With the current CRBR baseline design, the limit is 2.5 inches at 70°F.
5. The inlet nozzles for the assemblies, in conjunction with the reactor internals, shall be designed with sufficient aperture redundancy to preclude total inlet blockage and to provide for adequate cooling even after total blockage of one inlet passage.

6. Adequate precautions are taken via project procedures to preclude fuel, blanket and removable radial shield assembly (RRSA) blockages after assembly at the fabricator and prior to reactor insertion. These precautions include 1) an air flow test at the fabricator after component assembly, 2) controlled storage and shipment to the CRBRP site, and 3) visual inspection of inlet nozzles upon assembly receipt at the CRBRP site. These precautions preclude the necessity for evaluations of blocked assemblies during and after refueling.
7. To prevent loading of a fuel or blanket assembly into a position where it is undercooled, the following situations must be prevented by a properly designed discrimination system.
 - a. Fuel assembly insertion into a position where it would be undercooled, i.e., a position in which more coolant flow through the assembly is required for heat removal than can be admitted by the flow orifice in that assembly or receptacle.
 - b. Fuel assembly insertion into positions in the core that are provided for the control rod assemblies, blanket assemblies and removable shield assemblies, except for those positions where fuel and inner blanket assemblies are intentionally interchangeable.

- c. Blanket assembly insertion into positions that are provided for control rod assemblies, removable shield assemblies, or fuel assemblies, except for those positions where fuel and inner blanket assemblies are intentionally interchangeable.

4.2.1.1.3 Environmental and Material Considerations

The following design basis material properties shall be used for assembly design and analysis either directly or by modification of previous material property correlations.

Post irradiation test data do not represent in-reactor environment; they provide a conservative measure of in-reactor degradation effects as discussed below.

The major effects of in-reactor degradation are the enhancement of thermal creep rate and the reduction of tensile properties (strength and ductility) and creep rupture strength. As discussed in the Sections below, the causes of this degradation are depletion of interstitial elements due to sodium exposure and damage due to irradiation. Since the mechanical properties affected by in-reactor degradation cannot be physically monitored during reactor operation, post irradiation testing is required to obtain the appropriate data.

The use of post-irradiation test data for design-basis degradation effects is conservative. For interstitial loss and irradiation effects, the degradation is zero upon reactor insertion and reaches its maximum value at the end of a given residence time. It is at this maximum level of degradation that post-irradiation test data, which is used as the design basis, is acquired. Furthermore, if the test material was irradiated in flowing sodium, any synergistic interaction of irradiation and interstitial loss would be included in the post irradiation test data.

As an example, assume that the loading causing damage in-reactor remains constant. Then for this example, the cladding damage ratio would be represented by:

$$DR = \frac{1}{\tau} \int_0^{\tau} R(t) dt$$

where: τ = in-reactor residence time, and

$R(t)$ = the variation in degradation with time, t .

This damage ratio is a measure of the cladding damage averaged over the in-reactor residence period. It is further assumed that the actual in-reactor degradation is linear with time, ie:

$$R_{ACT}(t) = R_{EOL} t/\tau$$

Thus, for an actual irradiation period, the damage is

$$DR_{ACT} = \frac{1}{\tau} \int_0^{\tau} R_{ACT}(t) dt = \frac{1}{\tau} \int_0^{\tau} \frac{R_{EOL} t}{\tau} dt = \frac{R_{EOL}}{2}$$

using the assumptions given above.

However, for performance analysis studies, the design basis degradation determined from post-irradiation testing corresponding to residence time t is assumed to be:

$$R_{DES}(t) = R_{EOL}$$

Thus, for design performance analysis studies, the damage ratio is:

$$DR_{DES} = \frac{1}{\tau} \int_0^{\tau} R_{des}(t) dt = R_{EOL}$$

utilizing the assumptions given above.

Figure 4.2-1B shows the comparison of the actual and design basis damage ratios. The design basis cladding damage ratio at end of life is twice that actually accrued assuming time linear degradation. Using the same logic, similar results can be derived with any non-linear in-reactor degradation which increases. Thus, the application of irradiated materials properties in this manner to design performance analysis gives conservative results.

4.2.1.1.3.1 Irradiation Induced Creep and Swelling

The stress free swelling equations used in the CRBRP fuel and blanket assembly analyses are shown in Figure 4.2-3, while the irradiation induced creep and stress enhanced swelling equations which were used are given in Figure 4.2-4.

In the cladding analysis, irradiation induced creep is considered as a significant deformation mechanism. However, it is not currently considered to be ductility limited as stated in fuel rod design requirement 4 of Section 4.2.1.1. To date, there has been no evidence that prototypic cladding material will breach when a certain level of irradiation induced creep is exceeded.

4.2.1.1.3.2 Creep Rupture Properties and Thermal Creep

Creep rupture properties include primary and secondary thermal creep rates and rupture stress as a function of time. They are used primarily

to evaluate cladding integrity either by inelastic strain accumulation or cumulative damage analysis (see Section 15.1.2). Thermal creep is an insignificant deformation mechanism when compared to irradiation induced creep and swelling.

For conservatism, the thermal creep correlation for solution annealed 316SS is also used for 20% cold worked material for evaluation against the strain criteria. The thermal creep correlation is given in Ref. 1. The rupture strength-time correlation used for cumulative damage analysis is described in subsection 15.1.2.1.

4.2.1.1.3.3 Tensile Properties

Tensile properties used in the evaluation include the modulus of elasticity, proportional limit and ultimate tensile strength. The unirradiated modulus of elasticity is reported for both solution annealed and 20% cold worked 316SS in Ref. 153. The proportional limit and ultimate strength variation with temperature and irradiation are given in subsection 15.1.2.1.

4.2.1.1.3.4 Cladding Wastage

Cladding wastage is a broad term used to denote both material loss and degradation of properties due to the high temperature, high energy neutron flux, and sodium environment. Various mechanisms that have been identified include:

- a. Loss of material and surface depletion (chromium and nickel) due to sodium corrosion.
- b. Internal cladding attack by redistributed fission products.
- c. Loss of material due to fretting and wear.
- d. Degradation of material strength due to loss of carbon and nitrogen.
- e. Decrease in time to rupture and material strength due to irradiation.
- f. Manufacturing tolerances and defects.

The wastage associated with inelastic strain analysis is as follows:

1. Sodium corrosion allowances (item a) are consistent with the time and temperature dependent material loss of the LIFE-III National Fuel Rod Performance Code (see following subsection).
2. Allowances for fission product attack (item b) are consistent with the burnup and temperature dependent material loss of the LIFE-III code.

3. Tolerance and defect allowances (item f) are consistent with CRBRP cladding drawing tolerances and inspection techniques.
4. Other allowances (items c, d, and e) are simulated by an additional 2 mil material loss at 80,000 MWD/T peak burnup, use of solution annealed rather than cold worked thermal creep equations and a factor of ~ 3 on rupture strain. These allowances are consistent with FFTF fuel rod analysis assumptions.

In the context of fuel rod design, cladding wastage rates are utilized in the various analytical models which are used to evaluate fuel rod performance under a variety of expected environments. If the various parameters used in these analytical models are inadequate (including cladding wastage), the experimentally determined fuel rod performance will be less than that predicted by the models. Thus, the ultimate adequacy of the cladding wastage allowances are determined comparing experimental fuel rod performance and fuel rod performance calculated by the criteria of PSAR Section 4.2.1.1.2.2.

In this manner, the comparison of the analytical and experimental fuel rod performance presented in Section 4.2.1.1.2.2 confirms the adequacy of the cladding corrosion and wastage allowances. If these allowances were inadequate, i.e., if the cladding corrosion and wastage rates were appreciably greater than assumed, the fuel rods subjected to steady state tests would have failed sooner than predicted by the analysis. However, as noted in Section 4.2.1.1.2.2 for the cases where the experimental fuel rod assembly porosities were prototypic of CRBR values, the burnups attained by the fuel rods under steady state test conditions were well in excess of the calculated burnup.

Further verification of the adequacy of the cladding wastage allowance is found in the results of FFTF fuel rod transient tests. These tests are described in detail in Reference 57; the pertinent results are given in Tables 4.2-D and 4.2-E. For these tables the cladding strain limit criteria and the calculational techniques outlined in Reference 57 were used to calculate the expected rod failure limits. Cladding wastage effects were included in these calculations. Again, if the assumed cladding wastages would have been adequate, the tested rods would have failed at levels below those predicted by analysis. As shown in Tables 4.2-D and 4.2-E, only one of the rods tested failed below the predicted levels. This single failure appears anomalous, since a rod subjected to the same pre-transient environment but twice the transient stress level than this rod failed at higher temperatures. Thus, both steady state and transient test results indicate the design wastage allowances are adequate.

Neutron hodoscope data from HUT tests 5-3A and 5-5B, and a very recent LASL experiment (PINEX) qualitatively demonstrates that the time for fuel pin cladding failure as indicated by the thermocouples in the capsules corresponds directly with actual, real time observation of cladding failure. Detailed analyses of these data which quantitatively supports this conclusion is included in Reference 173.

For cladding cumulative damage analysis, the treatment of wastage is reported in subsection 15.1.2.1.

Fretting and Wear

The fuel rod cladding design-basis wastage allowance for fretting and wear referred to above is as follows:

- 0.5 mil at beginning of life for either fretting and wear or cladding scratch.
- 2.0 mils per 80,000 MWD/MT burnup linearly applied during life for fretting and wear.

Although the 2.5 mil wastage at end of life would be localized circumferentially near the wire wrap interface, it is conservatively applied to the full 360 degrees of cladding outside circumference.

The magnitude of the fretting-wear wastage allowance was based upon 316 stainless steel pin-disk tests performed in sodium at Westinghouse Research Laboratories (Reference 76). The oscillatory pin (6 cycles per minute) was 0.25 inch in diameter and ground to a 4-inch hemispherical radius. The disks were machined from bar stock with a flat test face dimension of 0.67 inch by 0.75 inch. Sodium oxygen content was less than 5 ppm. Average wear depths for prototypic loads and sodium temperatures are given in items 1 to 4 of Table 4.2-C. Similar tests at Karlsruhe with higher loads and cycles subsequently indicated a similar wear depth, see Reference 77 and item 5 of Table 4.2-C.

53 | The above data are nonprototypic with regard to geometry; the pin-disk tests were primarily intended to simulate fretting wear between fuel rod cladding and a spacer grid support system. However, fretting-wear tests utilizing prototypic cladding and wire wrap geometry have been performed in sodium (3-5 ppm oxygen) at ETEC (Reference 78). As the data (items 6 to 11 of Table 4.2-C) are similar to the preceding 1000 cycle data, it is believed that the major portion of the wear depth occurred during the early stages of the test and that it is not extremely sensitive to geometry.

The major driving force for fretting and wear in wire wrapped assemblies has been ascertained to be a combination of individual fuel rod and overall rod bundle flow induced vibration. This premise arises from the behavior of loosely packed rod bundles irradiated in EBR-II. For a given fuel rod geometry, flow induced vibration is in turn controlled by coolant flow velocity, wire wrap axial pitch and the amount of porosity per fuel rod ring in the rod bundle. The following features are being incorporated into the fuel assembly design to minimize flow induced vibration and the potential for fretting and wear:

- 51 |
1. The CRBRP utilizes 6 discrete flow orificing zones within the fuel assemblies so that overcooling (flow velocities higher than necessary) is minimized.

2. The shield block exit geometry and rod attachment assembly are designed to promote uniform flow distribution across the inlet of the fuel rod bundle.
3. The axial pitch of the fuel rod wire wrap is 11.9 inches, the same as FFTF.
4. The radial porosity between the fuel rod bundle and the duct is minimized by the selective assembly techniques described in Section 4.2.1.2.2.

The adequacy of items 3 and 4 in controlling fuel rod cladding fretting and wear has been confirmed in the prototypic EBR-II experimental sub-assemblies P13, P14, and P14A.

The purpose of the EBR-II experimental subassemblies P13, P14, P14A is included on page VC-46, and page III.C-3 of PSAR Reference 101. The irradiation schedule for these tests is included in Reference 162, page A-23. These tests have been completed and the assemblies have been examined. In a topical report, "Flow Induced Vibration of Fuel Rods in CRBRP", the relevance of these data for the CRBRP design in conjunction with other tests is discussed. This topical report was submitted in February, 1977. Examination of the P13 and P14 test assemblies revealed that a decrease of the radial porosity between the fuel rod bundle and the duct in these test assemblies did indeed prevent significant cladding and wire wear. The results from these tests are used to set the rod bundle porosity. Final confirmation will come from the FFTF operation or CRBRP surveillance. The results of these examinations and the testing status were reported at the "CRBRP Fuel Meeting" with NRC, October 13 and 14, 1976 in Bethesda, Maryland.

4.2.1.1.3.5 Effects of Fuel and Cladding Swelling

As noted in subsection 4.2.1.1.2.1, fuel-cladding interaction due to differential fuel and cladding swelling is a design basis operating condition. The magnitude of the fuel cladding interaction is to be calculated using the LIFE code which evaluates the thermal and mechanical effects of both the fuel and cladding as well as their interaction. This code has been adopted as the national LMFBR fuel pin performance code. All cladding material properties as well as the following fuel properties have been jointly agreed to by the National LIFE committee which includes representatives of DOE/RRT, AI, ANL, GE, HEDL and W-ARD:

- a) fuel mechanical properties including the effects of fuel cracking and subsequent healing,
- b) fuel restructuring including porosity, grain size and plutonium distribution,
- c) fuel swelling including the effects of hot pressing and solid fission products,

- d) fission gas release and the resulting plenum pressure, and
- e) gap conductance, fission gas thermal conductivity and conductance for fuel cladding contact.

It should be noted that the LIFE fuel rod performance predictions using the fuel properties above are based upon comparisons with actual rod performance determined through irradiation tests in EBR-II. In many cases, certain aspects of these tests are prototypic of CRBRP design conditions (see subsection 4.2.1.3 Irradiation Experience).

The changes in fuel properties with temperature and irradiation exposure described above can adversely affect the allowable power (or temperature) for fuel melting which as noted in subsection 4.2.1.1.2.2 is a design basis. The effect of initial O/M (oxygen/metal) ratio on the melting point is negligible while the melting temperature drops initially and then continues to decrease with burnup at a much lower rate. However, the fuel restructuring and gap closure effects calculated by the LIFE code tend to compensate somewhat for the decrease in power to melt. The evaluation of the power-to-melt of the CRBRP fuel rods is discussed in Section 4.4.3.3.6.

The LIFE code (Reference 175) consists of two interconnected sets of computational modules, thermal and mechanical. The thermal module calculates parameters such as fuel and cladding temperature, power to melt and fission gas release while the mechanical module calculates parameters such as fuel-cladding contact pressure, cladding stress and the resultant cladding deformation. In the current pre-release version of the LIFE code, LIFE III, the thermal module has all models in place. However, the iterative process of defining calibration constants, qualitative checking and verification of the mechanical module against experimental data over the entire range of expected CRBR environments is still in progress. Also, several mechanical design parameters, such as cladding wastage and plenum gas pressure, are presently calculated more conservatively in the fuel rod design codes FRST and FURFAN than in the LIFE III code. For these reasons, the following restrictions and modifications to the LIFE III code results were applied to the CRBRP first core fuel and blanket rod evaluations:

- a) The LIFE III code has been formulated, calibrated, and verified for steady state conditions only. Thus, this version of the LIFE code cannot be used to determine FCMI during rapid transient events.
- b) The LIFE III code models are capable of predicting steady state FCMI loads in blanket rods. This code can also calculate fuel and blanket rod responses to mid-life power increases which may occur over time periods of 10 hours or greater. However, these predictions must be used with judgement since the LIFE III code has neither been calibrated or verified to account for blanket rod effects in general or rod environment change rates of this magnitude in either fuel or blanket rods.

- c) The steady state FCMI pressures calculated by the LIFE code are adjusted to account for the differences in cladding wastage between the LIFE III code predictions and the fuel rod design code predictions.

These restrictions and adjustments will be re-examined and modified, if necessary, for later versions of the LIFE code.

For the fuel rod, analyses were performed for steady state FCMI loads at axial locations 12, 18, 27 and 36 inches above the bottom of the fuel pellet stack (i.e., at $X/L = 0.33, 0.5, 0.75$ and 1.0 , where L is the fuel pellet stack length of 36 inches). For the blanket rods, these calculations were performed for axial locations 29, 40 and 50 inches above the top of the rod lower end cap (i.e., at $X/L = 0.46, 0.62$ and 0.78 where L is the blanket pellet stack length of 64 inches). Prior experience indicated that the most significant FCMI effects occurred at these locations.

Item b) above notes that the LIFE III models are mathematically capable of predicting steady state FCMI in blanket rods. They can also predict effects of mid-life power increases which occur over time periods on the order of tens of hours or longer in both fuel and blanket rods. However, LIFE III calibration and verification has not included either of these considerations. Thus, while the LIFE III code was utilized in this study to investigate both blanket rod FCMI and effects of mid-life power increases in blanket rods, these results are preliminary and subject to changes in magnitude as more advanced versions of LIFE become available. To compensate for this uncertainty, the following procedures were followed in this study:

- a) The steady state FCMI adjustment noted in item c above which compensates for the conservative design cladding wastage was not applied to the blanket rods. This results in considerably higher calculated FCMI loads in the blanket rod cladding.
- b) In the LIFE III analyses, the rods which experience a mid-life power increase were brought to power at varying rates during the startup of the second cycle. As discussed in Section 4.2.1.3.1.1 below, this indicates the effects of programmed startup on FCMI loads, and suggests a method whereby excessive FCMI (if present) due to the mid-life power increase experienced by blanket rods may be minimized. Also power jumps greater than those actually calculated to occur are assumed in these evaluations. Thus, the calculated power jump effects on cladding performance are conservative, based on current models.

By taking this approach, the LIFE III results may be used to formulate qualitative conclusions about blanket rod behavior under certain conditions for which this version of the code has not been specifically calibrated.

4.2.1.1.3.6 Environmental Effects - Blanket Assemblies

The effect of operating environmental conditions in the blanket assemblies will be similar to those for the design equations and considerations for fuel appearing in Section 4.2.1.1.3. Four areas are different, however.

- 1) Because of low sodium flow in the radial blanket assemblies, the corrosion rate on the cladding will be lower than that for the fuel rod cladding. It has been noted that there is a linear flow rate dependency when the velocity is less than 10 ft/sec (subsection IV.H of Reference 58). Hence, corrosion values may be variable in the various orificing zones of the radial blanket.
- 2) Due to the chemical nature of the UO_2 , its initial O/M ratio, and the fission product spectrum in the blanket rods, it is anticipated that there will be less fuel-clad reaction for a given temperature condition and temperature gradient than for mixed oxide fuel rods.
- 3) Based on present CRBRP nominal and specification values of oxygen in sodium and blanket UO_2 , the theoretical uniform volume expansion would be 2% $\Delta V/V$ for extreme reaction conditions after a failure late in life (subsection 4.2.1.1.3.8).
- 4) As noted in subsection 4.2.1.1.3.5, the LIFE fuel rod performance predictions including the effects of fuel cladding interaction are based upon comparisons with actual rod performance determined through irradiation tests in EBR-II. These tests are prototypic of CRBRP fuel rod design conditions and may not apply to the blanket rod. (See subsection 4.2.1.4 Irradiation Experience.)

Further information on these differences is provided in the response to Question 241.74.

4.2.1.1.3.7 Fission Product Redistribution

The primary fission product which may affect the in-reactor performance of fuel rods is cesium (Ref. 2). Cesium can lead to the formation of low-melting mixed oxide compounds at the fuel-cladding interface and these compounds increase the intergranular attack of the cladding. Cesium can also react with fission-product molybdenum to form cesium molybdate. Under the radial thermal gradient in the fuel, this compound can transport molybdenum and oxygen to the fuel-cladding interface by vapor-phase transport. Cesium can migrate axially and react with axial-blanket uranium pellets to form cesium uranate. This reaction leads to swelling of the pellets. However, in cases where sufficient voidage is available near the insulator, failures should not occur even though extensive reaction may be observed. Some cesium reaction with the axial blanket is anticipated in the CRBRP fuel rods; therefore voidage must be available in the gap to preclude significant interaction with the cladding.

Axial migration is observed in fuel rods in which the initial O/M ratio of the fuel is < 2 (i.e., ~ 1.95). In fuel pins with initial O/M ratio closer to 2, the fission product cesium is observed to remain as Cs_2MoO_4 and not migrate to the insulator pellets. The formation of Cs_2UO_4 in blanket pellets also depends on the stoichiometry of the urania. Formation of significant amounts of Cs_2UO_4 is expected only if the urania is hyperstoichiometric.

Electron microprobe studies (Ref. 3) of radial cross sections of fuel rods have shown that fission-product cesium tends to concentrate in the cooler region of the oxide, especially in the region of the fuel-cladding interface. Also highest concentrations of fission-product molybdenum are found in the noble-metal alloy inclusion and in the cooler region of the fuel adjacent to the fuel-cladding interface. The CsMoO_4 is observed to be stable under conditions of low temperatures and high oxygen potentials (Ref. 4). Low oxygen partial pressures and/or high temperatures decrease the tendency to form gaseous Cs_2MoO_4 in the hot region of the fuel and thus hinder the migration of molybdenum. Under these conditions, the cesium will migrate axially to react with urania blanket pellets to form cesium uranate. Evaluation of the potential and magnitude of this effect is reported in item 5 of the Fuel Rod Steady-State Evaluation (Section 4.2.1.3). This evaluation also refers to the irradiation tests which will be used to update the migration phenomenon and associated understanding of fission product cladding reaction and interaction effects.

4.2.1.1.3.8 Performance of Defected Fuel and Blanket Rods

The CRBRP is being designed for operation with limited amounts of failed fuel, as described in Chapter 11. Fuel or blanket rod failures which exhibit only fission gas releases will not be removed from the core as they present no safety problem provided design basis limits are not exceeded (see Chapter 15.4). Fuel assembly failures having concurrent or subsequent indications of fuel exposure to sodium by a defined limit, are to be removed from the core. Development of this limit is dependent on the development of appropriate technology which will assure the benign nature of operation with limited fuel-sodium contact (see response to NRC Question 241.76). Failed fuel assemblies characterized as having gross fuel losses or exposure to sodium in excess of the limit are to be removed from the reactor vessel on a priority basis.

When the Delayed Neutron Detectors (DND's) indicate that there are gross fuel losses or excess sodium exposure, suspect assemblies which have been identified by the Fuel Failure Monitoring System will be removed from the core. Verification that the correct assembly has been removed will be obtained by reactor startup and monitoring of the DND's. The frequency of inspection will be controlled by the frequency of failures that exhibit gross fuel losses or excess sodium exposures as indicated by the DND's.

51

Amend. 52
Oct. 1979

This subsection reviews the available information concerning operation with fuel or blanket material exposed to sodium.

Out-of-pile and in-pile tests (GETR and EBR-II - References 5-9) have shown that both UO_2 and $(U,Pu)O_2$ will react with sodium, where the reaction product has the generic formula, Na_3MO_4 (where M is U or [U, Pu]). These tests and isothermal equilibration tests at Argonne National Laboratory (ANL) (Reference 10-14) have indicated that this compound forms in the presence of excess sodium under conditions where the oxygen activity is sufficient to stabilize the compound. Oxygen, which is the limiting specie, may come from either fuel, sodium or both.

The evaluation of possible reactions between fuel or blanket materials and sodium indicates that effects of the reaction can be deleterious, but proper control and additional testing and development can result in safe operation of an LMFBR with failed fuel or blanket rods. It is concluded that:

1. The reaction product between sodium and fuel or blanket material is Na_3MO_4 , where M is (U, Pu) or U, respectively.
2. If the oxygen concentrations in the sodium and the fuel or blanket material are greater than the respective equilibrium values, the reaction will proceed and form a stable product. If the oxygen content in either specie is below equilibrium value, a stable reaction product will not form.
3. The reaction product, Na_3MO_4 , has a density about one-half that of the reacting fuel or blanket material.
4. Volumetric swelling under uniform reaction conditions at equilibrium is approximately equal to the difference between the initial and equilibrium deviations from stoichiometry.
5. Volume expansion under uniform reaction conditions appears to reach a maximum value in time, consistent with the attainment of equilibrium.
6. The higher temperatures and higher initial O/M values are conducive to more rapid attainment of reaction equilibrium.
7. The O/M of fuel or blanket material increases with higher burnup.
8. Present LMFBR nominal and specification values of oxygen in sodium and fuel or blanket materials are higher than presently available experimental equilibrium values. Confirmation of this point is needed.
9. Theoretical uniform volume expansion of CRBR fuel and blanket pellets would be 5% and 2% $\Delta V/V$, respectively, for extreme reaction conditions after a failure late in life.
10. Sufficient data is not available to predict local swelling under non-uniform reaction conditions in CRBR fuel and blanket rods.
11. Many bare fuel rods have operated in fast reactors for periods up to 2 1/2 years after failure without reported difficulty or effects on reactor operation.

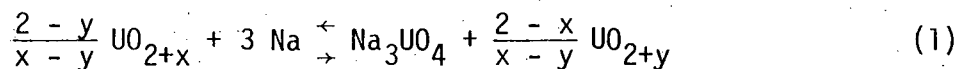
Irradiation tests, in sodium, of defected blanket rods are planned (See Section 1.5.1.5) to resolve the unknown described above. In addition, it is currently planned that run-beyond-failure irradiation testing of fuel will be done in EBR-II in support of the LMFBR program.

51

A detailed discussion of the considerations which led to these conclusions follows:

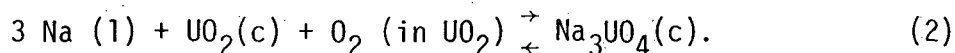
The Na-U-O System

Various compounds of Na with UO₂ have been reported in the literature to have densities (Table 4.2-1) lower than the density of UO₂ (~11 g/cc). Pepper (Ref. 9) et. al. and Blackburn (Ref. 14) et. al. studied the various regions of the Na-U-O system. These phase relations are shown in Figure 4.2-5 at about 800°C (1472°F). The three phase region of importance to the UO₂-sodium reaction is Na-UO₂-Na₃UO₄, since Na₃UO₄ has been established as the phase in equilibrium with UO₂ and Na in defected fuel or blanket elements. The mass-balance reaction between sodium and uranium oxide is



where 2+y is the final equilibrium stoichiometry of uranium oxide. Sodium will react with UO_{2+x} as long as the oxygen pressure, which is determined by temperature, oxygen concentration of UO_{2+x} and oxygen dissolved in sodium, is greater than that in equilibrium with the UO₂-Na-Na₃UO₄ three-phase system. The reaction will proceed until the oxygen pressure is reduced to the equilibrium value.

The equilibrium reaction in the three-phase region, Na-UO₂-Na₃UO₄, is



Measurements have been made at ANL (Ref. 15 to 18) to acquire the thermodynamic data for Na₃UO₄. Data from these studies were used to derive the following equation for the equilibrium oxygen pressure as a function of temperature and sodium activity.

$$\ln P(\text{O}_2) = \frac{-220,500}{RT} + \frac{62.7}{R} - 3 \ln a_{\text{Na}}, \quad (3)$$

where -220,500 is the difference in the enthalpies of formation for Na₃UO₄ and UO₂, and 62.7 is the corresponding difference in entropies of formation. If the liquid sodium is at the same temperature as the oxides, the last term is zero. When there is a temperature differential (where the fuel is hotter than the sodium), the sodium activity is equal to P_{Na}/P⁰_{Na}, where P_{Na} is the equilibrium sodium pressure at the temperature of the liquid sodium and P⁰_{Na} is the equilibrium pressure calculated for the temperature of the UO₂. For the Na-UO₂-Na₃UO₄ three-phase region, P_{Na} is given by

$$\log P(\text{Na}) = \frac{-5120}{T} + 4.35. \quad (4)$$

Combining equations (3) and (4), one can obtain the oxygen pressure in terms of sodium and UO_2 temperatures:

$$\ln P(O_2) = \frac{-290,800}{RT_{UO_2}} + \frac{70,300}{RT_{Na}} + \frac{62.7}{R} \quad (5)$$

The partial molar free energy of oxygen in urania as a function of temperature for various values of the O/U ratio are shown in Figure 4.2-6. From this data and equation (3) or (5), the equilibrium O/M values in the Na- UO_2 - Na_3UO_4 system can be calculated.

Based on the oxygen pressures in three-phase equilibrium Henry's Law and the solubility of sodium oxide, the equilibrium oxygen content (in ppm) of sodium in contact with UO_2 and Na_3UO_4 is given by (Ref. 15):

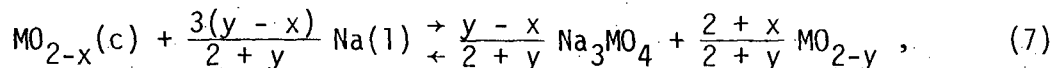
$$\ln[O] \text{ (ppm)} = \frac{-11,550}{T} + 14.33. \quad (6)$$

The U-Pu-Na-O System

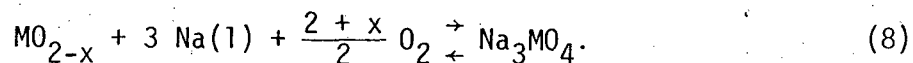
The reaction product of sodium and mixed-oxide fuel has been established as Na_3MO_4 , where M represents (U,Pu). It was also observed that the (Pu/U+Pu) ratio in the Na_3MO_4 phase was essentially the same as that of the mixed-oxide from which it formed.

As noted earlier, the oxygen required to form Na_3MO_4 in the sodium-mixed oxide reaction could come from either the mixed oxide, the sodium or both. However, if the initial oxygen of sodium is less than its equilibrium value when in equilibrium with $(U,Pu)O_2$ and Na_3MO_4 , the sodium cannot contribute oxygen to the reaction. Furthermore, if the oxygen content in sodium remains below the equilibrium value, the formation of a stable reaction product, Na_3MO_4 , is not possible.

Neglecting the oxygen content in sodium the reaction can be written as



where $(2-x)$ is the initial O/M ratio of the fuel and $(2-y)$ is the corresponding equilibrium value below which reaction with pure sodium cannot occur. To calculate oxygen pressures for Na_3MO_4 and mixed oxide, the difference between the free energies of formation of Na_3MO_4 and $(U,Pu)O_2$ is assumed to be the same as the difference between the free energies of formation of Na_3UO_4 and UO_2 . The equilibrium reaction in the three-phase region is



Equations (3) and (5) are also applicable in this case because it has been assumed that the U-Na-O system approximates the U-Pu-Na-O system for low concentrations of Pu. As before, with the partial molar free energy of oxygen in mixed oxide and equation (3) or (5), the equilibrium O/M ratio for the mixed oxide can be calculated.

There is a great variation in the measured oxygen potentials by various authors (Ref. 19 to 21). In this calculation however, Rand and Markin's (Ref. 22) data are used (Figure 4.2-7). Table 4.2-2 shows the calculated equilibrium O/M values for different fuel compositions along with some measured values (Ref. 16) and oxygen concentrations in Na in equilibrium with Na_3MO_4 .

Nature of Reaction Products

The principal characteristics of Na_3UO_4 are:

- fcc structure with $a = 4.77 \text{ \AA}$ to 4.80 \AA
- theoretical density of 5.6 g/cc
- melting temperature of 1420°C .
- for 80% TD, heat conductivity at 540°C is an order of magnitude less than that of UO_2 .

The Nature of Reaction and Relationship to Swelling

Previous discussions of the reaction between UO_{2+x} and Na, and $(\text{U,Pu})\text{O}_{2-x}$ and Na indicated the reactions will be limited by the available sodium or oxygen. In the case of failed fuel or blanket elements in a reactor, excess sodium will be present and hence, oxygen will be the reaction limiting specie. The reaction appears to start with the formation of a surface layer product followed by reaction within the fuel matrix at grain boundaries. The initial grain-boundary penetration proceeds by formation of a very thin intergranular layer. The intergranular layer thickness leads to cracking and further intergranular attack.

Theoretical volume expansion due to the reaction can be calculated based on the initial O/M of the fuel, theoretical densities of the reactants and reaction products, and the theoretical equilibrium O/M of the system. The degree of swelling thus depends on the amount of oxygen available in the system. The volumetric swelling observed at equilibrium is proportional to the divergence between the initial O/M of the fuel and the equilibrium O/M in the system. That is,

$$\% \Delta V/V \cong 100|x - y| ,$$

where x and y are the deviations from stoichiometry initially and at equilibrium, respectively.

Kinetics of the Reaction

The data for reaction rates of sodium with fuel or blanket material are still incomplete. Aitken (Ref. 5) has described the in-pile reaction rates of defected pins with sodium showing a one-fourth power time dependence. The proposed mechanism assumes the rate to be controlled by sodium diffusion through the reaction product layer. If this is the rate limiting mechanism, one would expect the product to form a layer of near-uniform thickness on the surface of the fuel. Since intergranular attack is observed, reaction control by sodium diffusion appears unlikely. However, if the diffusion of the sodium to the fuel through the product interface is faster than the oxygen diffusion within the fuel, then intergranular attack can be explained because oxygen is believed to diffuse more rapidly along grain boundaries than normal to grain surfaces.

Kinetic studies at ANL (Ref. 23) show that in most instances the curves of volume expansion versus time level off at each temperature to form plateaus. The volume expansions at the plateaus were in fair agreement with the maximum theoretical expansions calculated based on the equilibration studies. Therefore, it is assumed that the plateaus do represent the attainment of equilibrium conditions. The time to reach equilibrium depends on the reaction temperature and initial O/M of the fuel. The results indicate that the higher the temperature or the higher the O/M, the more quickly the reaction attains equilibrium.

The effect of fuel density on the volume expansion is not clear. In one test, high density pellets underwent larger volume expansions than less dense pellets. This can be explained on the basis that high density pellets contained smaller void volumes and hence, less of the expansion could take place internally by a process of void filling. The data also indicate a more rapid reaction for the higher density pellets.

Tests to determine the lower temperature threshold for the formation of the reaction product, Na_3MO_4 , indicate the reaction initially occurs in the range of 400 to 450°C. However, Housseau et. al. (Ref. 24) have reported an effect of fuel-sodium reaction on cladding in the range of 300 to 400°C.

Effect of Burnup on Reaction and Swelling

As burnup increases, the O/M of the fuel increases and various fission products are introduced in the fuel matrix. The increase in O/M will increase the oxygen available for the reaction, which increases the amount of swelling. This increased oxygen is due to a lower affinity for oxygen in the fission products than in the fuel. Fission products insoluble in the matrix are observed to have no effect on the reaction. However, soluble fission products, like rare earths and Zr, are observed to increase the swelling. Chemical analyses have failed to show any reaction products other than Na_3MO_4 and hence, the effects of soluble fission products are not clear. However, considerable acceleration of the reaction kinetics is reported (Ref. 24) in the presence of soluble fission products.

Limitations in the Application of Theory and Experimental Data

Inherent difficulties in accurate analysis of both the O/M ratio of mixed oxides after exposure to sodium, and oxygen concentrations in sodium after exposure to mixed oxides, have limited the amount of experimental data available to establish the oxygen level in sodium required to form the reaction product.

Based on the thermodynamic data, one can calculate the equilibrium oxygen pressure over the $\text{Na-MO}_{2-x}\text{-Na}_3\text{MO}_4$ system and then convert the oxygen pressure to equilibrium O/M based on the oxygen potential data for the fuel. The experimental oxygen potentials for mixed oxide fuel vary as much as 20 Kcal and exhibit great differences in temperature dependence. In most cases, the experimental determinations were done at higher temperatures, thus requiring extrapolation of the data to lower temperatures for the reaction equilibrium O/M calculations. Depending on which oxygen potential data for mixed oxide is selected, one can obtain significant increases (Martin and McIver's data) (Ref. 19), decreases (Woodley's data) (Ref. 21) and essentially no change (Blackburn model) (Ref. 16 and 17) in the O/M ratio with temperature at the three-phase equilibrium. Experimental determinations by Smith (Ref. 25) and Martin and Schilb (Ref. 23) show a decreasing O/M with temperature at the three-phase equilibrium.

The equilibrium O/M ratios given in Table 4.2-2 are calculated for fuel in contact with sodium. Since the LMFBR fuel is expected to have a radial temperature gradient from about 2800°K to 1300°K, the oxygen will be distributed non-uniformly in the fuel. Because of this non-uniform distribution of oxygen, the mole fraction of oxygen within the fuel is not necessarily the same as that at the interface. Thus, the total fuel oxygen content may differ significantly from those values given in Table 4.2-2. In addition, oxygen content of the fuel increases with burnup because the fission products have a lower capacity for oxygen than the fuel. Hence, the start-of-life oxygen content alone is not sufficient to define the conditions for sodium-fuel reaction in irradiated fuel.

The equilibrium oxygen content of sodium for fuel-sodium- Na_3MO_4 equilibrium is practically constant for either UO_2 or U-Pu oxide fuel. The calculated oxygen concentrations in the sodium are independent of the fuel oxygen potentials and therefore, are not affected by the uncertainties in the fuel oxygen potential. These calculations are based on the solubility of Na_2O in sodium, Henry's law, and oxygen pressures determined from equation 3 or 5. The calculated equilibrium oxygen content of the sodium, as shown in Table 4.2-2, is strongly dependent on the temperature at the sodium-fuel interface. Typical oxygen levels in cold-trapped sodium (like EBR-II or an LMFBR) are 1 to 2 ppm. This indicates that the sodium would act as a sink for oxygen above 700 to 800°K. In this instance, the excess oxygen for the reaction is supplied by the high O/M ratio of the fuel that results from oxygen redistribution and burnup in the fuel. However, the flowing sodium would tend to reduce any reaction product that might be

initially formed when the sodium contacts fuel. Since the amount of oxide fuel in the failed pin is small compared to the total flowing sodium, one might expect a limited reaction and therefore; extended operation of the failed fuel rod without any safety hazards.

Smith (Ref. 25) has experimentally determined the equilibrium oxygen concentrations in sodium for the fuel-sodium- Na_3MO_4 system using the vandaum wire equilibration method. The oxygen concentrations in sodium at the three-phase equilibrium varied from ~0.1 to 0.4 ppm in the temperature range of 650 to 900°C. The oxygen concentrations are given as a function of temperature by

$$\ln[\text{O}] \text{ ppm} = - \frac{5720}{T^{\circ}\text{K}} + 3.91.$$

where K is the fuel-sodium interface temperature. The important consequence of this result is that the sodium in typical cold-trapped systems will serve as a source of oxygen for the fuel-sodium reaction in the event of a breach of the cladding. The reaction product is stable under these conditions and increased swelling of the fuel (and therefore fuel rod) with time can be expected. Additional experimental work may be needed to confirm this experimental data.

Effects of Reaction on Cladding Strain (Review of Defected Fuel Rod Experience)

The available kinetic data (Ref. 23) indicate that the fuel-sodium reaction in the presence of excess sodium attains equilibrium within two to six days depending on the initial stoichiometry of the fuel and reaction temperature. The amount of sodium available will depend on the defect size and the sodium flow conditions.

Under uniform reaction conditions the swelling or fuel volume expansion due to reaction will be uniform. If there is no gap available, the volume expansion will force the cladding radially and the strain on the cladding can be assumed to be uniform and equal to the diametral expansion of the fuel. This situation is observed in sodium bonded mixed oxide fuel pins. In the B8 series (sodium bonded mixed-oxide fuel rod) tests diametral increases up to 12% were noted (Ref. 5). The observed changes were in reasonable agreement with the uniform swelling predictions when other deformations were considered.

For example, consider the case of a CRBRP fuel element failing late in life with a sizeable breach of the cladding such that uniform reaction of the fuel is assumed to occur and go to equilibrium. The O/M of the fuel increases during burnup from a specification value of 1.96 to 2.00, as shown in Figure 4.2-8 which will be the value at the time of failure and the start of the fuel-sodium reaction. Assuming an equilibrium O/M value of 1.95 for the fuel, the uniform volume expansion from the relationship given earlier will be 5% $\Delta V/V$, or about 1.67% diametral increase. In contrast,

the blanket material O/M increases from a maximum specification value of 2.01 to approximately 2.019 at the end of life. If failure occurs and reaction starts at this point in time, a uniform volume expansion of 1.9% is calculated at equilibrium where the O/M will be 2.00, as shown in Table 4.2-2. This results in a 0.63% diametral growth.

However, under conditions of a localized cladding breach, the reaction may not take place uniformly but may occur in a narrow sector near the defect. This gives rise to non-uniform fuel volume expansion leading to a non-uniform strain in the cladding near the defect. The non-uniform strain or localized strain would enlarge the defect and, under extreme conditions, potentially lead to a gross cladding rupture.

Several encapsulated rod failures and defected fuel rod tests have shown non-uniform strain near the defect due to sodium-fuel reaction (Ref. 8 and 26). However, none of these tests have shown gross rupture, primarily because the fuel rods were exposed to a limited quantity of static or flowing sodium, which limited the oxygen available from the sodium. The localized strains in the rods were at least three to four times that evaluated for theoretical fuel volume expansion. Values as high as 30% $\Delta D/D$ have been measured in some tests, as shown in Figure 4.2-9. The size of the cladding defect plays an important role in this type of non-uniform reaction. Murata et al. (Ref. 6) have emphasized the uncertainties associated with predicting the swelling resulting from in-reactor sodium-fuel reactions in defected fuel pins (B9A).

Specific data on the extent of sodium-fuel reactions resulting from bare fuel rod failures in fast reactors is essentially non-existent. Failed rods have operated in DFR for over 100 days with little or no deterioration observed after the post-failure operation (Ref. 27). Failures in Rapsodie and BR-5 driver fuel have also occurred and the fuel has remained in the reactor for even longer than 100 days, apparently without deleterious effects. These experiences give credence to the operation of fast reactors with failed fuel rods.

4.2.1.1.3.9 Fission Gas Release

The CRBRP fuel rod design is based on the principle that released fission gas communicates freely with the plenum during normal operation. This principle is used in the design of all operating light water and fast reactors and in those which are currently undergoing design or construction. The basis for using this principle is presented below:

1. It is well established that mixed oxide fuel is extensively cracked when brought to power. Crack healing will occur while the fuel is at power, but not all cracks will heal or heal completely, particularly in the cooler, outer regions of fuel and in the low power, top and bottom sections of the rod. The large body of post-irradiation examination results show that cracks caused during the rise to power (as distinguished from those caused by shutdown) are still present.

Thus, a network of fuel cracks will exist in the outer, cooler regions of the fuel which will maintain contact with the plenum even if the fuel-cladding gap is closed. Also, in the case of high power fuel rods which form a central cavity within the fuel column, experimental results (see 2 below) indicate that fine cracks or openings will exist, which permit communication of this cavity with the cooler regions of fuel and the plenum. The openings may exist anywhere along the cavity, at pellet interfaces for example, or near the ends of the cavity where the fuel temperatures are relatively low because of the axial power profile.

2. Communication between the plenum and fission gas released within the fuel column (to outer fuel regions or the central cavity) was demonstrated in two sets of experiments which employed continuous measurement of released fission gas. Both sets of experiments were designed to test fast reactor fuel and used fuel rod diameters, fuel compositions, and linear power typical of fast reactors.

- a. The first set of experiments (References 97 and 98) was performed in the BR-2 and used pressure sensors to continuously measure fission gas release. The experiments included twelve pins, two referred to as Mol 8B tests and ten as the Mol C tests. One of the Mol 8B tests achieved a maximum burnup of 115,000 MWD/T and the other 40,000 MWD/T (the pressure sensor failed). The ten Mol C fuel pin tests operated to burnups in the range of 74,000 to 96,000 MWD/T. Both Mol 8B pins showed central cavity formation. Post-irradiation examination of the Mol C tests have not been reported, but the linear powers are high enough to form central cavities in the fuel.

Both the Mol 8B and Mol C tests showed a continuous release of fission gas to the plenum while at power throughout life. The effects of shutdowns on gas release were negligible. The latter point is important because if any gas was trapped within the fuel column, it would have been released during shutdowns as a result of the extensive fuel cracking that occurs. These experiments, therefore, show that released fission gas is in communication with the plenum throughout life.

- b. The second set of experiments (References 98, 99 and 100) was performed in the Oak Ridge Reactors and used a helium gas sweep system introduced at the bottom of the fuel column in one case and at the top of the fuel column in the other case, and monitoring of the sweep gas for fission gas detection. Two fuel pin tests were performed, one using solid pellets, GB-10, and the other annular pellets GB-9. The latter test, therefore, does not directly apply to the question but is of interest. The GB-9 pin achieved a burnup of 55,000 MWD/T. The GB-10 pin is still undergoing irradiation and results have been reported for burnup to 7,000 MWD/T. The linear power in the latter test is high enough to form a central cavity.

In both cases, results showed a continuous release of fission gas while the pins were at power and negligible effects of shutdowns similar to the Mol 8B and C experiments. In the case of the GB-10 test where the sweep gas was introduced at the bottom of the fuel column at a pressure of 1,000 psig, the pressure drop through the fuel column was initially 70 psi and dropped to 10 psi as irradiation proceeded indicating that there is significant permeability in the column at low burnup.

Summary

In summary, post-irradiation examination of fuel indicates that fuel cracks are present during steady-state operation. These cracks provide communication to the plenum of gases released within the fuel column. Instrumented tests of fast reactor type fuel rods demonstrate that communication exists to burnups of 115,000 MWD/T. The low burnup fast reactor fuel results (GB-10 in particular) also show that communication exists.

Additional detailed analysis of fast reactor fuel pin tests will be performed to further verify the design bases for the FSAR and additional results from the instrumented tests will be monitored and analyzed.

4.2.1.1.4 Surveillance and Post Irradiation Examination of Fuel and Blanket Assemblies

Current designs and analytical predictions of the behavior of fuel assemblies and rods are based on models supported by experimental data. As more results become available from test programs including EBR-II and other fast reactor experiments, the models will be revised and modified to reflect the behavior and effects indicated by the new post-irradiation data. (See Sections 1.5 and 4.2.1.5 for a description of the fuel and blanket assembly development program.) Frequent assessment and correlation of the analytical codes will continue with the objectives of establishing firm design and performance limits, minimizing uncertainties in the analysis, and understanding rod and assembly behavior. However, restraints on the design and operating conditions of experimental assemblies partially preclude simulating CRBR conditions for all important parameters simultaneously. Therefore, it will be necessary to perform limited periodic examinations of the initial core assemblies. Such examinations will also be used to verify safe operation to the established operating limits; and to obtain data that could be used to establish improved design and operating limits. The following surveillance and post-irradiation examination plan is designed to satisfy these requirements and objectives.

This program is preliminary and the final selection of the surveillance schedule and examination plan (Table 4.2-3 is typical) will be dependent upon the available information from various sources (i.e., EBR-II, FFTF, etc.). The depth and extent of the finalized program will be formulated to provide verification information of parameters which are not available from other sources. Final surveillance and examination plans will be submitted consistent with the FSAR submittal.

The CRBRP can be operated with gas leakers; no reactor shutdown will be required for gas leakers except as noted in Section 7.5.4. The gas leaker is characterized by a fission gas monitor signal but no fuel-sodium reaction signal. Fuel assembly failures having concurrent or subsequent indications of fuel exposure to sodium above a defined limit, are to be removed from the core. Development of this limit is dependent on the development of appropriate technology and will permit operation with limited fuel-sodium contact. Failed fuel assemblies characterized as having gross fuel losses or exposure to sodium in excess of the limit are to be removed from the vessel on a priority basis.

When failures occur in assemblies, the method of detection will generally be either a cover gas monitor signal or a delayed neutron signal or both. The former indicates a release of fission gas from the failed rod, which will also expell a tag gas for assembly identification. The latter type of signal indicates the release of solid fission products to the primary sodium coolant and, most likely, the fuel material in the breached rod is in contact with the sodium, giving rise to the possibility of a reaction between sodium and the pellets (see Section 7.5.4).

All known defected fuel rods having fuel-sodium contact will be removed at each refueling until sufficient data are available to show that such fuel can be operated with predictable and safe results.

4.2.1.1.4.1 General Surveillance and Examination Plan-Fuel Assemblies

The assemblies to be selected for examination in the surveillance program should not have special handling, but should be typical and representative of the production lot of rods and assemblies. All CRBRP fuel assemblies will have a unique identification number legibly marked in arabic numerals and in coded notches on the outlet nozzle. For a given fuel assembly, this unique number provides traceability to the quality conformance inspection reports for that particular assembly. Fuel assemblies charged into the initial reactor loading will have quality conformance inspection requirements patterned after those required for the FFTF Driver Fuel Assemblies. These requirements have been incorporated in the materials and fabrication sections of the appropriate CRBRP fuel assembly equipment specifications.

The quality conformance inspection report and its associated documents for a particular fuel assembly compare the fabrication attributes or parameters, which occur in that assembly (e.g., dimensions, material properties, surface smoothness, etc.) to the nominal design parameters and tolerances. Thus, assemblies can be randomly selected for examination but without specific attention which would tend to make the assemblies non-typical prior to irradiation.

Fuel assemblies located in instrumented positions within the central part of the core should be used for the surveillance tests. They would provide representative thermal history of operation for assemblies with a variety of linear heat ratings, fluence, and burnup conditions.

Schedules of assembly discharges for examination should be planned to maximize the usefulness of the data obtained and to minimize the perturbation of the surveillance program on reactor and plant operation. Special reactor shutdowns or fuel handling activities will not be scheduled solely for discharge of surveillance assemblies.

Fuel assemblies should be removed at several different burnup values consistent with the constraints given above. It is anticipated that the first of these scheduled removals would occur after the first year cycle of operation at a burnup which corresponds to 25,000 to 30,000 MWD/T. Future removals will be dependent upon the need for verification information.

The examination of the surveillance assemblies is described in a later section. To maximize the utilization of results for each increment of burnup, all examination and testing should be accomplished as soon after discharge as possible, but certainly before the next planned incremental discharge. Furthermore, every attempt will be made to minimize the time required to initiate examinations.

4.2.1.1.4.2 General Surveillance and Examination Plan - Blanket Assemblies

The surveillance program must be carefully planned to yield information for critical times during initial operation of the reactor. Results of the examination will be evaluated and used to guide reactor operators through all phases of reactor operation from initial criticality and conservative performance to the ultimate goal of maximizing the plant operating factor with a statistically safe number of failed rods. The surveillance plan identified assumes that pertinent blanket rod tests will have been performed in EBR-II and FFTF with results capable of predicting CRBRP rod performance. If these tests are not available an alternate surveillance program will be developed.

Selection of Surveillance Assemblies

The assemblies to be selected for examination in the surveillance program should be typical and representative of the production lot of rods and assemblies. Radial and inner blanket rods selected for surveillance in the initial reactor loading should be well characterized and identified relative to fabrication attributes, but special handling that would introduce any bias in results should be avoided. The most desirable situation would be to examine assemblies and rods that span the applicable specification and drawing limits.

Radial and inner blanket assembly positions should be selected which provide the best characterization of the irradiation environment.

Operation Without Failure

Schedules of assembly discharges for examination should be planned to maximize the usefulness of the data obtained and to minimize the perturbation of the surveillance program on reactor and plant operation. Special reactor shutdowns or fuel handling activities should not be utilized solely for discharge of surveillance assemblies. Blanket assemblies should be removed at a minimum of two different (and adequately spaced) increments of exposure between initial insertion and the end of assembly life. The first blanket assembly should be removed shortly after the first cycle.

Operation With Failure

Surveillance and examination plans in CRBR will be prepared to handle the presence of failed rods which can occur during all periods of reactor operation. Unexpected failures occurring prior to reaching the design end-of-life burnup include rods suffering from "infant mortality" generally caused by undetected defects in material or workmanship, and rods experiencing transient conditions in the reactor. Failed assemblies may be discharged from the reactor at the next refueling after detection to determine the cause and nature of the failure. However, experiences from previous test programs should provide sufficient guidance to indicate safe operation can be achieved with such failures in reactor. It may be possible to allow surveillance assemblies to be operated to and beyond failure once the Demonstration Phase of the reactor operation is completed.

4.2.1.1.4.3 Typical Examination Requirements - Fuel and Blanket Assemblies

A typical example of a surveillance examination plan for fuel and blanket assemblies, rods, ducts and assembly end pieces is shown in Table 4.2-3. Following discharge, a visual examination and dimensional characterization of the assembly should be performed. Provisions should be available for shipment of the assemblies to hot cell facilities for detailed non-destructive and destructive examinations noted in the table.

Visual examination and bow and length measurements on the rods should be performed prior to removal of the spirally wrapped wire. In addition, the rods should be visually examined after wire removal for signs of wear or reaction on the cladding caused by the wires. Depending on the burnup and condition of any rod at the time of examination, more or less detail will be included in the items listed in the table for the rods. In particular, the extent of sectioning and cladding property tests may be varied as required by non-destructive test results. Similarly, destructive testing of ducts and end pieces will be accomplished only when observations and exposure conditions indicate the need.

Care must be taken throughout the examinations to be able to relate in-reactor orientation to component behavior.

4.2.1.1.4.4 Evaluation of Results - Core Fuel and Blanket Assemblies

The data obtained from this surveillance program will be analyzed in sufficient detail to permit evaluation of current conditions in the assemblies and to provide guidance for the extrapolation and estimation of behavior to higher exposure conditions. Test results from each incremental examination will undergo a timely evaluation to identify satisfactory performance to the next examination point or the possibility of a problem developing which could impact on assembly operation. Examination results will be compared and related to similar findings from experiments in test reactors to assist in the prediction of subsequent operation. The data will be utilized to improve design codes and behavior models which are actively used in the design of reactors.

The proper execution of a surveillance program on core fuel and blanket assemblies and rods in CRBRP will provide a sound basis for improving design lifetimes of assemblies and the overall fuel management and economics of the reactor. Timely data and immediate implementation of results will accelerate the schedule for improved operation of the reactor. Experiences and information developed from this program will also benefit the design and future operation of LMFBRs beyond the CRBRP.

4.2.1.2 Design Description

4.2.1.2.1 Core Design and Operation

The Clinch River Breeder Reactor fuel is a mixed (Pu-U) oxide. It is cooled with sodium. A schematic of the reactor is shown in Figure 4.2-36 to provide orientation for the fuel and blanket assembly locations. The core support plate and the core barrel form the principal locators for the fuel inside the vessel. The fuel, control, blanket, and removable shield assemblies rest on the core support structure. Hydraulic balance is employed to offset the upward forces resulting from the coolant flow through the fuel and blanket assemblies. Each of these reactor assemblies has two load pad areas which match the elevation of the core restraint former rings. The rings are supported by the core barrel which rests on and is attached to the core support plate.

The upper internals structure is located above the core. The structure laterally stabilizes the primary and secondary control rod shroud tubes and also provides secondary holddown for the fuel, most blanket and control assemblies. The four support columns of the upper internals have jacks for lifting the upper internals clear of the removable reactor assemblies for refueling. The in-vessel transfer machine (IVTM) rotates with the upper internals structure for removing and replacing of reactor assemblies at refueling. Fuel transfer and contingency storage positions are provided in the annulus formed between the core barrel and the reactor vessel thermal liner.

The active length of the core is 36 inches and the equivalent diameter of the fuel and inner blanket region is 79.5 inches. The fuel region initially consists of 156 fuel assemblies with a total fissile plutonium loading of 1502 Kg. The reactor core also initially contains 82 inner blanket assemblies, 126 radial blanket assemblies, and 312 removable radial shield assemblies. The total number of fuel and blanket assemblies varies slightly from cycle to cycle as described in Section 4.3. During initial reactor heat-up and sodium fill, the reactor core is completely occupied by core special assemblies (CSA). These core special assemblies are also utilized during special refueling operations (i.e., lower inlet module replacement) to support the core array while the spent core active assemblies are being replaced. The special assemblies are not utilized during normal refueling operations.

The reactor control systems include 9 primary and 6 secondary control assemblies. The two systems are independent and diverse. Both systems are capable of shutting down the reactor from full power to hot standby conditions. A core map is shown schematically in Figure 4.2-10A, while the fuel and blanket numbering scheme is shown in Figure 4.2-10B.

The reactor system is being designed to withstand the various loadings which result from the CRBRP steady state and transient duty cycle events. Details of the steady state nuclear, thermal-hydraulic and mechanical load environments during reactor operation are given in Sections 4.3, 4.4 and 4.2.1.3 respectively.

The umbrella transient duty cycle for the initial CRBRP core is described in Sections 4.4 and 4.2.1.3. This duty cycle covers the current categories of normal, upset, emergency, and faulted conditions as defined in Appendix B.

4.2.1.2.2 Fuel Assemblies

There are six different types of CRBRP fuel assemblies corresponding to the six flow orificing zones as described in Section 4.4.2.5. Coolant flow is controlled by orifice plates within the assembly.

The CRBRP fuel assembly design is based upon the FFTF driver fuel assembly design and LMFBR development experience with modifications necessitated by the breeding, operational and cost requirements of the CRBRP. A detailed comparison of the CRBRP and FFTF fuel assembly design details is given in Table 4.2-4. Welded into a compact structural unit, the fuel assembly can be handled by the refueling machines and provides a controlled path for the primary sodium coolant. As shown in Figure 4.2-11, each fuel assembly is comprised of the following subassemblies:

- A. 217 fuel rods that contain the fuel pellets,
- B. An inlet nozzle,
- C. A shield and orifice region,

- D. A rod attachment assembly,
- E. A duct, and
- F. An outlet nozzle.

The fuel rod design is illustrated in Figure 4.2-12. The mixed plutonium-uranium dioxide sintered powder fuel pellets supply heat and neutrons for breeding, the uranium dioxide axial blanket pellets above and below the fuel enhance breeding, and an upper plenum containing fission product gases generated during operation. Plenum volumes larger than FFTFs are required to allow for the higher fission gas pressures caused by somewhat higher operating temperatures and by potential operation to higher equilibrium burnup levels.

Pertinent safety features of the CRBRP fuel rods, similar to those in FFTF, are:

1. Normal high level quality assurance will be supplied to prevent mixing of the fuel pellet enrichment types or interchange of fuel and axial blanket pellets inside a fuel rod.
2. The fuel pellet column is retained in position during preirradiation shipping and handling by a preloaded helical compression spring made of Type 302 Stainless Steel. After insertion of the fuel rod into the reactor, the spring is flexible enough that it will not restrict the axial expansion of the fuel pellet column.
3. Each fuel rod contains a gas tag capsule which identifies failed fuel rods by a unique gas mixture for each assembly.
4. A wire wrap spacer system is employed to maintain required lateral spacing during normal and transient operation.

The fuel assembly inlet nozzle is designed to support and locate the assembly in the lower internals inlet modules, furnish a mechanical discriminator, provide a hydraulic balance system and allow the primary coolant flow to enter the assembly. These design features are accomplished by using the FFTF inlet nozzle design, except: a) the bypass flow is restricted by piston rings in both directions, and b) six discriminator posts are required to identify the six flow zone assembly types. A detailed description of the discriminator's geometry and functions is given in Section 4.2.1.2.5.

Fuel column holddown spring design calculations were performed following the standard, industry accepted analysis techniques in References 148 and 149. The following requirements were satisfied by the fuel pellet holddown spring (made from type 302 Stainless Steel):

- Prior to insertion into the reactor, the spring shall maintain pellet position during a maximum axial shipping and handling load of 6g.

- After irradiation and thermal induced changes of the spring properties, the spring shall accommodate a pellet column growth of 1.0 inch before compressing the spring to 90% of its solid height.
- The maximum material volume of the fission gas plenum components shall be equal to or less than 15% of the total fission gas plenum volume.

The difference between the minimum and the nominal spring preload provides allowances for:

- a) spring preload deviations at the specified deflection; and for
- b) variation of the compressed spring length caused by manufacturing tolerances.

The torsional wire stress in the spring at the maximum preload was verified to be less than the allowable value.

In addition, the following requirements were satisfied:

- A minimum coil-to-coil clearance during pre-irradiation shipping and handling loads shall be maintained; and
- The spring outside diameter increase due to compression shall not interfere with the minimum cladding inside diameter.

No tests of the fuel column hold down spring are planned except for the required QA tests during fabrication.

The primary coolant flows from the lower internals through slots in the receptacle side walls that match with slots on the side of the inlet nozzle into the fuel assembly. This coolant path is designed to prevent passage of foreign objects that may cause total or partial coolant flow blockage to a fuel assembly. In the lower internals the primary flow is strained to preclude passage of particles greater than 0.25 inches in diameter. The total area of the six inlet nozzle slots is 3.5 times greater than the assembly internal flow area. The geometrical configuration of the inlet slots precludes total blockage and disperses gas bubbles. Hydraulic and gravity forces acting on the fuel assembly determine the net hold down force which is used to keep the assembly seated in the receptacle and maintain correct axial location of the fuel. The FFTF-type piston ring seal and inlet slots continue to sustain the hydraulic holddown even if the fuel assembly should be lifted a maximum of 2.5 inches to contact the upper internals structure.

In the context of CRBR fuel assembly design, the term "hydraulic holddown" refers to the design features which assure that the hydraulic forces when acting in conjunction with gravity forces, keep the assembly seated in the lower inlet module. These design features are illustrated in Figure 4.2-11A and are explained below.

The fuel assembly is designed so that the hydraulic forces acting on it remain unchanged even in the event that the assembly is lifted from its seated position in the core. The inlet nozzle at the lower end of the fuel assembly is inserted into the cup-like receptacle of the lower inlet module (LIM). The fuel assembly cannot disengage from the LIM in an assembled reactor because it is trapped by the upper internal structure. However, sufficient clearance is provided between the fuel and upper internal structures to allow for axial expansion of the fuel assembly caused by thermal and fluence effects.

Coolant flow enters the inlet nozzle of the fuel assembly radially from holes in the sides of the LIM. A piston ring is used to seal the annulus between the nozzle and LIM to prevent this flow from entering the core interstitial region. Although nominally the sealing requirement is for a static seal, a piston ring type dynamic (moving) seal was selected. This piston ring is fitted inside a finished cylindrical bore in the LIM where borelength is greater than the clearance at the top of the fuel assembly. This arrangement ensures continuous sealing even if the fuel assembly should lift up from its seated position in the LIM. Necessarily, this piston ring is located above the nozzle inlet holes and the finished bore is located above the LIM radial flow holes.

Reduction of the hydraulic pressure load acting upward on the inlet nozzle is accomplished by venting the space at the lower end of the inlet nozzle to a low pressure region. A second piston ring seal is used near the bottom of the nozzle to separate the high pressure inlet flow from the vented space. This seal has the same requirements as does the other seal used between the inlet flow and the core interstitial space, with the exception that the piston ring and its mating bore must be located below the inlet flow paths.

The sum of the various vertical forces acting on the fuel assembly determines the net holddown force which keeps the assembly seated in the receptacle and maintains correct vertical location of the fuel. The weight of the assembly in air is approximately 450 lb., but it weighs only about 390 lb. when submerged in sodium because of bouyancy effects. Small differences in diameter between the top and bottom piston rings combined with the differential pressures acting on the assembly result in a net upward hydraulic force of about 50 lbs., which reduces the seating force of the assembly to roughly 340 lb. Because of the seating arrangement discussed above, this net seating force exists even if the assemblies are raised by some hypothetical mechanism to bring them into contact with the UIS. In addition, the inlet nozzle and LIM is designed to provide adequate coolant flow regardless of whether the assembly is seated or in contact with the UIS.

Coolant flow control and attenuation of damaging neutron fluence to the lower internals structure is provided by the shield block and orifice plates. The five flow rates required for proper cooling of the fuel assemblies are accomplished by varying the number of orifice plates and the number

and size of the holes in a plate. Staggering of the holes between the plates and shielding provide the maximum flow control by preventing flow streaming and limits the maximum length of foreign particles. Only objects smaller than the orifice holes in the individual orificing zones can enter the shield block. Axial grooves and numbers on each orifice plate assure hole staggering and plate identification when the plates are welded together to form a subassembly.

Recent nuclear experiments at ORNL indicate that one shield block with sufficiently long, straight through holes (or hole) will reduce the neutron streaming and flux to acceptable levels. The lower internals lifetime is longer than FFTF's, requiring more nuclear shielding provided by the lower axial blanket and longer shielding effective length. The shield block external geometry and the connection of the rod attachment assembly, duct and inlet nozzle to the shield block are the same as in the FFTF. The proper assembly of these components is done with normal high level quality control. When completed, the shield and inlet assembly can be inspected visually to confirm proper assembly.

When all the attachment rails have been pinned in place a plenum is formed between the attachment rails and shielding, providing mixing and uniform flow to the fuel rods. The attachment rails divide the flow. Only objects smaller than the sub-channel flow area can pass through the bundle. No over-heating of fuel rods will occur even if a large portion of the flow area at the attachment rails should become blocked by loose objects because flow redistribution will take place beyond the rails prior to the fueled section.

Similar to FFTF, a closed hexagonal duct surrounds the fuel rods and directs the primary coolant flow. The assembly duct wall also prevents the adjacent assembly from being in direct communication with molten fuel and/or coolant pressure resulting from fission gas ejection and possible interaction between molten fuel and the sodium coolant. It provides a means of absorbing the damage due to local pressure pulses caused by fission gas ejection and provides a delaying mechanism against melt-through to the assembly adjacent to the failed one. The load pads, thicker than FFTF's because of the larger core, are capable of transmitting the radial core restraint loads and assure that adjacent assembly ducts contact only at the pads to prevent hangups during refueling operations. Large contact areas minimize local bending stresses and reduce the probability of self-welding.

The across flats clearance between the fuel rod bundle and the duct will be controlled through selective assembly. The selective assembly will be as follows.

1. 217 fuel rods and a fuel assembly duct are selected from inventory. The fuel rods are not wrapped with the spacer wire at this point.

2. The diameter of each of the 217 fuel rods is measured at a number of axial locations.
3. The flat-to-flat inside dimension of the duct is measured at a number of axial locations.
4. From the measured dimensions obtained in steps 2 and 3, the arithmetic average rod diameter of the 217 fuel rods and the arithmetic average duct flat-to-flat inside dimension is calculated.
5. These average dimensions are entered into the graph of Figure 4.2-12A to determine the diameter of the wire wrap.
6. The wire wrap of the required diameter is attached to the fuel rods. Next the rod bundle is assembled, strip-by-strip onto the rod attachment assembly on the shield block. The duct outlet nozzle subassembly is then slid over the completed bundle and welded to the shield block.

The location and number of axial measurements on the rod and duct will be specified in the CRBRP fabrication requirements when sufficient statistical data from FFTF fuel assembly fabrication is accumulated.

The outlet nozzle is designed to guide the flow from the fuel assembly into the flow collector and instrumentation in the upper internals, to provide refueling features, and with the inlet nozzle and load pad, provide fuel assembly radial positioning and support. The outlet nozzle inside surface controls the coolant exit velocity to minimize the potential for outlet nozzle vibration and directs the flow into the proper flow collector and associated instrumentation. Design features of the outlet nozzle and inlet nozzle will be provided to preclude fuel rod damage in the unlikely event of an assembly entering an occupied position.

The outlet nozzle geometries that assist refueling are:

1. An inside surface groove to receive the refueling machines' grapple fingers.
2. A large exit diameter to guide the grapple nose into the nozzle when the IVTM and outlet nozzle are misaligned,
3. An external diameter that does not prevent a discrimination post on a neighboring assembly that is misaligned from being inserted,
4. Assembly tapers to guide a fuel assembly in and out of its receptacle or to guide neighboring assemblies during refueling, and

5. A transition from the outlet nozzle outside diameter to the load pad hexagonal geometry to provide a tapered surface that, when mated with the shielding transition region tapers on an assembly entering the core, will rotate the assembly to a correct azimuthal orientation.

After an assembly has been completely withdrawn from the core, axial grooves on the outlet nozzle can be interpreted to verify a specific type of core assembly, its serial number and the reference orientation by the refueling machine (See Section 9.1). Normal high level quality control and administrative procedures will be utilized to assure the identification notches on the outlet nozzle match with the flow orifices.

With the exception of the fuel and axial blanket pellets and the Inconel 718 piston rings and locking bar, all other fuel assembly components are austenitic stainless steel. These materials have been selected because of their toleration to the reactor operating conditions and the availability of prototypic operating experience being developed for the LMFBR fuels program. As in the FFTF driver fuel assembly design, the fuel rod cladding, end caps and wire wrap as well as the fuel assembly duct are Type 316, austenitic stainless steel nominally 20% cold worked. The inlet and outlet nozzles and shielding orifice subassembly are solution annealed Type 316. To minimize the potential for damage, galling and wear, the mating surfaces of the inlet nozzle and piston rings with the lower inlet module are chrome plated while the load pads on the duct and outlet nozzle are chrome-carbide coated.

The selection of chromium carbide coatings for the load pads in the outlet nozzle and duct is the consequence of an intensive program on friction, wear and self-welding, supported by the USDOE. From this program, test results showed that bonded chromium carbide based materials provided the lowest, most consistent friction coefficients. Further investigation of a variety of processes for applying chromium carbide based materials revealed that the detonation-gun process was able to provide a coating that could pass the friction, wear, sodium corrosion, thermal cycling, mechanical integrity and irradiation tests required to meet acceptance criteria. Additional information on this program and testing involved in the development, evaluation and qualification of chromium carbide coatings for sodium cooled reactor applications is given in Reference 165.

The selection of chrome plating for the inlet nozzle was based upon its successful performance for similar applications in EBR-II and verification testing for FFTF. Reference 48 reports that the compatibility of chromium plating with EBR-II primary sodium coolant was determined by two techniques. First, stainless steel components that had been chromium-plated were examined after years of exposure to primary sodium in the reactor. Second, a special subassembly was exposed to EBR-II primary sodium for 13 months in which a loss of chromium plating of as little as 10^{-6} in. could be detected by

gravimetric means. The results obtained indicate that chromium plating is completely compatible with the flowing EBR-II primary sodium coolant at temperatures at least as high as 840°F, which is higher than the CRBRP sodium inlet temperature of 730°F at the chromium plated inlet nozzle.

The FFTF testing consisted of withdrawal and insertion of a full size assembly under prototypic and experimental core configurations. Nozzles of 316 SS or chromium plated SS were used in contact with Inconel 718 liners (prototypic for FFTF and CRBRP). Tests were run in air and in high purity sodium at 400°F (refueling temperature). The occurrence of wear and material transfer on the nozzle, piston ring and liner surface, as well as axial withdrawal forces and lateral forces at the load pad and nozzle receptacle regions were determined as a function of the following FFTF parameters (which umbrella the CRBRP design and environment):

- nozzle design,
- nozzle surface material,
- deflection of the fuel assembly duct produced by thermal expansion, irradiation induced creep and/or swelling distortion,
- deflection of adjacent load pad configurations, and
- IVTM grapple misalignment

53 | Testing results verified that selection of the chromium plated surface in place of stainless steel (see Figures 2 and 3 in Reference 166) would provide superior resistance to nozzle wear damage, not cause damage to the long-life receptacle and provide withdrawal forces well below the IVTM (for CRBRP) and IVHM (for FFTF) capability.

Dissimilar materials mentioned above may be in contact as described below:

1. In the fuel rod attachment assembly, the Inconel 718-locking bar mates with surrounding parts made of type 316 stainless steel (316SS). The locking bar is located in a hole in the top of the attachment assembly.
2. The chrome plated Inconel 718 piston rings are located in grooves in the 316SS inlet nozzle.
3. The 316SS inlet nozzle mates with the Inconel 718 receptacle in the lower inlet module (LIM). The inlet nozzle is chrome plated at potential points of contact with the LIM.

51 | The materials indicated above were selected specifically to preclude galling and self-welding. In addition, the Above Core Load Pad and Top Load Pad are chrome-carbide hard surfaced to prevent galling and self-welding at inter-assembly contact points.

4.2.1.2.3 Radial Blanket Assembly

The functions of the radial blanket assemblies are:

- a. Provide, contain and position the fertile material for conversion to plutonium.
- b. Produce heat for the Primary Heat Transport System.
- c. Provide radial shielding of the core support structures and the radial shield.

A radial blanket assembly consists of 61 rods arrayed in a triangular pitch and supported in a hexagonal duct. The duct is axially and laterally positioned by the inlet nozzle at the lower end; additional lateral positioning is provided by 2 rows of load pads at intermediate elevations located on the outside of the assembly. The assembly is also axially positioned by the hydraulic balance system acting on the inlet nozzle. The outlet nozzle at the upper end has an internal shoulder to accommodate the refueling grapple.

Radial Blanket Rod

The radial blanket rod is shown in Figure 4.2-13. Each rod consists of cold worked stainless steel cladding surrounding depleted UO₂ pellets and a fission gas plenum above the fuel pellet column. The rods are fixed to the assembly at the lower end and spaced at intermediate points along the length with helical wire wrap with a 4 inch pitch. The radial blanket cladding tube prevents contact between the pellets and sodium, and prevents radioactive fission gas from being released to the primary system. The radial blanket pellets are manufactured from depleted uranium oxide with the dimensions given in Table 4.2-5. The fuel pellet column is held in place during shipping and handling by a helical coil holddown spring. The spring is designed to not interfere with the thermal expansion of the fuel pellet column during reactor operation. The dimensions of the cladding and rod are given in Table 4.2-5. The lower end cap provides a keyhole slot which mates with an attachment rail to positively locate the rod within the assembly. After the rod assembly, a tag gas is released into the fission gas plenum.

51

The spacer wire is made of cold-worked Type 316 stainless steel and is wound in a clockwise helical spiral around the blanket rods with sufficient preload to prevent wire slackening during operation. The wire is wound with a 4 inch pitch and the ends of the wire wrap are welded to the end plugs.

Radial Blanket Assembly

The radial blanket assembly is shown in Figure 4.2-14. The key dimensions are compiled in Table 4.2-5. The features of the radial blanket assembly are similar to the Core Fuel Assembly with the following exceptions:

1. The radial blanket rod bundle contains 61 rods.
2. All radial blanket assemblies are identical before irradiation.
3. The discriminator post is different, preventing insertion of a control, inner blanket or fuel assembly into a radial blanket location or a radial blanket into a control, inner blanket or fuel assembly location.
4. Four different orifices are built into the lower inlet modules of the radial blanket region of the reactor, see Section 4.4.

The radial blanket residence time in the inner row is four years. The lifetime in the outer row of radial blankets is limited to five years because experience and materials data for longer irradiations are not yet available. Radial blanket shuffling is not currently planned; however, shuffling or rotation of the radial blanket assemblies is possible if more detailed analysis reveals the desirability for such operations.

4.2.1.2.4 Inner Blanket Assembly Design

The inner blanket assemblies perform functions (a) and (b) of Section 4.2.1.2.3. They are located in the core where they are surrounded by fuel and control assemblies. The inner blankets use the basic features of the radial blanket assembly design; in particular, the blanket rod bundle configuration and duct design are identical for the two types of assemblies. With this approach the inner blanket design can be based on much of the development and test data which is being or will be generated for the radial blanket assembly. This minimizes the need for additional development (see Section 4.2.1.5).

The inlet nozzle, shield block, and orificing of the inner blanket is designed to interface with the inlet modules in the inner core region. To accomplish this design, features similar to those of the fuel assembly inlet and hardware are adopted. Unlike most of the radial blanket assemblies significant flow orificing will be incorporated into the lower end of the inner blanket assemblies.

The assembly discrimination system will prevent insertion of an inner blanket assembly into a fuel, control, or radial blanket assembly position.

4.2.1.2.5 Discrimination System for Correct Loading Assurance

The fuel and inner blanket assemblies are designed to be inserted in discrete positions throughout the reactor core. Each fuel and inner blanket assembly position in the core requires a particular assembly type.

The assembly type is determined by the required amount of flow through the assembly. There are a total of six distinct fuel assembly types and three distinct inner blanket assembly types. However, the discriminator on one of the inner blanket assembly types is the same as one of the fuel assembly discriminators. This is to allow alternation between an inner blanket assembly and a fuel assembly at uniquely defined core locations (see Figure 4.2-10A). Thus, eight different discriminator configurations, or eight different assembly types are located in the fuel/inner blanket region of the core. These eight different types of assemblies are located in a unique pattern that is repeated for each 60 degree sector of the core. Figure 4.2-10A shows a typical core segment containing all of the different types of assemblies.

All radial blanket assemblies are identical; the correct amount of flow for each blanket position is regulated by orifices located in the assembly and in the lower internals inlet module receptacle. Any radial blanket assembly can be inserted into any location in the radial blanket zone. The potential for and consequences of an incorrect radial blanket placement are discussed in Section 15.4.3.

To prevent overheating and possible melting of the fuel the following design basis of subsection 4.2.1.1.2.3 (item 6) must be satisfied and the following operational error must be prevented:

Inclusion of an incorrect type component into a fuel assembly which would result in improper fuel loading, improper flow orificing, or insertion into an undercooled position in the core.

The following subsections describe how the required protection is provided.

- a. Insertion of the fuel or inner blanket assembly into a fuel or inner blanket assembly position where it would be undercooled is prevented by a mechanical core location discrimination system. It consists of eight unique 2.35-inch long discriminator posts at the bottom end of the inlet nozzles that are distinguished by combinations of post and

blind axial hole diameters. This geometry was selected for its manufacturing simplicity and independence of orientation to the load pad hexagonal geometry. The discriminator posts interface with 2.30-inch high discriminator inserts which have matching hole and post diameters. The discriminator inserts are made of Inconel 718 and are located at the bottom of the receptacles in the lower internals inlet modules. The post and hole diameters vary to form the eight types of one-way fuel and inner blanket assembly discriminators identified in Figure 4.2-15. The diameters were chosen to minimize the refueling stresses for both the normal and mis-loaded condition. If a fuel or inner blanket assembly is inserted into an incorrect fuel or inner blanket assembly location, the discriminating features will not match; the receptacle insert will not accept the fuel or inner blanket assembly discriminator post and will stop the assembly 2.30-inches short of its fully inserted position. The resulting 2.30-inch height difference is detected by the in-vessel transfer machine axial position locating system. In addition the IVTM cannot release the assembly from the grapple. Thus, loading of a fuel or inner blanket assembly into an incorrect fuel or inner blanket assembly location is prevented.

- b. Loading of fuel and inner blanket assemblies into control assembly locations is prevented by a similar system of discriminators as described above.

The radial blanket and removable shield assembly inlet nozzle and receptacle diameters are smaller than the fuel assembly nozzle and receptacle diameters. Thus, insertion of a fuel or inner blanket assembly in these locations is precluded. Insertion of radial blanket or shield assemblies into fuel assembly locations is prevented by interference between the inserts in the receptacles for fuel and inner blanket assemblies and the inlet nozzles of the radial blanket and shield assemblies which do not have corresponding interfacing features. Incorrect insertion in these cases will also result in a height difference of 2.30 inches or more that is detected by the IVTM and which will prevent release of the assembly from the grapple.

- c. Each of the six unique fuel assembly types is composed of one of six unique types of inlet nozzles, one of six unique types of orifice assemblies, and a handling socket assembly that has a unique arrangement of identification notches for an individual fuel assembly.
- d. Each of the three unique inner blanket assembly types is composed of one of three unique types of inlet nozzles, one of three unique types of orifice assemblies, and a handling socket assembly that has a unique arrangement of identification notches for an individual inner blanket assembly.

Prevention of improper combination of these fuel assembly components with variable geometries for the purpose of distinguishing between orifice configurations, core lattice position and identification is insured by adhering to high level quality assurance procedures. These include measuring component dimensions and visual inspection of component features and identification markings. All variable geometry components have identification features or letters that are visible throughout the entire assembly process.

4.2.1.3 Design Evaluation

The fuel rods are designed and analyzed to meet the design criteria of Section 4.2.1.1.2.2 for the design environments which envelope the steady state and transient environment presented in Sections 4.3 and 4.4. The analytical methods utilized to assure fuel rod conformance with the cladding strain limit and CDF criteria are also described in Section 4.2.1.1.2.2. The conservatism of the rod performance capabilities calculated with CDF and strain limit analytical techniques and criteria will be verified by comparing actual fuel rod lifetimes from the steady state and transient test programs (References 162 and 168) with corresponding rod design lifetimes calculated using these techniques and criteria. To assure a valid verification, the test rod will:

1. Be subjected to steady state and transient environments whose severity levels envelope those of the CRBR design environment and
2. Provide sufficient data to allow conservative extrapolation to those CRBR conditions which cannot be duplicated in the current test facilities.

Thus, the analytical tools which are used to preclude failure of fuel during steady state and transient reactor operation will be verified by direct comparison with representative rod lifetime data.

The work performed to date towards verifying the analytical methods and criteria is described in References 75, 57 and Section V of Reference 58 and is summarized in Tables 4.2-B, 4.2-D, and 4.2-E.

The data used in this verification work was obtained from in-reactor test programs in which over 1000 rods have been tested in environments typical of the CRBRP, and from ex-reactor, materials property test programs in which hundreds of individual tests of several different types (e.g., stress rupture, FCTT, etc.) have been performed.

In Reference 75, a strain limit procedure for determining rod steady state lifetime similar to that described in Section 4.2.1.3.1.2 was utilized to calculate the design lifetimes of several EBR-II test rods which were exposed to a temperature and burnup range encompassing CRBRP operation. The major differences in the procedure used for experimental verification and the CRBR design procedure of Table 4.2-A are:

- a. Nominal cladding temperatures were utilized in the verification work calculations. The CRBR fuel rod design procedure utilizes the cladding design hot spot temperatures (see Section 4.4), and therefore would predict shorter lifetimes than the procedure used in the verification study.
- b. The thermal stress due to the temperature gradient across the cladding wall was neglected in the verification study. In the CRBRP design procedure, this thermal stress is assumed to be relieved entirely by ductility limited thermal creep. This assumption adds to the total cladding ductility limited strain, and therefore results in shorter fuel rod lifetime predictions with the CRBRP design procedure than with the verification procedure.
- c. No fuel cladding mechanical interaction (FCMI) was considered in the verification study. In the CRBR design procedure, FCMI loads are considered, and under certain conditions can reduce the calculated rod lifetime compared to fuel rods which are loaded by plenum gas pressure alone.

51 Even with these assumptions, the procedure and the corresponding strain limit were shown to be conservative as summarized in Table 4.2-B.

Further verification of the conservatism of the cladding lifetime determined by the strain limit techniques is found in the results of FFTF fuel rod transient tests. These tests are described in detail in Reference 57; the pertinent results are given in Tables 4.2-D and 4.2-E. For these tables the cladding strain limit criteria and the calculational techniques outlined in Reference 57 were used to calculate the expected rod failure limits. As shown in Tables 4.2-D and 4.2-E, only one of the rods tested failed below the predicted levels. This single failure appears anomalous, since a rod subjected to the same pre-transient environment but twice the transient stress level than the anomalous rod failed at higher temperatures. Thus, both steady state and transient test results indicate the cladding strain limit analysis techniques and design criteria are conservative.

Verification of various aspects of the CDF technique using a variety of materials test data is described in Section V of Reference 58. These verification studies have shown that:

- a. The cladding mechanical damage due to a series of loading conditions is the sum of the damage due to each load;
- b. The materials property models in the CDF procedure are basically correct;
- c. The method used in the CDF to analyze transients is correct;
- d. The distribution of experimentally observed failure times lies within the uncertainty bands around the nominal failure times predicted by the CDF procedure.

Preliminary work which compared experimentally observed rod lifetimes from steady state EBR-II tests with the lifetimes predicted for these rods by the CDF procedure also showed the CDF procedure to be conservative. This work will be updated in the future using more accurate values for the reactor environment, as noted below.

The rod cladding loads utilized in both the strain limit and CDF verification calculations summarized above was assumed to be due to fuel rod internal gas pressure only. Also, the combined steady state and transient experimental environments used in these verification studies do not completely envelope CRBRP conditions. Additional experimental fuel rod lifetime and cladding loading data must therefore be obtained before the verification of fuel rod design criteria and analysis techniques can be completed. Also, the published values for the in-reactor environments for the completed fuel rod tests of interest are preliminary. Further analysis verification work will be performed with the final environment values only. The general verification plan for the CDF related design procedure as it relates to the various aspects of design analysis verification is given in Items 3 and 4 of Table 4.2-65. The experiments to obtain additional data for verification

(References 162 and 168) and the refinement of the in-reactor environment values for completed fuel rod tests are currently in progress. Based on the information given in Table 4.2-65, a general plan for the CDF and strain limit design procedure verification activities is given in Table 4.2-5A. The fuel rod design analysis verification work will be completed and reported in the FSAR.

The purpose of the design analysis techniques and criteria (both CDF and strain limit) is to assure that the design lifetime of a particular rod design is sufficient to meet performance objectives (i.e., preclude failure). The verification calculations indicated above are intended to assure these calculated design lifetimes are conservative (i.e., that the fuel rod performance objectives will actually be met). The various models which are utilized in the design analysis techniques (e.g., material stress-strain curve, material UTS vs. temperature data) should be realistic, yet the design analysis procedure and criteria must be capable of precluding failure. The verification results obtained to date (see Tables 4.2-B, 4.2-D, 4.2-E, and Reference 58) indicate that this is indeed true for the models and techniques used in the CDF and strain limit design procedures. As noted above, these verification studies will be extended in the future to include experimental fuel rod environments which envelope both steady state and transient CRBR conditions. Thus, the viability of the analytical procedures and criteria can be adequately demonstrated without showing that each model within these analytical procedures is always conservative for every conceivable combination of environmental conditions. Alternatives and fallback positions are defined in Section 4.2.1.6 in the event that future testing and analytical efforts do not verify the adequacy of the preliminary design limits and techniques.

There is a direct relationship between the analytical fuel and blanket rod performance results, the reactor damage prevention methods (plant protection system), and reactor control points such as total plant power and core mixed mean outlet temperatures. The fuel and blanket rod are designed and analyzed to meet their design criteria for a specified steady state and transient core design environment. As discussed above, correlation with test results will verify the conservatism of the design procedures, and will assure that rods which meet these criteria will fulfill their performance objectives for the specified design environment. The plant protection system and control points are designed to limit the actual reactor steady state and transient environment to severity levels below those of the design environment. Thus, performance of the plant protection and control systems within their specifications will assure that the fuel and blanket assemblies operate within their design environment limits. This assurance of specified core environment levels, in combination with the verified fuel rod design procedures discussed previously, in turn assures that the CRBR fuel will meet its lifetime objectives.

4.2.1.3.1 Fuel and Blanket Rods

An analysis of the CRBRP fuel and blanket rod designs was performed to show that the design requirements of subsection 4.2.1.1.2.2 are satisfied for the worst initial core operating conditions. The analysis concentrated upon the steady state (normal) conditions and the design transients for upset and emergency conditions that were expected to be life limiting. The basis for this selection was experience from the FFTF fuel assembly design evaluation and the analysis of experimental oxide-fueled assemblies which are being irradiated in EBR-II. The steady state and transient analyses are described below; the analyses of the consequences of faulted and accident conditions are considered on an individual event basis in the appropriate subsections of Chapter 15.

In all design calculations, design basis temperatures and pressures were assumed which equal or envelope those described in Section 4.4. These temperatures and pressures, when utilized with design basis materials properties, cladding wastage rates, and fuel swelling models, resulted in design stresses and strains with conservative design margins. Stress effects on irradiation swelling and swelling effects on irradiation creep were included when needed to obtain conservative results.

In accordance with the design bases of subsection 4.2.1.1 detailed analyses were also performed for the blanket components in the areas of thermal hydraulics, stress, deflection, flow induced vibration, seismic response, and irradiation damage. The blanket assembly failure mechanisms considered were ductility limited creep rupture strain, overstressing due to steady-state and transient loads and temperatures, and interference between adjacent parts. Additional consideration must be given to the increased uncertainties in material properties over long radial blanket component lifetimes.

In these analyses, the postulated failure modes for the blanket assemblies and the fuel assemblies are generally the same. Therefore, the same basic analytical tools were used for the analysis of both. Some design conditions which are more severe in the radial blanket than in the fuel assembly are the large radial temperature gradients and larger required component lifetimes. The radial blanket can survive these conditions because the neutron fluxes, temperatures, and damaging effect of transients are less severe than in the fuel assembly region.

Amend. 53
Jan. 1980

4.2.1.3.1.1 Fuel and Blanket Rod Damage Mechanisms

54 | Steady State Loads

Based upon previous experience, the primary sources of steady state cladding damage that were considered in the first core evaluation included the following:

- A. Secondary stresses due to differential growth are generated by the radial temperature gradient through the cladding thickness. All cladding temperatures used in the analysis enveloped the design basis hot spot temperatures reported in Section 4.4.
- B. Fission gas release during life generates pressure stresses on the sealed fuel rod cladding. The fission gas pressures used were determined as discussed in Section 4.4.
- C. Wastage effects reduce cladding thickness and strength as described in subsection 4.2.1.1.3.4.
- D. Fuel-cladding contact pressure is generated by differential growth with respect to the fuel pellet. Fuel-cladding mechanical interaction was investigated by use of detailed fuel pin performance codes. Such codes are necessary to integrate the various phenomena occurring in the fuel and cladding which determine the stress at the fuel-cladding interface. The basic element of such codes is a thermomechanical stress strain analysis system which analyzes the interactions occurring between the fuel and cladding and within each of these components. The codes were used to incorporate thermal expansion, swelling, creep, and elastic deformations of the fuel and clad and hot pressing and restructuring of the fuel into columnar, equiaxed, and undisturbed zones.

The fuel swelling calculation is based on a phenomenological model of fission gas forming bubbles that achieve equilibrium with their surface tension and the hydrostatic stress in the fuel and are later released to the plenum. Since independent measurements do not exist, the fuel swelling and restructuring models are calibrated from measurements of irradiated fuel rods. These rods cover a broad range of operating conditions with linear power from 6 to 19 kw/ft; O_2 to 12_2 atom %; cladding temperature, 900 to 1300°F; fluence, 0 to 8×10^{22} n/cm² ($E > 0.1$ Mev); fuel density, 88 to 96% theoretical; and fuel centerline temperatures up to melting.

Fuel rod performance codes with their mechanical analysis and materials models determined from independent experiments and fuel swelling and restructuring calibrated to a variety of fuel irradiations are used to calculate fuel clad mechanical interaction (FCMI). This interaction is caused by differences in swelling between fuel and cladding. Cladding swelling

51

Amend. 54
May 1980

has an incubation period in which the swelling rate is low. During this time the fuel swelling generally closes the fabricated fuel-clad gap and generates a fuel-clad interaction stress. After the incubation period the increased clad swelling relieves the interaction stress. Under certain conditions, this increased cladding swelling results in re-opening the fuel clad gap. This has been observed experimentally with solution treated cladding in EBR-II.

The code used in the ongoing calculations of cladding loads is LIFE, Reference 175, (see Appendix A). LIFE was developed by Argonne National Laboratory as a fuel performance code with the capability of following the reactor power history. The magnitude and duration of the fuel-cladding mechanical contact are calculated with the LIFE code. LIFE has been adopted as the national fuel pin modeling code and is undergoing further development at ANL, W-ARD, HEDL, AI and GE. Limitations on the current version of the LIFE code (LIFE-III) and the methodology by which it is applied to fuel and blanket rod analysis is discussed in Section 4.2.1.1.3.5.

56 | Two types of rods were investigated for FCMI effects: those with the highest end-of-life damage due to fission gas loads, and those which experienced the highest percent increase in steady state power level between cycles. The first type of rods are the least capable of withstanding any additional loading of any variety. In the second type of rod, the power increase at middle-of-life could lead to FCMI due to fuel-cladding differential thermal expansion, particularly if previous conditions resulted in a closed fuel-cladding gap at the time of the power increase. For all rods, the axial locations which showed the most significant calculated FCMI loads were analyzed in detail for cladding damage. A corewide map of end-of-life cladding steady state CDF for the hot spot of the hot rod in each assembly is given and discussed in Section 4.2.1.3.1.2. The hot rod of radial blanket assembly 201, which experiences a 12% power jump between cycles 2 and 3, was chosen for investigation of power jump effects. In addition to experiencing a relatively high power jump, this rod also has one of the higher cladding CDF values at end-of-life.

53 | Steady state FCMI loads were calculated for the hot rods of fuel assemblies 10 and 14, inner blanket assembly 67, and radial blanket assembly 201 (see Figure 4.2-10B). These rods were found to sustain the highest cladding damage due to fission gas pressure alone (see Section 4.2.1.3.1.2.1 below). Between cycles, a 10 hour drop to zero power followed by a 10 hour rise to full power was assumed. The FCMI pressure values calculated by LIFE III for the fuel rods were adjusted to account for the greater cladding wastage which is assumed in the CRBR for design evaluations.
51 | For example, in the LIFE III calculations, the initial cladding thickness

of 15 mils typically decreased by a maximum of 2 mils at $X/L = .75$. In the fuel rod design code FRST (see Section 4.2.1.3.1.2.2 below), the initial cladding thickness of 13.5 mils typically decreased by 6 mils over the design lifetime at $X/L = 75$. To compensate for this effect, the FCMI loads calculated by LIFE for the fuel rods, were multiplied by the ratio of the average cladding thickness calculated by FRST to that calculated by LIFE III over the rod design lifetime for each rod and axial location considered. Pending calibration of the LIFE code for blanket rods, the blanket rod FCMI loads were not adjusted for cladding wastage when input to the design code for added conservatism.

The results of these calculations are shown in Figures 4.2-17A, 4.2-17B, 4.2-17C and 4.2-17D. These figures are plots of total internal cladding pressure (plenum gas pressure + FCMI pressure) at the three cladding axial locations under consideration. The straight line pressure histories are due to plenum gas pressure only while the non-linear portions of these pressure history plots indicate the occurrence of FCMI loading.

The effects of the mid-life power increase on FCMI in the hot rods of radial blanket assembly 201 was investigated with the LIFE-III code by varying the power ramp rate at the beginning of the third cycle. For this study, three third cycle startup programs were considered:

- Normal startup (3 loop operation)
- Fast startup (3% min.)
- Programmed startup

The three startup procedures used in the analysis are shown in Figure 4.2-16. The fast startup was based on the maximum possible ramp rate achievable in the reactor, i.e., 3% per minute. The programmed startup was based on an earlier fuel pin power-to-melt uncertainty analysis for CRBR (Section 4.4).

Figure 4.2-24 shows the maximum calculated FCMI loads during the third cycle startup for the three startup schemes described above. This figure demonstrates that the FCMI loading calculated by LIFE III due to mid-life power increases in radial blanket rods can be significantly altered by varying the rates at which these rods are brought up to power at the beginning of the cycle when the power increase occurs. The effects of these cladding loadings on rod lifetime, and the overall conclusions derived from these calculations are discussed in Section 4.2.1.3.1.2.

Based upon experience with FFTF and EBR-II fuel assembly design, the following mechanisms were expected to be of secondary importance with respect to cladding damage in CRBRP but important to overall fuel and blanket rod performance.

51

1. Cladding-Wire Wrap Interaction

Rod growth exceeding the wire wrap growth results in compressive and helical bending stresses in the rod and tensile stresses in the wire wrap. This loading might produce cladding damage or wire wrap breakage. Wire wrap breakage or slackening with respect to the cladding might allow either excessive vibration causing additional fretting and wear or fatigue damage, or alternatively slumping in such a way as to disrupt the inter-rod spacing and corresponding coolant flow.

2. Bundle-Duct Interaction

The fuel or blanket rod bundle cross-section could grow faster than the duct cross-section giving interference to such an extent that the fuel rods see localized stresses and strains at the planes of lateral support provided by the wire wrap. Conversely, the duct cross-section could grow at a faster rate than the fuel rod bundle giving increased clearance between the bundle and the duct. As a result, the fuel rod bundle may either vibrate giving increased fretting and wear and increased fatigue damage or the coolant flow may redistribute causing local fuel rod overheating in the center pins and leading once again to increased cladding damage.

3. Rod Bow

Fuel Rods

The fuel rod bow is dictated by the wire wrap pitch. One design requirement is that the fuel rod bow due to temperature gradients across the fuel rod and axial loads and the growth of the rods shall not decrease significantly the nominal coolant flow channel between adjacent fuel rods. Based on FFTF analyses, the above mentioned design requirement is expected to be satisfied and no limit on fuel pin performance imposed. Analysis and a prototypic irradiation test to confirm the above conclusion will be performed.

Blanket Rods

The contact forces between the blanket rods are caused primarily by bowing due to the radial thermal and flux gradients across the blanket assemblies. These contact forces control the cladding fretting wear, which is a component of the total cladding wastage rate. The bowing of the blanket rod should generally result in larger contact forces than in the fuel assembly. This is due to the larger temperature gradients across the blanket rods and the greater blanket rod stiffness as compared to the core fuel rods.

The contact forces between the blanket rods were calculated as a function of time over the blanket assembly lifetime for a row of nine rods using the ANSYS computer code. The blanket rods were modeled as a linear series of two-dimensional beam elements with regularly spaced friction link gap elements for lateral restraint. Loads were assumed to be due to axial and radial thermal and neutron flux gradients typical of the blanket assembly. The temperature gradients and displacement boundary conditions were chosen to give conservative results. Stress effects on irradiation swelling and swelling effects on irradiation creep were neglected. Except for short transient forces lasting for a few minutes, the maximum rod-rod contact force was found to be < 4 lb. and would result in less wear than that used in the cladding strain calculations where wear is calculated as a function of contact force.

In a blanket assembly, cladding temperature and neutron fluence increases as distance from the core center decreases (i.e., the temperature and flux gradients are positive towards the core center). The portion of the blanket rod cladding facing the core center thus tends to expand more than the cladding facing away from the core center. For an unconstrained geometry, this would cause the blanket rods to bow toward the core center during reactor operation (see Figure 4.2-88). However, because of the duct constraint, the rods were actually held relatively straight by the rod-rod and rod-duct contact forces. This results in the rod cladding facing the center of the core being subjected to a compressive stress, while the portion of the cladding facing away from the core is under a tensile stress. Based on the irradiation creep and swelling formulation given in Reference 153, irradiation creep and stress enhanced irradiation swelling tend to relax these stresses. As these stresses relax, the rod-rod contact forces are reduced. Thus, neglecting stress effected irradiation swelling, and swelling enhanced creep, results in higher rod-rod contact forces during the core residency time considered in the calculation, and is therefore a conservative approach.

4. Rod Vibration and Fatigue

Fuel Rods

The primary concerns regarding fuel rod vibration are fatigue failure of the cladding and wire wrap and the potential for excessive cladding and wire wrap fretting and wear which could reduce the load carrying capability of these components. Fuel assembly design features critical to fuel rod vibration, such as fuel rod diameter, cladding thickness, wire wrap diameter and axial pitch and bundle porosity, are identical to those used in the FFTF fuel assembly. Therefore, based upon FFTF water and sodium flow test results, no problems are expected in these areas. However, water flow tests and irradiation tests are planned to verify this conclusion (see subsection 4.2.1.5).

The FFTF Fuel Assembly Flow Vibration Test results are reported in great detail in Reference 169 and are summarized in Reference 170. The results from these flow vibration tests demonstrate that fuel rod vibrations in FFTF and CRBRP fuel assemblies will be small. The FFTF fuel assembly flow vibration test is directly applicable to CRBRP fuel design. The relevance of these data for CRBRP design and the correlation of these data with recent irradiation test data is discussed in the topical report "Flow Induced Vibration of Fuel Rods in CRBRP", submitted in February, 1977. The additional flow-vibration test of a CRBRP fuel assembly is planned to confirm that the rod vibration amplitudes are as low or lower than those measured in the FFTF fuel assembly flow vibration test.

The results of fuel rod bundle irradiation tests on cladding with vibratory wear, including all 37 rod bundles, are reported in Reference 101, Section VC-4. These results will also be discussed in the topical report, "Flow Induced Vibration of Fuel Rods in CRBRP". These 61 rod bundle irradiation tests designated as P13, P14, and P14A are being performed in EBR-II to substantiate the present assumption that a small rod-bundle-duct clearance will prevent significant rod vibratory wear. Preliminary results from interim examination of these tests were reported at the "CRBRP Fuel Meeting" with NRC, October 13 and 14, 1976 in Bethesda, Maryland (additional details are contained in the handout from that meeting HEDL-TI-76035-2, "Reference Fuel Steady State Irradiation Program" and Appendix). An examination of the P13 and P14 test at a burnup of 45,000 MWD/MTD exhibited insignificant cladding and wire wrap wear. In Table 4.2-67 the test parameters of the P13, P14 and P14A test assemblies are compared with those test assemblies which exhibited significant wear. The major differences in the design between both types of assemblies are the smaller initial porosity of the P13, P14 and P14A test series and the use of 20% cold worked type 316 stainless steel ducts. The use of this duct material in conjunction with cold worked cladding maintained or decreased the small initial rod bundle porosity with increasing burnup. In earlier tests the rods did exhibit vibratory wear because the large initial rod bundle porosity was amplified by inserting low swelling cold worked type 316 stainless steel cladding into a fast swelling type 304 stainless steel duct. A comparison of the rod bundle porosity of many assemblies in Figure 4.2-129 shows that those assemblies which experienced porosity greater than 6 mils per ring did experience vibratory wear. The irradiation and examination schedules for these tests are included in the Reference Fuel Steady State Irradiation Program Plan, Reference 162, Page A-23.

51

Amend. 51
Sept. 1979

A water flow test of a prototypic FFTF and nearly prototypic CRBRP fuel assembly showed that the maximum fuel rod vibration occurred at the top of the fuel rod bundle and was on the order of 2 to 5 mils peak-to-peak. A preliminary assessment revealed that the alternating stress and corresponding strain range associated with the range of peak amplitudes of vibration is 2.8 to 7.0 times lower than the fatigue endurance limit given in ASME Code Case 1331-8. For the wire wrap the ratio is from 2.2 to 5.4. It is expected that these ratios are sufficient to account for any degradation in fatigue strength due to sodium exposure and irradiation damage. Fuel rod vibration induced fatigue damage is therefore expected to be negligible. In-reactor confirmation will be obtained from FFTF driver assemblies and CRBRP In-Reactor Tests (in FFTF) in 1984.

Blanket Rods

At this time the maximum vibration amplitude of the blanket rod is not known. However, the vibration amplitude is limited by the available rattle space between radial blanket rods which is approximately 0.003 in. on the average. Vibrations with larger amplitudes could occur locally if the rod bundle is tightly compacted in other regions of the assembly cross section. However, it was noted that damaging core fuel rod vibration is not expected. Vibrations are less likely to occur in the blanket rod bundle because (a) the blanket fuel rods are stiffer, (b) blanket rod vibration frequencies are higher, (c) flow velocities are lower in the blanket assembly, (d) the thermal gradient is larger than in the fuel assembly bundle, and (e) the average radial rattle space for each rod is approximately the same in the fuel and blanket assemblies. All known correlations for flow induced rod vibration predict insignificant bending vibration amplitudes. However, vibration modes can be postulated other than the vibration of a single rod. When considered as an entity, the rod bundle is a mass-spring system which can vibrate laterally. The rod bundle has a relatively large mass and a small spring constant, and therefore has a low vibrational frequency. Vibration of the entire bundle could be caused by pressure differentials across the rod bundle or by transmission of reactor structural vibration.

Rod vibrations, if they occur, might potentially lead to local cladding wear. Fatigue failure or degradation of cladding strength is not likely to occur because the bending stresses and strains caused by postulated vibrations are small. For example, a 0.003 inch vibration amplitude over a 12 inch length causes a bending stress of only 4404 psi and 5.2×10^{-5} in/in. bending strain, which is far below the endurance limit of Type 316 SS. Therefore, no significant degradation of cladding strength due to radial blanket rod bending vibration is expected. The necessary conditions for cladding wear to occur, such as vibration amplitudes, surface conditions, and temperatures, are not well understood and will be evaluated as test data become available. Water flow and vibration testing will be completed in 1982. Confirmatory In-Reactor Tests (in FFTF) will be completed in 1985.

Flow vibration tests of a prototypic FFTF control rod absorber assembly have been performed and the results reported in Reference 29a. These results indicate rod vibration less than 1 mil RMS. The blanket rod assemblies will operate at flow rates equivalent to those utilized in Reference 29a, and the dimensions and stiffness of the tested rod bundle are of the same order of magnitude as those of the blanket rod bundle. Thus, the blanket rod vibration amplitude is also expected to be less than 1 mil RMS.

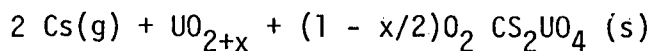
A blanket rod bundle flow test in air and in water will be performed. If a blanket rod bundle vibration test does become necessary, the vibration response of selectively instrumented blanket rods will be determined in this flow test, to demonstrate freedom from severe flow induced vibration within the available space.

Although blanket rod vibration is not expected to cause random failures, it is shown in Section 15.4 that random rod failures are not a safety hazard. Hence, blanket rod vibrations or their consequences likewise pose no safety hazard.

5. Cesium Migration and Axial Blanket Pellet Interaction

There are two general aspects of cesium migration and axial blanket interaction. The first deals with the complex combination of conditions that favor the Cs-UO₂ reaction. The second deals with those design parameters that would preclude a severe mechanical interaction if the CS-UO₂ reaction occurred.

The reaction of cesium with hyperstoichiometric urania was investigated at ANL. The experiments suggest the following equation for the reaction (Reference 2).



53 | The standard free energy of formation of cesium uranate is given by

$$G_{fo} = -453350 + 9.16T \text{ cal/mol}$$

Here

x = the deviation from stoichiometry

T = temperature in °K

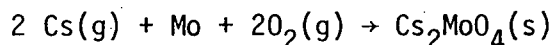
51 | g,s = gaseous and solid phases respectively

53|

If the fission product cesium is free to migrate to the cooler ends of the fuel pin it will react with urania to form Cs_2UO_4 whose molar volume is ~ 3.5 times more than that of the UO_2 .

Obviously, if there is insufficient voidage available to accommodate the Cs_2UO_4 reaction product, then a mechanical interaction with the cladding will result.

The propensity for the axial migration of cesium is sensitive to the prevailing operating conditions, particularly as they affect the availability of fission product molybdenum. Given the proper thermodynamic conditions, Cs and Mo will react with available oxygen to form Cs_2MoO_4 which will deposit at the fuel-cladding interface and subsequently react with the stainless steel. Thermochemical studies at ANL (Reference 159) have shown the following reaction:



54|

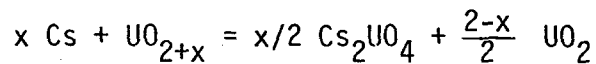
$$\Delta G_{f0} = -362000 + 85.68T \text{ (}^\circ\text{K)} \text{ cal/mol}$$

The Cs_2MoO_4 reaction competes for the molybdenum which may also combine with noble metals to be deposited as metallic inclusions within the (U, Pu) O_2 fuel. This alloying process is favored at high temperatures and low O/M ratios within the fuel. In this case, the gaseous cesium is free to migrate axially toward the cooler regions of the fuel pin. The conditions that partition the two competing molybdenum reactions are not known exactly. However, observations from EBR-II irradiated fuel pins (e.g. scheme shown in Figure 4.2-9A.

51|

Clearly, the Cs_2MoO_4 reaction is undesirable from the standpoint of cladding attack and a low O/M ratio is specified to minimize the reaction. Thus, for all practical purposes it must be assumed that the CsUO_2 reaction will occur in some CRBRP fuel pins. In this regard it must be assured that sufficient voidage is available for the Cs_2UO_4 product. Voidage is defined as that free space required to accommodate the Cs_2UO_4 reaction product and preclude a severe mechanical interaction with the cladding.

The formation of cesium-uranate also depends on the stoichiometry of the urania in the axial blanket pellets. Formation of a significant amount of Cs_2UO_4 is expected only if the urania is hyper-stoichiometric. The reaction of cesium with hyper-stoichiometric urania is limited by the excess oxygen in urania. The volume change that accompanies the formation of Cs_2UO_4 can be calculated from the following reaction:



The difference, ΔV , between the volume of reaction products and volume V inside the fuel pin is given by

$$\Delta V = V \left\{ \frac{\rho_{sm}}{V_{\text{UO}_{2+x}}} \left[\frac{x}{2} V_{\text{Cs}_2\text{UO}_4} + \left(1 - \frac{x}{2}\right) V_{\text{UO}_2} \right] - 1 \right\}$$

where

ρ_{sm} = fractional smeared density

$V_{\text{UO}_{2+x}}$ = molar volume of UO_{2+x} ($\sim 24.6 \frac{\text{CC}}{\text{mol}}$)

V_{UO_2} = molar volume of UO_2 ($24.6 \frac{\text{CC}}{\text{mol}}$)

$V_{\text{Cs}_2\text{UO}_4}$ = molar volume of Cs_2UO_4 ($85.3 \frac{\text{CC}}{\text{mol}}$)

By setting ΔV equal to zero in the above equation, the following expression relates the initial value of the smeared density and the initial value of the deviation from stoichiometry such that the maximum value (x_{max}) of deviation forms a mixture that exactly fills the available space. The expression is:

$$x_{\text{max}} = \frac{2V_{\text{UO}_{2+x}}}{V_{\text{Cs}_2\text{UO}_4} - V_{\text{UO}_2}} \left(\frac{1}{\rho_{sm}} - \frac{V_{\text{UO}_2}}{V_{\text{UO}_{2+x}}} \right)$$

If no credit is allowed for accommodation of the reaction product by the UO_2 pellet porosity, then ρ_{sm} becomes the ratio of pellet to cladding cross sectional area. This modification of the above equation is reflected in Figure 4.2-9B. Theoretically mechanical interaction between the Cs_2UO_4 reaction product and the cladding would not be expected until 100% of the voidage in the pellet to cladding gap was expended. However, as shown by the X on Figure 4.2-9B, reference fuel pin PNL-8-25 irradiated in EBR-II to a peak burnup of ~60 MWD/kg (Reference 160) did experience a slight local cladding strain in the vicinity of a cesium activity peak when on a nominal basis only 95% of the gap voidage had been consumed. Note that pin PNL-8-25 did not experience cladding breach. This difference in theoretical versus observed voidage to preclude mechanical interaction may be hypothesized as being due to pellet and cladding surface irregularities, non-uniform reaction product formation of the reaction product being less than 100% dense.

The above considerations have been factored into the design of the UO_2 CRBRP axial blanket pellets adjacent to fuel. Based upon fabrication experience with similar FFTF insulation pellets, the UO_2 pellet initial O/M ratio should be less than 2.005 and the ratio of cross sectional areas should be within the range of 88.4% to 92.2% (90.25% nominal). As shown in Figure 4.2-9B, this is well below the thresholds for severe mechanical interaction of the reaction product with the cladding.

With regard to the experimental data base and its uncertainty, the examination of reference fuel pins irradiated in EBR-II for cesium migration and insulator (blanket) pellet reaction is reported in Section VH of Reference 101. Of the approximately 100 pins examined after the wire wraps were removed, three high power, high burnup pins show both cladding strain and a sharp peak in cesium gamma activity at the interface between the bottom of the fuel column and the insulator pellets. However, none of the three had failed. To date, seven pins have been completely examined after being irradiated to high burnup (>50,000 MWD/T). All seven had operated at peak powers in excess of 11 kW/ft. Other high power pins have been examined at burnups from 60 to 50,000 MWD/T and lower power pins have been examined at burnups ranging from 2,000 to 43,000 MWD/T. None of the latter have shown cladding strain or cesium segregation at the insulator pellets. It is noted in Reference 101, that the three pins exhibiting strain due to cesium reaction PNL-5B-25, PNL-8-11 and PNL-8-25 were quite similar to other pins in the EBR-II subassemblies which showed no evidence of cladding strain due to cesium reaction.

531 The planned EBR-II and FFTF irradiation tests that will provide additional information on cesium migration and associated cladding reaction and pellet interaction effects is given in Revision 1 of the Reference Fuel Steady-State Irradiation Program Plan (Reference 162) which was provided in Response to Question 241.56. Specifically, Table 4.2-62 of the PSAR (Table II in the program plan) identifies the following areas of investigation:

51

II. Solid and Volatile Fission Product Migration

5. Cesium migration in long pins.
6. Effect of cesium migration in mechanical strain.
7. Confirmation of design fixes.
8. Effect of low O/M fuel (O/M<1.95).
9. Tests in FFTF (effect of peaked axial power profile).

IV. Fuel-Cladding Chemical Interactions

16. Effects on cladding mechanical properties.
17. Correlation of temperature and burnup effects.
18. Effect of O₂ potential (O/M and fission product spectrum).
19. Effects of getters.
20. Effects of all Pu fissioning in FFTF (EBR-II tests included enriched uranium).
21. Effect of FFTF axial power profile.

The schedule for EBR-II testing to support CRBRP FSAR submittal is given in Figure A-1 of the program plan (Reference 162) while the schedule for FFTF testing in support of CRBRP initial core operation is given in Figure A-3 of Reference 161. Figure A-2 gives the EBR-II irradiation experiments, described in Table A-1, which support activities II and IV above.

Fuel and Blanket Rod Cladding Design Transients

The CRBRP design duty cycle which is described in Appendix B classifies all operational events as normal, upset, emergency and faulted. Individual and faulted events are described and analyzed in the appropriate subsections of Chapter 15.

The upset and emergency events of the design duty cycle were first categorized according to their effect on cladding temperature and type of initiating mechanism. For the transients of Appendix B, the three categories are considered as follows:

Down Transients

Cladding temperature decreases to values below those for normal steady state operation. Because the cladding transient strength decreases with increasing temperature (see Figure 4.2-2B), significantly higher loading can be accommodated during reduced temperature operation. Therefore, in this preliminary assessment no additional cladding damage was associated with this type of transient.

Undercooling Type Up Transients

Cladding temperature increases to values above normal operation due primarily to a reduction in coolant flow. Fuel temperature does not change significantly. The damaging effect of these transients is due primarily to the increased fission gas pressure and reduced cladding strength.

Reactivity Insertion Type Up Transients

Both cladding and fuel temperatures increase above their normal operational values due to higher power generation without proportionately higher coolant flow. In addition to the damaging mechanism identified for undercooling transients, there is a potential for increased fuel-cladding mechanical interaction and additional fission gas release. Fuel-cladding mechanical interaction was neglected in this preliminary evaluation for reasons discussed later.

Ideally, each damaging up transient of Appendix B should be fully characterized and evaluated according to its effect on fuel rod cladding performance. However, the more practical approach is to umbrella these events in a conservative manner; that is, the damage due to the umbrella events would exceed the damage of the combined individual events. This would normally involve the following steps:

1. The major categories of damaging events would be subdivided according to transient duration. For example, fast acting transients which usually achieve higher cladding temperature would be categorized against longer acting lower temperature transients.

2. Each transient within these categories would be qualitatively examined for potential cladding damage with respect to its normal operating conditions at event initiation. Further subdivision may be required. For example, transients during startup with reduced temperature and power as initial conditions may be less damaging than normal full power operation.
3. Finally, within each category the transient which would probably produce the most damage would be selected as the umbrella transient. The umbrella event frequency would be established by encompassing all damaging events within that category.

Based on these considerations, the U-2b, OBE, E-16, and SSE (60% step) events were chosen as the most damaging events for each transient category. These events were therefore utilized in the fuel and blanket rod performance evaluations. These events are described in Table 4.2-59. The cladding temperature histories during the umbrella transients for both fuel and blanket rods are shown in Figure 4.2-24E through 4.2-24J.

No transient FCMI effects were included in the CDF analyses presented here. For these calculations, the very conservative cladding transient temperatures and duty cycle indicated above were assumed. For the cladding strain analyses, the procedure used to calculate transient FCMI for the FFTF evaluations was utilized (Reference 57 and 173). This procedure is described in Section 4.2.1.3.1.2.2 below.

As a better understanding of the transient behavior of prototypic irradiated cladding evolves, the design duty cycle is defined in more detail and the PPS design and trip settings are finalized, the fuel rod cladding transient analysis will be updated as follows:

1. The cumulative damage function analysis procedures and the inelastic strain criteria and associated procedures will be continually updated to incorporate all recent testing data relative to irradiated materials properties and fuel rod failure mechanisms.
2. The design duty cycle events will be examined more thoroughly for time effects, initial state points, and probable damage (e.g., effect of down transients) as indicated by the revised CDF analysis procedures.
3. More realistic umbrella events and frequencies will be defined based upon the above examination.

Sodium Voiding Accidents

The mechanical effects of gas bubble passage through the core have been treated in Section 15.4.1.5.6.

4.2.1.3.1.2 Rod Performance Analysis Results

4.2.1.3.1.2.1 Cladding CDF

The cumulative damage function (CDF) histories were calculated for the hot rods of the active core assemblies and checked against the CDF limit given in Section 4.2.1.1. For this assessment, only the effect of steady state and transient plenum gas pressure and steady state FCMI are specifically included.

Maximum design basis cladding temperatures were used in these analyses. Also, the properties and behavior of the cladding material at the 99% confidence limit were assumed, i.e., the probability that the most conservative value of each material property was used is 99%.

Clearly, this assumption defines the most conservative condition for evaluation of the design requirement case.

In general, results are conservative when an upper limit on rate correlations is used, and when a lower limit on strength correlations is used. An example of where using upper material property design limits is conservative is the calculation of internal and external cladding degradation. Maximum values of sodium corrosion, fretting wear, and fuel-cladding chemical interaction result in the minimum end of life cladding thickness. This results in conservatively high cladding stresses and a conservative lifetime prediction.

The cladding CDF evaluation assumes the upset transients are applied at equal time intervals throughout cladding life, with the emergency event applied at end-of-life. Cladding temperature increases during all transients were set equal to the maximum values. Degradation of the cladding materials properties due to the environment at the time of transient occurrence was included in all CDF calculations.

The FURFAN computer code (See Appendix A) is used to calculate the steady state and transient CDF histories (See Appendices A and F of Reference 58). Cladding temperatures, steady state plenum pressures, local rod burnup, and steady state FCMI pressure histories are input to this code. A minimum beginning-of-life cladding thickness of 0.0135 inch, which is consistent with cladding tolerance and defect allowances, is assumed. The cladding material wastage rates and mechanical properties are discussed in Section 4.2.1.1.

Initially, the cladding steady state CDF history at the hot spot due to plenum gas pressure only is evaluated for each hot rod in the core. These results are then used as bases for further analysis as follows:

1. The fuel and blanket rods with the highest end-of-life, steady state CDF are analyzed for transient effects using the FURFAN code.

2. The fuel and blanket rods with the highest end-of-life, steady state CDF are analyzed for steady state FCMI loads as described in Section 4.2.1.3. The total plenum gas plus FCMI loads are then utilized in FURFAN to assess the total cladding internal pressure effects on rod performance. Since FCMI occurs in general over the middle-to-lower sections of the rod, the CDF of the rod must be calculated at locations other than the cladding hot spot when assessing FCMI effects.
3. The fuel and blanket rods which experience the highest power increase between cycles are also analyzed for FCMI (see Section 4.2.1.3.1.1). If any appreciable FCMI occurs in these rods, the CDF histories due to total internal pressure are calculated for those axial locations where the FCMI exists.

Fuel Rods

The end-of-life, steady state CDF values for the hot rod of each fuel assembly in the core calculated according to the methods and assumption described above, are shown in Figure 4.2-25. The lifetime for these rods is defined as the duration of cycles 1 and 2 or 328 full power days (fpd).

The first core fuel rods all attain their goal design lifetime of 328 fpd when steady state plenum gas pressure loading only is considered.

Based on the steady state results of Figure 4.2-25, the hot rods of fuel assemblies 10, 11, 14 and 24 were analyzed for transient effects at the cladding hot spot. These rods have the highest calculated steady state CDF at the cladding hot spot at end-of-life. The transient duty cycle and the cladding temperature histories at the hot spot due to these transients are described in Sections 4.4 and 4.2.1.3.

The effects of the transient duty cycle on the fuel rod lifetime was assessed with the CDF transient limit curves. This technique is described in detail in subsection 11.C of Reference 58 and has been illustrated by an example in Section 4.2.1.1. Briefly, in this method, the maximum transient cladding temperatures and the maximum allowable transient cladding temperatures as determined by the CDF technique are plotted as a function of time on the same graph. The time at which the plots intersect determine the rod lifetime due to steady state and transient conditions. If the goal lifetime is achieved without these plots intersecting, the difference between the maximum and the allowable transient cladding temperature at the goal lifetime (i.e., 328 days) gives a measure of the cladding margin remaining at that time.

The transient limit curve for the hot spot location on the hot rod of assembly 14 is shown in Figure 4.2-26A. This curve shows that this rod achieves the goal lifetime of 328 days with a margin of 18°F at the hot spot. The remainder of the fuel rods considered achieve goal lifetime with larger calculated margins or at the lower peak power.

At rod locations below the hot spot, FCMI loads are calculated to occur in addition to the plenum gas pressure loads. Thus, even though the cladding temperatures at these locations are lower than at the hot spot, the increased loading may cause more rapid damage accumulation.

To investigate this possibility, the hot rod of fuel assembly 14 was selected for detailed calculation. This rod achieved goal lifetime with a small positive margin remaining at the hot spot, and therefore is one of the most severely loaded fuel rods in the core. For the CDF analyses, cladding design temperatures were utilized for the axial locations under investigation ($X/L = .33, .50$ and $.75$). The total cladding pressures are shown in Figure 4.2-17A. The transient limit curve technique was used to evaluate cladding performance at these axial locations.

The results of this calculation are shown in Figure 4.2-26B, which is the transient limit curve for the cladding axial location $X/L = .75$ of the rod under consideration. This figure shows this cladding location achieves goal lifetime with considerable cladding transient temperature margin. The end-of-life transient temperature margins for the $X/L = .33$ and $X/L = .5$ locations are even greater than for the $X/L = .75$ location.

Blanket Rods

The end-of-life, steady state CDF values for the hot rods of each blanket assembly, calculated according to the methods and assumptions described above, are shown in Figure 4.2-27. The lifetime for the inner blanket rods is the first two cycles, or 328 full power days. The inner row of the radial blanket has a four cycle lifetime, while the outer row of the radial blanket has a five cycle lifetime. For this study, the radial blanket inner row was analyzed for the first four cycles of operation, or 878 full power days, and the outer row of radial blankets was analyzed for the first five years of operation, or 1153 full power days.

For loading due to fission gas pressure only, the inner blanket hot rods generally have a lower steady state CDF at end-of-life than do the radial blanket rods. This also provides margin for any effects the inner blanket rods may experience due to the power increase which occurs after the first cycle of operation in many inner blanket assemblies (see Figure 4.2-16).

From the data of Figure 4.2-27, the hot rods of outer blanket assembly 201, and inner blanket assembly 67 were calculated to have the highest end-of-life CDF values at the hot spot for each blanket type. These rods were analyzed for transient effects at the hot spot using the methods and assumptions previously described for the fuel rods. The results of these analyses are shown in Figure 4.2-28A and 4.2-28B. These results show that these blanket rods achieve the goal life with the transient limit curves at end-of-life lying above the peak transient cladding hot spot temperature. The cladding hot spot transient temperature margins at end-of-life for the other blanket rods are greater than the hot spot margins for the hot rods of assemblies 201 and 67.

As noted in Section 4.2.1.1, the LIFE III code has not been calibrated for blanket rods. However, the magnitude of the calculated blanket rod FCMI loads as a function of rod power, temperature, etc., correlate well with the calculated fuel rod FCMI dependence on these parameters. This indicates the LIFE III models are mathematically capable of predicting blanket rod FCMI results. To compensate for the uncertainty in blanket rod FCMI magnitude due to lack of specific calibrations, the blanket rod wastage was assumed to equal the conservative design cladding wastage. This resulted in conservative calculated FCMI stresses.

The effects of these calculated steady state FCMI loads and the transient duty cycle on cladding lifetime at axial locations $X/L = 0.46$ and 0.62 were determined for the hot rods of outer blanket assembly 201 and inner blanket assembly 67. The cladding temperature assumptions and transient limit curve techniques utilized for these blanket rods are identical to those utilized for the fuel rods. The total cladding internal pressures are shown in Figures 4.2-17C and 4.2-17D for the axial locations considered. These calculations predict that at end-of-life, the steady state and transient CDF margins at these axial locations on both blanket rods exceed the CDF margins at the hot spot location.

Mid-Life Power Increase Effects

As noted in Section 4.2.1.1, the LIFE III code has not been calibrated to calculate the magnitude of FCMI loads for this type of environment change. However, the code models are capable of predicting the qualitative physical relation between FCMI and power change rate over the periods of time typical of reactor startup. Thus, for this study, blanket rod cladding performance with these startup programs at the beginning of the third cycle were calculated and compared. These startup programs were described in detail in Section 4.2.1.3.1.1.

The cladding CDF due to the most severe startup loading (100% power at 3% per minute) was calculated with the FURFAN code. Results of these analyses are shown in Table 4.2-10. Steady state CDF values are shown for 878 EFPD (4 cycles of operation) with and without accounting for the power jump. Comparison of the results shows that even in the worst case the mid-life power jump, per se, has no significant deleterious effect on the steady state performance capability (CDF) of the blanket rod.

4.2.1.3.1.2.2 Cladding Ductility Limited Strain

The FRST computer code (see Appendix A) was used to calculate fuel rod cladding ductility limited strain versus time. This code provides a means of calculating effects of time-varying cladding temperature, plenum pressure, cladding wastage, and fuel-cladding contact pressure on the cladding ductility limited strain as defined in Section 4.2.1.1.2.2. This is done by utilizing the cladding thermal and pressure loads which equal or envelope those of Section 4.4 in the solution annealed 316 SS thermal creep equation, referenced in Section 4.2.1.1. Cladding wastage and steady state fuel-cladding contact pressure effects are considered in the cladding load calculations. Irradiation creep and swelling strains are also calculated by FRST using the 20% cold worked 316 SS models. The FRST calculational procedure has been verified against both hand calculations and MINIGRO code results.

For conservatism, the FRST computer code used the material modeling assumptions presented in Section 4.2.1.1; all pertinent initial environmental conditions considered for the fuel rod cladding strain calculations are also described or referenced in this section.

A sub-routine to the FRST code which calculates the cladding plastic strain increment and thermal creep strain rate during the transient, was used to determine the effects of transients on cladding strain accumulation. For the cladding material, the solution annealed 316 SS thermal creep strain relation, specified in Section 4.2.1.1, and the stress-strain relationship given in Figure 4.2-2A, were assumed. Fission gas plenum pressure and FCMI at the time of transient occurrence is input to this sub-routine from the steady state analysis results. During a given transient, the sub-routine adjusts this pressure to reflect increased fission gas pressure, transient fuel-cladding differential expansion, and the time varying cladding temperature. During the transient, the code calculates the cladding stress, and utilizes this stress and the cladding temperature in the solution annealed 316 SS thermal creep equation to calculate the cladding strain rate due to the transient. Whenever the cladding stress exceeds the material proportional elastic limit given by the stress-strain-temperature relation of Figure 4.2-2A, the code uses the mathematical equation of this relation to calculate cladding plastic strain, and this value is added to the plastic strain to obtain the total cladding transient ductility limited strain. This technique, which is the same as used for FFTF, is described and verified in References 57 and 173.

A minimum beginning-of-life cladding thickness of 0.0135 inches was assumed, which allows for design tolerances and defect allowances. The cladding material wastage rates and mechanical properties are discussed in Section 4.2.1.2. The pertinent initial conditions used for these calculations were previously described in this section.

Strain Limit Analysis Results

Cladding ductility limited strain history calculations for steady state operation were first performed for the hot rods of the equilibrium core fuel assemblies assuming cladding loading due to plenum gas pressure only. The lifetime for these rods is defined as two equilibrium cycles, or 550 full power days. The results of the analyses are summarized on Table 4.2-11, which lists the end-of-life cladding ductility limited strain at the cladding hot spot for the hot rod of each assembly. The table shows that the highest steady state strain accumulated by any fuel assembly at the hot spot is 0.042%, versus an allowable of 0.2%.

Cladding ductility limited strain calculations for steady state operation were also performed for the hot rods of selected cycle 1 and 2 inner blanket assemblies (550 fpd life) and selected cycle 1 to 4 radial blanket assemblies (875 fpd life) using the FRST computer code. The outer row of radial blankets (1150 fpd lifetime) operate at much lower cladding temperatures and stresses than do the inner row of radial blankets, and therefore accumulate less cladding strain. The inner and radial blanket assemblies with the highest pressures and temperatures were analyzed because their maximum cladding strains enveloped those of the remaining assemblies. The results show that the inner blanket assemblies have steady state ductility limited strains well below their allowable limit of 0.2%. Radial blanket assemblies 201, 203 and 206 were analyzed, and found to have steady state cladding hot spot strains of 0.007%, 0.028%, and 0.022% respectively at end-of-life. These strains, which are expected to be the highest to occur in the radial blanket rods, are well below the design limit of 0.1%.

The cladding strains resulting from the combined gas pressure and FCMI loads were calculated at the $X/L = .33, .50, .75$ and 1.0 axial locations for the hot rod of fuel assembly 10, and at $X/L = 0.31, 0.62,$ and 0.81 for inner blanket assembly 67, and outer blanket assembly 206. As indicated above and in Table 4.2-11, these rods have the highest end-of-life cladding hot spot strains for their respective types. The total internal pressure histories at these axial locations for the rods of interest are shown in Figure 4.2-17B through 4.2-17D. For these calculations, cladding temperatures under the spacer wire with statistical hot channel factors at the 2σ confidence level were utilized. The results of these calculations are presented in Table 4.2-14. These results show that the fuel and blanket rods considered in this study achieved goal lifetimes with ductility limited strains less than the limit when FCMI pressures were included in cladding loads.

The effects of the design transient duty cycle of Section 4.2.1.3 on cladding ductility limited strain was also determined with the FRST code. The hot rods of fuel assembly 10, inner blanket assembly 67, and radial blanket assembly 206 were investigated at the axial locations previously noted. Transient FCMI effects were included as described above. The maximum total (steady state and transient) cladding ductility limited strain for all axial locations equalled 0.277% for the fuel rod, 0.028% for the radial blanket rod, and 0.004 % for the inner blanket rod. Since these strains are all less than the limit, all rods achieve goal lifetime.

4.2.1.3.1.2.3 Wire Wrap Loads

During the fuel and blanket rod design life, the relationship between spacer wire length and rod axial height changes. The predominant sources of this differential elongation are:

1. Differential wire and cladding thermal expansion;
2. Differential irradiation induced axial swelling of the wire and fuel rod cladding;
3. Change of the fuel rod cladding length due to internal fission gas pressure effects;
4. Increase of the fuel rod cladding diameter due to fission gas pressure and irradiation induced swelling which increases the required length of the wire helical path.

If the axial component of the wire growth is greater than the fuel rod cladding growth, wire slackening occurs. If the cladding growth is larger than the wire growth, then the wire and cladding are deformed to accommodate the differential growth. The four modes of deformation are:

1. Axial elongation of the wire;
2. Helical bending of the cladding which allows the wire to assume a shorter path;
3. Axial compression of the cladding;
4. Torsional deformation (twisting) of the cladding.

Excessively tight wire wrap may rupture, potentially causing increased cladding fretting wear, and potentially disturbing the flow path locally. To determine the wire load such that the axial components of wire and cladding elongation are compatible, wire stress, cladding stress, and cladding and wire deformation are calculated as a function of time with the WRAPUP D computer code (Reference 163). In the event the wire slackens to zero stress, the wire slack, which is the difference between the actual total wire length and the wire length necessary for complete contact of the blanket and fuel rods at zero stress, can also be calculated with the WRAPUP D code. The maximum wire stresses and strains are checked against the limits given in Section 4.2.1.1.

Uncertainties in wire-cladding interaction modes and in material responses to in-reactor environments are accounted for by adjustable input parameters to the WRAPUP D code. Until WRAPUP D verification against experimental data is accomplished to reduce these uncertainties, reasonable worst case combinations of material creep and swelling rates, wire-cladding frictional forces, and material wastage configurations are used to calculate

wire wrap lifetimes for the fuel and blanket rods. The details of how these combinations are achieved in the WRAPUP D code are described in Reference 163. For the WRAPUP D analysis of the CRBR fuel and blanket rods, conditions were chosen to produce maximum wire stress and maximum wire strain for the specified core environments as follows:

a. Maximum Wire Stress

This condition is produced by assuming maximum irradiation swelling, minimum irradiation creep, zero wastage at the wire-cladding interface line, zero wire-cladding slippage, and core midplane conditions (maximum wire-cladding temperature difference).

b. Maximum Wire Strain

This is achieved by assuming the same conditions as for the maximum wire stress, except that free wire-cladding slippage is utilized, and the rod axial temperature distribution is considered.

The justification for these assumptions is given in Reference 163.

To estimate the wire wrap performance of the fuel and blanket rods, the wire stress and ductility limited creep strain histories were calculated for the hot rods of fuel assembly 14, inner blanket assembly 67, and outer blanket assembly 203. As shown in Figures 4.2-25 and 4.2-27, these rods have relatively high end-of-life steady state CDF values for each rod type. Circumferentially averaged design cladding temperatures at the upper 2σ confidence limit were utilized in this calculation while the spacer wire temperature was assumed to the upper 2σ hot channel temperature (see Section 4.4). This results in a conservative temperature differential between the wire and the cladding. Fast neutron flux values from Section 4.3 were also utilized in these calculations. Previous studies have shown FCMI effects on wire loads to be negligible, so these effects were not considered.

The results of the wire wrap performance calculations are summarized in Table 4.2-15. This table also presents the wire stress and strain safety margins based on the criteria of Section 4.2.1.1. These results show the spacer wire on the rods investigated in this study meet their lifetime goals with wide margins of safety.

In addition to the wire failure mechanisms considered above, it is also possible for the wire wrap to grow in length relative to the cladding and become loose. It has been postulated that excessively loose wire could rub over the cladding, causing rod-rod cladding contact and hot spots. However, EBR-II experimental results (Reference 163) have shown that test rods with extremely loose wire wrap suffered no damage until assembly reconstitution loads caused wire displacements and cladding contact between rods. These test

rods were wrapped with solution annealed 316 stainless steel, and therefore experienced much more wire loosening than is possible in the CRBR rods, which are wrapped with 20% cold worked 316 stainless steel. Also, the CRBR fuel and blanket assemblies will not be disassembled and reconstituted during their lifetime. Finally, scoping calculations predicted wire wrap maximum slack in fuel and blanket rods to be less than 0.1 inch at end-of-life. For these reasons, wire loosening is not considered an important contributor of fuel rod failure.

Preliminary studies on the effects of transients on the wire wrap performance completed to date show that:

- a. Transient effects on the wire wrap are primarily due to differential thermal expansion between the wire and cladding and therefore are governed by the coolant-cladding temperature differential during the transient.
- b. The coolant-cladding temperature differential increases by a maximum of 15% above its steady state value for approximately 5 minutes during the worst duty cycle upset transient considered. Preliminary calculations show that the wire ductility limited strains due to this loading do not exceed the wire wrap transient design limit. These calculations will be performed using a validated version of WRAPUP D and updated environments and reported in accordance with the schedule for submittal of the FSAR.

Due to these considerations, a detailed analysis of the effects of wire rupture, especially simultaneous wire rupture, is unnecessary at this time.

The effect of temperature gradients across the rod on the wire stress was also neglected. Both effects cause higher stresses on the blanket wire wrap than on the fuel rod wire wrap because in the blanket assemblies:

- a. The wire diameter is smaller
- b. The rod stiffness is greater
- c. The temperature gradients across the rods are larger
- d. The wire pitch is smaller.

The potential consequence of wire loosening or rupture on the assembly performance is less severe than that for a small local flow blockage. The impact of local flow blockages and flow recovery are evaluated in Section 15.4.

4.2.1.3.1.2.4 Fatigue Effects in Fuel Rods

A scoping calculation was performed to assess the fuel rod cladding fatigue damage due to the current CRBRP duty cycle. The types of transients considered include:

- a. Normal scram followed by a normal startup to former power level.
- b. Reactor trip from full power followed by a subsequent startup to former power level.
- c. Reactivity insertion upset event, followed by a scram and subsequent startup to former power level.

For each type of transient considered, cladding fatigue loadings were assumed to be caused by:

- a. Plenum pressure changes
- b. Changes in the temperature gradient across the cladding
- c. Steady state fuel cladding mechanical contact pressure.

The strain versus cycles to failure curves and creep fatigue interaction assumptions of ASME Code Case 1592, Sections T-1413 and T-1423 were utilized for the cladding, since fatigue data on irradiated 20% CW 316 SS is limited. Such data that do exist (Reference 167) show this approximation to be conservative. The following assumptions were also made for this calculation.

- a. During the hold at hot standby (600^oF) between a scram and subsequent startup, no cladding thermal or irradiation creep occurs. The cladding thermal creep equation discussed in Reference 1 and the negligible fast neutron flux during hot standby shows this to be an acceptable assumption.
- b. After a combined scram and startup to the former power level, the cladding loading due to fuel-cladding mechanical interaction does not exceed that which existed prior to the scram. This assumption is consistent with results of LIFE code calculations.
- c. Fuel-cladding mechanical interaction (FCMI) effects during the upset reactivity insertion transients were not directly assessed. However, for the relatively small number of transients of this type postulated, FCMI cladding stresses would have to exceed the cladding proportional elastic limit for fatigue effects to be significant. The magnitude of this interaction is not quantified at this time, but it is under investigation (see Reference 168).

- d. The fatigue damage D to the fuel rod cladding for a particular strain range $\Delta\epsilon$ is expressed as

$$D_{\Delta\epsilon} = (n_i/N_i) \Delta\epsilon$$

where n_i is the number of applied cycles of the strain range, and N_i is the allowable number of cycles for that strain range. The total cladding fatigue damage is

$$D_t = \sum_{\Delta\epsilon} (n_i/N_i) \Delta\epsilon$$

which is the sum of the fatigue damage components due to the individual fatigue strain ranges. Per the methodology of Reference 167, the design limit is $D_t=1.0$.

The total fatigue damage to the fuel rod cladding due to the transients and loads listed above was calculated to equal

$$D_t \approx 4 \times 10^{-3}$$

and is summarized in Table 4.2-66.

As noted, this does not include the effects of transient FCMI stresses. Based on the methodology of Code Case 1592 to Section III of the ASME Code (Section T-1413 and T-1423), creep-fatigue interaction is negligible for this low value of fatigue damage. Thus, no cladding lifetime reduction is expected from fatigue effects, provided FCMI stresses do not significantly exceed the cladding proportional elastic limit.

The methodology for including fatigue effects into the CDF procedure is discussed in detail in PSAR Section 4.2.1.1.2.2.

4.2.1.3.1.2.5 Load Follow Capability

53 | The CRBRP plant control system and other permanent features are being designed to provide load following capability. However, at this point in time and current status of technical knowledge on the behavior of fuel assemblies under load follow conditions is essentially nonexistent. A tentative test program to verify load following capability is described in Table 4.2-9. Because the in-reactor simulation results were not available for initial core design, the fall back position can be either one of two possibilities:

51 |

- a. A verification of the in-pile performance utilizing a CRBRP fuel surveillance program and pertinent testing to confirm analytical predictions, followed by derating the core burn-up capabilities, if necessary.
- b. Not to load follow for initial cycles of CRBRP operation until the in-pile performance is simulated in FFTF and adequately understood.

4.2.1.3.2 Fuel and Blanket Assembly Structural Evaluation

4.2.1.3.2.1 Duct Dilation

Dilation of the hexagonal ducts can occur due to volumetric growth caused by irradiation swelling, thermal expansion, and thermal and irradiation creep due to internal coolant pressure. To preclude possible difficulties during refueling, current design practice requires the dilated duct diameter to be less than the assembly pitch except at the load pad areas. To assure the fuel and blanket assemblies meet this requirement, the duct dilation was calculated for selected assemblies over the axial region most likely to exceed the pitch line.

Duct dilation due to the thermal-hydraulic and nuclear environments was calculated as a function of time. The computer model used for these calculations is shown in Figure 4.2-29. The upper bound design basis creep and swelling correlations which were used in the duct dilation analysis are discussed in Section 4.2.1.1.3.1. The duct dilation calculational method was verified by comparing analysis results with independent calculations using similar input conditions. During steady state operation, the duct experiences a temperature that increases over the length of the active core and is nearly constant both below and above the active core. The pressure differential across the duct wall is greatest at the bottom of the duct and decreases along its length. For this study, the duct temperature and fast neutron flux distributions described in Sections 4.4 and 4.3 respectively, were utilized. Based on a scoping examination of the assembly ducts with the highest temperature-flux combination, the ducts of radial blanket assembly 201, inner blanket assembly 67 and fuel assembly 45 were chosen for detailed analysis.

The analysis results are shown in Figures 4.2-30, 4.2-31A, and 4.2-31B. Figure 4.2-30 illustrates the shape of the duct cross section after irradiation creep and swelling. The line at 108 mils in Figures 4.2-31A and B represents the allowable duct dilation based on the thermally expanded assembly pitch dimension. For all cases considered, the maximum duct expansion did not exceed this limit.

4.2.1.3.2.2 Rod Bundle-Duct Interaction

Due to the higher average rod temperatures, the fuel and blanket rod bundle cross sections can grow faster than the duct cross sections at the same axial location. This can cause interferences between the rod bundles and ducts, resulting in fuel and blanket rod distortions, additional cladding stresses, and increased cladding temperatures. However, as noted below, analytical and experimental results demonstrate that moderate amounts of rod bundle-duct interference will not significantly reduce rod lifetime.

The rod bundle growth is influenced by irradiation swelling of the rods and wires, by thermal expansion of both, and by irradiation induced creep of the cladding under internal pressure. Initially (at beginning of life), a gap exists between the duct and the rod bundle, assuming the bundle is in a perfectly straight, tight configuration. The minimum value of the gap is 0.015 inch in the fuel assemblies and 0.006 inch in the blanket assemblies. Significant compression of the rod bundles (i.e., rod bundle-duct interference) is achieved only after differential bundle-duct growth causes this gap to close, and the fully compressed rod bundle begins to press against the duct. This differential growth between the rod bundle and duct is accommodated by the following mechanisms:

1. helical distortion of the rods;
2. rod dispersion, i.e., displacement of the rods from their nominal locations in the bundle.

These mechanisms are all described in detail in Reference 172. Briefly, the rod helical distortion is caused by loads applied to the rods at the wire wrap contact points due to the bundle-duct interference (see Reference 172). This distortion stresses the rods, and in extreme cases can shorten the cladding lifetime by causing excessive strain accumulation. The rod helical distortion can be reduced by the dispersion mechanisms. However, excessive rod dispersion can decrease the coolant channel flow areas to the extent that cladding hot spots occur causing premature failure.

Previous studies (Reference 172) have demonstrated that for fuel rods, rod bundle-duct interferences on the order of one wire wrap diameter (0.056") cause neither excessive cladding stresses or hot spot temperatures. Thus, as a design guideline, maximum rod bundle-duct interaction is to be maintained less than one wire wrap diameter in the fuel assemblies. This same guideline is also currently applied to the blanket assemblies (where the wire wrap diameter is 0.033 in.), even though the blanket rod bundles are much stiffer than the fuel rod bundles, and no data comparable to that for the fuel rod bundle is currently available. The rationale behind applying this bundle-duct interference guideline to the blanket assemblies is discussed below.

To calculate the actual amount of bundle-duct interference in the CRBR core assemblies, the free cross-section expansion of selected rod bundles was calculated and compared to the dilation of the corresponding duct cross sections. Duct loading was assumed due to coolant pressure only, which resulted in conservatively high values of calculated bundle-duct interference. For a given assembly, the bundle-duct interference equals the rod bundle cross section dilation, minus the sum of the duct dilation and the initial bundle-duct clearance. Negative values of interference indicate that for the time and location considered, a net clearance between the rod bundle and duct still exists.

For this study, the rod bundle-duct interferences at end-of-life (the maximum value) were calculated for fuel assembly 45, inner blanket assembly 67, and radial blanket assembly 201. The rod bundle growth was based on the assembly nominal average cladding temperature, and the neutron flux environments presented in Section 4.3. Maximum rod material irradiation creep and swelling rates consistent with the relationships discussed in Section 4.2.1.1.3 were also assumed. The design minimum rod bundle-duct initial clearance values noted above were utilized in the interference calculation, along with the duct dilation values presented in Section 4.2.1.3.2.1.

The results of these analyses are shown in Figures 4.2-32 and 4.2-33. These results show that the maximum rod bundle duct interference in the fuel and blanket assemblies considered did not significantly exceed the guideline values of one wire wrap diameter. Also, the maximum fuel rod bundle-duct clearance did not exceed 6 mils/ring which is the empirically-determined porosity below which fretting wear is not expected to occur (see Figure 4.2-129 and Section 4.2.1.3.1.1).

Because of the relative stiffness of the blanket rod bundle as compared to the fuel rod bundle, the cladding stresses due to a given amount of helical distortion will be much higher in the blanket rods than in the fuel rods if no stress relaxation mechanisms are considered. However, irradiation creep relaxes much of the helical distortion stresses due to bundle-duct interaction in the fuel rods; it is anticipated that this will also occur in the blanket rods. In addition, local dimpling deformation of the cladding contributes somewhat to the compressibility of the rod bundle.

The limit on the blanket rod bundle duct interaction will be verified as a result of the following analytical and experimental process:

- The blanket rod bundle/duct interaction analysis will be repeated with updated material property data, temperatures, and models.
- The blanket rod bundle compressibility will be determined in a rod bundle compaction test, the results will be extrapolated analytically to inreactor conditions.

- The above two results will yield a bundle/duct interaction force and the resultant cladding stress. The cladding stress, which generally relaxes rapidly due to irradiation induced creep, will be considered in the design evaluation.
- As a result of this analysis, the adequacy of the minimum blanket rod bundle/duct clearance will be determined. It will be determined as part of the final blanket design process, and the results will be provided to the NRC in the FSAR. Further information is given in the response to Question 241.105.

Final experimental verification of the adequacy of the design will be obtained from irradiation testing of a radial blanket assembly (WBA-40) in FFTF.

4.2.1.3.2.3 Stress Analysis of Core Assembly Structural Components

As was the case for the rod evaluations, the CRBRP fuel and blanket assembly structural components were analyzed to show that the design requirements of subsection 4.2.1.1 are satisfied for the operating conditions of subsection 4.2.1.1 which, based upon previous experience, were expected to be life limiting.

These analyses were comprised of the following steps:

1. Determination of the most significant loading mechanisms;
2. Determination of the critical assembly structural regions;
3. Determination of the magnitudes of the enveloping loads and environments applied to these regions;
4. Formulation of suitable materials property models for the regions;
5. Calculation of the stresses, deflections, and damage in the components due to the loads and environments;
6. Comparison of the calculated stresses, deflections, and damage to the structural criteria of Section 4.2.1.1 to determine structural margins.

These steps were performed separately for the fuel and blanket assemblies, although the considerations and analysis techniques applied to both assembly types were similar. A brief description of the considerations and techniques is presented below, as well as summaries of the enveloping loads and margins for the limiting fuel and blanket assembly structural regions. The detailed analysis of the fuel assembly structure is given in Reference 171, while the corresponding stress report for the blanket assembly structure will be submitted prior to the FSAR.

4.2.1.3.2.3.1 Loads Specification

A typical core assembly in CRBRP is subjected to varying environment and load conditions depending upon its relative location and interface with other core and out of core components. The loads required for the structural analyses are core restraint loads, seismic loads, thermal loads and hydraulic loads. In addition, since the core assemblies operate in an irradiated environment, fluence and heat generation rates are also important. As a result of the requirements discussed in Section 4.2.1.1, the loads data must include values for all the environmental and loading conditions listed above.

4.2.1.3.2.3.2 Selection of Data Locations

The various assembly loads identified above are selected for specific radial locations across the core depending on the type of loading condition and the type of analysis for which these loads are needed. In addition, the selection is also based on assuming the "worst case" loads to occur in the assembly under the "worst case" environmental conditions.

Figure 4.2-11 shows the schematic elevation view of a typical fuel assembly. The critical locations along the fuel assembly where the loads are quantified are the shield block region, the duct mid core region (CMP)*, the load pad region (ACLP)+, and the outlet nozzle region (TLP)Δ. The shield block region is characterized by thick walls and relatively high coolant pressure and thermal gradients. The mid core region is characterized by peak material degradation due to irradiation effects resulting in loss of residual ductility. The load pad region is characterized by high seismic and core restraint loads whereas the outlet nozzle region is characterized by high temperatures and temperature gradients.

Additional fuel assembly components identified as requiring loads specification are the orifice plates and the fuel rod attachment assembly. The fuel assembly orifice plates are located at the top of the inlet nozzle. The nuclear, thermal and seismic load conditions are the same as in the inlet nozzle region. The fuel rod attachment assembly is located at the top of the shield block region. The nuclear, thermal and seismic load conditions are the same as in the shield block region. In addition, the dead weight of the fuel rod bundle (217 rods) supported by the attachment bar is approximately 235 lbs.

Based on the results of the fuel assembly structural analysis and an evaluation of the significant blanket assembly loads, the critical regions of the blanket assembly (Figure 4.2-14) identified for detailed load and structural analysis are the shield block region, the load pad region (ACLP)+, the outlet nozzle region (TLP)Δ, and the blanket rod attachment assembly. These regions have the same characteristics as their counterparts in the fuel assembly.

*Core Mid Plane
+Above Core Load Plane
ΔTop Load Plane

4.2.1.3.2.3.3 Loads and Environments for Core Assembly Components

The maximum calculated values of the loads and environments to which the fuel and blanket regions are subjected are given in Tables 4.2-8A, 4.2-8B, 4.2-8C, 4.2-12 and 4.2-13. These maximum values were often assumed to occur simultaneously and on the same assembly, although this does not actually happen. The details of the assembly component loading is discussed in Reference 171. Brief descriptions of how these loads and environments were determined are given below.

Nuclear Data

53 | The nuclear data utilized in these analyses in terms of assembly-average total flux, assembly-average fast flux fraction and axial distributions of total and fast flux in fuel and blanket assemblies equal or envelope that given in Section 4.3 for the most significantly loaded structural components. The fluences are calculated by assuming that the BOC flux distribution is appropriate for the first half of the cycle and the EOC flux distribution is appropriate for the second half of the cycle. Table 4.2-8A gives values of the design total and fast fluences at various axial locations for the fuel assembly, while the design total and fast fluences for the blanket assembly duct region and non-duct components are given in Table 4.1-12.

Steady State Thermal Environment

The steady state design temperatures utilized in these analyses equal or envelope those given in Section 4.4. For the fuel assembly components, the steady state duct temperatures and temperature gradients defined at BOC1 provide the worst case. Therefore, the steady state fuel assembly thermal conditions described in this section are based on BOC1 data. Both beginning and end-of-life temperature and temperature gradients are utilized in the blanket assembly region structural analyses.

Tables 4.2-8A and 4.2-12 give the maximum steady state temperatures, cross-assembly temperature gradients, and assembly-to-neighboring assembly temperature gradients for the fuel and blanket assembly regions, respectively. The maximum gradients were assumed to occur throughout the life of the assemblies.

Thermal Transients

51 | The duty cycle for fuel and blanket assemblies is defined in Section 4.2.1.3 and Appendix B. Given therein is the definition, classification and frequency of various thermal transients applicable to the fuel and blanket assembly structural components. In certain cases, the duty cycle evaluation requires that the mechanical loading associated with an earthquake be combined with the thermal loading due to transients.

As in the case of the fuel and blanket rods, umbrella transients were chosen for the various core assembly regions. These are the most severe 1 or 2 transients in each category which, for design purposes, are assumed to occur at a frequency equal to the total number of transients in the duty cycle. In the shield block and inlet nozzle region for the fuel and blanket assemblies, the umbrella thermal transients are U-18 (loss of offsite power), and E-4a (saturated steam line rupture). For the other fuel and blanket assembly regions, the E-16 transient (three loop natural circulation) was chosen as the umbrella thermal transient for both upset and emergency conditions. The fuel assembly region temperature and temperature gradient histories for these various transients are given in Reference 171. Similar data for the blanket assembly regions will be given in the blanket assembly structural analysis stress report.

Core Restraint Loads

Core restraint loads are developed due to duct-to-duct interaction at the load pads caused by cross flat temperature and flux gradients and swelling in core assemblies. Preliminary analyses indicate no duct-to-duct contact occurs in the mid core region. These loads have a peak value at beginning of life, decreasing rapidly in early life due to creep relaxation and subsequently increasing again slowly due to swelling. The loads reported here are the peak beginning of life loads.

The maximum design, interduct forces on the load pads are given in Table 4.2-8B and 4.2-12A for the fuel and blanket assemblies, respectively. The direction and application of these forces are shown in Figure 4.2-33A. Further details of the core restraint contact loads are given in Reference 171. The maximum bending moments in the core assemblies due to steady state temperatures and flux conditions and core restraint are also given in Tables 4.2-8A and 4.2-12 for the critical regions on the assemblies. The bending moment at the top load plane is zero for both assembly types.

Hydraulic Conditions

The maximum nominal duct coolant pressures at plant thermal hydraulic design conditions are given in Tables 4.2-8A and 4.2-12 for various assembly locations. The coolant pressure in the core assembly ducts decreases linearly with axial location to approximately 1 psi at the top of the rod bundle. The coolant pressures given in Table 4.2-8A for the orifice plate and rod attachment represent the coolant pressure drops across these components.

Seismic Loads

The seismic loads are loads generated in core assemblies due to seismic activity at the plant site. Based on the design duty cycle, the seismic events are represented by two earthquakes - the operating basis earthquake (OBE) and the safe shutdown earthquake (SSE) - and loads produced by the worst of the two earthquakes were accounted for in the analyses.

The horizontal seismic loads in fuel assembly ducts at the above core load pad were determined by a finite-element planar model of the core cross section referenced in (171). The loads from this model are the "likely worst case" interduct forces applied at the above core load pad under a lateral, unit gravitational, quasi-static loading in one horizontal direction. To apply the 1g ACLP loads from the finite element core model to the duct analysis, the following procedure was adopted:

- (a) The portion of the fuel assembly weight supported at the load pad was added to the calculated loads. This weight was distributed evenly at each load pad corner.
- (b) The 1g loads from the planar core model calculation were multiplied by the appropriate seismic acceleration factor for each load pad.
- (c) The seismic loads from the planar core model are applicable to the duct at the above core load pad. The top load pad forces were calculated by multiplying the above core load pad forces by a load factor which is equal to the ratio of the assembly weight supported at the top load pad divided by the assembly weight supported at the above core load pad. The top load pad seismic load effects were found to be negligible compared to the effects of other transients on this region.

Various core assembly locations were screened to determine the worst loaded duct. The interduct ACLP design seismic forces at these locations calculated according to the above procedure are given in Tables 4.2-8B and 4.2-13 and the tabulated forces are identified in Figure 4.2-33A. The maximum vertical forces due to OBE and SSE events at various characteristic locations are given in Table 4.2-8C for both the fuel and blanket assemblies.

For the core assemblies, the frequency of the OBE event is determined by prorating the given number of design events for the plant life (30 years) into the component lifetime in years and rounding up to the next higher whole number. Each event is characterized by 10 peak response cycles. The extremely unlikely SSE event is assumed to occur once.

4.2.1.3.2.3.4 Materials Property Considerations

For both the fuel and blanket assemblies, the duct (including the ACLP) is made of 20% cold worked 316 stainless steel (20% CW 316 SS). All other components considered in the structural analyses consist of solution annealed 316 stainless steel (SA 316 SS). The pertinent properties of these materials must be adjusted for temperature and fluence effects. The most important properties of these materials and the methods or sources from which their numerical values as functions of fluence and/or temperature are obtained as given below.

Thermal Properties

These values were obtained from Reference 153 for both material types. This reference also gives the temperature dependence of these properties.

Elastic Properties

These values and their temperature dependence were also obtained from Reference 153 for both material types.

Stress-Strain Curves

53|

Reference 153 data was utilized to construct the stress-strain curves for unirradiated 20% CW 316 SS and for unirradiated and irradiated SA 316 SS as a function of temperature and fluence. Reference 171 describes how the inelastic material properties were derived for irradiated 20% CW 316 SS from the data of Reference 176. Fluence effects were considered by utilizing the average values of the beginning and end-of-life stress strain curves. Data scatter was accounted for by utilizing the minimum property values for irradiated 20% CW 316 SS, 80% of the average values for unirradiated 20% CW 316 SS, and 90% of the average property values for irradiated and unirradiated SA 316 SS.

Fracture Strain

The true minimum irradiated fracture strain (ϵ_f , min) for both material types over the temperature range 800 to 1400°F as a function of fluence ($E > 0.1$ Mev, where (ϕt) is in units of 10^{22} n/cm²) and temperature (T , °F) is given by the following relations (see Reference 171):

$$\epsilon_{f, \min} = \epsilon_f^1 \text{ for } (\phi t) < (\phi t)_0$$

$$\epsilon_{f, \min} = \epsilon_f^1 \left[\frac{(\phi t)}{(\phi t)_0} \right]^n \text{ for } (\phi t) > (\phi t)_0$$

where,

$$\epsilon_f^1 = 0.45 \left[\frac{T}{1000} \right]^{-3.5} \text{ for } 800 < T \leq 1000$$

$$\epsilon_f^1 = 0.45 \frac{T}{1000}^{-5.5} \text{ for } 1000 < T < 1400$$

$$(\phi t)_0 = 1.4 - \frac{T}{1000} \text{ for } 800 < T \leq 1000$$

$$(\phi t)_0 = \frac{T}{1000} - 1 \text{ for } 1000 < T < 1400$$

$$n = -1.7 + \frac{T}{1000}$$

51 |

Amend. 53
Jan. 1980

Fatigue Properties

For both material types, the Manson Universal Slopes Method was used to construct fatigue curves from the elastic and inelastic property values of the materials. Irradiation and temperature effects were accounted for by including them in the pertinent properties. Multiaxial stress states were accounted for by applying the higher of the equivalent or maximum principal strain range to the fatigue curves. Data scatter was included by reducing the uniaxial fatigue life by a factor of 2 on strain range or a factor of 20 on life, whichever is more severe. This process is described in detail in Reference 177.

Stress Rupture

Stress rupture properties for irradiated SA 316 SS are based on the minimum properties given in Reference 175, while Reference 58 presents this data for 20% CW 316 SS.

4.2.1.3.2.3.5 Analysis Methods

53| The fuel and blanket assembly structural evaluation was performed in accordance with the criteria identified in Section 4.2.1.1 which assure that the intended function of these assemblies is not impaired over the CRBR first core, comprising a total of 328 full power days for the fuel and inner blanket assemblies, and 878 or 1153 days for the radial blanket assemblies. The criteria protect against the crack initiation failure modes of local ductile rupture and combined creep-fatigue damage. In addition, the excessive deformation failure modes of peak plus accumulated and residual deformation are protected against by the criteria. The core assembly structural evaluation was based on the loading magnitudes and currently available materials data identified above.

The detailed analyses of the fuel assembly structural components identified above are presented in Reference 171. A similar analysis for the blanket assembly components will be presented in the blanket assembly structural design support document, to be released prior to the FSAR. The analysis and evaluation techniques used for both assembly types are generally quite similar. A brief description of those assembly component structural analysis techniques is given below.

53|51 The structural evaluation approach adopted for the fuel assembly shield block, CMP and ACLP hex ducts, TLP outlet nozzle, attachment assembly, and orifice plate was to construct analytical models for the respective regions in relation to prominent design features and loading conditions which would provide worst case structural damage. This same approach was taken for the blanket assembly components, except for the blanket assembly attachment region for which an experimental determination of the worst case structural damage was made.

In the assembly component structural analysis and evaluation, a loading analysis was first made that considered the mechanical, seismic, core restraint, and thermal steady state and transient loads presented above in establishing the number of characteristics of a worst case transient sequence that umbrellas all expected transients for the region or component during the CRBR first core operation. Next, an inelastic structural analysis of the component or region was made for a single worst case time independent transient sequence and time dependent hold time to calculate the strains and dimensional changes from which total lifetime bounding values were calculated. The ANSYS Computer Program (Appendix A) was used extensively in the analytical approach adopted for the structural evaluation. This is a finite element structural analysis code, to which a component or region model, materials properties, and steady state and transient boundary conditions are input. With this code, the same model can be used to calculate component temperatures due to a boundary condition input, and the thermal stresses resulting from these temperatures. Both time dependent and steady state component structural analyses are performed, depending on the loading condition. Finally, the time dependent and steady state analysis results were compared to the criteria limits to determine the adequacy of the component or assembly region performance.

The procedure for evaluating peak plus accumulated and residual deformations in relation to deformation limits was relatively direct as the inelastic deformations due to the applied transient-hold cycles are known from the ANSYS displacement solutions. However, for comparisons of the stress and strain response with crack initiation failure mode criteria, the structural evaluation procedure is not direct because a detailed examination of local multiaxial stress and strain behavior in relation to uniaxial tensile and biaxial pressurized tube data is required prior to evaluating the local ductile rupture and combined creep-fatigue factors. Further, the component models include a large number of finite elements (see Figure 4.2-33B, for example) which must be screened to determine the worst location for crack initiation. Accordingly, an important consideration in performing a thorough structural evaluation of crack initiation is a means of processing the stress and strain response into a format that permits a ready comparison with allowable limits. In this evaluation, a special purpose damage processor was written to access the stress and strain response data determined by ANSYS for each converged time-independent and dependent solution throughout the worst case duty cycle and identified the element with the maximum local ductile rupture and combined creep damage factors. These worst damage factors were then compared to the criteria limits.

The structural performance of the blanket rod attachment assembly was assessed by a series of assembly drop tests. In these tests, a test assembly which included a prototypically loaded blanket rod attachment assembly was dropped from successively increasing heights up to a maximum drop height of 3 inches. This resulted in blanket rod attachment loadings far in excess of values expected to occur in service.

Several tests of duct sections and irradiated materials have been performed (Reference 178) and additional tests are planned to confirm the conservatism of the analysis and the adequacy of the design.

4.2.1.3.2.3.6 Design Margins

The bounding design margins for the critical fuel and blanket assembly components or regions due to the loadings discussed in Section 4.2.1.3.2.3.3 and based on the criteria presented in Section 4.2.1.1 are given in Tables 4.2-16 and 4.2-17. These results show that all components and regions considered achieved design lifetime within the limits prescribed by the structural design criteria of Table 4.2-7. The drop tests on the blanket rod attachment assembly indicated that no deformation of this component occurs up to a drop height of 3 inches. After a 3 inch drop on a rigid plate, which produces loads in this component far in excess of expected values, a slight buckling was observed in one part of the blanket rod attachment assembly which in no way would have impaired the function of the assembly. Thus, it is concluded that all structural components of the fuel and blanket assemblies meets their structural requirements.

4.2.1.4 Irradiation Experience

4.2.1.4.1 Fuel Rods

The design of mixed-oxide fuel rods has been developed from theoretical models and a broad range of irradiation experiment results. The theoretical developments of the phenomenological models considered in the evaluation of fuel rod behavior have been discussed in the literature. Verification and modification of these models is primarily based on the data and subsequent analyses derived from the irradiation tests performed in the U.S. and abroad. It is the purpose of this subsection to review the irradiation experience to date and the applicability of the test results to the CRBRP fuel rod or blanket rod design and their anticipated performance.

The LMFBR Fuel Development Program includes an extensive irradiation testing program for the verification of FFTF and CRBRP fuel rod design adequacy. The irradiation testing program includes steady state testing of fuel rod assemblies in EBR-II and encapsulated rods in the General Electric Test Reactor. Transient overpower and flow coastdown tests on fresh and irradiated fuel rods are conducted in capsules and self-contained loops in the TREAT facility. The transient testing program, has two major test series, engineering proof testing and transient overpower testing.

Figure 4.2-34 illustrates the numbers and schedules of tests which have been or are being conducted in the various development areas. The steady state irradiation testing program provides for design verification by testing

prototypic fuel rods at linear heat ratings, cladding temperatures and burnups representative of operating conditions expected in FFTF and CRBRP. 900°F operation refers to the initial operating conditions of the FFTF and 1100°F operation refers to rated FFTF core operating conditions. It should be noted that the FFTF fuel rod hot spot cladding temperature at 900°F operation corresponds to the CRBRP fuel rod cladding hot spot temperature at end of design life. The thirteen tests at the 900°F operation conditions include 37 and 61 rod EBR-II subassembly tests. Some of these are representative of earlier FFTF fuel rod designs (quarter-inch diameter rods clad in solution treated 304 or 316 stainless steel). These tests have been continued because they provide a broader data base for the formulation of fuel rod performance analysis models. The fuel rod hot spot temperature at 900°F operation corresponds to the CRBRP fuel rod cladding hot spot temperature at end-of-life. Although these lower temperatures simulate only end-of-life CRBRP conditions, the results are used in evaluating particular attributes (i.e., wastage) incorporated directly or indirectly into performance models and/or are used in design verification through extrapolational procedures. An example of how the data may be used in an overall sense has been given in PSAR Section 4.2.1.1.2.7 and also in the response to Question 241.85. The five tests in the 1100°F operation range are conducted in 37 rod EBR-II subassemblies.

The fuel design criteria of subsection 4.2.1.1.2.2 specified that no fuel melting should occur at a 15 percent overpower condition. In-reactor fuel rod tests to establish the thermal performance limits of the FFTF fuel have been conducted. These tests will provide information for designing CRBRP fuel. The six thermal performance tests include two 19-rod assemblies and a 37-rod instrumented subassembly in EBR-II and special capsule irradiation tests on vendor fuel in the GETR. General Electric Company's Breeder Reactor Operation has also conducted a thermal performance test of mixed oxide fuel rods in EBR-II which included rods manufactured by HEDL that were siblings to the rods used in the HEDL tests. Postirradiation examination of the rods is underway at LASL. Preliminary results further substantiate the earlier HEDL thermal performance test results. Both the capsule irradiation program for FFTF driver fuel rods and the irradiation program for vendor produced fuel pellets in EBR-II are described in detail in Task D - Vendor Fuel Irradiation of Reference 164. Tests within this task are conducted in the General Electric Test Reactor (GETR) and in EBR-II. Data for comparison of general performance of HEDL to vendor fuel to intermediate goal burnup is obtained at prototypic FFTF rated core heat rate and cladding temperatures in instrumented capsules irradiated in the GETR Radially Adjustable Facility Tube (RAFT) facilities. Thermal performance is compared in special capsules irradiated sequentially in the GETR trail-cable facility. Fast flux fuel performance is compared in a 37-rod, high cladding temperature test currently being irradiated in EBR-II.

Three main conditions of irradiation performance are being tested: 1) general performance of randomly selected rods at prototypic heat rates and to low and intermediate burnup in GETR-Raft Capsules, 2) thermal performance of randomly selected fuel to establish relative power-to-melt using GETR trail-cable capsules, and 3) low power, fast flux, high cladding temperature performance of randomly selected fuel in a 37-rod EBR-II test, HEDL-P-15.

As explained in Reference 164, four FFTF fuel rods were selected at random from available lots of accepted rods, two from each fuel vendor, and four comparison rods were fabricated by HEDL. All were encapsulated and irradiated in GETR-Raft facilities. Parts of HEDL-vendor rods were removed after ~ 10,000 and 36,000 MWD/MTM for disassembly examination and evaluation. Examination was scheduled to be completed during the first half of 1976 but has not yet been reported.

In the thermal performance series, four capsules of HEDL-vendor fabricated fuel and a calibration capsule of HEDL fabricated fuel were irradiated. On the basis of the calibration capsule results, the remaining capsules were tested to cause partial centerline melting of the fuel column. Destructive examination will establish the comparability of power-to-melt of HEDL and vendor fuel. Examination was scheduled to be completed during the first half of 1976. Recommendations on operation of FFTF cores 1-4 from the capsule tests are scheduled during the first half of 1978 (see Figure D-2, Reference 164). The results of these capsule tests will aid in the CRBRP fuel design by providing thermal performance data comparisons of vendor produced fuel versus the HEDL produced fuel that was tested previously. CRBRP will utilize the data to establish whether there is a larger or smaller margin to melt, and whether there is a typical effect on vendor fuel performance which must be taken into account through design margin adjustment. The EBR-II tests of vendor fuel will aid in a comparison of HEDL-vendor fuel fast flux performance including fission gas release confirmation at lower power, fuel stability and consistent migration and potential fuel cladding chemical interactions. The schedule for the HEDL-P-15 test is given in Figure A-2 of Reference 164.

Fuel rod ultimate life and fuel rod cladding failure mechanisms and modes are being determined in tests that are deliberately continued until cladding failure occurs. Plans are also being formulated for conducting irradiation tests on fuel rods which have failed to establish rod and fuel assembly behavior under these conditions. The HEDL fuel development program includes ten run-to-failure tests. Five failed rods are now under detailed examination. The consequences of mixed oxide fuel rods failing by natural causes have been consistently benign. There has been no failure propagation or explosive release of fission gases. The cladding defects are typically grain boundary separations, and are so small that special examination techniques have been developed to find them. Identification of EBR-II subassemblies which contained xenon tagged failed rods was quite straightforward. The RTCB task of the Reference Fuel Steady-State Irradiation Program (Reference 164), utilizes fuel rods containing prototypic cladding, a temperature range applicable to FFTF and CRBRP, and are contained in EBR-II subassemblies with other fuel rods of the same design and containing the same materials so that the data are significant and the subassembly spacing system is representative of current LMFBR design. Fuel rods selected

for RTCB testing in EBR-II are irradiated until a cladding breach is detected by fission gas release. After a breach is detected, the assembly is immediately removed from the reactor and the breached rod is identified. The breached rod and selected sibling rods are examined to establish the cause and mechanism of the breach. The results of these examinations together with the fabrication and irradiation variables form the basis for establishing fuel rod lifetime criteria and models for determining the excess lifetime beyond the design lifetime of the fuel rods. A specific example of the use of these and other obtained data has been given in PSAR Section 4.2.1.1.2.2.

The scope and up-to-date schedule for RTCB testing has been given in Reference 164 in more detail and the results of examinations of RTCB experiments have been reported in Reference 101. The RTCB assemblies for irradiation in EBR-II are shown in Table B-1 of Reference 164. A milestone schedule for the EBR-II testing is shown in Figure B-1 of Reference 164.

FFTF driver fuel rods manufactured by the two vendors supplying fuel for the FFTF and potentially CRBRP are being irradiated in capsules in the GETR to establish their irradiation performance in comparison with the HEDL-prepared fuel and fuel rods used throughout the irradiation testing program. Vendor-produced fuel pellets will also be irradiated in special rods in EBR-II to further demonstrate the satisfactory dimensional stability of the FFTF and CRBRP fuel. The five vendor fuel tests include two rods from each vendor irradiated in capsules in GETR. Three of these rods and their matching HEDL rods were discharged at goal exposures of ten thousand and thirty thousand MWd/T and are undergoing postirradiation examination. Performance of the vendor fuel rods has been completely satisfactory.

A more detailed description of the tests and test results obtained and illustrated in Figure 4.2-34 may be found in Reference 101.

In addition to the secondary references provided in Reference 101, a National Reference Fuel Steady State Irradiation Program Plan is being formulated and a summary provided to NRC in June, 1976. Program Plan sub-tasks are: Steady-State Irradiation Performance, Run-to-Cladding Breach, Run-Beyond-Cladding Breach, Vendor Fuel Irradiation, Fuel Performance Analysis and Prediction, and Load Following. The program activities are summarized in Table 4.2-62 which is taken from a preliminary draft of the program plan. The National Reference Fuel Steady-State Program Plan will include a schedule responsive to specific milestone needs of CRBRP. Test data from these programs will be reported periodically in status reports similar to Reference 101.

The National Reference Fuel Steady-State Irradiation Program includes a range of in-reactor environments that encompass those of CRBRP. Data from these tests will be used in developing and verifying the fuel performance models which will be utilized in CRBRP fuel design. An example of this application of steady state irradiation data is given in Section 4.2.1.1.2.2. In addition, the steady state program provides rods for transient testing.

Commitment to a precise method of utilization of the specific scientific information from each test is not feasible at this time because of the multiple alternatives that exist in applying the results to the design, follow on testing, surveillance, and reactor operations. However, preliminary planning for utilization of ongoing and planned EBR-II testing has been formulated and is provided for information in Table 4.2-65. This preliminary planning identifies a method of potentially verifying the adequacy of the CRBRP fuel design from the extensive EBR-II test programs without need for extensive follow-on effort.

Figure 4.2-35 illustrates the growing number of stainless-steel-clad, mixed oxide fuel rods in the U.S. Program which have been irradiated in EBR-II to greater than the FFTF/CRBRP initial peak fuel goal burnup of 80,000 MWd/T. This graph does not illustrate the larger statistics of the foreign programs, i.e., Dounreay and Rapsodie. However, each of the rods illustrated in this figure is much more extensively characterized both before and after irradiation, a feature which provides more precise information from each irradiation test in the U.S. Program. This does not imply that better characterization necessarily leads to better performance predictability over larger statistics. Rather more precise information may be derived from each irradiation test if thorough pre/post characterization work is utilized. Features which are characterized prior to irradiation vary somewhat in attributes but generally include the following:

- a. - pellet O/M ratio, density, smear density
- b. - pellet diameter
- c. - cladding outer/inner diameter
- d. - fuel column length
- e. - cladding mechanical properties
- f. - cladding chemistry

Features characterized following irradiation also vary but generally include:

- a. - fission gas release
- b. - fuel stability and consistent migration
- c. - pellet diameter and central hole dimensions
- d. - cladding profilometry and/or diameter
- e. - pellet density and/or column length change
- f. - fuel cladding chemical interaction
- g. - fuel/cladding gap

Significant results obtained from the steady state test program to date are summarized as follows:

1. Sodium corrosion, fuel-cladding chemical interaction, and manufacturing tolerances have all been demonstrated to be less than the current design wastage allowances.
2. Dimensional stability of the fuel has been predictable and satisfactory. There is no "Fuel Densification" problem.
3. Thermal performance capability revealed by integral tests has exceeded the design requirement for linear heat rating by 20%.

4. To the extent tested, natural fuel rod cladding failures were benign. This experience agrees well with results from foreign programs.

The fuel rods referred to in Figure 4.2-35, from the test programs of Figure 4.2-34, are described in reference 101. These fuel rods may be compared to the CRBRP fuel rod design parameters described in Table 4.2-4. The test environments given in Reference 101 may be compared to the steady-state operating conditions for CRBRP given in Table 4.2-61. Comparing the CRBRP conditions with those in reference 101, the major differences are in the fluence/burnup ratio, axial power distribution, and coolant velocity temperature combinations. FFTF fuel performance verification discussed above will provide more data to verify both the CRBRP fuel design and/or analytical methods.

The LMFBR fuel transient testing program being conducted by HEDL complements that being pursued by Argonne National Laboratory's reactor analysis and safety division. A commonality is provided to both programs by the HEDL EBR-II steady state irradiation testing program which is the source of irradiated prototypic fuel rods used in the transient tests.

The HEDL program includes two principal test series, engineering proof tests and transient overpower tests. The objective of the engineering proof test series is to confirm the ability of the FFTF and CRBRP fuel rod to withstand events terminated by the plant protection system (PPS), without exceeding their design limits. The test matrix which was based on very conservative design analyses of the FFTF fuel rod, includes fast and slow reactivity insertion ($\$3/\text{sec.}$ and $3\text{¢}/\text{sec.}$) and a loss of cooling test for variable fuel rod linear power, fluence to burnup ratio and cladding temperature. To the extent tested, the results showed that for the PPS terminated events, design limits for the FFTF fuel rod were only distantly approached. This test series also includes reirradiation to fuel clad breach, in EBR-II, of rods subjected to terminated events in TREAT, to further demonstrate the PPS terminated events have no deleterious effects on subsequent fuel rod performance and lifetime.

Overpower tests determine the fuel rod cladding failure threshold for terminated events. Data from these tests are used in the formulation of analytic models to describe fuel rod performance up to the point of cladding failure. Mechanisms which cause cladding failure and the location of the failure are of primary interest. Post failure behavior of fuel rods and assemblies under transient overpower conditions are addressed experimentally in the ANL-E Series tests. These tests are of primary interest for performing analyses of the more severe faulted conditions and hypothetical accidents. The test program matrix includes simulating $60\text{¢}/\text{sec.}$ and $\$3/\text{sec.}$ transient overpower conditions on encapsulated, previously irradiated prototypic FFTF/CRBRP fuel rods. An important parameter in the test program is the steady state irradiation linear heat rating of the rod because cladding failure threshold depends on the microstructure of the irradiated fuel. The test program also includes plans for a test of fuel rods with full-length FFTF/CRBRP fuel columns in a flowing sodium (MK-IIC) loop.

In evaluating the relative fuel damage potential for the transient events in the CRBRP design duty cycle, engineering judgement was applied. The general procedure and rationale used for determining the design basis umbrella transients for fuel performance analyses and transient testing is as follows:

1. For undercooling transients, maximum cladding temperature increase and transient duration (time) are the primary factors considered. Maximum cladding temperature increase is important because of the significant reduction in cladding tensile and rupture strength and significant increase in thermal creep rate with increasing temperature. Furthermore, maximum cladding temperature gives an indication of plenum temperature increase which, by the ideal gas law, would increase the fission gas pressure within the constant volume of the fuel rod. Time or duration of the transient is important because the creep rupture damage (thermal creep strain) is time dependent.
2. For overpower transients, maximum cladding temperature increase and transient duration are also considered. In addition, maximum fuel temperature and the fuel to cladding temperature difference are used to evaluate transient severity. Maximum fuel temperature is considered because as fuel temperature increases, the fission gas stored in the fuel either expands, increasing fuel cladding mechanical interaction (FCMI), or is released, increasing the fission gas loading. Fuel to cladding temperature difference is considered because it is the driving force for FCMI due to differential thermal expansion.

While a value for FCMI and the corresponding cladding damage may not be calculated for each transient in the CRBRP duty cycle, FCMI and cladding damage are definitely considered in formulating the CRBRP design-basis umbrella transients. The verification of the above rationale, consideration of second order effects (e.g., rate of change) and determination of the worst conditions for a given transient are provided by the LMFBR Mixed Oxide Fuel Transient Testing Program Plan described in Reference 168. The detailed logic for the integrated CRBRP/FFTF transient testing portion of this program is also given in Reference 168.

Briefly, there are two primary types of transient events considered in the Transient Testing Program: undercooling events and overpower events. For the undercooling events, there are four sets of tests currently planned; for the overpower events, there are seven test sets. Each set has a specific purpose. For the undercooling event test, these purposes are:

1. Determine the worst transient event;
2. Check for the worst time in the fuel rod life for the transient to occur;

3. Determine the margin to cladding failure after transient occurrence;
4. Check the effects of breached cladding on fuel rod transient behavior.

Four of the sets of overpower fuel rod tests have the same purposes as above. In addition, three other overpower test sets are planned to:

1. Determine the effects of rate of change on environment;
2. Determine the effects of prior transients;
3. Determine the effects of fuel microstructural changes.

The integrated CRBRP/FFTF Transient Testing Program is broad in scope. It is designed to determine the worst PPS terminated undercooling or overpower conditions or events. If the worst events for CRBRP are not encompassed by the current (PSAR) analyzed umbrella conditions, new umbrellas will be chosen and eventually analyzed.

51

As part of the National Reference Fuel Steady-State Irradiation Program and the National LMFBR Mixed Oxide Fuel Transient Performance Program, run-to and beyond cladding breach programs are planned for steady-state irradiation in EBR-II to meet the CRBRP requirements.

The Run-to-Cladding-Breach tests of the Reference Fuel Steady-State Irradiation Programs provide the experimental test data to establish the reference fuel lifetime, establish the cause and mechanism of the cladding breaches, establish the consequences of a steady-state cladding breach, and provide the requisite fuel pin lifetime statistics to develop and verify design and performance codes. The test program is designed to irradiate prototypic fuel pins in EBR-II until a cladding breach occurs in one fuel pin in the test assembly. Reference 101 discusses seven rods with breached cladding, confirming that: 1) a cladding breach has no deleterious effect on the subassembly hardware or on the neighboring fuel rods, 2) the leakage of fission gas through the breach is slow and gradual, 3) the fissures appear to form after considerable plastic deformation of the cladding, 4) there is no evidence that fuel sodium contact is an immediate consequence of a cladding breach.

34] The run-beyond cladding breach program activities are given in Table 4.2-62, items 39 and 40. The run-beyond-cladding-breach tests of the Reference Fuel Steady-State Irradiation Program provide the experimental basis for long-term operation of CRBRP with breached fuel pins residing in the core. Activities carried out under this task will: 1) include continued irradiation of fuel pins after they sustain an inreactor cladding breach and 2) provide predictability of events subsequent to a fuel pin cladding breach. An additional accomplishment under this Task will be to provide breached fuel pins to the transient test program. These breached fuel pins will be transient tested to confirm the satisfactory performance of breached fuel pins during a typical design basis Plant Protection System terminated transient.

The irradiation of breached fuel pins in EBR-II will provide: 1) reactor operational experience with breached fuel pins, 2) confirmation of the capability of reactor instrumentation to monitor fuel and fission product release from a breached fuel pin, 3) verification of the capability to detect a new cladding breach with a previously breached fuel pin residing in the core, 4) data on the growth of a cladding fissure after breach, 5) potential for fuel washout, and 6) insight into any possible tendency for failure propagation to neighboring fuel pins.

Extensive analytical and experimental results (summarized in Section 15.4) demonstrate that the probability of a local in-core fault leading to a condition where substantial damage is propagated throughout the assembly is extremely remote. In addition, many of the mechanisms involved in local failures are inherently benign and/or self-limiting.

The evidence presented in Section 15.4 shows that existing experimental data is adequate to confirm the safety of the reactor from the potential propagation of local faults.

A complimentary out-of-reactor program of testing cladding from irradiated fuel rods is being conducted in support of this effort. The significant results obtained from the HEDL transient testing program are summarized as follows:

1. Fuel microstructure of the steady state irradiation history of a fuel rod affects the fuel rod cladding failure threshold.
2. No significant fuel rod damage has been observed for PPS simulated terminated events.
3. An empirical correlation for fuel rod cladding failure threshold is being developed.

References 53 through 57 provide currently available fuel rod transient test data and descriptions of analytical models that have either been formulated from the data or evaluated against the data. In addition, a first phase verification of the Cumulative Damage Function procedure based upon some of this transient test data is presented in Section V of Reference 58. The complete verification plan for the fuel assembly (including the CDF design procedure) is provided in Table 4.2-65.

At this time, the LMFBR fuel development program has concentrated primarily on testing the FFTF fuel rod for FFTF initial and rated core operating conditions. This program provides useful information for initial design and analyses of the CRBRP design and operating conditions. However, as the CRBRP design and operating conditions evolve, the LMFBR fuel development program will be reviewed in detail. Where necessary, additional testing will be planned to support CRBRP cladding integrity limits, fuel assembly design bases and performance predictions.

As an example, for the current CRBRP design, initial Pu/(U + Pu) contents of 33 w/o are needed. Although the fuel programs previously mentioned have concentrated on Pu/(U + Pu) contents of 25 w/o, significant differences are not anticipated. Plans are underway to confirm these points. In particular, cladding wastage (FCCI), constituent migration, solid and volatile fission product migration, fuel rod thermal performance, and fuel/sodium (RBCB) tests are in the preliminary planning stages.

In addition, modest fabrication development testing is also in the preliminary planning stage to confirm that the higher Pu/(U + Pu) content does not result in unforeseen fabrication difficulties. These tests are primarily associated with potential inhomogeneous effects which could affect fuel pellet specifications.

The fuel rod tests in EBR-II described in References 162 and 168 can not be used directly to establish or extrapolate to the expected fuel failure statistics of the CRBRP core. These EBR-II experiments are in many instances intended to resolve key issues by providing data for models which are used to analyze fuel rod behavior and lifetime. For example, models for fission gas release, solid and volatile fission product migration, fuel cladding chemical interactions, thermal performance, bundle-duct interactions, etc., are all derived from the EBR-II experimental data. In addition, certain operations such as reconstitution take place in many of the EBR-II tests and are believed to have contributed to subsequent failures. Clearly, there will be no reconstitution of CRBRP assemblies. Hence, failures attributable to such a non-prototypic process are in no way representative of expected CRBR fuel rod performance.

In addition to the above considerations, certain results which are obtained can lead to improvements in the overall design. One example may be found in the bundle-duct interaction area, where significant learning was obtained, through failures, on the amount of wear as a function of bundle porosity (see References 101 and 176). The failures found led to a correlation which has, in turn, provided a superior support system. Obviously, failures of this type should not be attributed to designs employing the superior support system.

The operating CRBR fuel may also, through the design process, have built-in conservatisms which are not reflected in the EBR-II fuel rod failure statistics. For example, as part of the design analysis procedure, the CRBR fuel rods are assumed to operate at hot channel and hot spot temperatures at the upper 2σ level of uncertainty. To validate the calculated fuel rod performance, EBR-II tests are performed with nominal temperatures set equal to the expected CRBR 2σ hot spot/hot channel temperatures. Thus, the EBR-II test rod population is exposed to a more severe temperature environment relative to that of the CRBR fuel rods. Again, this prevents EBR-II test rod failure statistics from being directly applicable to CRBR fuel rods.

Because of all the above considerations, it is concluded that experimental EBR-II fuel rod failure rates are not typical of expected CRBR fuel rod failure rates. Therefore, EBR-II failure statistics cannot be used to formulate CRBR fuel rod failure statistics without excluding failures due to non-prototypic loads and environments, and accounting for significant differences in the environment distribution that each population of pins encounters.

In addition to the U. S. steady-state irradiation program, considerable data have been generated by the foreign programs on cold worked 316 stainless steel clad rods. Burnups of 100,000 MWD/MT have been achieved on PFR-type fuel pads in DFR. Although no bare fuel rods have been irradiated beyond failure in the U.S., foreign experience includes operations with failures for periods up to 2-1/2 years without apparent significant mechanical effects on the fuel assembly.

The results of foreign experience to high burnups (100,000 MWD/MT) and operation with failed fuel are described in Reference 27 and in References 102 and 103. As noted previously, this data is used to provide confidence that CRBRP design goals are achievable.

Test results from foreign programs are qualitatively assessed for trends in fuel and fuel assembly behavior. However, foreign fuel rod test data are not being used to quantitatively evaluate the performance of CRBR fuel rods, or to formulate analytical models used in their design. For this reason, a detailed comparison between foreign test programs and CRBR is not necessary.

51

4.2.1.4.2 Blanket Rods

The design of the CRBRP blanket rods has been developed from theoretical models based on mixed oxide fuel rod experiments and light water reactor fuel rod operating experience. No irradiation experience with prototypic blanket rods is available. This section reviews the irradiation experience which is applicable to the blanket rods.

In 1970, several experiments were initiated which contained mixed oxide fuel rods clad with reference 20% cold worked 316 stainless steel tubing. These experiments investigated the effects of varying the amount of cold work on the performance of the cladding at high temperatures and high fast fluences and studied the feasibility of increasing the cladding operating temperature up to 1385⁰F. Results from the fuel rod tests will be directly applicable to the blanket cladding design; however, the performance of the fuel pellets in these tests is not applicable to the radial blanket. In addition to the U. S. steady state irradiation program, considerable materials data have been generated by foreign programs on cold worked 316 stainless steel.

In February 1974, a 7 rod blanket test was inserted into the EBR-II reactor. The rods have diameters, temperatures, and power ratings similar to CRBRP blanket rods. The experiment is to determine the performance characteristics of blanket rods during steady-state operation and for a step increase in power late in life. The power step simulates the effects of assembly rotation, an out-in shuffling scheme, or a midlife power increase in the CRBRP.

The mixed oxide fuel rod irradiation tests provide basic design information for analytical modeling of fuel rods. The analytical design tools which are under development for fuel rods are also used for blanket rods. The basic information is generated in three development programs:

- 1) Reference Cladding and Duct Test Plan (transmitted to NRC via letter S:L:1112, dated June 7, 1976)
- 2) Reference Fuel Steady State Irradiation Program (Reference 162)
- 3) Reference Fuel Transient Testing Program (Reference 168).

The technical information that will be obtained from these programs and its utilization in fuel design are described in Section 4.2.1.4.1, including information on both cladding behavior and fuel behavior. The generated information will cover a parameter range which generally envelops the environmental conditions for blanket rods (e.g., temperatures, fluences, flux, burnup, sodium velocities). However, some blanket parameters (e.g., the long radial blanket operating time) are not enveloped and must be addressed by supplementary means. Table Q241.74-1 (see the response to Question 241.74) identifies technical

information obtained from fuel rod development that is applicable to areas of technical uncertainty for blanket rods. This table also shows how the information is supplemented by approved blanket rod irradiation tests designated as WBA-20, WBA-21, WBA-40 and WBA-41. The fuel rod test information and the blanket irradiation tests are also supplemented by out of reactor tests which are included in Table Q241.74-1 and are described in Table 4.2-20 of the PSAR.

The cladding materials data and other design information obtained from the Reference Cladding and Duct Program is incorporated in the design computer codes which are used for fuel and blanket rod design. The technical information incorporated in these codes is listed in Table Q241.74-1 and includes:

- Basic Cladding Material Properties (UTS, YS, Rupture Strength)
- Cladding Wastage (inside and outside)
- Cladding Damage and Failure Properties
- Cladding Swelling and Creep

The applicability of these data to blanket rod design will be assessed separately before submittal of the FSAR. Table Q241.74-1 also indicates how cladding data are supplemented by blanket rod irradiation test data. However, even these test programs do not eliminate the uncertainty caused by extrapolation of available cladding performance data from ~10,000 hours to the goal operating time of ~21,000 hours. Confirmation of the validity of the extrapolation will be obtained from irradiation of WBA-40 in FFTF, which will test operation of the CRBRP blanket.

This test and the other planned blanket irradiation tests were described at the CRBRP Fuel Meeting with NRC, October 13 and 14, 1976 in Bethesda, Maryland. (Additional details on test WBA-20 are contained in the handout from that meeting entitled "Radial Blanket Rod Test", H. D. Garkisch.)

4.2.1.5 Testing and Inspection Plans

4.2.1.5.1 Fuel Assembly Design Verification Tests

To verify the adequacy of design features unique to the CRBRP fuel assembly, a testing program has been identified. This program is based upon a thorough review of existing FFTF and LMFBR Base Technology programs for applicability to CRBRP fuel assembly design. For example, Table 4.2-18 addresses the application of the FFTF fuel assembly design verification tests. LMFBR Base Technology programs such as those discussed in subsection 4.2.1.3.1.3 and the National Irradiation Creep Experiments are expected to provide a better understanding of in-reactor behavior and performance potential. Verification of the specific CRBRP fuel assembly design would probably not be addressed. As a result of this assessment, the design verification tests of Table 4.2-19 have been identified. It is planned that all out-of-pile test

51

data resulting from the design verification program should be available prior to final design release and either verify the adequacy of the design feature in question or dictate required modifications for adequate design conservatism. For test data when not available prior to the fuel manufacturing release, the information will be used to limit performance objectives during the initial core operation.

The HEDL PPS terminated transient overpower (HOP) and undercooling (HUC) tests and the unterminated (up to cladding breach) transient overpower tests (HUT) that are planned to support CRBRP fuel rod design are given in the "Plan for National LMFBR Mixed Oxide Fuel Transient Performance Program" (also referred to as simply Program Plan). This Program Plan also supports FFTF, advanced oxide system design and general analytical methods development. A summary of transient tests that support CRBRP was provided to NRC in May, 1976. The impact of this test program and the associated transient testing schedule on the CRBRP design, is that the experimental data from the post EBR-II irradiation transient testing program will be utilized directly to support CRBRP design and FSAR submittal.

The general objectives of the LMFBR Mixed Oxide Fuel Transient Performance Program relative to CRBRP are as follows:

- 1) To acquire experimental data so that analytical models describing transient behavior of prototypic fuel and cladding can be developed and independently verified. The data shall envelope the expected range in the CRBRP design and steady-state and transient operational parameters.
- 2) To provide experimental data so that new or existing cladding damage models and the associated limits for each level of damage severity can be substantiated. Testing in this category would be aimed at determining the amount of damage accrued during a specific type of transient event as well as the allowable limit for a given damage severity level. Again, the expected range in CRBRP design and operational parameters shall be considered.
- 3) To furnish well-documented experimental data which will verify the adequacy of the CRBRP fuel rod design to accommodate design basis transients. Predicted design margins for CRBRP shall also be experimentally established.

The referenced Program Plan is responsive to the first two CRBRP objectives by including activities for transient performance code and associated analytical models development. Moreover, specific experiments are included in the Program Plan to provide data to resolve key uncertainties in current analytical models and to provide a wider range

of integral test conditions for transient performance code development, calibration and verification. The methods developed must be capable of analyzing single transients, multiple transients, and post-transients operation for fuel rod conditions up to and including cladding breach. Documentation of validated analytic methods is planned to meet objectives 1 and 2 consistent with CRBRP milestones. Results of tests that support FFTF and advanced oxide fuel designs will also be used in development of validated analytic methods.

The preliminary testing program and schedule to directly support objective 3 for CRBRP fuel design is also included in the Program Plan. Specifically, a set of steady-state irradiation conditions and a corresponding set of umbrella transients to envelope multiple testing needs are included in the Program Plan. This testing program is responsive to the specific CRBRP fuel rod design basis transients summarized in Table 4.2-59, and the tables and figures referenced therein. Approximately 25 transient experiments are planned to envelope the CRBRP design basis transients. This program is focused upon EBR-II irradiated fuel rod transient testing in support of the initial cycles of CRBRP operation. Transient tests will be performed primarily in TREAT with some testing in an appropriate loss of flow facility. This CRBRP transient testing program will guide the planning of future test programs as follows:

- 1) Test results will dictate which rod burnup or microstructural conditions are of primary significance for a given transient event,
- 2) Test results will provide severity comparisons so that the transient testing scope can be limited to a minimum number of worst events, and
- 3) Results of pre and post transient examinations in conjunction with the corresponding transient performance will provide guidance as to the key fuel or cladding parameters that must be measured during surveillance.

In summary, the current* CRBRP transient testing program is responding to CRBRP needs by supplying:

A set of well-documented experimentally-verified design tools to analyze the response of CRBRP fuel pins to design basis transients, and

Experimental evidence to demonstrate both the conservatism of the design analyses and the transient performance limits of fuel pins in CRBRP

* As knowledge is derived from early tests, the detailed test matrices in the Program Plan will be updated and changed as necessary to focus testing efforts on most pressing data needs. NRC will be advised of the changes.

4.2.1.5.2 Fuel Assembly Fabrication and Site Examination Quality Assurance Provisions

A. Fabrication Examination

A comprehensive quality assurance program will be employed during all phases of the fuel assembly fabrication to ensure compliance with design parameters to a high degree of certainty. During final design, the details of the program were documented as quality conformance inspection plans. In the formalization of these plans, all available Regulatory Guides and the DOE Reactor Development and Technology Standards used for FFTF fuel assembly fabrication were considered. For the fuel rods, fuel assembly duct tubes and fuel assembly hardware, dimensional inspection will typically be 100%. In Tables 4.2-59A and 4.2-59B are lists of typical inspection characteristics in the plan for the fuel rod and fuel assembly and their various components.

B. On-Site Acceptance Tests

To assure that damage during shipping, loading and unloading or from sabotage has not occurred, a standard inspection procedure will be performed on every fuel assembly entering the plant site. Similar to the inspection for incoming light water reactor and FFTF assemblies, this procedure consists of:

- a. Examination of the shipping container for broken seals, dents, penetrations, sheared bolts or any sign of shipment damage and verification that the shipping container shock indicators were not tripped.
- b. A standard visual inspection of the assembly for dents, nicks, and gouges, especially in the area of hexagonal load pad corners, shield block corners, the inlet nozzle, piston ring and discrimination post, and correct assembly identification by verifying handling socket identification, discrimination post geometry and assembly serial number.

Defects determined during visual examination shall be photographed and selective dimensional inspection of external features shall be performed using manual general purpose tools that are commercially available. This inspection would be performed to determine if defects are of such an insignificant nature to be acceptable. A photographic record will be maintained for all accepted defects.

4.2.1.5.3 Blanket Assembly Planned Design Verification Tests

The inner and radial blanket assemblies have no equivalent in the FFTF reactor. The assembly hardware (inlet nozzle, outlet nozzle, and duct) are similar to the CRBRP core fuel assembly hardware, however, significant differences between the fuel and radial and inner blanket assemblies require the design verification tests presented here. The blanket rods have outside diameters and fuel pellets which are similar to LWR fuel rods. Thus, this LWR fuel rod fabrication technology can be used to fabricate and inspect the blanket rods.

Planned blanket design verification tests are listed in Table 4.2-20 along with the activity descriptions and planned completion dates. These tests will be performed unless data can be obtained through analysis or from other tests. The load pad strength and duct bending stiffness test, and rod cladding rupture tests are component verification tests, determining the strength characteristics of important blanket components which differ significantly from corresponding core fuel assembly components. The rod irradiation in EBR-II will verify the performance of blanket rods in a fast sodium reactor environment. The performance of the entire blanket rod bundle in a fast sodium reactor will be tested by the rod bundle irradiation test in FFTF.

4.2.1.5.4 Blanket Assembly Examination Quality Assurance Provisions

A. Fabricator Acceptance Tests

A comprehensive quality assurance program will be employed during all phases of the blanket assembly fabrication to insure compliance with design parameters to a high degree of certainty. The program is planned to comply with stringent commercial fuel fabrication standards. The radial blanket fuel pellet characteristics will be measured using applicable sampling plans. The blanket rods, ducts and other hardware will generally have 100% dimensional inspection. Following is a list of typical inspections and the probable reference techniques specified (other techniques equal to or better than the listed techniques may be used):

- a. Blanket Fuel Isotopic Content: Applicable sampling plan; calculated from mass spectrometry for isotopic content and weight per unit length measurement.
- b. Blanket Fuel Pellet Density: Applicable sampling plan; calculated from dimensional and weight measurements and thermogravimetry for oxygen-to-metal ratio.
- c. Blanket Fuel Pellet Dimensions: Applicable sampling plan; thermogravimetry.
- d. Oxygen-to-Metal Ratio: Applicable sampling plan; thermogravimetry.
- e. Blanket Rod Component Placement: 100% radiographic of upper fuel column.
- f. Blanket Rod Dimensions: 100% standard gauging.
- g. Blanket Rod End Cap to Cladding Tube Weld: Lot qualification, metallographic examination, radiography, visual examination, and dimensional examination using go no-go gauge.

- h. Blanket Assembly Duct Tube Material Properties: Applicable lot sampling; chemical analysis for composition, applicable E-Spec for grain size, corrosion resistance, tensile testing, and hardness.
- i. Blanket Assembly Duct Ultrasonic Inspection: 100%; pulse-echo, in accordance with applicable E-Spec.
- j. Blanket Assembly Duct Dimensions: 100%; standard gauging.
- k. Blanket Assembly End Hardware Dimensions: 100%; standard gauging.

B. On-Site Acceptance Tests

To assure that damage during shipping, loading and unloading or from sabotage has not occurred, a standard inspection procedure will be performed on every blanket assembly entering the plant site. This procedure will consist of:

- a. Examination of the shipping container for broken seals, penetrations or any sign of shipment damage and verification that the shipping container shock indicators were not tripped.
- b. A standard visual inspection of the assembly for dents, nicks, and gouges, especially in the area of hexagonal load pad corners, shield block corners, the inlet nozzle, piston ring, and discrimination post; handling socket identification, discrimination post geometry and assembly serial number. Visual inspection of accelerometers on the assembly to confirm that the maximum allowable loads have not been exceeded.
- c. A standard dimensional inspection shall verify that the assembly straightness and overall twist are within the drawing tolerances.

Defects determined during visual examination will be photographed and measured. This inspection would be performed to determine if defects are of such an insignificant nature to be acceptable. A photographic record will be maintained for all accepted defects.

4.2.1.6 Alternatives and Fallback Positions

Design requirements and limits for fuel and blankets are defined in Section 4.2.1.1.2.2. Currently, two alternative limits are utilized

In assessing cladding integrity during normal, upset and emergency events. These are: 1) cumulative damage function (CDF) and 2) cladding strain (calculated as defined in Section 4.2.1.1.2.2). These limits are intended to preclude cladding failure. Preliminary verification of the limits and the techniques utilized in assessing CRBRP fuel and blanket rods against the limits are summarized in Section 4.2.1.1.2.2 for cladding strain, and Section V of Reference 58 for the CDF. Further development and verification of these limits and techniques based on the results of the irradiation experience summarized in Section 4.2.1.4 and the tests summarized in Section 4.2.1.5 is planned consistent with the schedule for submittal of the FSAR. In addition, the CRBRP design includes systems that will enable detection and location of failed fuel (see Section 7.5.5). A preliminary assessment of the performance of failed fuel is given in Section 4.2.1.1.3.8 and further data relative to operation with failed fuel will be available prior to the FSAR from run-beyond-cladding breach testing in EBR-II.

Within the framework of this overall approach, several alternatives and fallback positions are available for implementation if future testing and analytical efforts do not verify the adequacy of the preliminary design limits and techniques. Specifically, fallback positions are available in the following five areas:

1. Design Limits and Techniques
2. Design Features
3. FFTF Testing
4. CRBRP Surveillance
5. CRBRP Operating Limits

Fallbacks for Design Limits and Techniques

If the CDF and strain limits utilized in preliminary design cannot be adequately verified for final design purposes, four alternatives are available as fallbacks. These are:

1. Develop a new analytical technique based on a statistical approach and empirical data. Consistent with the event classification and cladding damage severity limits given in Table 15.1.2-1, a small fraction of fuel rod cladding failures are permitted during emergency events.

2. Reduce the allowable CDF and/or strain limit downward as required to conservatively envelop future test results.
3. Adopt completely either the CDF or the strain limit if the other cannot be verified.
4. Develop a new design criterion based on either an analytical or empirical approach.

These fallbacks will be implemented as required during the evolutionary design process prior to FSAR submittal.

Fallbacks for Design Features

The results of ongoing and planned tests can also be used to adjust features of the design. Figure 4.2-35A illustrates the relationship between the current design and licensing schedules and provides several examples of design features that could be adjusted as a result of ongoing tests. Such changes will be considered during the evolutionary design process that extends to a release to initiate fabrication of the CRBRP first core fuel.

Testing and Operational Fallbacks

The final three areas in which fallback positions are available involve FFTF testing and CRBRP operation and surveillance. Driver core assemblies, surveillance assemblies, and test assemblies in FFTF will provide significant experience and data on the performance of reference LMFBR fuel. Although these data will not be available until after fabrication of CRBRP first core fuel has begun, they will be available for FSAR submittal and review. The data can be used to confirm previous results, resolve any remaining issues and reduce uncertainties and design allowances.

53 | Data derived from surveillance of CRBRP operations and core assemblies can also be utilized as a fallback if the design limits and techniques cannot be completely verified prior to CRBRP operation (see Section 4.2.1.1.4). Such data can be used for final verification of overall performance; verification of the effects on performance, of differences between actual operating conditions and those used in design evaluations and development tests, and reduction of uncertainties and allowances.

51 | As a final fallback, the CRBRP operating limits can be adjusted. Reactor power, allowable fuel burnup, and operating temperature (either as a function of power or through the use of values measured during operation) can be adjusted consistent with the extent to which the design limits are verified.

Numerous combinations exist for the implementation of these final three fallback positions. In addition, the extent to which they are needed for verification purposes cannot be accurately assessed until final design and the ongoing and planned testing is completed. Plans to utilize these fallbacks for verification or to increase the ultimate operational limits for the reactor will be prepared on a schedule consistent with that for preparation of the FSAR.

4.2.2 Reactor Vessel Internals

4.2.2.1 Design Bases

4.2.2.1.1 Functional Requirements

Two major assemblies form the reactor internals support structure. These are the multiple component lower internals structure (LIS) and the multiple component upper internals structure (UIS). An additional major system is the core restraint system (CRS), which consists of the core formers and the removable radial shielding.

The lower Internals structure consists of the core support structure, lower Inlet modules, bypass flow modules, fixed radial shielding, fuel transfer and storage assembly, and horizontal baffle. Support for the core formers of the core restraint system is provided by the lower Internals structure.

The following are primary functional requirements for these components. Also included are the maintainability and surveillance requirements.

4.2.2.1.1.1 Core Support Structure

The core support structure consists of the core plate, the core barrel, and the module liners. The core plate and support cone form the upper surface of the Inlet plenum, provide the structure for the upper surface of the inlet plenum and provide the structure for the support of the core. The core barrel encloses the core and provides a base for the core former rings. The core support structure is welded to the support cone which is an integral part of the reactor vessel. The Core Support Structure to Core Support Cone and Core Support Cone to Reactor Vessel Welds are both in an area where the temperature is below 800°F and therefore the high temperature ASME Code Criteria is not applicable. The welds made to the Core Support Cone were analyzed utilizing the ASME Code Criteria and Material Allowables. As a permanent structure, it must be designed for the "stretch" conditions* and have a design life of 30 years. The core support structure has the following principal functional requirements:

- a) Provide support for the weight of the core assemblies, lower inlet modules, bypass flow modules, fuel transfer and storage assembly, horizontal baffle, fixed radial shielding, removable radial shielding, spacers and core formers.

*See Section 1.1

- b) Transmit reaction loads due to pressure differences, weights and seismic disturbances to the interface with the reactor vessel.
- c) Withstand all specified loading conditions without exceeding the design primary and secondary stress limits for the appropriate loading categories as specified in Section III of the 1974 Edition of the ASME Boiler and Pressure Vessel Code.
- 58| d) Provide the foundation for vertical and horizontal restraint of the core and removable radial shield assemblies.
- e) Control (limit) axial deflections of the core relative to the control rods, which are supported by the reactor closure head.
- 58| f) Provide a stable base for the core former structure.
- 58| g) Provide, together with features of the upper internal structure and the core former structure, adequate alignment between the upper and lower internals.
- 58| h) Provide features to preclude major flow blockage at the module liner inlet.
- 58| i) Distribute coolant to the lower inlet modules and bypass flow modules which distribute the coolant to the reactor assemblies.
- j) Distribute coolant to the fuel transfer and storage assembly, and to provide the coolant for the reactor vessel/liner annulus.
- k) Provide features to minimize gas entrapment during sodium fill.
- 58| l) Provide interface features with the horizontal baffle for the degree of sealing required to limit the metal temperature of the core barrel below the horizontal baffle.
- 58| m) Limit the maximum deflection of the CSS to 0.150 inch upward, under the maximum design ΔP .

4.2.2.1.1.2 Lower Inlet Modules (LIM)

58| The lower inlet modules are removable components of the lower internals structure (see Figure 4.2-40). They are designed to fit into and seal with the core support structure module liners with strainer holes in the modules aligning with coolant slots in the liners. Each module directs the coolant flow to seven reactor assemblies which could consist of fuel, control, blanket, and removable radial shielding assemblies and combinations thereof depending on core location. There are a total of 61
51| modules, the outer 24 of which will be designed to divert flow by bypass

orifices to provide coolant flow to the bypass flow module/removable radial shielding and the core barrel/reactor vessel annulus. Although the modules are 30 year life components, they will be designed to be removable. The inlet modules have the following principal functional requirements:

- a) Support, vertically position and restrain downward, position and restrain horizontally the reactor assemblies during assembly, operation and refueling of the reactor using hydraulic balance features where required.
- b) Distribute and provide coolant to the various reactor assemblies (fuel assemblies, blanket assemblies, control rod assemblies, and removable radial shielding).
- c) Provide a source of low pressure bypass coolant to the bypass flow module/removable radial shield assemblies and the core barrel/reactor vessel annulus.
- d) Provide features to assure correct placement of the reactor assemblies in a safe location.
- e) Maintain a pressure boundary between the high pressure region and low pressure region within the reactor vessel and limit the leakage flow across the boundary.
- f) Provide a low impedance flow path through the LIM for the Secondary Control Rod System bypass flow.
- g) Provide retention of loose debris greater than 0.25 in. in diameter to preclude blockage of the reactor assembly rod bundles.
- h) Provide for the retention of the modules during normal reactor operation using hydraulic balance features where required.
- i) Assure that the LIM can be removed through the Upper Internals Structure and the IVTM port.
- j) Maintain nominal primary coolant flow and preclude any adverse change of flow paths.
- k) Provide a capability to use multiple coolant flow sources in the core support structure module liner.

4.2.2.1.1.3 Bypass Flow Modules

The Bypass Flow Modules (BPFM) shown in Figure 4.2-41A, are supported by the Core Support Structure (CSS). The BPFM supports and positions the Fixed Radial Shield (FRS) and Removable Radial Shield (RRS)

assemblies. The BPFM is designed as a permanent component. The BPFM receives low pressure coolant from the inlet modules and distributes the coolant to the RRS assemblies. A total of 6 BPFM provides a flow to a total of 264 RRS and each is designed to meet the following functional requirements.

- a) Support and position a total of 44 removable radial shield assemblies per module during reactor assembly, operation, and refueling.
- b) Distribute and provide coolant to each of the radial shield assemblies supported.
- 58 | c) Provide features to insure placement of only removable radial shield assemblies into any of the receptacles in the bypass flow modules.
- d) Provide a redundant flow path for the coolant which feeds the RRS assemblies.
- 58 | e) Support and position the Fixed Radial Shield (FRS).
- f) Provide a thirty year life (22.5 full power years) with no planned maintenance.

4.2.2.1.1.4 Fixed Radial Shielding

The fixed radial shielding is located inside the core barrel beyond the radius of the removable radial shielding and rests on the bypass flow module and beneath the lower core former. The fixed radial shielding is designed for the 30 year plant life. The functional requirements for this component are:

- 58 | a) Provide in conjunction with the removable radial shielding assemblies, radiation protection for the core barrel and reactor vessel. This shielding will contribute to the overall reactor shielding system. The minimum ductility provided by the combination of the fixed and removable radial shielding is 10% residual ductility for the core barrel and reactor vessel. This value is based on the total elongation at end of design life and includes effects due to stretch conditions.
- b) Operate for a thirty year life at seventy-five percent plant capacity factor. The minimum ductility limit (based on total elongation) for the fixed radial shielding is 10%.

4.2.2.1.1.5 Fuel Transfer and Storage Assembly

Reactor refueling requires bringing new fuel into the reactor vessel and removing the spent fuel. The fuel is brought in and out through the vessel head by the ex-vessel transfer machine. A transfer position is required so that the ex-vessel machine can decouple and move out of the way so that the in-vessel transfer machine can grapple the assembly and continue the fuel handling operation.

Operational flexibility in scheduling fuel replacement requires the capability for interim storage of two irradiated fuel assemblies.

Accumulation of material property trend data requires a position for exposing the surveillance specimens to the appropriate environmental conditions.

The above needs are met by the fuel transfer and storage assembly which has the following principal functional requirements:

- a) Provide features which allow cooling of the stored fuel assemblies.
- b) Provide interface features that minimize leakage with the horizontal baffle.
- c) Provide support for the weight of the core component pot, stored core components and surveillance specimens and fixtures.

4.2.2.1.1.6 Horizontal Baffle

The horizontal baffle forms the upper boundary of the core barrel/reactor vessel annulus and physically separates the hot sodium in the outlet plenum from the cooler bypass flow sodium in the core barrel/reactor vessel annulus. The horizontal baffle has the following functional requirements:

- a) Limit heat flow from the outlet plenum sodium to the core barrel/reactor vessel annulus sodium to an acceptable level.
- b) Form an effective hydraulic barrier between the core barrel/reactor vessel annulus sodium and the outlet plenum sodium.
- c) Insure that temperature oscillations on metal surfaces in or adjacent to the coolant flow paths are compatible with the horizontal baffle service life requirements.
- d) Deleted
- e) Position and support the upper end of the fuel transfer and storage assembly.
- f) Provide a guide for entry of the core component pot and passage of sodium from the outlet plenum into the fuel transfer and storage assembly.
- g) Provide a thirty year service life (22.5 full power years) with no scheduled maintenance.
- h) Transmit the IVTM and EVTm transient mechanical loads from the fuel transfer and storage assembly to the core support structure and reactor vessel thermal liner.
- i) Provide access through the horizontal baffle base plate into the core barrel/reactor vessel annulus.

4.2.2.1.1.7 Upper Internals Structure (UIS)

The upper internals structure* is located in the reactor outlet plenum immediately above the core. This is an area characterized by a demanding thermal fluids environment. The structure must be designed to perform satisfactorily in this environment for the design life of 30 years while meeting the following functional requirements:

- a) Provide secondary core holddown for the fuel, blanket, and control assemblies.
- b) Provide support for routing reactor system instrumentation including that to selected fuel and blanket assemblies.
- c) Assure alignment of the control rod shroud tubes in the upper internals structure with the control rod ducts in the core.
- d) Provide means for ducting the core effluent to the upper regions of the outlet plenum so as to effectively mitigate stratification during the scram transient, and to promote mixing during normal operational sequences.
- e) Protect the control rod drivelines from potential flow induced vibration excitation from cross flow in the outlet plenum.
- f) Provide for mounting of the control rod scram arrest dashpots, and for reaction of the associated scram arrest loading.
- g) Provide access to the core to allow the withdrawal of a core support structure inlet module.
- h) Provide upper internals structure jacking mechanism (UISJM) mounted on the Intermediate Rotating Plug (IRP), which will engage with the upper internals support columns and lift the upper internals structure to permit rotation for refueling.
- i) Provide shielding approximating that of the uninterrupted head for the penetrations of the upper internals structure support columns through the intermediate rotating plug.

58

* For the sake of continuity and completeness, the UIS jacking mechanism is included herein with the UIS.

51

- j) Provide the penetration of the IRP by the upper Internals structure columns with seals and above the head shielding, so as to limit the irradiation dose to the head access area to be compatible with a total head dose rate of 25 mREM/hr.
- k) Provide a source of material for surveillance of the upper Internals structure.
- l) Provide for the routing and support of the diagnostic instrumentation required for initial confirmation of the satisfactory performance of both the upper Internals structure and the outlet plenum flow control features.
- m) Key the upper Internals structure to the core barrel such that the lateral movement is limited.

4.2.2.1.1.8 Core Restraint System

The core radial restraint system is comprised of formers mounted on rings in the core barrel, and all the core assemblies supported within those formers. Design of the system is based on the limited free bow concept. Since it is not economically feasible to replace the core restraint system formers during the life of the plant, these components shall be designed for a 30 year life. Principal functional requirements to the core restraint system are as follows:

- a) Provide means for the control of core motion so that it is both predictable and safe.
- b) The reactivity feedback attributable to the core restraint system shall be such that Criteria 9 and 10 are satisfied for reactor power range operations.
- c) Limit the potential magnitude of core compaction (and the resulting reactivity insertion) due to postulated stickslip motion to less than allowable values which assure that the fuel and cladding will not be damaged. The allowable step reactivity insertion magnitude is 60¢ at full power, and 85¢ at hot standby (5% power).
- d) Provision shall be made for release of core restraint inter-assembly loads, such that refueling insertion and withdrawal loads will not exceed 1000 lbs., including the buoyant weight of the assembly being handled.
- e) With the core in the refueling configuration, all core components handling sockets must be positioned within plus or minus 0.58 inches of true position.

- f) The core restraint system shall position the upper end of the control assembly ducts to within plus or minus 0.53 inches of true position.
- g) Positioning control of the fuel assembly duct nozzles shall be such as to minimize lateral hydrodynamic forces imposed on the upper internals structure instrumentation posts.
- h) The core restraint system shall be designed to prevent a general condition of duct-to-duct contact in the active core region.
- i) The design life for the core formers is 30 years for the 75% plant capacity factor.
- j) Design of the core restraint system shall be consistent with annual refueling.
- k) The dynamic radial deflection of the inner profile of the Upper Core Former (UCF) shall be less than ± 0.100 inch, relative to the UCF centerline during an SSE or OBE event.
- l) The Lower Core Former (LCF) radial deflection relative to the LCF centerline during an SSE or OBE shall be limited to less than ± 0.100 inch.
- m) Provide vertical load reaction to the core barrel.

4.2.2.1.1.9 Removable Radial Shield (RRS)

The removable radial shield assemblies are core assemblies (see Figure 4.2-43) which mechanically interface with the radial blanket assemblies, the core former structure, the lower inlet modules, the bypass flow modules, and the upper Internals. These assemblies have the following functional requirements:

- a) Provide radiation shielding to ensure the structural integrity of the reactor permanent components beyond the radius of the RRS for 30 years.
- b) Provide a compact structural unit that can be handled in and out of the reactor by the normal fuel handling equipment.
- c) Transmit lateral core restraint loads without contributing significantly to the magnitude of these loads.
- d) Provide flow paths for cooling of the RRS to preserve structural integrity.
- e) Provide a means for locating surveillance specimens in the RRS and a method for their expedient recovery.

The bases for these requirements are described in 4.2.2.1.2.9.

4.2.2.1.1.10 Core Former Structure (CFS)

The Core Former Structure provides the restraint to limit the bowing of the core assemblies for the Core Restraint System. The CFS consists of the Upper Core Former, the Support Ring, the Lower Core Former, keyway inserts and azimuthal spacers. The CFS has the following functional requirements:

- a) Provide peripheral constraint for the reactor core assemblies.
- b) Provide lateral location and restraint for the lower end of the Upper Internals Structure.
- c) Transmit the applied loads from the reactor core assemblies and the Upper Internals Structure to the Core Barrel including upward vertical loads.
- d) Provide a structural attachment for the Fixed Radial Shield.
- e) Provide a temporary vertical support for the Upper Internals Structure.

58| 4.2.2.1.1.11 Maintainability

The structures must be designed to facilitate sodium drainage.

Any structure or assembly which may ultimately require removal from the reactor vessel for maintenance or inspection must be removable through the head openings and must be provided with lifting lugs or fixtures for use during these operations.

58| 4.2.2.1.1.12 Surveillance

Irradiation damage data for specific locations is required such that changes in material properties can be monitored. Material surveillance coupons will be located such that accelerated irradiation data is available at the time of normal coupon inspection for a particular component/location of interest. This will enable a potential deteriorating condition to be detected before the next scheduled coupon inspection.

58| 4.2.2.1.1.13 Margin Beyond The Design Base Considerations

In addition to the functional requirements discussed previously, the core support structure and horizontal baffle shall be designed to satisfy the margin beyond design basis considerations of CRBRP-3 (Reference 10 of Section 1.6). Structural Margin Beyond Design Base (SMBDB) is not a design loading condition. However, it represents additional requirements to provide margin for highly improbable loading conditions. These loads are postulated to arise from a core related event during normal full power operation, independent of any other event.

4.2.2.1.2 Bases for Functional Requirements

Bases for the requirements of Section 4.2.2.1.1 are given below:

4.2.2.1.2.1 Core Support Structure

- a) Requirement - Provide support for the weight of the core assemblies inlet modules, bypass flow modules, fuel transfer and storage assembly, horizontal baffle, fixed radial shielding, removable radial shielding, spacers and core formers.

Bases - Self evident.

- b) Requirement - Transmit reaction loads due to pressure differences, weights and seismic disturbances to the interface with the reactor vessel.

Bases - Self evident.

- 58| c) Requirement - Withstand all specified loading conditions without exceeding the design primary and secondary stress limits for the appropriate loading categories as specified in Section III of the 1974 edition of the ASME Boiler and Pressure Vessel Code.

Bases - The various load combinations produce deflections of the CSS core plate and core barrel. The resulting deflections can be evaluated for their suitability so long as the structure returns to its zero position when the loads are removed. However, if yielding occurs the zero position and thus maximum deflection positions would be indeterminate and thus the predicted reactivity changes and relative clearances would be indeterminate. Thus, the CSS must be designed such that the primary stresses throughout the structure are below the material yield.

- 58| d) Requirement - Provide the foundation for vertical and horizontal restraint of the core and removable radial shield assemblies.

Bases - Internally or externally induced loads on the core (fuel, control and blanket assemblies) and removable shield assemblies would result in motions of these components which could have adverse reactivity effects unless the motion is limited by a stable base in both the vertical and horizontal positions. The CSS core plate and core barrel must be designed to limit these motions such that the resulting clearances of the control rod and control rod drive remain sufficient to provide reliable scram capability.

- 58| e) Requirement - Control (limit) axial deflections of the core relative to the control rods, which are supported by the reactor closure head.

Bases - Vertical pressure and/or mechanical loading causes the CSS to deflect vertically relative to the reactor vessel head. The fuel assemblies, which are supported by the CSS, move vertically with the CSS. The control rods however are supported from the reactor vessel head and thus do not move with the CSS. Deflections of the CSS produces differential axial motion of the core relative to the control rods, thereby producing a reactivity change in the core. The CSS must be designed to limit axial motion such that the resulting reactivity change does not result in exceeding the fuel damage limits for an upset event.

- f) Requirement - Provide a stable base for the core former rings.

Bases - The core former rings are positioned by the core barrel. The location and rigidity is critical as it limits the radial motion of the core. All transverse loads from the core are transmitted through the core former rings to the core barrel.

- 58| g) Requirement - Provide together with features of the upper internals structure and the core former structure, adequate alignment between the upper and lower internals.

Bases - Operation of the control rod driveline system is dependent on the alignment of the control rod guide tubes in the upper internal structure and the control assemblies located in the core support structure by the core plate and the core restraint system.

Monitoring of the outlet flow temperature from core assemblies is done by instrumentation located in the flow ducts of the upper internals structure. Accuracy of measurement is dependent on the alignment of these flow ducts with their respective core assembly outlet nozzles.

- h) Requirement - Provide features to preclude major flow blockage at the module liner inlet.

Bases - Blockage of coolant to the inlet module can create a hazardous condition by starving any one or more of the core assemblies within the module. This could occur regardless of the precautions taken during assembly and construction. Thus the CSS should have design features capable of capturing and retaining loose debris, upstream of the module inlet.

- 58| i) Requirement - Distribute coolant to the lower inlet modules and bypass flow modules which distribute the coolant to the reactor assemblies.

Bases - Adequate coolant is required to all reactor assemblies so that requirements on upper temperature limits on the various materials are not exceeded.

A relatively uniform flow is required at the inlet to fuel and blanket core zones.

- 58| 51| j) Requirement - Distribute coolant to the fuel transfer and storage assembly, and provide the coolant for the reactor vessel/liner annulus.

Bases - Remove decay heat generated by the storage of irradiated reactor assemblies, and provide coolant for the annulus between the reactor vessel and vessel thermal liner to limit the maximum temperature of the reactor vessel wall to an acceptable value.

- k) Requirement - Provide features to minimize gas entrapment during sodium refill.

Bases - If allowed to accumulate in the inlet plenum, trapped gas could be carried into the coolant stream and cause temporary coolant starvation to reactor assemblies. This would possibly overheat fuel cladding material beyond its upper temperature limit.

- l) Requirement - Provide interface features with the horizontal baffle for the degree of sealing required to limit the metal temperature of the core barrel below the horizontal baffle.

Bases - It is required that the core barrel temperature be at, or close to, the temperature of the adjacent core former rings to maintain the lateral location of the reactor assemblies. To meet this requirement, only inlet/bypass coolant can be in direct contact with the outside profile of the core barrel.

- m) Requirement - Limit the maximum deflection of the CSS to 0.150 inch upward under the maximum ΔP .

Bases - The maximum step reactivity insertion due to a downward deflection of 0.150 inches of the CCS plate is worth 17¢. For a 17¢ step reactivity insertion at full power, the hot channel maximum cladding temperature increase is less than 20°F.

4.2.2.1.2.2 Lower Inlet Modules

- a) Requirement - Support, vertically position and restrain downward, and position and restrain horizontally the reactor assemblies during assembly, operation, and refueling of the reactor using hydraulic balance features where required.

Bases - The pressure difference between the inlet and outlet plena is sufficient to raise some reactor assemblies from their required location. The function of the hydraulic balance system is to equalize (balance) the pressure forces on the fuel and blanket assemblies so that there is little or no lifting force. This design approach eliminates the need of a mechanical restraint to assure positive downward load and facilitates the removal and installation of reactor assemblies.

In the LIM design the criterion to be used is that the minimum net axial restraining force shall be downward and approximately equal to the buoyant weight of the lightest reactor assembly, which is the fuel assembly (387 lb. in Na.).

It is intended to use hydraulic balance when the combination of dead weight buoyancy and hydraulic loads produce a force which does not meet the above criterion. To facilitate design and fabrication, hydraulic balance will not be utilized for restraint of the radial blanket and removable radial shield assemblies where the criterion is met.

Control of reactor criticality requires accurate vertical and horizontal positioning of the reactor assemblies during assembly, operating and refueling.

- b) Requirement - Distribute and provide coolant to the various reactor assemblies (fuel assemblies, blanket assemblies, control rod assemblies and removable radial shielding).

Bases - The core location of each LIM dictates its coolant flow requirements. The modules provide flow control to radial blanket and removable radial shield assemblies by orificing. Coolant flow is delivered to the fuel, blanket, control and removable radial shield assemblies through various passages within the LIM.

- c) Requirement - Provide a source of low pressure bypass coolant to the bypass flow module removable radial shielding assemblies and the core barrel/reactor vessel annulus.

Bases - Components encompassing the core must be cooled to limit their temperatures to acceptable values. The coolant passages from the inlet plenum to these components is via the CSS and peripheral modules.

- d) Requirement - Provide features to assure correct placement of the reactor assemblies in a safe location.

Bases - The various reactor assemblies are required to be in discrete locations within the core to meet nuclear requirements and assure adequate cooling. Thus the LIMs will incorporate pin alignment devices to assure proper azimuthal orientation of the modules. Various discriminators will be assembled into each reactor assembly receptacle to ensure that only those assemblies can be interchanged which will not result in an undercooled assembly. The discriminators will have "no go" devices such that they will limit axial travel and prevent "seating" of an assembly when in an improper core location.

- e) Requirement - Maintain a pressure boundary between the high pressure region and low pressure region within the reactor vessel and limit the leakage flow across the boundary.

Bases - Flow leakage must be limited to ensure adequate flow of coolant to the fuel assemblies. The LIM is a 30 year component designed to be removable and yet it must maintain a pressure boundary between the high and low pressure regions. Therefore, where differential movement is expected between mating parts due to either thermal expansion or mechanical loads, dynamic sealing devices must be incorporated. Thus, the module will be designed to insure sealing utilizing piston rings and/or other sealing devices within the state of the art that can be used in the reactor environment.

- f) Requirement - Provide a low impedance flow path through the LIM for the Secondary Control Rod System bypass flow.

Bases - The secondary control rod system (SCRS) provides a back-up shutdown capability and utilizes a hydraulic assist for insertion of the control rod. Approximately 73 percent of the coolant flow is redirected downward to the module providing a large pressure drop across a piston attached to the control assembly. This pressure drop across the piston provides the insertion force required to assist insertion of the secondary control rods during a SCRAM. Therefore, the LIMs containing SCRSs will incorporate flow conduits designed to minimize flow losses through the module to the low pressure region in the CSS.

- g) Requirement - Provide retention of loose debris greater than 0.25 in. in diameter, to preclude blockage of the reactor assembly rod bundles.

Bases - Blockage of coolant flow in fuel assemblies can create a hazardous condition. Should loose debris be present during reactor operation despite the precautions taken during reactor construction and sodium fill, the LIM will trap loose debris greater than 0.25 in. diameter and prevent a flow blockage by means of strainer holes incorporated into the module stem.

- h) Requirement - Provide for the retention of the modules during normal reactor operation using hydraulic balance features where required.

Bases - It is desirable that no mechanical devices be used for retaining the LIM in the core support structure. Such devices

are difficult to engage or disengage with remote handling equipment and would impair the module removal capability. The use of a hydraulic balance module retention feature satisfied this requirement.

- i) Requirement - Assure that the LIM can be removed through the Upper Internals Structure and the IVTM port.

Bases - The LIM configuration, dependent on core location, may not be symmetrical about the longitudinal centerline. The c.g. eccentricity from this centerline will cause tilting of the module upon removal and installation. Handling tools and module design will be such that the module will be constrained within a dimensional envelope capable of passing through the most restrictive passage and components such as the IVTM port. This requirement is necessary in order to insure that the module can be removed from the reactor without the requirement for major disassembly of the reactor internals.

- j) Requirement - Maintain nominal primary coolant flow and preclude any adverse change of flow paths.

Bases - The LIM receptacle flow slot geometry, which interfaces with reactor assembly inlet nozzle slots, is designed so that flow is provided to the reactor assemblies in the event of inadvertent rise of the assemblies due to loss of hydraulic balance. Also, the strainer hole pattern in the LIM stem is designed to provide adequate flow through the LIM in the event of inadvertent rise of the LIM due to loss of its hydraulic balance.

- k) Requirement - Provide a capability to use multiple coolant flow sources in the core support structure module liner.

Bases - The LIM stem is provided with strainer hole pattern to interface with both the primary and secondary flow parts in the core support structure module liners.

4.2.2.1.2.3 Bypass Flow Module

- a) Requirement - Support and position a total of 44 removable radial shield assemblies per module during reactor assembly, operation, and refueling.

Bases - The shield assemblies as part of the core restraint system require vertical and horizontal positioning within certain tolerances to assure proper alignment of the core and conse-

quently control reactor criticality. In addition, the position of the removable radial shield assemblies must be such as not to interfere with insertion and removal of adjacent inner assemblies (radial blanket assemblies) during initial core loading and subsequent refueling conditions.

- b) Requirement - Distribute and provide coolant to each of the radial shield assemblies supported.

Bases - Bypass flow provided by the lower inlet modules to each of the bypass flow modules is distributed uniformly to the removable radial shield assemblies through the use of a low pressure plenum.

58

51

- 58 | c) Requirement - Provide features to insure placement of only removable shield assemblies into any of the receptacles in the bypass flow modules.

Bases - The fuel assemblies, radial blanket assemblies, and control assemblies must be prevented from being placed in a shield assembly location to assure safe operation. Thus a discrimination feature system will be provided within the bypass flow module receptacles to preclude the placement of any of the above core assemblies into a shield assembly location.

- d) Requirement - Provide a redundant flow path for the coolant which feeds the RRS assemblies.

Base - The RRS assemblies must have an adequate coolant flow to prevent excessive temperatures which could contribute to increased assembly bowing, creating problems with refueling. In the unlikely event of flow blockage into one BPFM, the redundant flow passages will allow sufficient coolant flow to that BPFM to keep the RRS assemblies within acceptable temperature ranges.

58 |

- e) Requirement - Support and position the Fixed Radial Shield (FRS).

Base - The FRS requires support and positioning in the vertical and horizontal direction within certain tolerances at the base of the FRS. The BPFM is that component which satisfies these requirements.

- f) Requirement - Provide a thirty year life (22.5 full years) with no planned maintenance.

Base - The design of the FRS is such that it will not be removed during the life of the reactor. Subsequently, the BPFM has to be designed such that it requires no maintenance for the life of the reactor.

38 |

4.2.2.1.2.4 Fixed Radial Shielding

- 58| a) Requirement - Provide in conjunction with the removable
radial shielding, radiation protection for
the core barrel and reactor vessel. This shielding will con-
tribute to the overall reactor shielding system. The minimum
58| ductility assured by the combination of the fixed and removable
radial shielding is 10% residual ductility for the core barrel
and reactor vessel. This value is based on total elongation at
end of design life and includes effects due to stretch
conditions.

36| Bases - The combination of removable and fixed radial shielding
must assure that the core barrel and reactor vessel remain
within ductile limits stated above. Should the ductility of the
material drop below the 10% level the ability of the material
to yield locally would be reduced. The lack of residual
ductility would add uncertainty to the integrity of the structure.

The ductility of the structural regions of the core barrel and
reactor vessel must be maintained at a level which will insure
that ductile failure mode analysis used in analyzing the
design remains valid.

- 58 |
- b) Requirement - Operate for a thirty year life at seventy-five percent plant capacity factor which also includes effects due to stretch conditions. The minimum ductility limit (based on total elongation) for the fixed radial shielding is 10%.

58 |

58 |

Bases - The combination of removable and fixed radial shielding must be designed such that the fixed radial shielding remains ductile within the limit stated above. The ability of the material to yield locally would be reduced if the ductility of the material dropped below the stated limit. This situation would produce uncertainties concerning the integrity of the structure.

The ductility of the structural regions of the fixed radial shielding must be maintained at a level which will insure that the ductile failure mode analysis used in analyzing the design remains valid.

4.2.2.1.2.5 Fuel Transfer and Storage Assembly

- a) Requirement - Provide features which allow cooling of the stored fuel assemblies.

58 |

Bases - The removed fuel assembly cannot be allowed to increase in temperature such that the gas pressure would build up and result in cladding failure. Additionally, a removed fuel assembly inherently contains useful information which could be compromised or destroyed if the fuel temperature subsequent to removal is permitted to exceed significantly the peak operating temperature. Thermal analysis has indicated that cooling of the transfer and storage assembly is required to remove the heat generated in a spent fuel assembly. Note that during normal refueling operations, no core assembly may be stored in the FT&SA while another assembly is being inserted or withdrawn from an in-core location.

- b) Requirement - Provide interface features that minimize leakage with the horizontal baffle.

51 |

Bases - The outlet plenum is filled with the hot core effluent, while the plenum underneath the horizontal baffle is filled with the cooler core inlet sodium. The upper portion of the fuel transfer and storage assembly is a part of the horizontal baffle and provides the guidance for insertion of the core component pot and the stored fuel into the fuel transfer and storage assembly. If significant leakage flow were permitted in between

the fuel transfer and storage assembly and the horizontal baffle it could lead to possible insufficient material fatigue strengths to withstand the potential hot and cold flow oscillation sweeping the interface surfaces between the horizontal baffle and the fuel transfer and storage assembly.

- c) Requirement - Provide support for the weight of the core component pot, stored core components and surveillance specimens and fixtures.

Bases - Self evident

58

4.2.2.1.2.6 Horizontal Baffle

- a) Requirement - Limit heat flow from the outlet plenum sodium to the core barrel/reactor vessel annulus sodium to an acceptable level.

Bases - Bypass flow in the core barrel/reactor vessel annulus cools components within and on the periphery of the annulus as well as the vessel and vessel liner. Therefore, heat flow across the baffle must be within limits which will provide acceptable bypass cooling flow temperature to components which utilize bypass flow for cooling.

- b) Requirement - Form an effective hydraulic barrier between the core barrel/reactor vessel annulus sodium and the outlet plenum sodium.

Bases - Random mixing of hot sodium flowing through and exiting through the fuel region and sodium rising in the annulus between the core barrel and the reactor vessel creates unstable flow conditions characterized by thermal plumes and/or widespread turbulence. In addition, bypass flow must be directed to provide coolant to the reactor vessel and liner above the baffle.

- c) Requirement - Insure that temperature oscillations on metal surfaces in or adjacent to the coolant flow paths are compatible with the horizontal baffle service life requirements.

Bases - Thermal stratification exists in the flow exiting the core. The flow through the radial blanket will be cooler than that in the main core region. The radial blanket flow will tend to be split off at elevation just above the core barrel (base of the UIS). This cooler flow will mix with that circulating in the outlet plenum, and thermal striping can result.

51

d) Deleted

49

e) Requirement - Position and support the upper end of the fuel transfer and storage assembly.

Bases - The upper end of the FT&SA must be located accurately both circumferentially and radially on a designated arc concentric with the reactor core vertical centerline.

f) Requirement - Provide a guide for entry of the core component pot and passage of sodium from the outlet plenum into the fuel transfer and storage assembly.

Bases - Guidance for the entry of the core component pot into the fuel transfer and storage assembly must be provided to permit in-core fuel transfer apparatus to correct for low order misalignment during fuel transfer and storage operations.

58

g) Requirement - Provide a thirty year service life (22.5 full power years) with no scheduled maintenance.

Bases - The horizontal baffle must operate in the reactor environment for this period of time without failure as this component cannot be replaced or fully inspected.

h) Requirement - Transmit the IVTM and EVTM transient mechanical loads from the FT&SA to the core support structure and reactor vessel thermal liner.

Bases - The In-Vessel Transfer Machine (IVTM) will transport a reactor assembly to the fuel transfer and storage assembly area, align the reactor assembly with a core component pot (CCP) and insert the assembly into the CCP. The grapple device holding the reactor assembly will contact the upper surface of the FT&SA inlet port nozzle on the horizontal baffle and overtravel vertically downward to actuate a release mechanism in the IVTM grapple. The Ex-Vessel Transfer Machine (EVTM) could misalign slightly and a core component pot hit the FT&SA inlet port nozzle.

41

58

Amend. 58
Nov. 1980

- i) Requirement - Provide access through the horizontal baffle base plate for access to the core barrel/reactor vessel annulus.

Bases - Access to the core barrel/reactor vessel annulus is required for in-service inspection.

4.2.2.1.2.7 Upper Internals Structure

- a) Requirement - Provide secondary core holddown for the fuel, blanket, and control assemblies.

Bases - It is possible to postulate mechanisms which would result in the core moving upwards within the core barrel. Among the mechanisms of concern is gradual undetected loss of hydraulic holddown (although no cause for such an event has been identified). Were this vertical motion to occur then it is possible to postulate sudden downward motion of the core in response to a seismic event. The amount of downward motion acceptable is governed by the resulting reactivity insertion and the associated effect on fuel damage. The upper internals holddown is required to limit the maximum possible upward motion of the core such that the sudden downward motion of the same magnitude will not result in the core damage limits being exceeded.

- b) Requirement - Provide support for routing reactor system instrumentation including that to selected fuel and blanket assemblies.

Bases - Above core thermocouples are required for monitoring and verification of acceptable core performance. Practical considerations of thermocouple replacement requires the use of dry-well housing tubes. Provision is being made to position a thermocouple over selected fuel and blanket assemblies to provide both surveillance/diagnostic information and reactor control.

- c) Requirement - Assure alignment of the control rod guide tubes in the upper internals structure with the control rod ducts in the core.

Bases - The control rod driveline passes through the upper internals structure and into the core. Lateral displacement of the upper internals structure relative to the core could cause structural loading between the driveline and the interfacing components. The frictional component of these loads retards rod insertion. Therefore, this effect must be controlled. In part, this control is achieved by limiting the lateral displacement of the upper internals structure relative to the core. The allowable

alignment error between the upper internals structure and the core is determined from the total reactor system alignment analyses, in which control rod driveline interactions from all sources are included. The maximum misalignments permitted in the reactor are shown in Figures 4.2-95A & B.

- d) Requirement - Provide means for ducting the core effluent to the upper regions of the outlet plenum so as to effectively mitigate stratification during the scram transient, and to promote mixing during normal operational sequences.

Bases - Sodium exiting from the core following the scram is cooler, and therefore denser than the sodium already in the outlet plenum. Because of this density difference, it is possible to postulate a condition in which the cool sodium settles to the bottom of the outlet plenum, forming a stratified condition.

At the instant of scram, kinetic energy is stored in the torodial sodium flow in the outlet plenum, and analysis indicates that this kinetic energy will act to promote mixing of the cool sodium exiting from the core with the hot sodium already in the outlet plenum via a flywheel effect. The degree to which this kinetic energy effect will be effective in preventing flow stratification is at present, unknown. To provide the required assurance against outlet plenum flow stratification, the upper internals structure is being designed to promote mixing. The effective control of stratification is essential to control the ramp rate of the transients experienced by the hot leg equipment. This control is required to minimize the component cumulative damage usage factors.

Since some uncertainty exists as to the behavior of the sodium in the reactor outlet plenum following a scram transient, flow stratification tests are planned to provide data which will be used to verify the effective operation of the upper internals structure mixing features.

Mixing of sodium streams at different temperatures could produce cyclic straining in structural members. Stainless steel components must be protected from this condition (thermal striping) to minimize accumulation of fatigue damage.

- e) Requirement - Protect the control rod drivelines from potential flow induced vibration excitation from cross flow in the outlet plenum.

Bases - Sodium exiting from the core flows vertically upwards to a plane beneath the suppressor plate where it turns and flows radially outwards. Cross flow in this area can cause flow induced vibration and unacceptable associated fretting damage in an unprotected control rod driveline. Fretting damage of this type could impair control rod system performance, and therefore must not be allowed to occur. The upper internals structure is required to isolate the control rod driveline from potential flow induced vibration excitation by providing shroud tubes which surround the driveline and isolate it from sodium cross flow.

- f) Requirement - Provide for mounting of the primary control rod scram arrest dashpots, and for reaction of the associated scram arrest loading.

Bases - Retardation of the downward velocity of the control rods following the scram is achieved by the use of sodium filled dashpots. These dashpots must be positioned in the sodium pool where they will always be primed, and in a region sufficiently remote from the core that they will not be significantly affected by irradiation induced ductility loss. These twin constraints placed the dashpots in the region of the upper internals structure. The structure must provide for positioning and retention of the dashpots, and also provide a structural path by which the scram arrest loads may be grounded to the reactor vessel mounting.

- g) Requirement - Provide access to the core to allow the withdrawal of a core support structure inlet module.

Bases - Geometric constraints on the rotating plugs dictate that the AHM be positioned such that it passes through the outer region of the upper internals structure. The size of the opening required in the upper internals structure is dictated by the functional requirement for inlet module removal and replacement.

- h) Requirement - Provide upper internals structure jacking mechanisms mounted on the IRP, which will engage with the upper internal support columns and lift the upper internals structure to permit rotation for refueling.

Bases - The upper internals structure has, at its lower end, keys which engage in slots in the upper core former ring during normal operation. Disengagement of the keys requires the upper internals structure be lifted vertically. The 9-1/2 inches vertical lift provided is sufficient to disengage the keys and provide an adequate working clearance between the upper internals structure and all projections on the core support structure.

- 58 | i) Requirement - Provide shielding approximating that of the uninterrupted head for the penetrations of the upper internals structure support columns through the intermediate rotating plug.

Bases - Radiological design requirements for the head access area dictate that the dose rates in this area shall not exceed 25 mREM/Hr. In order to meet this dose rate limitation, it is essential that there be no radiation streaming paths through the head.

- 41 | j) Requirement - Provide the penetration of the IRP by the upper internals structure columns with seals and above-head shielding that limit the radiation dose to the head access area dose rate of 25 mREM/Hr.

Bases - At the upper internals structure head penetrations, the primary containment boundary is extended upwards in the form of the UIS jacking mechanism housings. The potential exists for radioactive cover gas to penetrate the area between the outside of the upper internals structure support columns and the inside of the jacking housings. Penetration of radioactive cover gas to the area above the head must be minimized, since this is a source of radiation to the head access area. The upper internals structure column seals are provided to minimize cover gas leakage.

- 41 | k) Requirement - Provide a source of material for surveillance of the upper internals structure.

47 | Bases - The design of the upper internals structure is based on the assumption of ductile behavior in both time-dependent and time-independent failure modes. Ductility of the material can be reduced by the leaching of carbon and nitrogen by the dynamic sodium environment. Materials evaluations based on relatively short exposure time tests indicate that ductility loss will not be a problem in the upper internals structure. The surveillance specimens are required to confirm this behavior in the actual reactor operating environment over the full service life.

- l) Requirement - Provide for the routing and support of the diagnostic instrumentation required for initial confirmation of the satisfactory performance of both the upper internals structure and the outlet plenum flow control features.

Bases - The upper internals structure is designed to promote mixing and control stratification in the outlet plenum. Water simulation tests, and a small scale sodium test will be used to provide early confirmation of this aspect of the upper internals design. It is impossible, however, to fully simulate all aspects of the CRBR outlet plenum transient behavior in these tests. Full simulation will be obtained for the first time during the initial stages of CRBR operation. Thermocouples strategically located on the upper internal structure will monitor outlet plenum temperatures during the early stages of operation, and provide confirmation of the effective operation of the upper internals flow control features.

The upper internals structure may be subject to vibration excitation by impingement of the core outlet flow and cross flow in the upper plenum region. The structure is designed to have the stiffness required to minimize dynamic response to this excitation. During the design phase, water loop testing of upper internals structural models will be used to optimize the design from a vibration viewpoint and confirm acceptable vibration behavior of the final configuration. Accelerometers positioned within the CRBR upper internals structure will provide confirmation that the upper internals structure behaves in a manner similar to that predicted from the model tests.

- m) Requirement - Key the upper Internals structure to the core barrel such that the lateral movement is limited.

Bases - Keying the upper Internals structure to the upper core restraint former limits the lateral deflection of the lower end of the upper Internals structure during seismic excitation. This deflection control is essential to satisfactory operation of the control rod system.

4.2.2.1.2.8 Core Restraint System

- a) Requirement - Provide means for the control of core motion so that it is both predictable and safe.

Bases - Reactivity feedback in an LMFBR core is sensitive to core geometric changes. In the case of the CRBRP, uniform radial compaction of the core inserts reactivity at the rate of approximately 1/2¢ per mil of inward motion of the outer core radial boundary. The core restraint system is designed such that reactivity insertions from this source are sufficiently small so as to produce no damage to the core components. In addition, core design features are employed which enhance predictability of core movement and minimize the occurrence of spurious scrams due to incremental core motion.

- b) Requirement - The reactivity feedback attributable to the core restraint system shall be such that Criteria 9 and 10 are satisfied for reactor power range operations.

Bases - Satisfaction of the reactivity related design bases identified in Criteria 9 and 10 in Section 3.1.3.1.

- c) Requirement - Limit the potential magnitude of core compaction (and the resulting reactivity insertion) due to postulated stick-slip motion to less than allowable values which assure that the fuel and cladding will not be damaged. The allowable step reactivity insertion magnitude is 60¢ at full power and 85¢ at hot standby (5% power).

Bases - The important parameters for determining a step reactivity insertion limit are fuel temperature, cladding temperature, and sodium temperature.

Analysis presented in Section 15.2.3.3 of this document has shown that a step reactivity insertion of 60¢ at full power will not bring the fuel centerline temperature to the level that would initiate fuel melting, will not result in the clad reaching the emergency event temperature limit of 1600°F, and will not result in sodium boiling in the hot channel. These results were all achieved simultaneous with the assumption of an SSE seismic event which retards insertion of the control rods. An assumed 90¢ reactivity insertion by contrast does produce up to 25% melting of the fuel and peak clad temperatures up to 1700°F. A 60¢ step reactivity insertion limit provides a satisfactory margin against damage to the core components.

For a step insertion of 85¢ at hot standby (5% power) fuel cladding temperature, fuel temperature, and coolant temperature will not even reach normal full power temperature levels. Thus no damage would occur and the reactor would be shut down by the PPS system.

- d) Requirement - Provision shall be made for release of core restraint interassembly loads such that refueling insertion and withdrawal loads will not exceed 1000 lbs., including the buoyant weight of the assembly being handled.

Bases - This requirement is based on the field experience and recommendations of engineers with reactor refueling experience. The requirement for refueling loads to be kept at a low level is based on concern for the possible consequences of applying high loads to adjacent core assemblies scheduled for continued operation in the core and the reduced ductility of the core assemblies being removed. Limiting the insertion and withdrawal loads to 1000 lbs. maximum effectively precludes the potential for damage to either the core assembly being handled or the adjacent core assemblies.

- e) Requirement - With the core in the refueling configuration, all core component handling sockets must be positioned within ± 0.58 inches of true position.

Bases - The IVTM is being designed to locate and engage with the core components when the IVTM grapple head and the core component handling socket are misaligned by up to 1.75 inches. A conservative scoping analysis of the potential positioning errors in the IVTM grapple due to head tolerances, IVTM tolerances, and structural deformations gives a maximum IVTM grapple position error of ± 1.1 inches. This leaves an additional 0.65 inches for core component handling socket positioning errors. The core component handling socket positioning

requirement is set at +0.58 inches leaving a 70 mil contingency allowance that will not be exceeded using the most conservative assumptions relative to component tolerance stack up and structural deformation.

- f) Requirement - The core restraint system shall position the upper end of the control assembly ducts to within +0.53 inches of true position.

Bases - Deviation of the control assembly ducts from their true position results in clearances between the control rod driveline and the interfacing structures being reduced. Reduction of these clearances eventually leads to the generation of interaction loads between the driveline and the surrounding structure. The allowable limit to this clearance reduction is set by the effect that the resulting interaction loads have on control rod scram insertion times. A conservative scram dynamics analysis has shown that the +0.53 inch control assembly positioning error is compatible with acceptable control rod system scram performance. A larger control rod duct positioning error may be compatible with acceptable scram performance. Fixing the maximum allowable control rod duct positioning error at +0.53 inches represents a conservative design approach which assures that positioning errors in the control rod ducts will not impair in any way the functional capability of the control rod system.

- g) Requirement - Positioning control of the fuel assembly duct nozzles shall be such as to minimize lateral hydrodynamic forces imposed on the upper internals structure instrumentation posts.

Bases - Water loop testing of reactor internals dynamic models has shown impingement of the core effluent jets on the upper internal structure immediately above the core to be a potential source of upper internals structure vibration excitation. The potential for this excitation increases when the jets impinge on flat surfaces with hydrodynamic force generating capability. The UIS instrumentation posts and shroud tubes have small transverse dimensions and large vertical dimensions to provide the required bending strength while producing minimum drag. The requirement for core effluent position control assures that the main body of the effluent jet will pass cleanly between the instrumentation posts and shroud tubes, thereby minimizing the potential for hydrodynamic force generation.

- h) Requirement - The core restraint system shall be designed to prevent a general condition of duct to duct contact in the active core region.

59 | Bases - The purpose of this requirement is to assure that the functional capability of all core components is preserved. Potential failure mechanisms associated with a general condition of duct to duct contact are: duct brittle fracture under seismic loading, excessive duct deformation with the buildup of large interduct contact loads and adverse pin bundle-duct interaction. By limiting the degree of duct-to-duct contact, the functional capability of all core components is preserved.

- i) Requirement - The design life for the core formers is 30 years for the 75% plant capacity factor.

Bases - This requirement assures that the core formers will not need to be replaced during the design life of the plant. The primary incentive for this requirement is economic and operational benefits.

- j) Requirement - Design of the core restraint system shall be consistent with annual refueling.

Bases - This requirement provides consistency with established plant operating guidelines.

- k) Requirement - The dynamic radial deflection of the inner profile of the Upper Core Former (UCF) shall be less than ± 0.100 inch, relative to the UCF centerline during an SSE or OBE event.

Bases - Proper alignment of the control assembly handling socket is necessary to meet protection system (SCRAM) insertion rate requirements.

The insertion rates required during a seismic event are slightly lower than those required during non-seismic events (see Figures 4.2-93 and 4.2-94).

44 | For non-seismic events, control rod system alignment requirements are defined by Figures 4.2-95A and B. The contribution from the core restraint system and core former clearances and tolerances is limited to less than 0.530 for the control assembly handling socket to reactor vessel centerline.

However, for seismic events, a similar alignment limit was considered not to be applicable, since dynamic analysis is being performed to adequately account for deflections of each component interfacing with the control rod system. Qualitatively, the objective for the core former is to limit seismic deflections to as small as practical, within the various design restrictions. The 0.100 inch dynamic deflection limit is thus established as a reasonable design objective for such a large (150 inch O.D.) ring. It should be pointed out

that the UCF time vs. deflection history in relation to that for the control rod system and other interfacing components is also an important parameter in the scram analysis, and is not easily factored into a simple deflection requirement.

- 1) Requirement - The Lower Core Former (LCF) radial deflection relative to the LCF centerline during an SSE or OBE shall be limited to less than ± 0.100 inches.

Bases - The Lower Core Former, interfacing with the above core load pads on the reactor assemblies, performs a geometry control function. To limit the seismic loads on the assemblies and to limit the magnitude of and reactivity insertion during a seismic event, the LCF deflection must be limited. If the distance across the core former were significantly reduced due to an elliptical deflection of the ring, the reactor assemblies would be compacted, causing a reactivity insertion and higher loads on the load pads. By limiting the LCF deflection to less than 0.100, an increase in load pads is avoided since adequate clearances exist between load pads and between the outermost load pad and the Lower Core Former. This is shown in Figures 4.2-84 and 4.2-92. Preliminary core restraint models indicate that cumulative clearance is slightly more than 0.150 inches between the first row blanket assembly load pad and the LCF segment for on-power operation. Therefore, if the LCF deflects up to 0.100 inches, the compaction would primarily affect the shield and outer blanket assemblies and would not be expected to result in a significantly greater seismic reactivity insertion.

During low power operation, the gap existing in the outer core region is less than for on-power operation due to the outward assembly bow. This could result in a slightly larger seismic reactivity insertion; however, the allowable reactivity insertion is also larger for low power operation. Further evaluations are planned to better determine the effect of core former deflection on seismic reactivity insertions. These evaluations will lead to an improved definition of LCF deflection requirements.

There will be a seismic induced core compaction in an orthogonal direction which will occur even with zero LCF deflection. This is discussed in Section 15.2.1.3. The intent of the LCF deflection limit is to prevent an additional source of core compaction during a seismic compaction event.

14

- m. Requirement - Provide vertical load reaction to the core barrel.

Bases - The core former structure is subjected to mechanical loads caused by the incremental thermal growth of the fuel assemblies. Due to stick-slip friction of the assemblies and alternating heating and cooling cycles, a new upward force may be developed on the core former ring. Additionally, the SMBDB loadings can cause upward forces on the upper case former.

4.2.2.1.2.9 Removable Radial Shield (RRS)

- a) Requirement - Provide radiation shielding to ensure the structural integrity of the reactor permanent components beyond the radius of the RRS for 30 years.

Bases - The structural integrity of the reactor permanent components is based on the requirement that at the end of the 30 year life the minimum total residual elongation of the materials must be not less than 10%.

- b) Requirement - Provide a compact structural unit that can be handled in and out of the reactor by the normal fuel handling equipment.

Bases - Efficient and economical means of installing and removing the RRS by the fuel handling equipment. This is achieved by commonality with the fuel and blanket assembly design.

- c) Requirement - Transmit lateral core restraint loads without significant contribution to the magnitude of these loads.

Bases - The load buildup at "on power" conditions must be minimized to increase the margin of safety against duct crushing. Also, it is desired to attain lower withdrawal forces at reactor refueling conditions.

- d) Requirement - Provide flow paths for the sodium for cooling of the RRS to preserve the structural integrity.

Bases - Coolant flow must be provided inside the assembly to maintain the maximum material temperature below a reasonable limit ($\approx 1100^{\circ}\text{F}$), and to limit the maximum temperature gradients due to nuclear heating so that the resulting thermal stresses will not exceed the allowable limit.

- e) Requirement - Provide a means for locating surveillance specimens in the RRS and a method for their expedient recovery.

Bases - As described in 4.2.2.1.1.12, surveillance is required to obtain information on materials irradiation damage so that changes in material properties can be monitored and potential deteriorating conditions detected.

4.2.2.1.2.10 Core Former Structure (CFS)

- a) Requirement - Provide peripheral constraint for the reactor assemblies.

Bases - Positioning of the core former structure relative to the core maintains, as part of the core restraint system, proper core geometry during all modes of operation.

- b) Requirement - Provide lateral location and constraint for the lower end of the Upper Internals Structure.

Bases - Maintain alignment of the Upper Internals Structure for proper operation of the reactor control system. Interface constraints are imposed by the In-Vessel Transfer Machine, the reactor vessel, and the rotating plugs.

- c) Requirement - Transmit the applied loads from the reactor core assemblies and the Upper Internals Structure to the Core Barrel including upward vertical loads.

Bases - Transfer loads to the Core Support Structure, the primary structural support and positional reference for the Core Former Structure.

- d) Requirement - Provide a structural attachment for the Fixed Radial Shield.

Bases - Maintain lateral restraint at the upper end of the Fixed Radial Shield.

- e) Requirement - Provide a temporary vertical support for the Upper Internals Structure.

Bases - React the dead weight of the Upper Internals Structure during installation of reactor components.

4.2.2.1.3 Design Loading

The loading conditions to which the reactor internal structures may be subjected are categorized into Normal, Upset, Emergency, Faulted, and Design Conditions as defined in Section III NG & NB-3000 of the ASME Boiler and Pressure Vessel Code.

Table 4.2-21 provides for the 30 year life reactor internals components the design temperatures versus the predicted steady-state temperatures (including uncertainties) at the maximum temperature point of the components.

Design loading conditions are given for the two principal groups of reactor internals components, the upper internal structure and the lower internals structure.

The only structural component of the lower internals structures is the core support structure. Thus the temperature, pressure and static loads for the lower internals which follow are stated for the core support structure.

4.2.2.1.3.1 Core Support Structure

1. Temperature and Pressure

The CSS shall be designed to meet temperature and pressure conditions as follows:

Design Condition Parameters

Core Plate.....	775 ⁰ F
Module Liner.....	775 ⁰ F
Core Barrel.....	775 ⁰ F - 1015 ⁰ F
Support Cone.....	775 ⁰ F
Design ΔP.....	170 psi

Stretch Condition Parameters

Core Plate.....	715 ⁰ F
Module Liner.....	715 ⁰ F
Core Barrel.....	715 ⁰ F - 1015 ⁰ F
Support Cone.....	715 ⁰ F
Refueling Temperature.....	375 ⁰ F
Pressure Difference at Stretch Conditions.....	139 psi
Maximum Sodium Velocity.....	30 Ft/Sec.
System Design Life.....	30 Calendar Years

2. Mechanical Loads

The CSS shall be designed to support all of the reactor components during initial reactor assembly as follows:

	<u>CSS Static Loads</u>	<u>Dry Weight (lbs.)</u>
CSS.....		198,800
Inlet Modules (Based on Average Weights).....		72,100

CSS Static Loads Dry Weight (lbs.)

Fuel Assemblies.....	69,000
Blanket Assemblies.....	114,700
Primary Control Assemblies.....	9,250
Secondary Control Assemblies.....	2,100
Removable Radial Shield.....	125,460
Bypass Flow Modules.....	38,100
Core Former Structure.....	41,750
Horizontal Baffle.....	17,200
Fuel Storage and Transfer Assembly.....	4,800
Fixed Radial Shield.....	74,000
Upper Internals Structure.....	100,000

Transient mechanical loads imposed on the core support structure are due to fuel transfer operations and actuation of the control rod systems (PCRS&SCRS). The transient fuel transfer conditions are as follows: The first condition is that due to the invessel transfer machine (IVTM) in transferring fuel to or from the core. An axial load of 5,000 pounds maximum is anticipated for this operation. The second condition is that due to the IVTM in transferring fuel to or from the fuel transfer and storage assembly. The anticipated axial load for this operation is also 5,000 pounds maximum. These loads are the maximum down thrust of the IVTM including the weight of an assembly. The third loading condition is that imposed by the ex-vessel transfer machine (EVTM) in transferring fuel to or from the fuel storage assembly. A maximum axial load of 2,200 pounds is expected for such an operation.

A transient condition imposing mechanical loads on the LIS is the actuation of the SCRS. The end-of-scrum deceleration of each of the six SCRS imposes a 1,700 maximum pound axial load on the core support structure for a total axial load of 10,200 pounds. The fifth condition is the scram arrest load from each PCRS control rod. This load is conservatively calculated to be 5,000 pounds for each of 9 rods or 45,000 pounds maximum. This is a dynamic load applied for a very brief period.

Normal

Mechanical loads applied to the CSS during operation are reduced relative to the dead weight loads during assembly by the buoyancy of the core and core support structure in the sodium.

Upset

The CSS shall be designed for five (5) OBE events with ten (10) maximum peak response cycles each. Of the five (5) OBE events, four (4) of these OBE's shall be assumed to occur during the most adverse Normal Operating Conditions determined on the CSS design limit basis. The other one (1) OBE shall be assumed to occur during the most adverse Upset event, determined on the CSS design limit basis, and at the most adverse time in the upset event. The most adverse events to be combined with the OBE's shall be established during the structural evaluation and included in the formal stress report.

For structural systems which are attached directly to either the top of the core barrel or to the CSS plate, the horizontal and vertical OBE response spectra will be used. These spectra represent smoothed curves of acceleration response versus natural frequency of simple single degree of the freedom systems subjected to time-dependent excitation at the point in the overall reactor system where the spectra are being developed.

Emergency

There are no mechanical loads caused by the emergency conditions specified.

Faulted

The CSS shall be designed for one (1) SSE event with ten (10) maximum peak response cycles. This SSE event shall be assumed to occur during the most adverse Normal Operating Conditions determined on the CSS design limit basis. Furthermore, this same SSE event shall also be assumed to occur simultaneously with the saturated steam line rupture event and to start at the same time as this event. The most adverse event/events to be combined with the SSE shall be established during the structural evaluation and included in the formal stress report.

To meet the requirement of safe shutdown during and after an SSE, the nuclear core must be maintained in approximately the same axial and lateral position relative to the control rod as existed prior to the event. To meet this requirement, the CSS shall not exceed the limits of Section III, subsection NG of the Code for Faulted Conditions during and after an SSE. The maximum lateral displacement between the CSS and the vertical centerline of the stationary outer ring of the reactor vessel support during and after an SSE shall be minimized.

Amend. 51
Sept. 1979

4.2.2.1.3.2 Upper Internals Structure (UIS)

Outlet Temperature and Flow Profiles

The outlet temperature and flow profiles will be used to obtain steady-state thermal input for the design of the upper internals structure. Core temperature and flow patterns are symmetrical for 60° sectors of the core, and each 60° sector also has an axis of symmetry and may therefore be represented by a 30° sector.

Reactor vessel outlet temperature, mixed mean 995°F

Operating dead band +20°F

Temperatures in the sodium exiting from the core vary widely as reported in Section 4.4.3.3. Mixing of the core effluent with the bypass flow yields a mixed-mean temperature at the vessel outlet of 995°F + 20°F. The structure will also be designed to operate with a maximum thermal mismatch of 390°F between individual core and control assemblies. At the hot/cold interface between the radial blanket and the core, the sodium flow from adjacent assemblies may differ in temperature by up to 273°F. Mixing of these sodium streams on the surface of UIS structural members immediately above the core gives rise to thermal striping stresses.

Transients

Summarized below are the transients to which the upper internals structure was thermally and structurally evaluated. Due to recent changes in the plant duty cycle and further evaluation of plant performance, the plant duty cycle transients (Appendix B) are judged to have approximately the same severity as the transients for which the upper internals structure were evaluated. Final evaluation of the upper internals structure with the Appendix B duty cycle will confirm its structural adequacy.

Normal Transients

The following three design events equal or exceed the frequency and severity of all anticipated 'normal' thermal transients.

RV - 1N Dry heat up - 5 events

70° to 400°F at 10°F/Hr

RV - 2N Normal heatup - 670 events

400°F to 925°F at 150°/Hr

Ramp: 25° in 25 sec. at 1.0°/sec. 6 times/hr/event

50° in 50 sec. at 1.0°/sec. 1 time/event

RV - 3N Normal Load Follow - 12,000 events

925° to 1010° at 85°/1400 sec. 1 event/24 hr.

Upset Loading

The following three events equal or exceed the frequency and severity of all 'upset' thermal transients. In the case where values are given for more than one mixing value, the more severe case will be used for analysis.

RV-1U: Reactor Trip - 361 Events (Includes 11 emergency events)

Core outlet

Vessel outlet - 5% mixing

Vessel outlet - complete mixing

RV-3U: Uncontrolled Rod withdrawal @ full power - 26 events

Core outlet

Vessel outlet - 5% mixing

RV-4U: Uncontrolled Rod withdrawal @ Startup - 20 events

Core outlet

Vessel outlet 5% mixing

Emergency T and H Loading

The effect of the emergency transients identified is judged to be less severe than that of an upset reactor trip. Conservative account has been taken of these emergency events by adding eleven (11) events of transient RV-1E to 350 events of RV-1U for a total of 361 events of RV-1U.

Faulted T and H Loading

The following event is specified to assure that sufficient margin exists in the design to survive the 'faulted' transient event, however unlikely.

RV-1F Unmitigated Rod Drop - 1 Event

It is noted that there are reactor trips to prevent such a condition.

Mechanical Loads

During normal operation the upper internals structure must support its own weight and carry relatively small hydraulic forces.

Upset Mechanical Loads

The upper internals structure provides backup holddown capability in case of seismic disturbance or loss of hydraulic holddown. Seismic input produces the UIS mechanical upset conditions.

The structure shall also be designed for seismic loads which have been determined from a seismic analysis of the entire reactor system using the OBE floor response spectra as input to the reactor vessel support (99' elevation). Acceleration

history of the support point may be used in lieu of the floor response spectra. The structure when subjected to the OBE seismic loads shall satisfy the ASME Code criteria for upset conditions. Specific objects of this analysis are as follows:

The seismic response of the UIS must be evaluated both with engaged and disengaged radial keys.

In the engaged condition, freedom for lateral movement at the keys will be less than 0.060.

For OBE seismic loads the UIS must be designed to limit deflection during refueling to preclude impact between the UIS and the vessel thermal liner.

Emergency Mechanical Loads

The upper internals structure provides backup holddown capability in case of a seismic disturbance or loss of hydraulic holddown. The SSE seismic disturbances will be conservatively defined as an 'emergency' event instead of the allowable 'faulted' definition.

The upper internals structure shall be designed for seismic loads which have been determined from a seismic analysis of the entire reactor system using the SSE floor response spectra given above as input to the reactor vessel support (99' elevation). Acceleration histories at the support point may be used in lieu of the floor response spectra. The structure, when subjected to the faulted conditions SSE seismic loads, shall satisfy the ASME Code criteria for emergency conditions in the operating position.

Scoping analysis has shown that the vertical excitation is insufficient to cause core movement leading to loading of the upper internals structure. The maximum emergency condition vertical loading occurs in the event of a loss of hydraulic hold-down. The UIS is designed to carry the impact loading caused by arresting the upward velocity of core and blanket assemblies caused by loss of hydraulic holddown.

Faulted Mechanical Loads

The SSE earthquake has been transferred to the 'Emergency Loads' for definition, even though this is in fact a 'faulted' condition.

4.2.2.2 Design Description

4.2.2.2.1 Reactor Internals Structures

The structural components of the reactor internals are grouped into two major assemblies: the upper internals structure and the lower internals structure, Figure 4.2-36.

53 | The upper internals structure maintains alignment between the fuel/control assemblies and the control rods with their associated drive mechanism. Additionally, the upper internals structure collects the core coolant and channels it through the coolant tubes. Channeling the coolant flow parallel to the control rod driveline insures that cross flow induced vibration of the driveline is prevented. The channeled coolant also promotes mixing of the outlet plenum which mitigates the impact of thermal transients on the outlet plenum structures and nozzles.

The lower internals structure supports the reactor assemblies. Additionally, the lower internals structure limits fuel assembly radial motion, and distributes flow through the various core regions by means of modules sealed in the core support plate. The core support plate also has an integral core barrel which provides support for the core formers which limit core motion, the permanent shielding which shields the core barrel and vessel, and the in-vessel transfer and storage wells which provide a transfer station for the reactor assemblies.

58 | The reactor internals structures utilize a variety of structural materials which include:

Material

1. Type 304 SS
2. Type 316 SS
3. Type 304 SS w/Chrome Plate
4. Alloy 718
5. Alloy 600 (Locking Pin)
6. Type 316 SS with Haynes 273 weld deposit
7. Type 316 SS with Chrome Carbide hard surface
8. Alloy 718 with aluminized surfaces
9. Weld-deposited 308SS
10. Weld-deposited 316SS or 16-8-2
11. Type 316 SS with aluminized surfaces

Amend. 58
Nov. 1980

Much of the data available on neutron irradiation of materials used in the CRBR have been obtained at temperatures at which thermal aging effects might be expected. Whether the observations in such cases represent the simple sum of irradiation and thermal aging effects taken independently, or whether synergism is involved is not known. Consequently, no attempt has been made to differentiate between the two effects when evaluating irradiation experiments and making estimates of material radiation damage. A design ductility criteria is used for CRBRP reactor internals permanent components to assure structural integrity.

The design ductility criteria for the CRBRP reactor internal components are based on end-of-life residual total elongation of uniaxial tensile specimens. Values of 10% and 5% minimum residual total elongation are being used as a general design rule for the permanent components. The use of the 5% residual total elongation criteria is restricted to selected low stress areas in the Inlet module and fixed radial shield. Table 4.2-53 lists the general residual ductility criteria in use together with component material irradiation temperature, predicted maximum end-of-life fluence, predicted average neutron energy, and fluence limit for the stated minimum residual total elongation. The material fluence limits for the minimum total elongations indicated have been defined using an neutron energy-dependent technique developed in References 178, 179 and 180.

The data used in the determination of energy-dependent fluence limits have been acquired through irradiations in EBR-II, and are stored in the HEDL data bank. The available data on types 304, 316 and weld-deposited 308L stainless steel, the major materials from which the reactor internals are fabricated, are given in References 178, 179 and 180. Data on Alloy 718 are contained in References 178 and 179 only.

References 178 and 179 document the interim interpretation of behavioral trends in these materials for an ongoing irradiation effects program designed to provide an improved data base for evaluation of fluence limits using energy-dependent methods. Application of simple scaling procedures yielded relative damage cross sections which were found to incorporate separable spectrum and temperature dependencies. The irradiation effects program entitled "FFTF/CRBRP Structural Materials Irradiation Experiment", has been completed and the results published in Reference 188.

Reference 180 uses the results of References 178 and 179 as a guide in the analysis of a larger data base (Tables 4.2-54, 4.2-55 and 4.2-57) to develop stainless steel property correlations for engineering applications in reactor component design and analysis. Trend curves for nominal and minimum property values which incorporate effects of temperature, exposure and spectrum are defined.

Minimum ductility trend lines defined by Reference 178, 179 and 180 have been used in defining the energy-dependent fluence limits for the minimum residual total elongation of Table 4.2-53. Energy dependent fluence limits for the reactor internals structures are defined at worst case irradiation temperature, i.e., 700°F for the lower internals structures and 1200°F for the upper internals structure.

Lower internals stainless steel energy-dependent fluence limits are based on the data of References 179 and 180. Lower internals Alloy 718 energy-dependent fluence limits are represented by a single, conservative, value of 5×10^{21} n/cm². The Alloy 718 fluence limit assures a residual total elongation of 10% for average neutron energies less than 0.23 Mev (lowest mean energy of test data). The Alloy 718 fluence limit is based on establishing a minimum property line for the Alloy 718 data of Reference 179, using engineering judgement to account for increased data uncertainty associated with the data base.

Upper Internals structure stainless steel and Alloy 718 energy-dependent fluence limits are also represented by a single, conservative, value of 1×10^{21} n/cm². The fluence limit, representative of a level for onset of notable irradiation damage, assures no measurable loss in component ductility from that of the unirradiated material. The 1×10^{21} n/cm² fluence limit was chosen in order to restrict the allowable neutron exposure to low levels where irradiation damage can be ignored.

Existing 316 stainless steel and Alloy 718 radiation effects data of Tables 4.2-55 and 4.2-56 support a 1×10^{21} n/cm² fluence limit for average neutron energies greater than 0.4 Mev, but do not necessarily support a 1×10^{21} n/cm² fluence limit for average neutron energies typical of the upper internal structure, $\bar{E} < 0.1$ Mev.

Helium embrittlement effects which dominate physical property behavior at irradiation temperatures of the upper internals structure (1200°F max), are greater in a soft spectrum ($\bar{E} < 0.1$ Mev) than in a hard spectrum ($\bar{E} > 0.4$ Mev), for the same fluence level. Adjusting the Table 4.2-55 and 4.2-56 data to account for spectral effects results in a 1×10^{21} n/cm² fluence limit applicable to the upper internals structure. An irradiation effects program will be conducted using the FFTF MCDA-1 facility (late 1982) to support a 1×10^{21} n/cm² fluence limit for average neutron energies less than 0.1 Mev.

4.2.2.2.1.1 Lower Internals Structure

The lower internals structure consists of six components: the core support structure, the lower inlet modules, the bypass flow modules, the fixed radial shielding, the fuel transfer and storage assembly and the horizontal baffle. The core support structure, Figure 4.2-37, is the major support member of the lower internals structure.

58 | The core support structure is welded Type 304 stainless steel structure which includes the core support plate and the core barrel. The core support plate contains module liners which serve as receptacles for the lower inlet modules. The core support structure carries the weight of the other portions of the lower internals structure, the reactor removable assemblies (fuel, blanket, control and radial shield assemblies) and the core former structure. The core support structure provides the upper boundary of the vessel inlet plenum and distributes the coolant to the lower inlet and bypass flow modules. The core support structure transmits the dead weight hydrostatic pressure and seismic loads to the reactor vessel.

51 | The core support structure concept is based upon the FFTF core support structure, however, the FFTF manufacturing experience has been utilized to reduce the complexity of the core basket. The FFTF core basket was a core diameter size structure containing receptacles so that each reactor assembly could be "plugged" into the core basket. This single large core basket has been simplified by designing mini baskets (lower inlet modules). Each inlet module receives seven reactor assemblies. Each module in turn plugs into liners which are integral to the core support plate. The concept of these liners is shown in Figures 4.2-38 and 4.2-39. Each liner is a Type 304 stainless steel tube inserted into the support plate seated to the bottom of the plate by a flange and clamped to the support plate by a cap at the top of the liner. The cap complies with the ASME Code requirements for the use of the non-integral joints. The liner is sealed near the lower surface of the

plate to permit hydraulic balance of the lower inlet modules. The liner has an alignment feature mating with the support plate and an alignment feature for the lower inlet modules. These two alignment features assure that the lower inlet modules are positioned correctly. The reactor assembly discrimination feature precludes placing an assembly in an improper location. Auxiliary flow ports and debris barriers, as shown in Figures 4.2-38 and 4.2-39 have been provided in each module liner to preclude the possibility of large debris of any type from blocking all flow to one or more of the inlet modules. The auxiliary flow ports are located immediately below the CSS plate in a secondary inlet plenum formed by the hexagonal debris barriers, which separate the auxiliary flow ports from the primary flow ports and the radial ribs on the peripheral liners. The primary flow ports are designed to prevent large debris from entering the module liner stem and blocking the auxiliary ports from the inside and the peripheral ribs prevents debris from working its way in from the side of the array. In the event that one or more of the primary flow ports become blocked, the affected liner would then draw cooling sodium via the auxiliary flow ports from the secondary plenum. Sodium feed to this secondary plenum is by (1) the auxiliary flow ports in the unblocked liners and (2) the array of 2 inch diameter holes in the hexagonal debris barrier array.

Lower inlet modules support and position the reactor assemblies on the core support plate. These modules, as shown in Figure 4.2-40, distribute the coolant to the various reactor components: fuel assemblies, blanket assemblies, removable shield assemblies and control rod assemblies. Each module fits into a liner integral to the support plate and receives seven reactor assemblies and provides orificing that is unique to specific reactor assembly locations as shown in Figure 4.2-41.

Each of the LIMs feature one alignment pin and two shorter discriminator pins. Proper alignment of each LIM is assured through the mating of the alignment pin to the module liner hole. Each LIM group has two uniquely machined discriminator pins that mate with two uniquely drilled holes on each of the module liners. During installation, the alignment pin will properly align the LIM. However, complete installation will be prevented if the two discriminator pins do not line up with module liner holes.

Sufficient clearance exists between the LIM and the module liner, as well as pin/hole dimensions, to allow thermal expansion. The module liner has an interference fit with the Core Support Plate and it maintains a fixed position with the plate. Both the liners and the Core Support Plate experience similar steady state temperatures and are made from the same material, therefore, thermal expansion variations between the two are minimum.

Mechanical discriminating features are designed into each module to assure placement of the reactor assemblies into the proper region (i.e., fuel, blanket, and control) so that assemblies cannot be undercooled. Furthermore, mechanical discrimination assures the proper core lattice positions for fuel assemblies. Angular alignment to the module for the correct lattice position is assured by an alignment pin between the liner and the core support plate. The modules are shielded by the lower shield within the reactor assemblies so that the loss of ductility limit is not exceeded during the plant life. The modules are a welded 304 stainless steel structure and all 61 modules have the

same envelope dimensions. However, there are several distinct configurations due to the differing flow requirements of the reactor assemblies.

Loads from weight, hydraulic pressure drop and seismic acceleration are transmitted by the support plate to the reactor vessel. Sizing analysis for internal pressure, flow blockage, control rod drop, and seismic loads indicate that under normal operating loads with flow blockage the inlet module meets the ASME Section III criteria for primary stresses.

Six bypass flow modules, surrounding the lower inlet modules, distribute low pressure coolant received from the lower inlet modules to the removable radial shield assemblies. The bypass flow modules provide receptacles to accept the removable radial shield assemblies that are not positioned in the lower inlet modules.

51

The details of the FRS are provided in Section 4.2.2.2.1.4.

54

The general design rule of 5.0% minimum residual ductility insures that non-ductile fracture will not occur during short term loadings in reactor internal structures. This criterion is based upon the minimum residual total elongation of 10.0% and the established relationship between total and uniform residual elongation of $\epsilon_t = \epsilon_u + 5\%$ as noted in Table 4.2-53. This relationship is based upon the end-of-life tensile test data in Tables 4.2-54 through 4.2-57 and data from References 178, 179 and 180. It is conservatively based upon a data set showing the least uniform elongation for a total elongation of 10.0%. An evaluation of all current data indicates that when the degradation on ductility is greatest at a particular fluence level the uniform elongation tends to be a greater fraction of the total than this relationship indicates. Since this limit is based upon uniaxial test data a correction for the multiaxial state of stress for actual reactor component conditions is required. This correction can be performed using scientific paper 67-100-CODES-P1, "Applied Mechanics in the Nuclear Industry Applications of Stress Analysis". For a typical thermal stress conditions which causes an equibiaxial stress state the 5.0% would be reduced to 0.9%. The elongation available to insure ductile behavior can be determined by considering the factor of safety, consistent with the ASME Code Section III factor of safety protecting against ultimate failure. The use of the factor of safety of 3.0 would reduce the elongation for a equibiaxial state of stress to 0.30%.

The applied strain considered relevant to this elongation limit is the maximum value of the three principle strains and represents an accumulation of elastic plus plastic strain at the end of life. These limits would apply at a minimum to membrane plus bending strains regardless of whether the loading is primary or secondary. Thermal transient strains in reactor internal components are less than the 0.30% membrane plus bending. Therefore, from the tensile data base that is presently available, the ductility required at the end-of-life in reactor internal components is sufficient to insure their integrity when 10% residual total elongation is available and the criteria described is applied. In locations where significant fatigue damage occurs in the low cycle regime, which is also affected by the ductility of the material, corrections to the fatigue design curves are applied using accepted theories of fatigue design curve construction which are based upon reduction in area.

57 | A test program is presently in place which will experimentally characterize the fracture toughness of reactor component materials when subjected to a fast-neutron irradiation environment. This program includes tests of smooth, notched and welded specimens. The establishment of the fracture toughness and fatigue crack propagation characteristics will provide a basis for confirmation of the described criteria or the substitution of a more refined criteria.

4.2.2.2.1.2 Lower Inlet Module

51 | Sixty-one inlet modules support and position the reactor assemblies on the core support plate. These modules distribute the coolant to the following reactor components: fuel assemblies, blanket assemblies, removable shield assemblies, control rod

Amend. 57
Nov. 1980

assemblies, core barrel, pressure vessel thermal liner, fuel transfer and storage assembly and horizontal baffle. Each module fits into a liner integral with the core support plate and supports and positions seven reactor assemblies while providing orificing that is unique to specific reactor assembly locations. Figure 4.2-41 shows 1/6 of the core and indicates the relative position of fuel and radial blanket assemblies and orifice zones.

The module stem acts as a strainer which collects and prevents loose debris from directly blocking the various reactor assemblies.

Mechanical discrimination features are designed into each module to assure placement of the reactor assemblies into core lattice positions that will not result in assembly undercooling. Angular alignment of each module for its lattice position is assured by an alignment pin between the module liner and the module. The modules are welded 304 stainless steel structures. There are several internal configurations, excluding discrimination differences, due to the differing flow requirements of the reactor assemblies.

4.2.2.2.1.3 Bypass Flow Module

58 | The bypass flow modules shown in Figure 4.2-41A, are functionally similar to the lower inlet modules in that they provide support and position removable radial shield assemblies and direct low pressure flow to cool these assemblies. There are a total of 6 modules designed to rest on the core support plate and conform to the periphery formed by the 61 lower inlet modules. A flow pipe attached to the bottom of a bypass flow module mates with a hole in the core support plate. This provides a flow path for the coolant between the lower inlet module and bypass flow module.

58 | The bypass flow modules distribute reactor flow to 264 removable radial shield assemblies, 44 of which are in each module. Flow enters each of the six bypass flow modules through a bottom entry port. Each bypass flow module is hydraulically interconnected to the adjacent two bypass flow modules giving multiple flow sources for all the RRS assemblies served by the bypass flow modules. The removable radial shield assemblies fit into receptacles integral with the bypass flow modules. These receptacles are designed with a mechanical discrimination feature to assure placement of only the removable radial shield assemblies into the bypass flow module.

The low pressure existing within the region of the outer removable radial shielding results in negligible hydraulic forces and consequently a hydraulic balance system is not required. The assemblies are simply slip fitted into the receptacle permitting easy insertion and removal.

4.2.2.2.1.4 Fixed Radial Shield

The fixed radial shield is a segmented annular ring of type 316 stainless steel located between the removable radial shielding and the core barrel as shown in Figure 4.2-42. The segments rest on the bypass flow modules and extend upward to the lower core former structure. The segments are laterally positioned by captured pins at the lower end to the bypass flow modules and at the upper end to the former structure. The pinning arrangement accommodates differential thermal expansion and results in the

36

fixed radial shield being a simple unrestrained structure. The fixed radial shield weight is carried by the bypass flow modules and the seismic loads are transmitted through the core former structure and bypass flow modules to the core support structure. The fixed radial shield in conjunction with the removable shielding protects the core barrel and vessel from radiation damage to assure the retention of ductility for a design lifetime of thirty years.

58 |

4.2.2.2.1.5 Fuel Transfer and Storage Assembly

Reactor refueling requires bringing new fuel into the reactor vessel and removing the spent fuel. The fuel is brought in and out through the vessel head by an ex-vessel transfer machine and is handled inside the vessel by an in-vessel transfer machine. A fuel transfer position is required to set down an assembly so that one machine can decouple and move out of the way so the other machine can grapple the assembly to continue the fuel handling operation.

The component surveillance program necessitates placement of specimens outside the core barrel. The fuel transfer, fuel storage, and surveillance specimen positions are provided by the five wells in the reactor vessel/core barrel annulus.

The wells are fabricated of Type 304 stainless steel and are attached to the core barrel and the horizontal baffle. Thus all dead weight and earthquake loads are transmitted to the core support structure.

4.2.2.2.1.6 Horizontal Baffle

The horizontal baffle shown in Figure 4.2-44 forms the upper boundary of the core barrel/reactor vessel annulus and physically separates hot sodium in the outlet plenum from the cooler bypass flow sodium in the core barrel/reactor vessel annulus. The baffle maintains the temperature of the sodium in the core barrel/reactor vessel annulus close to reactor inlet temperature to reduce temperature differences across components below the baffle and to provide for decay heat removal from the irradiated reactor assemblies, stored in the fuel transfer and storage assembly. In addition, the boundary formed by the baffle forms a part of the flow path which diverts bypass flow between the reactor vessel and reactor vessel thermal liner, through uniformly spaced holes in the thermal liner below the baffle, to provide cooling for the reactor vessel and reactor vessel thermal liner. A small pressure differential must be maintained across the horizontal baffle to provide the head for this flow. The pressure differential, approximately 0.5 psi, causes leakage through the seals at the edges of the horizontal baffle base plate and at the FT&SA inlet port nozzles. However, the leakage is limited to 12.5% of bypass flow to insure that sufficient cooling flow is provided to the vessel and vessel thermal liner.

51 |

The horizontal baffle design incorporates a single 1.5 inch thick simply supported base plate restrained on the outer diameter by a segmented ring outer edge attachment. Each outer ring segment includes a top ring segment, a spacer block and a bottom ring segment, all of which are bolted to the vessel liner flange with a single bolt that extends through the ring segments and spacer block and into the vessel liner flange. At the inner diameter the base plate is supported on a ledge on the core barrel wall. It is held vertically by continuous ring that fits into a groove near the upper end of the core barrel. Circumferential motion of the base plate relative to the core barrel is restrained through a key. Radial movement of the base plate at its outer periphery is not restricted and wear resistant surfaces of Haynes 273 are provided on both sides of the plate at the inner and outer diameters and on the continuous ring and ring segments to accommodate relative radial and angular rotation displacements due to thermal and seismic effects at the outside diameter and angular rotation displacements due to thermal effects at the inside diameter.

The base plate normally operates with a 150-200°F temperature difference through the thickness. Since the upper surface is hotter, the plate will tend to develop an upwardly convex spherical curvature. The plate edges, however, are restrained vertically to the relative vertical thermal displacement between the vessel thermal liner flange and the core barrel ledge. As a result of the vertical restraint, a thermally induced vertical downward force will act on the vessel liner flange and an equal upward force will act on the core barrel.

These vertical reaction forces provide a positive seal at the base plate outer and inner diameters. During down transients, the direction of the holddown forces can reverse due to the reversal of the through-the-thickness temperature gradient. The core barrel ledge will be in compression (down load) and the upward load at the vessel liner flange is carried through the top ring segments.

The portion of fuel transfer and storage assembly associated with the baffle consists of five penetrations through the base plate at a radius of 85.62 inches with an inlet port nozzle at each penetration. The penetrations allow access to the portion of the FT&SA located in the core barrel/reactor vessel annulus. The nozzles are fabricated from Alloy 718 because of the thermal striping (alternate washing of a metal surface with hot and cold fluid) anticipated in the FT&SA inlet ports.

Six 8" diameter access ports are provided in the Horizontal Baffle, equally spaced around a circle. These ports are provided with removable plugs that are locked in place during reactor operation. The plugs can be removed during installation of the Horizontal Baffle to provide access to the core barrel/reactor vessel annulus.

The horizontal baffle, except for the Alloy 718 FT&SA inlet port nozzles, is fabricated from Type 316 stainless steel.

4.2.2.2.1.7 Upper Internal Structure

Principal features of the upper internal structure are illustrated in Figure 4.2-45. The main body of the load bearing structure is a Type 316 SS weldment comprised of four support columns, an upper plate, a lower plate, four curved shear webs, and a combining mixing chamber and holddown structure which also supports shear keys for locating with slots in the core restraint upper former.

Scoping stress analysis of the upper internal structure and its components has established the necessity for thermal shields for the support columns to upper plate welds and for the inner surfaces of the mixing chamber. Thermal shields for the upper plate to support column weld consists of 316 SS collars whose lower end rests on the upper plate external to the welds. The lower surface of the lower plate, which forms the upper boundary of the mixing chamber, is shielded by stainless steel insulator plates and alloy 718 liners, and the inner periphery of the chamber is protected by an alloy 718 shroud. Three arch shaped shear webs integrate the upper and lower plates with the support columns. A modified shear web is provided adjacent to the IVTM penetration in the lower plate. Core holddown loads are transmitted through the mixing chamber to the load bearing structure by instrumentation posts as shown in Figure 4.2-45A, and lower shroud tubes.

The mixing chamber and its components serve three purposes:

- a) to mix the core outlet sodium and duct it via chimneys into the outlet plenum,
- b) to provide structural members to transmit core holddown loads to the main load bearing structures, and
- c) to provide location and support for core instrumentation.

To provide a mixing function, the chamber is a volume surrounded at the top by the UIS lower plate, and around the periphery by a curved peripheral shroud. Both of these plates are lined with alloy 718 for resistance to thermal shock and striping. Inside the enclosed volume of the mixing chamber are instrumentation posts and lower shroud tubes, as shown in Figure 4.2-45B, which react the core holddown loads and transmit them to the load bearing structures. In addition to reacting core holddown loads, the instrumentation posts locate thermocouples in the outlet sodium from core assemblies and hold the thermal liners to the lower plate, as shown in Figure 4.2-45c. Those portions of the instrumentation post exposed to flowing sodium are made of alloy 718.

Amend. 51
Sept. 1979

The alloy 718 lower shroud tubes react the control assembly holddown, and if necessary, control assembly breakaway loads. They are mechanically attached to the inner rings of alloy 718 chimney support forgings in the upper and lower support plate as shown in Figure 4.2-45B. Tangential spokes connecting the inner and outer rings of these support forgings alleviate thermal stresses due to radial temperature differences by inducing relative twist between the rings. The support forgings are mechanically fastened to the lower support plate. The outer rings of the support forgings at the upper support plate are free to move vertically, compensating for differential thermal expansion between the shrouds and the basic structure, but are restrained from rotation and horizontal movement. Above the upper support plate, the lower control rod shroud tubes mate with larger diameter upper control rod tubes using slip fit connections. This assembly method permits the upper internals structure to be raised for refueling.

Flow chimneys are fixed to the outer ring of the support forgings, as shown in Figure 4.2-45B, and duct sodium flows from the mixing chamber into the outlet plenum as shown in Figure 4.2-45D.

A hole is provided through the support plate and outer perimeter of the mixing chamber to provide the in-vessel transfer machine (IVTM) with access to the reactor assemblies. During normal operation, this hole is filled with an IVTM port plug.

The IVTM port plug is included as a component of the UIS. It is supported by a riser of the small rotating plug (SRP) which is part of the reactor closure head assembly of the Reactor Enclosure System. The IVTM port plug, when removed, leaves an access hole extending through the SRP, the outlet plenum, and the UIS. The IVTM operates through this access hole in conjunction with the auxiliary handling machine (AHM) (both a part of the Reactor Refueling System) to remove reactor assemblies and items as large in cross section as the Lower Inlet Modules. When installed, the plug blocks flow through the mixing chamber wall thus preventing aberrant sodium flow and leakage. It also limits radiation streaming through the reactor vessel closure head assembly/IVTM port plug interface to safe levels.

The reactor system thermocouple instrumentation enters the reactor vessel through the support columns of the upper internals structure. Each thermocouple is routed to a position above a core assembly to monitor the outlet temperature as shown

in Figure 4.2-45D. Each support column houses up to eight stainless steel conduits each containing up to 4 thermocouple dry wells. Each dry well is made of stainless steel tubing and encloses one thermocouple. The conduits emerge through openings in the side of the support columns at a location below the upper plate of the upper internals structure. At their lower end the conduits engage the upper ends of the instrumentation posts. Individual thermocouple dry wells branch out from the conduit ends to specific positions (in the instrumentation posts). The ends of the dry wells, at the monitoring positions, are sheathed in Inconel 718 to reduce the thermal shock to the stainless steel thermocouple dry wells.

The complete upper internals structure is supported from the intermediate rotating plug via the upper internals structure jacking mechanisms. Three radial locating keys are positioned at the lower end of the structure. These are supported on Type 316 SS box weldment, which forms the outside of the mixing chamber. Mating keyways are provided in the top of the upper core restraint former ring. Keys are required in this location to insure that: 1) the overall structure is acceptably aligned with the core for control rod driveline connection and unimpaired motion; 2) instrumentation posts are properly positioned over the core assembly outlet nozzles; and 3) sufficient support is provided to the upper internals during the seismic event. The location keys can be disengaged by lifting the upper internals structure 9-1/2 inches from the operating position to allow free rotation of the rotating plugs during fuel handling operations.

Beyond the functional requirements, the operating environment in the reactor vessel outlet plenum imposes additional design requirements on the upper internals structure. Sodium streams, exiting from the core at differing temperatures, mix in the outlet plenum resulting in fluctuating temperatures on the surface of the upper internals structure. During the scram transient, the section of the upper internals structure immersed in the sodium pool is subjected to a rapid drop in surface temperature. Jet impingement forces from the core outlet flow, and upper plenum cross flow forces must be accommodated by the design. Experience in designing the instrument trees for FFTF has shown that consideration of environmental factors dictates the selection of many of the internals design features.

Effective utilization of the reactor vessel outlet plenum mixing volume is essential for mitigation of the transient experienced by the reactor vessel and the hot leg components. The upper internals.

51

Amend. 51
Sept. 1979

structure chimneys provide a means of forcing the required mixing, by ensuring that a major portion of the core effluent exits into the plenum at a high elevation. Flow stratification tests provided data used in evaluating the upper internals structure mixing performance.

The design of the main load bearing Type 316SS structure reflects the requirements for stiffness to control flow induced vibration and thin structural walls to minimize thermal stresses in the non-isothermal environment. Flow tests on an early upper internals structure design for the British PFR reactor substantiated the need for adequate structural stiffness. The lower portion of the load bearing stainless steel structure is in the form of a structural box which imparts stiffness without the use of heavy structural members. Careful attention has been given to matching member thicknesses at structural junctions to avoid transient thermal stresses resulting from inertia discontinuities. The shear webs are perforated to maximize the uniform response of the structure to transient sodium temperature changes.

Loads imposed by a postulated loss of hydraulic holddown are transmitted directly to the lower plate via the instrumentation posts. The upper internals structure is designed to survive without damage an operational basis earthquake with the lower locating keys disengaged.

Flow patterns in the region immediately above the core have been investigated in water table tests. These tests have shown that a toroidal flow pattern exists in the mixing chamber located directly above the core. A large portion of the stream to stream temperature differences are reduced in this chamber before the flow exits. Temperatures in these flow streams differ substantially, hence the mixing adjacent to the inner surface of the mixing chamber results in thermal striping. The material selected for the exposed surfaces in the mixing chamber must therefore have an endurance stress limit in excess of the maximum anticipated stress amplitude produced by fluid mixing. This requirement led to the selection of Alloy 718 for the exposed surfaces of mixing chamber components.

59 | 41 |
58 | 41 |

4.2.2.2.1.8 Core Restraint System

Design of the CRBRP core restraint system is based upon the limited free bow concept. Essential features of this concept are illustrated in Figure 4.2-47. Fixed peripheral formers provide lateral support to the core assemblies at two locations above the active core. A third support at the core support plate elevation completes the lateral support configuration.

Relief of restraint loads for refueling in the limited free bow core restraint concept is achieved by allowing the core assemblies limited freedom for unrestrained bowing during the core startup and shutdown transients.

The amount of free bow permitted is controlled by sizing the gaps between core assembly load pads, and between the peripheral load pads and the adjacent core formers. The upper bound of the allowable core and former gaps is defined by a conservative analysis of the effect on critical core components of a step compaction of the core through the range of free motion permitted by the gap configuration. The resulting core step reactivity insertion is not allowed to produce transient heating rates in the fuel which would result in the fuel pin upset condition damage limits being exceeded.

It is evident that the core restraint system in its entirety includes all the reactor assemblies plus elements of the core support structure and the upper internals structure. Only the core formers, their associated retention and positioning hardware and the removable radial shield assemblies are categorized as core restraint hardware.

41 |

58 | 49 |

4.2.2.2.1.9 Removable Radial Shield (RRS)

The RRS assemblies are removable core assemblies (see Figure 4.2-43) having a structure basically similar to the fuel and blanket assembly structures consisting of inlet nozzle, hexagonal duct tube and outlet nozzle. The shield material is made up of stainless steel rods within thin walled ducts. The assemblies are designed to be as flexible as possible in order not to contribute to the off-power restraint loads. A close-fitting support block is inserted inside the duct at the ACLP to provide axial restraint for the shield rods and to absorb seismic loads that are transmitted through the ACLP to the core former. Control of flow through the RRS is provided by a stack of orifice plates located inside the inlet nozzle.

4.2.2.2.1.10 Core Former Structure

The core former structure is composed of three substructures, the upper core former ring, a spacing cylinder, and the lower core former ring. The core former rings are comprised of profile milled segments assembled into continuous rings, as illustrated in Figure 4.2-46. The above core load plane former ring, called the lower core former ring, is mounted on a ledge machined in the inner diameter of the core barrel. The spacing cylinder, called the support ring, provides holddown for the lower core former ring and support for the top load plane former ring called the upper core former ring. The upper core former ring has six lugs that fit slots in the top of the core barrel to transmit seismic and other loads to the core barrel. A series of L-shaped keys are circumferentially slipped into the groove on the inside of the core barrel, between each of the six lugs, and trapped by means of a radially oriented dowell pin on either side of each slot. These L-shaped keys prevent vertical displacement of the core former rings. The upper core former ring is centered in the core barrel cavity by means of the six radial lugs. The lower core former ring is centered in the core barrel cavity by means of radial shims.

4.2.2.2.1.11 Maintainability

All the reactor internals except for the removable core assemblies, are designed for a 30 year life with no scheduled maintenance. However, provision has been made to permit removal of the lower inlet modules to assure full plant life and malfunction recovery capability. Contributing factors which may require malfunction recovery capability include:

1. Potential damage to the reactor assembly receptacles, as a result of insertion and removal of reactor assemblies.
2. Potential wear or partial plugging of strainers and orifices, as a result of coolant induced changes.

4.2.2.2.1.12 Surveillance

Material surveillance coupons are contained within special removable radial shield assemblies and a fuel transfer and storage assembly. In addition to these special assemblies, all irradiated removable assemblies will be available for material surveillance. The orifice plates of four removable radial shield assemblies are used to monitor carbon mass transfer effects of Type 304 stainless steel.

4.2.2.3 Design Criteria

The design criteria presented in this section are those that were in effect at the time analyses were performed. These analyses reflect the requirements of the ASME Code, which provides the basic design criteria for these components.

Fabrication of all of the reactor internals components is done by holders of Code Certificates of Authorization for fabrication of Core Support Structures and/or Class 1 Appurtenances. Construction is performed per the applicable requirement of the ASME Code Section III, Subsections (NA, NB, NG), with modifications as appropriate for each of the components. Modifications include permitting the use of Inconel 718 as a structural material and the use of austenitic stainless steel at temperatures above 800°F. Independent fabricator verification is performed by Code Authorized Inspectors or by the designer's representative. The fabricator and designer provide written certification that all applicable requirements of the Code have been met. Code stamping is performed only where permitted by the ASME Code rules.

4.2.2.3.1 Lower Internals Structures (LIS)

The LIS components and Core Former Structure (CFS) are evaluated as nuclear components in accordance with the rules of: The ASME Boiler and Pressure Vessel Code, Section III.

Where these rules cannot be applied, the following rules are invoked:

- a. Code Case 1592, Class I Components in Elevated Temperature Service, Section III.
- b. RDT F 9-4 Components at Elevated Temperature (Supplement to ASME Code Cases 1592, 1593, 1594, 1595, and 1596).
- c. RDT F 9-5, Guidelines and Procedures for Design of Nuclear Systems Components at Elevated Temperatures (Non-mandatory).
- d. The special purpose strain controlled high-cycle fatigue criterion discussed in Section 4.2.2.3.2.3 may be applied to 304 and 316 austenitic stainless steel at temperatures up to 1100°F.

Material properties not given in the Code are taken from the Nuclear Systems Materials Handbook, TID-26666, and Section 4.2.2.3.3.1 below.

4.2.2.3.1.1 Core Support Structure (CSS)

The CSS was analyzed using the following additional rules:

- a. The 1974 Edition of the Code, Subsection NB and selected portions of Subsection NG with Addenda through Summer 1975.
- b. RDT Standard E 15-2NB, November 1974, (Supplement to ASME Code Section III, Subsections NA and NB).

- c. Modification to the high temperature design rules for Austenitic Stainless Steel creep fatigue evaluation per Section 4.2.2.3.2.3.
- d. In the use of Code Case 1592, the effect of the sodium and radiation environment on material properties was evaluated as defined in Section 4.2.2.3.3.2.
- e. Because of radiographic examination limitations for the 20 inch thick weld between the core plate forging and the ring forging, progressive liquid penetrant examination was performed per paragraph NG-5231 as specified for Type I welds in Table NG-3352-1.

4.2.2.3.1.2 Lower Inlet Module (LIM), Bypass Flow Module (BPFM), and Core Former Structure (CFS)

The 1974 Edition of the Code with Addenda through Winter 1976 were used for the LIM, BPFM, and CFS analyses.

4.2.2.3.1.3 Horizontal Baffle (HB), Fuel Transfer & Storage Assembly (FT&SA), and Fixed Radial Shield (FRS)

The HB, FT&SA, and FRS are internal structures and are not covered by mandatory Code rules, but the Owner's designee has required that the rules stated in Section 4.2.2.3.1 be applied to the design and analysis of these components. The HB and FT&SA use the 1974 Edition of the Code with Addenda through Winter 1976, and the FRS uses the 1977 Edition of the Code with Addenda through Winter 1977.

4.2.2.3.1.4 Removable Radial Shield (RRS)

The RRS is a replaceable core component with a structure basically the same as those of the fuel and blanket assemblies. Therefore, the structural design criteria applicable for the RRS are also basically similar to those of the fuel and blanket assemblies, rather than those described in Section 4.2.2.3 for the permanent reactor vessel internal components and structures. The RRS design criteria are described in Section 4.2.1.1.2.2.2.

4.2.2.3.2 Upper Internals Structure (UIS)

Code criteria applicable to the analysis of the UIS are divided into two categories as follows:

4.2.2.3.2.1 Class 1 Appurtenances

Those portions of the UIS support columns located within the boundary of code jurisdiction for appurtenances and the IVTM port plug cap shall be analyzed as Class 1 appurtenances in accordance with:

- a. 1974 Edition of the ASME Boiler and Pressure Vessel Code, Section III, Subsection NB with addenda through Winter 1974 and,
- b. RDT Standard E15-2NB, November 1974.

4.2.2.3.2.2 Internal Structure

Even though the existing ASME Code does not provide rules for the analysis of components operating at temperatures in excess of 800°F, those portions of the UIS located within the primary pressure boundary shall be analyzed as Class 1 components in accordance with the following:

For temperatures below 800°F the 1977 Edition of the ASME Boiler and Pressure Vessel Code, Section III, with addenda through Summer 1977, Subsections NA and NG shall be used.

For temperatures in excess of 800°F the following shall be used:

- a. The 1977 Edition of the ASME Boiler and Pressure Vessel Code, Section III, with addenda through Summer 1977.
- b. Code Cases 1592, 1593, and 1594.
- c. RDT E15-2NB (Supplement to Section III).
- d. RDT F9-4 (Supplement to Code Cases 1592, 1593, 1594, and 1596).
- e. The Nuclear Systems Materials Handbook, TID 26666, "Inconel Alloy 718", Technical Bulletin T-39, International Nickel Company and the Alloy 718 design fatigue curve, Figure 4.2-48 shall be used.

59 | 4.2.2.3.2.3 Modifications to the High Temperature Design Rules for Austenitic Stainless Steel

Creep-Fatigue Evaluation

Creep-fatigue evaluations will be performed in accordance with the applicable criteria except as modified herein.

The creep-fatigue damage rules of Paragraph T-1400 of Code Case 1592 consider creep damage accumulations resulting from stresses which are clearly compressive to be equally as damaging as creep damage accumulations from tensile stresses. The damaging effects of compressive stresses in a high temperature environment are known to vary considerably from one material to another. Strain controlled fatigue test data of austenitic stainless steels (304 and 316 SS) consistently point to compressive residual stresses having little or no deleterious effect. There is also test evidence that suggests that when subjected to alternate hold periods in both tension and compression that hold in compression has a healing effect on the damage produced by the tensile hold. Based upon these data, the creep-fatigue damage rules are modified as described in subsequent paragraphs.

59 | The effects of the presence of stress concentrations on stress rupture properties are known to vary considerably with the material, geometry of the stress concentration, magnitude of the stress level, the environment, and life. In the case of austenitic stainless steels, test data consistently points to stress concentrations having a less severe effect on stress rupture strength than predicted using the analytical approaches of Code Case 1592 and RDT Standard F9-4 criteria, and in the case of 316 SST, there is a consistent trend to significant notch strengthening for some types of geometries, particularly with a service environment and life at the upper limit of those in the UIS. The rules of RDT Standard F9-4T and Code Case 1592 require comparing the peak stress to the Code strength which is based upon smooth specimen data. They do not recognize that peak stresses may have no adverse effect on stress rupture strength nor do they recognize that non-uniform stress states may alter the strength of the material. Based upon test data, the creep damage rules are modified as described in subsequent paragraphs to allow the use of a peak stress to rupture design curve.

Modifications to Creep-Fatigue Damage Rules

49 | In cases where, in the service life of the component, all three principal stresses are clearly compressive during a hold period, the creep-fatigue evaluation shall be modified as described herein. If prerequisites for the use of the modified rule are not met for a portion of a component's life, the creep-fatigue rules of T-1400 of Code Case 1592 shall be used without modification for that portion of the component's life. The modified rule is described in items (1) to (7), where (1) to (5) are prerequisite conditions, and item (7) is a final applicability criteria to be satisfied.

- (1) None of the three principal stresses is tensile during hold period.
- (2) The material is austenitic stainless steel type 304 or 316.
- (3) Metal temperature does not exceed 1200°F.
- (4) The structure does not require a Code Stamp under existing Code rules.
- (5) Simplified or rigorous inelastic analysis is used.
- (6) Subject to the above limitations, creep-fatigue damage may be calculated in accordance with T-1400 of Code Case 1592 as modified by the following steps.

Step 1 - Calculate the fatigue damage in accordance with T-1411, -1412, -1413, and -1414.

Step 2 - Calculate the creep damage in accordance with T-1411 and T-1420.

Step 3 - Multiply the cumulative creep damage by 1/f, taking f = 5, for those hold periods where the stress is compressive, i.e.

$$\frac{1}{f} \sum_{k=1}^{q_1} \left(\frac{t}{T_d} \right)^k, \text{ where } q_1 \text{ are the compressive holds.}$$

Step 4 - Calculate the total damage including creep damage from conditions where the principal stresses are not clearly compressive, i.e.,

$$\sum_{j=1}^p \left(\frac{n}{N_d} \right)^j + \frac{1}{f} \times \sum_{k=1}^{q_1} \left(\frac{t}{T_d} \right)^k + \sum_{k=q_2}^q \left(\frac{t}{T_d} \right)^k = D_e$$

Step 5 - The acceptability of the damage (D_e) is determined in accordance with T-1411. The creep-fatigue damage envelope is shown in Figure 4.2-47A (Figure T-1420-2 of Code Case 1592). If the total damage (D_e) falls within the envelope, the damage level is acceptable.

D_e is plotted on Figure 4.2-47A and the allowable damage (D) is the sum of the allowable creep and fatigue damage components at the intersection of the damage envelope and a line extended from the origin through D_e . See Figure 4.2-47A.

53 |

53 |

53 |

49 |

$$D = \sum \frac{n}{N_d} + \sum \frac{t}{T_D}$$

To meet criterion: $D_e \leq D$

- (7) A cycle limiting criterion is required to verify the applicability of the modified rule. The effective number of allowable design cycles is:

$$n_e = n \left(\frac{D}{D_e} \right)$$

Where n is the total number of significant strain cycles between hold periods. Low amplitude high cycle strain fluctuations (such as normal power fluctuations) need not be considered in n if they are elastic excursions that result in negligible fatigue damage.

For the modified rule to be applicable, n_e shall not exceed 3000 for type 316 stainless steel nor 6000 for type 304 stainless steel.

Modification of Creep Damage Rules

In cases where a local stress concentration exists, the creep-fatigue damage evaluation may be modified as described herein.

- (1) The material is austenitic stainless steel Type 304 or 316 solution treated.
- (2) The structure does not require a Code Stamp under existing Code rules.
- (3) Simplified or rigorous inelastic analysis is used.
- (4) Stress rupture test data of the same type of stress concentration with similar geometric proportions tested at prototypic temperatures are used as a basis for modification of the Code Strength. The test temperature may be higher than the service temperature in order to more closely simulate the actual component lifetime and the stress level.
- (5) The notched stress rupture data shall be from specimens which are comparably or more severely loaded than the component, i.e., membrane loading of a notched specimen should be more severe than a gradient loading.
- (6) The stress rupture test data include data up to 1/60 of the component lifetime at prototypic temperatures or the equivalent when a short-time high temperature combination is used to simulate the desired long-time service environment.
- (7) Subject to the above limitations, the creep damage may be calculated in accordance with F9-4T and Code Case 1592 with one of the following modifications.

- (A) Use a peak stress-to-rupture design curve based upon the stress-to-rupture design curve in Code Case 1592 adjusted for the influence of a non-linear stress state caused by the presence of a geometric stress concentration.
- (a) Determine the smooth specimen stress rupture strength curve by tests of the same material at the temperature of interest.
 - (b) Determine the stress rupture strength curve with the presence of the geometric stress concentrations under the same conditions in (a) with specimens of the same heat of material with the same histories. Analytically determine the peak stress rupture strength in terms of "peak stress" vs time to rupture.
 - (c) Ratio the Code Case 1592 stress-to-rupture design curve by the ratio of (b) divided by (a). This must be done for at least 3 points in time with a separation in time of at least two orders of magnitude. In cases where the strength ratio varies with lifetime, the lesser of the value extrapolated to the component lifetime or the experimental value for the longest duration tests shall be used.
 - (d) Use the greater of the creep damage using this modified rule and the creep damage using the stress unaltered by the stress concentration and the Code Case 1592 stress-to-rupture design curve.
- (B) If tests subject to the above limitations (1 through 6) show no decrease in rupture life for prototypic notch geometries, calculate the component creep damage neglecting the stress concentration due to the notch. No reduction in damage below the damage using the stress unaltered by the stress concentration and the Code Case 1592 stress-to-rupture design curve shall be used.

- (8) The total creep-fatigue damage is determined by adding to the creep damage and fatigue damage calculated in accordance with T-1411, -1412, -1413, and -1414 of Code Case 1592.
- (9) The allowable creep-fatigue damage (D) is determined from the lesser of the values from Figure T-1420-2 of Code Case 1592 (See Figure 4.2-47a) and an average of test values from creep-fatigue interaction tests of notched specimens.

High Cycle Strain Controlled Fatigue Limits

For those 304 and 316 Stainless Steel components which are outside ASME Code jurisdiction, the fatigue damage for strain controlled cyclic deformations in excess of 1×10^6 cycles may be evaluated using allowable strain ranges obtained from Figure 4.2-47B, provided metal temperatures do not exceed 1100°F. Fatigue life reduction factors must be applied independently for slow strain rates and hold times, in accordance with ASME Code requirements.

Equivalent strain range shall be used to evaluate whether or not the allowable strain range limits have been met. The equivalent strain range value for entering the curve shall be calculated in accordance with the procedures specified in ASME Code Case 1592 except that one of the following formulations shall be used:

Formula 1. When the elastic and plastic components of the total strain range are not known, the equivalent strain range shall be calculated as:

$$\Delta \epsilon \text{ equiv.} = \frac{\sqrt{2}}{2(1 + \nu)} \left[\Delta(\epsilon_1 - \epsilon_2)^2 + \Delta(\epsilon_2 - \epsilon_3)^2 + \Delta(\epsilon_3 - \epsilon_1)^2 \right]^{1/2}$$

where ν = Poisson's ratio for elastic strains.

Formula 2. When the elastic and plastic components of the total strain range are known, the equivalent strain range shall be calculated as the sum of equivalent elastic strain range.

$$\Delta \epsilon \text{ equivalent}^e = \frac{\sqrt{2}}{2(1 + \nu)} \left[\Delta(\epsilon_1 - \epsilon_2)^2 + \Delta(\epsilon_2 - \epsilon_3)^2 + \Delta(\epsilon_3 - \epsilon_1)^2 \right]^{1/2}$$

and equivalent plastic strain range

$$\Delta \epsilon \text{ equivalent}^p = \frac{\sqrt{2}}{3} \left[\Delta(\epsilon_1 - \epsilon_2)^2 + \Delta(\epsilon_2 - \epsilon_3)^2 + \Delta(\epsilon_3 - \epsilon_1)^2 \right]^{1/2}$$

where ν = Poisson's ratio for elastic strains.

Formula 3. The following formula is included as an alternative to formula 2 as it represents the method of calculating total equivalent strain range employed in some computer routines, e.g. ANSYS. The total equivalent strain range is calculated as:

$$\Delta \epsilon \text{ equiv.} = \frac{\sqrt{2}}{2(1 + \nu_g)} \left[\Delta(\epsilon_1 - \epsilon_2)^2 + \Delta(\epsilon_2 - \epsilon_3)^2 + \Delta(\epsilon_3 - \epsilon_1)^2 \right]^{1/2}$$

where ν_g is a generalized Poisson's ratio found as:

$$\nu_g = 0.5 - (0.5 - \nu) (E_s/E)$$

where ν = Poisson's ratio for elastic strains

E_s = The material secant modulus prior to the last plastic strain increment

E = The material elastic modulus

4.2.2.3.3 Additional Material Properties

4.2.2.3.3.1 Inconel 718 Fatigue Properties

The Alloy 718 design fatigue curves Figures 4.2-48 and 4.2-49 shall be used as interim data until their inclusion in the NSM Handbook. Modulus and mean stress corrections should be made to the data of Figure 4.2-49. The effects of the fabrication processes and service environment on the structural integrity of the UIS shall be considered. The effect

of grain size on the behavior of Alloy 718 shall also be considered. The ASTM grain size for Alloy 718 shall be specified to satisfy the fatigue environment existing in each part of the UIS design.

4.2.2.3.3.2 Environmental Effects on Material Properties

4.2.2.3.3.2.1 Sodium Effects

Most of the data used to define the allowable design stresses in the ASME Boiler and Pressure Vessel Code were obtained from mechanical tests conducted in air. The code requires the designer to account for environmental effects in his assessment of structural integrity.

This section describes the effects of the sodium environment upon the response and failure characteristic of the structural materials and the use of these sodium environmental factors in design evaluation. These factors are dependent only on the service temperature. The effects of loss of carbon plus nitrogen (C + N) on Types 304 and 316 stainless steel (annealed) are to lower the yield and ultimate strength, increase the elongation, and reduce the stress to rupture life.

References pertaining to effects of sodium, carbon and nitrogen on mechanical properties of materials are listed in references 104-135, 150-152 and 185.

Primary Stress Limits

The primary stress limits are based on S_u , S_y , S_r , onset of tertiary creep and stress to achieve 1% creep strain. In determining the primary stress limit, the stress to rupture value is degraded by:

- a fixed percent per Figure 4.2-48C for sodium exposure, and
- an amount per Figures 5.3-6 and 5.3-7 based upon the change in the average C+N concentration at the end of life.

The yield and ultimate strengths are degraded an amount per Figures 4.2-48L and 4.2-48M based on the average C+N concentration at the end of design lifetime.

Primary Plus Secondary Limits

When elastically calculated stresses are being evaluated, the design stress limits are modified based on the effect of the average C+N concentration on the S_u , S_y , and S_r properties. In addition, the effects of the exposure to sodium on the S_r value (Figure 4.2-48C) is considered.

When inelastic analysis is used to determine the actual strains for comparison to the inelastic strain limits, the effects of the average C+N content upon the response characteristics (e.g., stress-strain equation) is considered. As an alternate, the inelastic analysis may be performed using time and position dependent material properties which account for the current C+N profile.

Creep-Fatigue Damage

In performing the creep-fatigue evaluation, the effect of the local C+N concentration at the point of interest is considered.

Effects of Liquid Sodium on Mechanical Properties

Two effects may occur due to continued exposure to liquid sodium. These are surface effects and interstitial transfer effects.

1. Surface Effects

The interactions of the sodium environment with the material being tested, excluding interstitial transfer effects, may be defined as surface effects. Compared with air testing, liquid sodium may cause certain metallic elements to be transferred from the hotter to the cooler regions of LMFBR systems. In addition, surface oxidation in liquid sodium is greatly reduced when compared to air testing. These surface effects are insignificant in their influence on short-term tensile properties.

For time-dependent deformation, such as stress-rupture and fatigue, the effects of a liquid sodium environment are complex and need to be considered in detail. In the case of stress-rupture, it has been shown that for a given temperature and stress, rupture times in air are longer than those in liquid sodium. Figure 4.2-48C gives a sodium-environment correction factor which may be applied to the rupture strength data specified in ASME Code Case N-47 or Code Case 1592 for Types 304 and 316 austenitic stainless steel. This effect should be used in all evaluations where stress to rupture is involved.

Fatigue properties of materials can be greatly affected by the environment in which the properties are measured. The avoidance of excessive surface oxidation by testing in sodium (or inert gas) instead of in air increases the cycles-to-failure for a given strain range. No increase in the design fatigue limits due to exclusion of oxygen effects is taken at the present time.

2. Interstitial Transfer Effects

In an all-austenitic decarburizing LMFBR system, interstitial carbon and nitrogen are transferred from the hotter to the cooler regions. This leads to weakening in the decarburized and denitrided regions and to strengthening in the carburized and nitrided areas. In the case of fatigue behavior however, the effects of interstitial absorption at the surface are complicated because of two concurrent mechanisms. On the one hand, it can lead to enhanced crack nucleation at carbide particles and, on the other, surface strengthening during strain-controlled fatigue will increase the proportion of elastic straining which is less damaging than plastic deformation.

In austenitic/ferritic LMFBR systems, studies indicate that, in general, the austenitic materials will be carburized and the ferritic materials will lose interstitials. However, the cross-over carburization to decarburization is system dependent and it is likely that, in certain systems, at least some of the austenitic material will be decarburized.

Reference 185 and the following subsections describe procedures by which the extent of interstitial transfer for Types 304 and 316 stainless steel for LMFBR components can be determined, and from this, the effects on mechanical behavior may be calculated. Procedures are given for calculating surface and average interstitial concentrations and interstitial gradients for Types 304 and 316 stainless steel under decarburizing and denitriding conditions. Since these values are system dependent, the necessary system conditions must be supplied for the calculations.

Effects of Sodium Exposure on Short-Term Tensile Properties

Since the principal effect of sodium exposure in the high-temperature regions of an LMFBR is to remove interstitials, the short-term tensile behavior of Types 304 and 316 stainless steel may be estimated by directly considering the effects of (C + N) level on the mechanical properties. Such an approach is necessary because of the scarcity of

data on sodium-exposed materials. For solution treated Type 304 stainless steel, the average yield strength, ultimate tensile strength, and uniform and total elongation may be given by the equations in Table 4.2-30. For solution-treated Type 316 stainless steel, the equivalent equations are given in Table 4.2-31, and Figures 4.2-48L and M.

These equations are strictly valid for materials containing uniform distributions of interstitials, but they may be used to estimate the behavior of materials containing interstitial gradients. In these cases, the (C + N) concentration represents the bulk average interstitial concentration.

To determine the effect of decarburization on the minimum anticipated yield strength (S_y) for use with primary stress limit checks at a given temperature, the following procedure is used:

- (a) The average (C+N) concentration is determined using the technique described above.
- (b) The decreased yield strength due to interstitial depletion is calculated from the equations described above and in Reference 185 assuming that the starting interstitial level is known.
- (c) The S_y values in the ASME Code are then decreased to these modified values representing the sodium exposure effects.

When the starting carbon concentration in the component is less than 0.04 weight percent, the S_y values for L grade material are used. Decarburization and denitriding will require the L grade S_y values to be modified in a similar way to those for regular grade alloys described above.

Determination of the effects of interstitial transfer on the design stress, S_m , follows a similar procedure to that described above, with additional calculations of effects on the ultimate tensile strength. For ASME Class 1 components, the design stress, S_m , is defined as the lowest of the following stresses:

- (I) 1/3 of specified minimum UTS at room temperature
- (II) 1/3 of the UTS at temperature ($\frac{1.1}{3}$ for 304/316)
- (III) 2/3 of the specified minimum yield strength at room temperature

- (iv) 90% of the yield strength at temperature for austenitic stainless steels and 2/3 of the yield strength for other materials.

Effect of Sodium Exposure on Stress-Strain Curves

Data exist to show that, for Types 304 and 316 stainless steel, the following relationship is valid:

$$\sigma = A(t) \cdot e^n \quad (11)$$

where: σ = engineering stress

ϵ = engineering strain

$A(t)$ = a constant at constant temperature

n = a strain-hardening coefficient which may be temperature dependent

From Figure 4.2-48G the stress-strain relationship for a specified temperature and interstitial level may be computed using the equations in Table 4.2-30 for Type 304 stainless steel and those in Figures 4.2-48L and M for Type 316 stainless steel. Note that the calculated stress-strain curves are strictly valid for alloys containing uniform interstitial distributions.

However, approximate stress-strain curves may be obtained for materials containing interstitial gradients by inserting bulk average (C+N) concentrations into the equations.

For analysis in which the stress-strain characteristics are considered to vary as a function of (C+N) the value of each point of interest as a function of time may be determined. The equations mentioned above are used to determine the instantaneous stress-strain relationship.

Alternatively, if the stress strain curve is known for the material, it can be reduced by the sodium effects factor K_N which is obtained from the expression:

$$K_N = \frac{\sigma_y(C+N)}{\sigma_y(C+N)_0}$$

where

$\sigma_y(C+N)_0$ is the interstitial level of carbon plus nitrogen concentration before sodium exposure, and $\sigma_y(C+N)$ is determined from Figure 4.2-48L for the particular location of interest.

Effect of Interstitial Transfer on Stress-Rupture Properties

It can be shown that losses in carbon and nitrogen reduce the rupture strength of Types 304 and 316 stainless steel. Figures 5.3-6 and 7 give correction factors which are used to evaluate this effect.

In evaluating primary stress limits the first requirement is to calculate the new average (C+N) for the component of interest, using the technique described previously. Assuming that the rupture strength is determined by the bulk average (C+N), then the percentage decrease in rupture strength resulting from interstitial depletion is obtained from Figure 4.2-48J. This interstitial transfer factor is then added to the surface-effect factor to give the total modification to the stress-rupture curves given in ASME Code Case.

A similar analysis may be used to modify the S_t design stresses.

For creep-fatigue evaluation the rupture strength decrease at the point of interest is determined by reducing the Code value by a factor from Figures 5.3-6 and 7 using the (C+N) at that point.

Effect of Interstitial Transfer on Strain-Controlled Fatigue Properties

It is well known that fatigue failure is initiated at the metal surface. When a surface crack is formed, the stress concentration at the crack tip causes it to propagate relatively quickly until complete failure occurs. The total cycles-to-failure may be given by the sum of N_i and N_p , where N_i is the number of cycles to cause crack initiation and N_p is the number of cycles to cause the crack to propagate to failure.

An indication of the effect of interstitial transfer can be seen in the Type 316 stainless steel fatigue data in Figures 4.2-48I and 4.2-48K. For room temperature and 1200°F tests in air, the fatigue life is larger for the lower interstitial concentrations. This is likely to be caused by the smaller amount of carbide in low-carbon material since previous work has shown that fatigue cracks are preferentially formed at this brittle phase.

For CRBRP components in the high-temperature locations, where surface interstitial losses occur, the fatigue life would be expected to increase. Because of the absence of applicable data on strain-controlled fatigue behavior in sodium it is not currently possible to quantify this effect. It appears, however, that a substantial increase in fatigue life will result for materials exposed to high-temperature sodium environments. However, until there are data to predict the magnitude of this effect, and the role of nitrogen is known, it is suggested that no correction for interstitial transfer be made to the fatigue curves.

Corrosion Effects

The design of the internals will account for the corrosion effects of flowing liquid sodium. Figure 4.2-48A and 4.2-48B are included for Type 304 and 316 SS (Ref. 50) and Inconel 718 (Ref. 51). It can be seen from the curves that negligible corrosion effects will occur for those materials even at the maximum design temperature of 1208°F. It should be noted that the austenitic stainless steel corrosion rate has been normalized with respect to oxygen content in the sodium, whereas nickel base alloys, such as Inconel 718 have corrosion rates independent of oxygen content. Few specific data are available for the Type 304 SS w/chrome plate and the Inconel 600; however, those materials are located in a relatively low temperature (775°F) region of the reactor and the available data (Ref. 52) lead to the conclusion that negligible corrosion effects are to be anticipated over the life of the reactor.

3. Combined Surface and Interstitial Transfer Effects on 316 SS Stress Rupture Strength

Stress rupture strength of 316 SS is affected by both surface and interstitial transfer effects in a sodium environment. The following approach should be used in combining these effects on stress rupture and S_t allowables.

Define the % change in rupture strength per subparagraph 1 above for surface effects.

Define the % change in rupture strength per subparagraph 2 above for interstitial transfer effects.

Define the total rupture strength degradation (F) by the following:

$$F = (F_{NI}) (F_{NS})$$

where

$$F_{NI} = (100 - \% \text{ reduction due to interstitial transfer effects})/100$$

$$F_{NS} = (100 - \% \text{ reduction due to surface effects})/100$$

4.2.2.3.3.2.2 Irradiation Effects

The effect of irradiation on material properties is obtained from Reference 1. When additional considerations are necessary, a description is provided in the appropriate component evaluation.

4.2.2.3.3.3 Friction, Wear, and Self Welding Considerations

The CRBRP Lower Inlet Module and Fuel Assembly components which interface or contact during normal operation at a temperature 730°F include:

<u>Fuel Assembly</u>		<u>Lower Inlet Module</u>
Inconel 718 w/chrome plate piston ring	-against-	Inconel 718 receptacle
Type 304 SS w/chrome plate fuel nozzle	-against-	Inconel 718 receptacle

No data is available for the above interfacing couples. However, data on less compatible types have been documented. Previous experience in EBR II (Ref. 48) combined with data obtained from tests at ARD (Ref. 49) indicate that self welding will not occur at temperatures below 800°F. The EBR II experience included chrome plated Type 304SS working against uncoated Type 304SS. ARD experience included Type 304 against Type 304 and alloy A 286 at pressure up to 30,000 psi for 6 months. Thus, it has been concluded that the additional precautionary measure of hard coating and the use of dissimilar metals will preclude the galling and self welding of the interfacing material at the expected operating temperature of 775°F. Tests are being conducted on all CRBRP material pairs including those listed above.

Information on the friction, wear, and self-welding properties of various mating materials in the reactor internals obtained through a national program which took into account specific component requirements may be found in References 79 through 94. The materials couples tested include Inconel 718/Inconel 718 (Refs. 79-86, 89, 91); chromium carbide/chromium carbide (Refs. 81, 94), Type 316SS/Type 316SS (Refs. 80, 90); Inconel 718/Chromium Plate (Refs. 90, 94); Haynes 273/Inconel 718 (Refs. 86, 91); Inconel 718/Type 304SS (Ref. 79); Inconel 718/Type 316SS (Refs 80, 89); Inconel 718/Ni Resis (Ref. 91); 17-4 PH/Inconel 718 (Ref. 91); and Stellite 6B/Inconel 718 (Refs. 79, 92). Friction and self-welding data are available at temperatures up to 1200°F where testing has been performed in both liquid sodium and sodium vapor environments. Most of the tests have been conducted on as-received material, but a small amount of data exists for sodium pre-exposed and for neutron-irradiated samples. Although there appears to be a slight deterioration in friction properties due to sodium pre-exposure, none at all seem to result from neutron irradiation.

The above referenced test data comprise several hundred pages of test results. To assure disassembly after operation of certain reactor internals (replacement of core assemblies, lifting upper internals), reduction and use of this test data for design information is described below:

The principal reactor internals components involved in normal dis-assembly (refueling) operations are: the Upper Internals Structure (UIS), the Core Former Structure (CFS) and the Core Restraint System (CRS). In these items, sliding motion occurs in two friction couples; between the UIS keys and the CFS keyways and the second between reactor assembly duct load pads. Neither of these couples is a safety related item in that motion between mating parts of the couples needs to occur only during reactor refueling operations. Any increased friction would be an operational concern only.

1. Friction Couples

531 Preliminary selection of the mating couple materials has been
531 made for the preliminary designs of the UIS, CFS and reactor
assembly duct load pads. The UIS key to CFS keyway couple is
Haynes 273 against Alloy 718 at $400 \pm 50^{\circ}\text{F}$ in sodium with
approximately one year soak at approximately 1000°F . The
couple between the load pads is chromium carbide against
chromium carbide at $400 \pm 50^{\circ}\text{F}$ with approximately one year
soak at the assembly outlet sodium temperatures. Coefficients
of friction to be used in preliminary design are shown in
Tables 4.2-31A, and 31B. Test data will be used as the design
is preliminary, final selection of mating materials is yet
to be made, and the use is not safety related.

2. Antigalling Characteristics

Tables 4.2-31A and 31B show friction testing data of candidate samples.

3. Irradiation Stability

No irradiation test data is available for Haynes 273 against Haynes 273. However, the maximum fluence at the UIS key to CFS keyway location is 1.4×10^{19} n/cm². The probability for radiation damage at this fluence is very small.

51 Table 4 lists coefficients of friction measured after irradiation of the chromium carbide test specimens in EBR II to approximately 1×10^{22} n/cm². Additional chromium carbide specimens are being irradiated in EBR II to higher fluences.

4.2.2.4 Evaluation

4.2.2.4.1 Lower Internals Structure

This section discusses the stress and thermal analyses of the following components:

- Core Support Structure
- Lower Inlet Module
- Bypass Flow Module
- Fixed Radial Shielding
- Fuel Transfer and Storage Assembly
- Horizontal Baffle
- Core Former Structure

These components were all analyzed for the critical loading condition and shown to meet the governing structural criteria. Further details are reported in each subsection.

59

4.2.2.4.1.1 Analysis of Core Support Structure (CSS)

Alternate Low Temperature Design Criteria

Section III of the ASME Code provides stress limits for austenitic steels for temperatures up to 800°F. The design temperature of the lower CSS is 775°F; however, during some thermal transient events the maximum metal temperature does exceed 800°F for short periods of time.

Since the time-dependent failure modes were shown to be significant for the CSS by satisfying the conditions of Test No. 4, Code Case 1592 and RDT F9-4, the alternate structural limits of the code case were employed in the CSS evaluation.

Geometry

The core support structure (CSS) concept considered in this analysis is shown in Figure 4.2-50. The CSS consists of a perforated support plate, core barrel, and lower inlet module liners. Portions of the support core and reactor vessel, are included in the analytical model, and all of these components are referred to as the "core support structure" in this analysis.

Thermal Analysis

Two thermal models were developed to calculate transient temperatures in the CSS. A 30 degree sector model (TAP-A computer code) was used to calculate temperatures in the perforated support plate and an axisymmetric model (ANSYS finite element code) was used to determine temperatures in other CSS components. The element geometry of the thermal models is identical with the corresponding stress models shown in Figures 4.2-52 and 4.2-54.

The sector and axisymmetric models were used to analyze the CSS-6N (N-4a as described in Appendix B of this PSAR), CSS-2U (U-2e), CSS-4U (U-18) and CSS-1E (F-4a) design transients for the CSS. It was shown that these four transients conservatively umbrella all of the plant duty cycle events.

Reactor inlet plenum mixing analyses were performed to determine the transient sodium boundary temperatures for the CSS. Convective heat transfer coefficients were calculated for the CSS surfaces exposed to flowing sodium. Interface conditions with the lower inlet modules (LIMs) were determined with detailed local models.

Structural Analysis Models

The ANSYS finite element computer program in conjunction with the "equivalent solid plate" method of analysis for perforated plates (Article A-8000 of Ref. 33) was used to perform the detailed structural analysis of the core support structure. Two types of finite element models were used in this analysis. The axisymmetric model (Figure 4.2-51) was used to calculate stresses in parts of the CSS other than in the perforated region.

The perforated plate region of this model defined by R* in Figure 4.2-51 was modeled by using the equivalent solid plate method of analysis for perforated plates. In this method, the perforated plate is replaced by a solid plate which is geometrically similar to the perforated plate but has modified values of elastic constants. The effective elastic constants E^* and ν are functions of the ligament efficiency, η . The deflections computed using conventional methods are correct; however, the actual values of the stress intensities in the perforated plate are determined by applying multiplication factors to the nominal stresses computed for the equivalent solid plate. The second model used in the analysis is shown in Figure 4.2-52. This model essentially substructures the perforated region of the core support plate by having boundary conditions applied at the sector periphery correspond to conditions at the equivalent location in the axisymmetric model for the transient time being analyzed. A third model was used in the analysis which is unrelated to the previously described models. Figure 4.2-53 illustrates the lower inlet module liner model used for calculating both primary and secondary stresses. In addition, the key structural evaluation sections are detailed to identify critical regions in the structure.

Structural Analysis

The CSS was analyzed for pressure, dead weight, OBE and SSE seismic, and the thermal transients using the structural models previously described.

The dead weight load used in this analysis is obtained by adding elements to the model shown in Figure 4.2-50 to correctly simulate the masses of the core assemblies, lower inlet modules, bypass flow modules and core former structure. The modified finite element model is shown in Figure 4.2-54.

The CSS axisymmetric model (Figure 4.2-54) was used to evaluate the primary stresses due to the seismic loads using ANSYS. Results of the seismic analysis indicated that OBE and SSE stresses are generally low, with the minimum margin-of-safety being conservatively calculated as 0.77 for the faulted event.

Thermal stresses were calculated in the CSS for the thermal transients using the CSS axisymmetric and sector models with the internal temperatures which were calculated in the thermal analysis.

Structural Evaluation

Five sections in the CSS axisymmetric model shown in Figure 4.2-51 and 10 sections of the core support plate sector model shown in Figure 4.2-52 were selected for the structural evaluations. These sections represent the high stress areas in the CSS structure, and their selection was based on a thorough review of the finite element stresses for pressure, dead weight, seismic, and the thermal transients.

The primary plus secondary stress intensity limit of 1.5 S_m was reduced to 1.35 S_m in the perforated region of the core support structure. This reduction was made to account for the actual bending shape factor for the geometry of the ligament. The 1.5 shape factor is only applicable for a rectangular cross section.

The primary, primary plus secondary, and fatigue evaluation results are summarized in Table 4.2-23. These data are limited to the maximum of each stress intensity category for the locations identified in the table. Simplified Inelastic analysis techniques were utilized to show that the areas with primary plus secondary stress intensity values exceeding the 3 S_m allowable limit are acceptable. A fatigue factor of 0.9 was used in evaluating the fatigue damage in the area of the full penetration weld, Section C-C, Figure 4.2-51. This factor is imposed to meet the requirements in paragraph 4.2.2.3.1.1 for the method of examination employed.

4.2.2.4.1.2 Analysis of Lower Inlet Module (LIM)

51 | The LIM was analyzed to the requirements for the criteria listed in Section 4.2.2.3.1.2. Because of the complicated geometry of the LIMs and the varying thermal/hydraulic environment on each of the 61 units, a number of finite element models were developed for the analysis. Two separate LIM designs are analyzed which envelop the existing configurations. These two basic cases analyzed are for a peripheral module and a central module (See Figure 4.2-50). Cross-sections at four different elevations were analyzed with at least one finite element model generated at each section for both cases.

Primary stresses in the LIM are due to deadweight, differential pressure, seismic events and IVTM loads, while secondary stresses are generated by thermal loading. In particular, the U-18 (Loss of all offsite power) and the F-4a (Saturated steam line rupture) thermal events from Appendix B were analyzed since these were shown to be enveloping down and up umbrella events respectively.

59 | Results of the load controlled portion of the analysis indicate that all applicable requirements are satisfied with the minimum margin-of-safety being 1.09 in the conservatively modeled upper body region of the LIM. Similarly, secondary stresses are relatively low in the component with the greatest fatigue damage occurring in the peripheral module stem and having a magnitude of 0.354.

4.2.2.4.1.3 Analysis of Bypass Flow Modules (BPFM)

59 | Geometry

38 | The BPFM geometry and relationship to adjacent components is shown in Figures 4.2-41A & 4.2-41B. Each individual module is composed of an upper forging with holes for the RRS assembly receptacles, side wall plates, and a bottom plate as shown in the section view of Figure 4.2-41B. The geometries of two analytical models are shown in Figures 4.2-63A & 4.2-63B.

Thermal Analysis

51 | The ANSYS finite element program was used to perform the heat transfer analysis of the BPFM for the most adverse thermal transients considered. Two finite element models were developed to calculate the transient temperatures. The outside half of the BPFM was modeled for two-dimensional analysis to determine the critical region in the BPFM due to the most severe transient event. A one-eighth section, three dimensional finite element model was developed for the critical region evaluations.

38 | The U-18 duty cycle was concluded to be the most adverse transient for the BPFM. The most severe temperature gradients occur in the interval

900-1000 seconds, near the termination of the steep down temperature transient. From this data the Intervals Stress Analysts identified the region of the BPFM requiring further detailed analysis.

Figure 4.2-63A shows the three-dimensional thermal model of the BPFM developed cooperatively with the Stress Analysts. In addition to one corner of a BPFM, the model includes the core barrel and stagnant sodium at the side and end walls. Comparison of the two-dimensional analysis temperature contours with those from a similar plate of the three-dimensional analysis shows good agreement between the models.

Structural Analysis

59 | The structural integrity of the BPFM was evaluated to Subsection NG, Section III, of the ASME Boiler and Pressure Vessel Code. Along with the thermal transients, the seismic loads, differential pressure load, loads due to core former misalignment and duct bowing, and transient mechanical loads due to the transfer operations of the Removable Radial Shield (RRS) assemblies have been investigated.

The functional requirements of the module to module connecting lugs and pins and the BPFM/CSS connecting pins were evaluated for seismic loads using a 3-D finite element model composed of the six interconnected modules. The structural evaluation results for the most critical loads (OBE) versus the Code criteria are given in Table 4.2-29A, showing positive margins in every area.

9 | For the evaluation of the BPFM body, a perforated thick plate model was used to study the IVTM transient mechanical load. The differential pressure load was evaluated using the one-eighth 3-D BPFM Solid Model (shown in Figure 4.2-63B) plus the perforated thick plate model. Thermal transient stresses were evaluated using the one-eighth BPFM solid model in conjunction with all of the above mentioned mechanical stresses. The BPFM inlet port region where the bypass flow is fed into the BPFM mixing chamber from the CSS was also analyzed, using an axisymmetric finite element model. This region proved to be the most critical area of the BPFM body.

59 | 38 | 38 | The minimum margin of safety in the structure is 0.23 for the bearing stress between the BPFM body and the CSS. The minimum margin of safety in the entire component is 0.64 for the primary stress intensity category. A simplified elastic-plastic analysis was performed to show that the structure does shake down to elastic action during its service life. The maximum calculated creep fatigue damage is 0.27 compared with an allowable of 1.0. In conclusion, the BPFM has been shown to meet all of its design requirements.

4.2.2.4.1.4 Analysis of the Fixed Radial Shield (FRS)

59 | This section summarizes the stress analysis performed on the Fixed Radial Shield (FRS) and is based on the requirements of the criteria listed in Section 4.2.2.3.1.3. The load controlled portion of the analysis was

conducted using the 3-D solid finite element model shown in Figure 4.2-75. Since the three segments of the shield are identical, only one sector is modeled. Deadweight, vertical seismic and landing loads on the structure are minimal and do not generate any significant stresses. The only primary load then considered is horizontal seismic. The primary stress tabulation at the critical locations in the FRS is shown in Table 4.2-29D. All primary limits are satisfied for the FRS and its attachment pins. Mode frequency analysis conducted on the FRS indicates a fundamental mode frequency of 67 Hz, precluding any possibility of dynamic amplification.

Strain-controlled stresses in the FRS were also calculated using finite element modeling techniques. The primary source of elevated temperatures in the FRS is due to nuclear heating where the center of the shield remains hot while the surfaces are cooled from being washed by sodium. By analyzing steady-state, U-18 and U-2B transients, the most critical thermal events are analyzed. Effects of neutron irradiation and sodium exposure are shown to either be small or to make the evaluation non-conservative, and were therefore ignored. Results of the secondary stress analysis indicate that creep/fatigue damage effects are small (0.055 out of an 0.9 allowable) and that strain limit requirements are satisfied.

4.2.2.4.1.5 Analysis of the Fuel Transfer and Storage Assembly (FT&SA)

The fuel transfer and storage assembly (FT&SA) was analyzed to the requirements listed in Section 4.2.2.3.1.3. Analyses performed show that the FT&SA satisfies ASME Boiler and Pressure Vessel Code Limits for primary type loadings. For this structure, primary loads include deadweight, OBE & SSE seismic and external pressure. A finite element model using 3-D beam elements is shown in Figure 4.2-76 which is used to determine load-controlled stresses. Results of a mode frequency analysis indicated a fundamental mode frequency of 30 Hz. Seismic stresses calculated in the tubes were shown to be small. Primary stresses in the lower support block region of the FT&SA are also shown to be small as indicated in Table 4.2-29E.

Finite element analyses were also used to generate temperatures and thermal stresses in the FT&SA. The thermal stress analysis of the tubes was conducted elastically for steady-state and the U-4 transient discussed in Appendix B.

The U-4 transient enveloped all thermal events to which the FT&SA is exposed. Results of the thermal stress analysis indicate that the creep/fatigue damages are well within the interaction envelope of code case 1592. In addition, the strain limit requirements are satisfied for the most critical section. Thermal analysis of the lower support block was conducted using a finite element model of a cross-section of the block. Results of this deformation controlled stress analysis indicate relatively low stress levels. Due to the low service temperature of the block no creep damage will occur. The fatigue damage was also low with a value of .149.

59

4.2.2.4.1.6 Analysis of the Horizontal Baffle (HB)

The Horizontal Baffle (HB) was analyzed to the criteria outlined in Section 4.2.2.3.1.3. Analysis results show that the HB satisfies the ASME Boiler and Pressure Vessel Code Criteria. HB plate stresses were obtained using finite element modeling techniques. Primary loads considered include deadweight, pressure, fuel transfer machine loads and seismic events. It was shown that there will be no dynamic amplification and the rigid plate can be analyzed seismically using maximum support accelerations. Table 4.2-29F indicates results of the load controlled analysis for the HB plate for loadings discussed above. All primary limits for the HB and interfacing components have been satisfied.

Loadings considered for the strain-controlled portion of the analysis are due to the plate preload and thermal transients. The transients examined in the analysis are the U-1, U-4 and E-2 events discussed in Appendix B, and envelop all thermal events. The thermal stress analysis was also conducted using finite element techniques. Structural evaluation of the results of the strain-controlled analysis indicate that all areas of interest demonstrate structural adequacy by elastic analysis except the HB plate. Resulting steady-state stresses and transient strain ranges are small enough so that the creep/fatigue damages are within the limits of Code Case 1592. A thermal striping assessment was made, results of which indicated negligible fatigue damage since the maximum potential is 4⁰F. Since the elastic stresses calculated in the HB plate were too high to meet the limits for elastic analysis, a simplified inelastic analysis was undertaken to demonstrate the structural adequacy of the part. Results show that total strain accumulated throughout the life of the component satisfy the allowables of 1%, 2% and 5% on average, linearized and peak respectively. The creep fatigue requirements are also satisfied.

4.2.2.4.1.7 Analysis of the Core Former Structure (CFS)

This section summarizes the results of the Core Former Structure (CFS) stress analysis. The evaluation is made to requirements of criteria used in Section 4.2.2.3.1.2. Primary stresses in both the upper and lower core former rings are determined by generating a 2-D in-plane finite element model. This model consists of beam elements with varying cross-sections to simulate both the irregularly shaped core former ring and the segmented inserts. Loads are applied to the upper ring through the 3 UIS keyways and 6 core barrel lugs, and to the lower ring through 12 equally spaced compression only azimuthal spacers. These loads are due to deadweight, seismic events, core misalignment and core reaction.

Mode frequency analysis was conducted on both the upper and lower geometries. The minimum fundamental mode was 66 Hz, on the upper ring, placing the structure in the zero period acceleration domain.

59 Results of the load controlled analysis determined that all primary limits were satisfied as required by the applicable criteria.

The deformation controlled stresses and strains were determined by a 2-D axisymmetric model of a cross section of the ring. The model used for both the thermal and thermal stress analyses of the ring is shown in Figure 4.2-77.

Thermal boundary conditions applied to the upper core former model were fluid temperatures applied through a convection coefficient in several different regions of the model as shown in the figure. The structure was analyzed elastically for the U-1b, U-2b, U-18 and E-16 thermal events which may be conservatively used to umbrella all other loadings.

All regions of the CFS were shown to be adequate using elastic analysis methods except the top surface of the upper ring. This area was shown to be adequate by simplified inelastic methods. The fatigue damage at this location was .414 with a creep damage of .239. This combination of damages falls within the creep fatigue interaction envelope of Code Case 1592.

4.2.2.4.2 Upper Internals Structure

This section presents the analysis performed in support of the final design of the Upper Internals Structure (UIS) and used to demonstrate the adequacy of this component for the expected service conditions and environment. The adequacy of the design is based primarily upon meeting the criteria of Section III of the ASME Boiler and Pressure Vessel Code, including Code Case N-47, and supplemented by RDT Standards F9-4T and F9-5T and special project structural design rules presented in Section 4.2.2.3.2 and 4.2.2.3.3. These special project structural design rules have been developed based on material properties testing. A summary of the components analyzed, material properties, structural design criteria, mechanical loads, thermal environment, methods of analysis and structural analysis is presented herein.

4.2.2.4.2.1 Components Analyzed

The major components of the UIS are identified in Figure 4.2-45. A brief outline of the functions of the UIS is given in Section 4.2.2.2.1.7. A list of the components of the UIS analyzed to demonstrate structural adequacy of the design are:

- o Lower Plate and Ligament
- o Upper Plate
- o Support Columns
- o Shear Webs
- o Core Barrel Key

- o Instrumentation Posts
- o Upper and Lower Shroud Tubes
- o Chimney Assemblies
- o Mixing Chamber Thermal Liners
- o IVTM Port Plug
- o IVTM Port Plug Cover

4.2.2.4.2.2 Material Properties

The ASME Code is the prime source for materials properties. For material properties not specified in Section III of the code or applicable code cases, the mechanical properties are based on the Nuclear Systems Materials Handbook TID-26666, RDT Standard F9-4T, RDT Standard F9-5T or the sources given in Section 4.2.2.3.3.

There are no irradiation effects on the mechanical properties of Inconel 718 or 316 stainless steel at the highest fluence levels attained at the end of its 30 year service life. The maximum fluence level is less than:

$$1 \times 10^{21} \text{ n/cm}^2$$

Type 316 stainless steel is a non-age hardenable alloy. Therefore, no significant changes in strength or hardness should result from long term exposures at temperatures up to 1100°F. Inconel 718 is an age hardenable alloy, however, the age hardening process does not result in significant reductions in mechanical properties when subjected to temperatures up to 1100°F for component lifetimes. No allowances have been made for the effects of thermal aging on the properties of either alloy. However, experimental material properties programs to study the behavior of both alloys due to the thermal environment and sodium exposure are discussed in Section 1.5.

The sodium effects of Section 4.2.2.3.3.2.1 are implemented in creep-fatigue damage evaluations of 316 stainless steel.

| CONTENTS OF THIS PAGE HAVE BEEN INTENTIONALLY DELETED.

Cyclic Hardening

A factor K_C is applied to alter the stress-strain curve yield surface.

where:

$$K_C = (-0.144 + 3.094 \Delta\epsilon)^{1/2} \text{ for } \Delta\epsilon > 0.36\%$$

If the strain range $\Delta\epsilon$ is $\leq 0.36\%$, then $K_C = 1.0$.

High Cycle Design Fatigue Strength

Stainless steel materials subjected to high cycle thermal fluctuations and flow induced vibration phenomena require a fatigue strength evaluation beyond the Code Case 1592 (N-47) curve limit of 10^6 cycles. The Code Case 1592 (N-47) curve is extrapolated beyond 10^6 cycles using a slope on cycles of -0.12 for load controlled situations. In cases where conditions are strain controlled, the special purpose high-cycle fatigue criterion, as described in 4.2.2.3.2.3, is used beyond 10^6 cycles.

4.2.2.4.2.3 Structural Design Criteria

The portion of the UIS within the reactor vessel operates at elevated temperatures above 800°F . Under these circumstances the UIS is classified as an elevated temperature structure and is designed and analyzed as an ASME - III Code Class 1 component.

Alternate structural design criteria have been adopted in the cumulative creep-fatigue damage rules of Code Case 1592 (N-47) and RDT Standard F9-4. These criteria assume that in compressive hold, creep rupture damage is 20% as damaging as the damage caused by the same sustained stress in tension. It applies for austenitic stainless steel (Types 304 and 316) at metal temperatures less than 1200°F (649°C). At times in the duty cycle when sustained stresses are tensile, damage is computed in accordance with Code Case 1592 (N-47).

4.2.2.4.2.4 Mechanical Loads

Design Loads

The design condition loads are the dead weight and pressure. The design temperature of the UIS is 1220°F.

Normal Loads

During normal operation, the UIS carries no mechanical load except its own weight and loads due to actuation of the control rod system. The upper shroud tubes carry the dashpot loads resulting from the primary control rod scram arrest accelerations, and the lower shroud tube is designed to react a 19,000 pound upward load incurred in exercising the control rod breakaway joint.

The UIS is designed to preclude the occurrence of adverse structural and dynamic effects due to flow induced vibration. Where possible, the entire structure and its components are designed such that their natural frequencies do not coincide with any vortex shedding frequencies. Component mechanical stresses caused by flow induced vibration are required to meet the limits of the ASME Boiler Code Section III and Code Case 1592 (N-47) for normal conditions to ascertain structural integrity with regard to fatigue.

During refueling operations, the UIS is raised and lowered so that the rotating plugs may be positioned to provide access to various reactor locations. Misalignment of the UIS keys with respect to the keyways in the CFS will cause loads between the keys and keyways. Both the normal and frictional force resulting from this misalignment are considered in the analysis.

Upset Loads

The upset mechanical loads on the UIS are the seismic input for the operating basis earthquake (OBE). The UIS is designed for OBE in accord with the criteria described in Section 3.7.

Emergency Loads

The UIS is designed to accommodate loads due to loss of primary holddown (hydraulic balance). Loss of hydraulic balance is classified as an emergency event and is assumed to occur five times, but for conservatism it is analyzed as an upset event.

The UIS is designed to withstand the effects of a safe shutdown earthquake (SSE). The SSE is a faulted condition, however, to be conservative, the UIS is designed to satisfy the ASME Code criteria for emergency conditions when in the operating configuration and subjected to the SSE loads.

59 | 4.2.2.4.2.5 Thermal Environment

Operating conditions for the UIS are specified in a 30 year histogram using the ASME Code categories of normal, upset, emergency, and faulted conditions for the mechanical loads and steady state and transient temperatures. Plant capacity is 75% giving a full power life of 22.5 years.

Normal Loads

59 | The UIS is designed to accommodate thermal striping during normal operation. The UIS surfaces directly exposed to the more severe thermal striping are the instrumentation posts, control rod shroud tubes, keys, the internal surfaces of the chimneys, and the UIS mixing chamber. Sodium exiting from the chimneys will subject the support columns to thermal striping.

59 | The reactor operating temperature, for long term steady state effects in a cumulative damage analysis, is based on reactor coolant outlet temperature of 1000°F with a 2σ uncertainty.

57 | 59 | During refueling operations, which are normal operating conditions, the UIS will be at the refueling temperature of 400°F.

Normal operating temperature transients such as startup and shutdown are less severe than the upset and emergency events and are enveloped by them.

Upset and Emergency Loads

57 | Steady state temperatures with 2 uncertainties for a reactor outlet nozzle temperature of 1015°F are used to begin transient analysis of UIS components.

For most areas of the UIS the most severe thermal transient among the Upset (U) and Emergency (E) Duty Cycle events is an uncontrolled rod withdrawal from full power. For the lower shroud tube, the E-16 emergency transient, three loop natural circulation, is also severe. All other UIS transients are grouped with respect to severity under these transients. The fluid temperature changes are less severe farther from the fuel exit as a result of mixing with control assembly flow and blanket assembly flow. These other assemblies also have less severe changes occurring at their exits. The heat transfer analyses of different areas of the UIS account for all these differences.

Faulted Loads

Two faulted events are identified in the UIS duty cycle. Only one occurrence of either of these events is considered. Faulted events are not considered in cumulative damage calculations.

4.2.2.4.2.6 Methods of Analysis

Elastic analysis, simplified inelastic and rigorous inelastic analysis have been used to develop the detail design which meets all its structural requirements. The simplified inelastic analysis used for the UIS are 1) Neubers method, this method is presented in Code Case 1592 (N-47) in Section T-1430, and 2) Simplified inelastic analysis of plates and cylinders under thermal transient loadings. This technique is used in the program HOTDAMG described in Appendix A. This method utilizes a strain correction factor which is a function of the elastically calculated stress and the yield stress to account for plasticity.

The rigorous inelastic analysis for the UIS was performed using finite element analysis methods. ANSYS and WECAN (both described in Appendix A) have been utilized for this type of analysis. Verification problems have shown that both programs are adequate for detailed inelastic analysis.

Computer Codes

The following computer codes are utilized in the heat transfer and structural analysis of the upper internals structure:

ANSYS
HOTDAMG
WECAN
TAP-A
TRUMP
VARR-11
TEMPEST

Descriptions of these computer codes are given in Appendix A.

4.2.2.4.2.7 Structural Analysis

The detail rigorous analysis can be divided between overall analysis and detail part analysis. The seismic analysis, duty cycle evaluation, and

overall thermal stress analysis are overall analyses. Other items discussed are detail part analyses.

Seismic Analysis

The UIS column seismic loads are obtained from the reactor system seismic analysis. The seismic analysis for the remainder of the UIS, was performed with a 180° finite element model of the structure with all of the details essential to dynamic analysis. Modal analysis of the UIS Model for both operating and refueling configurations is performed to obtain natural frequencies and mode shapes.

Seismic Response Spectrum Analysis is used to evaluate primary stresses in the UIS due to seismic excitation. The analysis is performed utilizing the CRBRP Seismic Design Criteria and the dynamic models identified above. Further details are described in Section 3.7. The displacements were checked to verify that impact did not occur at close clearance locations. Stresses due to horizontal support point motion and due to dead weight, are added by absolute value to response spectrum analysis stresses to give final values for comparison to the criteria.

Duty Cycle Evaluation

The UIS is subjected to a large number of Upset and Emergency condition thermal transients. The purpose of the duty cycle evaluation is to reduce the number of events to be applied in the analysis of each area of the structure to only one or two events so as to obtain an equivalent creep and fatigue damage for the entire duty cycle. In a high temperature component time dependent response and environmental effects become governing factors. Residual stresses, holdtime between cycles, elastic-plastic strain, cyclic-hardening, and creep/fatigue interaction must all be properly accounted for. In general, simplified creep-fatigue damage evaluations have been used to perform the duty cycle reduction and determine the umbrella transients.

Overall Thermal Stress Analysis

The UIS gross model is generated from, 1) shell elements for the lower and upper plates, shear web and skirt, 2) pipe elements for the columns, and 3) rigid beam elements to connect the columns to the plates and shear web. The primary purpose of the elastic lower plate model is to provide boundary forces for the more detailed inelastic lower plate model at various times during the U-2b transient (see Appendix B for description of this transient). Since the entire UIS is included in the model, it is possible to obtain boundary forces for other components such as the column center region and the column/top plate joint.

The analysis consists of generating temperatures at various times in the U-2b transient from thermal data obtained from the overall model thermal/structural Interface analysis. These temperatures are applied to the overall structural model. The forces produced at the boundaries of the individual components by the thermal loadings are then applied to the more detailed models of these components.

Lower Plate Analysis

The main purpose of the lower plate inelastic thermal stress analysis is to, 1) provide nodal forces for the ligament analysis due to the transient, 2) ascertain adequacy of the lower plate to react the loss of hydraulic holddown load, and 3) determine if the lower plate satisfies the ratcheting criteria.

The boundary forces are obtained from the UIS overall structural model analysis together with temperatures provided by T/H Analysis.

Lower Plate Ligament Analysis

The critical lower plate ligament is analyzed for the steady state, the critical thermal transient and the applied interaction loads from the lower plate model. A 3-D finite element model is used in the analysis. The results are then compared to the allowables to determine the lifetime of the lower plate.

Upper Plate Analysis

The upper plate overall stresses are evaluated in the analysis of the overall model. A 2-D finite element model of this area is used and transient solutions obtained for the governing transient. In addition, the seismic stresses and steady state thermal stresses from the overall model were superimposed on the detail model.

Column Center Region

The creep-fatigue damage in the column center region due to the critical transient combined with the seismic loads was calculated. Inelastic stress analysis is performed with a through thickness 1-D model applying the critical thermal transient combined with the highest possible seismic load.

Shear Webs

The shear web and its attachment to the lower and upper plates have been considered in the gross model.

Core Barrel Key

The core barrel key is included in the gross model used for seismic analysis. In addition, detailed creep-fatigue analysis of the Haynes 273 hardfacing on the keys is performed using the results from a 3-D finite element model. The thermal stress analysis is based on the critical transient. The creep-fatigue evaluation used a fatigue curve derived from monotonic tensile properties using the "Method of Universal Slopes". Additional structural reliability was generated by a test program which included both low cycle fatigue due to reactor transients and high cycle fatigue due to normal load fluctuations.

Instrumentation Post

The analysis of the instrumentation post considers steady state and U-2b, and E-16 transient thermal loadings, stripping, seismic conditions, loss of hydraulic holddown loads, and loads induced in the instrumentation posts by bowing of the UIS lower plate liners. Appropriate 2-D finite element models are used to represent different portions of the post.

Upper and Lower Shroud Tubes

The upper and lower shroud tubes are both Inconel 718 due to the severe steady state and stripping environments. The lower shroud tubes are double wall construction in order to minimize the thermal stresses induced by the severe steady state gradients. These thermal loadings have been defined through the use of small scale thermal hydraulic models. The results of the thermal stress analysis considering both reactor transients and the interference fit between the mating tubes shows an acceptable creep-fatigue damage. These analyses are performed using 2-D finite element models and elastic analysis.

Chimney Assemblies

The Inconel 718 chimney shell was analyzed for steady state and transient conditions. The critical part of the assembly is the spider forging which was analyzed using a 3D finite element model for both steady state and thermal transients.

Mixing Chamber Thermal Liners

The mixing chamber thermal liners are Inconel 718 and are analyzed for the steady state and transient environment using simplified analysis techniques. In general, these parts have low cumulative damage by comparison to other parts.

IVTM Port Plug and IVTM Port Plug Cover

The principal loadings for the IVTM Port Plug and IVTM Port Plug Cover are due to seismic events. Dynamic analysis using finite element models is performed for this condition and the results have been used to design the attachments to the reactor head.

51

4.2.2.4.3 Core Restraint System Evaluation

4.2.2.4.3.1 Summary of Results

51| The adequacy of core restraint system performance is based on comparison of core restraint system model results with the requirements defined in Section 4.2.2.1.2.8. The core restraint system results include the effects of uncertainties in the model environmental data, material properties and core component dimension. Uncertainties are combined statistically but always in a way to produce a conservative result relative to the defined requirement. The following comparison of core restraint performance to the system requirements utilizes data for the first core of CRBRP.

a) Reactivity

Feedback reactivity attributable to core assembly motions is assumed to occur either predictably, as a result of power-to-flow variations during the reactor startup process or unexpectedly, due to the sudden movement of the core assemblies within the confines of load plane gaps illustrated in Figure 4.2-84.

As discussed in Section 4.2.2.4.3.3, the reactivity feedback due to predictable assembly motions such as those which occur during reactor startup, may be positive or negative. Performance results show that the positive feedback effect is limited to power-to-flow ratios less than 0.7 and that the rate of positive reactivity insertion is a function of the core assembly duct temperature patterns, assembly motion reactivity coefficients and the lifetime status of the core assemblies. Assembly motion reactivity patterns with uncertainty effects included are provided for use in the evaluation of the reactor control system, plant protection system and reactor stability. These evaluations demonstrate that Criteria 9 and 10 in Section 3.1.3.1 are satisfied.

The analysis of sudden reactivity insertions utilizes conservative assumptions with regard to assembly positioning, interaction and dimensions which although plausible are all extremely unlikely. The event is also assumed to occur at the worst time in assembly life. This very conservative design procedure is used to set the cumulative load plane gap at the ACLP so that a sudden (or step) reactivity insertion at full power no greater than 60¢ is predicted. This design procedure insures that the step reactivity insertion limit at power levels of one megawatt or less is automatically satisfied.

b) Core Component Contact Loads and Distortions

The core restraint system model described in Section 4.2.2.4.3.3 is also used to predict interassembly contact loads, core to peripheral support component loads and overall assembly distortions

arising from radiation induced creep and swelling in the core assembly ducts. Uncertainties in dimensions, environment, material properties and the model are all considered to arrive at enveloping contact loads. Contact loads are predicted for both normal and non-seismic off-normal events for both on-power and off-power (refueling) conditions. Non-seismic loads obtained from this model are combined with seismic and other loads as indicated in Section 4.2.1.3.2.3.3. These combined loads are used in the structural evaluation of reactor system components which interface with the core restraint system. Loads calculated at refueling conditions are utilized to demonstrate that the refueling limit for assembly insertion and withdrawal is satisfied. System model results predict core assembly bowing and dilation effects as influenced by the environmental conditions (temperature and flux) within the core. Core assembly distortions are predicted to be sufficiently small so that the interassembly contact limits and the assembly handling envelope limits are satisfied.

c) Top End Misalignments

The evaluation of misalignment of the core assembly handling socket is based on stackup of top load plane gaps from a given assembly to the farthest location on the upper core former ring. Thermal and dimensional uncertainties and permanent component misalignment effects are also included. This very conservative procedure is used to set the top load plane gaps to insure that assembly top end misalignment limits are satisfied.

d) Duct-To-Duct Contact

Interassembly contact at non-load plane locations due to the combined effects of bowing and duct dilation is also computed. Present evaluations indicate that local non-load plane contact between assemblies will initiate between fuel assemblies during the second cycle of irradiation. The results show, however, that no general duct-to-duct non-load plane contact pattern is established.

4.2.2.4.3.2 Material Properties

The analyses of this section utilize material properties found in Reference 181 for irradiation swelling and creep. Analyses were performed using nominal forms and with uncertainties conservatively applied.

4.2.2.4.3.3 Analysis of Assembly Bowing and Duct Dilation

Core restraint analyses were performed using the NUBOW-3D core restraint system analysis computer code (see Appendix A). The code analyzes a 30° sector of the core restraint system including irradiation and mechanical influences as shown in Figure 4.2-85.

53| Assembly duct temperature data and neutron flux data used in the core restraint analysis are shown in Section 4.4.3.3.5, "Core Assemblies Duct Temperatures", and Section 4.3.2.9, "Vessel Irradiation". These data were applied over a time period corresponding to two cycles of reactor operation to determine the thermal, irradiation swelling, and creep bowing response of the modeled assemblies. Examples of assembly bowing profiles and interassembly loads are presented in Figures 4.2-88 and 4.2-89 for the following conditions in the operating cycle:

1. At power, start of cycle one.
2. At power, end of second cycle (328 days).

51| Assembly Bowing and Interassembly Load Patterns

Influencing the bowing profiles in the time domain were the effects of irradiation swelling and creep. The effect of irradiation creep is to relax loads caused by on-power thermal bowing, while swelling act to bow the assemblies in the direction of increasing lateral thermal and flux gradient. Figure 4.2-90 illustrates the interassembly load pattern at ACLP due to on-power thermal bowing loads. Irradiation creep effects occur almost immediately, however, a delay or incubation period is required before swelling effects become pronounced. For the row 9 assembly, swelling became significant during the second cycle of operation (compare Figures 4.2-88 and 4.2-89).

Sudden Core Radial Motion

61| The presence of interassembly gaps at the above core load plane gives rise to the potential for inward radial motion of the core assemblies. A positive reactivity insertion due to assembly motion requires a general radial inward movement of the core. A conservative design procedure employed in CRBRP is to set the ACLP load plane gaps so that the maximum sudden inward motion of the core assemblies within the confines of the ACLP radial gap would result in a step reactivity insertion no greater than 60¢ when the reactor is at full power. The assembly motion necessary to cause a step insertion of this magnitude is improbable. During reactor startup, the establishment of temperature gradients across the assemblies will cause them to bow generally inward tending to close ACLP gaps in the core region in a predictable and controllable manner. Once the ACLP gaps are closed, further inward motion of the core assemblies is not possible. Consequently, the only possible way for a sudden inward core motion to take place is for the core not to compact radially inward at the ACLP as it is brought to power. The only non-compaction effects which have been identified and experienced in core array mechanical interaction testing are the combination of high friction ($\mu > 0.6$) and assembly azimuthal rotation.

59| Consequently, in the analysis of the step insertion event it is assumed that during the insertion of assemblies into the core, the assemblies are rotated uniformly so that the interassembly load plane gap is eliminated.

It is further assumed that the friction coefficient is sufficiently high that thermal bowing forces generated as the reactor is brought to power will not be sufficient to overcome load pad frictional forces and realign the assemblies. Secondly, it is assumed that when full power is achieved, a seismic event occurs which produces forces sufficient to overcome the load pad frictional forces and realign the core assemblies into their nominal orientation. The rotational alignment of the core is assumed to occur suddenly, displacing the core radially inward.

The conservatism of this procedure can be illustrated by examining the assumptions which are employed in the step insertion procedure.

- 1) Core assembly load pads and the core formers are assumed to be at their nominal dimensions. Fabrication experience indicates that the as-built assembly load pad dimensions in the aggregate will be larger than nominal and that the core former ring smaller than nominal thus the as-built load plane gap is likely to be smaller than the nominal load plane gap. Furthermore, tolerance effects between adjacent assembly faces would result in the smaller of the distribution of interassembly gaps controlling the compaction process. The net effect of load pad tolerances would be to reduce the load plane gap.
- 2) Load plane surfaces are coated with a low friction hard surface coating of chromium carbide. The mean friction coefficient of this surface coating in the reactor operating range is 0.2 to 0.4. Analytical and experimental evidence on core array mechanical simulations indicates, that for this range of friction coefficient, non-compaction effects are not significant.
- 3) The rotational alignment of assemblies within the core is expected to be distributed statistically about the nominal orientation as determined by the core assembly and core former load plane as-built surface dimensions. No operational bias has been identified which could preferentially orient the core assemblies so as to close the load plane gap but still permit installation and removal of assemblies into and from the core.

Reactor Assembly Bowing Reactivity

During a change in reactor power-to-flow ratio, temperature gradients change or develop across assembly ducts, causing the assemblies to bow. Lateral motions of the core regions of these assemblies result in a reactivity change. This reactivity change differs from that discussed in the previous paragraph in that it is assumed to occur in a predictable and controllable manner in response to duct temperature changes.

Figure 4.2-92A depicts the row average assembly bowing patterns and corresponding reactivity effects that develop during a power to flow ratio

transition. At near-zero power-to-flow ratios, the assemblies tend to bow freely within the constraints of the interassembly and peripheral load plane gaps. The presence of a peripheral gap at the TLP core former ring permits a net outward motion of the core region of the outer core fuel and radial blanket assemblies producing a negative reactivity effect as shown for the 0.2 power-to-flow ratio pattern. When the closure of TLP gaps from the outer blanket rows to TLP core former ring prevent further outward motion, the core regions of the outer core fuel and radial blanket assemblies bow inward as shown for the 0.4 power-to-flow ratio pattern. The net inward motion of the fuel and radial blanket assemblies continues until the ACLP gaps close from the center of the core to the radial blanket rows. During this phase the bowing reactivity contribution is positive. Subsequent increases in power-to-flow ratio result in more complex S-shape bowing patterns and a net outward motion of the active core regions of the high worth fuel and radial blanket assemblies. During this phase, the bowing reactivity contribution is negative as depicted for the power-to-flow ratio equal to 1.0 pattern in Figure 4.2-92A.

Figure 4.2-92B shows the bowing reactivity characteristics which are predicted for nominal thermal, nuclear and load pad dimensional data at various times in the fuel assembly lifetime. Differences between the bowing reactivity patterns are attributable to the irradiation effects of creep and swelling in the reactor assembly ducts. Early in fuel assembly life (125 and 250 days in Figure 4.2-92B), the high worth assemblies at the fuel-radial blanket interface are bowed outward at the ACLP at refueling conditions as a result of irradiation creep. On a subsequent reactor startup (power-to-flow transition), these high worth assemblies traverse inwardly to a greater extent than initially straight assemblies. Later in the fuel assembly lifetime (500 days in Figure 4.2-92B), the high worth assemblies at the fuel-radial blanket interface bow inward at the ACLP at refueling conditions as a result of swelling. The startup bowing reactivity late in the fuel assembly life resembles the characteristic behavior of initially straight assemblies.

Figure 4.2-92C shows the bowing reactivity characteristics which are predicted for various assumptions of nuclear and thermal data, load pad mechanical interaction and dimensional uncertainties.

The curves in Figures 4.2-92B and 4.2-92C, when combined with other significant reactivity effects such as the Doppler effect, are used in the reactivity feedback evaluations which are provided in Sections 4.3.2.8, Reactor Stability, 7.7.1.2, Reactor Control System and 15.1.4.5, Reactor Assembly Bowing Reactivity Considerations.

Withdrawal Loads at Refueling

The frictional components of assembly withdrawal loads are obtained from the NUBOW-3D analysis. The effects of uncertainties are combined statistically

and the sodium buoyant assembly weights are added to the friction forces as shown below:

$$F_w = \sum \mu_i (\sum F_j)_i + U + W$$

where: F_w is the withdrawal load, μ_i are friction coefficients at load planes, F_j are the duct normal forces at load plane i , U is the uncertainty adder and W is the assembly sodium buoyant weight.

Midcore Duct-to-Duct Contact

Duct-to-duct contact at the core midheight was investigated via NUBOW-3D. It was found that assembly bowing alone was not sufficient to cause midcore contact. However, with duct dilational behavior modeled, midcore contact does occur in the outer core region. Nominal calculations predict the first occurrence just after the end of cycle 2 (~335 vs. 328 days). This is a duct midheight pressure bulge-to-pressure bulge type of contact from internal pressure driven creep dilation, and is not likely to cause high contact loads.

Conclusions and Future Work

Assembly motion reactivity effects are conservatively predicted by current analytical procedures. The results shown indicate that reactivity related core restraint requirements of Section 4.2.2.1.2.8 are satisfied.

Core component contact loads and distortions are predictable using current analytical methods. Additional work is planned to verify dilation induced duct-to-duct contact predicted in NUBOW-3D with more detailed models.

Additional areas where further work is planned include:

- 1) Detailed analysis of core restraint performance beyond core 1.
- 2) The simulation of fuel management in the NUBOW-3D model.
- 3) Verification and improvement if necessary of the duct dilation induced duct-to-duct contact model.

4.2.2.4.4 Removable Radial Shield Assembly (RRS)

The RRS configuration is shown in Figure 4.2-43. The structural analyses included two critical regions of the RRS, the Above Core Load Pad (ACLP) of the duct and the outlet nozzle. The selection of these two regions was based on structural analyses of the basically similar fuel and blanket assemblies which indicated that the assemblies inlet regions comprising the inlet nozzle, orifice assembly and transition had very high design margins, while operating under more severe environmental conditions than the RRS. The above mentioned structural analyses indicate that the ACLP is the critically loaded region.

In the ACLP analyses, maximum values from all loading sources were assumed to occur simultaneously at the single assembly subject to the worst environmental conditions. The various loading conditions considered were seismic, core restraint, and steady-state and transient thermal loads. Three different sets

of thermal-hydraulic conditions were considered from which the worst combinations of maximum duct midwall and cross-duct gradient temperatures was obtained. Stresses, strains and damage were determined for the ACLP resulting from the above loading sources and conditions.

An ANSYS finite element computer code was used for the RRS duct stress analyses. Based on the results of this analysis, inelastic and fracture toughness analyses of the ACLP were also performed.

The inelastic analyses were performed to determine strain and damage of the ACLP using the CHERN elastic-plastic-creep computer code. Two separate sets of analyses were performed, one representing BOL conditions, and one representing EOL conditions corresponding to a design life of 10 years. Twenty out of the 190 loading cycles of the unit histogram (see Figure 4.2-43A) were run for each of the two conditions to overcome the transient portions of the elastic-plastic-creep domain, and the remaining 170 cycles were conservatively duplicated by the 20th cycle. Both the calculated total maximum strain and the calculated maximum creep-fatigue damage when compared with the minimum allowable values yield positive design margins equal to 14.0 and 0.14, respectively.

A fracture toughness analysis of the duct ACLP was also performed, since the minimum elongation in the load pad at end of life is $\leq 3\%$, and brittle fracture is a potential failure mode. For this analysis, an initial flaw size and shape, and two orientations were assumed, consistent with the requirements defined in RDT E6-20T (now NE E6-20T). The analyses consisted of the following steps:

- a) The critical stress intensity factor K_{IC} for BOL and EOL material conditions were derived from data on unirradiated sub-compact test specimens made from FFTF duct material.
- b) The stress intensity factor for the assumed semi-elliptical flaw under tensile stress was determined.
- c) A crack propagation analysis was performed to determine the crack growth under the applied duty cycle.
- d) The maximum stress intensity factor K was determined for the final flaw size obtained from the crack propagation analysis.
- e) Finally, the margin of safety was determined by comparing the calculated maximum EOL stress intensity factor K_{max} with the allowable design value which was obtained by applying a design margin of 1.5 on the calculated critical stress intensity factor K_{IC} . This evaluation yielded a positive margin of safety equal to 5.7.

4.2.2.5 Welding and Seizing of Reactor Internal Parts

The design considerations for welding and seizing of rotating or moving parts for reactor internals are presented in Table 4.2-64.

4.2.2.6 Thermal Striping Evaluation of Reactor Internals

4.2.2.6.1 General Methodology for Thermal Striping Evaluation

The general method used to evaluate components for thermal striping is illustrated in Figure 4.2-130. The steps involved are as follows:

- a) The maximum potential for thermal striping is identified. This potential is the calculated temperature difference in sodium coolant from adjacent streams. Included in the temperature difference are 2 σ uncertainties.
- b) Scale model tests are run as appropriate and the component thermal striping factors are measured. The measured striping factors are combined with the maximum striping potential to generate a thermal striping temperature time history and define a maximum fluid ΔT .
- c) The thermal striping temperature time history is used as the boundary temperature in a transient thermal analysis of selected component. This analysis calculates the magnitude of the fluctuating difference in the surface temperature and the mean temperature ($T_s - T_m$).
- d) The range of $T_s - T_m$ is used to determine a stress or strain range which is used in the fatigue evaluation of the structure.

There are primarily 4 methods used to evaluate structures for thermal striping.

1st Method

This is the most simplified and conservative method used. In this method the maximum fluid ΔT (Hottest fluid Temp. - Coldest Fluid Temp) is compared to an allowable metal ΔT . (Temp. of the metal surface - metal mean temp). The method for determining allowable metal ΔT is described in Section 4.2.2.6.4.

If ΔT fluid $<$ ΔT metal allowable the structure is adequate for striping.

Discussion of Conservatism:

There are several factors which cause this method to be conservative.

1. Using fluid temperatures is conservative, since this assumes an infinite film coefficient and neglects the mean temperature effects on strain. Since striping is a fast transient the mean temperature effect will be small for most cases. However, the film coefficient effect can be significant.
2. Using the observed maximum and minimum as umbrella temperatures is conservative since each cycle would not have this maximum strain range.
3. Assuming a biaxial stress state is conservative for some locations such as at corners, where there is no biaxial stress state.
4. Conservatism, incorporated into the design such as factors on design fatigue curves and temperature uncertainties.

2nd Method

The second method is used when the 1st method does not show the structure adequate. This method is to use the film coefficient and the materials thermal properties to determine the actual metal surface temperature. The metal surface ΔT is then compared to the allowable metal ΔT (Surface-mean) used in method 1. If $\Delta T_{\text{metal surface}} < \Delta T_{\text{metal allowable}}$ the structure is acceptable for striping.

Discussion of Conservatism

Conservatism is the same as for method 1 but excluding item 1.

3rd Method (Detailed Analysis)

This method is used when methods 1 and 2 are not adequate to show that the structure is acceptable and there is reason to believe it can be shown adequate with this method. This method involves the evaluation of actual temperature data from prototypic tests. In this evaluation instead of using the hottest and coldest fluid temperatures, the fluid temperature data is first converted to metal temperatures by thermal solutions. Then the metal temperature peaks are umbrellaed i.e., all temperature peaks between specified values are grouped and given the highest absolute temperature within the group. These umbrella temperatures are used to calculate strain ranges for each group.

$$\epsilon_{r_i} = \frac{\alpha \Delta T_{\text{metal}}}{(1 - \nu)}$$

α = Instantaneous coefficient of thermal expansion
 ν = Poisson's ratio
 ϵ_r = Strain range

Where ΔT_{metal} = Difference between the max and min temperature variation of the metal within the group (conservative).

The number of cycles within each group (n_i) is projected throughout the reactor life. The allowable number of cycles (Nd_i) for the strain range in the corresponding group is obtained from the applicable fatigue curve. The total striping fatigue damage is, $D_{\text{fatigue}} = \sum_1^i n_i / Nd_i$

This damage will then be added to the creep-fatigue damage calculated for other transients. If the damage calculated here is within the creep-fatigue damage envelop, Figure 4.2-47A, the striping is considered acceptable.

Conservatism

Items 3) and 4) from Method 1

There is still some conservatism in umbrellaing the temperatures, but not as significant as before.

4th Method (Alternate Detailed Analysis)

Again this method is used only when methods 1, 2, or 3 are not adequate to show the structure acceptable. This method is used when the geometry of the structure is such that the previously discussed methods are overly conservative i.e., thin walled structures where mean temperature effects can be substantial, and corners where biaxiality effects vanish. Either effects tend to reduce the stress and strain.

For this method detailed finite element models are developed to determine the thermal and stress response of the structure for the specific striping environment. The stress and strain ranges determined from the models are then used to evaluate the fatigue damage due to striping.

Conservatism

See Item 4, from Method 1.

4.2.2.6.2 Maximum Potential Fluid ΔT s

To evaluate the effects of thermal striping on reactor internals, a first step is to determine the maximum potential for thermal striping that exists at each selected component. This maximum potential is the maximum temperature difference (ΔT) between the different sources of sodium in each region, including 2σ uncertainties. For example, the striping potential at a lower shroud tube is the ΔT between the control assembly (C/A) -2σ exit temperature and the hottest adjacent fuel assembly (F/A) $+2\sigma$ exit temperature. The striping potentials are developed using a conservatively high core ΔT that represents a 115% power condition. This core ΔT is about 60°F higher than expected in the CRBRP. A listing of the maximum potential fluid for different components is included in Table 4.2-68.

4.2.2.6.3 Maximum Fluid ΔT s

The maximum fluid ΔT at a given location is determined empirically as a fraction of the maximum potential fluid ΔT . Water model testing was performed in 1) a full scale mockup of a cluster of seven removable assemblies and in 2) the quarter scale IRFM (Integral Reactor Flow Model) at HEDL. Hot and cold water exiting the core assembly outlet nozzles at appropriate flow rates simulate the assembly to assembly ΔT . Fast response thermocouples near the surfaces of the components models provide the time history of the fluid temperature fluctuations normalized to determine a normalized striping factor.

The results of these tests provide a measure of the maximum fluid ΔT at critical locations.

7-Assembly Tests

The 7-assembly test model is a full scale model of the reactor internals configuration above a cluster of 7 core assemblies including the assembly exit nozzles. Configurations tested include the following components above the central of the 7 core assemblies.

- o Lower shroud tube and primary control rod driveline.
- o Lower shroud tube and secondary control rod driveline.
- o Lower shroud tube at core periphery without control rod driveline.
- o Instrumentation post.

Figure 4.2-131 is a sketch of the 7-assembly test model. The configuration shown here is with an instrumentation post. In this configuration the thermal striping factors are measured on the instrumentation posts for the different combinations of fuel assemblies and blanket assemblies that are below it.

Integral Reactor Flow Model - Thermal Striping

The integral reactor flow model (IRFM) is a 360 degree 0.248 scale model of the CRBRP outlet plenum and its internal components which models significant hydraulic and vibrational characteristics of the CRBRP. Sodium in CRBRP is modeled by water in IRFM. An overall view is shown in Figure 4.2-132. Fuel, control, and blanket assemblies are represented by tubes orificed at the bottom to give the proper flow distribution. The top ends of all core outlet nozzles are prototypic to produce the proper velocity profile. Four different zones (fuel assemblies, inner blanket and control assemblies, radial blanket assemblies, and removable radial shield assemblies) were provided with different specified flows and temperatures and were varied to model striping conditions at various core life conditions.

The frequency and amplitude of fluid temperature oscillations were monitored on the outlet plenum permanent reactor structures. Thermal striping in these regions are due to temperature differences between the fluids exiting the fuel assemblies, the radial blanket assemblies, the inner blanket assemblies, the control assemblies and the removable radial shield assemblies.

In addition to the striping measurements at the reactor components, measurements were made in the outlet plenum using radial traversing probes. The axial location of these probes is illustrated on Figure 4.2-133.

Test Results

The results of these thermal striping tests are listed on Table 4.2-68 in the form of normalized striping factors. The factors are a fraction of the striping potential with a factor of 1.0 being 100% of potential. Results from the traversing probes in the outlet plenum are illustrated on Figure 4.2-134 in the form of striping ΔT contours. The striping levels on all components outside of this region, such as the reactor vessel thermal liner, the suppressor plate, and the primary piping, are within the range of allowables as shown on Table 4.2-69.

4.2.2.6.4 Striping Limits for Alloy 718 and Stainless Steels 304 and 316

Many reactor internal components experience strain controlled cyclic deformations in excess of 1×10^6 cycles. From the available fatigue data, reference 182, the allowable strain or stress range for 1×10^6 cycles or more approaches the endurance limits of each of the concerned materials. These allowable strain or stress limits can be converted into limits on the metal surface to mean temperature range (ΔT total). The allowable striping ΔT metal can be conservatively determined from the endurance stress or strain ranges for a fully constrained biaxial stress case, e.g. thick flat plate. The following relations are used;

$$\Delta T_{\text{metal}} = (1-\nu) \frac{\Delta \sigma_r}{E \alpha_i} \quad (\text{a) (stress formula)}$$

$$\Delta T_{\text{metal}} = (1-\nu) \frac{\Delta \epsilon_r}{\alpha_i} \quad (\text{b) (strain formula)}$$

where ΔT_{metal} - Metal surface temperature minus the mean temperature
See Figure 4.2-130, Section C

$$\Delta \sigma_r = \text{endurance stress range (25}_a\text{)}$$

$$\Delta \epsilon_r = \text{endurance strain range}$$

$$\alpha_i = \text{instantaneous coefficient of thermal expansion}$$

$$\nu = \text{poisson's ratio}$$

$$E = \text{modulus of elasticity}$$

This limit represents one of the most conservative cases as discussed in Method 2 in 4.2.2.6.1. If the striping ΔT metal on the component is below this limit, no further analysis is necessary.

In some applications the alternating stress or strain is accompanied by mean stress or strain. The mean stress or strain effect is detrimental and the allowables should be adjusted accordingly.

For 304 and 316 stainless steel the design endurance strain ranges can be obtained from Figure 4.2.47B, provided that the metal temperatures do not exceed 1100°F. The striping ΔT metal limits are given in Table 4.2-69 with selected mean strain effects.

The allow 718 fatigue curve is shown in Figure 4.2-48. The striping stress limits are developed from the endurance stress range of the up-to-date data provided in Reference 183. The high cycle (10^8 or more cycles) design fatigue strength curve with no mean stress is shown in Figure 4.2-49. Corrections for mean stress effects should be made by calculating a reduced allowable alternating stress intensity, s_a' , as follows:

$$s_a' = s_a \times \frac{200,000 - s_{max}}{200,000 - 2s_a}$$

where

- s_a = the lowest allowable alternating stress intensity from Figure 4.2-49 for the metal temperature range of interest, psi
- $s_{max.}$ = the maximum calculated stress intensity during the stress cycle, psi
- s_y = material yield stress for the metal temperature range of interest, psi

The above equations for s_a' are used with the following restrictions:

- A. If $2 s_a \geq s_y$ or $2 s_a > s_{max.}$, $s_a' = s_y$ and the equation is not used.
- B. If $s_{max.} \leq s_y$ and $2 s_a \leq s_{max.}$, the equation is directly applicable.
- C. If $s_{max.} > s_y$ and $2 s_a < s_y$, use $s_{max.} = s_y$ in the equation.

The striping ΔT metal limits are obtained for any s_a' by applying equation (A). The allowable T metal range for a fully constrained biaxial case with zero mean stress is shown in Figure 4.2-135 for allow 718. To obtain the allowable ΔT metal from Figure 4.2-135 the metal temperature used is the value within the striping range that yields the lowest allowable ΔT metal range. (The data base includes ASTM grain sizes of 5 through 10 with an average grain size of 7)

The effects of the fabrication processes and service environment on the structural integrity of the involved component shall be considered. The effect of grain size on the behavior of Alloy 718 shall also be considered. Some of the UIS liner plates cannot be purchased with an ASTM Grain size finer than 2, therefore a reduction in the allowable stress range is required. The allowable metal ΔT for a required reduction of 32% is shown in Figure 4.2-136 which does not include mean stress effects. When other grain sizes are used the allowable must be adjusted accordingly. Data used to determine the grain size effects on the endurance limit are from References 4.2-186 & 187.

4.2.2.6.5 Summary of Thermal Striping Results

The thermal striping evaluation methods and results are summarized in Table 4.2-68 for the permanent reactor internals. The general conclusion from this table is that all the permanent reactor internals are acceptable for their thermal striping environments. As cited previously and indicated by Figure 4.2-498, the striping values for all reactor components outside the Upper Internal Structure and above the Horizontal Baffle are below the allowable limits for stainless steel.

4.2.3 Reactivity Control Systems

The mechanical designs of the reactivity control systems consist of the primary control rod system (PCRS) and the secondary control rod system (SCRS). Each mechanical system consists of a control rod drive mechanism (PCRD for primary, SCRDM for secondary) mounted on the top of the reactor vessel closure head; a control rod driveline (PCRD for primary, SCRDM for secondary) connecting the mechanism to the absorber in the core region; and a control assembly (PCA for primary, SCA for secondary) located in the core region. The control assembly consists of a movable absorber pin bundle called the control rod and outer duct assembly.

These control rod systems perform the following functions upon signal from the Instrumentation and Control Systems:

Primary Control Rod System

1. Provide the primary shutdown (scram) system for the off-normal conditions.
2. Provide normal operational control.
3. Provide normal reactor startup and shutdown reactivity control.
4. Provide additional margin for control in the event of any anticipated reactivity fault.

Secondary Control Rod System

1. Provide the secondary shutdown system for off-normal conditions.
2. Provide reactor shutdown independent of the primary system.
3. Provide additional margin for shutdown in the event of any anticipated reactivity fault.

Primary Control Rod System Codes

The analytical codes being used to evaluate and verify the design of the primary control rods are as follows:

- 1) THI-3D; Steady-State Thermal-Hydraulic Multichannel Analysis.
- 2) COBRA; Steady State and Transient Thermal-Hydraulic Analysis of Rod Bundle Elements.
- 3) FORE-II; Transient Thermal-Hydraulic Analysis.
- 4) CRSSA; Thermal-Hydraulic and Mechanical Analyses over the Primary Control Assembly Lifetime.
- 5) CRAB; Steady State Hydraulic and Scram Dynamics Analyses of the Primary Control Assembly

A brief description of each of these codes is presented in Appendix A, "Computer Codes of the PSAR".

16

4.2.3.1 Design Basis

4.2.3.1.1 General Safety Design Criteria

The General Safety Design Criteria are discussed in detail in Section 3.1.3, subsection III, Protection and Reactivity Control Systems, and are outlined here for completeness. Specific criteria which are a part of the design basis for the reactivity control systems mechanical components are:

1. Criterion 20 - Protection System Independence
2. Criterion 21 - Protection System Failure Modes
3. Criterion 23 - Protection System Requirements for Reactivity Control Malfunctions
4. Criterion 24 - Reactivity Control System Redundancy and Capability
5. Criterion 25 - Combined Reactivity Control Systems Capability

These criteria are augmented by the following requirements:

1. The speed of response of the control rod system, acting as part of the Plant Protection System, shall be sufficient to assure that the Damage Severity Limits of Table 4.2-35 are not exceeded. Specific requirements for speed of response are presented by Figure 4.2-94 for the SCRS.

The allowable damage limits are related to the frequency of the transient condition so that anticipated events do not lead to a reduction in the effective fuel lifetime. RDT Standard C16-1T, Dec. 1969, is used as the basis for the primary control rod system damage severity limits, without a stuck rod. (See Table 4.2-35.) To provide conservative plant protection, the same primary system damage limits are required to be satisfied under the assumption of a stuck rod. The primary system has the function of limiting fuel damage to design limits for anticipated events. Failure of the primary system is an extremely unlikely event. Consequently, the secondary system, which is needed for shutdown only if the primary system fails, need only limit damage to the major incident limit of an extremely unlikely event. For additional conservatism in limiting plant damage for an anticipated event, the limits of Table 4.2-35 require only minor incident damage for the secondary system. The combined probability of an extremely unlikely fault event concurrent with failure of the primary system is exceedingly low and is not applied as a design basis.

- 51 | 2. For an Operational Basis Earthquake (OBE), an anticipated fault, both control rod systems shall be capable of functioning, including reactor scram, both during and after the earthquake. Reactor shutdown shall be achieved assuming loss of offsite power and/or a step reactivity insertion (maximum of 30¢) coincident with the earthquake (concurrent events defined as an unlikely fault) without exceeding the damage severity limits of a minor incident for primary system shutdown and of a major incident for secondary system shutdown.

51 | For a Safe Shutdown Earthquake (SSE) (extremely unlikely fault), either control rod system shall be capable of shutting down the reactor during the earthquake but is not required to function after the earthquake other than passively assuring that shutdown is maintained. Reactor shutdown shall be achieved assuming concurrent loss of offsite power and a step reactivity insertion (maximum of 60¢) coincident with the earthquake without exceeding the damage severity limits of a major incident for both systems.

The requirement for functioning of the secondary system in an SSE provides an additional protective margin beyond that of Table 4.2-35.

3. No electric or other external (to the mechanical control rod system) power shall be required for a scram of any control rod.

4.2.3.1.2 Control Rod System Clearances

The specific goal in establishing control rod system clearances is to ensure safe and reliable shutdown and control capability for the reactor. To this end, the basis for establishing clearances fall into the following general categories:

Limit scram retarding forces resulting from misalignment of components.

Limit scram retarding forces resulting from material effects from thermal, radiation, and other environmental characteristics.

Assure normal operation of the control rod systems under misaligned and environmental conditions.

Control Systems clearance requirements and their bases are summarized in Table 4.2-36.

4.2.3.1.3 Mechanical Insertion Requirements

This section describes mechanical insertion requirements with regard to scram speed of response, alignment requirements, scram arrest, normal insertion and withdrawal speeds, and coefficient of friction considerations.

Scram Speed of Response

The minimum scram speeds of response for the control rod systems are as follows:

1. The primary and secondary control rod systems shall satisfy the scram Insertion speed requirements of Figure 4.2-93 and Figure 4.2-94, respectively.
2. Figure 4.2-93 includes 0.1 second unlatch time delay between start of CRDM stator current decay and start of the primary control rod motion. Figure 4.2-94 includes 0.1 seconds unlatch time delay between current interruption to the solenoid valves and start of secondary control rod motion.
3. The control rod systems shall include limit stops to assure that the control rods cannot be withdrawn above the design basis maximum withdrawal stroke. The control rod drive mechanisms shall limit driveline and control rod withdrawal, when the driveline and control rod are coupled, to a value of 37.5 inches for the primary system and to a position such that the absorber operating position is above the fuel and upper blanket interface for the SCRS. The maximum withdrawal position shall be developed to ensure insertion requirements are met for the secondary system. Scram speed requirements shall be satisfied for fully withdrawn control rods assumed to be at the maximum withdrawal position.
4. Once the scram signal has been input to the control rod systems, there shall be no way to over-ride or countermand the signal or to delay completion of the scram cycle.

The scram requirements of Figures 4.2-93 and 4.2-94 are values that represent the minimum insertion speeds required to assure that the damage severity limits of Table 4.2-35 are not exceeded for all design basis transients. Iterative transient evaluations such as for the transient evaluated in Chapters 15.1 and 15.3 of this PSAR have led to the specified minimum insertion rates. Anticipated transients such as the loss of offsite power have been particularly influential in establishing the requirements of Figure 4.2-93 and 4.2-94.

These requirements are to be satisfied under all potential control rod positions within the design limits established by requirement 3 above and within worst case positional uncertainties for banked primary system control rods. The nominal delay times of 0.1 second for requirement 2 are specified for consistency with the insertion speeds. Potential tradeoffs between the delay time and insertion speed requirements may be made while assuring that the overall insertion time requirements are met.

46| Scram during a seismic event is not specifically required unless an event coincident with or caused by the earthquake leads to a reactor trip requirement. The seismic speed of response requirements of
46| Figures 4.2-93 and 4.2-94 are preliminary values to assure that the appropriate damage limits are not exceeded for the infrequent seismic event. The specific seismic scram requirements of Section 4.2.3.1.1 lead to a slightly slower speed of response for the OBE than for the non-seismic events in the case of the PCRS (see Fig. 4.2-93), but
46| coincidentally equal speed of response for both OBE and non-seismic events in the case of the SCRS (see Fig. 4.2-94). For the SSE, which is an extremely unlikely fault, the higher allowable damage severity limit (see Table 4.2-35) permits the slightly slower
46| speed of response requirements given in Figures 4.2-93 and 4.2-94 for the SSE. For the secondary system, major incident damage limits apply to both OBE and SSE.

46| The required insertion speeds for full power and low power or low flow transients are shown in Figures 4.2-93 and 4.2-94. The speed of the PCRS is only slightly dependent on flow with insertion speeds tending to increase with decreasing flow rates. The minimum PCRS worth available for shutdown is slightly smaller at low power due to the increased rod insertion required to compensate the negative power coefficient between zero and full power. Thus, the speed of response requirements for the PCRS in Figure 4.2-93 reflect only the difference in total reactivity assured for reactor shutdown (see Section 4.2.3.3.1.3).

46| The SCRS utilizes hydraulic scram assist for which the insertion speeds tend to decrease with lower flow rates. Therefore, a specific requirement for low flow speed of response has been developed for the SCRS based on satisfying appropriate damage limits for low power initiated transients. The requirements have been specified for 40% flow on the basis that plant operating procedures specify a minimum of 40% flow for low power operation and approach to critical startup procedures.

The upper limit on control rod travel is required to prevent the absorber region of the control rod from accidentally being separated from the fueled core region by a gap exceeding the design bases. If a scram were called for when a large gap existed, a longer delay time would result before the control rod entered the core. Operation above the specified withdrawal limit is to be prevented by appropriate mechanism and control assembly design limits. The mechanical limit stop may be an upper stop in the control assembly preventing further withdrawal of the control rod or an electrical limit switch which the operator cannot bypass during operation.

Misalignment

The control rod systems shall be capable of satisfying all normal operation and scram insertion requirements under the maximum misalignment design conditions given in Figures 4.2-95A and 95B. Misalignment causes drag forces which tend to inhibit rod insertion. Consequently, the control rod systems must be designed to meet minimum scram requirements under maximum misalignment conditions.

SCRDM/SCRD Misalignment

The reactor system misalignments are specified as cylindrical or conical envelopes in which the individual components may assume any arbitrary position. Different combinations of the individual component misalignments produce different degrees of interference with the driveline. The effects of the interference can be assessed in terms of the contact loads and drag forces. Analysis shows that the interference loads and deflections resulting from the specified reactor system misalignment will be relatively small and will not impact the structural integrity or functional performance of the SCRS driveline.

The analysis involved a search for contact points between the driveshaft and the misaligned interfacing components, calculations for the deflections, contact loads and drag forces, and evaluation of their impact on the driveline structural and functional performance. The analysis was repeated for various combinations of the component misalignments to determine the reactor misalignments producing the maximum interference loads on the drive shaft. Next the effect of these misalignments on the driveshaft/sensing tube interfaces was evaluated. Finally, the sensing tube/tension rod interference loads were calculated. The analysis was performed for the normal operating conditions misalignments and the refueling condition misalignments which envelop the "hot standby" condition misalignments.

SCA Misalignments

The upper duct and the guide tube in the lower duct in the Secondary Control Assembly (SCA) define the control rod insertion path into the core. The scram-clearance analyses demonstrated adequate operating clearances between the control rod and the guide ducts to permit free passage of the rod into the core at any time during the design life.

During operation, the original fabrication clearances are reduced due to thermal and irradiation induced deformations, and free passage is not assured even if the control rod diameters remain smaller than the guide tube and duct

diameters. This is because the operational deformations include axial bending in addition to the diametral distortions, and the differences in the bowing profiles of the control rod and the guide ducts (upper duct and the guide tube) have a potential for producing a forced three-point contact. A forced three-point contact between the guide tube/duct and the control rod is not acceptable because the resulting rod decelerations and their impact on the scram time are not readily evaluated. The analyses demonstrated that a forced three-point contact will not occur between the control rod and the guide ducts after allowing for the fabrication tolerances and operational deformations.

The effect of fabrication and assembly tolerances on the control rod was accounted for by using the maximum diameters in the tolerance bands and assuming the control rod wrapper tube to be bowed in the form of a circular arc to reflect the straightness tolerances. The thermal bow due to diametral temperature gradients was assumed to be in the same direction as the fabrication bow. The piston swelling was based on $+3\sigma$ uncertainty levels in the correlation.

The effect of the fabrication and assembly tolerances on the guide tube/duct was accounted for by using the minimum diameters in the tolerance bands and assuming the guide tube and upper duct to be bowed in the form of circular arcs to reflect the straightness tolerances. The analysis included possibilities of the bows of the two components being in the same direction and in the opposite directions. The guide tube deformations due to creep under external pressure were calculated using $+3\sigma$ uncertainty level creep rates and initial ovality based on the fabrication tolerances on the tube diameter. The analysis was based on the assumption of plane strain deformations of individual cross-sections. Swelling related increases in the tube/duct diameters were ignored. The operational bowing of the SCA duct and the guide tube resulting from thermal and irradiation induced deformations was calculated in an overall core inter-assembly analysis. This bowing was combined with the fabrication bow in a manner leading to maximum mismatch between the control rod and guide tube profiles through parametric analyses.

The interference analyses to calculate the clearances between the distorted ducts and control rod were performed using the SCRAMLAR Code, which adds the effects of the different sources of deformations to obtain the distorted control rod and guide tube/duct profiles and diameters and calculates the least possible clearance between the guide path and the control rod during scram travel. The results show acceptable margins against a forced three-point contact between the control rod and guide tube/duct for 328 days and 550 days operation.

Figures 4.2-95A and 95B provide schematics (Operating and Refueling Conditions) of the reactor system static misalignment sources (and their magnitudes) that can produce mechanical contact causing scram retarding drag forces. This schematic illustrates that the major sources of misalignment are the accumulation of fabrication tolerances in the reactor vessel closure head which limit the accuracy of lateral and angular location of the CRDM nozzle with respect to the reactor vessel reference centerline, and the accumulation of core component inter-assembly clearances that permit mispositioning of the control assembly handling sockets with respect to the reactor vessel reference centerline. The total misalignment drag forces resulting at these locations must be consistent with the insertion requirements and the available scram forces. The actual operational misalignments of the various components of the reactor system are defined by the magnitude of Figure 4.2-95A; however, the magnitudes and the orientations of these individual misalignment sources may be randomly distributed within this available envelope for each individual control rod location.

Scram Assist

The control rod systems shall provide scram assist features to enhance the scram speed of response.

The primary system provides a spring scram assist over approximately the first 27 inches of travel from the fully withdrawn position, with a 362 lb minimum force at the fully withdrawn position. The secondary system scram assist initially provides approximately 248 lb hydraulically applied at Thermal Hydraulic Design Value conditions. This ensures that the scram requirements will be met for the SCRS.

A scram assist feature improves the shutdown system safety aspects in two ways. First, the scram speed is improved from the greater unbalanced force provided by the scram assist. Second, scram stroke completion is more positively assured because a greater drag force would be needed to stop the control rod than for a gravity only scram. A scram assist active over approximately 27 in. from the fully withdrawn position provides positive force over sufficient distances to insert the absorber into the high reactivity worth region beyond the core midplane.

Insertion and Withdrawal Speeds

1. The design withdrawal speeds for the control rod systems shall assure conservatively small rates of reactivity insertion and the maximum withdrawal capability of the mechanisms, in case of overspeed signal from the controller, shall assure that the rate of reactivity insertion is less than 30¢/sec.

51 |

- a) The PCRS maximum withdrawal and insertion rates have been conservatively established as 9 in. per minute maximum design speed, and 73 in. per minute for the maximum speed limit in the event of an overspeed signal from the controller.
- b) The SCRS withdrawal and insertion rates have been conservatively established as 9 inches per minute for the design speed and 20 inches per minute for the limiting mechanism capability in the event of an overspeed signal from the controller.

- 2. The PCRDM shall be designed for selectable rod movements between 0.36 and 9.0 inches per minute to accomplish the normal operational reactivity control functions related to plant load follow, burnup compensation, startup and normal shutdown, with incremental steps of 0.025 inches in order to provide fine resolution reactivity control.

The maximum design basis withdrawal speeds of 9 inch per minute for both the PCRDM and the SCRDM have been selected to assure maximum reactivity insertion rates of only a few cents per second. This speed assures that ample time exists for reactor shutdown response before a large reactivity insertion can occur even in the event of an uncontrolled rod withdrawal. For the very unlikely event of an overspeed signal from the controller, the maximum PCRDM speed limit restricts the maximum reactivity insertion rate to approximately 33¢/second, which is well within the Plant Protection System capability.

54 |

The 0.025 inch incremental step size (applicable to PCRS) is based on the requirement to have the magnitude of the incremental worth adjustment significantly less than the total dead band of the power controller. The controller dead band is +2% at full power and the power coefficient is such that approximately 2.0¢ worth is equivalent to 1% at full power. The maximum primary control rod worth is less than \$3.53 which corresponds to an average reactivity of approximately 16¢ worth per inch. The 0.025 inch incremental control rod step size in combination with the 16¢ average worth per inch leads to a linear reactivity resolution of 0.40¢ worth per control rod step which is significantly less than the 8.0¢ worth of the controller dead band.

54 | 51

Insertion and Withdrawal Forces

54 |

- 1. To provide extra shutdown margin for the reactors, each control rod system shall provide a minimum insertion force capability for a 1000 lb. force applied to the control rod in an attempt to free a stuck rod by driving in with the mechanism.

2. Each control rod system shall provide a minimum withdrawal force capability to assure control rod withdrawal under worst case assumptions of alignment, drag forces, flow conditions and duct bowing.
3. The control rod systems shall be designed to assure that the control rods cannot be significantly lifted (floated) from the fully inserted position under maximum control assembly pressure drop conditions. This requirement shall apply to all rods in each system with the driveline connected to the control rod or to refueling conditions for which the driveline is disconnected and withdrawn to its refueling position. Significant lifting is defined as the withdrawal distance that would reduce shutdown reactivity margins by more than the excess margin provided by the stuck rod requirement used to establish rod worths.

The above reactivity limit on rod lifting defines limits on rod motions that might occur as a result of inadvertent flow rate increases with the drivelines disconnected, even if full flow is initiated in the shutdown refueling condition. (However, it is noted that to initiate full flow in this condition would require multiple operator errors and the violation of interlocks).

- 51 |
4. Each control rod system design shall provide capability, as a non-routine operation, of permitting refueling withdrawal of the driveline and replacement of the control assembly in the event of failure of the driveline coupling to release the control rod, or a control rod stuck in any position.

A primary control rod stuck in the withdrawn position, or a coupling failure would prohibit the rotation of the reactor closure head required for normal refueling operations. This requirement is to provide capability for an abnormal operation permitting appropriate separation of the driveline and control rod.

Coefficients of Friction

53 | Scram insertion speeds shall be assured for a coefficient of friction of 1.5 for sliding contact and 1.0 for dynamic impact contact (such as in a seismic event), or other values as established by appropriate test programs.

51 | Seismic excitation of the reactor system results in the structure surrounding the control rod and absorber and driveline being subjected to dynamic lateral displacements. The result of this exci-

tation is that the surrounding structure impacts the driveline and absorber at the guide points, thereby generating impulsive lateral interaction loads which characteristically exist for less than a millisecond. Specific loading effects at the point of impact related to the presence of the coolant and the local dynamic deformation of the material cannot be separated uniquely. However, both are embodied in an "Effective Coefficient of Friction", applicable to impact load condition, which is expected to be substantially less than the design value of a 1.0. A test, described below, was performed to determine this "Effective Coefficient of Friction".

61 | Coefficient of sliding friction test data from sources external to CRBRP indicate that friction coefficients for material couples occurring in the control rod systems are substantially below 1.5 (Ref. 40). These tests were performed using a pin slider on a flat plate under steady loading. These data, contained in References 79 and 80, are summarized in Table 4.2-36A. This table contains data taken at temperatures ranging from 400°F to 1160°F and represents the maximum observed dynamic friction for each couple. The ETEC data for Inconel 718/718 did not represent the maximum observed value during sliding, but rather the combination of the initial and final values. These data appear to be inconsistent with the other data for Inconel 718/718.

61 | To resolve this inconsistency and to create a large body of applicable data for a variety of material couples appropriate to the control rod systems, a series of tests on the sliding coefficient of friction using a pin slider on a flat plate have been performed. These data, presented in Table 4.2-36B, represent the average value of the sliding coefficient of friction for each material couple for a variety of temperatures, pin pressures and over two stroke lengths. For certain couples such as Inconel 718/718 and Inconel 718/316SS the complete tests were repeated and two lines of data appear in Table 4.2-36B. Average values of the sliding coefficient of friction are presented because these data are more appropriate to the conditions that exist during scram than the momentary peak values or the initial and final values presented in Table 4.2-36A. Also, data in Table 4.2-36B has been presented as a function of temperatures and pin pressure to allow review of these functional variables. Since the data in Table 4.2-36B show no significant dependence on temperature, the upper three sigma data have been averaged over temperature for each of the material couples in Table 4.2-36B. The results are shown in Table 4.2-36C for comparison with the prior, less extensive Table 4.2-36A. These data demonstrate a dependence on pin pressure with the lower pin pressures having the higher coefficients of sliding friction. This pressure dependence occurs frequently in pin on plate measurements and may not be a material couple characteristic. There also appears to be a slight correlation with stroke length. In this case, the longer stroke length of .750 inches would be more appropriate for the control rod system during scram.

59

In summary, the data presented in Table 4.2-36B and 4.2-36C represent the most recent and most appropriate values of sliding friction data for the material couples used in the control rod system. The upper three sigma values of Table 4.2-36B, as selected for the most appropriate analysis conditions, are the recommended values for design analyses.

Tests were performed to determine the effective coefficients of friction under dynamic impacting conditions such as would occur between the PCRS fixed boundaries and the translating elements during a seismic event. In these tests, the effective dynamic coefficient of friction was determined by solution of the equations of motion based on measured impact loads and drop times of test rods subjected to lateral dynamic excitation (Ref. 182). These tests were simplified simulations of the circular PCRS driveline and hexagonal control rod oscillating within their respective constraints. To reduce complexity but still retain the principal dynamic effects on the coefficient of friction, the test articles were a straight circular rod traveling through three bushings, and a hexagonal rod traveling in a hexagonal duct. Bushing clearances were chosen to provide both lateral and rotational impact under lateral dynamic input similar to PCRS driveline response to seismic excitation. The hexagonal rod to duct clearances were typical of PCA design clearances. Material couples were prototypic of the PCRS (i.e., Inconel 718 on Inconel 718, circular, and Inconel 718 and 316 SS, hexagonal).

51 59

59 | The test media were air, water and liquid sodium. Only the circular rod was tested in sodium to determine the differences, if any, between the water and sodium media.

59 | The input was a simple sinusoid at a frequency typical of the PCRS predicted response to seismic excitation. Different frequencies and amplitudes were tested. Input was applied to the test vessel simulating the PCRS fixed boundaries which are excited in an earthquake. Bushing and hex duct loads were monitored by strain bolts to determine the drop rod impact magnitudes.

59 | The tests have been completed. Table 4.2-36E summarizes the resultant coefficients of friction. It can be seen that the dynamic coefficient of friction is significantly less than the 1.0 design value specified in the absence of corroborative test data for a lower value. 51 | The effective friction coefficients from these tests are used for seismic 59 | scram insertion speed analyses.

Antigalling Characteristics

51 | Table 4.2-36D summarizes the FFTF Prototype Control Rod System Tests and the completed CRBRP Prototype Control Rod System Tests. Throughout all these tests, there were no failures to scram and no galling was found except for a slight effect in the FFTF tests between the control assembly wear pads and the outer duct which did not impare scram performance. For CRBRP, this wear effect was eliminated by including a rotational joint in the control rod shaft. In all tests except the CRBRP Unlatching Test, the environment simulated a reactor environment of liquid sodium with an argon cover gas. In all cases the sodium pool temperature ranged from 400^oF to 1100^oF. In the CRBRP Unlatching Test the liquid medium was water and a dummy weight was used to simulate a PCA.

The prototypic FFTF CRDD accumulated a total travel of 23,635 feet and 828 scrams, and the CRD/CA disconnect coupling was operated 50 times. When Phase 2 of the CRBRP tests have been completed, all CRBRP Prototype Units will have exceeded the CRBRP requirements of 17,000 feet of travel and 750 scrams over the 30 year life of the mechanism.

59 | These test results for the PCRS design and associated material couples show negligible galling. Consequently, galling will not significantly affect PCRS performance.

Irradiation Stability

As stated in an earlier paragraph, the friction coefficient was only slightly affected by sodium exposure and there was no effect due to irradiation. In addition, the control rod drive mechanism and the control rod driveline fluences are too low for the radiation to

affect their performance. Core assembly irradiation induced swelling has been conservatively included in the design process to establish the clearances for control assembly components.

Based on the above test data, subsequent analysis and utilization of this data in the CRBRP design, the operability of the reactivity control systems and their disassembly after reactor operation seemed assured. However, to provide the desired assurance, additional testing described in Section 4.2.3.4 and Appendix C, Section C.5.1.2 has been established for the CRBRP Primary Control Rod System. These tests will
51 | provide additional data regarding the operability of CRBRP at LMFBR operating temperatures.

4.2.3.1.4 Positioning Requirements

The positioning requirements for the control rod systems are:

1. Both the primary and secondary control rod system shall each provide two independent position indication systems and a means for verification of coupling and disconnect between the driveline and control rod.
2. Each control rod system shall provide capability for measurement of scram insertion times for individual control rods with the reactor shutdown (not more than 5% power) and flow not more than 40%.
3. One of the position indication systems for each control rod system shall have a minimum indication accuracy of ± 0.5 inch for the full-in and full-out position of the control rods and ± 1.25 inches over the full control rod stroke. These accuracies apply to the positions of the translating assemblies (drivelines) relative to the CRDM housings.
4. One of the primary control rod system position indication systems shall provide an accuracy of ± 0.15 inch for the leadscrew relative to the full insertion position.
5. One of the secondary control rod system position indication systems shall provide an accuracy of ± 0.5 inch at the full-in, withdrawn operating and refueling positions.

Two independent position indication systems are provided for each system to give positive verification of control rod position and a means to check operation of each system by comparison with the other system. These systems are expected to monitor the positions of the control rod drivelines (leadscrews). Consequently, an additional indicator is provided to verify connection and disconnection operations between the driveline and control rod.

Testing capability for control rod scram performance is planned for all plant conditions between cold shutdown and full power conditions. Measurements of individual control rod scram insertion times are required to ensure this capability and to provide periodic checks for abnormal control rod performance.

Position accuracy of ± 0.5 inch at full insertion is provided to verify the fully inserted positions for reactor shutdown and to assure insertion positions for control rod disconnect and subsequent refueling operations. Accuracy in the fully withdrawn position is specified to assure adequate positioning for potential scrams from the parked position. These positions are also used for safety interlocks with the reactor control and refueling systems.

The primary control rod system is used for establishing criticality and subsequent power control operations. While the rod position indication

is not fed back directly to the reactor control system, the operator utilizes the position data to evaluate the plant and to interpret reproducibility of reactivity control. The relative position indication accuracy of ± 0.1 inch leads to reactivity reproducibility of approximately 1¢ for the highest worth rod in the primary system. In addition, the position indication is utilized for logic interlocks and alarm as described in Section 7.7.1.3.

4.2.3.1.5 Structural Requirements

Control Rod Drive Mechanisms

The primary and secondary control rod drive mechanisms are designed to the following classes of components:

1. ASME Boiler and Pressure Vessel Code, Section III, 1974 edition, Class 1. For the primary control rod system, the mechanism motor tube, motor tube hold-down ring, nozzle extensions and position indicator housing form a part of the pressure retaining boundary. For the secondary control rod system, the extension nozzle, the hold-down ring, the upper SCRDM housing, the upper portion of the lower SCRDM housing, and the connector plate form a portion of the pressure retaining boundary.
2. Seismic Category 1. The control rod systems are required to remain functional and shutdown the reactor in the event of an SSE. (See Section 3.2.1 for detailed discussion).
3. Safety Class 1. The control rod systems are categorized as Class 1 because of their control and shutdown functions. (See Section 3.2.2 for detailed discussion).

The primary control rod drive mechanisms shall be designed to the load conditions of Table 4.2-37. For these loading conditions, pressure boundary components shall meet the structural requirements of Section III of the ASME Pressure Vessel Code together with applicable code cases and amendments to the code by RDT Standards. The portion of the Secondary Control Rod System that is coded in accordance with the ASME B&PV code and hence forms a part of the pressure retaining boundary shall be designed to the load conditions of Table 4.2-37. The structural requirements of Section III of the ASME Pressure Vessel Code together with applicable code cases and amendments to the code by RDT Standards shall be met.

The governing stresses in the mechanism are the time independent effects of primary mechanical loads, secondary thermal loads and fatigue. Use of the methods of these codes together with consideration of material effects such as

carbon and nitrogen depletion, thermal aging, and environmental correction factors to account for material interaction with sodium leads to conservative structural designs of the mechanisms.

The primary and secondary control rod drive mechanisms shall have a design life of 30 years. This lifetime is consistent with the design lifetime of the reactor. Interim maintenance of some replaceable components will be required in order to achieve this lifetime.

The PCRDM and SCRDM shall remain structurally intact and attached to the reactor vessel, and shall not permit sodium leakage under Structural Margin Beyond the Design Base conditions. (See Reference 10a, Section 1.6). This requirement provides added margin of safety for an event for which no causative mechanism is known.

The PCRDM and SCRDM shall be designed such that no mechanical failure can result in any parts becoming missiles.

Control Rod Driveline

The primary control rod driveline (PCRD) and the secondary control rod driveline (SCRD) shall meet the intent of the structural requirements of Section III, ASME Pressure Vessel Code, together with applicable Code Cases (1592), and amendments by applicable RDT Standards. The stress and stability criteria for evaluation of the design shall be as specified in the above codes for all significant loading conditions including those identified in Table 4.2-37. Material physical property changes due to irradiation, thermal, and sodium environments shall be considered in evaluating the design.

The ASME Code specifies conservative allowable stresses for various loads and combinations of loads. The compressive load limit shall be no greater than $1/3$ the buckling stability load of the driveline, and the design stress intensity limit shall be the lower of $1/3$ ultimate or $2/3$ yield stress. Satisfaction of the criteria assures that conservative margins exist for all conceivable loads including rod ejection for which no causative mechanism is known.

The design lifetimes of the primary and secondary drivelines shall be as shown in Table 4.2-38. The design lifetime requirements are conservative with regard to material considerations, taking into account the irradiation environments of these components (Table 4.2-39).

The following SCRS description is included in response to NRC Regulatory Guide 1.87, "Guide for Construction of Class 1 Components in Elevated Temperature Reactors," which supplements ASME Section III Code Case 1592. Code Case 1592 is used in analysis of those sections of the SCRS driveline which operate at temperatures above 800°F. The drive mechanism operates at temperatures below 450°F and is not in scope of Code Case 1592. The control assembly is not in the scope of the ASME Code because of the irradiation effects. The most highly stressed section of the driveline operating at temperatures exceeding 800°F is the joint between the lower and upper tension rods. The lower and upper tension rods are under uniaxial tension produced by the pneumatic pressure in the scram cylinder. Load transfer between the two halves of the tension rod is through a mechanical coupling where multiple flanges at the

ends of the two halves are engaged in grooves in a split shell which is held together by a lock sleeve. The stress levels in this section were calculated by multiplying the uniform tensile stress in the principal section of the tension rod by elastic stress concentration factor. This is equivalent to elastic analysis. Equal load distribution was assumed between the three flanges at the end of each half of the piston rod. The Code allowable stress limits were conservatively based on temperature estimates which assumed no mixing in the coolant from the core exit to the sodium surface level. That is, the Code stress allowables for 1080°F based on "no mixing" assumption were used instead of the 1000°F value corresponding to the expected plenum temperature, which is applicable continuously throughout the design life.

Control Assemblies

The structural design basis for the control assembly is very similar to the design basis for the fuel and blanket assemblies given in Section 4.2.1.1. Applicable criteria from Section 4.2.1.1 are given below as supplemented by additional criteria unique to the control assembly.

1. Operating Conditions and Loads

The control assemblies shall be designed to operate over a minimum design life goal of 328 full power days (FPD) corresponding to operation over the first two cycles of 128 FPD and 200 FPD together with capability for a minimum of one cycle of 275 FPD for later cores. The mechanical design of the primary control assemblies shall be based on a lifetime goal of 550 FPD. This requirement is established so as to not preclude two cycle operation in the event it can be shown that nuclear effects on B₄C pellets and absorber pins are not limiting to two cycles operation.

51

For design analysis at steady state and anticipated fault (upset event) conditions, control assembly temperatures shall be based on expected plant operating conditions and semistatistical hot channel factors at the upper 2σ confidence level. For unlikely and extremely unlikely faults (emergency and faulted events) for which a single worst case event is considered in the design basis duty cycle, the upper limit on plant conditions (T&H design values) and hot channel factors at the upper 3σ confidence level shall be utilized. Damage associated with long term steady state operation or accumulated over a number of anticipated events would be associated with average temperature behavior so that a 2σ confidence level is conservative for these conditions. However, a single worst case event such as an unlikely fault tends to be life limiting with potential safety consequences so that very conservative 3σ confidence levels are applied for these events.

Normal, upset, emergency and faulted events shall be utilized in evaluating the control assembly performance and safety aspects as noted in Section 4.2.3.1.6.2. Appropriate accident events of Section 15.4 shall also be considered on an individual event basis.

The following loading mechanism shall be considered in the absorber pin design:

- a) Clad pressure loads in the sealed absorber pins produced by helium released from captures in the B₄C absorber. Clad loading due to differential pellet and clad growth will be minimal due to the pellet clearance requirements given in Table 4.2-36.

- b) Primary and Secondary clad stresses generated by radial, axial and circumferential thermal and flux gradients in the clad material. These stresses will be relaxed by pin bowing, irradiation creep and thermal creep. At shutdown conditions, residual stresses associated with these relaxation mechanisms will be present.
- c) Interaction forces between the clad and wire wrap generated by differential axial and radial growth. Interaction forces between the pins and inner duct will be controlled to a small value by the clearance requirements of Table 4.2-36, and will be considered in the structural evaluation of the primary control assemblies.
- d) Potential fatigue stresses resulting from flow induced vibrations and transient events.

Evaluation of the control assembly included the following loading considerations as a minimum design basis in addition to the absorber pin loading mechanisms described above:

- a) Duct loads introduced by the core restraint system as a result of assembly bowing and/or seismic events. Note: This design aspect is not currently finalized; this work will be completed prior to issuance of the FSAR.
- b) Forces induced by sodium flow and associated pressure drops through the assembly including pressure differences across the duct walls and nozzles as well as axial lift forces offset by the assembly weight and hydraulic holddown features. The secondary control assembly shall consider irradiation creep deflection of the inner cylindrical guide tube caused by the external pressure loading on this tube.
- c) Secondary stresses due to the steady state and transient temperature gradients through the component thickness.
- d) Maximum insertion, withdrawal and dynamic loads applied through the refueling equipment and during refueling operations. The design shall accommodate maximum shipping and handling loads based on 6g axial and 2g lateral accelerations.
- e) Maximum insertion and withdrawal loads applied by the CRDM's (see Table 4.2-37) and scram arrest loads.

2. Design Criteria

Control assembly structural criteria are specified for the absorber pins and the balance of the assembly. Absorber pin criteria are similar to and are based on a common methodology with fuel rod criteria. Table 4.2-37A provides the absorber pin structural criteria.

The balance of the assembly criteria have been patterned after ASME Section III Code requirements, with modifications to account for the reduced ductility of irradiated material. The Code based design stress limits are derived from consideration of ductile failure modes only. Their use in core component design is restricted to applications in which it can be demonstrated that ductile failure mode analysis is applicable. Factors considered in this evaluation are the effects of irradiation, stress multiaxiality, and straining rate on the fracture elongation of the material. Where ductile behavior cannot be guaranteed, additional design limits are imposed to provide safeguards against brittle failure.

Table 4.2-37B provides the balance of the assembly structural criteria.

Thermal and hydraulics design criteria have also been established for the control assemblies in addition to the operating conditions previously discussed. The following are the T&H criteria specified:

- a) No centerline absorber melting at an upper 3 confidence level shall be permitted at either a 15% overpower condition or under transient conditions including upset and emergency events. This requirement is specified as a conservative design basis since test data is not currently available on B₄C behavior at incipient melting conditions.
- b) As a design guideline, the maximum cladding midwall temperature during an emergency event shall be less than 1600°F for any extended period of time.
- c) For faulted conditions, the sodium temperature shall be maintained below its boiling point, saturation temperature at the existing pressure.
- d) Hot channel factors shall be determined by taking into account PCA and SCA tolerances and flow channel closure due to absorber pin bowing or differential radial growth of the clad, wire wrap and inner duct.

3. Safety Related Design Features

In addition to the control assemblies safety features for shutdown and reactivity control, the design shall include the safety features for the fuel assembly given in 4.2.1.1.2.3 together with the following requirements:

- a) A discrimination system shall be provided to insure against a refueling error which could result in a significant reactivity error or undercooling of the control assemblies. This system shall prevent the following situations:

Insertion of any assembly other than a control assembly into a control assembly position.

Insertion of a control assembly into a fuel assembly position or a wrong control assembly position (i.e. interchange of a primary and secondary control assembly).

- b) The relative location of the absorber pellet column within the pin shall be maintained under shipping, handling and scram arrest loadings by a properly designed axial spring support system.

4.2.3.1.6 Environmental Requirements

The control rod system shall provide safe reliable shutdown and control capability when subjected to the following environmental conditions with the ability to withstand the total loss of N_2 cooling without a loss of CRDM safety function.

The external surfaces of the Control Rod Drive Mechanisms are exposed to the head access area environment at temperatures between 70 and 265°F during full power operation. The internal atmosphere of the CRDM is inert gas at temperatures ranging from 70 to 450°F. Normal primary mechanism internal pressures range from 15 to 30 psia.

The control rod drivelines are exposed to an environment of liquid sodium containing 2 (>800°F) to 5 (<800°F) PPM oxygen over the lower 60 percent of its length (approx.). The remaining upper portion is exposed to an atmosphere of inert cover gas and sodium vapor.

The control assemblies are exposed to an environment of liquid sodium containing 2 (>800°F) to 5 (<800°F) PPM oxygen.

The design of the CRBRP Primary CRDM/CRD is conceptually the same as that used on the FFTF program. This design employs some proven design concepts, (References 145, 146 and 147) that inhibit the upward movement of sodium vapor laden cover gas by reducing the annulus width while increasing the length thereby minimizing the effect of natural convection.

To further insure the reliability of the Primary CRDM/CRD a continuous purge system consisting of recycled cover gas will be utilized to provide a constant downward flow through the annuli into the reactor.

In addition, testing has been incorporated into the CRBRP reliability program which is aimed specifically at determining the effect of sodium vapor condensation on the Primary CRDM/CRD. A failed-bellows environment test will be conducted in which a prototype PCRDM/PCRD will be operated in a sodium vapor-argon gas environment with a failed main bellows. This test will confirm acceptability of operation with a failed bellows.

In addition, a duplicate test has been performed on the FFTF program which provides preliminary data regarding the basic design adequacy.

Secondary Control Rod System

Condensation of sodium vapor in the reactor head area around the Secondary Control Rod Driveline will have no influence on scram release of the Secondary Control Rod because only the tension rod needs to move (<0.09 inch) to allow the latch to release the control rod. The tension rod is located within the sensing tube which is, in turn, enclosed in the driveshaft. The regions between these shafts and tubes are sealed by bellows, and consequently, sodium vapor is prevented from entering these regions and condensing there. The clearances between the outside of the driveshaft and the upper internals structure are relatively large in the region above the liquid sodium level. Consequently, accumulation of sodium vapor condensation will not inhibit drive-in of the driveshaft for normal reactor shutdown. Furthermore, these regions are normally kept well above the sodium solidification temperature and so the vapor that does condense will be in liquid form rather than as a frost. Because of these considerations, sodium vapor condensation is not expected to adversely affect the ease of movement or operation of the Secondary Control Rod Drive Mechanism and Driveline nor adversely affect scram release of the Secondary Control Rod.

A failed-bellows test was conducted to demonstrate the extent of sodium ingress into the SCRDM/SCRD moving parts and to demonstrate the degree to which performance is degraded following prolonged operation with failed bellows. Operation with the defected bellows for 11 months had no detectable effect on the scram performance and the mechanism performance. The sodium ingress to the mechanism was negligible. The sodium ingress to the upper driveline was sufficient to reduce the sensing tube travel, resulting in the loss of the direct position indication of the control rod coupling head within the latch. The reduced sensing tube travel had no effect on the ability to couple to the control rod or on the scram performance. The reduced sensing tube travel was attributed solely to the operation with the detected driveline lower bellows.

4.2.3.1.6.1 Nuclear Environment

Table 4.2-39 represents a preliminary evaluation of the axial distribution of the total and fast neutron flux along the Row 4 control rod system for the control rod in a fully withdrawn position at the end of Cycle 4. The fluxes at other control locations will be less than the values given for the Row 4 control rod system at this time in life.

4.2.3.1.6.2 Control Rod Systems Duty Cycle

The CRBRP duty cycle consists of normal, upset, emergency, and faulted events. From this complete duty cycle a lesser number of umbrella transient events is selected and a histogram prepared for use in the evaluation of the capability of the control rod system design to satisfactorily withstand the effects of the thermal transient requirements. A histogram for the primary and secondary CRDM and CRD which depicts a reactor operating cycle that begins during a dry reactor heatup and terminates during a dry reactor cooldown is shown in Figure 4.2-96. A tabulation of these umbrella transient events is included in Table 4.2-40.

The service life of the primary and secondary systems is derived from the duty cycle in Figure 4.2-96. Table 4.2-38 summarizes the required service life of the components of the primary and secondary systems. Allowance is made in the design of the mechanisms for the replacement of certain replaceable components at periodic maintenance intervals, based on experience gained from initial inspections. The design life of the drivelines shall be maximized to the extent possible with a goal of no required replacement during the 30 year plant life, with minimum lifetimes as shown in Table 4.2-38.

4.2.3.1.6.3 Thermal and Hydraulic Environment

The evaluation of the effects of the thermal and hydraulic environment on the control rod system components shall be based on consideration of both steady state and transient conditions. This evaluation required consideration of the simultaneous temperature versus time and flow versus time relationships for the sodium coolant exiting the control assemblies, the sodium coolant exiting from the surrounding fuel assemblies, as well as the control rod moving downward during a scram.

The steady state temperature distribution of the control rod system must be determined from evaluation of the following thermal and hydraulic parameters:

The Reactor Steady State Thermal Environment (see Figure 4.2-97) defines the steady state temperature distribution.

The steady state mass flow rate and temperature of the sodium flowing through the control assembly, and the mixing of this sodium with the adjacent assemblies sodium in the 2 inch space below the shroud tube.

The location of the bleed holes in the driveline shroud tube.

Thermal transient conditions are defined by the duty cycles described previously.

4.2.3.1.7 Material Selection and Radiation Damage

Material choices for control rod systems were based on prior experience and data from FFTF (Ref. 1, 40, and 41), and on the goal of maintaining adequate mechanical properties in an atmosphere of inert gas, sodium vapor, and liquid sodium. Additional discussion of the interaction of the sodium environment with austenitic stainless steel is presented in Sections 5.3.2.2.2 and 5.3.2.2.3.

Control Rod Drive Mechanisms

The primary mechanisms utilize Type 403 SS in the motor tube and segment arms for its ferro-magnetic properties. In addition, both Types 403 SS and 17-4 PH are utilized in highly stressed areas such as the segment arms, and leadscrews, because of their high strength. The secondary mechanism will utilize many different types of materials. Selected load-carrying members are made from high strength materials suitable for the conditions.

Regarding Type 17-4 PH material for the PCRDM, only the leadscrew will be fabricated from this metal and exposed to elevated temperatures. The 17-4 PH material being utilized in the leadscrew will be procured and heat-treated per ASME Standard SA-564 as modified by RDT Standard M7-6. The latter standard permits only two heat treat temperatures; 1100°F and 1150°F. The FFTF mechanism leadscrew was purchased and heat treated to the same specifications. In service, the maximum temperature experienced by the lower portion of the leadscrew, which is fabricated from 17-4 PH, will be in the temperature range of from 400 to 450°F. This maximum temperature will be experienced only when the control rods are fully inserted. During reactor operation, with the rods fully or partially retracted, the service temperature of the leadscrew will be less than the 400 to 450°F region. This latter condition should account for the major exposure time for this 17-4 PH material.

In selecting the 17-4 PH material for this application, the early experience (References 140, 141 and 142) with this alloy involving embrittlement was considered, especially when the material is aged at a relatively low temperature such as 950°F and subjected to a service temperature in the 600 to 800°F range. Based on the high aging temperature of 1100°F coupled with a service temperature of 450°F or lower, embrittlement was not considered a problem. It was concluded that below 550°F the embrittlement is minimal. The position is substantiated by the data presented in References 143 and 144.

The exposure time required to cause room temperature charpy impact values to fall below 15 ft. lbs is shown in Figure 4.2-97A together with the exposure time to deplete room temperature impact values by one half shown in Figure 4.2-97B. This indicates that at temperatures below 500°F, essentially no effect on impact strength is observed.

Driveline and Bellows

Material choices for the drivelines and bellows were predicted on maintaining adequate margins of strength in the high temperature sodium and irradiation environment. Inconel 718 is utilized for the PCRS to take advantage of its high strength and hardness and its favorable wear and antigalling characteristics. The Primary CRDM bellows consist of a main bellows, a disconnect actuating rod bellows, and a position indicator rod bellows. All of the bellows are Inconel 718, and located above the sodium level in a low-level irradiation environment. The main bellows is cycled as the control rod system is moved. The outer two bellows cycle only for the refueling or maintenance modes. Before installation in the mechanism, all bellows are required to pass a 20 cycle breaking test with subsequent leak testing. Table 4.2-36D summarizes FFTF and CRBRP CRDM testing completed. These tests have been completed without a bellows failure. Details of additional FFTF bellows testing is described below.

59

35

The prototype design test objectives are to confirm the design and operating characteristics of the PCRS in a sodium-argon environment of the design basis service life, including a minimum of 17,000 feet of travel and 732 scrams. The reliability objective is to confirm the shut-down reliability of the PCRS.

14

35

Three prototypic FFTF CRDM bellows were life tested over a vessel containing a pool of sodium with argon cover gas and one bellows was tested in argon gas. The tests included cyclic tests and scram tests. The FFTF life requirements were identified as 20,000 feet of travel, and 1500 scrams, which represents twice the expected usage in service. No testing was performed in sodium, since sodium immersion is not a service condition. The results of the bellows tests are summarized below:

<u>Bellows No.</u>	<u>Environment</u>	<u>Scrams</u>	<u>Ft. of Travel (does not include Scram Travel)</u>
S/N 001	Argon	1200	19,000
S/N 002	Argon-Sodium vapor @ 450 ⁰ F	2500	23,000
S/N 003	Argon-Sodium vapor @ 450 ⁰ F	2250	20,700
S/N 004	Argon-Sodium vapor @ 450 ⁰ F	1530	13,770

<u>Bellows No.</u>	<u>Comments</u>
S/N 001	Indicated a leak after 1200 scrams and 19,000 feet of travel
S/N 002	Completed the test with no indications of failure, but helium leak test later indicated leakage
S/N 003	Subsequent helium leak test confirmed leakage
S/N 004	Failed after 1530 scrams and 13,770 feet of travel. Subsequent helium leak test confirmed leakage.

14

Three of four of these bellows exceed the CRBRP travel requirements, and all exceed the scram requirement.

PCRS operation or scram performance is not expected to be sensitive to a failed bellows condition for operating periods of at least one year. Testing with a purposely failed bellows in Phase IV of the FFTF Control Rod Environmental Life Test was completed in June 1976. The FFTF Control Rod System performed satisfactorily with a failed bellows. In addition to the FFTF failed bellow tests, the CRBRP CRDM will be tested for operation with a failed main bellows to represent a year of in-service operation under this condition.

Although no bellows testing in an irradiated environment has been performed, irradiation is not expected to detrimentally affect the Inconel 718 bellows since the flux level will be low. The environment conditions for the CRDM bellows are less than 2.5×10^5 n/cm²/sec total flux. The fluence for this condition after 30 years will be about 1.8×10^{14} n/cm².

No data are available for Inconel 718 irradiated at the low fluence service conditions. Data for substantially more severe irradiation exposures are given in References 72 and 73. The very low levels of irradiation of the CRDM bellows would not be detrimental to bellows strength, ductility, or performance.

Couplings

The material selected for the primary control rod driveline coupling is Inconel 718, based on the same criteria as the driveline material choices. The PCRD coupling will be only infrequently actuated and is not required to release during scram. Thus, high strength retention in hot sodium is the primary consideration in the choice of Inconel 718 for the primary coupling. Type 304 stainless steel is utilized in the compression sleeve around the coupling, taking advantage of its greater thermal expansion vs. Inconel 718 to create a thermally locking joint.

The secondary driveline/control assembly coupling includes the coupling head at the upper end of the control rod, the collet gripper that engages the head, and a cam that serves in the actuation of the assembly and performs the release function for scram. Therefore, friction, wear, and self-welding considerations are important in the choice of materials for the secondary coupling. Selection of materials was based on results of a prototypical test program conducted to examine the material combinations and functional performance for the coupling components.

The three components of the secondary coupling was fabricated from Inconel 718 in the aged condition. Selection of Inconel 718 was based upon the results of the national program on friction and wear, (see Section 4.2.3.3, Table 4.2-50, and Ref. 42 and 43) which identified this alloy as exhibiting low friction and low self-welding tendencies in sodium.

Additional comments regarding self-welding considerations for the Secondary Control Rod System are found in Section 4.2.3.3.2.4.

Control Assembly

Structural material for the control assembly must have good stability in sodium, resistance to deleterious irradiation effects and good high temperature strength. Cold worked Type 316 stainless steel exhibits the above characteristics to a greater degree than other candidate materials with significant irradiation experience and is, therefore, the material of choice for the control assembly and absorber pin cladding. Structural materials used for the control assembly are consistent with fuel and blanket assembly designs discussed in Section 4.2.1. Material properties utilized in the control assembly design and analysis are discussed for the core assemblies in Section 4.2.1.1.

B₄C was selected for the absorber material to fully utilize the developmental and applied effort on this material under the FFTF program. B-10 enriched B₄C will be used for the CRBRP absorber. Ref. 44a and 153 describes the B₄C data currently being applied on the CRBR program.

Wear Surfaces

A number of components in the control rod systems will experience sliding contact with adjacent components, or will remain in static contact for long durations in sodium or sodium vapor. Low friction and wear materials have been selected for critical wear surfaces.

The only material couple involved in the operating parts of the primary coupling is Inconel 718/Inconel 718. This particular materials combination has been subjected to extensive testing in sodium and has proven to have excellent resistance to self-welding. Test conditions have included

temperatures of 850 and 1050°F, for contact pressures of 16,000 and 148,000 psi, and times up to 6 months, with separations being performed at the exposure temperature (References 136 and 137). Other tests, primarily aimed at collecting sliding friction data, indicated that no self-welding took place after 1 week in 1100°F sodium under pressures up to 5000 psi (Reference 138). These findings by ARD experimenters, are in line with those of a German laboratory, which found that no self-welding occurred after 168 hours in 1292°F sodium under a contact pressure of 7000 psi (Reference 139).

From the above observations, it is apparent that Inconel 718/Inconel 718 materials couples will perform more than adequately in applications where resistance to self-welding is a major requirement.

A failure of the coupling to decouple has no safety consequence. Although the CRD must be disconnected from the control assembly to permit refueling, the breakaway joint (discussed in Section 4.2.3.1.3) may be utilized in the unlikely event that a failure to decouple did occur. Refueling could then proceed normally.

At potential high wear points in the primary system, resulting from the operating requirements of the system, low wear material couples have been selected. For in-sodium applications, including the control assembly wear pads, Inconel 718 in contact with 316 SS is the material of choice due to its favorable wear, anti-galling characteristics and stability in sodium. Above the bellows, materials such as Stellite 6B and modified 440C are utilized for their superior abrasion resistance. Typical applications in the primary system include Stellite 6B for the mechanism leadscrew bushings in contact with 17-4 PH leadscrew, and Stellite 6B for the torque taker in contact with the Inconel 718 torque taker tube. Areas above the bellows employ dry film lubricant extensively.

For the secondary system, critical surfaces such as the control rod wear-pads will be fabricated from low friction and galling resistant materials such as Inconel 718.

4.2.3.2 Description and Drawings

The two redundant control rod systems, called the primary and secondary control rod systems, are shown schematically in the reactor in Figure 4.2-98. Table 4.2-41 illustrates the diversity in these systems. Reactor shutdown can be achieved by either system with the other system completely inoperable and with the highest worth rod stuck in the system which is operable. This redundancy assures safe and reliable shutdown capability.

The two shutdown systems are completely independent including the Plant Protection System (Section 7.1) which provides separate signal and command arrangements for each of these systems.

Each system consists of a control assembly, a control rod driveline and a control rod drive mechanism. The control assembly, located in the core, consists of a movable absorber pin bundle called the control rod and an outer duct assembly. The control rod driveline provides a linkage between the control rod and the control rod drive mechanism, located above the reactor closure head, which positions the control rod at appropriate axial core positions.

The control rod systems operate on the principal of varying the neutron absorption in the core by movement of the control rods in and out of the core. The primary system provides a means for starting up the reactor, regulating the power level of the reactor and compensating the reactivity loss due to fuel burnup as well as functioning as the primary shutdown system. The secondary system provides reactor shutdown in the extremely unlikely event of failure of the primary system to shutdown the reactor.

4.2.3.2.1 Primary Control Rod System

The 9 core locations comprising the Primary Control Rod System (PCRS) are shown in Figure 4.3-1. The three major components of primary control rod system are shown schematically in Figure 4.2-100. The PCRS design is essentially the same as the FFTF CRS design in order to maximize the use of the FFTF design, analysis, and testing experience. Figures 4.2-101 through 4.2-104 show the principal design features of the primary control rod system.

4.2.3.2.1.1 Primary Control Rod Drive Mechanisms

Principal features of the Control Rod Drive Mechanism (PCRDM) are shown in Figures 4.2-101, 102 and 103.

The PCRDM is an electro-mechanical actuating device which utilizes a collapsible rotor roller nut drive, and is actuated by signals from the reactor control system. These signals cause the stator to be energized and magnetically actuate the rotor assembly arms, causing the roller nuts to engage the threaded portion of the leadscrew. Rotation of the electrical field of the stator causes rotation of the roller nuts with respect to the leadscrew which is rotationally restrained. This rotation raises or lowers the leadscrew whereas, stopping the rotation causes the rotor assembly to hold the leadscrew at any desired position. De-energizing the stator causes the roller nut to disengage the leadscrew, causing the leadscrew, driveline and the control rod absorber to drop into the core at a rapid rate of insertion (scram). Heat from the stator is removed by the recirculating gas cooling system (see PSAR Section 9.16.2.2). Loss of stator cooling will not inhibit the ability of PCRDM to perform its safety function. Two independent control rod position indicating systems are incorporated in each control rod drive mechanism.

The primary safety function is to safely and reliably control and shutdown the reactor. The function of the mechanism, while engaging the leadscrew or disengaging for a scram, is sometimes also referred to as a "latching" or "unlatching". The scram function is described in detail in following sections and the mechanism components are shown in referenced figures. Other functions of the mechanism may also be referred to as a latch. However, the scram function of the mechanism is the only function directly associated with shutdown and control of the reactor.

Other design functions of the CRDM are:

Position and hold the control rod at desired elevations in the core.

Insert and withdraw the control rod in appropriate increments.

Release the control rod for rapid insertion (scram) following a reactor trip.

Provides a means for uncoupling the control rod for refueling and recoupling after refueling.

Indicate control rod position by two independent systems.

Bellows seals placed between the PCRDM and the PCR in the reactor vessel prevent the sodium vapor laden cover gas from entering the mechanism cavity. A positive pressure of inert gas is maintained within the CRDM above the bellows.

51 | The internals of the mechanism operate in an inert gas at 2 to 15 psig pressure. The reactor cover gas pressure at the bellows is essentially atmospheric so the bellows normally are subjected to a maximum pressure differential of 15 psi.

Material choices for the CRDM are summarized in Section 4.2.3.1.7.

The PCRDM consists of four major subcomponents: roller nut drive, absolute position indicating system, relative position indicating system and the seal system.

A seismic support for the mechanism nozzles will be provided on the reactor head to ensure adequate support under seismic loading conditions. It will support the CRDM nozzles at approximately 80 inches above the head. This seismic support will also provide radiation shielding in the Head Access Area.

Roller Nut Drive

51 | The drive mechanism is a collapsible rotor, roller nut type having the stator outside the pressure boundary and the rotor and rollers inside operating in an inert atmosphere. The design features of the mechanisms are similar to the FFTF mechanism; however, design changes have been made to provide greater drive motor power for the increased weights of the CRBR CRD and control assembly. The rollers engage the threaded lead-screw and drive the driveline assembly up or down. The drive motor is a 6 Phase 4-pole DC type that can be indexed in 15 degree increments (0.025 inch leadscrew steps). Gas forced through a housing about the stator cools the stator coils.

The rotor assembly is composed of an axially located hollow tube or spider on which are pivoted two rotor segment arms or shells that are semicircular in cross section. Two rollers are mounted in windows in the lower end of each rotor arm. In addition, four double springs are captured between the arms, tending to force the arms apart. When the stator is energized, the upper ends of the arms are pulled outward by the magnetic field, the lower arms are pivoted inward engaging the rollers with the thread on a leadscrew. The bottom end of the leadscrew is connected to the control rod through the driveline assembly.

When the power to the mechanism stator is cut off, the magnetic field holding the upper ends of the rotor arms outward collapses. The springs separate the lower arms and the rollers release the leadscrew, allowing it, the driveline and control rod to drop into the core. A scram assist spring is provided to supplement the gravity drop over the first 27 inches of rod travel on a fully withdrawn rod.

Separation of the lower segment arms activates out motion limiter pawls which engage the leadscrew to limit upward motion of the control rod when the rollers are disengaged. These pawls are spring-loaded for positive engagement to retard upward motion. However, for rod insertion, they allow the leadscrew, driveline and control rod to ratchet into the core with minimal drag.

51 | The four rollers are mounted in the rotor arms on ball bearings to carry the axial loads. The axes of the rollers are inclined by the leadscrew helix angle and the vertical position of the rollers is offset by one-fourth the leadscrew pitch (0.6 in.) to align them with the double thread of the leadscrew. Axial and radial rotor loads are transmitted to the mechanism housing through a large bearing below the rotor segment arm pivot pins (Figure 4.2-101). A smaller radial bearing is located near the top of the housing, just above the synchronizer bearing which serves to coordinate the radial motion of the rotor segment arms. Bearing lubrication is of the dry film type.

Relative Position Indication System

The relative position indication system consists of an electromagnetic sensor that counts the number of passes of the magnetic poles of a position indicator rotor attached to the top of the drive mechanism rotor.

The number and fraction of revolutions, multiplied by the 0.6 inch pitch of the leadscrew, indicates the distance of rod withdrawal from the fully inserted position. If a scram occurs, the indicator will lose its position reference and be referenced from an extreme rod position. This is the more accurate of the two position indication systems. The position indication accuracy of the present design is ± 0.150 inch.

51 |

Absolute Position Indication System

The absolute position indication system measures the position of the CRDM leadscrew directly through sensor elements located on the inside of the position indicator housing. The sensing elements are reed switch type sensors, selected for CRBRP based on FFTF experience. This system does not lose its reference position following a reactor trip.

51 | The position indication accuracy is specified in Section 4.2.3.1.4. The absolute position indicating system has provisions for "full-in" and "full-out" indication and for confirming positive coupling with the control rod.

Seal System

The purpose of the seal system is to prevent sodium vapor from the reactor from entering the drive mechanism cavity and depositing on the internal working components of the control rod drive mechanism. Three separate bellows are used in the seal system. The large bellows seal the driveline to the upper bellows support, and must operate over a range of approximately 37.5 inches with a 2 to 15 psi pressure differential across it. Two smaller bellows seal the coupling actuator shaft and the position indicator rod which run coaxially within the driveline. These bellows flex only during coupling and uncoupling of the driveline and control rod.

51 |

A torque restraint is provided in the space outside of the large bellows to prevent the CRDM leadscrew, bellows and driveline from rotating. Torque taker keys on the driveline ride in full-stroke vertical keyways in the torque tube (see Figure 4.2-102).

51 |

A pressure switch is located in the CRDM pressure enclosure. This switch is designed to sense the reduced pressure associated with a bellows leak. When such a leak is sensed, an alarm will be sounded notifying personnel of a bellows failure and that replacement is necessary.

A continuous purge system using recycled cover gas is provided to prevent sodium vapor and radioactive cover gas from rising through the annuli of the CRDM to an elevation above the reactor head. The purge supply is connected to each CRDM extension nozzle and produces a predominantly downward flow of recycled cover gas through the small annuli between the driveline, shield plug and shroud tube. This system is also effective in the event of a failed bellows in preventing sodium vapor from entering and depositing in the drive mechanism cavity.

4.2.3.2.1.2 Primary Control Rod Driveline

51 | The Primary Control Rod Driveline (PCRD) is an approximately 37 ft. long hollow shaft which connects the mechanism leadscrew with the control rod (Figures 4.2-102 and 103). The PCRD is made of Inconel 718, and its total weight is approximately 315 pounds.

The control rod disconnect coupling is located at the lower end of the PCRD and is shown on Figure 4.2-103. A manual disconnect tool, similar to the FFTF disconnect tool, is used to couple and uncouple the control rod. The design of the coupling elements of the disconnect is essentially the same as the design used on commercial pressurized water reactors and on FFTF.

A position indicator rod or telltale rod (see Figure 4.2-103) passes through the coupling and contacts a surface on the control rod shaft. This position indicator rod extends into the PCRD leadscrew and is used to verify that the control rod remains fully inserted when the driveline is disconnected and raised for refueling.

The piston-type dashpot, identical to the dashpot used on the FFTF PCRD, is a part of the driveline (see Figure 4.2-103). The dashpot has a radially free floating cup which is vertically supported on a seat in the upper guide tube and a piston which moves with the overall driveline assembly. The dashpot is designed such that the piston travels the full driveline stroke but only provides a 9 inch dashpot stroke. The upper end of the cup is perforated to reduce weight and to prevent fluid from being trapped during the remainder of the piston travel. The inside diameter of the cup is tapered in the last 9 inches to restrict flow between the piston and the cup and provide retarding force. The upper and lower cap of the dashpot cup center it on the piston and outer tube. The piston which is an integral part of the main structural member of the driveline, is also tapered so that a large clearance exists between the cup and the

piston at the beginning of the dashpot stroke, which is reduced as the piston travels its length. The tapered piston configuration provides the capability of supplying a fairly constant decelerating force over the entire stroke.

4.2.3.2.1.3 Primary Control Assemblies

The Primary Control Assembly (PCA) contains boron carbide in a movable pin bundle, with core reactivity controlled by moving the pin bundle axially. Absorber assemblies are replaced in the core during reactor refueling. The absorber assemblies are designed to:

Provide neutron absorber material to control reactivity for reactor startup, power level control, fuel burnup compensation, and reactor shutdown.

Provide passages to guide and control the sodium coolant.

Provide shielding to protect the core support structure from excessive neutron fluence.

Provide features for proper interfacing with other core components, the core support structure, the fuel handling machine, and the core restraint system.

Mate with the PCRD to form a portion of the control rod system.

51 | A pictorial drawing of the control assembly is shown in Figure 4.2-104. The control assembly is a hexagonal component consisting of the control rod (movable 37 pin bundle) assembly and the outer duct assembly. The control rod consists of the absorber pellets, absorber pin cladding, the pin support structure, wear pads, control rod shaft, rotational joint and the female driveline coupling. The outer duct assembly consists of the control assembly handling socket (flow outlet nozzle) outer duct, radiation shielding, inlet flow orifices and inlet nozzle. Externally the control assembly is nearly identical, geometrically, to the core fuel assembly. The assemblies are supported at their inlet nozzles by the lower core support structure inlet modules. The upper ends of the core assemblies of the reference design are restrained radially by a passive core restraint system (see Section 4.2.2) at two elevations; namely, the above core load plane and the top load plane. Load pads are provided on the core assembly ducts at these two core restraint elevations and former rings are provided between the core assemblies and the core barrel to limit radial misalignment.

51 | The control rods must move axially within the outer ducts of the control assemblies from the fully inserted to the fully withdrawn positions. Positive position stops are provided in the handling socket

51 | to limit the control rod travel. The overall length of the control assembly is 168 inches. The center of the 36 inch absorber pellet column is located at the center of the 36-inch core fuel height in the fully inserted position. For the fully withdrawn position the bottom of the absorber pellet column is located at the top of the fuel pellet region. Radial misalignments between the control assemblies and the driveline have been established by alignment studies which are presented in Section 4.2.3.1.1.

51 | Control Rod and Control Rod Shaft

The principal component of the control rod is the absorber pin bundle. The structural support for the pin bundle is an inner duct tube which encloses the absorber pins. The inner duct is attached to the top and bottom grid plates which align the pins. The top grid plate and inner duct are welded to an adaptor plate. The adaptor plate is connected to the bottom of the control rod shaft with a rotational joint (See Figure 4.2-104). This swivel type joint prevents end moments from being carried into the control rod from the control rod shaft and driveline. This feature minimizes normal forces and frictional forces between the wear pads and the control assembly outer hexagonal duct thereby reducing outer duct wear and scram retarding forces. A female coupling is provided at the upper end of the control rod shaft for joining with the male coupling of the CRD. The inner duct wall thickness has been determined based on the applied loads, clearances for duct bowing and radial coolant pressure differential. The thin wall inner duct together with the rotational joint increase the bundle flexibility and reduce resistance to control rod travel in a bowed outer duct. The coolant bypass flow minimizes thermal bowing of the inner and outer ducts. Hydraulic tests on the FFTF control rod have confirmed the design methods for pressure drop and flow through the control assembly. Final confirmation of pressure drop and flow characteristics of the CRBR control assembly with the labyrinth wear pads will be provided by the ongoing CRBR PCA hydraulic tests.

51 | Labyrinth seal wear pads are provided at the top and bottom of the inner duct. These wear pads guide the movement of the pin bundle within the outer duct, establish the clearance to minimize contact between the inner and outer ducts, enhance bundle to assembly flow split, and provide a hard material wear interface with the outer duct.

Absorber Pins

The absorber material portion of the pin consists of a stack of boron carbide pellets (92 ± 2 percent theoretical density), 36 inches long. Gas plena are provided in the absorber pin to limit internal gas pressure build-up caused by helium generation. The total plenum lengths are 14.2 and 24.3 inches for the bottom and top plenum, respectively. Within the upper plenum there is a spacer and spring to keep the boron carbide pellets and lower plenum spacer compressed during handling and at impact after scram. The absorber pellet stack consists of hot pressed boron carbide pellets, enriched to approximately 92% B¹⁰.

Absorber pins are arranged on a triangular pitch to diameter ratio of 1.05. Each of the absorber pins in the interior rows of the pin bundle is helically wrapped with a wire to provide lateral spacing along its length and promote coolant mixing. The exterior row of pins is wrapped with elliptical cross section wire with reduced minor diameter to provide clearance between the pins and inner duct to accommodate normal swelling. Reduction of the wire size in the peripheral pins minimized overcooling of the side channels and provides improved flow distribution to the interior channels. The wire is pulled through and welded at its end to the bottom end cap and is laid along and welded to the upper end cap. The pins are approximately 78 inches long within an overall bundle length of 80 inches. The cladding is 0.602-inch nominal outside diameter by 0.49 inch thick and is 20 percent cold drawn Type 316 stainless steel. The cladding tube and end caps provide structural support and hermetic sealing for the absorber pellets and spacer components. The pins are supported at the top plate by a weld and are free to expand through the bottom plate. This puts the pin in tension during deceleration at scram arrest since the control rod stop is located in the outlet nozzle.

Outer Duct Assembly

In the assembled configuration, the pin bundle is held inside the outer duct assembly by the outlet nozzle which has an internal shoulder serving as the interface for the refueling gripper. An interior shoulder in the nozzle serves as the full insertion stop for the control rod. The principal structural member is the 0.120-inch wall thickness, 20 percent cold worked Type 316 stainless steel duct tube which extends from the outlet nozzle at the top to the radiation shield at the bottom. The duct wall is increased in thickness locally to approximately 0.21 inch at the load pads. The load pads mate with similar pads on surrounding fuel assemblies to provide lateral positioning of the core components and to transfer the loads developed through interaction with the core restraint system.

Neutron Shield Block

The shield block is a hexagonal block, 4.575 inches across flats, approximately 22 inches long including a hex to round transition over the bottom 6 inches. An internal cavity in the circular section contains the orifice plate assembly. A single flow hole, 1.5 inches in diameter, extends through the length of the shield concentric with the shield. The lower end of the shield block is welded to the inlet nozzle which provides the interfaces with the inlet modules. These interfaces include six inlet flow ports, external piston rings limiting leakage flow to the low pressure region of the reactor to maintain hydraulic balance and the discrimination features.

Assembly Discrimination

51 | Two unique noninterchangeable discriminator types are provided for the control assembly discriminator types to preclude insertion of a control assembly into a non-control assembly core location and also preclude insertion of any other type of reactor assembly (fuel, blanket or removable radial shield) into a control assembly core location.

51 | In addition, these two unique control assembly discriminator types preclude insertion of each type of control assembly into an incorrect control assembly location. The two types of control assemblies that require discrimination from each other are as follows:

1. Primary control assemblies that are to be located in Row 4 or Row 7 corners, only.
- 51 | 2. Secondary control assemblies that are to be located in Row 7 flats only.

51 | The geometries of the control assembly discriminators are similar to that shown in Figure 4.2-15 for the fuel assemblies. However, the diameters of the discriminator posts on the control assemblies are sufficiently different from the corresponding diameters on the other types of reactor assemblies to preclude incorrect insertion of an assembly during refueling. The discriminator system will stop the insertion of any assembly into an incorrect assembly location 2.35 inches short of its fully inserted position. This resulting 2.35 inch height difference is detected by the In-Vessel Transfer Machine (IVTM) axial position locating system and the IVTM will not release the assembly from the grapple.

4.2.3.2.2 Secondary Control Rod System

51 | The Secondary Control Rod System (SCRS) (shown schematically in Figure 4.2-105) provides six two-position control rods that move from their full-out position to their full-in position to shutdown the reactor. Each control rod is held in its full-out position by a scram latch that engages the control rod's top end. The scram latch is located at the bottom end of a drive shaft extending through the reactor closure. The Secondary Control Rod Drive Mechanism (SCRDM) that positions the drive shaft and latch is mounted above the reactor head. The control rod has gravity and hydraulic pressure forces from the coolant pressure drop across the core which are applied to the control rod in a direction that tends to drive it into the core. The latch holds the control rod in the full-out position against those forces.

The SCRS hardware includes the following major items:

1. The Secondary Control Assembly (SCA) that has a hexagonal configuration similar to fuel assemblies and contains the movable control rod (Figure 4.2-106).
2. The Secondary Control Rod Driveline (SCRD) that extends through the reactor closure and seals the reactor cover gas (Figures 4.2-107a and 4.2-107b).
3. The Secondary Control Rod Drive Mechanism (SCRDM) mounted to the reactor closure top side and connected to the drive shaft seal assembly (Figures 4.2-108a and 4.2-108b).

The SCRS utilizes hydraulic forces to assist scram action. The control rod moves axially within the control assembly guide tube. During normal reactor operation, the rod is supported above the core by the latch that is actuated by a pneumatic cylinder. Appropriate flow paths and orifices within the assembly allow the reactor coolant to flow from the high pressure plenum to the region above the piston. Sodium below the piston is ducted to the low pressure plenum.

Therefore, a pressure drop in the downward (scram) direction exists across the control rod piston continuously during normal operation. Upon receipt of a scram signal, the control rod is released by depressurization of the latch-actuating cylinder and is forced down by the hydraulic pressure force and gravity into the core region. Coincident with scram initiation, the primary coolant pumps are tripped, that is, turned off; however, the transient pressure decay is relatively slow with respect to the SCRS scram speed, so that sizeable scram assist pressure forces exist throughout the scram stroke. This relatively slow decay of the scram assist pressure due to the primary coolant pump coast down also applies when consideration is given to the postulated undercooling accident.

The latch can be actuated to release the control rod by venting the pressure in the pneumatic cylinder. The weight of the rod and the hydraulic forces cause the grippers to spread and release the rod.

To retrieve the rod from the full-in position, the latch is lowered by the SCRDM. Upon engagement of the latch with the control rod, the pneumatic cylinder is pressurized to secure the rod in the latch. The SCRDM is then actuated to raise the control rod slowly out of the core region to its normal full-out position. In this position the latch is located just below the top of the handling socket as shown in Figure 4.2-105.

For head rotation, the control rods are released and the drivelines below the closure are withdrawn well into the upper Internals structure to provide protection for them during head motion.

4.2.3.2.2.1 Secondary Control Rod Mechanism

Extension Nozzle - The extension nozzle that is attached to the reactor head provides the support and mounting feature for the SCRDM and its attached SCRD and control rod. The mechanism holddown ring at the nozzle upper end attaches the SCRDM to the nozzle in a manner similar to that used by the primary drive mechanism.

Sealed Housing - A two part sealed housing (upper drive housing and lower drive housing) forms the outer shell of the SCRDM that will contain the argon pressure that backs up the main shaft bellows. An integral flange at the housing's mid-section mounts and seals the SCRDM to the extension nozzle. The sealed housing upper end is capped off by the connector plate. The fixed end of the main shaft bellows attaches and seals to the lower end of the sealed housing. The sealed housing is pressurized through a connector in the top connector plate. The housing pressure is maintained at approximately 5 psi above the reactor cover gas pressure. Should a bellows or any other gas seal fail, the leak will be detected, and an alarm sounded, by a system that continuously monitors argon flow in and out of the SCRDM.

Mechanism Frame - The main structural framework for the SCRDM is provided by the mechanism frame (see Figures 4.2-107b, 108a and 108b). The frame is composed of two rails (beams), end plates, mid-supports, and a number of rail cross tie brackets. These components, bolted and keyed together, form a structurally rigid open frame. The rails provide the guidance for the coil cord assembly and the carriage assembly. The lower end plate contains the leadscrew thrust bearings. The mid-supports contain the needle bearings and provide radial support for the leadscrews at their midpoint. The mechanism frame is coupled to the lower housing where the load is transferred to the extension nozzle. The coupling is made with a flange (formed by brackets at the frame mid-length) clamped to a ledge on the lower drive housing.

Leadscrews - The axial motion for the drive is generated by twin ball-nut leadscrews. Bearing support is provided at three elevations. The lower bearings are in a duplex arrangement that takes the axial load and gives a rigid support for column loading considerations. The mid-support bearings use needle bearings for a thin cross section and provide lateral support. The positioning carriage ball-nuts travel between the lower two bearings. Each leadscrew is rated for 10,000 pounds column loading and 25,000 pounds tensile static load. The leadscrew has 0.2-in. lead per revolution. The upper bearings provide radial support at the gear drive.

Motor and Locking Device - Power to the leadscrews is provided by an electric motor. Two idler gears from the motor pinion gear transfer the torque to the leadscrews. Two methods are provided for preventing the driveline and carriage from coasting downward. During normal operation (when power to the motor is available), the electrical braking capability of the motor is used. During installation and refueling (when power is not available), the motor shaft lock device is used. This device, by mechanical means, prevents motor shaft rotation. The lock device will maintain its functional state (locked or unlocked) without the application of power.

Latch Mechanism - The latch mechanism is mounted to the upper side of the positioning carriage and provides the function of operating the control rod release latch at the end of the drive shaft. The main components of the latch mechanism are the position indication devices, the pneumatic actuator, and the scram valves. The motion of the concentric shafts inside the drive shaft are indicated by two LVDTs (linear variable differential transformers).

The pneumatic actuator utilizes high pressure argon in order to apply a tensile force to the tension rod to keep the latch locked. The scram valves that vent the pneumatic actuator, which in turn releases the control rod latch, are mounted below the pneumatic actuator. Guides, located above the scram valves on the positioning carriage, engage with the frame guide rails to provide a stable motion path for the positioning carriage and latch mechanism.

The scram valves are redundant and testable. A system of two-out-of-three logic permits any one of the three solenoids to be actuated for test purposes without causing scram. However, actuation of any two of the three solenoids is sufficient to release the control rod. The valves are instrumented to monitor response during testing. This feature permits periodic testing of the scram valves thereby enhancing reliability of the system.

Electrical Lead Coil - The electrical cables needed for the latch mechanism LVDTs and scram valves and the pneumatic tubes needed for the pneumatic cylinder and driveline internal pressurization are routed to the latch mechanism by a helical coil assembly.

Position Indication - Two separate indication systems are provided for indicating carriage position. The two systems consist of (1) a signal

converter driven by the motor input signal which displays a derived carriage position, and (2) a rotary encoder providing continuous absolute position indication (reference position is not lost with power failure) over the full stroke.

The rotary encoder's function is checked by redundant verifier switches actuated as the carriage passes a predetermined position. This initiates a comparison of the encoder reading against a calibrated value. This checking function is intended as an advisory indication only.

The carriage position is also indicated by two proximity switches mounted at elevations corresponding to the control rod fully inserted position and the driveline refueling position. The upper limit switch stops the carriage at the position required for refueling. The lower limit switch stops the carriage at a position such that the lower driveline nose cone remains a short distance above the fully inserted control rod. An override permits the driveline to be driven down until the nose cone contacts the top of the control rod.

Connector Plate - Hermetically sealed, electrical connector feedthroughs are threaded into the top plate and sealed by welding. Connectors from the SCRDM cables can be attached to the feedthroughs on the lower side of the connector plate before it is mounted to its housing. Room is provided at the top of the drive to accommodate the cable length needed for this operation.

4.2.3.2.2.2 Secondary Control Rod Driveline

Latch - The control rod scram release latch is located at the bottom end of the driveline. The coupling head on the control rod is gripped by the latch gripper fingers that are held in the locked position by the latch tension rod. Less than 0.1 inch downward stroke of the gripper fingers and latch tension rod will release the control rod by permitting the control rod coupling head to slide out of the gripper fingers. The upper end of the latch tension rod is coupled to the pneumatic actuator discussed in Section 4.2.3.2.2.1. The pneumatic actuator has a stroke range of plus or minus one inch, as compared to the 1/4-in. gripper motion thus allowance is provided for differential thermal expansion over the driveline length. Since the latch tension rod is tensioned by the pneumatic actuator the pneumatic actuator piston can shift either up or down slightly to accommodate drive line expansions and contractions and still maintain a relatively constant force on the latch tension rod.

The angle surfaces contacting the gripper fingers are designed to operate over a coefficient of friction range of 0.2 to 2.0. The latch has been designed to be capable of carrying a 500 pound downward load on the latch fingers from the control element. Preliminary estimates indicate an applied load of approximately 330 pounds at reactor full power of which 250 pounds is developed by the hydraulic scram assist feature of the SCRS. The remainder is due to gravity loads.

The presence of the control rod coupling head within the latch fingers is indicated by a mechanical extension of the sensing tube that contacts the top of the coupling head. The sensing tube has a stroke range of minus 0.5-in. and plus 1.0-in. from the latched position shown on Figure 4.2-107a.

Rigid Drive Shaft Section - At the minus 344-in. elevation, where the relative motion between the core assemblies and the upper core support structure is postulated, the drive shaft portion of the driveline has a thick wall to protect the latch tension rod inside. The surrounding core support structure and control assembly handle are expected to deform before the drive shaft crushes, thereby keeping the latch tension rod free to release.

Bellows - The latch tension rod and sensing tube are sealed with metal bellows located at two elevations: the lower end of the upper driveline above the three-shaft coupling and the upper end near the positioning carriage. The volume inside the drive shaft between these two sets of bellows will be pressurized with argon from a source outside the SCRDM. The internal drive shaft pressurization is higher than the maximum pressure at the latch end.

Three-Shaft Coupling - The three shaft coupling (shown on Figure 4.2-107a) joins the lower driveline to the upper driveline. This coupling enables disassembly and assembly of the lower driveline without affecting the remainder of the driveline and mechanism.

Coupling of the tension rod is performed by butting the two ends together, engaging the split shell retainer halves in the tension rod grooves, and lowering the lock sleeve to encompass the retainer halves. The lower end of the lock sleeve is deformed to retain it over the split shell. The coupling concept used for the tension rod is also used for the sensing tube. The driveshaft connection is made with a coupler tube. The tube is bolted to the lower driveline. Attachment of the coupler tube to the upper driveline utilizes two sets of split rings and a threaded locknut. The locknut in combination with the split rings couples the tube to the upper driveline.

Head Shielding - The head shield plug design is similar to the primary system shielding design.

Attachment to SCRDM - The SCRDM attaches to the bottom of the SCRDM positioning carriage by a bolted flange.

4.2.3.2.2.3 Secondary Control Assembly

The control assembly consists of a hexagonal duct that is similar to the fuel ducts, a nosepiece, a shield, a guide tube, a control rod, and an upper handle. The principal dimensions of these components are summarized in Table 4.2-42.

The control rod is composed of 31 absorber pins surrounded by a circular wrapper and includes a piston assembly at the bottom and a damper assembly at the top. Each absorber pin contains a 36-inch column of enriched B₄C pellets, and the minimum total B¹⁰ loading in the control rod is 4.66 kg. The absorber pin has a gas plenum above and below the pellet column with thin walled spacer tubes in each to maintain position. The upper plenum also contains a holddown spring.

The piston assembly has an inlet plenum region to provide good flow distribution for the coolant as it enters the piston region from the guide tube. There is a small clearance between the piston assembly and the guide tube above and below the inlet region. The lower region requires small clearances to create high pressure drop for hydraulic scram assist. The upper region has small clearances to minimize leakage flow around the outside of the control rod.

39] The damper assembly above the absorber pins contain the damper and dashram, a coupling head to mate with the latch, and an exit plenum for the flow through the absorber pin bundle. The damper is made up of a series of plates and belleville-type springs. Two types of plates are alternately stacked with the springs. All plates have a hole in the middle to accommodate a shaft. The shaft has a plate at one end and an arresting arm at the other. After the rod has traveled 90% of the scram stroke, the arresting arm contacts the downstop and starts to compress the stack of springs and plates. Sodium between the plates is expelled, slowing down the rod. The exterior of the housing containing the springs and plates is tapered to act as a dashram. The dashram starts to slow the rod when it enters the guide tube by reducing the annular flow area between the rod and guide tube.

A downstop is attached to the outer duct such that the boron carbide is fully inserted in the core when the control rod is resting on the downstop and the damper is compressed. The top end of the guide tube is also attached to the downstop, while the lower end of the guide tube contains a shield plug which has a sliding fit with the nosepiece. The guide tube has ports to provide upflow for cooling the control rod and downflow around the piston for hydraulic scram assist. The guide tubes' ports are adjacent to the inlet region of the control rod when the rod is in the withdrawn parked position.

39] The shield plug at the lower end of the guide tube has a hole through the middle to permit downflow to the low pressure plenum. The shield is sized to provide a steel volume fraction of 73% averaged over the 20 inch shield height and the 4.76 inch assembly pitch. The shield plug also has grooves in its perimeter to permit the upflow from the nosepiece inlet to traverse the shield region.

39] The nosepiece contains two concentric flow regions. Coolant from the reactor high pressure plenum enters the outer flow region of the nosepiece through inlet ports. Sodium flows upward through the shield grooves and then between the guide tube and outer duct until it reaches the ports in the guide tube.

Part of the flow goes through and around the control rod to cool the absorber pins and exits the assembly around the latch seal. Most of the coolant at the guide tube ports flows downward around the piston, through the shield and inner flow region of the nosepiece, and into the reactor low pressure plenum.

4.2.3.3 System Evaluation

4.2.3.3.1 Primary System Evaluation

4.2.3.3.1.1 Alignment Analysis

53 | This section presents the results of an evaluation of the forces which occur due to lateral misalignment of the CRBRP primary control rod system components. These forces act to retard control rod translation during scram and therefore must be considered in the Scram Analysis (Section 4.2.3.3.1.3).

All the effects contributing to drag forces (product of a lateral load and a coefficient of friction) were considered including lateral bending effects, torsional windup of the driveline, constant operational effects (e.g., out-motion limiter pawl ratchetting along the leadscrew) and PCA duct bowing. The lateral bending loads resulting from system misalignment were determined by a static analysis using the ANSYS finite element structural computer code (APP-A) to model the PCRS. The worst case misalignment of the fixed (non-moving) boundary of the PCRS was determined to be the refueling misalignment, Figure 4.2-95B. This misalignment envelope was further defined by determining the shape of the upper shroud tube, assumed to be initially straight, when forced to interact with a misaligned non-translating assembly (NTA) and constrained to the defined end points according to Figure 4.2-95B. The NTA, consisting of the upper bellows support, torque tube, shield plug, shield plug extension and shield tube, was assumed to be misaligned in the direction opposite to the direction of the installed shroud tube.

53 | A finite element model of the translating assembly (leadscrew, driveline, dashpot cylinder and piston) was prepared and forced to conform to the envelope defined by the misalignments from Figure 4.2-95B design clearances and the analysis of the NTA above (see Figure 109a). The translating assembly itself was assumed to be misaligned, Figure 4.2-109b, as determined by an analysis of tolerances of the component parts. This resulted in a system of static forces required to elastically bend the translating assembly into conformance with the fixed envelope (Figure 4.2-109c). Analyses as described above were performed for each significant withdrawal position (6 total) from fully inserted to fully withdrawn.

59 | Assumptions salient to the lateral misalignment force analysis were as follows:

1. The control rod system is at a uniform temperature which corresponds to the "worst case" refueling conditions for misalignments (see Figure 4.2-95B). Axial thermal expansion of the components has been ignored.

59

2. Linear interpolation between the maximum misalignment values of the top and bottom of the control assembly is valid.
3. The dashpot cylinder is forced over to one side of the shroud tube and parallel to the slope of the shroud tube.
4. The NTA and TA are initially misaligned as in Figures 4.2-109a & b, and these are the worst possible configuration.
5. The stiffness of the disconnect actuating rod internal to the control rod driveline is negligible when compared to the outer tube.
6. The sum of the absolute values of the reaction forces acting on the T.A. will be greatest (largest retarding forces) for the two-dimensional case with the greatest curvature in the elastic curve of the control rod.

51

The total lateral loads calculated for each withdrawal position are summarized in Table 4.2-43.

The same analysis was performed for the PCRS sodium test misalignment conditions, which envelop the design basis in order to determine the validity of the worst case assumptions made. These assumptions were a) the position of the dashpot and b) worst case NTA and TA misalignments. Table 4.2-43a summarizes the analysis bases and the resulting total forces for the fully inserted position.

Subsequent system tests at the misalignments defined by Figure 4.2-95a resulted in a measured drag load of approximately 10 pounds. This confirmed that the dashpot moves laterally as designed (i.e. is not fixed as assumed) and that the assumption of combined worst case misalignment of the translating and non translating assemblies is extremely conservative.

Only slight variation in the calculated lateral loads was observed over the control rod stroke except near the full insertion position. The end of stroke drag forces are effective only over the last six inches where the control rod coupling can contact the inside diameter of the scram arrest flange.

The maximum coefficient of sliding friction from the available data (see Section 4.2.3.1.3) was used for each of the material couples in the primary control rod system. These coefficients are greater than the 3σ values given in Table 4.2-36A. Table 4.2-43 summarizes the lateral misalignment drag loads at each withdrawal position.

Torsional effects are minimized by the Rotational Joint at the top of the absorber bundle. Torque taker clearances and normal manufacturing twist of the absorber ducts can lead to twist of the driveline which is torsionally restrained by the Torque Taker at the top and by the hexagonal control rod at the bottom. The Rotational Joint provides the azimuthal degree of freedom to relieve the potential driveline torsion, as well as providing lateral degrees of freedom which minimize moment transmission between the shaft and the control rod. Tests performed on prototype Rotational Joints (Ref. 177) established that the maximum torque transmitted through the joint was 20.5 inch pounds. This was observed after an extended soak period in sodium and represented only a momentary "static" friction peak which immediately reduced to approximately 8 inch pounds torque. Because of the nominal cross corner hex diameter of 4.6 inches, the maximum torsional contribution to lateral load is 9 lbs. acting momentarily at the beginning of a scram.

The out-motion limiter pawl drag must be considered in the scram retarding forces acting on the translating assembly. This load results from the spring loaded pawls ratchetting along the leadscrew as it scrams. The magnitude of this load is approximately 14 lb.

Control assembly duct bowing can modify the system of misalignment drag forces by changing the material couples and slightly altering the available clearances. Two point contact occurs when the inner and outer ducts are in contact. Depending on the misalignment condition, duct to duct contact relieved the contact at one or both of the wear pads. Only a very small incremental change in misalignment or duct bowing can cause a change from wear pad to duct to duct contact. Thus, the principal contributor from duct bowing results from the change in material couples, i.e., from Inconel 718/316 Stainless Steel to 316/316. In rod withdrawal positions greater than approximately 6 inches, only about 7% of the total drag loads occur at the wear pads. Between 6 inches withdrawn and fully inserted approximately 20% of the total drag occurs at the PCA wear pads. Therefore, since the coefficient of friction for the 316/316 couple is approximately 16% lower than for the 718/316 couple, the loads due to duct bowing decrease and are estimated at approximately -1 lb. for withdrawn positions and -8 lbs. for near and fully inserted positions. These forces were neglected in the scram analysis.

The drag forces used in the scram analysis for the PCRS are given in Table 4.2-43. Drag forces are less than 135 lbs. for the control rod stroke from full out to approximately 6 inches withdrawn and increasing to about 290 lbs. at full insertion.

4.2.3.3.1.2 Control Assembly Bowing Analysis

Assembly bowing results from three factors: flux gradients across the assembly causing differential irradiation swelling, thermal gradients across the assembly, and mechanical loading from adjacent assemblies together with creep or plastic deformation. The movable control rod is suspended from the rotational joint which provides sufficient degrees of freedom to prevent large moments in any plane being transmitted through the joint to the shaft. Thus, control rod bowing is not mechanically influenced by the shaft nor by adjacent assemblies because of the clearances between it and the outer duct. The outer duct is restrained at the inlet nozzle, the above core load pad (ACLP) and the top load pad (TLP). Therefore, the outer duct bow is dependent on a static equilibrium condition with adjacent assemblies, and the magnitude of bowing deflection at any axial position is limited by this condition and the clearances of the core restraint system at operating conditions.

The control rod moves inside the outer duct, positioned and guided by the Inconel 718 labyrinth seal wear pads at the top and bottom of the rod (Fig. 4.2-104). The nominal diametral (flat to flat) clearances between the control rod and duct are 0.100 inch at the bottom wear pad, 0.120 inch at the top wear pad to allow for radial thermal growth relative to the bottom, and 0.297 inch inner duct to outer duct clearance. The

limiting bowed condition is three point contact, defined as contact between both wear pads and the outer duct on one side of the rod, and duct to duct contact on the opposite side (see Section 4.2.3.1.2). Beyond this condition, the drag loads are directly proportional to control rod stiffness.

The control rod preliminary bowing analyses model was derived from the core restraint system analyses (Section 4.2.2). The model is a 3 assembly model for simplicity, which was shown to predict essentially the same interassembly loads and deflections as the much more complex row model used for core restraint system analysis. The model includes all the phenomena contributing to bowing as discussed above.

Worst case bowing tends to occur in the Row 7 corner control rod due to maximum flux and thermal gradients at that location, relative to other control assembly locations. Therefore, the analysis for the Row 7 Corner assembly conservatively envelopes all other primary control assemblies, and is used as the basis for demonstrating satisfactory performance for all PCAs.

54 | The maximum transverse thermal gradient in the control rod occurs during full power operation with the rod at or near full insertion and the rod misaligned such that both top and bottom wear pads contact the outer duct toward the center of the core. This condition is shown in Figure 4.2-111(a). For purposes of this evaluation, it has been conservatively assumed that the R7C rods can be in fully inserted position during power operation. It is expected that the R7C rods will be withdrawn at least 13.6 (18.6 nominal) inches at the beginning of the minimum withdrawal cycle (BOC-4) for full power operation.

The direction of potential reaction forces for the assumed initial condition are indicated by the arrows in the sketches (Fig. 4.2-111). Both the inner and outer ducts are assumed to be straight for the initial configuration. The outer duct then bows convex toward the center of the core under the influence of transverse thermal gradients and irradiation induced differential swelling. Swelling induced bow tends to become significant only toward the end of one year of operation. The inner duct is assumed to remain straight for this configuration resulting in the point contact conditions shown in sketch (B). The reaction loads for sketch (B) would be small and similar in magnitude to sketch (A).

51 | If the rod is assumed to be misaligned so that both wear pads contact the outer duct on the side away from the core centerline, a small reverse thermal gradient (high on the outside) can occur across the rod (Sketch F, Fig. 4.2-111). The resulting small control rod reverse bow

together with any outer duct bow, which must be convex relative to the core centerline at power operation, redistribute the bypass flow to reach a thermal equilibrium condition similar to a straight rod. Therefore, it is concluded that the worst case assembly bowing condition is achieved by assuming no operational bowing of the control rod, while permitting the outer duct to bow as dictated by the adjacent assemblies. Predictions of control rod bowing utilizing the maximum transverse thermal gradients predicted for the rod over a range of radial misalignments and rod withdrawal and using extremely conservative flux data have indicated that the rod bows less than 0.01 inch (deviation from a straight line connecting the end points) in a direction parallel to the outer duct bow. Therefore, the assumption of no control rod operational bow has been analytically confirmed.

Outer duct bowing is primarily dictated by interactions with adjacent assemblies. However, the thermal and flux gradients across the assembly do contribute to a small extent to the equilibrium bowed condition. For bowing predictions a combination of high flux and high temperature was conservatively assumed in the analysis despite the fact that these maxima occur at different rod withdrawal conditions and therefore do not concurrently exist in actual operation. In addition, a low flux case was assumed which maximizes the flux gradient across the adjacent fuel assembly, together with the further conservatism of assuming that the adjacent fuel assembly is initially pre-bowed for one cycle to cover the possibility of non-batch refueling.

The three assembly bowing model together with its assumptions introduces conservatism into the analysis. Since assembly interaction effects dominate control assembly duct bowing, the inherent assumption of two face stiffness leads to greater predicted bow. In-service, assemblies adjacent to the four duct faces not in the plane of bowing add stiffness to the assembly and reduce the magnitude of the bow. This conclusion is supported by preliminary data from the Core Restraint Test Facility, and will be further verified as more data becomes available.

51 Figure 4.2-110 is a predicted outer duct bow for 275 FPD operation in a homogeneous core layout configuration again based on flux data which is conservative by a factor of approximately 1.5. Bowing analyses performed for heterogeneous core layout configurations have resulted in greater end of life clearances between the control rod and the outer duct than obtained using Figure 4.2-110 results. Key elevations are indicated on this figure including the position of a fully inserted rod, the above core load pad (ACLP) and the top load pad. Since the clearance evaluation is a balance of available design clearances and reductions in these clearances from various effects, it is clear that the worst case (greatest reduction of clearance) is with the rod fully inserted. This can be determined by connecting the intersection of the control rod full-in end points with a straight line and gaging the deviation from this straight line to the bowed configuration. Clearly as the rod is withdrawn, the deviation decreases, therefore the clearance increases.

59

51

Figure 4.2-110A is a plot of the outer duct bow adjacent to a fully inserted rod - i.e. the maximum deviation from the straight line noted above, superimposed on the clearance envelope of straight inner and outer ducts under the following assumptions:

- a) The wear pads are in contact with the outer duct on the same side. (Thus the clearance at 80 inches and 0 inches is zero.)
- b) The wear pads are at their maximum tolerance.
- c) The inner duct OD is at its maximum tolerance.
- d) The outer duct ID is at its minimum tolerance.

Additional assumptions relating to manufacturing are made as follows:

- a) The wear pads are azimuthally misaligned by the maximum tolerance.
- b) The inner duct is non-straight by maximum manufacturing tolerance and is assembled so that the bow opposes the predicted outer duct bow.
- c) Outer duct manufacturing bow tolerances have been assumed to be cumulative with the predicted operational bow. This is extremely conservative since analyses have shown that the end of life bowed configuration is not significantly altered by assuming an initially bowed configuration due to manufacturing tolerances.

The assumptions on manufacturing tolerances all reduce design clearances and are identified on Figure 4.2-110A. The following conclusions can be drawn from Figure 4.2-110A:

- a) Two point (duct-to-duct) contact would occur under the assumptions of these analyses. The load from this contact will be small due to the freedom given by the rotational joint.
- b) Three point contact does not occur. In fact, a large margin to three point contact exists as gaged against the maximum bow in 275 FPD operation.

Therefore, it is concluded that bowing will not detract from the scram performance of the PCA. The large margins and very conservative assumptions lead to a high confidence in this conclusion.

4.2.3.3.1.3 Scram Analysis

This section describes the scram analyses performed for the primary control rod system to demonstrate the expected rates of reactivity insertion during a reactor scram. Considered in this section are available shutdown reactivities, typical rod positions, control rod scram speeds and scram reactivity insertion rates.

Typical Rod Withdrawal Positions

Rod positions at the time of the scram may vary significantly due to: withdrawal over the fuel cycle, potential variations in rod bank positions, uncertainties in rod worths and variations in the fuel cycle length between the first and later cores. This time to insert the first dollar of shutdown reactivity in the reactor scram is typically of greatest importance as this first dollar is sufficient to turn around the power peak or fuel temperature increase for most transients. Table 4.2-44 shows typical rod withdrawal positions over the first five operating cycles. BOC-5 has been shown to be the worst case for the slowest first dollar insertion and is therefore the basis for the scram insertion analysis.

Control Rod Scram Speed

Control rod insertion speeds are calculated by the CRAB-II computer code which solves the equations of motion considering all the forces acting on the PCRS translating assembly, both scram assisting and scram retarding. Section 4.2.3.3.1.1 presents the analysis of the scram retarding forces, and Table 4.2-43 gives the total drag force as a function of withdrawal.

Validation of the CRAB-II code for predicting speed of insertion was done using test data from the PCRS system tests. Figure 4.2-112 shows insertion profiles from various withdrawal positions based on the drag forces given in Table 4.2-43. Figure 4.2-113 demonstrates the ability of CRAB-II to predict actual test data using conditions expected to occur in the core. Also shown in Figure 4.2-113 is the CRAB-II predicted speed of insertion using the conservative design conditions described in Section 4.2.3.3.1.1. The difference between the two curves represents the conservative margin for speed of insertion used in the scram analysis. Figure 4.2-113a demonstrates the ability of CRAB-II to predict test data over a range of flow rates and insertion times.

Scram Reactivity Insertion Rates

Scram reactivity insertion rates have been calculated based on the displacement/time profiles given in Figure 4.2-112, the cycle dependent rod positions of Table 4.2-44 and the minimum and expected bank worths appropriate to each cycle with the single most reactive rod stuck. The results of these calculations are shown in Figure 4.2-114. Although BOC-5 procedures the minimum shutdown, BOC-4 has been included to show the change in scram insertion from BOC-5 to BOC-4. All other cases insert reactivity faster due to higher worths or farther initial rod withdrawal.

An evaluation of the inherent shutdown margin can be obtained by comparing the minimum reactivity insertion with the expected reactivity insertion. The

minimum reactivity insertion represents a 3σ worst case evaluation of maximum excess reactivity and minimum control rod worth, while the reactivity insertion represents nominal core conditions. Additional margin on reactivity insertion for both minimum and expected conditions is included in these curves by using speed of insertion calculated with the conservative design conditions of drag shown in Figure 4.2-113.

End of cycle reactivity insertions are significantly greater due to increased shutdown margins and faster rod speeds due to greater scram assist forces at these positions.

All curves in Figure 4.2-114 have assumed a delay of 0.1 seconds from the advent of a scram signal to the start of rod motion. Actual test data from the PCRS system tests has shown this unlatch time to be 0.0486 ± 0.0002 seconds. Thus, on a 3σ basis, the scram insertion curves in Figure 4.2-114 could be moved to the left by 0.05 seconds.

It is therefore concluded that the primary control rod system satisfies the speed of response requirements given in Section 4.2.3.1.3 for all conditions.

4.2.3.3.1.4 Seismic Scram Analysis*

An analysis was performed to determine the effect of a safe shutdown earthquake (SSE) on the CRBRP Primary Control System's scram capability. Lateral contact forces on the translating assembly were determined for a severe three second segment of the SSE which was then used in evaluation of scram performance under seismic conditions.

The worst time to initiate a scram in this 3 sec. time interval was identified by determining the time required to scram 9 inches. This criterion was used because it represents the required rod travel of the rods to insert approximately one dollar of reactivity. A 1.2 second load time history whose initial point is the worst scram initiation time was then used repetitively until the rods were fully inserted. A dynamic impact coefficient of friction of 0.5 was used since this value is conservative relative to the coefficient of friction averaged over the length of the PCRS (see paragraph 4.2.3.1.3).

The ANSYS computer program was used to perform the seismic analysis, using the semi-linear transient dynamic (time history) option of the program. An overall reactor system model was first used to determine the motions of the important components. The gross motions of the system components were then used as input functions in a decoupled primary control rod system model to determine the response of the leadscrew, driveline and control assembly within the PCRDM, shroud tube and control assembly duct.

The nonlinear primary control rod system model and its use in the seismic impact analysis are discussed in Section 3.7.3.15.3. The results of this analysis used in the scram calculations are the contact forces (vs. time) during the seismic event.

*See footnote to Section 3.7.3.15.

The scram analysis was performed using the CRAB computer code (See App. A) incorporating the dashpot model and time variant scram retarding force capability. The results of the SSE scram insertion predictions are compared with the seismic scram requirements in Figure 4.2-119. BOC-5 was determined to be the time in life which produced the minimum reactivity insertion due to bank position and available worth. An evaluation of the inherent shutdown margin can be obtained by comparing the minimum reactivity insertion with the expected reactivity insertion. The minimum reactivity insertion represents a 3 σ worst case evaluation of maximum excess reactivity and minimum control rod worth, while the expected reactivity insertion represents nominal core conditions.

It is concluded that the primary control system satisfies the SSE scram insertion requirement of Figure 4.2-93. The reactivity effects of the slightly increased scram time are evaluated in Section 15.2.3.3.

The seismic scram analysis is a conservative evaluation of scram capability under SSE environment in that a conservative calculation of loads and scram initiation time was employed.

4.2.3.3.1.5 Control Assembly Analyses

Absorber Pin

The primary control assembly utilizes enriched B₄C (approximately 92 atom percent ¹⁰B in Boron). Data on helium release, thermal conductivity and pellet swelling, required for absorber design, are available in References 44 and 44a.

Currently committed B₄C tests providing EBR-II irradiation data in support of CRBRP control assembly design are given in Table 4.2-46A. The table summarizes each test using the HEDL name for the test. Typical test parameters for pellet temperature, pellet diameter and B-10 captures completion dates for the EBR-II irradiations.

The tests of Table 4.2-46A will extend the irradiation data well above the pellet temperature and pellet sizes anticipated for the primary control assembly. The BICM-1 test has provided data to 80X10²⁰ B-10 captures/cc, which is comparable of first core burnups for CRBRP. The BV-2 test for vented pins will provide data on pellet swelling for burnups typical of 275 FPD cycle operation. The tests of Table 4.2-46A cover the operating range for the primary control assembly over its required lifetime.

The planned EBR-II B₄C irradiation tests do not include in-reactor transient cycling of absorber rods. Out-of-pile testing of irradiated pellets has been performed under the HEDL development program to determine gas release under transient thermal conditions. Preliminary results indicate that helium release upon temperature increases occurs over a relatively long time (on the order of 15 minutes) characteristic of a Primary Control Assembly thermal transient. Since B₄C temperature increases during transients are small (<100 F) the incremental gas increase from a transient is a small effect. Incremental gas release

during transients based on the thermal transient tests are included in the pin lifetime analyses. Since the absorber pins are designed to preclude pellet to clad interactions or B_4C melting under worst case transient conditions, gas release is the only B_4C variable required to be assessed in transient analyses.

53 | Further performance data for the PCA will be obtained from the
PCA Irradiation Test (see Section 4.2.3.4.1.1) which will provide integrated
51 | lifetime performance data for near prototypic environments and operating
parameters.

51 | Table 4.2-46 summarizes performance parameters for the absorber
pins. The thermal-hydraulic parameters are discussed in Section 4.4.
For the current design, the plenum lengths have been established by
the maximum available pin length, and the clad stresses at the end of
one operating cycle are less than 5,000 psi as shown in Table 4.2-46.

51 | Preliminary strain analyses of the pin have indicated that there
is only minimal accumulated strain at the end of the lifetime requirements.
Additional analysis utilizing the cumulative damage function approach
has been performed which also verifies the lifetime capability of the
pins. Use of the CDF for the absorber cladding requires that the duty
cycle be separated into various stress state/time segments superimposed
on the steady state operating conditions. This introduces conservatism
in the analysis since conservative estimates of stress and time form
the basis for the analysis. Effects such as sodium interaction with the
cladding and pin-duct interactions are included in the lifetime evaluation.
 B_4C swelling is calculated to assure that no force contact occurs
between the pellets and the cladding (see Table 4.2-36) thus reducing
the margin for error in the calculations. Figure 4.2-111a shows pellet
swelling and associated pellet to clad gap for rod in the Row 7 corner
location. Figure 4.2-111b shows axial B-10 burnup profiles for each
rod position in the equilibrium cycle.

54 | 53 | 51 | Based on the results of the preliminary analyses performed, it
is concluded that the pellet/clad gap clearance requirements are satisfied
for the required 328 FPD lifetime with an initial gap of 0.028 inches
(Figure 4.2-111a). The initial gap must be increased to allow for
additional pellet swelling over the goal lifetime of 550 FPD.

Structural Evaluation

51 | A preliminary elastic analysis was performed to evaluate the
structural adequacy of the control assembly outer ducts. Design stress
limits were derived using the criteria defined in Table 4.2-37B. Both

ductile and brittle failure modes were considered in deriving these criteria. Material data was taken from Ref. 1 for the worst case thermal and irradiated state of the critical duct sections evaluated, that is, the lower duct welds and the ACLP. Plastic analysis, including creep and swelling effects, is not expected to significantly change the result of the elastic analysis.

51 | The results of the analysis for fuel ducts are presented in Tables 4.2-7 and 4.2-8. These results are applicable to the control rod duct since the control assembly utilizes the fuel ducts. It can be seen that positive margins exist for all loading conditions and stress categories. The control assembly duct does not attain the same temperatures as the fuel duct, thus the allowable stress and the margins of safety are greater for the control assembly. For the ACLP region of the duct, the increase in material allowable due to the lower control assembly duct temperatures, as shown in Figure 4.4-29, will raise the margins both for primary plus bending and primary plus secondary categories. In addition, the CDF will decrease from the already comfortable value to much less than 1 for both peak and seismic loading conditions.

51 | Analyses were performed to evaluate the effects of scram impact on the control assembly and the outer duct. These analyses indicate that scram impact does not pose a problem for the control assembly duct.

53 | The leadscrew-driveline-control rod assembly and the duct were modeled as a dynamic system (Figure 4.2-120). A driveline initial velocity of 25 ips was assumed to provide added analytical margin over the 14 ips design final velocity of the driveline and the FFTF dashpot test results of 9 ips. The results of this preliminary analysis are as follows:

51 | 1. There is insignificant rebound (both in magnitude and frequency) of the control assembly following impact on the scram arrest flange. In addition, the outer duct does not appear to be overstressed. Additional effort is in progress to establish acceptability of the end-of-life residual ductility.

51 | 2. The "breakaway" link (see Section 4.2.3.1.3) at the base of the control rod shaft is not dynamically overstressed upon scram impact. The dynamic weight of the control rod is less than the force at which the "breakaway" feature is designed to rupture (16,500 pound predicted force, 19,000 pound maximum) to satisfy the stuck rod or stuck coupling requirement referenced above.

3. The impact of the disconnect coupling actuating shaft is slight and does not damage the rod for an initial velocity of 25 ips, and does not occur at the design velocity of 14 ips.

4. There are large margins of safety for the driveline expansion sleeve and the position indicator rod for an impact at 25 ips.
5. The control rod welds (adapter plate-to-duct and pin-to-adapter plate) have adequate margins of safety based on 25 ips impact velocity.
6. Absorber cladding stress is insignificant in scram impact.
7. There is sufficient absorber pellet preload to prevent pellet separation and interpellet impact.

4.2.3.3.1.6 PCRD and PCRD Structural Analysis

51 | The CRBRP control rod system utilizes a modification of the FFTF mechanism to benefit from FFTF design and development experience. A complete structural analysis of the FFTF mechanism is reported in Ref. 41. Review of this analysis and scoping analyses of CRBRP primary control drive mechanisms indicate that loading requirements except the seismic requirements, are very similar to FFTF requirements.

59 | 51 | The mechanism is designed to withstand all loads stemming from SSE, and safely shutdown the plant. Seismic analysis has indicated that all seismic loading conditions are within allowable limits.

59 | Preliminary analyses have been performed to determine the structural adequacy of the control rod driveline, based on conservative assumptions of minimum material properties and maximum loads on stressed components. These evaluations considered the maximum load applied to the driveline by the motor including a stuck rod, latching and a cold stator. These loads are the peak tensile, compressive and buckling loads, and envelope all other loads encountered by the driveline. Table 4.2-47 summarizes the applied and allowable loads and stresses for the PCRD and PCRD components for the peak loading conditions. Only the maximum loading conditions have been addressed in this assessment of the PCRD/PCRD structural analysis. It can be seen in Table 4.2-47 that the maximum load or stress for these conditions does not exceed the allowable loads and stresses.

59 | 4.2.3.3.1.7 Overall System Performance Evaluation

Potential for Functional Failure of Critical Components

51 | As stated in Appendix C, a Failure Model and Effects Analysis of the control rod system were performed. In this analysis, each basic

component was considered separately to determine the type of failure, its causes, its effects on system performance, and the probability of occurrence. With regard to the primary mechanism and driveline, the analysis yields the conclusion that functional failures of the components are either extremely unlikely or have insignificant effects on system performance.

51 |

The primary safety functions of the CRDM and PCRD are reliable scram, and accurate, repeatable positioning. Therefore, the components which could conceivably inhibit these functions must be active in these functions. These components are the segment arms, including springs, pivot pin and synchronizer bearing, the scram spring, and the driveline coupling. Effects of failure of these components and other components such as bellows and stator cooling system are evaluated below.

Segment arm functional failure is failure to separate and release the leadscrew. This could result from segment arm spring failure, synchronizer bearing failure, or pivot pin lockup. There have been no known segment arm spring failures in 15 years of collapsible rotor mechanism experience and analysis of the FFTF mechanism has shown capability to scram with at least one failed segment arm spring under the conservative assumption of worst case bearing friction. Bearing and pivot pin failure would occur only if debris jammed the bearing, or gross dimensional inaccuracies occurred. There is no known source for debris, and dimensional variation is limited by rigorous quality inspection. Structural failure of the bearing is extremely unlikely, as the bearing is only slightly stressed.

A seal system has been provided in the CRDM to prevent sodium vapor from entering the roller nut area (see Seal System, Paragraph 4.2.3.2.1.1). However, in the extremely unlikely event that sodium vapor could be deposited in the roller nut area, testing has indicated (Ref. 11) that a roller nut type of CRDM scrams with no statistically significant scram time degradation in a sodium vapor-inert gas environment; that CRDM performed the required withdrawal, insertion, and scram functions satisfactorily while being cycled through 9600-ft and scrambled 1070 times with a 340-lb driveline weight attached. Testing with a purposely failed bellows in Phase IV of the FFTF Control Rod Environmental Life Test was completed in June 1976. The FFTF Control Rod System performed satisfactorily with a failed bellows.

51 |

Loss of stator coolant could ultimately result in stator failure and rod drop as the CRDM is fail-safe to stator failure. Monitoring of the stator coolant temperature will be utilized to permit corrective action to prevent a spurious scram.

A malfunction of the coupling would be sensed at connection after refueling by means of the position indicator rod at the center of the driveline. The coupling is designed to lock by differential thermal expansion for worst case clearance. Preliminary analysis has shown that the coupling lockup temperature at beginning of life is approximately 500°F for minimum clearance and approximately 700°F for maximum clearance. Thus, the control rod coupling is tight at operating temperatures above 700°F. Thermal expansion of the driveline could result in small positioning errors which will be evaluated in light of the control rod reactivity worth-position relationship.

51

Finally, an FFTF mechanism has been life-tested through 1500 full-length scrams, 20,000-ft of travel and 30,000 start-stop cycles without functional failures. Additional life tests are in progress for the CRBRP PCRDM.

Sensitivity to Mechanical Damage

Preliminary structural analysis has shown the primary mechanism adequate under seismic (SSE) conditions. Testing in similar mechanisms has been completed in which substantially greater shock loads than the SSE were imposed without failure. Therefore, the structural adequacy of the mechanism has been firmly established.

There is no conceivable driveline failure mode which would prevent scram. That is, even a gross rupture of any part of the driveline causes the control element to drop. Failure of the dashpot could cause a hard impact at the end of scram, however, the source of such a failure cannot be identified.

The positioning function of the driveline could be impaired should the dashpot cup bind at the top of its 1-1/2 in. travel. This failure mode is judged as being insignificant since there is a large clearance (0.41 in.) between the cup and the shroud tube. The only circumstances which could cause binding are: a) debris of sufficient size wedged into the gap at the end of the upstroke, and b) mechanical damage so severe as to produce enough distortion of the driveline to bind against the shroud tube. The latter has been ruled out previously in the evaluation of the CRD under the worst case design loading and particles greater than 0.25 in. diameter are screened out by the inlet module area. Also, the full-stroke displacement of the dashpot cup (1-1/2 in.) is sufficient to cause significant loss of reactivity insertion in a scram if the dashpot cup fails to seat.

It is therefore judged that there is very little sensitivity to mechanical damage affecting reactivity control or shutdown capability of the primary CRDM and CRD. Detailed evaluations will be performed in the design and testing efforts to further support these conclusions.

Potential for Excess Reactivity Additions

51 | The maximum design withdrawal speed of the mechanism is 9 ipm. The reactivity insertion associated with this withdrawal rate is evaluated in Section 4.2.3.1.1. The maximum uncontrolled withdrawal rate of the primary control rod system is 73 ipm, limited by the rollout characteristics of the mechanism. For this to occur, four separate and unrelated failures would have to simultaneously occur in the mechanism controller, including output signal oscillation at a frequency greater than the power supply source frequency. Additionally, the uncontrolled motion would be confined to only one rod, due to the single rod stepwise function of the controller. Because of the number of simultaneous failures required to cause a rapid withdrawal, this event is judged to be extremely unlikely. However, the reactivity effects of such an event are discussed in Section 15.2.2.3 and have been found to be within the capabilities of the plant protection system to prevent fuel damage.

Potential for Rod Ejection

Inadvertent lifting or ejection of the control assembly is not considered credible because of the low pressure design of the reactor system. The weight of the control assembly (including the driveline) is approximately 400 lbs. There is no conceivable uplift force of a similar magnitude. In spite of this, an out-motion pawl is added for another layer of conservatism to limit outmotion speeds.

At refueling when the control assembly is disconnected from the driveline, a situation may be postulated in which full pump flow is started by an unknown mechanism. A control assembly flow rate of about 58,445 lb/hr is required to lift the control rod with the driveline disconnected. The preliminary maximum flow rate is 51,493 lb/hr for these postulated conditions which result in a flotation margin of 1.14. Table 4.2-48 compares predictions of the flotation conditions with the FFTF control assembly flow tests. This comparison shows that the flotation conditions are predicted to an accuracy of better than 5% on both flow rate and pressure drop. Consequently, flotation of the control rod cannot occur even with the driveline disconnected. A major structural failure of the lower axial shield orifice assembly would have to occur before flow rates approaching flotation conditions would be possible. Therefore, rod ejection is not considered credible and is not included as a design basis.

CRDM Housing Leak

51 | The CRDM pressure boundary design incorporates a buffered seal configuration to prevent leakage of reactor cover gas into the head access

area. The buffer zone consists of an Argon gas atmosphere above the bellows and the Bellows Support/Extension Nozzle Seal. These boundaries are shown pictorially in Figure 4.2-102 and schematically in Figure 4.2-102A. This seal configuration places two seals in series between the Cover Gas region and the Head Access Area. With this series seal configuration, the static pressure in the buffer region between the series seals can be continuously monitored with pressure transducer type instrumentation. Continuous monitoring of the buffer zone pressure will reveal seal leakage in any of the buffer zone seals and permit remedial action before failure of the other series seal can cause leakage to the Head Access Area.

Seals between the Buffer Zone and the Cover Gas include the three welded metal bellows units and the Conoseal between the Upper Bellows Support cylinder and the Extension Nozzle (see Figures 4.2-102 and 120A). The welded bellows are included in this seal boundary to permit motion required for the CRDM leadscrew stroke, actuation of the control rod disconnect coupling, and motion of the position indicator rod. The Upper Bellows Support/Extension Nozzle Conoseal joint is required to complete the seal between the Buffer Zone and the Cover Gas. The seals on the opposite side of the buffer zone, namely, the Upper CRDM Mechanism Seals, between the Buffer Zone and the Head Access Area, include the Motor Tube/Extension Nozzle, the Position Indicator Housing/Motor Tube, the pressure switch and several Voishan Seals, all shown schematically in Figure 4.2-120A.

51 The seal boundaries are filled with an atmosphere of inert argon gas at a pressure slightly higher than that of the reactor cover gas. This inert argon buffer gas protects the CRDM rotor assembly and lead-screw-roller nut assembly from the deleterious effects of the reactor cover gas environment. In addition, the pressure of the buffer gas is continuously monitored by a pressure switch located at the top of the CRDM housing. In the event of a deterioration of either one of the redundant seal boundaries in the CRDM sealing configuration, the resulting decrease
51 | in the pressure of the buffer gas would be detected by this pressure switch and appropriate corrective action could be initiated while the remaining seal maintained the integrity of the reactor primary system boundary. The reliability of the pressure switch which monitors the argon buffer gas can be demonstrated by means of existing reliability data for similar electro-mechanical components and/or component tests. The low probability of failure that is anticipated for a simple electro-mechanical device such as the pressure switch, when combined with the extremely low probability of a simultaneous leakage failure of the two redundant seal boundaries, eliminates the consideration of an undetected leakage
51 | of reactor cover gas into the head access area as a credible event. The design requirement leakage rate for the CRDM housing is based on a helium leak rate of 1×10^{-4} cm³/sec maximum for each CRDM at normal reactor operating

Amend. 51
Sept. 1979

pressures. This design leakage rate is based on the demonstrated leak rate data for the mechanical compression seals and bellows units, and is considerably less than the portion of the total cover gas leakage into the head access area that has been allocated to the CRDM housings. In addition, the integrity of the CRDM housing seal configuration will not be significantly degraded (relative to the allowable leakage under SMBDB conditions) by the effects of the SMBDB loading condition which includes a reactor vessel after pressure of 300 psi maximum which corresponds to a steady state pressure acting on the underside of the head.

4.2.3.3.1.8 Previous Experience and Development Work

As previously noted, the Primary Control Rod System design is similar to the FFTF Control Rod System. The FFTF Control Rod System testing and analysis to date has confirmed the acceptability of this type of system for LMFBR application. The FFTF analysis and test data have been and will continue to be used in the design and analysis of the CRBRP Primary Control Rod System and Components.

Prior to the selection of the collapsible rotor roller nut type Control Rod Drive Mechanism for the FFTF application, this type of mechanism was used in naval pressurized water reactors for at least 15 years. The environment of the PWR drive mechanisms is not the same as the inert gas atmosphere of the FFTF and CRBRP applications. However, the FFTF development testing of the collapsible rotor roller nut mechanisms in inert gas/sodium environments has indicated the analysis techniques utilized in confirming scram reliability of this type of mechanism in PWR applications is valid for LMFBR applications. This analysis which was done for the FFTF Control Rod System and will be done for CRBRP, utilizes friction coefficient data developed in the FFTF friction and wear test program conducted at WARD, HEDL, and ETEC.

4.2.3.3.2 Secondary System Evaluation

4.2.3.3.2.1 Tolerance Analysis

Accurate knowledge of the control rod position above the core of an operating plant is needed to assure that performance requirements can be met. Dimensional loop tolerance from the control rod, up the driveline, through the SCRDM to the reactor head, down through the vessel to the core support structure has been analyzed to predict the effects of fabrication tolerances and temperature changes from shutdown to full power on control rod position relative to the core. This analysis indicated the need to reduce the effect of that total loop tolerance. To minimize the cumulative effects of the various tolerance conditions and to increase the confidences with which the position of the control rod is known, a means is provided to accurately establish the location of the top of the control rod when the plant is shutdown. This location is established in the following manner. The drive shaft will bottom out on the control rod under motor insertion stall forces. This assures a reference position for the control rod with respect to the control assembly. The drive mechanism position indication can be read for this reference point from which subsequent control rod withdrawal movement is measured. This approach bypasses the tolerance buildup that could develop from considering the entire dimensional loop and gives a more accurate indication of control rod position. Additional tolerance analysis important to the proper operation of the SCRS is addressed in the following paragraphs.

In the latch, the gripper moves within the driveshaft and contacts a shoulder in the driveshaft at the gripper's upper end when the latch is engaged. During engagement, the control rod coupling head contacts the lower end of the gripper fingers, and the coupling head forces the gripper fingers radially apart until their outer surface contacts a cam surface on the driveshaft. Tolerances on the driveshaft between the upper shoulder and cam face on the corresponding gripper features shall be such that the resulting radial position of the gripper fingers will fall within safe bounds when loaded by the coupling head. A 0.146 in. radial outward movement from the nominally engaged position of each gripper finger is required to release the coupling head. The cam angle is such that a 2:1 relation of finger movement to axial movement will exist. The coupling head and gripper fingers are designed such that contact stresses remain within acceptable limits.

One of the objectives considered when the damper design was selected was that the design reduced the close fits and high tolerances required for most hydraulic dampers. The minimum radial gap for the tapered dashram part of the damper is 0.083 in., which is relatively large compared to typical dashpot designs. Along the stack of the damper plates, the radial gap clearance

between the plate outside diameter and the cylindrical housing inside diameter changes from a minimum 0.010-in. gap to a maximum 0.125-in. gap. These clearances are above the minimum usually used in liquid sodium design.

The amount of movement the pneumatic cylinder piston must undergo to fully engage the control rod coupling head with the collet is a function of the tension rod strain in addition to the 0.25 in. of motion required to raise the collet. For the 1920 pound design tensile load, the rod will stretch approximately 0.166 in. at a temperature of 1000°F. The compressive reaction to this 1920 pound load occurs in the drive shaft, and results in a decrease of 0.016 in. in the length of the drive shaft. Thus, the stroke of the piston must allow for 0.432 in. of motion between the loaded and unloaded conditions. Since the current piston design can produce plus or minus one inch of motion, no problems are foreseen. In addition, the current design also has a threaded adjustment at the tension rod-piston coupling to accommodate tolerance build-up conditions.

An analysis of the available clearances between a bowed channel guide tube and the control rod within, has been performed considering the Row 7 duct bow. No interferences were found to exist. Therefore, no resistance to scram occurs as a result of bowing.

4.2.3.3.2.2 Scram Analysis

The Secondary Control Rod System is designed to shut the reactor down with any five of the six control rods scrambling. There are only two normal positions for the control rod in the SCRS, full-out or full-in. Scram is accomplished by releasing the latch and allowing the rod to drop into the core. The assembly flow is ducted to the control rod so that hydraulic pressures provide a scram assist force in addition to the control rod weight.

Control Rod Insertion Speed

Control rod insertion speeds are calculated by the DYNALSS computer code which solves the equations of motion considering all forces acting on the control rod including hydraulic scram assist force. The SCA design creates a high pressure region in the upper SCA and a low pressure region in lower SCA. The pressure differential across the control rod piston results in a net downward hydraulic force. The downward hydraulic force exists only at the very early stage of insertion to provide an initial scram assist force on the control rod. As the rod moves, the flow paths around the control rod and their resistances change. This, in turn, varies the flow distribution and the hydraulic forces. The code traces the control rod position, calculates the flow resistances and flow distribution, and determines the detailed hydrodynamic response of the control rod as it moves into the reactor core. The code provides options to accept either time-dependent pressures or flows at the SCA inlet, lower and upper outlet as input boundary conditions for scram dynamics calculations.

Validation of the code for predicting the control rod insertion speeds in the absence of seismic loadings was made against test data from the SCRS prototype tests. Measured time-dependent flow or pressure data for the inlet and outlet lines are inputted into the code as boundary conditions for the sodium tests loop scram calculations. Figure 4.2-121 shows the insertion of the rod from the initiation of the rod motion for scrams from steady 40% and 100% flow with testing temperature at 900°F and non-seismic conditions. The figure demonstrates the ability of the code to predict scram insertion performance closely for any given set of time-dependent pressure or flow data at the SCA inlet, lower and upper outlet.

The seismic effect on the control rod insertion is obtained from a seismic time history analysis of the secondary control rod assembly. This analysis determines the lateral contact loads of the control rod with the guide tube. These results in combination with a conservative friction coefficient are used to determine a conservative seismic induced drag load on the control rod during insertion for OBE and SSE conditions. These drag load values are inputted to the code which then predicts the control rod insertion time under OBE and SSE seismic conditions.

Scram Reactivity Insertion Rates

The SCRS scram insertion performance in the reactor was determined for the worst case transients and for steady state flow conditions by inputting seismic drag load data and time-dependent SCA boundary pressures calculated from reactor plena pressures. SCA boundary pressures for a steady state scram in the reactor remain constant during the scram. On the other hand, SCA boundary pressures for a transient scram are changing during the scram. The loss of all off-site power transient (U-18) with minimum reactor system resistance conditions as pre-transient reactor flow conditions has been identified as the worst case among all the cases evaluated. The time-dependent plena pressures during the transient are the result of simultaneous coastdown of all sodium pumps. As the high pressure drops off, the hydraulic scram assist force on the control rod decreases. The transient scram from full reactor flow coincident with OBE and SSE events was then calculated at three standard deviations above the mean. A steady state scram with minimum reactor system resistance conditions from 40% reactor flow coincident with OBE and SSE events was also calculated at three standard deviations above the mean. The statistical calculations of the scram insertions include uncertainties associated with operating parameters, temperature flow split and modeling. In addition, the minimum reactor system resistance conditions used for generating SCA boundary pressures are the limiting conditions to result in minimum pressure drop in the reactor system.

The displacement/time profiles obtained from the calculations described above were then converted into reactivity insertion/time profiles using the secondary control rod minimum worth insertion profile. The results of these calculations and their comparison with the minimum reactivity insertion requirements described in Section 4.2.3.1.3 are shown in Figures 4.2-122a & b. All calculated reactivity insertion curves in Figures 4.2-122a & b account for a combined reactivity insertion delay time of the Secondary Control Rod Drive Mechanism response time (unlatching time) and control rod traveling time of

the first 1-1/2 inches. The SCRDM response time is the interval from the scram initiation to the start of control rod motion. At nominal withdrawn parked position, the bottom of the absorber pellets is located 1-1/2 inches above the top of the reactor core. Therefore, the reactivity insertion will not begin until the control rod travels 1-1/2 inches into the core. An SCRDM response time of 0.060 seconds was used for all these calculations. The mean SCRDM response time measured in the SCRS prototype tests was 0.044 seconds and the maximum time (three standard deviations above the mean) was 0.056 seconds.

Figures 4.2-122a and b show that all the predicted reactivity insertion curves at three standard deviations above the mean met the scram insertion requirements. It is, thus, concluded that the secondary control rod system satisfies the minimum scram insertion speed requirements of Figure 4.2-94.

4.2.3.3.2.3 Control Assembly Analyses

Each secondary control assembly has a flow rate of 69,170 lb/hr., 73% under THDV conditions of which flows around the piston and into the low pressure plenum. The flow through the control rod is 9130 lb/hr and the remaining flow is leakage around the outside the control rod. Other pertinent operating parameters are summarized in Table 4.2-49.

To achieve the hydraulic scram assist force of 248 lb., a pressure drop of approximately 20 psi occurs across the piston at the design flow rate of 50,710 lb/hr to the low pressure plenum.

The peak absorber centerline temperatures of 1824oF for the hot spot and 1692oF for nominal conditions occur only at the bottom pellet of the absorber pellet stack since the B₄C is fully withdrawn from the core under operating conditions. The axial B₄C temperatures decrease rapidly in moving away from the top of the core. The solidus temperature of boron carbide can vary from 3880oF to 4440oF (depending on the stoichiometry) which is well above the 1824oF peak temperature. This is a centerline temperature that only occurs at the beginning of life when there is a large gas gap between the boron carbide pellet and the cladding, so there is no problem with cladding interaction.

The SCA absorber pin lifetime design is currently not finalized; this information will be provided prior to issuance of the FSAR.

SCA Guide Tube Analysis

The Secondary Control Assembly (SCA) guide tube provides mechanical guidance for the control rod during insertion and withdrawal, and also provides a cylindrical boundary which in conjunction with the control rod scram piston develops a hydraulic scram assist force on the control rod. Insertion of the control rod is assisted also by the force of gravity. Reactor sodium coolant flow, admitted into the annulus formed by the SCA outer duct and guide tube through the inlet ports in the SCA nosepiece, is the fluid source providing the differential pressure across the scram piston. The sodium coolant flow is admitted into the guide tube interior through guide tube ports located above the withdrawn parked position of the scram piston. Normal leakage flow past the scram piston is discharged to the low pressure plenum through a flow passage in the shield plug attached to the lower end of the guide tube. The guide tube, as a result of the pressure drop across the scram piston carries a slight (21-34 psi) external pressure over its lower length below the scram ports. The approximate length from the scram ports to the shield plug is 36 inches with the overall guide tube length being 74 inches. The guide tube wall thickness is 0.109 inches. Sodium flow in the annulus between the outer duct and guide tube above the port elevation is vented into the guide tube via a vent hole immediately below the downstop joining the top of the guide tube to the outer duct. Due to this vent hole there is no pressure force acting on the guide tube wall above the scram port elevation. With respect to maintaining guide tube functional requirements, deformation due to creep induced by the reactor environment is of principal analytic concern.

The guide tube may have an ovalized cross-section based on the worst case geometrical tolerances. Starting with these tolerances and using the maximum flux and temperature around the guide tube circumference at each elevation, a plane strain analysis was performed to calculate the guide tube deformations and resulting reduction in the guide tube/control rod clearances along the minor diameter of the ovalized guide tube due to the in-reactor creep deformations under the external coolant pressure. These reductions in the guide tube diameters were included in the analyses to demonstrate absence of forced three-point contact between the control rod and the guide tube during the control rod scram travel. In-reactor deformation rates at $+3\sigma$ uncertainty levels were used in the analysis.

The margins against time-independent buckling were shown to be large.

4.2.3.3.2.4 Overall System Performance Evaluation

Potential for Functional Failure of Critical Components

The Reliability Design Support Document (RDSD), planned for completion by the end of CY 1983, will provide the basis for this section's information. This information will be provided in the FSAR.

Component Strength Adequacy

The Secondary Control Rod System Components were designed to allowable stress/strain limits derived using the criteria defined in Section 4.2.3.1.5, Subsection 2. Both ductile and brittle failure modes were considered in deriving these criteria.

Potential for Functional Failure of Latch

The latch must: a) function to hold the control rod above the core during normal reactor operation; i.e., remain latched, b) function to release the control rod to effect scram; i.e., unlatch, and c) function to recouple the control rod to the drive shaft for retrieval prior to reactor start-up; i.e., relatch. Of these three, only the release function for scram carries significant safety implications.

The two potential failure modes considered to be of primary importance in the release function are extreme friction coefficients and self-welding of the surfaces in intimate contact (between the collet grippers and cam surface, and between the coupling head and the collet grippers, as shown in the schematic view of Figure 4.2-125). Component development tests of the scram latch configuration for the SCRS verified the adequacy of design of this component.

The concern of extreme friction coefficients was addressed by designing the latch to operate properly over a wide range of friction coefficients: from 0.2 to 2.0. It should be noted that the two pair of contacting surfaces can experience different friction coefficients. The design is such that the friction coefficients need not be the same on both surfaces for proper release. In fact, the friction coefficients on the two surface pairs can vary independently over the range specified without jeopardizing proper latch operation. The selection of the geometry of the mating surfaces to achieve accommodation of a maximum allowable friction coefficient of 2.0 is discussed in (Ref. 47). The specification of the lower limit for acceptable friction coefficient is motivated by the desire to have a reasonably low actuation force, and by the fact that no tests to date with the candidate materials have shown that friction coefficients below 0.2 will occur. A greater range of friction coefficients requires increased actuation forces to keep the latch closed.

For example, the required total actuation force (for the design basis coupling head load of 500#) to be applied to the tension rod is shown in Figure 4.2-126 as a function of friction coefficient for two cases: a) maximum allowable friction coefficient is 2.0, and b) maximum allowable friction coefficient is 3.08. Selected materials combinations were tested to verify the expected friction coefficient. These test results for the selected material combination, Inconel 718 on Inconel 718, were in the lower region of the design range 0.2 to 2.0 and compared favorably with data as reported in Table 4.2-50 for the candidate materials.

Avoidance of problems associated with self-welding depends upon the mechanical design concept, proper material selection, and upon achieving proper geometry of the surfaces so that contact stresses are limited to sufficiently low values that neither produce severe distortions nor favor self-welding. As noted in Table 4.2-51, Inconel 718 on Inconel 718 indicates desirable performance under the operating conditions expected for the latch. Similarly, Inconel 718 on Inconel 718 exhibits relatively low breakaway friction coefficients as shown in Table 4.2-50. Breakaway friction coefficients are a measure of self-welding tendencies during long-term holds. Furthermore, the geometry of the contacting surfaces is selected to give relatively low Hertz contact stresses of approximately 70,000 lb/in² as calculated by classical Hertz contact stress analysis. The surface of the gripper pads in contact with the cam is spherical, and the cam is conical. The inner surface of the gripper, the one in contact with the coupling head, is cylindrical with a circular cross section whereas the coupling head is spheroidal with a large radius in the vertical plane. Because of this geometry between the coupling head and the gripper, the point of contact at this interface is not critical; the radius of curvature of the gripper pad is concave and uniform everywhere, and hence, regardless of the location of the contact point, the contact stresses are the same. Consequently, if manufacturing errors result in slight mislocation of the gripper with respect to the cam surface, and the coupling head and gripper contact point differ somewhat from the design point, virtually no change in stress will result. A thorough test program was conducted involving operation of prototype latches in an environment and under conditions typical of reactor operation. Post-test examination of the latch demonstrated insignificant wear characteristics and, in conjunction with the friction coefficient measurements made during the test, provided assurance that the latch is properly designed for the application.

Because self-welding is a diffusion phenomenon, higher temperature and contact stresses are generally considered to favor self-welding due to the fact that these conditions promote diffusion across the contact area. Latches typically sustain high contact stresses and so might be considered candidates for self-welding problems. However, it is important to recognize that relatively high contact stresses are accompanied by relatively large (on a microscopic scale) elastic strains and associated storage of strain energy. This strain is available to rupture any self-weld bonds that might have occurred during intimate contact. If it is assumed that a self-weld bond has occurred on the latch contact areas, the forces acting on the latch as a result of only the gravity forces on the control rod have been calculated to be capable of inducing tensile stresses on the order of 1,200,000 psi on the postulated

self-weld bond. Clearly such a high stress cannot be sustained by any self-weld bond, and the bond would be ruptured, and the rod would be released. Consequently, it can be concluded that even if self-welding were to occur, the consequences would be limited to slightly greater wear on the latch components due to adhesive wear characteristics. If for some other reason, latch release were not achieved, then the primary control rod system would shut down the reactor.

Sensitivity of the Systems to Mechanical Damage

The Secondary Control Rod System is being designed to withstand significant mechanical damage and still permit scram.

Analysis has shown that 1.15-in. of relative lateral deflection between the bottom of the head and the top of the control assembly handling socket must occur before significant loads can be developed. At that point, the bottom of the driveline will have rotated one degree from its vertical orientation. The control rod coupling head has been designed to accommodate this rotation without inducing loads into the control rod.

The control assembly load pad capacity loading is not currently finalized, but will be determined after core restraint loads are available. This information will be provided in the FSAR.

Potential for Excess Reactivity Additions

The planned SCRS operation is to withdraw the control rods to their full-out position before the reactor becomes critical. During reactor operation at more than 5% power, the SCRS control rods are always out of the core. When the control rod is in normal parked position at the top of the core (bottom of B₄C nominally 1.5 inches above top of fuel), the top of the damper assembly is 0.75" from the bottom of the handle extension. Since the damper assembly cannot fit within the handle extension, the control rod cannot be withdrawn farther than 0.75 inch beyond its normal withdrawn position. Movement of the control rod from the top of the core to 0.75 inch beyond the top of the core would be only a small reactivity addition. During shutdown, downflow provides a downward force on the assembly which increases as the flow increases. The operation and design of the SCRS precludes reactivity addition due to unexpected control rod withdrawal.

The design nominal withdrawal speed of the SCRDM is 9 ipm, which is the same as the Primary Control Rod System maximum design withdrawal speed. Reactivity insertion rates associated with this withdrawal speed have been shown to be acceptable (Section 4.2.3.1.3).

Potential for Rod Ejection by Pressure Forces

The Secondary Control Rod System uses a net downward hydraulic pressure force for scram assist. This downward force is achieved by restricting the flow area at the top exit of the assembly (the latch seal), and by having flow communication with the low pressure plenum. The downward flow to the low pressure plenum undergoes a large pressure drop when it passes through the narrow clearance between the piston at the bottom of the control rod and the guide tube. With this configuration, the downward hydraulic force on the control rod increases as the flow rate increases, so a flow increase does not present a rod ejection hazard.

The piston that creates the large pressure drop in the downward flow must be between the flow ports in the guide tube and the low pressure plenum to achieve the downward force. The control assembly design precludes the piston ever rising above the guide tube ports. There is more than 1.25 in. between the bottom of the port and the bottom of the piston, so the piston would have to be raised more than that amount before it could expose the port directly to the low pressure plenum. The clearance between the top of the damper assembly and the lower end of the top handle extension is only 0.75". Even if the driveline were withdrawn beyond the normal parked position, the control rod would contact the top handle extension at 0.75" and prevent any further withdrawal. The piston is thus prevented from being above the ports.

The seal around the driveline (the latch seal) maintains a large flow restriction at the top assembly outlet. This seal is the principal contribution to pressure drop in the upward flow. The seal cannot be withdrawn from the assembly without scrambling the control rod because the damper will contact the handle extension. If the driveline is inserted so that the latch seal drops below the handle extension, the driveline still provides adequate flow resistance to prevent an upward hydraulic force on the control rod.

The only time the driveline is completely withdrawn from the assembly is during refueling, when the reactor is shut down and the pumps are operating at low flow. However, the control rods are not lifted even if the pumps are operated at full-flow conditions. This situation can only occur when the rods are fully inserted. With the driveline removed, more flow exits at the top of the assembly, and it passes through the narrow annulus between the dashram and the guide tube. The flow undergoes a large pressure drop at the dashram, and this creates a lifting force on the control rod. However, this lifting force is approximately 25% of the assembly's weight when the pumps are operating at full-flow conditions.

SCRDM Housing Leak

The details of the two seal boundaries forming and housing buffered seal and leak detection vary between the PCRDM and SCRDM.

- a) In the SCRDM the first seal boundary consists of three metal bellows and two metal mechanical compression seals. These elements in conjunction with the drive housing structure and driveline structure, seal off the total area inside the drive mechanism nozzle. At the top inside surface of the drive mechanism nozzle, two metal mechanical compression seals are located with the housing pressure ported between the seals to form a buffered seal configuration. Of this seal pair, the lower seal is adjacent to the reactor cover gas and is part of both the first seal boundary and the upper seal boundary, which is described below. The drive housing pressure, which is higher than the reactor cover gas, acts as a buffer against the cover gas so that any leakage is into the reactor. To follow the first seal boundary path through to the drive centerline, the next portion is a mechanical

compression seal between the lower end of the lower drive housing and the long stroke of the bellows lower end fitting. The drive housing pressure acts across this seal with respect to the cover gas, and thus acts as a buffered seal. The top end of the long stroke bellows attaches to the driveline. The cover gas occupies the inside of the bellows and the drive housing pressure surrounds the outside. The driveline configuration extends across the inside of the long stroke bellows to complete the first seal boundary. The driveline contains two internal concentric shafts, one for latch actuation and the other to indicate the control rod coupling head presence within the latch. These shafts within the driveline are sealed with respect to each other with two metal bellows at each end of the upper driveline. The bellows at each end of the driveline allow it to be internally pressurized to a higher pressure than the drive mechanism housing. The second seal boundary, or the primary system boundary, consists of the three metal compression seals (the upper seal of the nozzle to housing seal pair, the lower to upper housing seal and the upper housing to connector plate seal). The electrical and pneumatic inputs through the connector plate are sealed with welded seals and o-ring compression seals.

An o-ring sealed pressure relief valve, set at 25 psi, is mounted in the center access hole of the connector plate. This relief valve provides over pressure protection for the SCRDM housing in the event of an SCRS argon control system failure which could introduce limited flow but potentially high pressure argon into this closed volume.

- b) The volume enclosed by these two seal boundaries contains the motor, leadscrews, and position indicators. This volume, like the PCRDM, is purged with clean argon gas that is monitored to detect leaks. The difference in monitoring is that in the SCRDM the buffer gas flow rate is measured.

4.2.3.3.2.5 Previous Experience and/or Development Work with Similar Systems and Materials

Various control rod drive systems have received significant development and accumulated extensive experience through the years. EBR-II, Fermi, and FTR are the major U.S. programs that provide control rod drive experience for LMFBR conditions, with FTR being the most applicable.

EBR-II has operated for many years and accumulated reliable drive performance. The main shaft long-stroke bellows of EBR-II are located above the reactor head, as are the SCRS bellows, and the EBR-II experience has demonstrated that sodium vapor migration up the long narrow annulus to the bellows, is minimal and has not caused a problem. The EBR-II control rod is attached to the drive shaft by a gripper mechanism that even though its design is not the same as the SCRS latch and it does not release for scram, it still confirms that latch or gripper mechanisms can function reliably in liquid sodium.

The Fermi reactor utilized a latch at the drive shaft end to release the control rod for scram. After development, the final latch configuration performed well. The reported failure of a latch to scram was the result of a failed bellows exclusive of the latch mechanism. The Fermi latch design differs from the SCRS latch, but its success again adds to the confidence of using latch mechanisms for LMFBR control rod drive systems. The failed bellows prevented the Fermi latch from releasing by permitting liquid sodium to rise in the driveline. The sodium contacted air and reached a cooler elevation where a sodium freeze plug was created inside the drive shaft that prevented the latch release. Subsequent modification to the Fermi drives pressurized the drive shaft with argon and provided leak detection. The SCRS design has incorporated both driveline pressurization and leak detection.

The FFTF roller nut drive is the most recent drive development work, and it is also the CRBRP primary control rod drive. Several of its features will be applicable to the SCRS even though the SCRS is being designed to be diverse from the roller nut drive. The static metallic reactor core gas seals used for FFTF will be applicable for the SCRS. The design and testing experience on FFTF has provided candidate materials for satisfying difficult design requirements for operation in sodium. Inconel 718 was selected for the FFTF drive shaft material and is also planned for some of the SCRS driveline components. The fuel assembly and control assembly load pads require a low coefficient of friction material that will withstand high compressive loads and not exhibit self-welding in high temperature sodium. For the FFTF, chromium carbide was found to be a suitable coating that can be applied to the stainless steel base material. This chromium carbide coating is applied to the SCA load pads. The FFTF main bellows have undergone development that will apply to the SCRS. The SCRS design has maintained the same outside and inside diameters as used for the FFTF bellows. The SCRS stroke is longer but the SCRS bellows do not have to follow the rapid scram motion as do the FFTF bellows.

Boron carbide has been the near universal selection for the absorber material for LMFBR reactors both in this country and abroad. Both FFTF and the SCRS are utilizing this absorber material, so the design data and development experience will be applicable to the SCRS.

4.2.3.4 Testing and Inspection Plan

The testing and inspection plan described herein for the reactivity control system is divided into five areas which verify the design of the systems and the quality of the components installed in the reactor. These five areas are an extensive performance test program, plant tests, surveillance, acceptance tests, and post-irradiation examination.

4.2.3.4.1 Performance Test Program

Extensive testing programs are planned for evaluation of the reliability and design of both reactivity control systems. These tests will include individual component tests and complete prototype systems tests.

4.2.3.4.1.1 Primary Control Rod System

The PCRS testing program consists of the following major testing activities:

A) Component Tests: The following component design test and/or analysis program was established to provide design verification of the PCRS components.

1. Dynamic Seismic Friction Test

This test was performed to evaluate the effective coefficient of friction between a rod and its guide bushings under impact loading conditions. Data obtained are used to provide friction coefficients for seismic scram insertion analyses.

2. Control Assembly Hydraulic (Flow) Test

Test results will be used to verify the pressure drops, flow and vibration characteristics of the primary control assembly design under prototypic flow conditions.

3. Control Assembly Pin Compaction Test

Test has provided data to determine inter-pin and pin-to-duct loads for the primary control assembly analyses.

4. Control Assembly Rotational Joint Test

Test has provided performance data on the rotational joint which confirmed the reduction in control assembly wear and reliable operation of the joint.

5. B₄C Data Test

The base technology irradiation test program being conducted by HEDL includes acquisition of data required for design verification of CRBR control assemblies (see Table 4.2-46A).

6. Friction and Wear Tests

The base technology materials test program being conducted at ETEC and ARD provides data for the material couples selected for fabrication of the primary control rod system.

7. Control Assembly Analytical Methods

Provides an analytical model calibrated with test results for predicting primary control assembly thermal-hydraulics performance, lifetime characteristics and scram dynamics behavior.

- B) System Level Tests: A series of Primary Control Rod System Prototype Tests have been performed to verify that the Primary Control Rod System performance is consistent with its design requirements under design basis operating conditions. The Control Rod Drive Mechanism was evaluated in a CRDM Accelerated Unlatching Life Test. This test program verified the unlatch performance characteristics of a prototype primary control rod drive mechanism over twice the design lifetime travel and scrams. The Accelerated Life Test involved testing of a full size prototype primary control rod system in sodium, sodium vapor, and argon gas environments that simulate operations in the Clinch River Breeder Reactor Plant. Phase I testing in this series completed 1/2 of the PCRS lifetime scrams, 1/3 of the leadscrew travel requirement, and about 5 times the PCA travel requirements. Phase II of this series will extend total test scrams and travel beyond CRBRP lifetime requirements.

During System Level Tests of the Primary Control Rod System, each subsystem was also tested, including the position indication system and the dash pot. Four prototype systems were tested and the results show PCRS performance including position indicator accuracy and dash pot performance were within this design requirements.

- C) PCA Irradiation Test: A PCA irradiation test is scheduled to be inserted in the FFTF for 600 FPD. The intent of this test is to provide near-prototypic irradiation performance data on the PCA absorber assembly to support the PCA lifetime evaluations. The test assembly will contain 37 pins of enriched B₄C and will function as an integral part of the FFTF Secondary Control Assembly Bank. The parameters of the test assembly have been selected to provide data prototypic of the PCA for burnup, fluence, B₄C and cladding temperatures and cladding strain. Data from this test are expected to be available in 1986.
- D) Other Tests: See Appendix C for Reliability Test Program.

4.2.3.4.1.2 Secondary Control Rod System

The SCRS testing program consists of the following major testing activities:

- A) Latch Tests: Component development tests of the scram latch configuration for the secondary control rod system verified the design of this component.
- B) Damper Tests: Component development tests of the damper configuration for the secondary control rod system verified the design of this component.

- C) Position Indication Tests: Prototype system level testing the secondary control rod system verified the design of this subsystem.
- D) SCA Static Flow Tests: The static flow test has been performed to verify design calculations for hydraulic forces and flow splits through the secondary control rod.
- F) Prototype Tests: Four complete prototype secondary control rod systems were tested in sodium and verified compliance with the design life requirements under prototypic (except radiation) environmental conditions.
- G) Coil Cord Tests: The latch mechanism that moves with the driveline requires pneumatic and electrical service that is supplied by a coil cord. Component development tests of the coil cord configuration for the secondary control rod system and prototype system level testing verified the assembly procedures and design of this component.
- H) Latch Seal Tests: Testing provided information necessary to (1) properly size and shape the latch seal flow restriction and (2) to determine the leakage rate through the driveline flow limiters.
- I) Nosepiece Flow Tests: The nosepiece flow test provided hydraulic characteristics of an SCA nosepiece assembly.
- J) Argon Control System Tests: Testing has been performed to verify that the Argon Control System (ACS) can control the argon pressure and flow in the three regions of the SCRS and detect leakage to or from each of the three argon pressure volumes.

4.2.3.4.2 Plant Tests

Plant testing is divided into two categories. The first category is Start-up Test where the reactivity control systems components are carefully evaluated to verify conformance with the functional design parameters after initial installation in the reactor. The second category of Plant Testing is selected parameter tests performed during shutdown and refueling to assure there has been no significant degradation of the system since the Start-Up Tests.

Start-Up Tests

Plant start-up testing for the control rod systems will consist primarily of installed performance tests. The specific design parameters to be measured in

the PCRS will include scram insertion time, control rod adjustment rates, control rod worth, running and holding current for CRDM stator coils, and stator coil temperature.

Design parameters to be measured in the SCRS will include scram insertion time, control rod withdrawal rate, latch operation, control rod worth, housing temperatures, scram valve solenoid holding current, motor torque necessary for rod withdrawal, housing and driveline leak tightness and scram cylinder pressure.

Tests During Shutdown and Refueling

To assure there has been no degradation of the reactivity control systems, selected design parameters will be periodically measured during reactor operation. Tests which require access to the mechanism or which will interfere with safe reactor operation, will be performed during shutdown and refueling periods. For the PCRS, the following shutdown tests will be performed: scram insertion time, roller nut drop out current, stator checks, withdrawal speed and position indicator checks. For the SCRS, the following tests will be performed: scram insertion time, motor torque and speed latch operation, and position indication operation.

4.2.3.4.3 Surveillance

Surveillance During Operation

Surveillance during operation covers those conditions which can be monitored or inspected while the plant is in operation through the use of instrumentation or other means provided in the plant equipment design. By periodic surveillance, data will be accumulated which will indicate a drift or change in operating parameters. The more significant PCRS conditions to be surveyed are: detection of loss of internal PCRD pressure including ruptured bellows through CRDM pressure switch; position indicator or drive malfunction by comparison of position indicator readouts; operability of parked control rods by slight in and out jogging movements; and CRDM stator/cooling system malfunction by monitoring of stator thermocouples.

The conditions in the SCRS to be surveyed are: temperatures within the SCRDM housing, the electrical holding current for the scram valve solenoid, and the quantity of make-up argon gas required to maintain the SCRDM housing and SCRDM pressurization, valve poppet position during test and hold, control rod position, and latch and coupling head position.

Surveillance During Shutdown and Refueling

This surveillance covers control rod system components which can only be inspected by removal from the reactor. Inspection requirements vary in this category due to the downtime requirements of the plant. However, they can be summarized in the following groupings:

o Disassembly surveillance during normal refueling periods

No disassembly surveillance is planned during normal refueling. If, however, the normal tests performed during refueling or operation indicate some degradation in the operation of one or more PCRDM's, a selected removal and inspection of the suspected components may be performed.

o Disassembly surveillance after replacement

On a planned schedule, a mechanism and driveline will be removed and replaced so that it may be partially disassembled and inspected. These extensive inspections will include the following types of examinations: condition of leadscrews, springs, welded joints, wear surfaces, and wiring. During these inspections, expendable items, defective components, and those with limited design life, will be replaced to requalify the mechanism and driveline for reactor service.

4.2.3.4.4 Acceptance Tests

Acceptance tests will be performed both at the fabricator's site and at the CRBRP site after shipment. These acceptance tests follow stringent inspection and quality assurance procedures established for all stages of fabrication beginning with material procurement.

A. Fabricator Acceptance Tests

The fabricator shall perform acceptance tests on plant equipment to establish that the performance of each unit is within acceptable limits. The acceptance limits shall be determined from the performance requirements of the equipment specifications.

For the primary CRDM/CRD, these acceptance tests will include (but not be limited to):

- a) Proof pressure test of primary pressure boundary components
- b) Stator insulation and winding resistance
- c) Scram insertion characteristics from withdrawal heights of 10 inches and 36 inches
- d) Unlatch time at standard operating conditions of stator temperature and voltage
- e) Minimum latch current
- f) Minimum static and dynamic drop out current
- g) Position indicator accuracy
- h) Action of outmotion latch pawl

Supplier acceptance tests for the SCRDM and SCRD are shown below:

- a) Resistance and Capacitance Tests
- b) Hypot Test (Pin to Ground)
- c) Hypot Test (Pin to Pin)
- d) Pneumatic Connection Tests
- e) Driveline Pressure Volume Leak Test
- f) Pressure Boundary Seal Helium Leak Test
- g) Thermocouple Test
- h) LVDT Displacement Test
- i) Position Indication Test
- j) Motor Test
- k) Motor Shaft Lock Device Test
- l) Scram Test
- m) Poppet Movement Tests (PMT)
- n) Position Indication Switches Continuity
- o) Minimum Pressure Hold Level
- p) Scram Valve/Cylinder Pressurization
- q) Leak Test
- r) Vibration Sensor Test A

For the Primary Control Assemblies, fabricator acceptance tests for pin cladding and B₄C pellets will follow the guidelines of RDT M3 - 28T, May 1972, for cladding and RDT E6 30T, May 1973 for B₄C pellets - and will be fully documented in the FSAR. It is currently expected that the fabricator acceptance test requirements will cover the following as a minimum:

B₄C Pellets:

- 1) Pellet geometry
- 2) Density
- 3) B-10 content
- 4) Stoichiometry
- 5) Chemical Impurities

Pin Cladding, Pin Assembly, and Final Assembly

- 1) Geometry and Dimensional Checks
- 2) Bonding Gas Analysis as appropriate
- 3) Cladding Metallurgy (grain size, Intergranular attack)
- 4) Cladding Mechanical Properties
- 5) Weld Integrity
- 6) Ultrasonic Inspections
- 7) Cleanliness
- 8) B-10 Content
- 9) Weights

Inspections (such as mechanical properties) will be based on sampling plans for lot qualification which will be documented in the FSAR.

Critical parameters such as B-10 content will be determined in 100% inspections.

Similar fabricator acceptance tests will apply for the SCA.

B. On-Site Acceptance Tests

In addition to the acceptance tests to be performed by the equipment fabricator prior to shipment, receiving inspection and/or acceptance testing will be performed on each item of plant equipment when it arrives at the site. The purpose of these on-site inspections and tests will be to verify that the performance of the equipment has not deteriorated during shipping to the site, or while in storage.

Requirements for on-site acceptance tests have not yet been identified for the CRDM's and CRD's. Required testing beyond normal inspections for shipping or handling damage will be identified prior to the FSAR. Inspections for shipping damage will be visual check for dents, mars, breach of containment, extraneous materials in the shipping container and verification of acceptable shipping loads by checking the trip accelerometer in the container.

For the primary control assembly, the following on-site acceptance tests will be performed on each unit:

- a) Examination of the shipping container for broken seals, dents, penetrations, sheared bolts or any sign of shipment damage and verification that the shock indicators were not tripped.
- b) A visual inspection of the assembly for dents, nicks, and gouges, especially in the area of hexagonal load pad corners, shield block corners, the inlet nozzle, piston ring and discriminator post, and correct assembly identification by verifying handling socket identification, discrimination post geometry and assembly serial number.
- c) A control rod stroke functional test for detecting excessive drag forces between the inner and outer ducts.

Defects determined during visual examination will be photographed and measured. This inspection would be performed to determine if defects are of such an insignificant nature to be acceptable. A photographic record will be maintained for all accepted defects.

Similar on-site acceptance tests will be performed for the secondary control assemblies.

4.2.3.4.5 Post-Irradiation Examinations

Post-irradiation examinations will be performed on control assemblies from representative positions in the core for both the primary and secondary control assemblies. All assemblies in early cores will be given visual, bow, and dimensional checks before shipping for disposal. A few selected assemblies will be shipped to hot cell facilities for more detailed examinations.

The detailed examinations will include: gas release measurements from the absorber pins; bowing of the inner and outer ducts; B-10 burnup analysis and sectioning and examination for portions of the

various components by metalography and autoradiography. Physical property tests will be performed on the absorber pin cladding, pellets, the absorber duct, the control rod shaft, and other significant areas of the assemblies. Physical property examination will include tensile tests, stress rupture tests, ductility, and notch tensile tests, chemical analysis, and wear and erosion examinations. The results from these post-irradiation examinations will be used to verify performance predictions. If examinations of the discharged assemblies indicate confidence in extending the assembly life for an additional cycle, one assembly of each type may be retained in the core for an additional cycle to verify the extended life potential.

4.2.3.5 Instrumentation

4.2.3.5.1 Primary Control Rod System Instrumentation

The instrumentation for the primary control rod system consists of two independent control rod position indication systems as well as a pressure switch to monitor the integrity of the CRDM bellows sealing arrangement and thermocouples to monitor the temperature of the CRDM stator windings.

4.2.3.5.1.1 Absolute Control Rod Position Indication System

The absolute rod position indication system (of the primary control rod system) measures the leadscrew position by means of ultrasonics and magnetics to provide a signal indicative of rod position.

In this indication system, a magnetic wire is housed in a tube that extends into the inside diameter of the leadscrew. Electrical pulses sent through the wire cause a magneto - strictive twisting of the wire at the point where the wire is adjacent to a magnet mounted on top of the leadscrew. The resultant sonic pulses are detected at the top of the wire and are timed electronically to indicate the distance to the point of origin. This time/distance indication is converted to a D.C. signal which is analogous to rod position.

4.2.3.5.1.2 Relative Control Rod Position Indication System

The relative control rod position indication system measures the position of the corresponding leadscrew by means of counting the number of revolutions of the CRDM rotor assembly. The number of revolutions is determined by means of an electromagnetic sensor that counts the revolutions of an indicating disk attached to the rotor assembly. The number and fraction of rotor assembly revolutions, multiplied by the 0.60-in. pitch of the CRDM leadscrew, provides an indication of the leadscrew position as measured from the fully-inserted position. The

six poles of the indicating disk in conjunction with the 0.60-in. pitch of the leadscrew provides a resolution of ± 0.10 -in. and an accuracy of ± 0.15 -in. for this indication system. However, if a scram or misstepping occurs, the relative position indication system loses its zero-position reference and must be reset at the full-inserted control rod position.

4.2.3.5.1.3 CRDM Pressure Switch

The upper mechanism assembly is in a sealed environment pressurized with argon gas to protect the rotor assembly and leadscrew from the deleterious effects of the sodium vapor in the reactor cover gas. The argon pressure is monitored by a pressure switch located at the top of the CRDM motor tube housing. In the event of a failure of the bellows sealing arrangement for the upper

mechanism, the higher pressure argon gas will leak into reactor cover gas volume, and the resulting decrease in argon pressure will be detected by the pressure switch so that corrective action can be initiated.

4.2.3.5.1.4 CRDM Stator Thermocouples

The CRDM stator coils are equipped with thermocouples to monitor the temperature of the stator windings. In the event of a loss of flow of the stator coolant gas, the resulting increase in stator temperature will be detected by the thermocouple so that corrective action can be initiated.

4.2.3.5.2 Secondary Control Rod Instrumentation

The instrumentation for each of the six SCRDMs of the Secondary Control Rod System consists of an absolute SCRDM carriage position indication system, carriage position lights, sensing tube and latch/unlatch indication systems to detect whether the driveline is coupled to the control rod, pressure switches for monitoring the integrity of the SCRDM bellows sealing arrangements, and thermocouples for monitoring the internal temperatures of the SCRDM, and an acoustic monitor to indicate that the SCAs have bottomed during scram time testing.

4.2.3.5.2.1 Leadscrew Absolute Encoder Position Indication System

The driveline motion is provided through two parallel leadscrews. An encoder geared directly to one of the leadscrews provides the driveline position indication. The driveline position indication is used when coupling the latch to the control rod and raising the control rod to its operational withdrawn (top) position, and for withdrawing the driveline to the fully retracted refueling position.

The operation withdrawn (top) position is determined by comparing the absolute position indication signal with an acceptable withdrawn position switch setting.

4.2.3.5.2.2 Cam Actuated Switch Position Indication System

Four cam actuated indicator switches are used. Two switches are for a limit switch function to indicate the driveline positions which are the near full-down with the control rod in the core, and withdrawn for refueling with the control rod disconnected from the driveline. These two cam actuated indicator switches will operate indicator lights on the control room operator panel showing the two driveline positions, and function in the control logic circuit to automatically stop the drive motor at the stroke end points.

The other two cam actuated indicator switches are used to check the function of the absolute encoder. The two switches are mounted just below the operational withdrawn (top) position. The encoder function is checked as the carriage actuates these two switches. This initiates a comparison of the encoder reading against calibrated values.

4.2.3.5.2.3 Scram Latch Indication System

The latch design provides a mechanical feature that contacts the top end of the control rod coupling head over a range of positions on either side of the latched position. The motion of the coupling head is transmitted to the SCRDM by a sensing tube within the driveline. An LVDT (linear variable differential

transformer) attached to the upper end of the sensing tube provides an indication of the location of the control rod coupling head with respect to the latch. This indication is used for the coupling operation wherein the coupling head is first sensed as the driveline approaches, and shows when the driveline is in the correct position for actuating the latch gripper. When the coupling is completed, the sensing tube provides continuous indication that the control rod is connected to the driveline and therefore, serves an important safety-related function.

The tension rod that couples the scram latch at the driveline bottom end to the pneumatic actuator within the SCRDM, has its position indicated by a linear variable differential transformer (LVDT) located in the SCRDM. With pneumatic pressure (argon) applied to the pneumatic actuator, the tension rod pulls on the latch gripper to retain the control rod coupling head within the latch. The position of the tension rod provides the indication that the latch gripper is in the state that holds the control rod. This indication, coupled with the sensing tube indication that shows when the control rod coupling head is within the latch, assures the control rod is known to be properly latched to the driveline.

4.2.3.5.2.4 SCRDM Pressure and Leakage Monitoring

The SCRS utilizes three different argon pressure levels. The lowest pressure, approximately 5 psig above the reactor cover gas pressure, fills the SCRDM housing and provides a low pressure differential across the main driveline bellows to assure leakage into the reactor if a leak should develop. The mid-pressure, approximately 65 psig, internally pressurizes the driveline to assure a latch bellows leak will not permit liquid sodium to rise inside the driveline if a bellows leak should occur. The highest pressure, approximately 220 psig, is supplied to the pneumatic actuator to keep the scram latch energized. Each of these pressures is static once equilibrium is reached and the pressures are monitored in the SCRS equipment room. The system will include a leak detection capability for each pressure zone to warn of any bellows failure or other possible leak.

4.2.3.5.2.5 SCRDM Thermocouples

The temperature within the SCRDM is measured by thermocouples located on the motor housing, at mid-elevation near the pneumatic actuator valve, and near the bottom of the SCRDM housing.

4.2.3.5.2.6 Acoustic Monitor

An acoustic monitor (accelerometer), will measure scram times to obtain comparative surveillance data through the drive lifetime. The impact of the control rod meeting the control assembly downstop will produce vibrations that would be sensed. This has been verified by prototype testing.

REFERENCES

- *1. See references 59 and 75.
 2. C. E. Johnson, "Fission-Product Redistribution and Cladding Interaction", in "Reactor Development Program Progress Report, July, 1973", ANL-RDP-18, August 1973, p. 5.1.
 3. M. G. Chasanov, C. E. Johnson, P. E. Blackburn, and others, "Chemical Engineering Division Fuels and Materials Chemistry Semiannual Report, July-December, 1972", ANL-7977, April, 1973.
 4. I. Johnson, "Fission-Product Redistribution and Cladding Interaction", in "Reactor Development Program Progress Report, January, 1974", ANL-RDP-24, February, 1974, p. 5.2.
 5. E. A. Aitken, S. K. Evans, G. F. Melde, and others, "Reactions of Sodium with Mixed-Oxide Fuels", in Proceedings of the Conference on Fast Reactor Fuel Element Technology, pp. 459-478, American Nuclear Society, 1971.
 - *6. R. E. Murata, C. N. Craig, H. C. Pfefferlen, and others, "Effect of Stoichiometry on the Behavior of Mixed-Oxide Fuel During Extended Operation in Failed Pins", GEAP-13730, July, 1971.
 7. P. E. Bohaboy, C. N. Craig, G. L. Stimmel, "Performance of Failed Plutonium-Uranium Oxide Fuel Elements in Flowing Sodium", Trans. of the Amer. Nucl. Soc. 15, p. 196 (1972).
 8. D. E. Plumlee, P. E. Novak, "(Pu, U) O₂-Sodium Reactions: Effect of Fuel Parameters", GEAP-13729, September, 1971.
 9. R. T. Pepper, J. R. Stubbles, and C. R. Tottle, "The Constitution of the Sodium-Rich Region of the Sodium-Uranium-Oxygen System", Appl. Mater. Res. 3, pp. 203-207 (1964).
 10. E. A. Aitken, "Thermodynamic Analysis of Possible Chemical Interactions in the System: UO₂-PuO₂ Fuel-Sodium-Stainless Steel", GEAP-5683, July, 1968.
 11. T. Lauritzen, "Compatibility of Urania-Plutonia Fuels with Stainless Steel and Sodium", GEAP-5633, June, 1968.
 12. "Reactor Development Program Progress Report, February, 1971", ANL-7783, March, 1971.
 13. P. A. G. O'Hare, W. A. Shinn, F. C. Mrazek, and others, "Thermodynamic Investigation of Trisodium Uranium (V) Oxide (Na₃UO₄). 1. Preparation and Enthalpy of Formation", J. Chem. Thermodyn. 4, pp. 401-409 (1972).
- * References annotated with an asterisk support conclusions in the Section. Other references are provided as background information.

REFERENCES (Continued)

14. P. E. Blackburn, A. E. Martin, J. E. Battles, and others, "Sodium-Fuel Interactions," in Proceedings of the Conference on Fast Reactor Fuel Element Technology, pp. 479-493, American Nuclear Society, Hinsdale, Ill. (1971).
15. P. E. Blackburn, C. E. Johnson, I. Johnson, and others, "Chemical Engineering Division Fuels and Materials Chemistry Semiannual Report, July-December, 1971," ANL-7877, April, 1972.
16. M. G. Chasanov, C. E. Johnson, J. E. Battles, and others, "Chemical Engineering Division, Fuels and Materials Chemistry Semiannual Report, January-June, 1972," ANL-7922, October, 1972.
17. M. G. Chasanov, C. E. Johnson, P. E. Blackburn, and others, "Chemical Engineering Division Fuels and Materials Chemistry Semiannual Report, July-December, 1972," ANL-7977, April, 1973.
18. P. E. Blackburn, C. E. Johnson, J. E. Battles, and others, "Chemical Engineering Division Fuels and Materials Chemistry Semiannual Report, January-June, 1971," ANL-7822, September, 1971.
19. T. L. Markin and E. J. McIver, "Thermodynamic and Phase Studies for Plutonium and Uranium-Plutonium Oxides with Application to Compatibility Calculations," in Plutonium 1965, pp. 845-857, The Institute of Metals, London, 1967.
20. N. A. Javed and J. T. A. Roberts, "Thermodynamic and Defect-Structure Studies in Mixed-Oxide Fuels," ANL-7901, February, 1972.
21. R. E. Woodley, "Equilibrium Oxygen Potential Composition Relationships in $U_{0.75}Pu_{0.25}O_{2-x}$," HEDL-SA-269, 1970.
22. M. H. Rand and T. L. Markin, "Some Thermodynamic Aspects of (U, Pu) O_2 Sodium Solutions and Their Use as Nuclear Fuels," in Thermodynamics of Nuclear Materials, 1967, pp. 637-650, International Atomic Energy Agency, Vienna, 1968.
23. M. G. Chasanov, C. E. Johnson, N. D. Dudey, and others, "Chemical Engineering Division Fuels and Materials Chemistry Semiannual Report, January-June, 1973," ANL-8022, December, 1973.
24. M. Housseau, J. F. Marin, F. Anselin, and others, "Etude Des Reactions Entre Le Combustible (U, Pu) O_2 Et Le Sodium" in Fuel and Fuel Elements for Fast Reactors, Vol. 1, pp. 277-291, International Atomic Energy Agency, Vienna, 1974.
25. D. L. Smith, "Oxygen Interactions Between Sodium and Uranium-Plutonium Oxide Fuel," Nucl. Technol. 20, pp. 190-199, December, 1973.

REFERENCES (Continued)

26. K. E. Gregoire, P. E. Novak, R. E. Murata, "Failed Fuel Performance in Naturally Convecting Liquid Metal Coolant", GEAP-13620, June, 1970.
27. K. Q. Bagley, E. Edmonds, H. J. Powell, and others, "Fuel Element Behavior Under Irradiation in DFR", in Fuel and Fuel Elements for Fast Reactors, Vol.1, pp. 87-100, International Atomic Energy Agency, Vienna, 1974.
28. V. R. Marian and J. V. Marron, "Core Restraint System Tests and Analysis, Phase I: Planar Externally Clamped Core", GEAP-10798, March, 1973.
29. "Oxide Fuel Element Development Quarterly Progress Report for Period Ending June 30, 1974", WARD-OX-3045-14, September, 1974. (Availability: USAEC Technical Information Center).
- 29a. HEDL-TME-73-46, "Flow Induced Vibration Tests of a Prototypic FFTF Control Rod Absorber Pin Bundle Assembly", June 1973.
30. Deleted
31. C. R. Brinkman and G. E. Korth, "Strain Fatigue and Tensile Behavior of Inconel 718 from Room Temperature to 650°C", ANCR-1125, August, 1973.
32. "AEC Fuels and Materials Development Progress Report No. 79", GEMP-1013, June, 1969.
33. Rules for Construction of Nuclear Power Plant Components, ASME Boiler and Pressure Vessel Code, Section III, The American Society of Mechanical Engineers, New York, 1971.
34. R. T. Collins, G. W. Smith, and E. E. Spier, "Manual for Structural Stability Analysis of Sandwich Plates and Shells", NASA-CR-1457, December, 1969.
35. P. Seide, "A Survey of Buckling Theory and Experiment for Circular Conical Shells of Constant Thickness", in Pressure Vessels and Piping: Design and Analysis, Vol. 1, pp. 590-615, The American Society of Mechanical Engineers, New York, 1972.
36. G. Gerard, Introduction to Structural Stability Theory, McGraw-Hill, New York, 1962.
37. V. I. Weingarten and P. Seide, "Buckling of Thin-Walled Truncated Cones", NASA-SP-8019, September, 1968.

16

57

REFERENCES (Continued)

38. J. L. Houtman, "Inelastic Strains from Thermal Shock", Mach. Des 46, pp. 191-194 (1974).
39. J. M. Creer, J. A. Watt, and J. M. Yatabe, "Thermal Mixing in FFTF Secondary Piping Tees", HEDL-TME-73-21, January, 1973.

REFERENCES (Continued)

40. R. N. Johnson, "A Status Report on Friction, Wear, and Self-Welding Program in Support of FFTF Components", HEDL-TME-72-82, Rev. 1 (Availability: USAEC Technical Information Center).
41. "FFTF CRDM Design Report", Royal Industries, Santa Ana, Calif., Royal Industries Report 128 X900, April, 1972.
- *42. "LMFBR Alternate Shutdown System Development and Testing, Eighth Quarterly Report, October-December, 1973", GEAP-13824-8, January 1974.
- *43. "LMFBR Alternate Shutdown System Development and Testing, Ninth Quarterly Report, January-March, 1974", GEAP-13824-9, April, 1974.
- *44. "A Compilation of Boron Carbide Design Support Data for LMFBR Control Elements", HEDL-TME-75-19, March 15, 1975. (Availability: USAEC Technical Information Center).
- 44a. ANS Transactions, Volume 26, 1977.
- *45. "LMFBR Alternate Shutdown System Development and Testing, Sixth Quarterly Report, April-June, 1973", GEAP-13824-6, July, 1973.
- *46. "LMFBR Alternate Shutdown System Development and Testing Seventh Quarterly Report, July-September, 1973", GEAP-13824-7, October, 1973.
- *47. "LMFBR Alternate Shutdown System Development and Testing, Fifth Quarterly Report, January-March, 1973", GEAP-13824-5, April, 1973.
48. W. E. Ruther, H. A. Taylor, "Compatibility of Chromium Plating with EBR-II Coolant", ANL-8011, April, 1973.
49. J. Y. Chang, P. N. Flagella, S. L. Schrock, "Self-Welding Evaluation for A286 and Type 304 Stainless Steel in Flowing Sodium at 800 F", WARD-NA-3045-5, September, 1973.
50. C. Bagnall, D. C. Jacobs, "Relationships for Corrosion of Type 316 Stainless Steel in Liquid Sodium", WARD-NA-3045-23, 1975.
51. "Sodium Technology Program Quarterly Progress Report for Period Ending January 31, 1974", WARD-NA-3045-9, April, 1974.
52. W. E. Ruther, T. D. Claar, S. Greenberg, R. V. Strain, "Materials-Coolant Interactions in EBR-II", ANL-7670, March, 1970.
53. "Fuel Pin Transient Behavior Technology Applied to Safety Analyses", HEDL-SA-771, November, 1974.

* References annotated with an asterisk support conclusions in the Section. Other references are provided as background information.

REFERENCES (Continued)

54. "Microstructural Dependence of Failure Threshold in Mixed Oxide LMFBR Fuel Pins", HEDL-TME 75-9, October, 1974.
55. "Mechanical Properties During Simulated Overpower Transients of Fast Reactor Cladding Irradiated from 700-1000^oF", HEDL-TME 75-28, June, 1975.
- 57 | 56. "Base Technology FSAR Support Document-Prefailure Transient and Failure Threshold Behavior", HEDL-TME 75-47, November, 1975.
57. "Evaluation of FFTF Fuel Pin Transient Design Procedures", HEDL-TME 75-40, August, 1975. (See also reference 173.)
- 57 | *58. D. C. Jacobs, "The Development and Application of a Cumulative Mechanical Damage Function for Fuel-Pin Failure Analysis in LMFBR Systems", CRBRP-ARD-0115, August 1976.
- *59. R. Sim, A. Veca, "FFTF Fuel Pin Final Design Support Document", Westinghouse Advanced Reactors Division Internal Memorandum, FCF-213, December, 1971. p. 2.1 and 2.2.
- *60. R. D. Coffield, P. L. Wattelet, "An Analytical Evaluation of Fuel Failure Propagation for the Fast Flux Test Facility", WARD-2171-11, December, 1970.
61. W. H. McCarthy, K. J. Perry, G. R. Hull, J. W. Bennett, "Examination of F3A Series Unencapsulated Mixed-Oxide Fuel Pins Irradiated in EBR-II", Nuclear Technology, 16, pp 171-186 (1972).
62. B. F. Rubin et. al., "Fuel-Cladding Mechanical Interaction in LMFBR Fuel Rods", Nuclear Technology 16, pp 89-99 (1972).
63. R. F. Hilbert, E. A. Aitken, P. R. Pluta, "High Burnup Performance of LMFBR Fuel Rods - Recent GE Experience", Transactions of the American Nuclear Society 20, pp 315-318 (1975).
64. R. G. Sims, S. Vaidyanathan, "Cladding Loading Sensitivity for LMFBR Fuel Rods", GEAP-13969, January, 1974.
65. G. E. Culley, J. E. Hanson, W. L. Partain, J. H. Scott, A. E. Walter, "Fast Reactor Safety Implications of Recent Assessments of Fuel Pin Transient Behavior", Proceedings of International Conference, Engineering of Fast Reactors for Safe and Reliable Operation, II pp. 626-641, Gesellschaft Fur Kernforschung M.B.H., Karlsruhe, 1973. (CONF-72-1006).

51 | * References annotated with an asterisk support conclusions in the Section. Other references are provided as background information.

REFERENCES (Continued)

66. S. Chen, "Vibrations of Nuclear Fuel Bundles", Nuclear Engineering and Design 35, pp 399-422 (1975).
67. K. G. Eickhoff, C. Betts, F. E. Buckley, C. E. Yliffe, G. McAreavey, J. O. Poinder, H. Hughes, D. White, "Theoretical and Experimental Studies Supporting the Design of Fast Reactor Fuel Elements", Proceedings of a Symposium on Fuel and Fuel Elements for Fast Reactors I, pp 329-349, International Atomic Energy Agency, Vienna, 1974.
68. J. Van Miegroet, D. Dewaldelcer, A. Michel, K. Kummerer, G. Van Massenhove, "Design and Preparation of the MOL-78 Irradiation Experiment", Proceedings of a Symposium on Fuel and Fuel Elements for Fast Reactors I, pp 163-183, International Atomic Energy Agency, Vienna, 1974.

51

REFERENCES (Continued)

69. J.P. Mairion, J.C. Cauvin, P. Cheneloault, R. Delmas, A. Lhermenier, "Irradiation D'Une Aiguille Rompue Dans un Circuit de Sodium (Irradiation of a Broken Fuel Pin in a Sodium Circuit)", Proceedings of a Symposium on Fuel and Fuel Elements for Fast Reactors I, pp 261-275, International Atomic Energy Agency, Vienna, 1974. 12
70. HEDL-TME 71-114, "CCTL Mark II Subassembly Shipping Procedure, Testing and Shipping Report", August, 1971.
71. HEDL-TME 74-8, UC-79a, b, h, "CCTL Mark II and II-A Final Examination", February, 1974.
72. Claudson, T.T., "Effects of Neutron Irradiation on the Elevated Temperature Mechanical Properties of Nickel-Base and Refractory Alloys", "The Effects of Radiation on Structural Materials", ASTM STP 426, American Society for Testing and Materials, 1967.
73. Claudson, T.T., and Pessl, H.J., "Irradiation Effects on High-Temperature Reactor Structural Metals", Flow and Fracture of Metals and Alloys in Nuclear Environments", ASTM STP 380, American Society for Testing and Materials, 1965. 14
74. Strandring, J., Bell, T.P., Tickle, H. and Glendinning, A., "Effects of Neutron Irradiation on Creep-Rupture Properties of Type 316 Stainless Steel Tubes", Irradiation Effects in Structural Alloys for Thermal and Fast Reactors ASTM STP 457, American Society for Testing Materials, 1969, pp. 414-428.
75. Jackson, R.J., "Evaluation of FFTF Fuel Pin Design Procedure Vis-a-Vis Steady State Irradiation Performance in EBR-II", Addendum to HEDL-TME-75-48.
76. Bowen, P. H., Adhesive Wear (Galling) of Materials in Liquid Sodium, Report 70-1B5 - NAWAR-RT, Westinghouse Research Laboratories, May, 1970.
77. Kleefeldt, K., Investigation of Wear and Friction Between Fuel Rod Bundles and Spacer Grids in Sodium, Report KNK-1290, Karlsruhe Nuclear Center, October, 1970. (EURFNR-854)
78. Liquid Metal Engineering Center, Annual Technical Progress Report, January - December, 1972, LMEC-73-1, February 28, 1973, pp. 1-138 to 1-144. 15

REFERENCES (Continued)

References

79. LMEC-70-10, "Friction and Wear Screening Tests of Materials in Sodium", (July, 1970), pp. 63, 67, 70, 71, 122 to 127, 134, 139 to 141.
80. LMEC-70-13, "Liquid Metal Engineering Center (LMEC) Semi-annual Technical Progress Report January - June, 1970", (September, 1970, pp. 111).
81. LMEC-72-1, "Liquid Metal Engineering Center (LMEC) Annual Technical Progress Report January - December, 1971" (March, 1972), pp. 1-94 to 1-97, 1-100 to 1-119, 1-123.
82. LMEC-73-1, "Liquid Metal Engineering Center (LMEC) Annual Technical Progress Report, January - December, 1972", pp. 1-156 to 1-165, 1-170 to 1-172.
83. LMEC-74-1, "Liquid Metal Engineering Center (LMEC) Annual Technical Progress Report, January - December, 1973", pp. 1-112 to 1-138, 1-140 to 1-150.
84. LMEC-75-1, "Liquid Metal Engineering Center (LMEC) Annual Technical Progress Report, January - December, 1974", pp. 1-126, 1-128 to 1-134, 1-144, 1-147 to 1-150.
85. WARD-NA-3045-13, "Friction and Wear Testing in Support of FFTF Components. Interim Summary Report, August 1974", pp. 34, 38, 39, 43, 44, 47 to 50, 53, 58, 60 and Appendices A and B.
86. WARD-NA-3-45-16, "Sodium Technology Program Friction, Wear and Self-Welding Quarterly Progress Report for Period Ending July 31, 1974", pp. 2-7 to 2-9, 2-16 to 2-20, 2-27 to 2-30.
87. WARD-NA-3045-19, "Sodium Technology Program Friction, Wear, and Self-Welding Quarterly Progress Report for Period Ending October 31, 1974", pp. 2-9, 2-15, 2-16.
88. WARD-NA-3045-24, "Sodium Technology Program Friction, Wear, and Self-Welding Quarterly Progress Report for Period Ending January 31, 1975", p. 2-7.
89. WARD-NA-3045-27, "Sodium Technology Program Friction, Wear, and Self-Welding Quarterly Progress Report for Period Ending April 30, 1975", pp. 2-9 to 2-11, 2-13, 2-24, 2-27 to 2-28, 2-30 to 2-32, 2-37, 2-40.
90. AI-AEC-3037, "Annual Technical Progress Report, Sodium Technology and Cover Gas Seal Development Programs GFY 1972", pp. 64 to 70, 74 to 80.

REFERENCES (Continued)

91. AI-AEC-13110, "Annual Technical Progress Report, Sodium Technology and Cover Gas Seal Development Programs, GFY 1973", pp. 83 to 85, 87, 93, 94, 101 to 104, 111 to 114, 121 to 123.
92. AI-AEC-13132, "Annual Technical Progress Report, Sodium Technology and Cover Gas Seal Development Program, GFY 1974", pp. 57, 60, 67, 73, 75, 80.
93. AI-AEC-13143, "Quarterly Technical Progress Report, Sodium Technology and Cover Gas Seal Development Programs, October - December, 1974", pp. 71, 74, 75, 86, 88.
94. AI-ERDA-13147, "Quarterly Technical Progress Report, Sodium Technology and Cover Gas Seal Development Programs, January - March, 1975, pp. 51 to 55, 65, 70, 71.
95. B. F. Langer, "Applied Mechanics in the Nuclear Industry: Applications of Stress Analysis", Westinghouse Scientific Paper 67-1D0-CODES-P1, Spetember 25, 1967.
96. Den Hartog, Advanced Strength of Materials, McGraw-Hill, New York, 1975 p. 75.
97. P. Weimar and H. Sebening, "The Design, Irradiation and Post-Irradiation Examination of UO_2/PuO_2 Fuel Pins Irradiated in Experiment Mol 8B," EURFNR-1245, January 1975.
98. H. Zimmermann, "Fission Gas Behavior in Oxide Fuel Elements for Fast Breeder Reactors," EURFNR-1228, October 1974.
99. A. W. Longest, et al. "Gas Cooled Reactor and Thorium Utilization Programs," ORNL 4760, pp. 149-163, January 1973.
100. A. W. Longest, et al, "Gas Cooled Reactor and Thorium Utilization Programs," ORNL 4911, pp. 213-215, March 1974.
101. HEDL-TME-75-48, "HEDL Steady State Irradiation Testing Program" Status Report through February 1975, December 1975.
102. N.V. Krasnoyarov, "Investigation of the BOR 60 Reactor Fuel and Absorbing Elements", BNES Conference on Fast Reactor Power Stations, London, England, March 11-14, 1974, pp. 319-324.
103. V.M. Grayzev, et al., "Five Years of Nuclear Power Plant Operation of the BOR-60", US/USSR Seminar on Fast Breeder Reactor Construction and Operating Experience, Obninsk, USSR, June 2-5, 1975, pp. 36-147.

15

16

20

REFERENCES (Continued)

104. A Feduska, S. Orbon, S. L. Schrock and S. A. Shiels, "Interstitial Transfer Program Impact Assessment Report - Part I, Application of Data to FFTF Components, Topical Report", WARD-NA-3045-3, August, 1973.
105. P. Soo and W. H. Horton, "The Effect of Carbon and Nitrogen on the Short-Term Tensile Behavior of Solution-Treated Type 304 Stainless Steels", Topical Report, WARD-NA-3045-2, July, 1973.
106. See Reference 153.
107. M. Kangilaski, J. S. Perrin and R. A. Wullaert, "Response of Different Microstructures to Irradiation-Induced Embrittlement at Elevated Temperatures", Quarterly Progress Report - Irradiation Effects On Reactor Structural Materials, August, September, and October, 1969, BNML-1268, December, 1969, p. 5-27.
108. D. Fahr, "Analysis of Stress-Strain Behavior of Unirradiated Type 316 Stainless Steel", Fuels and Materials Quarterly Progress Report for Period Ending December 31, 1971, ORNL-TM-3703, March, 1972, p. 96.
109. P. Patriarcha, A. L. Lotts and C. M. Cox, "LMFBR Fuel Element Design and Model Development", Fuels and Materials Development Program Quarterly Progress Report for Period Ending June 30, 1970, ORNL-46001, November, 1970, p. 65.
110. P. Rodriguez, "High-Temperature Creep Behavior of Type 304 Stainless Steel in Argon-Oxygen Environments of Different Oxygen Partial Pressures", ORNL-TM-1124, May 5, 1965.
111. D. S. Wood, M. Farrow and W. T. Burke, "A Preliminary Study of Helium Environment on the Creep and Rupture Behavior of Type 316 Stainless Steel and Incoloy 800", in Effects of Environment on Material Properties in Nuclear Systems, The British Nuclear Society, London, 1971, p. 213.
112. D. S. Wood, M. Farrow, A. B. Baldwin and W. T. Burke, "Creep Rupture Properties of Some High Temperature Reactor Circuit Materials in Helium", TRG Report 2411 (R), April, 1973, to be published in Proceedings of Int'l. Conference on Creep & Fatigue in Elevated Temp. Applications, Sept., 1973, Philadelphia.
113. L. H. Kirschler, R. H. Hiltz and S. J. Rogers, Final Report on the Effect of High Temperature Sodium on the Mechanical Properties of Candidate Alloys for the LMFBR Program, MSAR 70-76, May, 1970.
114. W. F. Simmons and J. A. Van Echo, Report on the Evaluated Temperature Properties of Stainless Steels, ASTM Data Series Publication, #DS 5-S1, 1965.

115. F.C. Monkman, P.E. Price and M.J. Grant, "The Effect of Composition and Structure on the Creep Rupture Properties of 18-8 Stainless Steels", 48, 418 (1956).
116. J.K.Y. Hum and N.J. Grant, "Austenite Stability and Creep-Rupture Properties of 18-8 Stainless Steels", Trans. ASM, 45, 105 (1963).
117. E.E. Bloom and J.O. Stiegler, "The Effect of Fast Neutron Irradiation on the Creep-Rupture Properties of Type 304 Stainless Steel at 600°F", Irradiation Effects on Structural Alloys for Nuclear Reactor Applications, ASTM Special Tech. Publication, #STP 484, 1970, p. 451.
118. P.D. Goodell, T.M. Collen and J.W. Freeman, "The Influence of Nitrogen and Certain Other Elements on the Creep-Rupture Properties of Wholly Austenitic Type 304 Stainless Steel", Trans. ASME, 89, 517 (1967).
119. P.C.L. Pfeil and D.R. Harries, "Effects of Irradiation in Austenitic Steels and Other High-Temperature Alloys", Flow and Fracture of Metals and Alloys in Nuclear Environments, ASTM Special Tech. Publication, #STP 380, 1965, p. 202.
120. A.J. Lovell and R.W. Barker, "Uniaxial and Biaxial Creep Rupture of Type 316 Stainless Steel After Fast Reactor Irradiation", Irradiation Effects on Structural Alloys for Nuclear Reactor Applications, ASTM Special Tech. Publication, #STP 484, 1970, p. 468.
121. P.G. Stone, "The Effect of Carbon, Nitrogen and Boron on Elevated Temperature Properties", High-Temperature Properties of Steel, British Iron and Steel Assoc., 1966, p. 33.
122. R.W. Swindeman and R.D. Waddell, "Mechanical Properties of Type 304 Stainless Steel", Fuels and Materials Development Program Quarterly Progress Report for Period Ending September 30, 1971, ORNL-TM-3550, December, 1971, p. 175.
123. Steels for Elevated Temperature Service, 1965 Edition, U.S. Steel Corporation.
124. J.M. Beeston and C.R. Brinkman, "Axial Fatigue of Irradiated Stainless Steels Tested at Elevated Temperatures", Irradiation Effects on Structural Alloys for Nuclear Reactor Applications, ASTM Special Tech. Public. STP 484, 1971, p. 419.
125. J.T. Berling and T. Slot, "Effect of Temperature and Strain Rate on the Low Cycle Fatigue Resistance of AISI 304, 316 and 348 Stainless Steels", GEMP-642, not dated.
126. D.L. Keller, Progress on LMFBR Cladding, Structural, and Component Materials During July, 1971, Through June, 1973, BMI-1928, July, 1972.

127. K. Kanazawa and S. Yoshida, "Effect of Temperature and Strain Rate on the High Temperature, Low Cycle Fatigue Behavior of Austenitic Stainless Steels", International Conference on Creep and Fatigue in Elevated Temperature Applications, Inst. Mech. Engrs., 1973, p. 226-1.
128. R.C. Andrews and L.M. Kirschler, "Design Properties of One Heat of 2½ Cr-1 Mo Steel and 316 Stainless Steel in High Temperature Air, Helium and Sodium Environments." MSA Research Corp. Topical Report No. 7. September, 1966.
129. AEC Fuels and Materials Development Program, GEMP-1004, March 1968.
130. R.A.T. Dawson, W.J. Elder, G.J. Hill and A.T. Price, "High-Strain Fatigue of Austenitic Steels", Thermal and High-Strain Fatigue, Inst. of Metals Monograph No. 32, 1967, p. 239.
131. S.S. Manson, "Avoidance, Control and Repair of Fatigue Damage", in Metal Fatigue Damage, ASTM Special Tech. Public. STP 495, 1971, p. 254.
132. T. Udoguchi, Y. Asada and I Ichino, "A Frequency Interpretation of Hold-Time Experiments on High-Temperature Low-Cycle Fatigue of Steels for LMFBR", International Conference on Creep and Fatigue in Elevated Temperature Applications, Inst. Mech. Engrs., 1973, p. 211.1.
133. L.A. James and R.L. Knecht, "Structural Crack Growth", Quarterly Progress Report - Irradiation Effects on Reactor Structural Materials, May, June, July, 1973, HEDL-TME 73-67, September, 1973, p. HEDL-54.
134. R.B. Snyder, K. Nateson and T.F. Kassner, "A Generalized Method of Computing Carbon - Diffusion Profiles in Austenitic Stainless Steels Exposed to a Sodium Environment", ANL-8015, June, 1973.
135. C.R. Brinkman and G.E. Korth, "Heat-to-Heat Variations in the Fatigue and Creep-Fatigue Behavior of AISI Type 304 Stainless Steel at 593°C", J. of Nuc. Mat., 48, 293 (1973).

25

136. WARD-NA-3045-7, "Sodium Technology Program Quarterly Progress Report for Period Ending October 13, 1973," (January 1974).
137. WARD-NA-3045-19, "Sodium Technology Program Friction, Wear and Self-Welding Quarterly Progress Report for Period Ending October 31, 1974," (February 1975).
138. WARD-NA-3045, "Friction and Wear Testing in Support of FFTF Components Interim Summary Report August 1974", by W. L. Wilson, B. MINushkin, G. Chelen (November 1974).
139. K. Bendorf, "Experimental Investigations of Self-Welding of Structural Materials Under Sodium", Nuclear Engineering and Design 14, pp. 83-98 (1970).
140. W.C. Clarke, Jr., "A Study of Embrittlement of a Precipitation Hardening Stainless Steel and Some Related Materials", Trans. AIME, 245, 1969, p. 2135.
141. M.H. Jones, et. al, "Effects of Variation on Normalizing and Tempering Procedure on Stress Rupture Strength, Creep Embrittlement and Notch Sensitivity for a CR - Mo - V and a 17 CR - 4 Ni - Cu Steel", Trans ASM, 47, 1955, p. 926.
142. Armco 17-4 PH Precipitation-Hardening Stainless Steel Sheets and Strip, Product Data Bulletin S-9A, Armco Steel Corporation, Middletown, Ohio, 1966.
143. P.W. Johnson, Jr., "Stainless, Bar and Wire, 17-4 PH-Effect of Exposure at 500/800°F on Mechanical Properties", Armco Steel Co. Report No. 1, June 11, 1969.
144. P.W. Johnson, Jr., "Stainless, Bar and Wire, 17-4 PH-Effect on Expansion at 500/800°F for Mechanical Properties", Armco Steel Co. Report No. 2, June 19, 1970.
145. FFTF Primary CRDM/CRD Environmental Life Test.
146. Foster, K. W. and Kurzeka, W. J., "Control Rod for a 500-MWe Sodium Cooled Fast Breeder Reactor," ASME Paper 72-WA/NE-2, November 1972.
147. LMEC 70-1 and LMEC 71-7
Liquid Metal Engineering Center Semiannual Technical Progress Report.
148. "Design Handbook, Springs Custom Metal Parts", Associated Spring Corporation, Bristol, Conn., 1970.
149. Wahl, A. M., Mechanical Springs, 2nd Edition, McGraw-Hill, Handbook, 1963.

150. E.A. Whitlow and E. Berkey, "Microstructural and Compositional Changes in Sodium-Exposed Stainless Steel by Scanning Electron Microscopy", in Chemical Aspects of Corrosion and Mass Transfer in Liquid Sodium, S. Jansson (Edit.), AIME, 1973, p. 65.
151. K. Goldmann, M. Kolodney, W. Arbiter and G. Stern, "Some Fundamental Aspects of Carburization and Decarburization of Chromium Steels in Sodium Systems, in Chemical Aspects of Corrosion and Mass Transfer in Liquid Sodium, S. Jansson (Edit.), AIME, 1973, p. 177.
152. J.T. Barnby and F.M. Peace, "The Effect of Carbides on the High-Strain Fatigue Resistance of an Austenitic Steel" Acta Met., 19, 1351 (1971).
153. TID-26666, "Nuclear Systems Materials Handbook", Volume 1, Section 5, Property Code 2206 (F-1), Hanford Engineering Development Laboratory, 1974.
154. GEAP-14031-1, Core Restraint Engineering, August-October, 1974 First Quarterly Report, General Electric Fast Breeder Reactor Department, November 1974.
155. GEAP-14031-3, Core Restraint Engineering, February-April 1975 Third Quarterly Report, General Electric Fast Breeder Reactor Department, June, 1975.
156. GEAP-14031-4, Core Restraint Engineering, May-July 1975 Fourth Quarterly Report, General Electric Fast Breeder Reactor Department, August 1975.
157. GEAP-13986, Core Restraint System Tests and Analysis, Phase III Planar Externally Clamped Large Core, General Electric Fast Breeder Reactor Department, December 1973.
158. Olson, N.C., C.M. Walter and W.N. Beck, "Statistical and Metallurgical Analyses of Experimental MARK-1A Driver Fuel Element Cladding Failures in the Experimental Breeder Reactor II", Nuclear Technology (28) p. 134-151, January, 1976.
159. Haguard, B.R., "Reference Core and Structural Materials Monthly Status Letter, July, 1976", Document TC-575-7, Hanford Engineering Development Laboratory.
- 44 | 160. R. A. Karnesky et. al., "Cesium Migration in Mixed Oxide Fuel Pins", ANS Transactions 22, p. 229, 1975.
161. I. Johnson and E. C. Johnson, "Cesium Interaction with Irradiated Oxide Fuel Pins", ANS Transactions 17, p. 194-195, 1973.
162. Reference Fuel Steady-State Irradiation Program Plan, TC-573, Revision 1, Hanford Engineering Development Laboratory, March, 1976.

25

29

REFERENCES (Continued)

163. WARD-D-0149, E. C. Schwegler, "Wire Wrap Cladding Interactions in LMFBR Fuel Rods", Submitted to NRC October, 1976.
164. See #162.
165. R. N. Johnson, et.al., "Development of Low Friction Materials for LMFBR Components", Int. Conf. Liquid Metal Technology in Energy Production, Seven Springs, Champion, PA, May 3-6, 1976.
166. R. B. Richman, O. S. Fiskum, "Full Scale Withdrawal Testing of FFTF/LMFBR Fuel Assemblies", Trans. Am. Nuclear Society, 1975 Winter Meeting, Volume 22, Page 222-224.
167. ORNL-4998, Mechanical Properties Test Data for Structural Materials-Quarterly Progress Report to 7/31/74, page 3.
168. "Plan for the National LMFBR Mixed Oxide Fuel Transient Performance Program", March, 1977.
169. W. C. Kinsel, et. al., "FTR Fuel Assembly Vibration Tests", HEDL TME-75-49, August, 1976.
170. W. C. Kinsel, et.al., "Flow-Induced Vibration of Spiral Wire-Draped Fuel Assemblies", ASME Paper 75-WA/HT-76.
171. WARD-D-0204, T. V. Prevenslik, et.al., "CRBRP Fuel Assembly Structural Analysis in Support of the Final Design Review", January, 1978.
172. CRBRP-ARD-0150, E. C. Schwegler, "Fuel Rod Bowing", November 1976.
173. HEDL-TI-75001-122, "FFTF FSAR Supplement 12, Part 2, Response to NRC 9, Set 7", September, 1977.
174. D. V. Nelson et.al., "Development of Structural Design Criteria for Highly Irradiated Core Components", Paper 78-PVP-78, Pressure Vessel and Piping Division of the ASME, June, 1978.
175. M. C. Billone et.al., "LIFE-III Fuel Element Performance Code", ERDA-77-56, July 1977.
176. WARD-D-0166, H. D. Garkish, "Flow Induced Vibration of Fuel Rods in CRBRP - A Status Report", December, 1976.
177. CRBRP-ARD-0190, "Control Assembly Rotational Joint Verification Test Final Report", January, 1979.

178. A. L. Ward and L. D. Blackburn, "Ductility and Strength of FFTF/CRBRP Structural Materials Irradiated in Various Spectra, Interim Report", HEDL-TME-78-51, August 1978. (Availability, USDOE Technical Information Center).
179. A. L. Ward and L. D. Blackburn, "Ductility and Strength of FFTF/CRBRP Structural Materials Irradiated in Various Spectra, Second Interim Report", HEDL-TME-79-19, July, 1979. (Availability, USDOE Technical Information Center).
180. L. D. Blackburn, "Strength and Ductility of Fast Reactors Irradiated Austenitic Stainless Steels", HEDL-TME-79-21, August 1979.
181. TID-26666, "Nuclear Systems Materials Handbook", Volume 1, Property Codes 2206 (E-1) and 3304 (E-1), Hanford Engineering Development Laboratory, 1974.
182. A. Batenburg, H. O. Lagally, R. J. Simko, "Coefficient of Dynamic Friction via Analog Computer Data Reduction", ASLE Paper 80-LC-8B-1, August 1980.
183. T. T. Claudson, "Quarterly Progress Report: Irradiation Effects on Reactor Structural Materials, February - April, 1973, "HEDL-TME-73-74, pp. 53-60, May 1973.
184. KEI-64-80, Letter from D. D. Keiser to C. E. Gilmore, DOE/10, "Preliminary Alloy 718 ASME Code Case Package, "May 6, 1980. (Proprietary DOE)
185. R. A. Leisner, "Effect of Carbon and Nitrogen and Sodium Environment on the Mechanical Properties of Austenitic Stainless Steels", WARD-NA-94000-5, December, 1980.
186. C. R. Brinkman, "Material Data Base Used for Design and Elevated Temperatures for Long Term and Cyclic Loading", CRBRP/NRC Meeting on HTS Materials and Structures, April 6-7, 1982.
187. Huntington Alloys, Inconel Alloy 718 product brochure, 10M 10-73, T39, 1973.
188. L. D. Blackburn, A. L. Ward and D. L. Greenslade, "Ductility and Strength of FFTF/CRBRP Structural Materials Irradiated in Various Spectra, Final Report", HEDL-TME-80-81, December 1980.

*References annotated with an asterisk support conclusions in the section. Other references are provided as background information.

TABLE 4.2-A

Design Procedure for Steady State Creep Analysis

<u>Calculated Parameter</u>	<u>Required Assumptions</u>	<u>Comment</u>
Strain Rate	Thermal Creep Rate for Solution Annealed 316 Stainless Steel	Overpredicts Irradiated 20% CW 316 SS Creep Rate
Temperature	Upper 2 σ Local Hotspot Over Design Life	97.5% of Time Temperature is below this requirement.
	Total Gradient Totally Relaxed by Thermal Creep	Primarily Relaxed by Non-Damaging Irradiation Creep
Fission Gas	Upper 2 σ Limit, Linear by Cycle	Linear Behavior more Conservative than Actual Exponential Increase
Fuel Loading	Worst Prediction Considered	Worst Combination of Irradiation Induced Creep and Swelling and Fabrication Variables
Cladding Wastage	Upper Limit on Tolerance, Wear, Defects, Sodium Corrosion and Fission Product Attack	Approximately 40% of Original Cladding Thickness is Assumed Not Effective at End of Design Life
Stress Limit	Below Proportional Limit	No Plastic Strain Allowed

4.2-331

51

Amend. 51

Sept. 1979

TABLE 4.2-D

OVER-TEMPERATURE TRANSIENT EXPERIMENTS

<u>EBR-II ASSEMBLY</u>	<u>PEAK MWD/KG</u>	<u>ANL LOF TEST*</u>	<u>NO. OF RODS WHICH FAILED BELOW, AT, OR ABOVE DESIGN PREDICTION</u>		
			<u>BELOW</u>	<u>EQUAL</u>	<u>ABOVE</u>
UNIRRADIATED		L2, R3, R4, R5	0	0	18
PNL-11	30.0	L3 (PNL-17)	0	1	11
NUMEC-F	40.0	L4	1	2	34
PNL-10	50.0	NONE	0	0	24

*NOTE: All above design limit.

TABLE 4.2-E

RAPID REACTIVITY INSERTION EXPERIMENTS

DESIGNATION	TYPE TEST	KW/FT	ROD PARAMETERS		SECONDS TO BREACH	
			MWD/KG	% SD.	ACTUAL(1)	DESIGN(2)
H3, PNL 17-24	T \$0.5/S	8.5	31.0	88.9	NF*	NF
HOP 3-2A, p. 23A-27	T \$3.0/S	12.0	21.4	87.3	NF	0.42
HOP 3-2B, p. 23A-30	T \$3.0/S	12.0	44.0	87.3	NF	0.43
H5, PNL-17-25	U \$0.5/S	8.1	29.5	88.6	1.9	1.78
H4, NUM-F-51	U \$0.5/S	10.6	39.5	85.5	0.94	0.62
HUT 5-3A, PNL-10-17	U \$0.5/S	8.1	50.1	85.7	3.2	2.70
HOP 3-3C PNL 17-34	U \$3.0/S	8.0	29.7	88.8	0.80	0.65
EG-NUM-F-56	U \$3.0/S	11.5	42.6	85.5	0.59	0.41

* No Failure

- (1) Experimentally determined time to cladding breach.
 (2) Time to cladding breach calculated from strain limit criteria in Reference 173.

Table 4.2-1

DENSITIES OF COMPOUNDS IN THE U-Na-O SYSTEM

<u>COMPOUND</u>	<u>DENSITY</u> <u>g/cc</u>
UO_2	10.97
$NaUO_3$	7.26
$Na_2U_2O_7$	6.17
Na_2UO_4	5.51/5.73
Na_4UO_5	4.71
Na_3UO_4	5.6

TABLE 4.2-2

CALCULATED AND EXPERIMENTAL ISOTHERMAL OXYGEN CONTENTS
FUEL AND SODIUM FOR FUEL SODIUM REACTION

Temperature		Equilibrium Oxygen Pressure + (atm.)	$-\Delta G(O_2)$	O/M Ratio for $U_{0.8}Pu_{0.2}O_2$		C/M Ratio for $U_{0.75}Pu_{0.25}O_2$	O/M Ratio for UO_2		Oxygen Conc. in Na, * (ppm)
°K	°C			Calc. ††	Measured	Calc. ††	Calc.	Measured	
600	327	2.4×10^{-67}	183	1.92	--	1.90	2.00	--	.007
700	427	7.3×10^{-55}	177	1.93	--	1.913	2.00	--	.114
800	527	2.9×10^{-47}	170	1.94	1.955	1.925	2.00	--	.90
900	627	1.4×10^{-47}	164	1.945	--	1.931	2.00	2.00	4.47
1000	727	3.3×10^{-35}	158	1.95	--	1.938	2.00	2.00	16.12
1100	827	7.8×10^{-30}	151	1.955	1.958	1.944	2.00	2.00	46.00
1200	927	3.5×10^{-27}	145	1.96	1.959	1.950	2.00	2.00	110.50

+ Calculated from equation(6)

†† From Rand & Markins data

* Calculated from equation(3)

4.2-337

Amend. 51
Sept. 1979

TABLE 4.2-4
COMPARISON OF
CRBRP AND FFTF FUEL ASSEMBLY DETAILS

<u>Parameter</u>	<u>CRBRP Value</u>	<u>FFTF Value</u>
Number of low enrichment assemblies	0	28
Number of high enrichment assemblies	156	45
Rods per assembly	217	Same
Rods (total number)	33,852	15,841
Rod outside diameter (in.)	0.230	Same
Rod radial spacing	0.056 inch wire wrapped around fuel rod cladding in clockwise helical spiral with pitch of 11.9 inch	Same
Rod triangular pitch (in.)	0.2877	Same
Clearance between fuel rod assemblies at wires (nominal, in.)	0.0017	Same
Clearance between fuel rods (nominal, in.)	0.0577	Same
Cladding thickness (nominal, in.)	0.015	Same
Cladding thickness (minimum, in.)	0.014	Same
Rod axial support	17 key shaped rails through keyhole slots in bottom end caps	Same
Rod length (in.)	114.40	93.40
Pellet Column Length (in.)	64 including two 14 inch axial blankets	49 including two 5.7 inch Inconel 600 Reflectors

TABLE 4.2-4 (Continued)

<u>Parameter</u>	<u>CRBRP Value</u>	<u>FFTF Value</u>
Fission Gas Plenum Length (in.)	48.0	42.0
Fission Gas Plenum Available Volume-Cold (in. ³)	1.287	1.158
Lower axial blanket length (in.)	14	0.8
Lower axial blanket composition	Depleted uranium dioxide	Same
Core region length (in.)	36	Same
Core Pellet material	Plutonium-uranium dioxide	Same
Core Pellet Diameter (in.)	0.1935	0.1945
Pellet Length (in.)	0.205 to 0.283	Same
Density:		
Nominal (percent of theoretical)	91.3	90.4
Cold smeared (percent of theoretical)	85.5	Same
Plutonium Content:	32.8	19.8 and 24.2
Diametral gap between fuel cladding and fuel pellet (nominal, in.)	0.0065	0.0055
Upper axial blanket length (in.)	14	0.8
Upper axial blanket composition	Depleted uranium dioxide	Same
Axial Blanket Pellet Diameter (in.)	0.1900	Same

51

TABLE 4.2-4 (Continued)

<u>Parameter</u>	<u>CRBRP Value</u>	<u>FFTF Value</u>
Axial Blanket Pellet Length (in.)	0.31 to 0.46	0.4
Nominal density (percent of theoretical)	96.0	95.5
Diametral gap between fuel cladding and axial blanket pellets (nominal, in.)	0.0100	Same
Inlet Nozzle Discrimination Post Max. Dia. (in.)	1.956	1.985
Number of orifice zones	6	3
Number of shield blocks	1	3
Shield block total length (in.)	20.0	21.5
Shield block effective length (in.)	14.7	13.1
Shield block outside hex (in.)	4.695	4.665
Load pad, outside dimension across flats (in.)	4.745	4.715
Duct across flat, dimension (inside, in.)	4.335	Same
Duct wall thickness (in.)	0.120	Same
Load pad thickness (nominal, in.)	0.205	0.190
Fuel rod growth clearance (in.)	2.1	1.00
Outlet nozzle ID (nominal, in.)	3.60	2.80

TABLE 4.2-4 (Continued)

<u>Parameter</u>	<u>CRBRP Value</u>	<u>FFTF Value</u>
Outlet nozzle OD (nominal, in.)	3.90	Same
Misaligned grapple pickup capability	1.75	1.25

TABLE 4.2-5

NOMINAL RADIAL BLANKET ASSEMBLY DESIGN PARAMETERS

Assemblies (number)	126
Blanket Rods per Assembly (number)	61
Number of Flow Orificing Zones	4
Pitch to Diameter Ratio	1.072
Blanket Rod Spacing	Wire-Wrap, 0.033" dia. wire with 4" pitch
Blanket Rod Length, Inch	116.5
Cladding and Duct Material	20 percent cold worked Type 316 Stainless Steel
Rod Outside Diameter, Inch	0.506
Cladding Thickness, Inch	0.015
Fuel Pellet Column, Inch (uranium-dioxide)	64
Pellet Diameter, Inch	0.470
Pellet Length, Inch	0.5 to 1.0 at supplier's option
Pellet Density, % theoretical	95.6
Smear Density, % theoretical	93.2 (dish voids not considered)
Pellet Material	Depleted UO ₂
Diametral Gap between Cladding and Pellet (Initial, cold), Inch	0.006
Distance across Flats on Duct Inside, Inch	4.335
Duct Wall Thickness, Inch	0.120
Number of Radial Blanket Rows	2
Fuel Arrangement	Column of Cylindrical Pellets

TABLE 4.2-5 (Continued)

36	Fission Gas Cold Available Plenum Volume, in. ³	8.12
	Fill Gas	He
	Fill Gas Pressure, atm (at ambient temp.)	1
36	Spacer Material	316 SS - 20% CW
	Assembly Pitch, inch	4.760

| 13

TABLE 4.2-5A

General Plan for Verification of Fuel Design Analysis and Criteria

<u>Activity</u>	<u>Pertinent Tests</u>	<u>Utilization of Results</u>
1. Comparison of FURFAN and FRST with experiments (steady-state)	Reference Steady State Test Program (Reference 162)	FSAR evaluations
2. Comparison of FURFAN and FRST with experiments (transient)	Reference Transient Test Program (Reference 168)	FSAR evaluations
3. Comparison of WRAPUP predictions with experiments (steady-state)	Reference Steady State Test Program (Reference 162)	FSAR evaluations

51
4.2-345

Amend. 51
Sept. 1979

TABLE 4.2-6 DELETED

TABLE 4.2-7

CRBR CORE ASSEMBLY STRUCTURAL INELASTIC CRITERIA AND LIMITS

Type of Failure	Mode	Criteria	Limit
Crack Initiation	Local Ductile Rupture	$F_{DR} = \text{Max of } \left\{ \begin{array}{l} \bullet \frac{(c_{\text{max principal}}) TF}{0.3 \epsilon_f} \\ \bullet \frac{(c_{\text{max principal}}) TF}{\epsilon_u} \end{array} \right\}$ <p>where,</p> <p>ϵ_f = True Min. Fracture Strain ϵ_u = True Min. Uniform Elongation TF = Triaxiality Factor $TF = \frac{\sqrt{2} (\sigma_1 + \sigma_2 + \sigma_3)}{\sqrt{(\sigma_1 - \sigma_2)^2 + (\sigma_2 - \sigma_3)^2 + (\sigma_3 - \sigma_1)^2}}$ $\sigma_1, \sigma_2, \sigma_3$ = Principal Stresses $c_{\text{max principal}}$ = Maximum Principal Strain (Peak + Accumulated)</p>	1
	Creep Fatigue	$F_{CFD} = a/b = \text{Minimum of } \left\{ \begin{array}{l} \bullet \frac{7/3 D^C + D^F}{D^C} \\ \bullet \frac{D^C + 7/3 D^F}{D^F} \end{array} \right\}$ <p>where,</p> <p>D^C = Creep Damage Factor $D^C = \int_{tr} \frac{dt}{tr}$ tr = Rupture Time Based on Equivalent Stress or Max. Positive Principal Stress D^F = Fatigue Damage Factor $D^F = \sum_{NF}^n$ n = No. of Cycles N_f = Allowable No. of Cycles Based on range of equivalent or Max. Principal Strain</p>	1
Excessive Deformation	Peak + Accumulated	$\delta^{P+A} / PADL$ <p>where,</p> <p>$PADL$ = Peak + Accumulated Non-Uniform Deformation Limit, Excluding Irradiation Creep and Swelling</p>	1
	Residual	δ^R / RDL <p>where,</p> <p>RDL = Residual Non-Uniform Deformation Limit, Excluding Irradiation Creep and Swelling</p>	1

TABLE 4.2-8A

SUMMARY OF DESIGN LOADING CONDITIONS FOR FUEL ASSEMBLY STRUCTURAL ANALYSIS

Region or Component	Design Fast Fluence n/cm^2	Steady State Temp. (Inner Surface) $^{\circ}F$	Cross-Duct Temp. Gradient $^{\circ}F$	Inter-Assembly Temp. Gradient $^{\circ}F$	Core Restraint Bending Moment in-lb	Coolant Pressure psi
Shield Block Region	3.15×10^{21}	730	NA*	NA	NA	NA
Mid-Core Region	9.29×10^{22}	895	50	126	30700	31.2
Load Pad Region	3.0×10^{22} **	1084	118	219	48860	1.46
Outlet Nozzle Region	7.12×10^{20}	1116	134	214	NA	NA
Orifice Plate Region	6.61×10^{19}	730	NA	NA	NA	41.6
Rod Attachment Assembly	3.15×10^{21}	730	NA	NA	NA	43.8

* Not Applicable.

** The ACLP material properties for the structural damage calculation were based on a design EOL fast fluence of $3.0 \times 10^{22} n/cm^2$, which is in excess of the maximum fast fluence which actually occurs at this location.

TABLE 4.2-8B

DESIGN SEISMIC AND CORE RESTRAINT LOADS OF THE FUEL ASSEMBLY ACLP

<u>Load*</u> <u>Designation</u>	<u>OBE</u> <u>Load</u> <u>(lbf)</u>	<u>SSE</u> <u>Load</u> <u>(lbf)</u>	<u>Core Restraint</u> <u>Load</u> <u>(lbf)</u>
F ₁	4156	5823	432
F ₂	1184	1658	298
F ₃	3156	4422	298

51 *Load Direction and Points of Application to ACLP are shown in Figure 4.2-33A.

TABLE 4.2-8C

SEISMIC LOADS IN VERTICAL DIRECTION
(LOAD IN POUNDS)

Axial Location	OBE	SSE
Top Load Pad	35	55
Above Core Load Pad	110	170
Shield Block	180	280
Inlet Nozzle	290	460

51

TABLE 4.2-9
TESTING FOR LOAD FOLLOW

Activity Title	Activity Description	Supported Activity
Fuel Rod Ratcheting	Out-of-pile tests to determine cladding creep and stress relaxation due to internal pressure and thermal cycling prototypic of CRBRP load follow conditions	Reload Core Preliminary Design
Fuel Rod Load Follow Testing	Perform in-reactor fuel rod load follow simulation to determine effects of critical design parameters. These tests in conjunction with suitable analyses will establish limits for plant load follow operation. The test program will utilize instrumented assemblies in EBR-II and RAFT capsules in GETR.	Reload Core Fuel Rod Design
Fuel Rod Load Follow Verification	Perform fuel rod load follow simulation in FFTF instrumented open test assemblies to verify adequacy of reload design for plant load follow operation.	Reload Core Fuel Assembly Design Verification
Fuel Bundle - Duct Interaction Tests	Test utilizing prior sodium exposed fuel bundle to determine axial force in compressed duct required to overcome friction.	Reload Core Preliminary Design

4.2-351

51

Amend. 51
Sept 1970

TABLE 4.2-9A

TYPICAL NEUTRON ENVIRONMENT IN THE CRBR SHIELD ASSEMBLIES

RRSA Region	Elevation (inch)	Total Neutron Flux, $E > 0.0$ MeV (n/cm ² -sec)		Fast Neutron Flux, $E > 0.1$ MeV (n/cm ² -sec)	
		Maximum	Minimum	Maximum	Minimum
Outlet Nozzle	-344.15	2.3×10^{11}	8.1×10^{10}	1.5×10^{10}	3.0×10^9
Sodium Filled Duct	-405.15	6.1×10^{13}	8.1×10^{12}	1.5×10^{13}	1.1×10^{12}
Above Core Load Pad	-411.15	1.4×10^{14}	7.0×10^{12}	4.4×10^{13}	1.4×10^{12}
Shield Pad (Core Mid Plane)	-437.15	1.2×10^{15}	2.4×10^{13}	5.1×10^{14}	5.7×10^{12}
Inlet Nozzle Transition	-469.15	1.3×10^{14}	5.5×10^{12}	3.4×10^{13}	1.1×10^{12}
Inlet Nozzle	-512.15	1.3×10^{11}	1.5×10^{11}	1.2×10^{10}	9.9×10^9

TABLE 4.2-9B

SHIELD ASSEMBLY INELASTIC STRAIN CRITERIA

<u>Category</u>	<u>Normal Upset Limits</u>	<u>Normal, Upset and Emergency Limits</u>
Membrane Plastic Strain Limit	≤ 0.25	≤ 0.35
Total Inelastic Strain Limit	≤ 0.5	≤ 0.7
Creep-Fatigue Damage	—	Defined in Table 4.2-7

TABLE 4.2-10

STEADY STATE CDF VALUE FOR THE HOT ROD OF
BLANKET ASSEMBLY 201 OF THE FIRST CORE

<u>AXIAL LOCATION</u>	<u>CASE I*</u>	<u>CASE II**</u>
0.46	0.0106	0.0137
0.62	0.187	0.205

51

* Case I does not include effect of power jump.

** Case II includes effect of power jump.

TABLE 4.2-11

WORST FUEL ASSEMBLY HOT ROD STEADY STATE
DUCTILITY LIMITED STRAINS AT HOT SPOT

<u>Fuel Assembly</u>	<u>End-of-Life Strain at Hot Spot</u>
10	0.042%
12	0.030%
14	0.038%
25	0.034%

51

TABLE 4.2-11A

Characterized Cladding Breach Summary

Breach Fuel Pin	Cladding Material	Fluence 10^{22} n/cm ² E>0.1 Mev	Peak MW Cladding Temp. °F	% Strain @ Breach		Postulated Cause of Breach
				Inelastic	Total	
D-5	316 L-SA	13.0	1076	5.6	~5.9	Ductility exhaustion at cladding notch
PNL 5-1	304-SA	8.6	905	1.1	3.4	Pin-to-pin contact
PNL 10-14	316 - 20% CW	5.0	1022	~0	<0.2	Cladding wear
N-E-122	316 - 20% CW	3.2	1112	~0	<0.2	Unidentified
P-12A-63K	316 - 30% CW	2.3	1247	2.3	~2.4	Cladding recrystallization
EBR-II Driver Fuel	304 L-SA	3.0 to 4.4	890 ^(a) 1047	1.2 to 2.3	1.0 to 3.9	Intergranular crack propagation

(a) Cladding I.D. Temperature

TABLE 4.2-12

SUMMARY OF DESIGN LOADING CONDITIONS FOR BLANKET ASSEMBLY STRUCTURAL ANALYSIS

Region	Blanket Assembly Type	Design Fast Fluence n/cm ²	Steady State Temp. (Inner Surface) °F	Cross-Duct Temp. Gradient °F	Inter-Assembly Temp. Gradient °F	Core Restraint Bending Moment in-lb	Coolant Pressure psi
Shield Block Region	Inner	0.4x10 ²²	730	NA*	NA	NA	NA
	Radial	0.55x10 ²²	730	NA	NA	NA	NA
Load Pad Region	Inner	3.0x10 ^{22**}	927	33	146	29940	1.0
	Radial	3.0x10 ^{22**}	971	79	(both)	1450	0.5
Outlet Nozzle Region	Inner	0.18x10 ²⁰	972	17	216	NA	NA
	Radial	0.37x10 ²⁰	975	28	(both)	NA	NA

* Not Applicable.

** The ACLP material properties for the structural damage calculations were based on a design EOL fast fluence of 3.0×10^{22} n/cm², which is in excess of the maximum fast fluence which actually occurs at this location for both blanket types.

TABLE 4.2-13

DESIGN SEISMIC AND CORE RESTRAINT LOADS AT THE BLANKET ASSEMBLY ACLP

<u>Load*</u> <u>Designation</u>	<u>OBE</u> <u>Load</u> <u>(lbf)</u>	<u>SSE</u> <u>Load</u> <u>(lbf)</u>	<u>Core Restraint</u> <u>Load</u> <u>(lbf)</u>
F ₁	4278	5995	310
F ₂	2975	4169	297
F ₃	3064	4294	297

51

*Load Direction and Points of Application are shown in Figure 4.2-33A.

4.2-356

Amend. 51
Sept. 1979

TABLE 4.2-14

EOL Steady State Cladding Strains Due to FCMI and Plenum Pressure

<u>F/A X/L</u>	<u>F/A 10</u>	<u>B/A X/L</u>	<u>IB/A 67</u>	<u>RB/A 206</u>
0.33	$4.2 \times 10^{-2}\%$	0.31	0	0
0.50	$4.2 \times 10^{-2}\%$	0.62	$4 \times 10^{-3}\%$	$6 \times 10^{-3}\%$
0.75	$3.7 \times 10^{-2}\%$	0.81	$1.1 \times 10^{-6}\%$	$2.2 \times 10^{-2}\%$
51 1.0	$4.2 \times 10^{-2}\%$			

TABLE 4.2-15

CRBR FIRST CORE WIRE WRAP PERFORMANCE SUMMARY

	<u>F/A 10</u>	<u>IB/A 67</u>	<u>RB/A 203</u>
Maximum Wire Stress	11.7 KSI	14.2 KSI	10.5 KSI
Wire Stress Limit	21 KSI	21 KSI	21 KSI
Wire Stress M.S.*	.79	.48	1.0
Maximum Wire Strain	$2.5 \times 10^{-4} \%$	$6.4 \times 10^{-6} \%$	$1.2 \times 10^{-4} \%$
Wire Strain Limit	0.6%	0.3%	0.3%
Wire Strain M.S.	>100	>100	>100

*M.S. = Margin of Safety = $\frac{\text{Allowable Stress (or Strain)}}{\text{Maximum Stress (or Strain)}} - 1$

51

TABLE 4.2-16

FUEL ASSEMBLY BOUNDING MARGIN OF SAFETY SUMMARY

F/A Region	Margin of Safety*			
	Crack Initiation		Excessive Deformation	
	Local Ductile Rupture	Combined Creep-Fatigue Damage	Peak plus Accumulated	Residual
Shield Block	2.80	61.62	4.75	2.13
CMP Hex Duct	12.76	191.3	37.4	∞
ACLP Hex Duct	10.49	91.68	4.65	1.58
TLP Outlet Nozzle	0.37	0.29	3.0	1.86
Attachment Assembly	82.33	925,925	10.11	∞
Orifice Plate	4.03	291,544	0.43	1.52

$$*Margin\ of\ Safety = \frac{Allowable\ Value}{Calculated\ Value} - 1$$

51

TABLE 4.2-17

BLANKET ASSEMBLY BOUNDING MARGIN OF SAFETY SUMMARY

B/A Region	Margin of Safety*			
	Crack Initiation		Excessive Deformation	
	Local Ductile Rupture	Combined Creep-Fatigue Damage	Peak plus Accumulated	Residual
Shield Block	3.22	5.13	0.48	0.81
ACLP Hex Duct	21.22	97.04	0.128	0.066
TLP Outlet Nozzle	0.14	415	0.69	0.16
Attachment Assembly	Acceptable per drop test results			

51

* Margin of Safety = $\frac{\text{Allowable Value}}{\text{Calculated Value}} - 1$

TABLE 4.2-18

ASSESSMENT OF APPLICABILITY OF FFTF DESIGN VERIFICATION TESTS

<u>FFTF Design Verification Test</u>	<u>Applicability to CRBRP Fuel Assembly Design</u>
Fuel Assembly Life Tests	Generally applicable. Isothermal test temperature is non-prototypic, shield block and outlet nozzle configurations are non-prototypic.
Prototype Fuel Assembly Water Vibration Test	Fuel rod and assembly length, mass distribution, and shield-orifice and outlet nozzle configurations are different.
Fuel Assembly Nozzle Insertion Tests	Inlet nozzle to receptacle interface is prototypic. Assembly length, bowed shape, load pad and handling socket configurations are different.
Fuel Duct Load Capacity Test	CRBRP load pad thickness is larger; combined loading effects may be non-prototypic. Generally applicable.
Floating Collar Behavior Test	Currently not included in CRBRP reference design.
Piston Ring Sealing and Sodium Life Test	Directly Applicable.
Hydraulic Balance Sodium Erosion Test	Directly Applicable.
Orifice Pressure Tests	Not applicable since CRBRP utilizes a different configuration.
Bypass Flow Nozzle Leakage Test	Directly Applicable.
Pressure Drop and Flow Characterization	Applicable where geometries are similar.
Small Bundle Heat Transfer Tests	Directly Applicable.

4.2-361

Amend. 51
Sept. 1979

TABLE 4.2-18 (Continued)

<u>FFTF Design Verification Test</u>	<u>Applicability to CRBRP Fuel Assembly Design</u>
Duct Load Pad Friction, Wear and Materials Evaluation	Directly Applicable.
Material Property Characterization	Directly Applicable.
Fuel Irradiation Program.	Most information is applicable either directly or by inference to CRBRP conditions.

4.2-362

Amend. 51
Sept. 1979

TABLE 4.2-19

PLANNED CRBRP FUEL ASSEMBLY DESIGN VERIFICATION TESTS

Activity Title	Activity Description	Completion Date	Provides Input To
Fuel Assembly Flow Test in Water	Full scale 217 rod water test to determine flow distribution, pressure drop, rod vibration, potential for fretting and wear, and assembly and rod dynamic characteristics.	Complete	Final Design Verification
Outlet Nozzle Flow Test in Water	Component test to assess effect of geometry on flow distribution and pressure drop in water.	Complete	Final Design
54 Inlet Nozzle and Orifice-Shield Test in Water and in Sodium	Component test to assess effect of geometry on flow distribution and pressure drop and cavitation in water and cavitation damage in a long term sodium test.	Water Test 9/80 Sodium Test 6/81	Final Design Final Design Verification
54 High Temperature Duct Loading Test	Long term duct load pad test for prototypic geometry and temperatures and combined bending, crushing, torque and axial loading to determine load limits and deformation.	7/80	Final Design Verification
54 11:1 Scale Wire Wrap Bundle Air Flow Test	Air flow tests performed to reduce uncertainties in fuel assembly subchannel flow and mixing characteristics.	Phase I - Complete Phase II - 12/81	Final Design
54 54 51 Irradiation Tests in FFTF	Verify predicted behavior of CRBRP fuel assembly under prototypic operating conditions.	8/85	Prior to Reactor Operation

4.2-363

Amend. 54
May 1980

TABLE 4.2-18 (Continued)

<u>FFTF Design Verification Test</u>	<u>Applicability to CRBRP Fuel Assembly Design</u>
Duct Load Pad Friction, Wear and Materials Evaluation	Directly Applicable.
Material Property Characterization	Directly Applicable.
Fuel Irradiation Program.	Most information is applicable either directly or by inference to CRBRP conditions.

4.2-362

Amend. 51
Sept. 1979

TABLE 4.2-19

PLANNED CRBRP FUEL ASSEMBLY DESIGN VERIFICATION TESTS

Activity Title	Activity Description	Completion Date	Provides Input To
Fuel Assembly Flow Test In Water	Full scale 217 rod water test to determine flow distribution, pressure drop, rod vibration, potential for fretting and wear, and assembly and rod dynamic characteristics.	Complete	Final Design Verification
Outlet Nozzle Flow Test In Water	Component test to assess effect of geometry on flow distribution and pressure drop in water.	Complete	Final Design
Inlet Nozzle and Orifice-Shield Test In Water and In Sodium	Component test to assess effect of geometry on flow distribution and pressure drop and cavitation in water and cavitation damage in a long term sodium test.	Complete Sodium Test 9/83	Final Design Verification
High Temperature Duct Loading Test	Long term duct load pad test for prototypic geometry and temperatures and combined bending, crushing, torque and axial loading to determine load limits and deformation.	9/83	Final Design Verification
11:1 Scale Wire Wrap Bundle Air Flow Test	Air flow tests performed to reduce uncertainties in fuel assembly subchannel flow and mixing characteristics.	Complete	Final Design
Irradiation Tests In FFTF	Verify predicted behavior of CRBRP fuel assembly under prototypic operating conditions.	8/85	Prior to Reactor Operation

4.2-363

Amend. 71
Sept. 1982

TABLE 4.2-20

PLANNED CRBRP BLANKET DESIGN VERIFICATION TESTS

Activity Title	Activity Description	Completion Date	Provides Input To
Assembly Flow and Vibration Test In Water	Full scale assembly test to determine rod and assembly vibrations and pressure losses in the assembly.	4/83	Final Design Verification
Component Pressure Drop Test	Flow test in water various blanket assembly components, measuring the pressure losses as a function of flow rate.	9/83	Final Design
Load Pad Strength and Duct Bending Stiffness Test	Component test to determine the strength of a cold worked duct and load pad for various loading conditions and temperatures.	9/83	Final Design Verification
Rod Cladding Rupture Test	Component test to determine the strength of the cold worked cladding for several combinations of temperature and time and to establish a conceptual stress rupture time curve.	Complete	Final Design Verification
Rod Irradiation Test In EBR-II	Determine the performance characteristics of radial blanket rods in a reactor environment including the effects of a power jump.	Complete	Final Design Verification
Fabricate Rod Bundle Irradiation Test In FFTF	Provide prototype fabrication experience for blanket assemblies.	Complete	Assembly Fabrication

4.2-364

Amend. 71
Sept. 1982

TABLE 4.2-21

DESIGN TEMPERATURES VS PREDICTED STEADY-STATE TEMPERATURES
FOR PERMANENT REACTOR INTERNALS COMPONENTS

Component	Design Temperature (°F)	Predicted 'Maximum' S.S. Temperature (1) (°F)	Minimum Margin (°F)
Core Support Structure			
Core Plate	775	750 ⁽²⁾	25
Module Liner	775	750 ⁽²⁾	25
Core Barrel	1060	1010	50
Bypass Flow Module	775	750 ⁽²⁾	25
Fixed Radial Shield	950	932	18
Horizontal Baffle Assy.			
FT&SA Support Block	775	750 ⁽²⁾	25
HBA Base Plate	1020	1015 ⁽²⁾	5
Core Former Structure			
Lower Ring	928	928	-
Cylinder	937	937	-
Upper Ring	1076	1076	-
Lower Inlet Module	775	755	20
Upper Internals Structure	1220	1191	29

Notes:

- (1) All values shown include a 2σ uncertainty.
- (2) Coolant temperature. Actual component temperature slightly lower.

TABLE 4.2.22 IS DELETED.

TABLE 4.2-23

CORE SUPPORT STRUCTURE STRESS AND FATIGUE DAMAGE SUMMARY FOR
NORMAL AND UPSET CONDITIONS

<u>CUT</u>	<u>STRESS CATEGORY</u>	<u>CALCULATED VALUE</u>	<u>ALLOWABLE VALUE</u>	<u>MARGIN-OF- SAFETY *</u>
A thru E	P_m	5734 psi	14,800 psi	1.58
Figure 4.2-51	$P_L + P_b$	8760 psi	21,230 psi	1.42
	$(P_L + P_b + Q)_r^{**}$	94,050 psi	49,185 psi	N/A
	$\Sigma(n/N)$.57	.90	(+)
1 thru 10	P_m	2357 psi	14,800 psi	5.28
Figure 4.2-52	$P_L + P_b$	13,344 psi	19,980 psi	.50
	$(P_L + P_b + Q)_r^{**}$	83,809 psi	49,350 psi	N/A
	$\Sigma(n/N)$.80	.90	(+)
1 thru 18	P_m	<10,486 psi	15,000 psi	>.43
Figure 4.2-53	$P_L + P_b$	10,486 psi	>15,000 psi	>.43
	$(P_L + P_b + Q)_r^{**}$	83,333 psi	49,350 psi	N/A
	$\Sigma(n/N)$.41	.90	(+)

*MARGIN-OF-SAFETY = $\frac{\text{ALLOWABLE STRESS INTENSITY}}{\text{APPLIED STRESS INTENSITY}} - 1$

** Since $(P_L + P_b + Q)_r > 3S_m$, simplified elastic-plastic analysis is used.

61

TABLES 4.2-24 through -29
HAVE BEEN DELETED

PART NAMES	MODEL USED	STRESSES (PSI)				CRITERIA (PSI)			
		MEMBRANE	MEMBRANE + BENDING	BEARING	SHEAR	Sm	1.5 Sm	Sy	0.6 Sm
BPFM	INTEGRATED 3-D SEISMIC MODEL	2,154	2,246	13,565	7,235	15,040	22,560	16,740	9,024
SEISMIC LUG		4,484	13,791	3,948	2,548	15,040	22,560	16,740	9,024
SEISMIC SHEAR PIN		14,155	23,379	8,151	6,919	61,833	$K_t S_t =$ 78,522	130,700	37,100

Table 4.2-29a. BPFM Stress Summary (OBE)

59 |

TABLES 4.2-29b and -29c
HAVE BEEN DELETED

4.2-375
(next page is 4.2-376a)

Amend. 59
Dec. 1980

TABLE 4.2-29D
EVALUATION SUMMARY OF THE LOAD CONTROLLED STRESSES (FOR FRS)

<u>Material</u>	<u>Condition</u>	<u>Temp. (°F)</u>	<u>Evaluated Results (PSI)</u>	<u>Criteria (PSI)</u>	<u>Margin*</u>
316 SS	Normal & Upset (OBE)	1000	$P_m = 3202$ $P_L + P_b = 5840$	$S_{mt} = 154000$ $K_t S_t = 22330$	>3 2.82
	Faulted (SSE)	1000	$P_m = 4828$ $P_L + P_b = 8808$	$1.2 S_t = 22200$ $1.2 K_t S_t = 26307$	>3 1.99

*Margin = $\frac{\text{Allowable}}{\text{Actual}} - 1$

4.2-376a

59

Amend. 59
Dec. 1980

TABLE 4.2-29E
RESULTS OF LOAD-CONTROLLED ANALYSIS: LOWER SUPPORT BLOCK

Material: 304SS

Condition No.	Temp. (°F)	(1,2) Stress Intensity (P_m) (psi)	Allowable (psi)	(3) Allowable Stress Origin	Use Fraction Sum Calculation		
					Time of Loading t_i (hrs)	Allowable Time t_{ia} (hrs)	t_i/t_{ia}
Design	775	1880	15,100	S_o @ 800°F	-	-	-
A	755	1880	15,100	S_{mt} @ 800°F	262,900	∞	0.0
B/C	755	1880	15,100	S_{mt} @ 800°F	1	∞	0.0
D	1120	1880	22,800	$.6S_r$ @ 1000°F for 1 hr.	-	-	-

$$\sum \frac{t_i}{t_{ia}} = 0$$

Notes:

- (1) SSE loads were combined with design condition loadings to conservatively bound all the conditions.
- (2) The stresses in this column are actually $P_L + P_B$. To be conservative, they have been treated as P_m , therefore $P_L + P_B$ criteria is automatically satisfied.
- (3) Allowables are conservatively taken at higher temperature values.

4.2-376b

Amend. 59
Dec. 1980

TABLE 4.2-29F
RESULTS OF LOAD-CONTROLLED ANALYSIS: HORIZONTAL BAFFLE PLATE

Material: 316SS

Condition No.	Temp. (°F)	(1) Stress Intensity (P_m) (psi)	Allowable (psi)	(2) Allowable Stress Origin	Use Fraction Sum Calculation		
					Time of Loading t_i (hrs)	Allowable Time t_{ia} (hrs)	t_i/t_{ia}
Design	1020	10030	12140	S_o @ 1105°F	-	-	-
A	1000	10030	14800	S_{mt} @ 1105°F	262,900	10^6	0.263
B/C	1105	10030	14800	S_{mt} @ 1105°F	1	50,000	0.0
D	1120	10030	27900	$.6S_r$ @ 1150°F for 1 hr.	-	-	-

$$\sum \frac{t_i}{t_{ia}} = .263$$

Notes:

- (1) SSE loads were combined with design condition loadings to conservatively bound all the conditions.
- (2) Allowables are conservatively taken at higher temperature values.

4.2-376c

59

Amend. 59
Dec. 1980

TABLE 4.2-30

EFFECT OF (C + N) LEVEL ON TENSILE PROPERTIES OF
TYPE 304 STAINLESS STEEL

Mechanical Property	Equation	Standard Deviation
53 Yield Strength, KSI	$89.952 + 181.167 (C + N) - 0.082 T (C + N) - 4.269 T^{1/2} + 0.058 T$ where T is $^{\circ}R$	2.236
53 Ultimate Tensile Strength, KSI	$-1.806 - 227.391 (C + N) + 1634.644 T^{-1/2}$ $+ 0.626 T (C + N) - 2.607 \times 10^{-4} T^2 (C + N)$ where T is $^{\circ}R$	2.645
53 Total Elongation, %	$29.595 - 89.898 (C + N) + 628.443 T^{-1/2}$ where T is $^{\circ}R$	2.955
53 Uniform Elongation %	$25,748 - 78.211 (C + N) + 546.745 T^{-1/2}$ where T is $^{\circ}R$	2.955

Temperature range validities:	yield strength	75 - 1200°F
	ultimate tensile strength	200 - 1100°F
	total elongation	400 - 1200°F
	uniform elongation	400 - 1050°F

4.2-377

Amend. 53
Jan. 1980

TABLE 4.2-31

EFFECT OF (C + N) LEVEL ON TENSILE PROPERTIES OF
TYPE 316 STAINLESS STEEL

Mechanical Property	Equations		Standard Deviation
Total Elongation %	$28.000 - 99.139 (C + N) + 653.926 T^{-1/2}$	where T is °R	6.703
Uniform Elongation, %	$24.780 - 87.738 (C + N) + 578.725 T^{-1/2}$	where T is °R	6.703
Temperature range validities:		total elongation	535 - 1760°R
		uniform elongation	960 - 1510°R

4.2-378

Amend. 66
Mar. 1982

TABLE 4.2-31A

SUMMARY OF FRICTION RESULTS FOR IRRADIATED DUCT LOAD PAD MATERIAL (REFERENCE 89)

Test	Materials Combination (pin/plate)	Test Conditions						Breakaway (a)			Friction Results					
		Contact Pressure/Load (psi/lbs)	Avg. Vel. (ipm)	Stroke Length (pin dia./in.)	O ₂ Conc. by VWED (ppm)	Temp. (°F)	* Rubbing Experienced (Cycles)	Dist (Ins.)	Time (hrs)	μB	Max. Observed Dynamic Friction Coefficient			Avg. Dynamic Friction Coefficient		
										Init.	Max.	Final	Init.	Max.	Final	
(6-5)-I2	CRC/CRC (b)	300/39.5	1.0	0.8d/0.4	0.45 ± 0.03	450	38	30		0.20	0.26	0.26	0.16	0.21	0.21	
		0	0	0		800	0	0		--	--	--	--	--	--	
		300/39.5	1.0	0.8d/0.4		450	38	30		0.32	0.35	0.33	0.29	0.29	0.28	
		300/39.5	1.0	0.8d/0.4		700	38	30		0.37	0.55	0.52	0.33	0.44	0.44	
		300/39.5	1.0	0.8d/0.4		1000	38	30		0.54	0.64	0.64	0.40	0.50	0.50	
		300/39.5	1.0	0.8d/0.4	0.66 ± 0.05	1160	625	500	144	1.79	0.56	0.67	0.65	0.43	0.55	0.55
		300/39.5	1.0	0.8d/0.4		1160	30	24	4B	1.09	--	--	--	--	--	
		300/39.5	1.0	0.8d/0.4		1160	30	24	26.5	1.02	--	--	--	--	--	
		300/39.5	1.0	0.8d/0.4		1160	30	24	116	1.17	--	--	--	--	--	
		300/39.5	1.0	0.8d/0.4		1160	625	500	156	1.11	0.48	0.63	0.62	0.38	0.52	0.52
		300/39.5	1.0	0.8d/0.4		450	38	30		0.45	0.45	0.42	0.40	0.40	0.37	

(a) Static dwell times were performed following rubbing periods indicated (zero tangential load).

(b) Both pin and plate specimens consist of 1/2-inch diameter spots of CRC material applied to a 5/8-inch diameter disk of Type 316 stainless steel. The combination used in this test was: CN-1b/CN-1a left side couple, CN-1a/CN-1b right side couple. Material was irradiated in EBR-II in a sodium bonded capsule to an exposure of approximately 1.0×10^{22} n/cm² at 1083°F.

TABLE 4.2-31B
 SUMMARY TABLE OF FRICTION IN SODIUM
 (Reference 88)

(Atoms International Test Data)

Test		Test Conditions						Friction Results						Comments†		
No.	Materials*		Temperature (°F)	Load/Pressure (lb)/(psf)	Average Velocity (in./sec)	Stroke Length (Pin diameter)	Rubbing Experienced Number of Strokes/Distance (in.)	Dwell (hr)	Break-away Friction	Static Friction			Dynamic Friction			
	Pin	Plate								Average Initial	Maximum Observed	Average Final	Average Initial		Maximum Observed	Average Final
4-1	Haynes 273 WD, 13f B316	Haynes 273 WD, 8f B304	450	58.9/300	0.07	d/2	25/12.5	18	0.34	0.29	0.37	0.34	0.34	0.36	0.36	No prior wear cycles.
							175/87.5	158‡	0.56	0.31	0.31	0.27	0.46	0.54	0.54	Rubbing experience includes prior 25/12.5 at 450°F + 125/62.5 at other temperature levels.
			800				100/50	66	0.71	0.54	0.54	0.41	0.71	0.71	0.51	Rubbing experience includes 75/37.5 at lower temperature levels.
			1100				150/75	18	0.93	0.59	0.76	0.76	0.76	0.85	0.85	Rubbing experience includes 125/62.5 at lower temperature levels.

*See Material and Source (Table V-16) and Symbol Descriptions (Table V-17)

†Refer to Matrix and Temperature Test Profile for complete test sequence (Figure V-10)

‡20-hour dwell at 400°F preceded by 138 hour dwell at higher temperatures (800 to 1160°F)

4.2-379a

53

15

Amend. 53
 Jan. 1980

TABLE 4.2-32 and 4.2-33 DELETED

TABLE 4.2-34

RESULTS OF DILATION ANALYSIS (MID-FLAT DILATION)

Case	Assembly* Ref. No.	Face	Elevation Above Bottom of Lower Axial Blanket (in)	Pressure Differential (psi)	Temperature (°F)	Fast Flux (n cm ⁻² sec ⁻¹ x 10 ¹⁵)	Dilation After 1 Cycle (in)	Dilation After 2 Cycles (in)	Dilation After 3 Cycles (in)
1.1	C1	--	23	3.5	759	3.174	0.0183	0.0241	0.029
1.2		--	32	3.5	788	3.712	0.0219	0.0331	0.044
1.3		--	41	3.2	816	3.211	0.0220	0.0369	0.052
2.1	F4	2	23	35.4	784	2.795	0.0283	0.0502	0.072
2.2		2	32	32.1	844	3.269	0.0376	0.0895	0.143
2.3		2	41	28.8	916	2.829	0.0318	0.1121	0.198
2.4		2	50	25.5	970	1.469	0.0239	0.0363	0.098
3.1	F1	2	23	42.9	760	3.173	0.0312	0.0519	0.073
3.2		2	32	39.0	796	3.712	0.0395	0.0763	0.114
3.3		2	41	35.0	836	3.211	0.0371	0.0862	0.136
4.1	F6	3	23	22.0	782	1.263	0.0186	0.0222	0.029
4.2		5	32	20.0	850	1.500	0.0202	0.0283	0.048
4.3		5	41	17.9	922	1.297	0.0215	0.0247	0.061
5.1	B1	2	23	15.9	788	0.823	0.0196	0.0213	0.025
5.2		2	32	14.1	858	0.972	0.0212	0.0230	0.032
5.3		2	41	12.3	936	0.837	0.0226	0.0238	0.026
6.1	F1	5	23	42.9	774	3.222	0.0330	0.0584	0.084
6.2		5	32	39.0	819	3.769	0.0415	0.0947	0.146
6.3		5	41	35.0	890	3.260	0.0432	0.1296	0.215
6.4		5	50	31.0	932	1.693	0.0239	0.0480	0.106

53

*Refer to Figure 4.2-85 for assembly location and face numbering scheme

4.2-381

Amend. 53
Jan. 1980

TABLE 4.2-35

PRIMARY AND SECONDARY SHUTDOWN SYSTEM DAMAGE SEVERITY LIMITS

	Damage Severity Limit			
	Primary System Only Functioning		Secondary System Only Functioning	
	Without Stuck Rod	With Stuck Rod	Without Stuck Rod	With Stuck Rod
Normal: Operational (2)	Not Applicable	Not Applicable	Not Applicable	Not Applicable
Upset: Anticipated Faults	Operational Incident	Operational Incident	Minor Incident (1)	Minor Incident (1)
Emergency: Unlikely Faults	Minor Incident	Minor Incident	Major Incident	Major Incident
Faulted: Extremely Unlikely Faults	Major Incident	Major Incident	Major Incident	Major Incident

(1) Failure of the primary system to scram when required for an anticipated fault is defined as an extremely unlikely event (faulted condition). However, the damage severity limit for the secondary shutdown system is conservatively specified to assure fuel pin integrity even for the concurrent anticipated fault and failure of the primary shutdown system.

(2) No action required by Plant Protection System during Normal Operation.

4.2-382

Amend. 76
March 1983

TABLE 4.2-36

CONTROL ROD SYSTEMS CLEARANCE REQUIREMENTS

Components	Requirements	Basis
Inner Duct Wear Pads to Inner Duct	<p>1) No three point contact allowed (i.e., wear pads to one side and duct to opposite side) under worst case swelling and creep conditions.</p> <p>(Ref. Figure 4.2-111 configuration E).</p>	<p>1. Drag forces resulting from 3 point contact are proportional to the control assembly stiffness. Consequently, sufficient clearance must be provided to preclude this condition of potentially high scram retarding drag forces at all times in component life.</p>
	<p>2) Combined inner and outer duct bowing for the PCA shall not increase drag forces such that acceptable scram speed of response cannot be assured. For preliminary design considerations, appropriate clearances shall be provided to assure that the maximum drag force from duct bowing is less than 25 lb_f.</p>	<p>2. Additional drag force due to duct bow can be tolerated while satisfying scram speed of response requirements. Clearances are established commensurate with acceptable scram times. The preliminary 25 lb_f limit assures that duct bowing is a small contribution (<15%) to the total PCRS drag force.</p>
	<p>3) Combined control rod and guide tube bowing for the SCA shall not increase drag forces such that acceptable scram speed of response cannot be assured.</p>	<p>3. Clearances established commensurate with acceptable scram times.</p>
B ₄ C Absorber Pellets to 316 SS Cladding	<p>1) Sufficient clearance shall be provided to preclude forced contact between pellets and cladding.</p>	<p>1) Minimize uncertainties in clad lifetime predictions. Due to B₄C/316 SS interaction under pressure, clad thickness is difficult to estimate. Consequently, sufficient clearance is established to preclude contact under worst case absorber swelling.</p>

4.2-383

Amend. 76
March 1983

TABLE 4.2-36 (Continued)

Components	Requirements	Basis
Absorber Pin Wire Wrap to Inner Duct	1) Provide sufficient clearance to limit inner duct deformation such that wear pad to inner and outer duct clearance requirements are satisfied and to preclude reduction in clad lifetime.	1) Limit duct bow and pin stress. Significant interaction between duct and pins contributes to duct bow (therefore increasing drag forces), establishes high stress points on cladding, and inhibits free axial expansion of pins.
Absorber Pin to Spacer Grid	1) Provide sufficient clearance to allow free axial expansion at all times.	1) Limit pin stress.
Driveline to Shroud Tube	1) Provide sufficient clearance to prevent contact between driveline and shroud tube at points other than normal guidance features (i.e., shroud tube bushing, driveline wear bushing and driveline latch housing guide ribs) under maximum misalignment conditions. (Not required during seismic event).	1) Limit misalignment drag forces.
PCRD Piston to Dashpot Cup	1) Provide sufficient clearance to ensure that significant deceleration occurs only in last 9 inches of travel and that impact velocity is no greater than 14 ips.	1) Assure that dominant absorber reactivity worth is inserted before deceleration and provide acceptable scram arrest impact loads on the PCA.
PCRDM Leadscrew to Guide Bushings	1) Limit clearance such that leadscrew is aligned for proper scram release while not impeding scram by high drag forces.	1) Reliable scram performance.

4.2-384
 (Next page is 4.2-387)

Amend. 76
 March 1983

TABLE 4.2-36A

FRICITION COEFFICIENTS

<u>Material Couple</u>	<u>Application</u>	<u>Friction Mean</u>	<u>Coefficients Standard Deviation</u>	<u>Upper Three Sigma Limit</u>	<u>References</u>
53 Inconel 718/ Inconel 718	CRD to Dashpot Cut or Shroud Tube	Combined* 0.45 ETEC 1.53 WARD 0.45	0.2 0.21 0.15	1.05 2.16 0.9	7-8, 1-13
Type 316SS/ Type 316SS	Duct to Duct	0.7	0.18	1.24	2, 12
Haynes 273/ Inconel 718	CRD Dashpot Cup to Dashpot Cut Seat	0.64	0.21	1.27	8, 13
Inconel 718/ Type 304SS	CRD Compression Sleeve	0.85 (Only 2 Samples)	0.25	1.6	1
Inconel 718/ Type 316SS	CA Wear Pads Outer Duct	0.62	0.09	0.89	2, 11
Inconel 718/ Ni Resist	Torque Tube to Torque Taker	0.2	0.16	0.68	13
17-4 Ph/ Inconel 718	CRDM Bellows/ Leadscrew	0.64	0.16	1.12	13
Stellite 6B/ Inconel 718	Torque Keyway and Torque Taker	0.37	0.01	0.4	1, 14

*It should be noted that only 36 data points were utilized to obtain the distribution with a mean of 1.53 while 440 points are available for the distribution with a mean of 0.45. The combined data is overwhelmed by the large amount of data at the lower values. The higher values appear in just the ETEC data.

TABLE 4.2-36B
 AVERAGE FRICTION COEFFICIENTS
 FROM
 W-ARD TEST DATA

STROKE = .750 IN.

AVERAGE FRICTION COEFFICIENT Material Couple		Enviorn-ment		P = 100 psi								P = 1500 psi							
				TEST 1				TEST 2				TEST 1				TEST 2			
				400°F		800°F		800°F		1100°F		400°F		800°F		800°F		1100°F	
				μ	$\mu \pm 3\sigma$	μ	$\mu \pm 3\sigma$	μ	$\mu \pm 3\sigma$	μ	$\mu \pm 3\sigma$	μ	$\mu \pm 3\sigma$	μ	$\mu \pm 3\sigma$	μ	$\mu \pm 3\sigma$	μ	$\mu \pm 3\sigma$
316SS/316SS	Liq. Na	.81	.87	.88	.98	.80	.87	.87	.91	.73	.76	.74	.77	.73	.75	.75	.77		
Inconel 718/ Inconel 718	Liq. Na	.80 .63	.85 .69	.79 .70	.86 .77	.69 .74	.73 .79	.65 .70	.70 .73	.71 .58	.75 .61	.71 .60	.75 .62	.61 .62	.65 .66	.63 .66	.67 .68		
Inconel 718/ 316SS	Liq. Na	.87 .84	.92 .90	.89 .86	.95 .94	.92	1.02	.89	.95	.86 .79	.90 .83	.82 .77	.87 .84	.74	.80	.77	.81		
Inconel 718/ Haynes 273	Liq. Na	.70	.76	.67	.73	.79	.85	.78	.81	.66	.70	.69	.73	.73	.78	.70	.72		
*Stellite 6/ 17-4 PH	Argon	.24	.29	.27	.32					.17	.21	.13	.14						

STROKE = .188 IN.

316SS/316SS	Liq. Na	.95	1.02	1.07	1.17	.82	.87	.88	.92	.80	.84	.82	.86	.77	.81	.76	.79
Inconel 718/ Inconel 718	Liq. Na	.88 .73	.94 .80	.82 .73	.89 .78	.73 .83	.79 .89	.69 .72	.82 .75	.79 .66	.85 .70	.74 .66	.79 .69	.70 .67	.73 .70	.65 .67	.68 .69
Inconel 718/ 316SS	Liq. Na	.94 .92	1.01 1.00	.94 .91	1.00 .96	.99	1.06	.85	.89	.90 .87	.94 .92	.81 .79	.86 .83	.80	.84	.74	.78
Inconel 718/ Haynes 273	Liq. Na	.77	.83	.90	.96	.76	.80	.70	.73	.78	.82	.75	.81	.75	.79	.68	.70
*Stellite 6/ 17-4 PH	Argon	.21	.26	.17	.21					.18	.21	.13	.15				

*Run at 150°F and 400°F with 17-4 PH vitrolubed.

(next page is 4.2-391)

4.2-388

59

TABLE 4.2-36C
SUMMARY OF AVERAGE
FRICTION COEFFICIENTS

Material Couple	Environment	UPPER THREE SIGMA DATA	
		P=100 psi	P=1500 psi
<u>STROKE = .750 IN.</u>			
316SS/316SS	Liquid Na	.91	.76
Inconel 718/ Inconel 718	Liquid Na	.77	.67
Inconel 718/ 316SS	Liquid Na	.95	.84
Inconel 718/ Haynes 273	Liquid Na	.78	.73
<u>STROKE = .188 IN.</u>			
316SS/316	Liquid Na	1.00	.83
Inconel 718/ Inconel 718	Liquid Na	.83	.73
Inconel 718/ 316SS	Liquid Na	.99	.86
Inconel 718/ Haynes 273	Liquid Na	.83	.78

59

Amend. 59
Dec. 1980

TABLE 4.2-36D

FFTF AND CRBRP PROTOTYPE CONTROL ROD SYSTEMS TESTS

<u>FFTF Prototype Tests</u>						
<u>Phase</u>	<u>Test Description</u>	<u>Temp. Range</u>	<u>Feet of Travel</u>	<u>Scrams</u>	<u>Disconnect Operations</u>	
59 53 I	Flow Rates - 0 - 90 GPM Scram Heights - 9, 18, 27, 35, 36" Misalignment - Misaligned	400 to 1100°F	3,420	188	1	
59 53 II	Flow Rates - 0 - 100 GPM Scram Heights - 9, 18, 27, 35, 36" Misalignment - Aligned	400 to 1100°F	2,730	157	33	
59 53 III	Flow Rates - 0 - 100 GPM Scram Heights - 9, 18, 27, 35, 36" Misalignment - Gross Misalignment	400 to 1100°F	14,400	428	15	
59 53 IV	Flow Rates - 0 - 100 Scram Heights - 9, 18, 27, 35, 36" Misalignment - Aligned with Failed Bellows	400 to 1100°F	3,085	55	1	

100 GPM is 110% of Nominal Coolant Flow

53|

Amend. 59
Dec. 1980

15

TABLE 4.2-36D (Continued)

CRBRP PROTOTYPE TESTS

<u>Phase</u>	<u>Test Description</u>	<u>Temp. Range</u>	<u>Feet of Travel</u>	<u>Scrams</u>	<u>Disconnect Operations</u>
Complete	Accelerated Unlatching Life Test (Prototype Unit 1)	N/A* (H ₂ O)	35,451	1868	60
I	PCRS Accelerated Life Test (Prototype Unit 2)	400 to 1100°F	5,878	470	42
I	Failed Bellows Test (Prototype Unit 3)	400 to 1100°F	9,146	680	40
I	Real Time Test (Prototype Unit 2)	400 to 1100°F	5,418	368	40

59 *PCRDM and its supporting nozzle were maintained at prototypic temperatures by means of heaters. The drive-line and dummy weight to simulate the control rod weight were in a water environment for this test.

4.2-393a

Amend. 59
Dec. 1980

TABLE 4.2 - 36E
 MAXIMUM EFFECTIVE COEFFICIENT OF
 FRICTION DATA
 FOR DYNAMIC IMPACT LOADING

<u>Material Couple</u>	<u>Configuration</u>	<u>Medium</u>	<u>Max *</u>
I 718/I 718	Round	Air	.37
I 718/I 718	Round	Water	.35
I 718/316 SS	Hexagonal	Air	.63 **
I 718/I 718	Round	Sodium	.46
I 718/304 SS	Round	Air	.45
I 718/304 SS	Round	Water	.40

* Values represent the maximum observed in any test.

** Includes effect of slight duct material yielding resulting from test article configuration. Actual coefficient of friction will be less.

TABLE 4.2-37

CONTROL ROD DRIVE SYSTEM MAXIMUM LOADING CONDITIONS

Condition	Load (lb)		Basis
	Primary	Secondary	
Insertion	1000 (Min.)	1000 (Min.)	Primary and secondary system minimum insertion load.
	Max. Under	1800 (Max.)	Secondary System calculated max. based on motor controller torque limits.
Withdrawal	1500 (Min.)	900 (Min.)	Primary and secondary system values dependent on further detailed design and test measurements.
	Max. Under	2700 (Max.)	Secondary system calculated values based on motor controller torque limits.
Minimum Breakaway Joint Strength	16000	16,000	Minimum design strength of breakaway joint (CA to CA shaft) to provide for drive shaft separation with stuck control rod.
Maximum Breakaway Joint Strength	19000	19,000	Maximum design failure load of breakaway joint to provide for drive shaft separation with stuck control rod.
PI Compression	1000 (Max.)	None	Maximum load to free control rod coupling.
Assembly of Components	Variable	Variable	Torquing preloads required in assembling.
Seismic	OBE	OBE	Seismic design data bases are discussed in Section 3.7.
	SSE	SSE	
Thermal	Under evaluation	Not Finalized	Thermal stress information will be provided in the FSAR.
Rod Expulsion	1800 (Max.)	1500 (Min.)	Conservative design against rod expulsion such that maximum control assembly pressure drop cannot cause significant control rod transients.
Scram	Under evaluation	1700 (Max.)	Forces calculated from deceleration of translating assembly on scram stop.
Structural Margin Beyond Design Basis	Internal reactor vessel pressure (300 psi).	Internal reactor vessel pressure (300 psi).	Sealing integrity for CRDM housing and nozzle required under SMBDB conditions.
			Mechanical and hydraulic loads resulting from SMBDB including acceleration vs. time history loading are considered in design basis.

4.2-395

Amend. 76
March 1983

TABLE 4.2-37A

CONTROL ASSEMBLY - ABSORBER PIN STRUCTURAL CRITERIA

Conditions

Criteria

54 | Steady State

P_m or $P_m + P_b < S_p$ $S_p =$ Proportional elastic limit. These limits apply only after initial ascent to Full Power. ASME Code Section III Subsection NB and Code Case 1592 limits apply during Preoperational Handling and Checkout.

Steady State and Upset

$F_D \leq D$ $F_D =$ Damage factor determined similar or equivalent to procedure of Paragraph T-1411 of Code Case 1592. K' factors do not apply. Factor F_D to be based on average stress across a section. For D refer to Figure T-1420-2 of Code Case 1592.

Steady State, Upset, and Emergency

The following limits on the combined primary (local) membrane plus bending plus secondary stress intensity range shall be satisfied:

$\epsilon_u > 1\%$ The combination of $(P_L + P_b/K_t)/\sigma'_y$ and $(Q_R)_{max}/\sigma'_y$ stress intensities shall be restricted to within 80% of the shakedown boundary based on elastic-perfectly plastic material behavior with the flow stress taken to be σ'_y . For axisymmetric structures away from discontinuities the Bree elastic-plastic shakedown diagram can be used.

$\epsilon_u < 1\%$ $(P_L + P_b + Q)_{max} < 0.75 S_u$ for steady state and upset conditions
 $< 0.90 S_u$ for emergency conditions

Notes: S_y values may be used when σ'_y (cyclic yield strength) is not available
 K_t is defined in Code Case 1592
 $(Q_R)_{max}$ is maximum range of secondary stress intensity

$$\sum_{\tau} \left[\frac{\epsilon^C}{\epsilon'_u \tau} + \frac{\epsilon^P}{\epsilon'_u \tau} \right] < 0.9$$

$\epsilon^C =$ thermal creep, $\epsilon^P =$ plastic strain, $\tau =$ time

$\epsilon_u =$ uniform elongation, $\bar{\epsilon} =$ average strain rate,
 TF - triaxiality factor (stress state),

and $\epsilon'_u = \epsilon_u (TF, \bar{\epsilon})$

CDF - cumulative damage function similar to that applied to the fuel pin (as described in Part 5 of Section 4.2.1.1.2.2) with applicable material properties.

CDF ≤ 1.0

51 | Steady State, Upset, Emergency, and one worst case transient event

53

TABLE 4.2-37B

CONTROL ASSEMBLY - BALANCE OF ASSEMBLY STRUCTURAL CRITERIA

ϵ_u	Maximum Temperature $\leq 800^{\circ}\text{F}$	Maximum Temperature $> 800^{\circ}\text{F}$
$\epsilon_u \geq 5\%$	<p>A1 - ASME Code Section III, Subsection NB Rules plus:</p> <ol style="list-style-type: none"> 1. The effect of irradiation swelling and creep deformations shall be evaluated. 2. Design stress levels shall be based on ASME Code Section III, Subsection NB, unless test data in NSMH indicates use of higher allowables. 3. The mean stress correction for fatigue evaluations is to be based upon the cyclic stress-strain curve. 4. The fatigue evaluation shall be based upon test data for irradiated material or upon the ASME Code curve for unirradiated material, modified by the method of characteristic slopes for predicting fatigue failures based on ductility and fracture data from tests on irradiated material. 	<p>A2 - Rules of A1 plus:</p> <ol style="list-style-type: none"> 1. Code Case 1592. 2. RDT Standard F9-4T. 3. The effect of loss of carbon, nitrogen etc. to be considered when determining allowables. 4. Irradiation swelling and creep deformations to be considered in creep collapse analysis. 5. Inelastic strain accumulation must be computed as a function of temperature, stress state, geometry, and time under consideration. No fluence consideration is required.
$3\% \leq \epsilon_u < 5\%$	<p>B1 - Rules of A1 plus: When the option to invoke justifiable higher irradiated allowables is utilized:</p>	<p>B2 - Rules of A2 and B1.</p>

4.2-397

TABLE 4.2-37B (Continued)

ϵ_u

Maximum Temperature $\leq 800^\circ\text{F}$

Maximum Temperature $>800^\circ\text{F}$

B1 - Rules of A1 plus: (Cont'd)

1. No primary plus secondary stress is permitted to exceed that associated with strain of $\epsilon_u / 2$
2. Primary membrane stresses shall not exceed the lesser of 1/3 UTS or 2/3 of the proportional stress limit.
3. Linearized primary membrane plus bending stresses shall not exceed the lesser of 1/2 UTS or the proportional limit stress.

C - Rules of B1 and B2 for their respective temperature ranges plus:

1. Brittle fracture shall be considered as a potential failure mode.
2. Where low ductility components are subject to shock loads, failure due to the superposition of transient stress waves shall be considered.

$\epsilon_u > 3\%$

53 |

51

4.2-398

Amend. 53
Jan. 1980

TABLE 4.2-38

CONTROL ROD SYSTEMS SERVICE LIFE

		Design Life Years	Total Start/Stop Cycles	Total Lifetime Scrams	Lifetime Travel (FT)	Connect Disconnects Cycle	Full Stroke Scrams Dashpot
Primary System	Mechanism	30	8×10^6	732 ⁽³⁾	17,000	---	---
	Driveline	10	2.7×10^6 ⁽¹⁾	244 ^{(1),(3)}	5,700 ⁽¹⁾	60 ⁽⁴⁾	244
	Control Assembly	1	2.7×10^5 ⁽²⁾	26 ^{(2),(3)}	570 ⁽²⁾	6 ⁽⁴⁾	---
Secondary System	Mechanism	30	13,900	700 ^{(3),(6)}	7,700	1067 ^{(6),(7)}	---
	Driveline	10	4,650	260 ⁽³⁾	2,360	360 ⁽⁷⁾	---
	Control Assembly	1	930 ⁽²⁾	50 ^{(2),(3)}	500 ⁽²⁾	12 ⁽⁴⁾	---

1. Based on minimum 10 year life.
2. Based on life of 2 years.
3. Includes 5 isothermal scrams per year.
4. At refueling temperature.
5. Based on minimum 5 year life.
6. Based on routine maintenance for the 5 year life mechanism components that perform a scram function. This routine maintenance will extend the total lifetime to 30 years, to match overall mechanism design life.
7. Includes scrams, test scrams, and normal shutdown.

TABLE 4.2-39
NUCLEAR ENVIRONMENT

<u>Elevation (in)</u>	<u>Total Neutron Flux⁺ (n/cm²/sec.)</u>	<u>Fast Neutron Flux⁺ E < 0.1 MeV (n/cm²/sec.)</u>	<u>Comments</u>
+200	See Note 1	See Note 2	Top of CRDM
+100	See Note 1	See Note 2	Stator
+40	See Note 1	See Note 2	Scram Spring/Bellows Interface
+0.0*	See Note 1	See Note 2	Torque Taker/Bellows Interface
-74.65	2.5×10^5	6.3×10^2	Point on Driveline at Bottom of Reflector (Max.)
-190	5.1×10^8	5.2×10^3	Driveline Dashpot Seat (Max.)
-218	2.6×10^9	1.3×10^5	Guide Tube/Upper Internals Interface (Max.)
-350	3.0×10^{12}	3.8×10^{11}	Control Rod/Driveline Coupling (Max.)
-437.15	4.7×10^{15}	2.8×10^{15}	Core Midplane (Max.)
-512.15	9.6×10^{11}	1.2×10^{11}	Bottom of Control Assemblies (Max.)

* Top of closure head

* Fluxes based on equilibrium cycle

Note 1 - Neutron dose levels above the closure head in the vicinity of the control rod drive mechanisms may range from 100 mr/hr to < 2 mr/hr. A shield system/seismic support will shield areas above ~ 100 inches. The corresponding total neutron flux range is approximately 2×10^4 n/cm²/sec. to 2×10^2 n/cm²/sec.

51 Note 2 - The above total fluxes (Note 1) correspond to a fast neutron flux < 2×10^2 n/cm²/sec.

TABLE 4.2-40

GROUPING OF PLANT DUTY CYCLE
EVENTS INTO CRD UMBRELLA TRANSIENTS

1. CRD Transient Desgnt.	*** Duty Cycle Events Umbrellaed	30 Year* Umbrella Transient Frequency	Initial State Point	Final State Point
<u>NORMAL EVENTS:</u>				
CRD-1N (N-1a) Dry Heatup and Cooldown	N-1a(5)	5	Ambient or Refueling (Dry)	Refueling (Dry) or Ambient
CRD-2N (N-2a) Startup, Refueling to Hot Standby	N-2a(140)	140	Refueling	Hot Standby
CRD-3N (N-2b/U-2F) Startup, Hot Standby to 40% Load with excessive step	N-2b(720),** N-2a(140)	860	Hot Stand- by	40% Load
CRD-4N (N-3a) Shutdown, Hot Standby to Refueling	N-3a(60), U-11a(18), U-11b(18), U-11c(9), U-19a(9), U-19b(9), U-19c(9), E(7), F(1)	140	Hot Stand- by	Refueling
CRD-5N (N-3b) Shutdown, 40% Load to Hot Standby	N-3b(210), N-3a(60), U-15a(50), U-22(9)	329	40% Load	Hot Standby
CRD-6N (N-4a) Loading	N-4a(9300), N-5(750) Following Startup (840)	10,890	40% Load	100% Load
CRD-7N (N-4a) Unloading	N-4a(9300),N-5(750), U-15a(50),U-22(9), Preceding Shutdown (312)	10,421	100% Load	40% Load
CRD-8N (N-4b) Load Fluctuations	N-4b(46,500)	46,500	100% Load or 80% Load	80% Load or 100% Load
CRD-9N (N-6) S.S. Temperature Fluctuations	N-6(30 x 10 ⁶)	30x10 ⁶	100% Load	100% Load

51

TABLE 4.2-40 (Cont'd.)

1. CRD Transient Desgnt.	*** Duty Cycle Events Umbrellaed	30 Year* Umbrella Transient Frequency	Initial State Point	Final State Point
CRD-10N (N-7) S.S. Flow induced vibrations	N-7(10 ¹⁰)	10 ¹⁰	100% Load	100% Load
<u>UPSET EVENTS:</u>				
53 CRD-1U (U-1b) Reactor Trip from Full Power with Minimum Decay Heat	U-1a(180), U-1b(0), U-3b(15), U-4a(6), U-4b(15), U-5a(10), U-6(10), U-8(15), U-9(15), U-10a(12), U-10b(6), U-10d(6), U-11a(18), U-11b(18), U-11c(9), U-14(24), U-15b(10), U-19a(9), U-19b(9), U-19c(9), U-20b(5), U-21a(15), U-23(9)	425	100% Load	Hot Standby
CRD-2U (U-2b) Uncontrolled Rod Withdrawal from full power	U-2a(10), U-2b(10), U-3a(6)	26	100% Load	Hot Standby
CRD-3U (U-21b) Inadvertent opening of superheater outlet safety/power relief valve	U-7a(5), U-7b(5), U-13(18), U-20a(5) U-21b(9)	42	40% Load	Hot Standby
CRD-4U (U-2d) Uncontrolled Rod withdrawal from startup	U-2c(10), U-2d(10)	20	Hot Standby	Hot Standby
CRD-5U (U-2e) Plant Loading at maximum rod withdrawal rate	U-2e(10)	10	40% Load	100% Load
51 CRD-6U (U-18) Loss of preferred and alternate preferred power	U-5b(5), U-12(9), U-18(16)	30	100% Load	Hot Standby

Amend. 53
Jan. 1980

TABLE 4.2-40 (Cont'd.)

1. CRD Transient Desgnt.	*** Duty Cycle Events	30 Year* Umbrella Transient Frequency	Initial State Point	Final State Point
2. Duty Cycle Events	Umbrellaed			
3. Description				

EMERGENCY EVENTS:

CRD-1E (E-4c) Rupture between Superheater Outlet and Isolation Valve	E-2, E-3a, E-3b, E-4a, E-4b, E-4c, E-4d, E-5, E-6, E-8, E-9a, E-9b, E-9c, E-10, E-11, E-13a, E-13b, E-14	7	100% Load	Hot Standby
CRD-2E (E-16) Three loop natural circulation	E-7, E-15, E-16, E-17, E-18	7	100% Load	Hot Standby
CRD-3E (E-1) Primary Pump Mechanical failure	E-1	7	100% Load	Hot Standby

FAULTED EVENTS:

CRD-1F (F-2) DHRS Activation without SGS cooldown	F-2	1	100% Load	Hot Standby
---	-----	---	-----------	-------------

NOTES: * To obtain an event frequency for a period other than 30 years, divide the 30 year frequency by the number of periods in 30 years and use the next higher integer frequency if the results are not an integer.

** The N-2b frequency of 710 from OPDD-10 does not include startups for a faulted event and the nine U-22 events.

*** Duty cycle events are defined in PSAR Appendix B.

TABLE 4.2-41

COMPARISON OF PRIMARY AND SECONDARY CONTROL ROD SYSTEMS

	<u>Primary</u>	<u>Secondary</u>
<u>Control Assembly (CA)</u>		
Control Rod	37 Pin Bundle	31 Pin Bundle
B ₄ C Enrichments	92%	92%
Control Rod Guide Geometry	Hexagonal	Cylindrical
Control Rod Stroke	36.0" to 37.8"	37.5" Nominal
<u>Control Rod Driveline (CRD)</u>		
CA Coupling	Rigid Coupling	Flexible Collet Latch
CRDM Connection	CRD Leadscrew to CRDM Roller Nuts	SCRD Attached to SCRDM Carriage with Pneumatic Activation to SCRDM Latch thru Slender Rod
CA Disconnect for Refueling	Manual	Automatic
<u>Control Rod Drive Mechanisms (CRDM)</u>		
Type of Mechanism	Collapsible Rotor-Roller Nut	Twin Ball Screw with Translating Carriage
Overall Mechanism Stroke	37.5 Inches	67.5 Inches
Cover Gas Seal	Bellows	Bellows
<u>Scram Function</u>		
Scram Release	Magnetic, Release CRDM Roller Nuts	Pneumatic, Release SCRDM Latch in SCA
Scram Assist	Spring in CRDM	Hydraulic in SCA

TABLE 4.2-41 (Continued)

<u>Scram Function</u>	<u>Primary</u>	<u>Secondary</u>
Scram Speed Dependence on Flow Rate	Increases with Decreasing Flow Rate	Increases with Increasing Flow Rate
Scram Assist Length	27 Inches	Initial acceleration for normal scram; Full stroke if scram motion were impeded.
Scram Deceleration	Hydraulic Dashpot in CRD	Hydraulic Spring Damper in SCA
Scram Motion Thru Upper Internals	Full Stroke	~0.1 Inch (Tension Rod within SCRD)

Operational Functions

Independent Shutdown Capability	Yes	Yes
Burnup Control	Yes	No
Power and Reactivity Control	Yes	No

TABLE 4.2-42

SECONDARY CONTROL ASSEMBLY DIMENSIONS

Control Assembly

Outside Distance Across Flats	4.575 Inches
Inside Distance Across Flats	4.335 Inches
Overall Length	168.0 Inches

Guide Tube

O.D.	4.298 Inches
I.D.	4.080 Inches
Clearance Between Guide Tube and Channel	0.0185 Inch
Clearance Between Guide Tube and Piston	0.070 Inch

Control Rod

Outside Diameter of Control Rod Duct	3.777 Inches
Inside Diameter of Control Rod Duct	3.697 Inches
Number of Pins	31
Pin Pitch-to-Diameter Ratio	1.05
Pin O.D.	0.5526 Inch
Pin Clad Thickness	0.029 Inch
Total Pin Length	56.792 Inches
Plenum Length (Upper/Lower)	8.087 Inch/ 9.250 Inch
Insulator Pellet Length (Upper/Lower)	0/0.5 Inch
Active Absorber Length	36.0 Inches
Pellet Diameter	0.470 Inch
B-10 Loading (minimum)	4.66 Kg
Wire Wrap Diameter	0.0276 Inch
Wire Wrap Pitch	18.38 Inches
B-10 Enrichment	92%

TABLE 4.2-42a
PRIMARY CONTROL ASSEMBLY DIMENSIONS

Control Assembly

Outside Distance Across Flats	4.575 inches
Inside Distance Across Flats	4.335 inches
Overall Length	168.0 inches

Inner Duct/Outer Duct Clearances (Diametral)

Upper Wear Pad	0.120 inches
Lower Wear Pad	0.100 inches
Duct to Duct (Across Flats)	0.297 inches

Control Rod

Outside Distance Across Flats Inner Duct	4.038 inches (NOM)
Inside Distance Across Flats of Inner Duct	3.950 inches (NOM)
Inner Duct Wall Thickness	0.044 inches (NOM)
Number of Pins	37
Pin Pitch-To-Diameter Ratio	1.05
Pin O.D.	0.602 inch
Pin Clad Thickness	0.049 inch
Total Pin Length	78.445 inches
Plenum Length (Upper/Lower)	22.700 inches 14.220 inches
Insulator Pellet Length	0.700 inch
Active Absorber Length	36.0 inches
Pellet Diameter	0.4500 inch
Pellet Density	92% Theor.
B ¹⁰ Loading (92% enriched)	5.57 KG (NOM)
Wire Wrap Diameter (Interior/Edge)	0.030/0.015 inch
Wire Wrap Pitch	12.75 inches
Pin Bundle Clearance (Diametral)	0.034 inch

53

51

TABLE 4.2-43

PRIMARY CONTROL ROD SYSTEM LATERAL MISALIGNMENT FORCES

Rod Position (Inches Withdrawn)		Drag Force (lbf.)
0	Minimum radial clearance (C.R. coupling O.D. to scram arrest flange I.D.)	291
6	Increased radial clearance (C.R. shaft O.D. to scram arrest flange I.D.)	232
10	Just prior to dashpot deceleration	125
15	Typical position of Row 7 Corner control rod at start of cycle	131
30	End of cycle control rod position	101
37	Maximum withdrawal	108

53 | 51

* Based on lateral misalignments from Figure 4.2-95B.

TABLE 4.2-43a

EFFECT OF WORST CASE MISALIGNMENT ASSUMPTION

Configuration	System Misalignment According to Fig. 4.2-95B	Non-Translating Assembly Misalignment	Translating Assembly Misalignment	Fixed Dashpot Cup Assumed	Total Lateral Forces Predicted (lbf.)
Analysis of PCRS in CRBRP	Yes	Yes	Yes	Yes	291
Analysis of PCRS Tests Case 1	Yes	Yes	Yes	Yes	300
	Yes	Yes	Yes	No	102
	Yes	No	No	No	7.2
Test Results from PCRS Tests	Yes	As-built	As-built	Validity of Assumption Checked by test. Dashpot is <u>not</u> fixed.	10

59 53

4.2-409

51

59

Amend. 59

TABLE 4.2-44

PCRS CYCLE DEPENDENT WITHDRAWAL POSITIONS
(IN INCHES)

CYCLE	ROW 4	ROW 7			
	BOC & EOC	Minimum		Expected	
		BOC	EOC	BOC	EOC
1	36	16.0	20.9	18.9	24.2
2	36	15.1	22.4	18.1	26.9
3	36	12.9	23.3	16.2	27.7
4	36	12.5	21.1	16.6	26.9
5	36	12.6		15.9	

NOTE: Scram analyses of paragraph 4.2.3.3.1.3 have been based on minimum rod withdrawals approximately 0.4 inches greater than this table. The effects of this difference on scram speeds are negligible compared to the existing margins relative to requirements.

51

TABLE 4.2-45 DELETED

Amend. 51
Sept. 1979

TABLE 4.2-46

PRELIMINARY PERFORMANCE PARAMETERS FOR PCA ABSORBER PINS

NOTES: * Not an operating condition-for reference only

<u>PARAMETER</u>	<u>Row 4</u>	<u>Row 7 Corner</u>
B-10 Load (BOC Kg)	5.57	5.57
Withdrawn Position		
BOC 3 (inches)	36	20.8
EOC 3 (inches)	36	28.4
Total Absorber Power		
Full Insertion (KW)*	619* (EOC 4)	628* (BOC 3)
Withdrawn Position (KW)	75 (EOC 4)	375 (BOC 3)
Coolant Flow (THD)		
Total Assembly (lb/hr)	47,000	47,000
Pin Bundle (lb/hr)	28,670	28,670
Pellet Burnup		
Peak Pellet - Captures/ccx10 ⁻²⁰	75 (EOC 4)	115 (EOC 3)
Avg. for Stack-Captures/ cc x 10 ⁻²⁰	13 (EOC 4)	40 (EOC 3)
Helium Release Fraction		
Avg. for Pellet Stack	.15 (EOC 4)	.21 (EOC 3)
Pin Pressure and Stress		
Pressure (psi)	268 (EOC 4)	1037 (EOC 3)
Hoop Stress (psi)	1257 (EOC 4)	4860 (EOC 3)
Pin Lifetime	>275 FPD	>275 FPD

51 | Based on preliminary analysis of heterogeneous core conditions.

Amend. 51
Sept. 1979

TABLE 4.2-46A

Currently Committed B₄C Tests Supporting CRBRP Control Assembly Design

HEDL Test	Typical Test Parameters			Status and Comments
	Pellet Temp. °F	Pellet Dia. Inch	8-10 Captures per cc x 10 ⁻²⁰	
BICM-2 (YY06)	1800°F	0.300	50-60	Test complete. Data confirms HEDL design correlations.
BHTE	2400°F to 3600°F	0.25 to 0.6	20, 30, 50	Test in progress, 20 x 10 ²⁰ captures/cc data available 10/78.
BOPT-1	1450°F to 1950°F	0.636 0.617 0.450 0.430	10, 20, 50, 75	Test complete. 75 x 10 ²⁰ captures/cc data available 10/78.
BICM-1 (YY02)	1150°F 1650°F	0.300	20-80	Test complete. Results used in HEDL design correlations.
BV-2	1400°F 1600°F	0.44 0.62	20, 50, 110	Vented pins, 50 x 10 ²⁰ captures/cc data available 10/78. 110 x 10 ²⁰ captures/cc data available 8/79.
BRIR	1050°F 1650°F	0.362	95, 115, 180	Test in progress, 95 & 115 x 10 ²⁰ captures/cc data available 10/78. 180 x 10 ²⁰ captures/cc complete 1980.

4.2-413

53

Amend. 53
Jan. 1980

15

TABLE 4.2-47

CRDM DESIGN STRUCTURAL ANALYSIS SUMMARY

<u>Component</u>	<u>Allowable Stress or Load</u>	<u>Calculated Stress or Load</u>	<u>Margin</u>
<u>Pressure Boundary Components:</u>			
Motor Tube	60,000 psi	29,540 psi	103%
Position Detector Housing	60,000 psi	29,200 psi	105%
Nozzle Extension	25,000 psi	21,616 psi	15.6%
<u>Non-Pressure Boundary Components:</u>			
<u>Rotor Assembly Bearings:</u>			
Radial Bearing	7,594 lbs	<1,000 lbs	>659%
Synchronizer Bearing	12,476 lbs	<2,000 lbs	>524%
<u>Segment Arm Assembly:</u>			
Segment Arm Springs	70,000 psi	66,442 psi	5.4%
Synchronizer Pin	1.903 kips	.950 kips	100%
Segment Arm Pivot Pin	13,541 lbs	4,081 lbs	232%
<u>Out Motion Limiting System:</u>			
Out Motion Pawl	124,875 psi	56,555 psi	121%
Out Motion Pivot Pin	83,850 psi	45,219 psi	85%
Rotational Stop Latch	24,600 psi	21,201 psi	16%
Scram Assist Spring	70,000 psi	65,070 psi	7.6%
Leadscrew	24,600 psi	18,806 psi	31%
51 59 CRD Disconnect Fingers	53,633 psi	35,100 psi	53%

TABLE 4.2-48

COMPARISON ANALYSIS-HEDL EXPERIMENTS
FOR FFTF CONTROL ASSEMBLY

INCEPTION OF FLOATATION CONDITIONS

	Flow Rate (gpm)	ΔP (psi)
THEORETICAL PREDICTION	145	10.5
HEDL EXPERIMENTAL DATA	140-143	10.1 - 10.2
ERROR	1.5 - 3.6%	2.9 - 3.8%

TABLE 4.2-49

SECONDARY CONTROL ASSEMBLY OPERATING PARAMETERS (THDV)

Flow Rates:

Flow Around Latch Seal:

Control Rod Flow 9,130 Lbs/Hr.

Bypass Flow Around Rod 9,330 Lbs/Hr.

Total Flow Around Latch Seal 18,460 Lbs/Hr.

Flow to Low Pressure Plenum 50,710 Lbs/Hr.

Total Assembly Flow 69,170 Lbs/Hr.

Hydraulic Scram-Assist Force 248 Lbs.

Total Heat Generation 57 KW

Peak Linear Power 4.0 KW/Ft.

Average Control Rod Outlet Temperature 829°F

Average Assembly Outlet Temperature 854°F

Peak Clad Mid-Wall Temperature

Nominal 858°F

Hot Spot 903°F

Absorber Pin Lifetime *

Average Gas Release Rate In Peak Pin *

Absorber Center Line Temperature

Nominal 1692°F

Hot Spot 1824°F

*Design not currently finalized; this information will be provided in the FSAR.

TABLE 4.2-50

AI FRICTIONAL DATA

	<u>Friction Efficients</u>			<u>Temperature (°F)</u>
	<u>Breakaway</u>	<u>Static</u>	<u>Dynamic</u>	
Inconel 718/LC-1C ^a on 316	0.54	0.45	0.53	1000
Inconel 718/Inconel 718	0.41	0.58	0.73	1000
LC-1C/LC-1C on 316, ND ^b	0.61	0.34	0.36	1000
LC-1C/LC-1C on 718, ND	0.73	0.37	0.42	1000

- a. LC-1C is CR₃C₂ with 15% NiCr binder, D-gun coated.
 b. ND - Non-dimensional finish.

TABLE 4.2-51

SELF-WELDING TEST RESULTS AFTER 3 AND 6 MONTHS
AT 1050°F IN FLOWING SODIUM

Test No. ^a	Material Combination	Compressive Contact Load ^b lb/in (psi)	Test Period Month	Sample Geometry	Breakaway Force (lb)
7-54	I-718 on I-718	24,300 (150,000)	6	Curve on Flat	>0
7-55	I-718 on I-718	14,200 (16,000)	6	Curve on Curve	368 ^c
7-57	Stellite 6 on Stellite 6	9,600 (12,000)	6	Curve on Curve	368 ^c
7-51	Stellite 156 on Stellite 156	31,840 (16,000)	3	Flat on Flat	1,720 ^c

- a. As given in WDTRS #1.27 Revision 5, Table 7.
- b. Line contact load based on Hertzian stress given in parentheses. The Hertz contact stresses in the SCRS latch are approximately 70,000 psi.
- c. To be evaluated after disassembly of the test chamber before a firm conclusion of self-welding can be made.

TABLE 4.2-52

REFERENCES SUPPORTING CRBRP FUEL ROD LOADING
(See Response to Question 241.68)

Loading Category	FFTF Design	EBR-II Irradiation	Exemplary References	
			U.S. LMFBF Program	Foreign LMFBF Program
1. Fuel-Cladding Differential Expansion	59	62	64, 65	67, 68
2. Fission Gas Released from Fuel	59	61, 63	64, 65	67, 68
3. Differential Thermal & Irradiation Induced Expansion	59	---	64	67, 68
4. Support System Interaction				
A. Fuel Rod-Spacer	59	63	64	67
B. Bundle-Duct	59	63	64	---
5. Flow Induced Vibration	59	---	66	67
6. Accident Loading				
A. Fission Gas Ejection	60	---	65	69
B. Fuel Coolant Interaction	60	---	---	69

4.2-420

Amend. 51
Sept. 1979

TABLE 4.2-53

REACTOR INTERNALS IRRADIATION ENVIRONMENT & DESIGN CRITERIA

CRBRP Structural Component	Sub-Component	Material	Irradiation Environment				Design Criteria	
			Irrad. Temp. Range (a)		Maximum Total Fluence (n/cm ²) ^(b)	Average Neutron Energy (MeV)	Minimum Residual Total Elongation (%)	Energy ^(c) Dependent Fluence Limit (n/cm ²)
			Lower Bound (°F)	Upper Bound (°F)				
Core Former Structure	Support Ring	SS304	700	950	6.3×10^{21}	0.03	10	4.1×10^{22}
	Support Ring Weld	SS308	700	950	6.3×10^{21}	0.03	10	9.4×10^{21}
	Lower Former Ring	SS316	700	900	1.6×10^{22}	0.08	10	3.5×10^{22}
Fixed Radial Shield	Segment at Core Midplane	SS316	700	900	3.6×10^{22}	0.08	10	3.6×10^{22}
	Lower Retention Pin	INC718	700	700	3.6×10^{20}	0.04	10	5.0×10^{21}
Lower Inlet Module	Holddown Ring	SS304	700	800	5.4×10^{21}	0.06	10	2.3×10^{22}
	Receptacle	INC718	700	800	4.1×10^{21}	0.05	10	5.0×10^{21}
	Body/Stem Weld	SS308	700	800	2.5×10^{19}	0.03	10	1.0×10^{22}
Bypass Flow Module	Top Forging	SS304	700	800	1.2×10^{21}	0.04	10	3.3×10^{22}
	Locking Collar	INC718	700	800	1.5×10^{21}	0.04	10	5.0×10^{21}
	Seismic Lug Weld	SS308	700	800	5.4×10^{20}	0.04	10	1.0×10^{21}

4.2-421

57

57

Amend. 57
Nov. 1980

57 | 54

TABLE 4.2-53 (Continued)

REACTOR INTERNALS IRRADIATION ENVIRONMENT & DESIGN CRITERIA

CRBRP Structural Component	Sub-Component	Material	Irradiation Environment				Design Criteria	
			Irrad. Temp (a)		Maximum Total Fluence (n/cm ²) (b)	Average Neutron Energy (MeV)	Minimum Residual Total Elongation (%)	Energy Dependent Fluence Limit (n/cm ²) (c)
			Lower Bound (°F)	Upper Bound (°F)				
Core Support Structure	Core Barrel	SS304	700	850	6.0×10^{21}	0.12	10	1.3×10^{22}
	Core Barrel Weld	SS308	700	850	5.5×10^{21}	0.12	10	5.7×10^{21}
Fuel Transfer & Storage Assy	Tube	SS304	700	800	2.8×10^{21}	0.24	10	7.2×10^{21}
	Dashpot	INC718	700	800	2.6×10^{20}	0.08	10	5.0×10^{21}
Horizontal Baffle	Plate	SS316	700	1000	1.4×10^{20}	0.02	10	5.8×10^{22}
	Plate Weld	SS316/16-8-2	700	1000	1.4×10^{20}	0.02	10	2.9×10^{22}
	Entry Port Nozzle	INC718	700	1000	3.0×10^{20}	0.03	10	5.0×10^{21}
Upper Internals Structure	Inst. Post.	INC718	750	1200	4.3×10^{20}	0.05	10	1.0×10^{21}
	Core Inst.	SS316	750	1200	4.2×10^{20}	0.05	10	1.0×10^{21}
	Core Inst. Weld	SS316/16-8-2	750	1200	3.4×10^{20}	0.04	10	1.0×10^{21}
Control Rod Driveline	Thermal Shield	INC718	900	1200	2.9×10^{20}	0.03	10	1.0×10^{21}
	Compression Tube	SS304	900	1200			10	1.0×10^{21}

(a) Normal full power condition temperature limits rounded off to nearest 50° interval.

(b) Fluence based on typical equilibrium cycle average flux (nominal) for 22.5 full power years at 975 MWt and 3-stored fuel assemblies.

(c) Fluence limit based on lower bound energy dependent ductility/fluence trend lines at worst case irradiation temperature condition (700° or 1200°F)

4.2-422

Amend. 54
May 1980

TABLE 4.2-54

POSTIRRADIATION TENSILE PROPERTIES OF ANNEALED TYPE 304 STAINLESS STEEL

EXPERIMENT IDENTIFICATION	SPECIMEN IDENTIFICATION	IRRADIATION CONDITIONS							TEST CONDITIONS		TEST RESULTS ^(a)							
		EDR COORDINATES R, cm	II COORDINATES Z, cm	FLUENCE, $10^{22} n/cm^2$ ($E > 10^{-10}$ MeV)	FLUENCE, $10^{22} n/cm^2$ ($E < 0.1$ MeV)	dpa	E, MeV	TEMP. OF.	TEMP. OF.	STRAIN RATE, SEC ⁻¹	σ_u , 1000 psi	σ_y , 1000 psi	σ_u , 1000 psi	ϵ_u (PLASTIC)	ϵ_t	RA	TEST IDENTIFICATION	COMMENTS ^(b)
X009	A5-2	17.0	+19.6	1.1	0.84	3.8	0.615	900	70	2.7x10 ⁻⁵	39.4	70.0	100.5	0.541	0.618	0.769	HO 6076	
	A5-2	16.5	+19.6	1.1	0.85	3.8	0.615	900	572	2.7x10 ⁻⁵	50.0	66.5	77.4	0.100	0.161	0.670	HO 6080	
	A5-4	17.0	+4.3	1.7	1.5	7.7	0.837	1030	572	2.7x10 ⁻⁵	30.4	39.0	67.9	0.205	0.273	0.691	HO 6081	
	A2-3	16.6	+11.9	1.5	1.3	6.2	0.771	970	700	2.7x10 ⁻⁵	26.2	35.3	66.1	0.222	0.279	0.667	HO 6079	
	A2-4	16.6	+4.3	1.7	1.6	7.6	0.839	970	800	2.7x10 ⁻⁵	26.5	35.9	64.7	0.225	0.284	0.657	HO 6082	
	A5-5	17.0	+9.7	1.6	1.4	6.7	0.795	970	900	2.7x10 ⁻⁵	27.2	39.1	64.0	0.197	0.243	0.576	HO 6086	
	A5-3	17.0	+11.9	1.5	1.3	6.1	0.769	960	1000	2.7x10 ⁻⁵	24.6	39.3	56.4	0.120	0.143	0.305	HO 6087	
	A6-4	16.5	+4.3	1.7	1.6	7.8	0.840	930	1100	2.7x10 ⁻⁵	19.9	36.3	46.5	0.661	0.680	0.224	HO 6117	
	A1-3	17.5	+11.9	1.4	1.2	6.0	0.765	900	1200	2.7x10 ⁻⁵	13.2	30.1	37.6	0.037	0.054	0.147	HO 6094	
	A1-4	17.5	+4.3	1.7	1.5	7.6	0.834	1000	1300	2.7x10 ⁻⁵	15.7	27.3	29.9	0.020	0.050	0.108	HO 6103	
	A6-5	16.5	-9.7	1.6	1.4	7.1	0.800	1000	1400	2.7x10 ⁻⁵	14.2	21.1	21.6	0.006	0.060	0.157	HO 6078	
	A6-3	16.5	+11.9	1.5	1.3	6.3	0.772	900	1500	2.7x10 ⁻⁵	9.8	13.1	13.2	0.004	0.094	0.157	HO 6077	
	A2-2	16.6	+19.6	1.1	0.85	3.8	0.614	1000	1600	2.7x10 ⁻⁵	4.0	7.7	8.5	0.034	0.091	0.100	HO 6116	
	X010	A3-2T	29.9	+20.3	2.3	1.7	7.1	0.495	820	800	3x10 ⁻⁵	60.8	60.8	80.3	0.036	0.082	0.578	HO 7719
A3-4T		29.9	-8.9	3.4	2.7	12.1	0.615	860	800	3x10 ⁻⁵	70.6	86.4	88.4	0.013	0.050	0.471	HO 7721	
A3-3T		29.9	+5.1	3.5	2.9	12.9	0.635	860	800	3x10 ⁻⁵	66.2	80.9	83.4	0.018	0.059	0.510	HO 7720	
X014	12-5-1	6.0	-14.7	1.1	0.94	4.6	0.753	980	70	4x10 ⁻⁵	48.3	75.4	102.9	0.365	0.457	0.730	HO 6192	
	12-4-2	6.0	-4.7	1.3	1.2	6.0	0.843	950	572	4x10 ⁻⁵	37.3	52.9	75.6	0.161	0.193	0.529	HO 6191	
	12-4-1	6.0	-4.7	1.3	1.2	6.0	0.843	960	932	4x10 ⁻⁵	28.7	47.0	66.6	0.106	0.220	0.460	HO 6190	FEP
	12-2-2	6.0	+17.0	0.93	0.78	3.7	0.708	950	932	4x10 ⁻⁵	11.7	--	60.0	0.354	0.404	0.573	HO 6186	
	12-2-1	6.0	+17.0	0.93	0.78	3.7	0.708	950	930	4x10 ⁻⁵	47.1	61.1	69.8	0.004	0.139	0.512	HO 6187	
	12-1-2	6.0	+27.5	0.61	0.43	1.8	0.465	850	1010	4x10 ⁻⁵	27.1	47.0	60.8	0.204	0.260	0.512	HO 6185	FEP
	12-1-1	6.0	+27.5	0.61	0.43	1.8	0.465	850	1110	4x10 ⁻⁵	18.0	37.6	49.3	0.151	0.171	0.384	HO 6185	FEP
	9-4-2	3.9	-3.8	1.4	1.2	6.1	0.844	950	1200	4x10 ⁻⁵	11.2	15.8	33.3	0.163	0.172	0.319	HO 6168	FEP
	9-4-1	3.9	-3.8	1.4	1.2	6.1	0.844	975	1200	4x10 ⁻⁵	21.3	30.0	39.1	0.028	0.108	0.213	HO 6167	FEP
	9-1-2	3.9	+27.5	0.62	0.43	1.8	0.464	850	1700	4x10 ⁻⁵	17.3	27.6	37.8	0.174	0.200	0.343	HO 6164	FEP
	9-2-2	3.9	+17.0	0.94	0.78	3.7	0.710	900	1380	4x10 ⁻⁵	9.0	12.4	18.1	0.076	0.105	0.165	HO 6169	FEP
9-2-1	3.9	+17.0	0.94	0.78	3.7	0.710	940	1380	4x10 ⁻⁵	9.4	14.5	19.4	0.008	0.143	0.222	HO 6165	FEP	
X018	1-5-41	4.2	+45.2	0.89	0.47	1.7	0.272	825	800	3x10 ⁻⁵	42.3	53.0	72.7	0.214	0.295	0.659	HO 7490	
	1-5-40	4.2	+45.2	0.89	0.47	1.7	0.272	825	800	3x10 ⁻⁵	36.9	53.2	73.9	0.106	0.143	0.618	HO 7729	
	1-6-40	4.2	+40.5	1.1	0.61	2.3	0.310	825	800	3x10 ⁻⁵	40.2	58.7	74.3	0.082	0.120	0.603	HO 7730	
	1-6-41	4.2	+40.5	1.1	0.61	2.3	0.310	825	900	3x10 ⁻⁵	35.2	56.6	69.0	0.149	0.242	0.600	HO 7491	
	1-6-42	4.2	+40.5	1.1	0.61	2.3	0.310	825	1000	3x10 ⁻⁵	47.2	54.7	61.7	0.100	0.166	0.415	HO 7492	
	1-6-43	4.2	+40.5	1.1	0.61	2.3	0.310	825	1100	3x10 ⁻⁵	35.1	48.6	52.0	0.020	0.046	0.138	HO 7675	
	1-7-41	4.2	+35.7	1.3	0.81	3.1	0.350	825	900	3x10 ⁻⁵	44.7	61.3	70.7	0.121	0.218	0.650	HO 7493	
	1-8-41	4.2	+30.9	1.6	1.1	4.2	0.414	845	1000	3x10 ⁻⁵	46.6	61.4	65.8	0.072	0.117	0.789	HO 7494	
	1-10-42	4.2	+21.4	2.3	1.8	7.8	0.520	1010	900	3x10 ⁻⁵	50.4	66.3	73.4	0.021	0.160	0.455	HO 7495	
	1-10-41	4.2	+21.4	2.3	1.8	7.8	0.520	1010	1000	3x10 ⁻⁵	53.0	63.8	66.6	0.022	0.053	0.224	HO 7076	
	1-10-40	4.2	+21.4	2.3	1.8	7.8	0.520	1010	1100	3x10 ⁻⁵	50.0	60.1	60.7	0.003	0.013	0.098	HO 7077	
	1-11-41	4.2	+16.6	2.8	2.3	11.1	0.721	1060	1100	3x10 ⁻⁵	26.0	38.1	39.7	0.038	0.034	0.155	HO 7078	
	1-12-41	4.2	+11.9	3.4	2.9	14.3	0.787	1110	1100	3x10 ⁻⁵	38.6	44.5	48.7	0.017	0.032	0.155	HO 7079	
	1-14-41	4.2	+2.4	3.9	3.5	17.8	0.847	1140	1200	3x10 ⁻⁵	24.4	34.2	43.8	0.046	0.065	0.122	HO 7060	
X019	A26-2T	25.4	+53.3	0.63	0.30	1.0	0.208	800	800	2.7x10 ⁻⁵	26.9	35.3	71.5	0.104	0.142	0.692	HO 7731	
	A26-4T	25.4	+36.8	1.2	0.71	2.7	0.325	780	800	2.7x10 ⁻⁵	25.3	35.1	75.7	0.110	0.141	0.621	HO 7732	
	A26-5T	25.4	+27.9	1.6	1.1	4.5	0.427	770	800	2.7x10 ⁻⁵	52.2	71.1	91.5	0.043	0.072	0.527	HO 7733	
	A26-7T	25.4	+15.2	2.6	2.2	9.8	0.653	750	800	2.7x10 ⁻⁵	77.8	97.8	98.5	0.003	0.036	0.429	HO 7734	
	A26-8T	25.4	+6.4	3.3	2.8	13.5	0.735	730	800	2.7x10 ⁻⁵	93.9	126.3	126.6	0.003	0.033	0.454	HO 7735	
	A26-9T	25.4	-1.3	3.5	3.0	14.3	0.750	720	800	2.7x10 ⁻⁵	90.9	128.8	129.3	0.003	0.031	0.475	HO 7735	

4.2-423

Amend. 51
1070

TABLE 4.2-54 (CONTINUED)

POSTIRRADIATION TENSILE PROPERTIES OF ANNEALED TYPE 304 STAINLESS STEEL

EXPERIMENT IDENTIFICATION	SPECIMEN IDENTIFICATION	IRRADIATION CONDITIONS						TEST CONDITIONS		TEST RESULTS (a)							TEST IDENTIFICATION	COMMENTS (b)
		COORDINATES R, CM	Z, CM	FLUENCE, 10 ²² NEUTRONS/CM ² (E > 0.1 MeV)	FLUENCE, 10 ²² NEUTRONS/CM ² (E < 0.1 MeV)	DOSE	E, MeV	TEMP. OF, °C	TEMP. OF, °F	STRAIN RATE, SEC ⁻¹	σ _p , 1000 psi	σ _y , 1000 psi	σ _u , 1000 psi	ε _u (PLASTIC)	ε _t	RA		
A222	9624-1	31.8	+50.0	0.23	0.12	0.4	0.216	815	600	2	6.8	27.9	62.9	0.351	0.410	0.699	HO 7578	
	14024-1	29.7	-45.2	0.31	0.16	0.5	0.207	715	900	3x10 ⁻⁵	25.2	34.3	56.6	0.292	0.364	0.756	HO 7498	
	14024-2	29.7	-45.2	0.31	0.16	0.5	0.209	715	1000	3x10 ⁻⁵	30.0	37.4	57.2	0.260	0.341	0.594	HO 7459	
	9624-5	31.8	-35.8	0.35	0.20	0.7	0.245	725	500	3x10 ⁻⁵	20.5	31.9	60.9	0.222	0.287	0.642	HO 6705	
	14024-3	29.7	-39.9	0.40	0.22	0.8	0.249	725	1000	3x10 ⁻⁵	9.8	16.4	54.5	0.322	0.300	0.640	HO 6707	
	14024-4	29.7	-38.8	0.40	0.22	0.8	0.245	725	1100	3x10 ⁻⁵	12.2	14.5	44.4	0.193	0.224	0.748	HO 6708	
	14024-5	29.7	-35.8	0.40	0.22	0.8	0.248	725	1200	3x10 ⁻⁵	9.8	15.0	33.0	0.065	0.169	0.171	HO 6709	
	9624-4	31.8	-34.1	0.43	0.26	0.9	0.275	725	500	3x10 ⁻⁵	13.4	19.3	33.4	0.222	0.300	0.725	HO 6706	
	14024-3	29.7	-34.1	0.48	0.29	1.0	0.283	725	700	3x10 ⁻⁵	12.0	20.2	33.2	0.321	0.378	0.736	HO 6710	
	10024-1	32.9	-27.8	0.52	0.33	1.2	0.320	750	800	3x10 ⁻⁵	32.5	46.5	67.0	0.160	0.231	0.675	HO 6713	
	10024-2	32.9	-27.8	0.52	0.33	1.2	0.323	750	900	3x10 ⁻⁵	32.6	50.0	64.9	0.179	0.257	0.672	HO 6714	
	9624-5	31.8	-27.8	0.55	0.25	1.3	0.334	735	1000	3x10 ⁻⁵	45.3	50.0	60.5	0.172	0.235	0.545	HO 7465	
	9624-3	31.8	-27.8	0.55	0.36	1.3	0.334	735	1200	3x10 ⁻⁵	27.2	34.4	35.2	0.009	0.072	0.155	HO 6726	
	10024-3	30.8	-27.8	0.56	0.38	1.4	0.383	820	1000	8	3.2	22.3	57.0	0.270	0.339	0.650	HO 7577	
	10024-1	30.8	-27.8	0.56	0.39	1.4	0.383	820	1000	14	4.8	19.1	51.9	0.329	0.376	0.625	HO 7575	
	10024-1	32.9	-23.0	0.62	0.42	1.6	0.375	750	500	3x10 ⁻⁵	44.4	55.5	75.0	0.144	0.214	0.704	HO 6711	
	10024-2	32.9	-23.0	0.62	0.42	1.6	0.375	750	700	3x10 ⁻⁵	36.6	54.9	72.3	0.143	0.215	0.659	HO 6712	
	15024-1	30.8	-23.0	0.70	0.49	1.9	0.413	740	1100	3x10 ⁻⁵	31.8	44.6	47.4	0.079	0.061	0.314	HO 7457	
13024-4	26.6	+16.8	0.91	0.72	3.1	0.579	955	900	3x10 ⁻⁵	16.0	23.7	59.3	0.233	0.272	0.398	HO 6703		
13024-1	23.6	-16.8	0.97	0.77	3.3	0.577	955	1000	3x10 ⁻⁵	21.3	28.9	54.2	0.154	0.211	0.447	HO 6702		
A22	A28-2	27.3	+45.3	0.16	0.098	0.3	0.251	800	800	3x10 ⁻⁵	10.5	19.4	61.2	0.352	0.425	0.647	HO 6493	ED
	A28-3	27.3	+35.1	0.24	0.15	0.6	0.333	800	1000	3x10 ⁻⁵	56.2	22.4	66.2	0.331	0.418	0.641	HO 6494	ED
	A28-4	27.3	+24.9	0.35	0.25	1.0	0.459	800	1000	3x10 ⁻⁵	20.1	31.2	55.4	0.245	0.331	0.603	HO 6495	ED
	A28-8	27.3	-12.7	0.54	0.44	2.0	0.647	800	1000	3x10 ⁻⁵	32.7	46.2	60.8	0.157	0.235	0.603	HO 6496	ED
A24	21024-5	30.0	-50.0	0.76	0.37	1.2	0.192	725	800	3.5x10 ⁻³	36.6	43.3	67.2	0.195	0.247	0.715	HO 6535	
	21024-1	30.0	-50.0	0.76	0.37	1.2	0.192	725	800	5x10 ⁻²	40.7	45.9	64.6	0.157	0.200	0.634	HO 6532	
	22024-1	31.3	-50.0	0.70	0.35	1.1	0.193	725	800	1	35.7	45.9	64.9	0.177	0.244	0.650	HO 6540	
	22024-3	31.3	-50.0	0.70	0.35	1.1	0.193	725	800	10	41.1	45.6	65.6	0.195	0.267	0.702	HO 6545	
	21024-4	30.0	-50.0	0.76	0.37	1.2	0.192	725	1000	3.5x10 ⁻²	37.0	42.1	58.5	0.150	0.199	0.610	HO 6531	
	21024-2	30.0	-50.0	0.76	0.37	1.2	0.192	725	1000	5x10 ⁻²	42.3	46.2	55.6	0.161	0.240	0.705	HO 6533	
	22024-2	31.3	-50.0	0.70	0.35	1.1	0.193	725	1000	1	42.0	48.4	61.5	0.147	0.210	0.650	HO 6537	
	22024-4	31.3	-50.0	0.70	0.35	1.1	0.193	725	1000	10	37.9	44.3	59.5	0.163	0.241	0.672	HO 6549	
	16024-1	32.7	+50.0	0.67	0.34	1.2	0.215	825	800	3x10 ⁻⁵	28.9	35.3	65.5	0.242	0.297	0.699	HO 6566	
	16024-2	32.7	+50.0	0.67	0.34	1.2	0.215	825	1000	3x10 ⁻⁵	26.8	33.7	54.5	0.107	0.236	0.333	HO 6565	
	21024-1	29.0	-34.1	1.5	0.88	3.1	0.262	745	800	3x10 ⁻⁵	47.5	51.7	71.4	0.220	0.277	0.671	HO 6563	
	21024-2	29.0	-34.1	1.5	0.88	3.1	0.262	745	1000	3x10 ⁻⁵	37.4	45.7	50.8	0.112	0.158	0.195	HO 6562	
	16024-3	32.7	+34.1	1.3	0.77	2.8	0.306	825	800	3.5x10 ⁻²	46.1	51.6	67.1	0.143	0.199	0.675	HO 6529	
	16024-1	32.7	+34.1	1.3	0.77	2.8	0.306	825	800	5x10 ⁻²	43.3	48.6	65.1	0.125	0.190	0.447	HO 6534	
	16024-1	32.7	+34.1	1.3	0.80	2.9	0.311	825	800	1	52.1	53.9	72.3	0.140	0.207	0.607	HO 6537	
	22024-1	31.3	+34.1	1.4	0.84	3.1	0.317	830	600	1	52.6	62.0	72.1	0.090	0.157	0.779	HO 6547	
	22024-2	31.3	+34.1	1.4	0.84	3.1	0.317	830	800	10	55.5	60.3	71.9	0.133	0.190	0.621	HO 6546	
	16024-3	32.1	+34.1	1.3	0.80	2.9	0.311	825	600	10	53.9	60.8	72.6	0.193	0.311	0.631	HO 6551	
	16024-4	32.7	+34.1	1.3	0.80	2.9	0.311	825	1000	3.5x10 ⁻³	42.7	46.9	58.9	0.157	0.230	0.748	HO 6548	
	16024-2	32.7	+34.1	1.3	0.77	2.8	0.306	825	1000	5x10 ⁻²	46.9	52.5	55.5	0.102	0.265	0.683	HO 6525	
	16024-5	32.1	+34.1	1.3	0.80	2.9	0.311	825	1000	5x10 ⁻²	45.5	53.3	65.9	0.127	0.179	0.745	HO 6526	
	16024-7	32.1	+34.1	1.3	0.80	2.9	0.311	825	1000	1	53.8	57.9	66.2	0.102	0.170	0.639	HO 6528	
	16024-5	32.7	+34.1	1.3	0.77	2.8	0.311	825	1000	1	43.3	48.9	62.8	0.140	0.195	0.683	HO 6530	
	16024-4	32.1	+34.1	1.3	0.80	2.9	0.311	825	1000	10	48.0	52.8	65.4	0.140	0.210	0.672	HO 6543	
22024-1	31.3	+23.0	2.0	1.4	5.6	0.429	855	800	3x10 ⁻⁵	36.6	50.5	69.8	0.099	0.127	0.619	HO 7727		
22024-3	31.3	+23.0	2.0	1.4	5.6	0.429	855	600	3x10 ⁻⁵	51.9	64.4	74.6	0.137	0.193	0.659	HO 6564		

4.2-424

Amend. 51
Sept. 1979

TABLE 4.2-54 (CONTINUED)

POSTIRRADIATION TENSILE PROPERTIES OF ANNEALED TYPE 304 STAINLESS STEEL

EXPERIMENTAL IDENTIFICATION	SPECIMEN IDENTIFICATION	IRRADIATION CONDITIONS							TEST CONDITIONS		TEST RESULTS (a)							
		Irr. II COORDINATES R, cm Z, cm		FLUENCE $10^{22} n/cm^2$ (E > 0.1 MeV)	FLUENCE $10^{22} n/cm^2$ (E > 0.1 MeV)	dpa	E, MeV	TEMP. OF	TEMP. OF	STRAIN RATE SEC ⁻¹	σ_p , 1000 psi	σ_y , 1000 psi	σ_u , 1000 psi	ϵ_u (PLASTIC)	ϵ_t	RA	TEST IDENTIFICATION	COMMENTS (b)
1041 (CONT.)	17724-3	33.3	+23.0	1.8	1.3	4.7	0.388	855	600	3.5×10^{-3}	45.9	53.4	69.2	0.141	0.197	0.007	HO 9527	
	17724-5	33.3	+23.0	1.8	1.3	4.7	0.388	855	800	5×10^{-2}	48.4	55.1	65.8	0.144	0.196	0.057	HO 9525	
	16724-1	32.7	+23.0	1.9	1.3	5.0	0.400	875	800	1	47.5	53.2	70.2	0.147	0.213	0.634	HO 9542	
	16724-3	32.7	+23.0	1.9	1.3	5.0	0.400	875	800	10	46.2	54.3	71.1	0.140	0.205	0.650	HO 9552	
	22724-4	31.3	+23.0	2.0	1.4	5.6	0.429	855	1000	2×10^{-5}	59.4	59.7	63.5	0.063	0.099	0.398	HO 9551	
	17724-4	33.3	+23.0	1.8	1.3	4.7	0.388	855	1000	3.5×10^{-3}	43.7	48.9	60.5	0.116	0.171	0.757	HO 9526	
	17724-2	33.3	+23.0	1.8	1.3	4.7	0.388	855	1000	5×10^{-2}	47.6	51.7	61.5	0.150	0.237	0.693	HO 9524	
	16724-2	32.7	+23.0	1.9	1.3	5.0	0.400	875	1000	1	43.7	50.6	64.1	0.166	0.253	0.603	HO 9541	
	16724-5	32.7	+23.0	1.9	1.3	5.0	0.400	875	1000	1	47.0	50.9	55.8	0.126	0.174	0.675	HO 9548	
	16724-4	32.7	+23.0	1.9	1.3	5.0	0.400	875	1000	10	38.9	48.4	62.4	0.163	0.234	0.669	HO 9544	
22724-2	31.3	+23.0	2.0	1.4	5.6	0.429	855	1200	3×10^{-5}	31.7	37.6	---	0.017	0.029	0.228	HO 7726		
1067	35-T-021A	15.2	-57.6	0.12	0.05	0.2	0.162	700	600	3×10^{-5}	13.8	21.7	65.0	0.445	0.526	0.046	HO 7507	
	35-T-027A	14.4	-57.6	0.12	0.05	0.2	0.162	700	700	3×10^{-5}	13.7	21.7	64.5	0.446	0.527	0.051	HO 7554	
	35-T-018A	15.2	-57.6	0.11	0.05	0.2	0.153	610	600	3×10^{-5}	10.0	16.5	64.6	0.443	0.519	0.634	HO 7555	
	35-T-019A	14.4	-57.6	0.11	0.05	0.2	0.154	810	900	3×10^{-5}	12.0	20.1	61.0	0.364	0.440	0.656	HO 7556	
	35-T-024A	15.2	-21.0	0.50	0.38	1.7	0.576	745	700	3×10^{-5}	40.7	51.2	74.3	0.230	0.301	0.594	HO 7516	
	35-T-043A	14.4	-21.0	0.51	0.39	1.7	0.570	745	900	3×10^{-5}	38.1	50.0	67.5	0.249	0.332	0.529	HO 7518	
	35-T-027A	15.2	-21.0	0.46	0.36	1.6	0.558	795	600	3×10^{-5}	36.0	49.4	72.0	0.260	0.342	0.640	HO 7512	
	35-T-010A	14.4	-21.0	0.47	0.37	1.6	0.559	795	600	3×10^{-5}	33.8	49.6	69.8	0.215	0.305	0.576	HO 7515	
	37-4-21	13.7	-2.3	0.64	0.76	3.8	0.057	975	1100	3×10^{-5}	20.3	33.5	46.6	0.049	0.066	0.258	HO 7566	
	35-T-030	15.2	-2.3	0.62	0.73	3.7	0.050	975	1100	3×10^{-5}	19.5	26.2	45.0	0.035	0.056	0.138	HO 7728	
1137	87-06	15.7	-54.6	0.17	0.07	0.2	0.174	710	650	4.5×10^{-5}	13.8	20.7	69.0	0.232	0.266	0.650	HO 8175	
	87-03	15.7	-54.6	0.17	0.07	0.2	0.174	710	900	4.5×10^{-5}	12.6	18.8	62.9	0.245	0.273	0.693	HO 8177	
	87-10	15.7	-52.1	0.18	0.08	0.3	0.184	710	1200	4.5×10^{-5}	11.3	16.3	35.6	0.117	0.155	0.244	HO 8179	
	87-07	15.7	-49.2	0.21	0.10	0.3	0.198	710	600	4.5×10^{-5}	17.5	24.7	68.1	0.220	0.256	0.650	HO 8176	
	87-14	15.7	-49.2	0.21	0.10	0.3	0.190	710	900	3×10^{-5}	19.5	26.0	62.0	0.111	0.170	0.691	HO 8178	
	87-09	15.7	-49.2	0.21	0.10	0.3	0.199	710	1000	4.5×10^{-5}	16.6	23.0	60.3	0.201	0.244	0.642	HO 8173	
	84-1	15.1	-43.2	0.26	0.13	0.5	0.230	725	800	4.5×10^{-5}	8.9	10.2	65.5	0.260	0.299	0.642	HO 8113	
	84-02	15.1	-36.1	0.32	0.18	0.6	0.275	725	1200	4.5×10^{-5}	9.1	13.6	34.8	0.138	0.165	0.241	HO 8174	
	84-11	15.1	-35.2	0.31	0.22	0.8	0.362	805	900	4.5×10^{-5}	26.0	36.9	70.1	0.174	0.214	0.619	HO 8159	
	84-13	15.1	-35.2	0.34	0.22	0.8	0.362	805	1000	4.5×10^{-5}	23.3	34.1	53.3	0.165	0.199	0.577	HO 8171	
	84-12	15.1	-35.2	0.34	0.22	0.8	0.362	805	1000	3×10^{-5}	24.4	31.7	57.1	0.230	0.363	0.600	HO 8169	
	84-16	15.1	-35.2	0.34	0.22	0.8	0.362	805	1000	3×10^{-5}	24.6	33.8	50.2	0.243	0.299	0.492	HO 8165	
	84-14	15.1	-32.7	0.33	0.25	1.0	0.399	805	1200	4.5×10^{-5}	16.6	25.9	36.4	0.062	0.119	0.275	HO 8172	
	84-10	15.1	-29.8	0.42	0.29	1.2	0.429	805	600	4.5×10^{-5}	33.4	45.0	76.8	0.192	0.261	0.610	HO 8160	
	84-12	15.1	-29.8	0.42	0.29	1.2	0.429	805	900	4.5×10^{-5}	25.6	42.2	66.9	0.132	0.176	0.645	HO 8170	
	84-15	15.1	-29.8	0.42	0.29	1.2	0.429	805	1000	3×10^{-6}	24.4	37.2	55.9	0.152	0.183	0.309	HO 8164	
	84-17	15.1	-29.8	0.42	0.29	1.2	0.429	805	1000	3×10^{-4}	30.9	39.5	60.2	0.221	0.281	0.575	HO 8166	
1195	84-30	3.9	+31.0	0.39	0.25	1.0	0.413	770	70	3×10^{-5}	37.7	54.1	92.2	0.646	0.733	0.036	HO 6537	304L, ED
	84-31	3.9	+31.0	0.39	0.25	1.0	0.413	770	450	3×10^{-5}	34.7	42.3	55.7	0.241	0.312	0.740	HO 6535	304L, ED
	84-32	3.9	+31.0	0.39	0.25	1.0	0.413	770	850	3×10^{-5}	38.5	41.6	62.4	0.173	0.240	0.754	HO 6530	304L, ED
	84-25	3.9	+35.2	0.45	0.32	1.3	0.465	765	450	3×10^{-5}	39.0	53.8	74.3	0.180	0.273	0.756	HO 6542	304L, ED
	84-26	3.9	+25.2	0.45	0.32	1.3	0.466	765	650	3×10^{-5}	39.8	51.1	65.5	0.145	0.204	0.767	HO 6541	304L, ED
	84-27	3.9	-16.7	0.72	0.63	3.0	0.712	700	70	3×10^{-5}	63.4	84.6	102.0	0.350	0.455	0.797	HO 6539	304L, ED
	84-3	3.9	-16.7	0.72	0.63	3.0	0.712	700	450	3×10^{-5}	58.5	75.6	83.5	0.081	0.158	0.715	HO 9755	304L, ED
	84-4	3.9	-16.7	0.72	0.63	3.0	0.712	700	700	3×10^{-5}	52.0	77.2	85.9	0.078	0.131	0.642	HO 6531	304L, ED
	84-5	3.9	-16.7	0.72	0.63	3.0	0.712	700	850	3×10^{-5}	54.9	66.5	70.1	0.071	0.140	0.631	HO 6532	304L, ED
	84-12	3.9	-16.7	0.72	0.63	3.0	0.712	700	1000	3×10^{-5}	49.6	59.3	60.7	0.052	0.130	0.645	HO 6533	304L, ED
	84-15	3.9	-7.1	0.95	0.82	4.1	0.830	715	70	3×10^{-5}	71.5	101.6	112.4	0.334	0.494	0.772	HO 6534	304L, ED

4.2-425

Amend. 51
Sept. 1979

TABLE 4.2-54 (CONTINUED)

POSTIRRADIATION TENSILE PROPERTIES OF ANNEALED TYPE 304 STAINLESS STEEL

EXPERIMENT IDENTIFICATION	SPECIMEN IDENTIFICATION	IRRADIATION CONDITIONS						TEST CONDITIONS		TEST RESULTS (a)									
		EBR COORDINATES R, cm	Z, cm	FLUENCE, $10^{22} n/cm^2$ (E-M)	FLUENCE, $10^{22} n/cm^2$ (E-M)	dpa	E, MeV	TEMP., OF	TEMP., OF	STRAIN RATE, SEC ⁻¹	σ_b , 1000 psi	σ_y , 1000 psi	σ_u , 1000 psi	ϵ_u (PLASTIC)	ϵ_t	RA	TEST IDENTIFICATION	COMMENTS (c)	
I195 (CONT.)	84-17	3.9	-7.1	0.95	0.82	4.1	0.830	715	450	3x10 ⁻⁵	73.2	97.6	104.9	0.032	0.072	0.211	HO 6593	304L, ED	
	84-18	3.9	-7.1	0.95	0.82	4.1	0.830	715	700	3x10 ⁻⁵	61.8	84.6	85.0	0.033	0.090	0.634	HO 6535	304L, ED	
	84-19	3.9	-7.1	0.95	0.82	4.1	0.830	715	850	3x10 ⁻⁵	64.2	78.9	79.2	0.011	0.072	0.211	HO 6539	304L, ED	
	84-1	3.9	-24.2	0.40	0.23	0.9	0.327	835	600	3x10 ⁻⁵	24.0	38.9	70.7	0.343	0.407	0.659	HO 9753	ED	
	84-2	3.9	-24.2	0.40	0.23	0.9	0.327	835	700	3x10 ⁻⁵	16.7	25.2	68.1	0.345	0.451	0.675	HO 9754	ED	
	84-3	3.9	-24.2	0.40	0.23	0.9	0.327	835	800	3x10 ⁻⁵	24.0	33.1	65.1	0.324	0.347	0.715	HO 9755	ED	
	84-4	3.9	-24.2	0.40	0.23	0.9	0.327	835	900	3x10 ⁻⁵	29.9	36.3	63.9	0.294	0.365	0.656	HO 9756	ED	
	44-3	5.8	+49.6	0.20	0.10	0.4	0.242	875	900	3x10 ⁻⁵	20.3	26.4	65.9	0.294	0.354	0.551	HO 9756	ED	
	44-4	5.8	+49.6	0.20	0.10	0.4	0.242	875	1000	3x10 ⁻⁵	18.3	24.6	61.8	0.245	0.322	0.325	HO 9756	ED	
	44-1	3.9	-24.4	0.40	0.30	1.2	0.394	835	600	3x10 ⁻⁵	27.3	36.4	69.5	0.301	0.348	0.694	HO 9757	ED	
	44-2	3.9	-24.4	0.40	0.30	1.2	0.394	835	1000	3x10 ⁻⁵	25.8	36.2	61.7	0.257	0.285	0.490	HO 9759	ED	
	43-1	3.9	-27.0	0.53	0.37	1.5	0.436	835	800	3x10 ⁻⁵	27.8	38.9	70.6	0.260	0.332	0.504	HO 9759	ED	
	43-2	3.9	-24.6	0.58	0.43	1.8	0.482	835	1000	3x10 ⁻⁵	35.5	43.6	61.2	0.192	0.241	0.333	HO 9759	ED	
	43-7	3.9	-17.9	0.70	0.56	2.5	0.607	835	800	3x10 ⁻⁵	44.6	54.6	74.5	0.155	0.230	0.546	HO 9759	ED	
	43-8	3.9	-19.5	0.70	0.56	2.5	0.607	835	1000	3x10 ⁻⁵	33.6	49.6	63.4	0.149	0.179	0.410	HO 9759	ED	
	43-15	5.8	+47.2	0.22	0.11	0.4	0.258	875	900	3x10 ⁻⁵	20.5	27.1	64.3	0.274	0.323	0.562	HO 9756	ED	
	43-14	5.8	+44.8	0.24	0.13	0.5	0.274	875	900	3x10 ⁻⁵	16.7	25.3	65.5	0.323	0.362	0.592	HO 9754	ED	
	43-13	5.8	+42.4	0.25	0.15	0.6	0.294	875	900	3x10 ⁻⁵	20.1	27.4	64.3	0.291	0.343	0.541	HO 9754	ED	
	43-9	5.8	+40.1	0.28	0.18	0.7	0.314	875	800	3x10 ⁻⁵	19.0	26.5	64.7	0.310	0.379	0.552	HO 9752	ED	
	43-10	5.8	+40.1	0.28	0.18	0.7	0.314	875	900	3x10 ⁻⁵	21.5	25.8	66.2	0.366	0.403	0.512	HO 9753	ED	
	43-11	5.8	+40.1	0.28	0.16	0.7	0.314	875	1000	3x10 ⁻⁵	18.6	24.6	58.1	0.240	0.303	0.438	HO 9753	ED	
	43-12	5.8	+40.1	0.28	0.19	0.7	0.314	875	1100	3x10 ⁻⁵	18.6	27.1	47.2	0.134	0.143	0.141	HO 9759	ED	
	43-1	3.9	-24.6	0.50	0.43	1.8	0.482	835	800	3x10 ⁻⁵	27.1	44.1	70.9	0.242	0.305	0.648	HO 9751	ED	
	46-7	3.9	-24.6	0.50	0.43	1.8	0.482	835	1000	3x10 ⁻⁵	33.3	45.9	64.3	0.195	0.248	0.373	HO 9752	ED	
	49-3	5.8	+49.6	0.20	0.10	0.4	0.242	875	900	3x10 ⁻⁵	18.0	27.1	69.0	0.367	0.446	0.631	HO 9758	ED	
	48-4	5.8	+49.6	0.20	0.10	0.4	0.242	875	1000	3x10 ⁻⁵	16.3	20.5	60.5	0.222	0.262	0.439	HO 9757	ED	
	I198	84-8	3.9	-47.1	0.77	0.36	1.4	0.242	780	450	3x10 ⁻⁵	31.7	45.2	60.5	0.191	0.253	0.739	HO 6549	304L, ED
		84-1	3.9	-47.1	0.77	0.36	1.4	0.242	750	600	3x10 ⁻⁵	36.9	43.3	59.3	0.167	0.243	0.746	HO 6547	304L, ED
84-9		3.9	-41.4	0.92	0.45	1.7	0.259	780	450	3x10 ⁻⁵	32.5	51.3	69.0	0.167	0.235	0.739	HO 6550	304L, ED	
84-10		3.9	-33.6	1.1	0.60	2.1	0.287	780	450	3x10 ⁻⁵	46.3	57.5	55.1	0.125	0.172	0.772	HO 6551	304L, ED	
84-7		3.9	-33.6	1.1	0.60	2.1	0.287	780	800	3x10 ⁻⁵	50.0	57.7	58.9	0.110	0.165	0.705	HO 6548	304L, ED	
47-1		5.9	-23.4	2.1	1.5	6.9	0.525	950	1000	3x10 ⁻⁵	24.5	36.7	50.5	0.081	0.102	0.139	HO 6511		
47-6		5.9	-18.7	2.5	2.0	9.3	0.660	900	1000	3x10 ⁻⁵	31.7	40.0	51.1	0.063	0.080	0.096	HO 6512		
47-7	5.9	-18.7	2.5	2.0	9.3	0.660	980	1000	3x10 ⁻⁵	33.3	40.6	59.3	0.15	0.201	0.591	HO 9310			
503 (CONT.)	2A-1	23.0	-31.5	1.8	1.1	4.1	0.329	700	700	6x10 ⁻⁵	52.4	85.8	90.5	0.025	0.047	0.439	HO 6454		
	2A-4	23.0	-31.5	1.8	1.1	4.1	0.329	700	900	6x10 ⁻⁵	66.3	79.5	80.5	0.013	0.024	0.550	HO 6453		
	2A-1	23.0	-31.5	1.5	1.1	4.1	0.329	700	1100	6x10 ⁻⁵	44.3	60.2	50.6	0.005	0.030	0.107	HO 6451		
	6A-4	23.0	-31.5	1.5	1.1	4.1	0.329	700	1300	6x10 ⁻⁵	14.6	21.1	26.6	0.053	0.094	0.183	HO 6455		
	2A-2	23.0	-31.5	1.8	1.1	4.1	0.329	700	1500	6x10 ⁻⁵	9.3	10.7	11.5	0.013	0.077	0.220	HO 6452		
	25-1	23.0	-22.0	2.7	2.0	8.3	0.509	700	500	6x10 ⁻⁵	55.0	104.0	104.4	0.005	0.041	0.453	HO 6459		
	23-2	23.0	-22.0	2.7	2.0	8.3	0.509	700	700	6x10 ⁻⁵	69.9	90.3	96.8	0.032	0.079	0.639	HO 6454		
	25-3	23.0	-22.0	2.7	2.0	8.3	0.509	700	900	6x10 ⁻⁵	77.0	95.7	95.7	0.002	0.023	0.607	HO 6450		
	25-4	23.0	-22.0	2.7	2.0	8.3	0.509	700	1100	6x10 ⁻⁵	44.9	60.4	60.4	0.032	0.011	0.114	HO 6451		
	63-1	23.0	-22.0	2.7	2.0	8.3	0.509	700	1300	6x10 ⁻⁵	21.5	34.9	35.0	0.005	0.009	0.111	HO 6453		
	63-2	23.0	-22.0	2.7	2.0	8.3	0.509	700	1500	6x10 ⁻⁵	13.6	--	20.1	0.001	0.003	0.005	HO 6452		
	63-3	23.0	-22.0	2.7	2.0	8.3	0.509	700	1700	6x10 ⁻⁵	3.5	6.2	6.4	0.005	0.023	0.099	HO 6452		
	25-1	23.0	-8.0	4.0	3.5	16.7	0.757	720	700	6x10 ⁻⁵	81.0	107.5	108.3	0.002	0.019	0.417	HO 6455		
	25-2	23.0	-8.0	4.0	3.5	16.7	0.757	720	900	6x10 ⁻⁵	69.5	95.8	95.0	0.002	0.017	0.237	HO 6456		
	25-3	23.0	-8.0	4.0	3.5	16.7	0.757	720	1100	6x10 ⁻⁵	43.4	58.3	55.3	0.001	0.005	0.077	HO 6453	FEP	
25-4	23.0	-8.0	4.0	3.5	16.7	0.757	720	1300	6x10 ⁻⁵	19.1	30.3	30.8	0.003	0.002	0.054	HO 6454	FEP		

4.2-426

Amend. 51
Sept. 1979

TABLE 4.2-54 (CONTINUED)

POSTIRRADIATION TENSILE PROPERTIES OF ANNEALED TYPE 304 STAINLESS STEEL

EXPERIMENT IDENTIFICATION	SPECIMEN IDENTIFICATION	IRRADIATION CONDITIONS						TEST CONDITIONS		TEST RESULTS ^(a)							COMMENTS ^(b)
		EFFECTIVE DOSE COORDINATES		FLUENCE ⁽¹⁾	FLUENCE ⁽²⁾	dpa	E. MEV	TEMP. OF	TEMP. OF	STRAIN RATE	σ_p	σ_y	σ_u	σ_u (PLASTIC)	ϵ_c	RA	
		R. cm	Z. cm	($\times 10^{19}$ NeV)	($\times 10^{19}$ NeV)					1000 psi	1000 psi	1000 psi					
SEC3 (CONT.)	6C-1	23.0	-8.0	4.0	3.5	16.7	0.757	720	700	6×10^{-5}	14.6	19.5	67.1	0.405	0.429	0.732	HO 6495
	6C-2	23.0	-8.0	4.0	3.5	16.7	0.757	720	900	6×10^{-5}	13.6	16.8	61.2	0.416	0.435	0.726	HO 6495
	6C-3	23.0	-8.0	4.0	3.5	16.7	0.757	720	1000	6×10^{-5}	9.2	16.1	38.6	0.135	0.151	0.437	HO 6497
	6C-4	23.0	-8.0	4.0	3.5	16.7	0.757	720	1300	6×10^{-5}	9.2	15.5	22.5	0.090	0.099	0.192	HO 6498
	2D-1	23.0	0	4.3	3.7	18.2	0.790	730	500	6×10^{-5}	80.5	103.4	109.4	0.600	0.624	0.437	HO 6455
	2D-4	23.0	0	4.3	3.7	18.2	0.790	730	700	6×10^{-5}	69.5	105.0	105.4	0.600	0.621	0.593	HO 6457
	6D-2	23.0	0	4.3	3.7	18.2	0.790	730	500	6×10^{-5}	61.4	95.8	96.1	0.605	0.602	0.318	HO 6458
	6D-3	23.0	0	4.3	3.7	18.2	0.790	730	1100	6×10^{-5}	49.4	57.0	57.0	0.620	0.605	0.116	HO 6511
	2D-2	23.0	0	4.3	2.7	16.2	0.790	730	1300	6×10^{-5}	22.6	25.6	25.6	0.600	0.603	0.073	HO 6459
	6D-1	23.0	0	4.3	3.7	18.2	0.790	730	1500	6×10^{-5}	15.6	19.2	19.2	0.600	0.603	0.049	HO 6512
	6D-4	23.0	0	4.3	3.7	18.2	0.790	730	1700	6×10^{-5}	3.3	5.7	6.0	0.601	0.613	0.032	HO 6493
	2E-1	23.0	+21.0	2.5	2.0	8.4	0.553	820	500	6×10^{-5}	59.2	84.9	87.3	0.613	0.616	0.620	HO 6467
	2E-2	23.0	+21.0	2.5	2.0	8.4	0.553	820	700	6×10^{-5}	61.0	81.6	85.5	0.643	0.655	0.637	HO 6468
	2E-3	23.0	+21.0	2.5	2.0	8.4	0.553	820	900	6×10^{-5}	58.2	76.6	78.5	0.622	0.646	0.360	HO 6469
	2E-4	23.0	+21.0	2.5	2.0	8.4	0.553	820	1100	6×10^{-5}	39.9	58.6	59.3	0.604	0.613	0.195	HO 6470
	6E-1	23.0	+21.0	2.5	2.0	8.4	0.553	870	1300	6×10^{-5}	19.2	31.4	31.9	0.639	0.628	0.210	HO 6471
	6E-2	23.0	+21.0	2.5	2.0	8.4	0.553	870	1500	6×10^{-5}	11.0	13.8	14.2	0.605	0.656	0.276	HO 6472
	6E-3	23.0	+21.0	2.5	2.0	8.4	0.553	870	1700	6×10^{-5}	3.0	5.7	6.1	0.605	0.623	0.159	HO 6500
	2F-1	23.0	+48.0	0.91	0.47	1.7	0.241	870	900	6×10^{-5}	35.7	49.3	74.6	0.725	0.772	0.614	HO 6473
	2F-2	23.0	+48.0	0.91	0.47	1.7	0.241	870	1100	6×10^{-5}	25.1	40.0	49.0	0.606	0.125	0.395	HO 6474
	2F-3	23.0	+48.0	0.91	0.47	1.7	0.241	870	1300	6×10^{-5}	15.1	26.7	30.1	0.647	0.679	0.184	HO 6475
	6F-1	23.0	+48.0	0.91	0.47	1.7	0.241	870	700	6×10^{-5}	13.0	17.8	63.5	0.415	0.458	0.500	HO 6501
	6F-2	23.0	+48.0	0.91	0.47	1.7	0.241	870	900	6×10^{-5}	10.7	16.3	61.3	0.334	0.361	0.533	HO 6502
	6F-3	23.0	+48.0	0.91	0.47	1.7	0.241	870	1100	6×10^{-5}	8.0	12.7	35.5	0.180	0.193	0.421	HO 6503
	6F-4	23.0	+48.0	0.91	0.47	1.7	0.241	870	1300	6×10^{-5}	0.4	12.3	22.4	0.692	0.111	0.341	HO 6504
	2G-1	23.0	+74.0	0.35	0.13	0.4	0.121	870	500	6×10^{-5}	21.0	27.6	64.6	0.364	0.407	0.784	HO 6476
	2G-2	23.0	+74.0	0.35	0.13	0.4	0.121	870	700	6×10^{-5}	17.8	26.4	64.5	0.361	0.385	0.713	HO 6477
	2G-3	23.0	+74.0	0.35	0.13	0.4	0.121	870	900	6×10^{-5}	18.7	26.0	63.7	0.379	0.360	0.684	HO 6505
	6G-1	23.0	+74.0	0.35	0.13	0.4	0.121	870	1100	6×10^{-5}	15.4	22.8	43.4	0.178	0.199	0.505	HO 6506
	6G-2	23.0	+74.0	0.35	0.13	0.4	0.121	870	1300	6×10^{-5}	14.5	19.4	23.9	0.641	0.665	0.262	HO 6507
	6G-3	23.0	+74.0	0.35	0.13	0.4	0.121	870	1500	6×10^{-5}	7.6	11.3	12.2	0.631	0.104	0.761	HO 6508
	6G-4	23.0	+74.0	0.35	0.13	0.4	0.121	870	1700	6×10^{-5}	2.9	5.7	6.3	0.639	0.666	0.131	HO 6509
S13 CRP-18 THIMBLE	ASA-1	23.3	-27.3	5.1	3.4	13.2	0.398	700	700	4.5×10^{-5}	87.3	113.1	114.9	0.603	0.624	0.293	HO 9578
	ASA-2	23.3	-27.3	5.1	3.4	13.2	0.398	700	1100	4.5×10^{-5}	65.7	73.5	73.5	0.601	0.603	0.241	HO 9580
	ASB-1	23.3	-27.3	6.7	5.1	21.8	0.545	700	700	4.5×10^{-5}	73.1	112.3	113.9	0.605	0.636	0.346	HO 9579
	ASC-1	23.3	-27.3	8.5	7.1	33.1	0.693	700	700	4.5×10^{-5}	82.0	109.0	110.4	0.605	0.629	0.389	HO 9580
	ASC-2	23.3	-27.3	8.5	7.1	33.1	0.658	700	1100	4.5×10^{-5}	51.0	--	53.1	0.600	0.603	0.609	HO 9581
	ASD-1	23.3	0	9.7	8.3	40.4	0.765	710	700	4.5×10^{-5}	87.3	123.0	125.5	0.600	0.631	0.170	HO 9581
	ASE-1	23.3	0	10.0	8.7	43.0	0.790	730	700	4.5×10^{-5}	81.0	111.7	112.1	0.603	0.620	0.724	HO 9582
	ASE-2	23.3	0	10.0	8.7	43.0	0.790	730	1100	4.5×10^{-5}	47.1	--	48.1	0.600	0.604	0.300	HO 9582
	ASF-1	23.3	+13.7	6.0	6.7	31.2	0.657	760	800	4.5×10^{-5}	65.7	92.8	95.5	0.600	0.630	0.157	HO 9583
	ASF-1	23.3	+20.5	6.1	4.7	20.4	0.563	815	600	4.5×10^{-5}	62.2	78.0	80.6	0.600	0.617	0.306	HO 9584
	ASH-1	23.3	+27.3	4.7	3.3	13.3	0.447	845	800	4.5×10^{-5}	57.7	77.9	82.1	0.614	0.645	0.404	HO 9585
	ASH-1	23.3	+35.6	3.5	2.1	8.1	0.345	850	900	4.5×10^{-5}	38.0	66.8	72.4	0.638	0.660	0.400	HO 9586
	ASJ-1	23.3	+52.7	1.8	0.87	3.0	0.213	870	900	4.5×10^{-5}	26.4	45.5	68.2	0.697	0.143	0.455	HO 9587
	ASK-1	23.3	+59.5	1.4	0.61	2.0	0.178	875	900	4.5×10^{-5}	20.5	40.9	60.7	0.143	0.177	0.500	HO 9588
	ATL-1	23.3	+66.4	1.1	0.43	1.4	0.148	875	500	4.5×10^{-5}	20.3	37.8	59.0	0.130	0.160	0.424	HO 9589
	A415-1	23.3	+112	-0.02	-0.01	--	--	--	800	800	4.5×10^{-5}	20.2	33.0	68.8	0.232	0.271	0.426
A415-2	23.3	+112	-0.02	-0.01	--	--	--	800	1100	4.5×10^{-5}	20.0	32.7	51.3	0.105	0.130	0.375	HO 9577

4.2-427

Amend. 51
Sept. 1979

TABLE 4.2-54 (CONTINUED)

POSTIRRADIATION TENSILE PROPERTIES OF ANNEALED TYPE 304 STAINLESS STEEL

EXPERIMENT IDENTIFICATION	SPECIMEN IDENTIFICATION	IRRADIATION CONDITIONS							TEST CONDITIONS		TEST RESULTS (a)							
		EDR II COORDINATES R, cm Z, cm		FLUENCE 10 ²² n/cm ² (E>0.1 MeV)	FLUENCE 10 ²² n/cm ² (E>0.1 MeV)	dpa	E, MeV	TEMP., °F	TEMP., °F	STRAIN RATE, SEC ⁻¹	σ_p , 1000 psi	σ_y , 1000 psi	σ_u , 1000 psi	ϵ_u (PLASTIC)	ϵ_t	RA	TEST IDENTIFICATION	COMMENTS (b)
341 (SA-1) PHENOL	B501	10.8	-51.0	2.6	1.2	4.0	0.190	700	1100	4.5x10 ⁻⁵	43.3	55.2	57.5	0.007	0.020	0.173	HO 5615	
	B502	10.8	-42.5	3.6	1.8	6.4	0.230	700	1100	4.5x10 ⁻⁵	57.1	67.3	68.1	0.003	0.011	0.192	HO 5616	
	B503	10.8	-34.0	4.9	2.9	10.8	0.323	700	700	4.5x10 ⁻⁵	74.5	104.9	109.0	0.006	0.026	0.294	HO 5607	
	B504	10.8	-26.0	6.7	4.6	19.8	0.453	700	700	4.5x10 ⁻⁵	72.9	106.1	112.5	0.005	0.024	0.229	HO 5608	
	B505	10.8	-18.0	9.5	7.8	30.0	0.571	700	700	4.5x10 ⁻⁵	82.4	111.6	116.1	0.005	0.037	0.216	HO 5609	
	B506	10.8	-9.5	12.5	11.0	55.1	0.817	715	70	4.5x10 ⁻⁵	100.0	141.0	155.0	0.049	0.281	0.240	HO 5605	
	B507	10.8	-9.5	12.5	11.0	55.1	0.817	715	700	4.5x10 ⁻⁵	84.6	111.5	119.2	0.007	0.023	0.250	HO 5610	
	B508	10.8	0	13.6	12.3	52.7	0.652	750	700	4.5x10 ⁻⁵	86.9	102.0	105.7	0.005	0.029	0.235	HO 5611	
	B512	10.8	+9.5	12.2	10.8	53.6	0.915	795	70	1.3x10 ⁻²	97.6	121.9	132.1	0.033	0.112	0.071	HO 5606	
	B511	10.8	+9.5	12.2	10.8	53.6	0.915	795	800	4.5x10 ⁻⁵	66.0	92.8	99.6	0.005	0.025	0.254	HO 5613	
	B5J1	10.8	+18.0	8.7	7.1	33.1	0.671	840	800	4.5x10 ⁻⁵	64.8	92.4	96.1	0.004	0.017	0.185	HO 5612	
	B6J2	10.8	+18.0	8.7	7.1	33.1	0.671	840	900	4.5x10 ⁻⁵	50.0	76.5	82.6	0.005	0.015	0.118	HO 5614	

SYMBOLS ARE DEFINED AS FOLLOWS:

- σ_p IS STRESS AT PROPORTIONAL ELASTIC LIMIT
- σ_y IS 0.2% OFFSET YIELD STRESS
- σ_u IS ULTIMATE TENSILE STRESS
- ϵ_u IS ELONGATION AT MAXIMUM LOAD
- ϵ_t IS TOTAL ELONGATION
- RA IS REDUCTION OF AREA

(b) COMMENT CODES ARE AS FOLLOWS

- FEP - SPECIMEN FAILED AT EXTENSOMETER POINTS
- PIA - POSTIRRADIATION ANNEAL PRIOR TO TEST
- ED - FLUENCES BASED ON DOSIMETRY IN EXPERIMENT
- 304L - MATERIAL IS GRADE 304L STAINLESS STEEL
- FOG - SPECIMEN FAILED OUTSIDE OF GAGE LENGTH

4.2-428

Amend. 51
Sept. 1979

TABLE 4.2-55

POSTIRRADIATION TENSILE PROPERTIES OF ANNEALED TYPE 316 STAINLESS STEEL

EXPERIMENT IDENTIFICATION	SPECIMEN IDENTIFICATION	IRRADIATION CONDITIONS							TEST CONDITIONS		TEST RESULTS ^(a)							
		EPR II COORDINATES R, cm Z, cm		FLUENCE $10^{22} n/cm^2$ (E>10 ⁻¹⁰ MeV)	FLUENCE $10^{22} n/cm^2$ (E>0.1 MeV)	dpa	E, MeV	TEMP. OF	TEMP. OF	STRAIN RATE, SEC ⁻¹	σ_u , 1000 psi	σ_y , 1000 psi	σ_u , 1000 psi	ϵ_u (PLASTIC)	ϵ_t	RA	TEST IDENTIFICATION	COMMENTS ^(b)
1018	1-25-61	4.2	-50.0	0.78	0.36	1.6	0.200	700	800	3×10^{-5}	13.5	18.3	69.9	0.360	0.424	0.621	HO 7157	
	1-25-62	4.2	-50.0	0.78	0.36	1.6	0.200	700	1200	3×10^{-5}	13.7	17.7	41.1	0.032	0.107	0.390	HO 7160	
	1-24-61	4.2	-45.0	0.94	0.47	1.7	0.228	700	800	3×10^{-5}	16.7	23.6	75.6	0.252	0.352	0.557	HO 7156	
	1-24-61	4.2	-45.0	0.95	0.47	1.7	0.228	700	1200	3×10^{-5}	12.6	13.5	40.1	0.007	0.112	0.268	HO 7159	
	1-23-61	4.2	-40.6	1.1	0.59	2.2	0.264	700	800	3×10^{-5}	32.5	42.7	78.3	0.219	0.277	0.442	HO 7155	
	1-23-62	4.2	-40.6	1.1	0.59	2.2	0.264	700	1200	3×10^{-5}	19.4	27.4	41.4	0.075	0.031	0.215	HO 7158	
	1-22-61	4.2	-35.6	1.4	0.78	2.9	0.314	730	700	3×10^{-5}	49.3	61.2	83.5	0.193	0.272	0.615	HO 7367	
	1-22-62	4.2	-35.6	1.4	0.78	2.9	0.314	730	950	3×10^{-5}	38.0	56.0	79.5	0.250	0.344	0.515	HO 7271	
	1-22-63	4.2	-35.6	1.4	0.78	2.9	0.314	730	1100	3×10^{-5}	32.5	52.8	60.4	0.076	0.109	0.154	HO 7268	
	1-21-64	4.2	-30.9	1.6	1.0	4.0	0.373	820	800	3×10^{-5}	57.4	71.6	91.3	0.178	0.267	0.615	HO 7269	
	1-21-63	4.2	-30.9	1.6	1.0	4.0	0.373	820	1050	3×10^{-5}	45.9	68.2	79.6	0.113	0.181	0.419	HO 7074	
	1-21-62	4.2	-30.9	1.5	1.0	4.0	0.373	820	1200	3×10^{-5}	31.5	42.4	45.2	0.024	0.045	0.211	HO 7092	
	1-21-61	4.2	-30.9	1.5	1.0	4.0	0.373	820	1200	3×10^{-5}	11.4	13.9	35.0	0.112	0.134	0.197	HO 7097	PIA 2000°F/1 HR
	1-21-5C	4.2	-30.9	1.6	1.0	4.0	0.373	845	1200	3×10^{-5}	30.9	43.2	45.3	0.037	0.035	0.138	HO 7087	
	1-20-6C	4.2	-26.1	2.0	1.4	5.6	0.455	940	1200	3×10^{-5}	38.5	47.2	53.6	0.013	0.034	0.171	HO 7086	PIA 2000°F/1 HR
	1-20-61	4.2	-26.1	2.0	1.4	5.6	0.455	900	1200	3×10^{-5}	12.0	14.1	34.2	0.103	0.171	0.211	HO 7016	
	1-19-7B	4.2	-21.4	2.4	1.8	8.0	0.566	960	800	3×10^{-5}	63.1	75.9	91.2	0.112	0.191	0.516	HO 7068	
	1-19-7A	4.2	-21.4	2.4	1.8	8.0	0.566	960	900	3×10^{-5}	61.5	75.3	88.5	0.110	0.199	0.505	HO 7070	
	1-19-5D	4.2	-21.4	2.4	1.8	8.0	0.566	960	1050	3×10^{-5}	59.6	70.2	81.5	0.075	0.135	0.320	HO 7073	
	1-19-5A	4.2	-21.4	2.4	1.8	8.0	0.566	960	1100	3×10^{-5}	41.9	65.6	69.9	0.021	0.045	0.268	HO 7065	
1-19-6Z	4.2	-21.4	2.4	1.8	8.0	0.566	960	1200	3×10^{-5}	36.6	50.6	52.5	0.011	0.027	0.091	HO 7060		
1-19-7C	4.2	-21.4	2.4	1.8	8.0	0.566	1010	1200	3×10^{-5}	34.2	45.8	50.5	0.017	0.032	0.154	HO 7063		
1-19-61	4.2	-21.4	2.4	1.8	8.0	0.566	960	1300	3×10^{-5}	11.2	14.4	33.5	0.038	0.113	0.278	HO 7055	PIA 2000°F/1 HR	
1-18-61	4.2	-16.6	3.0	2.5	12.0	0.714	1020	1050	3×10^{-5}	44.5	55.7	69.1	0.050	0.040	0.303	HO 7072		
1-18-6C	4.2	-16.5	3.0	2.5	12.0	0.714	1090	1200	3×10^{-5}	25.4	38.1	45.4	0.029	0.047	0.076	HO 7084		
1-17-63	4.2	-11.9	3.5	3.0	14.9	0.785	1080	800	3×10^{-5}	42.2	53.5	61.5	0.139	0.162	0.553	HO 7154		
1-17-6Z	4.2	-11.9	3.5	3.0	14.9	0.785	1090	1200	3×10^{-5}	29.3	42.6	46.9	0.018	0.028	0.114	HO 7069		
1-17-6C	4.2	-11.9	3.5	3.0	14.9	0.785	1150	1200	3×10^{-5}	21.4	28.4	40.6	0.082	0.104	0.138	HO 7042		
1-17-61	4.2	-11.9	3.5	3.0	14.9	0.785	1060	1200	3×10^{-5}	11.0	14.1	33.4	0.034	0.112	0.195	HO 7094	PIA 2000°F/1 HR	
1-16-61	4.2	-7.1	3.8	3.4	16.9	0.827	1110	1100	3×10^{-5}	33.3	48.1	55.0	0.031	0.044	0.187	HO 7081		
1019	A12-2T	26.5	+53.3	0.60	0.29	1.0	0.207	800	800	2.7×10^{-5}	12.4	21.5	79.6	0.236	0.278	0.642	HO 7315	
	A12-4T	26.5	+36.8	1.1	0.69	2.5	0.321	700	800	2.7×10^{-5}	25.1	43.2	59.6	0.130	0.170	0.628	HO 7316	
	A12-5T	26.5	+27.9	1.6	1.1	4.3	0.421	770	800	2.7×10^{-5}	53.3	62.2	90.4	0.095	0.130	0.518	HO 7317	
	A12-7T	26.5	+15.2	2.5	2.1	9.2	0.635	750	800	2.7×10^{-5}	76.8	98.5	102.5	0.013	0.050	0.408	HO 7318	
	A12-9T	26.5	+6.4	3.2	2.7	12.6	0.711	730	600	2.7×10^{-5}	74.2	110.1	112.1	0.009	0.042	---	HO 7319	
	A12-9T	26.5	-1.3	3.3	2.8	13.3	0.726	720	800	2.7×10^{-5}	87.6	103.5	109.7	0.006	0.040	0.502	HO 7320	
1021B	6F26-1	4.4	-27.8	3.2	2.1	8.6	0.423	760	800	3×10^{-5}	65.0	67.8	95.9	0.044	0.081	0.577	HO 9220	
	6F26-2	4.4	-27.8	3.2	2.1	8.6	0.423	760	900	3×10^{-5}	60.2	67.8	95.1	0.045	0.050	0.520	HO 9221	
	6F26-1	4.4	-23.0	3.9	2.9	12.3	0.522	760	600	3×10^{-5}	71.1	92.8	100.9	0.027	0.063	0.480	HO 9222	
	6F26-2	4.4	-23.0	3.9	2.9	12.3	0.522	760	900	3×10^{-5}	67.2	69.0	92.8	0.018	0.051	0.480	HO 9223	
	6F26-3	4.4	-27.8	3.1	2.2	9.0	0.459	875	800	3×10^{-5}	36.6	44.9	78.0	0.156	0.150	0.594	HO 9261	
	6F26-4	4.4	-27.8	3.1	2.2	9.0	0.459	870	1200	3×10^{-5}	36.6	40.9	52.0	0.031	0.040	0.350	HO 9262	
	6F26-1	4.4	-23.0	3.8	2.8	12.3	0.547	870	900	3×10^{-5}	26.5	45.7	78.3	0.157	0.253	0.569	HO 9274	
	6F26-2	4.4	-23.0	3.8	2.8	12.3	0.547	870	1000	3×10^{-5}	35.8	44.7	71.5	0.125	0.140	0.285	HO 9225	
1021C	4016-1	4.3	-38.8	2.6	1.4	5.2	0.281	735	800	3×10^{-5}	52.0	69.1	87.0	0.094	0.134	0.602	HO 9072	
	4016-1	4.3	-34.1	3.1	1.6	6.9	0.331	735	800	3×10^{-5}	52.8	79.1	91.3	0.041	0.085	0.594	HO 5373	
	7116-1	6.5	-27.8	3.9	2.6	10.4	0.420	760	700	3×10^{-5}	68.3	85.4	98.5	0.045	0.078	0.537	HO 7333	
	7116-2	6.5	-27.8	3.9	2.6	10.4	0.420	760	800	3×10^{-5}	66.7	87.8	98.9	0.047	0.071	0.553	HO 9274	
	5016-1	7.9	-38.8	2.6	1.4	5.1	0.275	640	700	3×10^{-5}	48.8	68.3	87.8	0.095	0.127	0.602	HO 7302	

4.2-429

Amend. 51
Sept. 1979

TABLE 4.2-55 (CONTINUED)

POSTIRRADIATION TENSILE PROPERTIES OF ANNEALED TYPE 316 STAINLESS STEEL

EXPERIMENT IDENTIFICATION	SPECIMEN IDENTIFICATION	IRRADIATION CONDITIONS							TEST CONDITIONS		TEST RESULTS ^(a)							
		EDR COORDINATES R, cm	II COORDINATES Z, cm	FLUENCE, $10^{22} n/cm^2$ (E > 0.01 MeV)	FLUENCE, $10^{22} n/cm^2$ (E > 0.1 MeV)	dpa	E, MeV	TEMP., °F.	TEMP., °F.	STRAIN RATE, SEC ⁻¹	σ_u , 1000 psi	σ_y , 1000 psi	σ_u , 1000 psi	ϵ_u (PLASTIC)	ϵ_c	RA	TEST IDENTIFICATION	COMMENTS ^(b)
	5015-2	7.9	+38.8	2.6	1.4	5.1	0.275	840	900	3×10^{-5}	52.0	65.8	83.1	0.034	0.122	0.520	HO 9075	
	7406-1	6.5	+35.8	2.4	1.5	5.5	0.327	850	800	3×10^{-5}	41.5	51.4	80.6	0.120	0.159	0.551	HO 9007	
	7408-3	6.5	+38.8	2.4	1.5	5.5	0.327	850	900	3×10^{-5}	36.1	51.0	80.7	0.124	0.159	0.504	HO 9077	
	4406-1	4.3	+38.8	2.5	1.5	5.5	0.327	865	900	3×10^{-5}	44.7	48.9	79.9	0.124	0.152	0.495	HO 9076	
	7409-2	6.5	+38.8	2.4	1.5	5.5	0.327	850	1200	3×10^{-5}	25.6	45.6	54.2	0.019	0.025	0.265	HO 7004	
	4416-1	4.3	+34.1	3.0	1.9	7.4	0.375	865	900	3×10^{-5}	34.2	53.7	79.7	0.111	0.143	0.504	HO 9078	
	7712-1	6.5	+27.8	3.8	2.6	10.8	0.460	865	600	3×10^{-5}	47.8	64.2	87.0	0.102	0.127	0.551	HO 7008	
	7712-2	6.5	+27.8	3.8	2.6	10.8	0.460	865	1000	3×10^{-5}	44.7	60.0	79.1	0.092	0.105	0.305	HO 9040	
	5124-1	7.9	+27.8	3.7	2.6	10.7	0.451	860	1000	3×10^{-5}	43.6	61.8	70.5	0.076	0.100	0.423	HO 9079	
	7806-1	6.5	+16.8	6.3	5.3	25.0	0.759	1365	1100	3×10^{-5}	14.0	21.2	57.4	0.070	0.077	0.190	HO 7035	
	7806-2	6.5	+16.8	6.3	5.3	25.0	0.759	1365	1400	3×10^{-5}	12.6	17.7	20.2	0.002	0.011	0.011	HO 9091	
	7816-4	6.5	+16.8	5.0	4.9	23.2	0.713	1365	1300	8.9×10^{-2}	12.2	21.3	50.8	0.251	0.295	0.244	HO 9090	
	7816-3	6.5	+16.8	5.0	4.9	23.2	0.713	1365	1300	2.2×10^{-2}	14.6	21.3	52.2	0.235	0.304	0.374	HO 9061	
	7816-2	6.5	+16.8	5.0	4.9	23.2	0.713	1365	1300	5.0×10^{-2}	6.6	16.6	48.8	0.610	0.620	0.408	HO 9074	
	7816-1	6.5	+16.8	5.0	4.9	23.2	0.713	1365	1300	0.15	13.8	22.0	51.2	0.237	0.267	0.553	HO 9050	
	7826-2	6.5	+12.0	7.4	6.4	31.7	0.787	1365	1200	3×10^{-5}	14.2	21.3	41.8	0.015	0.040	0.208	HO 7003	
	7826-1	6.5	+12.0	7.4	6.4	31.7	0.787	1365	1400	3×10^{-5}	12.6	18.7	24.8	0.025	0.033	0.122	HO 9082	
	7834-1	6.5	- 7.3	8.4	7.6	38.3	0.851	1365	1100	3×10^{-5}	14.6	22.0	54.5	0.042	0.070	0.203	HO 7055	
	7834-2	6.5	- 2.3	8.4	7.6	35.3	0.851	1365	1400	3×10^{-5}	12.2	17.2	19.0	0.006	0.008	0.005	HO 7033	
X022	15016-11	30.8	+38.8	0.37	0.21	0.7	0.247	730	70	3×10^{-5}	26.8	35.4	82.0	0.464	0.547	0.724	HO 6907	
	15016-12	30.8	+35.8	0.37	0.21	0.7	0.247	730	600	3×10^{-5}	19.3	23.4	73.0	0.455	0.525	0.550	HO 6908	
	15016-13	30.8	+32.8	0.37	0.21	0.7	0.247	730	800	3×10^{-5}	20.7	24.7	72.2	0.432	0.504	0.674	HO 6909	
	15016-14	30.8	+33.8	0.37	0.21	0.7	0.247	730	900	3×10^{-5}	20.5	24.7	72.0	0.417	0.500	0.653	HO 6910	
	15016-15	30.8	+39.8	0.37	0.21	0.7	0.247	730	1000	3×10^{-5}	15.8	22.6	69.0	0.364	0.470	0.634	HO 6911	
	12016-9	31.8	+38.8	0.35	0.20	0.7	0.245	725	1000	3×10^{-5}	13.8	17.0	62.4	0.323	0.416	0.705	HO 6922	
	12016-6	31.8	+32.8	0.35	0.20	0.7	0.245	725	1100	3×10^{-5}	15.0	17.3	54.4	0.278	0.327	0.333	HO 6919	
	12016-10	31.8	+35.8	0.35	0.20	0.7	0.245	725	1100	3×10^{-5}	14.6	16.6	59.3	0.279	0.410	0.634	HO 6920	
	12016-7	31.8	+38.8	0.35	0.20	0.7	0.245	725	1200	3×10^{-5}	14.2	15.2	39.4	0.145	0.181	0.211	HO 6920	
	12016-8	31.8	+38.8	0.35	0.20	0.7	0.245	725	1400	3×10^{-5}	10.0	13.7	22.6	0.056	0.117	0.107	HO 6921	
	12026-1	31.8	+23.0	0.65	0.46	1.7	0.394	740	1050	3×10^{-3}	27.2	42.8	73.8	0.215	0.290	0.577	HO 6920	
	12026-2	31.8	+23.0	0.65	0.46	1.7	0.394	740	1100	3×10^{-3}	27.6	38.0	64.4	0.300	0.419	0.642	HO 6901	
	12026-3	31.8	+23.0	0.65	0.46	1.7	0.394	740	1200	3×10^{-3}	25.2	35.9	59.8	0.259	0.279	0.405	HO 6902	
	12026-4	31.8	+23.0	0.65	0.46	1.7	0.394	740	1400	3×10^{-3}	12.8	18.2	69.7	0.105	0.136	0.132	HO 6903	
	13026-6	28.6	+23.0	0.77	0.56	2.2	0.450	740	1100	3×10^{-5}	24.4	34.4	60.1	0.246	0.296	0.415	HO 6904	
	13026-7	28.6	+23.0	0.77	0.56	2.2	0.450	740	1200	3×10^{-5}	18.7	27.5	44.4	0.159	0.127	0.122	HO 6905	
	13026-8	28.6	+23.0	0.77	0.56	2.2	0.450	740	1400	3×10^{-5}	10.9	16.1	24.0	0.077	0.108	0.114	HO 6906	
	14026-1	29.7	+38.8	0.39	0.23	0.8	0.290	815	600	3×10^{-5}	10.7	22.0	65.8	0.432	0.465	0.634	HO 6908	
	14026-2	29.7	+38.8	0.39	0.23	0.8	0.290	815	1000	3×10^{-5}	11.8	23.5	71.8	0.460	0.513	0.650	HO 6909	
	14026-3	29.7	+38.8	0.39	0.23	0.8	0.290	815	900	3×10^{-5}	16.7	19.6	69.7	0.410	0.510	0.660	HO 6916	
14026-4	29.7	+38.8	0.39	0.23	0.8	0.290	815	1000	3×10^{-5}	15.7	19.3	65.7	0.351	0.510	0.671	HO 6917		
14026-5	29.7	+34.1	0.47	0.29	1.1	0.330	815	70	3×10^{-5}	19.7	31.7	65.0	0.433	0.613	0.724	HO 6915		
14026-1	29.7	+34.1	0.47	0.29	1.1	0.330	815	1000	3×10^{-5}	12.6	17.0	53.3	0.326	0.408	0.658	HO 6924		
14026-14	29.7	+34.1	0.48	0.30	1.1	0.334	805	1100	3×10^{-3}	17.8	20.6	54.9	0.265	0.306	0.374	HO 6920		
14026-2	29.7	+34.1	0.47	0.29	1.1	0.330	815	1100	3×10^{-3}	13.0	15.8	58.0	0.330	0.365	0.600	HO 6925		
14026-15	29.7	+34.1	0.48	0.30	1.1	0.334	805	1200	3×10^{-3}	15.0	16.9	41.2	0.114	0.157	0.252	HO 6931		
14026-4	29.7	+34.1	0.48	0.30	1.1	0.334	805	1200	3×10^{-3}	16.8	20.0	55.2	0.264	0.355	0.637	HO 6928		
14026-3	29.7	+34.1	0.47	0.29	1.1	0.330	815	1200	3×10^{-3}	12.0	16.4	54.5	0.235	0.351	0.504	HO 6925		
14026-16	29.7	+34.1	0.48	0.30	1.1	0.334	805	1400	3×10^{-3}	10.3	14.0	22.5	0.055	0.111	0.107	HO 6932		
14026-9	29.7	+34.1	0.48	0.30	1.1	0.334	805	1400	3×10^{-3}	11.2	14.0	35.0	0.139	0.169	0.198	HO 6929		
14026-4	29.7	+34.1	0.47	0.29	1.1	0.330	815	1400	3×10^{-3}	10.6	14.6	34.0	0.139	0.163	0.195	HO 6927		
14026-9	29.7	+27.8	0.58	0.40	1.5	0.397	800	900	4.5×10^{-5}	24.4	32.5	71.4	0.275	0.330	0.658	HO 9008		

4.2-430

Amend. 51
Sept. 1979

TABLE 4.2-55 (CONTINUED)

POSTIRRADIATION TENSILE PROPERTIES OF ANNEALED TYPE 316 STAINLESS STEEL

EXPERIMENT IDENTIFICATION TICKET	SPECIMEN IDENTIFICATION	IRRADIATION CONDITIONS							TEST CONDITIONS		TEST RESULTS ⁽⁴⁾								
		GCR IN COORDINATES R, cm Z, cm		FLUENCE 10 ²² n/cm ² (E>0.1 MeV)	FLUENCE 10 ²¹ n/cm ² (E>0.1 MeV)	dpa	E, MeV	TEMP., °F	TEMP., °F	STRAIN RATE, SEC ⁻¹	σ _p , 1000 psi	σ _y , 1000 psi	σ _u , 1000 psi	e _p (PLASTIC)	e _t	RA	TEST IDENTIFICATION	COMMENTS ⁽⁵⁾	
1041	14216-15	21.7	+23.0	0.69	0.50	2.0	0.462	800	900	4.5x10 ⁻⁵	30.9	39.8	73.7	0.270	0.302	0.642	HO 9089		
	12716-6	21.8	+23.0	0.63	0.45	1.7	0.419	820	1100	3x10 ⁻⁵	22.4	36.0	60.2	0.175	0.193	0.293	HO 6512		
	12716-7	21.8	+23.0	0.63	0.45	1.7	0.419	820	1200	3x10 ⁻⁵	24.4	36.2	48.0	0.075	0.098	0.187	HO 6513		
	12716-8	21.8	+23.0	0.63	0.45	1.7	0.419	820	1400	3x10 ⁻⁵	12.6	20.8	24.4	0.045	0.066	0.098	HO 6514		
	14216-1	21.7	+16.6	0.92	0.72	3.0	0.551	970	70	3x10 ⁻⁵	31.7	42.8	85.0	0.378	0.466	0.650	HO 6518		
	14216-2	21.7	+16.6	0.92	0.72	3.0	0.551	970	600	3x10 ⁻⁵	23.6	32.0	71.3	0.244	0.303	0.555	HO 6517		
	14216-3	21.7	+16.6	0.92	0.72	3.0	0.551	970	800	3x10 ⁻⁵	24.0	31.3	72.2	0.224	0.276	0.545	HO 6518		
	14216-4	21.7	+16.6	0.92	0.72	3.0	0.551	970	900	3x10 ⁻⁵	19.9	29.1	67.6	0.185	0.337	0.480	HO 6519		
	14216-5	21.7	+16.6	0.92	0.72	3.0	0.551	970	1950	3x10 ⁻⁵	19.2	28.7	63.5	0.175	0.232	0.536	HO 6524		
	14216-6	21.7	+15.8	0.87	0.58	2.9	0.553	970	1000	3x10 ⁻⁵	27.2	33.2	63.3	0.178	0.194	0.353	HO 6520		
	14216-2	21.7	+16.3	0.87	0.58	2.9	0.553	970	1100	3x10 ⁻⁵	22.4	31.6	54.1	0.168	0.121	0.309	HO 6521		
	14216-3	21.7	+16.3	0.87	0.58	2.9	0.553	970	1200	3x10 ⁻⁵	18.7	31.9	43.9	0.044	0.055	0.228	HO 6522		
	14216-4	21.7	+16.6	0.87	0.58	2.9	0.553	970	1400	3x10 ⁻⁵	15.3	24.4	25.5	0.023	0.056	0.081	HO 6523		
	14216-1	21.7	+12.0	1.1	0.84	3.7	0.601	970	1100	3x10 ⁻⁵	19.1	29.0	60.7	0.218	0.320	0.502	HO 6525		
	14216-4	21.7	+12.3	1.0	0.82	3.6	0.602	970	1200	3x10 ⁻⁵	20.3	30.1	55.6	0.204	0.292	0.447	HO 6526		
	14216-5	21.7	+12.0	1.0	0.82	3.6	0.602	970	1400	3x10 ⁻⁵	15.7	26.5	38.0	0.020	0.163	0.252	HO 6527		
	1057	19216-1	21.1	+38.8	1.1	0.61	2.0	0.245	745	900	3x10 ⁻⁵	30.1	45.8	80.5	0.512	0.637	0.602	HO 9028	
		19216-1	21.1	+34.1	1.3	0.78	2.7	0.274	745	900	3x10 ⁻⁵	40.3	54.9	82.5	0.360	0.403	0.577	HO 9029	
19216-1		21.1	+27.8	1.7	1.1	3.9	0.331	775	800	3x10 ⁻⁵	43.1	54.4	66.2	0.156	0.201	0.650	HO 9028		
21216-1		21.0	+27.8	1.9	1.2	4.5	0.353	765	900	4.5x10 ⁻⁵	58.5	72.4	87.4	0.163	0.157	0.455	HO 9029		
19216-1		21.1	+21.0	2.0	1.4	5.2	0.389	775	800	3x10 ⁻⁵	45.5	61.0	85.8	0.118	0.167	0.402	HO 9028		
21216-2		21.0	+23.0	2.3	1.6	6.2	0.428	765	900	4.5x10 ⁻⁵	45.5	82.1	91.1	0.040	0.063	0.437	HO 9021		
21216-1		21.0	+16.8	1.2	0.70	2.5	0.289	830	1600	3x10 ⁻⁵	30.9	40.6	71.5	0.171	0.223	0.300	HO 9027		
21216-1		21.0	+14.1	1.4	0.80	3.3	0.327	830	1300	3x10 ⁻⁵	28.5	44.7	74.0	0.145	0.179	0.350	HO 9028		
21216-1		21.2	+27.8	1.9	1.3	4.9	0.404	850	800	3x10 ⁻⁵	29.5	38.2	75.4	0.152	0.181	0.252	HO 9025		
21216-2		21.2	+27.8	1.9	1.3	4.9	0.404	850	900	3x10 ⁻⁵	27.8	37.0	75.0	0.163	0.170	0.390	HO 9026		
21216-4		21.2	+27.8	1.9	1.3	4.9	0.404	850	1000	3x10 ⁻⁵	30.9	37.8	65.4	0.160	0.113	0.252	HO 9029		
19216-1		21.1	+27.8	1.6	1.1	4.1	0.364	840	1000	3x10 ⁻⁵	30.9	45.9	73.6	0.200	0.359	0.447	HO 9024		
21216-2		21.0	+27.8	1.8	1.2	4.7	0.393	840	1000	3x10 ⁻⁵	39.8	49.6	72.0	0.291	0.348	0.244	HO 9026		
21216-1		21.2	+23.0	2.2	1.6	6.5	0.472	850	900	3x10 ⁻⁵	27.2	41.9	75.9	0.176	0.210	0.561	HO 9026		
21216-2		21.2	+23.0	2.2	1.6	6.5	0.472	850	1000	3x10 ⁻⁵	29.3	41.5	69.2	0.059	0.111	0.378	HO 9027		
19216-1		21.1	+23.0	1.9	1.4	5.2	0.413	840	1000	3x10 ⁻⁵	34.2	49.8	74.6	0.216	0.298	0.358	HO 9025		
21216-2		21.0	+23.0	2.1	1.5	6.1	0.456	847	1000	1.7x10 ⁻²	48.3	55.4	74.3	0.170	0.227	0.642	HO 9028		
21216-1		21.2	+27.8	1.9	1.3	4.9	0.404	850	1200	3x10 ⁻⁵	21.5	35.9	49.4	0.031	0.039	0.567	HO 7027		
21216-1		21.0	+16.8	2.8	2.2	9.1	0.542	1065	1000	3x10 ⁻⁵	19.9	28.9	67.6	0.132	0.156	0.268	HO 9030		
21216-2		21.0	+16.8	2.8	2.2	9.1	0.542	1065	1100	3x10 ⁻⁵	15.8	25.6	57.8	0.102	0.120	0.211	HO 9031		
21216-3	21.0	+16.8	2.8	2.2	9.1	0.542	1065	1200	3x10 ⁻⁵	17.6	25.7	44.3	0.081	0.114	0.295	HO 9032			
21216-4	21.0	+16.8	2.8	2.2	9.1	0.542	1065	1300	3x10 ⁻⁵	15.4	22.5	35.0	0.053	0.105	0.211	HO 9029			
21216-1	21.0	+12.0	3.2	2.6	11.1	0.591	1065	1300	4.5x10 ⁻⁵	16.3	21.0	34.2	0.061	0.077	0.205	HO 9070			
21216-5	21.0	+2.4	3.6	2.9	13.1	0.637	1065	1300	4.5x10 ⁻⁵	14.2	18.9	34.2	0.054	0.058	0.154	HO 9071			
1067	33-3-1	6.5	+17.0	4.3	3.6	16.9	0.702	1220	1200	3x10 ⁻⁵	28.5	39.0	48.0	0.026	0.031	0.154	HO 9084		
	33-3-5	6.5	+12.0	5.1	4.4	21.8	0.787	1230	1200	3x10 ⁻⁵	32.5	41.9	49.4	0.015	0.021	0.157	HO 9085		
	33-2-5	6.5	+17.0	4.0	3.3	15.7	0.707	1520	1500	3x10 ⁻⁵	13.0	18.7	20.2	0.011	0.023	0.132	HO 9086		
	33-2-5	6.5	+12.0	4.9	4.3	20.9	0.787	1520	1500	3x10 ⁻⁵	11.8	17.1	19.1	0.014	0.020	0.081	HO 9087		
1067	38-AE-1	15.6	+9.5	0.73	0.64	3.2	0.395	975	800	3x10 ⁻⁵	27.6	38.5	75.0	0.228	0.281	0.667	HO 7176		
	38-AE-6	15.6	+9.5	0.73	0.64	3.2	0.395	975	1000	3x10 ⁻⁵	21.2	36.8	65.5	0.134	0.157	0.336	HO 7177		
	38-AE-7	15.6	+4.8	0.79	0.71	3.6	0.842	975	1100	3x10 ⁻⁵	25.6	39.5	59.1	0.071	0.082	0.309	HO 7178		
	38-AE-8	15.6	0	0.82	0.73	3.7	0.855	975	1200	3x10 ⁻⁵	22.8	35.4	47.5	0.025	0.045	0.171	HO 7179		

4.2-431

Amend. 51
Sept. 1979

TABLE 4.2-55 (CONTINUED)

POSTIRRADIATION TENSILE PROPERTIES OF ANNEALED TYPE 316 STAINLESS STEEL

EXPERIMENT IDENTIFICATION	SPECIMEN IDENTIFICATION	IRRADIATION CONDITIONS						TEST CONDITIONS		TEST RESULTS ^(a)							
		EBR II COORDINATES R, cm Z, cm		FLUENCE, $10^{22}n/cm^2$ (E=10-10 MeV)	FLUENCE, $10^{22}n/cm^2$ (E>0.1 MeV)	dpa	E, MeV	TEMP., °F	TEMP., °F	STRAIN RATE, SEC ⁻¹	σ_p , 1000 psi	σ_y , 1000 psi	σ_u , 1000 psi	ϵ_u (PLASTIC)	ϵ_t	RA	TEST IDENTIFICATION
(a)	SYMBOLS ARE DEFINED AS FOLLOWS:																
	σ_p IS STRESS AT PROPORTIONAL ELASTIC LIMIT																
	σ_y IS 0.2% OFFSET YIELD STRESS																
	σ_u IS ULTIMATE TENSILE STRENGTH																
	ϵ_u IS ELONGATION AT MAXIMUM LOAD																
	ϵ_t IS TOTAL ELONGATION																
	RA IS REDUCTION OF AREA																
(b)	COMMENT CODES: PIA - POSTIRRADIATION ANNEAL PRIOR TO TEST																

4.2-432

Amend. 51
Sept. 1979

TABLE 4.2-56

TENSILE PROPERTIES OF IRRADIATED INCONEL 718
(Annealed 1750°F/0.5 Hr. - Aged 1325°F/8 Hr. + 1150°F/10 Hr.)

(from HEDL-SA 1059)

Irrad. Temp. °C	Fluence- Total	$10^{22}n/cm^2$ E>0.1 MeV	Test Temp. °C	$\dot{\epsilon}$ Sec ⁻¹	Strength - MPa (Ksi)					Elongation-%		Reduction of Area-%	Site Sequence
					PEL	0.2% Yield	Ultimate	Total	Unif.				
391	0.93	0.80	22	3×10^{-5}	791 (114.7)	1153 (167.2)	1300 (188.5)	10.3	6.4	27.9	HO 4804		
			232		803 (116.4)	1017 (147.5)	1153 (167.2)	10.5	6.9	32.8		4805	
			427		818 (118.7)	1006 (145.9)	1107 (160.6)	8.4	4.0	26.8		4806	
			427		695 (100.8)	942 (136.6)	1121 (162.6)	8.4	5.7	26.8		4824	
			538		803 (116.4)	1009 (146.3)	1118 (162.2)	4.1	2.7	11.5		4807	
			649				0.7	0.7	2.5	--		--	
404	0.55	0.41	22	3×10^{-5}	796 (115.4)	1027 (149.0)	1245 (180.5)	17.2	12.8	35.8	4803		
			232		859 (124.6)	1021 (148.1)	1255 (182.0)	17.8	14.4	32.8	4809		
			427		661 (95.9)	897 (130.1)	1107 (160.6)	19.3	14.3	26.8	4810		
			538		616 (89.4)	884 (128.2)	1071 (155.3)	12.8	11.2	17.1	4811		
			649		622 (90.2)	797 (115.6)	879 (127.5)	6.1	4.7	11.5	4861		
593	0.86	0.71	22	3×10^{-5}	656 (95.1)	910 (132.0)	1305 (189.3)	24.5	21.3	38.5	4818		
			232		610 (88.5)	814 (118.0)	1160 (163.2)	24.4	22.3	30.3	4819		
			232		616 (89.4)	863 (125.2)	1208 (175.2)	21.7	18.9	33.3	4822		
			427		701 (101.6)	854 (123.8)	1136 (164.7)	21.4	17.4	27.9	4851		
			538		644 (93.4)	814 (118.0)	1086 (157.3)	18.1	17.0	22.1	4852		
			593		587 (85.2)	769 (111.5)	968 (140.4)	9.0	8.1	18.0	4820		
			593		678 (98.4)	832 (120.7)	1039 (150.7)	7.7	7.4	13.1	4850		
			593		599 (86.9)	812 (117.8)	1027 (149.0)	9.4	8.7	9.0	4823		
			649		554 (80.3)	738 (107.1)	825 (119.7)	4.4	3.2	7.3	4821		
			593		1.78	1.30	22	3×10^{-5}	628 (91.1)	914 (132.5)	1281 (185.8)	21.2	19.5
232	718 (104.1)	912 (132.3)		1232 (178.7)			20.3		18.7	25.2	4841		
427	746 (108.2)	893 (129.5)		1140 (166.8)			18.1		15.8	22.1	4915		
538	684 (99.2)	841 (122.0)		1080 (156.7)			14.6		13.2	17.1	4857		
593	658 (95.5)	877 (127.2)		1029 (149.2)			5.5		5.0	1.6	4838		
649	656 (95.1)	791 (114.7)		838 (121.6)			2.5		2.3	0.8	4840		
649	3.13	2.65	22	3×10^{-5}	712 (103.3)	996 (144.4)	1274 (184.8)	17.0	12.7	28.7	4844		
			232		718 (104.1)	910 (132.0)	1232 (178.7)	20.3	18.7	25.2	4842		
			427		684 (99.2)	946 (137.0)	1191 (172.8)	16.0	14.3	19.5	4839		
			538		--	--	--	3.1	3.1	4.1	--		
			649		650 (94.3)	866 (125.6)	945 (137.1)	1.7	1.6	3.2	4914		
			649		847 (122.9)	877 (127.2)	877 (127.2)	0.3	0.3	2.4	4913		
			649		684 (99.2)	850 (123.3)	850 (123.3)	0.1	0.1	0.8	4912		

4.2-433

Amend. 51
Sept. 1979

TABLE 4.2-56 (CONTINUED)
HIGH STRAIN RATE TENSILE PROPERTIES OF IRRADIATED INCONEL 718

Irrad. Temp. °C	Fluence-Total	$10^{22}n/cm^2$ $E>0.1$ MeV	Test Parameters		Strength - MPa (Ksi)				Elongation-%		Reduction of Area-%	Site Sequence
			Temp. °C	$\dot{\epsilon}$ -Sec ⁻¹	PEL	0.2% Yield	Ultimate	Total	Unif.			
396	0.86	0.71	232	7.4×10^{-3}	803 (116.4)	1014 (147.0)	1170 (169.7)	7.2	5.9	26.2	HO 4847	
	0.86	0.71	427		780 (113.1)	982 (142.5)	1081 (156.8)	5.7	4.4	28.7		
	0.86	0.71	649		960 (139.3)	982 (142.4)	1001 (145.2)	3.9	3.2	14.7		
396	0.86	0.71	232	1.0	1042 (151.2)	1135 (164.6)	1253 (181.7)	9.6	5.7	30.9	4905	
	0.93	0.80	427		925 (134.1)	1051 (152.4)	1135 (164.6)	5.8	3.6	18.7	4904	
	0.86	0.71	649		834 (120.9)	989 (143.4)	1011 (146.7)	4.7	3.8	27.9	4906	
593	0.94	0.81	232	7.4×10^{-3}	667 (96.7)	845 (122.5)	1164 (168.8)	17.0	15.6	27.9	4849	
	0.94	0.81	593		622 (90.2)	801 (116.2)	1038 (150.6)	13.2	13.2	22.1	4846	
	0.96	0.83	649		650 (94.3)	823 (119.3)	1044 (151.4)	10.2	10.2	18.7	4845	
593	0.93	0.86	232	1.0	840 (121.9)	950 (137.8)	1228 (178.1)	16.8	14.1	41.3	4894	
	0.97	0.84	538		729 (105.7)	827 (120.0)	1074 (155.7)	16.5	13.3	24.6	4897	
	0.98	0.86	593		791 (114.7)	859 (124.6)	1057 (153.3)	18.0	16.2	24.6	4895	
	0.97	0.84	649		803 (116.4)	851 (123.4)	1037 (150.4)	12.6	12.0	18.9	4896	
593	1.48	0.99	232	7.4×10^{-3}	757 (109.8)	900 (130.5)	1219 (176.8)	16.7	15.5	35.0	4858	
	2.44	1.96	593		791 (114.7)	904 (131.1)	1107 (160.6)	12.5	10.7	23.8	4856	
	1.48	0.99	649		672 (97.5)	801 (116.2)	994 (144.2)	7.7	7.6	11.5	4859	
593	1.35	0.88	232	1.0	820 (118.9)	897 (130.1)	1185 (171.9)	19.5	16.9	39.0	4902	
	1.48	0.99	593		780 (113.1)	853 (127.3)	1011 (146.7)	14.2	10.6	32.0	4901	
	1.25	0.80	649		603 (87.4)	729 (105.7)	989 (143.5)	19.0	19.0	26.8	4903	
649	3.34	2.89	232	7.4×10^{-3}	925 (134.1)	1087 (157.7)	1289 (181.0)	10.9	9.1	22.8	4854	
	3.34	2.89	649		791 (114.7)	955 (138.5)	1094 (158.6)	6.4	4.8	13.1	4853	
649	3.34	2.89	232	1.0	989 (143.4)	1108 (160.7)	1274 (184.8)	12.5	9.4	28.7	4898	
	3.42	2.98	538		847 (122.9)	989 (143.4)	1173 (170.1)	11.1	8.1	27.9	4900	
	3.42	2.98	649		855 (124.0)	1009 (146.3)	1152 (167.1)	8.7	8.0	13.3	4899	

4.2-434

(from HEDL-SA 1059)

Amend. 51
Sept. 1979

TABLE 4.2-57

IRRADIATED WELD MATERIAL TENSILE PROPERTIES.

(from HEDL-TME 74-25)

Specimen Ident.	Condition	Test Temp. (°F)	Tot. ϕ t (10^{22} n/cm 2)	Irrad. Temp. (°F)	Strength (1000 psi)			Ductility (%)			
					PEL	YS2	UTS	UNI	TOT	RA	
<u>Weld "A" - Transverse, all-weld, 1/8" dia. gage</u>											
35-T-W10 (H07509)	AW	600	.45	800	52.8	69.6	77.9	6.2	14.4	61	
35-T-W11 (H07557)	AW	700	.45	800	53.5	70.9	78.0	3.8	10.5	57	
35-T-W13 (H07552)	AW	800	.45	800	48.0	66.9	75.5	4.8	11.0	68	
35-T-W19 (H07559)	AW	900	.45	800	52.8	67.2	70.8	2.9	9.7	74	
35-T-W9 (H07510)	AW	600	.10	700	45.5	58.3	71.8	9.6	16.5	65	
35-T-W17 (H07575)	AW	700	.10	700	35.8	56.8	71.3	10.7	16.5	76	
35-T-W18 (H07576)	AW	800	.10	800	36.6	51.3	67.8	12.8	19.2	75	
35-T-W46 (H07577)	AW	900	.10	800	39.0	53.9	68.5	11.8	17.3	64	
35-T-W52 (H07725)	AW	1100	.70	1100	31.9	41.4	52.2	3.9	5.9	53	
<u>Weld "B" - Transverse, all-weld, 1/8" dia. gage</u>											
4.2-435	35-SA1-W10 (H07517)	AW	600	.45	800	41.2	56.0	73.2	15.1	17.0	44
	35-SA1-W13 (H07560)	AW	700	.45	800	39.8	55.0	75.4	14.7	15.5	37
	36-SA1-W11 (H07561)	AW	800	.45	800	40.6	56.4	78.3	18.1	19.5	36
	36-SA1-W19 (H07562)	AW	900	.45	800	39.8	54.8	66.3	9.6	10.7	39
	35-SA1-W9 (H07503)	AW	600	.10	700	25.6	43.1	73.0	19.9	23.0	40
	36-SA1-W17 (H07579)	AW	700	.10	700	28.5	41.5	70.5	18.7	19.1	35
	35-SA1-W8 (H07572)	AW	800	.10	800	26.8	38.1	66.1	24.2	25.2	39
	35-SA1-W15 (H07574)	AW	900	.10	800	28.1	39.1	67.6	22.1	23.8	35
	35-SA1-W22 (H07583)	AW	1100	.70	1100	19.5	30.9	46.8	7.1	8.0	23
<u>Weld "C" - Transverse, all-weld, 1/8" dia. gage</u>											
	35-M1-W16 (H07514)	AW	600	.45	800	49.6	62.6	76.1	11.0	16.6	51
	35-M1-W17 (H07563)	AW	700	.45	800	52.8	65.0	70.2	4.6	9.1	52
	36-M1-W24 (H07564)	AW	800	.45	800	43.1	59.9	65.6	9.3	13.6	55
	36-M1-W25 (H07565)	AW	900	.45	800	44.7	59.1	77.6	7.4	13.6	58

AW - as weldedAmend. 51
Sept. 7

TABLE 4.2-57 (CONTINUED)

Specimen Ident.	Condition	Test Temp. (°F)	Tot. ϕ t (10^{22} n/cm ²)	Irrad. Temp. (°F)	Strength (1000 psi)			Ductility (%)		
					PEL	YS2	UTS	UNI	TOT	RA
35-M1-W15 (H07506)	AW	600	.10	700	27.6	42.6	66.7	21.6	27.0	60
35-M1-W23 (H07582)	AW	700	.10	700	32.5	44.9	68.5	21.8	27.2	49
35-M1-W13 (H07581)	AW	800	.10	800	28.5	40.6	66.7	22.3	28.2	50
37-M2-W11 (H07587)	AW	1100	.70	1100	24.4	37.3	43.6	5.9	10.9	35

Weld "D" - Transverse, all-weld, 1/8" dia. gage

35-SE1-W19 (H07511)	AW	600	.45	800	39.8	62.6	80.3	15.0	19.0	42
35-SE1-W24 (H07566)	AW	700	.45	800	40.6	59.1	77.6	16.6	21.2	58
36-SE1-W39 (H07568)	AW	800	.45	800	43.8	59.3	77.6	14.5	18.1	46
36-SE1-W40 (H07567)	AW	900	.45	800	38.2	58.2	74.8	14.2	20.4	52
35-SE1-W17 (H07513)	AW	600	.10	700	43.0	49.8	71.8	18.5	23.7	62
37-SE2-W13 (H07528)	AW	1100	.70	1100	28.1	40.8	52.2	6.0	9.8	46

Weld "I" - Transverse, all-weld, 1/8" dia. gage

SET-05 (H08150)	AW	800	.55	900	28.0	59.1	75.2	8.0	9.8	34
SET-06 (H08151)	AW	1200	.55	900	34.9	45.7	47.2	1.0	7.6	50
SET-19 (H08152)	AW	800	.23	800	37.3	48.8	70.7	14.1	16.7	43
SET-20 (H08153)	AW	1200	.23	800	25.6	36.3	39.4	2.2	9.2	46

Weld "J" - Longitudinal, all-weld, 1/8" dia. gage

SEL-01 (H08156)	AW	600	.55	900	43.2	59.2	81.6	11.8	15.2	42
SEL-02 (H08157)	AW	800	.55	900	46.5	62.2	76.8	10.9	13.6	37
SEL-03 (H08158)	AW	900	.55	900	38.8	61.2	74.6	8.5	11.7	50
SEL-04 (H08159)	AW	1000	.55	900	43.9	59.4	65.8	8.0	11.7	50
SEL-05 (H08160)	AW	1200	.55	900	30.9	40.9	42.9	1.2	12.8	47
SEL-10 (H08161)	AW	600	.18	900	39.4	53.0	76.9	14.4	17.1	55
SEL-11 (H08162)	AW	800	.18	900	43.9	52.7	72.4	16.2	18.9	48
SEL-12 (H08163)	AW	900	.18	900	39.8	51.8	70.9	14.0	16.8	50
SEL-13 (H08164)	AW	1000	.18	900	20.7	35.0	61.8	17.5	20.3	59
SEL-14 (H08165)	AW	1200	.18	900	30.9	39.0	41.5	2.1	20.1	48
SEL-19 (H08166)	AW	800	.23	800	34.2	52.8	73.2	15.1	17.9	48
SEL-20 (H08167)	AW	1200	.23	800	26.1	38.5	40.4	1.5	18.2	44

54 |

TABLE 4.2-58 - DELETED

4.2-437

Amend. 54
May 1980

THIS PAGE INTENTIONALLY BLANK

4.2-438

Amend. 51
Sept. 1979

TABLE 4.2-59

CRBRP DESIGN BASIS TRANSIENTS TO BE ENVELOPED IN FUEL
 ROD TRANSIENT TESTS

<u>Event Category</u>	<u>Simulated CRBRP Event</u>	<u>Description</u>
Upset	U2-b	Uncontrolled rod withdrawal from 100% power with delayed manual trip. Operation at 115% power for 5 minutes. This is most damaging fuel rod upset overpower transient.
Upset	OBE	Operating basis earthquake with 30¢ step reactivity insertion.
Emergency	E-16	Three loop natural circulation. Most damaging undercooling emergency event.
Faulted	\$2/Sec. Ramp	PPS Design Transient
Faulted	SSE (60¢ step)	Safe Shutdown Earthquake with 60¢ step reactivity insertion. Slightly more severe than \$2/sec ramp. (Umbrellas 60¢ step (non-seismic) which is emergency PPS design event.

TABLE 4.2-59A

QUALITY CONFORMANCE INSPECTION CHARACTERISTICS - FUEL ROD AND COMPONENTS

<u>Fuel Rods</u>	
General	End Cap-to-Clad Welding Qualifications
Fuel Rod Component Placement	Weld Throat Thickness
Components and Materials	Destructive Test
Gas Tagging	Nondestructive Test
Tag Gas Composition	Weld Surface
Number of Rods per Tag	Internal Weld
Fuel Rod Dimensions	Destructive Test
Length	Nondestructive Test
Fuel Rod Bow	Weld Diameter
Concentricity	Wire Wrapping
End Cap Angular Orientation	End and Weld Location
Fuel Pellet Stack	Overall Length
Pellet Type	Orientation
Other Conformance	Number of Turns
Weight	Tension
Length and Pellet Spacing	Wire-Cladding Gap
Before Rod Assembly	End Cap-to-Wire Wrap Welding
After Rod Assembly	Qualification
Volatiles Content	Wire Weld Strength
Gas	Surface Characteristics
Moisture	Cleanliness
Oxygen-to-Metal Ratio	Surface Passivation
Axial Blanket Pellet Stack	Residual Chloride and Fluoride
Conformance	Components
Weight	Fuel Rods
Length	Radioactive Surface Contamination
Volatiles Content	Smearable
Gas	Fixed
Moisture	Surface Defects
Oxygen-to-Metal Ratio	Surface Roughness
Fuel Rod Fissile Content	Identification
Bonding Gas	Workmanship
Composition	Assembly Sequence
Welding Chamber Helium Purity	Tag Gas Weight
Pressure	Capsule Loading
Fuel Rod Integrity	Gas Release
	Lotting
	Handling and Storage During Processing
	Archive Samples

TABLE 4.2-59A (Continued)

Fuel Pellets

Plutonium Form and Properties
 Isotopic Concentration
 Other Characteristics
 Uranium Form and Properties
 Fuel Pellet Fissile Concentration
 Uranium Concentration
 Fuel Pellet Plutonium Concentration
 Individual and Total Impurities
 Lot
 Core Zone
 Americium Content
 Oxygen-to-Metal Ratio
 Pellet
 Lot Average
 Gas Content
 Moisture Content
 Pellet
 Lot Average
 Homogeneity - Figure of Merit
 Plutonium Concentration Regions
 Grain Size, Porosity, Secondary
 Phases
 Fuel Pellet, Weight Per Unit Length
 Fuel Pellet Dimensions
 Length
 Diameter
 Dish Diameter
 Dish Depth
 Perpendicularity
 Pellet Weight
 Surface Condition
 Defects
 Appearance
 Cleanliness
 Process Sequence
 Pellet Manufacture
 Lotting and Identification
 Storage During Processing
 Archive Samples

Axial Blanket Pellets

Uranium Form and Properties
 Purity - Minimum Uranium
 Individual Impurities
 Oxygen-to-Metal Ratio
 Gas Content
 Moisture Content
 Weight per Unit Length
 Diameter and Length
 Maximum Radius or Chamfer
 Perpendicularity
 Surface Condition
 Process Sequence
 Pellet Manufacture
 Lotting and Identification
 Storage During Processing
 Archive Samples

Tag Gas Capsule

Dimensions
 Capsule Materials
 Tag Gas Composition
 Blending Gas
 Isotopic Ratios
 Xe to Kr Ratio
 Impurities
 Tag Gas Capsule
 Capsule Integrity
 Identification
 Cleanliness
 Residual Cl and F1-Components
 Surface Roughness
 Weld Procedure
 Laser Drilling Procedure
 EB Weld Thickness
 Weld Integrity
 Maximum Diameter
 Helium Leak Test
 Tag Gas Capsule Filling
 Lotting
 Archive Samples

TABLE 4.2-59A (Continued)

Uranium Dioxide

Maximum Particle Size
 Particle Distribution
 Surface Area
 Isotopic Content
 Impurity Levels
 Oxygen-to-Metal Ratio
 Uranium Content
 Sinterability
 Analytical Samples
 Sampling
 Lotting

Plutonium Dioxide

Sieve Analysis
 Particle Distribution
 Surface Area
 Plutonium Isotopic Concentration
 Americium Content
 Impurity Levels
 Oxygen-to-Plutonium Ratio
 Plutonium Content
 Packed Materials
 After Calcining
 Loss on Ignition
 Sinterability
 Screening
 Blending
 Analytical Samples
 Sampling
 Lotting

Tubing (Cladding)

Chemical Composition
 Ingots
 Finished Tubing
 Cold Work
 Tensile Properties
 Hardness
 Ductility and Soundness
 Flaring
 Burst Pressure
 Grain Size
 Inclusion Content
 Intergranular Attack
 Carbide Precipitation
 Corrosion Resistance
 Surface Condition
 Surface Roughness
 Tube Hollows
 Finished Tubing
 Surface Marring
 Residual Cl and F1
 Passivation
 Cleanliness
 Ovality
 Wall Thickness and Eccentricity
 Straightness
 Penetrant Examination
 Halogens and Sulfur
 Tube
 Finished Tubing
 Ultrasonic Examination
 Melting
 Tube Making
 Heat Treatment
 Lotting
 Identification

TABLE 4.2-59A (Continued)

Wrap Wire

Chemical Composition

 Ingots

 Finished Wire

Cold Work

Tensile Properties

Hardness

Ductility

Grain Size

Inclusions

Intergranular Attack

Carbide Precipitation

Corrosion Resistance

Surface Condition

Surface Roughness

Surface Marring

Residual Cl and F

Cleanliness

Dimensions

Heat Treatment

Lotting

Identification

TABLE 4.2-59B

QUALITY CONFORMANCE INSPECTION CHARACTERISTICS FOR FUEL ASSEMBLY AND COMPONENTS

<u>Fuel Assembly</u>	<u>Duct Tubes</u>
Fuel Assembly Components	Chemical Composition
Component Materials	Cold Work
Components	Mechanical Properties
Fuel Assembly	Hardness
Gas Tag	Grain Size
Enrichment/Component Match	Inclusions
Fuel Rod Position	Intergranular Attack
Fissile Content	Carbide Precipitation
Fuel Rods	Corrosion Resistance
Assembly	Surface Condition
Americium Content	Surface Roughness
Fuel Rods	Surface Marring
Assembly	Residual Cl and F1
Dimensions	Cleanliness
Lengths	Dimensions
Weld Surfaces	Wall Thickness
Straightness	Penetrant Examination
Alignment	Ultrasonic
Twist	Melting
Tight Bundle and Duct Tube Gap	Tube Making
Fuel Assembly Weight	Heat Treatment
Cleanliness	Lotting
Residual Cl and F1	Repair and Rework
Surface Texture	Archive Sample
Surface Marring	Identification
Identification	
Fuel Assembly	
End Components	
Workmanship	
Processes	
Machining	
Welds	
Process	
Archive Samples	
Air Flow Test	
Handling and Storage During Processing	
Fabrication Records	
Packaging	

TABLE 4.2-59B (Continued)

<u>Piston Rings</u>	<u>Hard Facing</u>
Chemical Composition	Chemical Composition
Grain Size	Particle Size
Tensile Properties	Strength
Hardness	Hardness
Surface Requirements	Metallographic
Surface Roughness	Surface Condition
Surface Marring	Surface Roughness
Surface Indications	Surface Marring
Dimensions	Cleanliness
Outside Diameter	Residual C1 and F1
Roundness	Dimensions
Flatness	Hard Surface Application
Hook Free Gap	Lotting
Width	Identification
Thickness	Archive Samples
Coating Thickness	
Perpendicularity	
Cleanliness	
Heat Treatment	
Coating	
Lotting	
Identification	

TABLE 4.2-60 and 4.2-61 DELETED

TABLE 4.2-62

National Reference Fuel Steady State Program Activities Summary

I. Fission Gas

1. Release to gas plenum during low power (<8 kW/ft) operation.
2. Quantities and location of gas retained in fuel.
3. Release to gas plenum during power cycle.
4. Improved gas release models

II. Solid and Volatile Fission Product Migration

5. Cesium migration in long pins
6. Effect of cesium migration on mechanical strain
7. Confirmation of design fixes
8. Effect of low O/M Fuel ($O/M = 1.95$).
9. Tests in FFTF (effect of peaked axial power profile).

III. Fuel Stability and Constituent Migration

10. Evaluation
11. Radial and axial distribution of oxygen.
12. Correlation of fuel fabrication parameters and fuel column length changes.
13. Effect of O/M on fuel and oxygen migration.
14. The effect of the axial blanket.
15. Tests in FFTF (effect of peaked axial profile).

IV. Fuel-Cladding Chemical Interactions

16. Effects on cladding mechanical properties.
17. Correlation of temperature and burnup effects, particularly at burnups >5 a/o.
18. Determination of effect of O_2 potential (O/M and fission product spectrum).
19. Effects of getters.

TABLE 4.2-62 (CONTINUED)

20. Effects of all Pu-fissioning in FFTF (EBR-II tests included enriched uranium).
21. Effect of FFTF axial power profile.

V. Thermal Performance

22. Evaluation of existing tests on power-to-melt and effect of burnup (up to ~ 8 a/o).
23. Lower-power (< 8 kW/ft) fuel restructuring and radial relocation data to high burnup (up to ~ 8 a/o).
24. Effect of low O/M (< 1.96).
25. Power-to-melt verification in FFTF.

VI. Steady-State Performance

26. Determine steady-state design margin.
27. Provide basis for steady-state lifetime prediction.
28. Provide data to develop breaching criteria:
 - a. Fission gas pressure
 - b. Strain data over the irradiation period and at failure
 - c. Post-test mechanical properties
 - d. Failure mechanisms.
 - e. Stress histories
 - f. Fuel-cladding mechanical interaction.
 - g. Creep plastic interaction.
 - h. Effects of swelling gradients.
29. Validate and update design procedures and performance prediction methods.
30. Validate thermal hydraulic predictions with in-reactor instrumented tests in FFTF and post-irradiation examination data from EBR-II and FFTF.
31. Demonstrate proof-of-performance of FFTF and CRBR fuel in FFTF on a statistical level.

VII. Bundle-Duct Interactions and Spacer Systems

32. Validate design fix for bundle vibration and wear observed in EBR-II.

TABLE 4.2-62 (CONTINUED)

33. Validate predicted duct dimensional changes in EBR-II and FFTF.
34. Improve design criteria for bundle-duct interaction.
35. Evaluate performance of backup spacer systems.

VIII. Cladding Performance Characterization

36. Continue to generate data from irradiated fuel pin sections and subassembly ducts to evaluate swelling and creep correlations.
37. Continue to generate mechanical property data from fuel pin sections to evaluate fuel adjacency effects and lot-to-lot variations.
38. Assess Na-cladding interaction models against in-reactor data.

IX. Run-Beyond-Cladding Breach

39. Evaluate potential for fuel washout and consequences
40. Determine susceptibility for propagation of a breach to neighboring pins.

20

TABLE 4.2-63 DELETED

TABLE 4.2-64

58

DESIGN CONSIDERATIONS FOR SELF-WELDING AND SEIZING OF ROTATING OR MOVING PARTS

<u>LOCATION</u>	<u>PROBLEM</u>	<u>DESIGN</u>	<u>COMMENT</u>
Core Support Structure Module Liner Holes	Seizing	Stainless base metal with chrome plate on vertical contact surfaces.	No seizing expected because operating temperature is less than 800°F.
Lower Inlet Modules	Seizing	Module - CSS: Chrome plated Inconel piston rings, hardface land, 0.035" diametral gap (min.) Module - Core Assy: Alloy 718 base metal on vertical contact surfaces.	No seizing expected because operating temperature is less than 800°. No seizing expected because operating temperature is less than 800°F.
58 Fuel Transfer and Storage Assembly	Seizing	Stainless base metal.	No seizing expected. Tolerance large enough to permit easy removal of CCP.
UIS			
Jacking Mechanism Seals			
	Seizing	Elastomers: Standard vertical low pressure gland provided (both surfaces). EPR type material with compatible lubricant (light film).	No seizing expected because of low temperature operation (150°F). AI tests indicate negligible wear and seizing.
	Seizing	Piston Rings: Precipitation Hardened Stainless Steel	No seizing expected because of low temperature operation (400°F). Movement seizing not expected with this design concept which employs a scraper ring.

58

25

4.2-445

Amend. 58
NOV. 1980

<u>LOCATION</u>	<u>PROBLEM</u>	<u>DESIGN</u>	<u>COMMENT</u>
IVTM Port Plug			
A. Plug	Seizing/ Self-Welding	IVTM Port Plug - UIS: Stainless base metal. Haynes 273 hardcoat.	No self-welding or seizing expected because of hardcoated surfaces.
B. Seals	Seizing	Elastomers: Standard vertical low pressure gland provided (both surfaces). EPR type material with compatible lubricant (light film).	No seizing expected because of low temperature operation (150°F).
UIS Shroud Tubes			
A. Slip Fit Connec- tion	Seizing/ Self-Welding	Alloy 718 Upper Shroud Tube Telescopes over Alloy 718 Lower Shroud Tube.	No seizing or self-welding is expected due to material combination. Relative motion occurs during reactor refueling at 400°F.
B. Shroud/ Drive- line Assy.	Seizing/ Self-Welding	All parts in sodium are Alloy 718. Hardcoat surfaces.	Material combinations selected to prevent seizing and self-welding.
UIS Keys/CFS Keyway	Seizing/ Self-Welding	Stainless base metal with Haynes 273 hard surface key in Alloy 718 keyway.	Material combination selected to prevent seizing and self-welding.
Thermocouple Installation in Drywells	Seizing	Stainless base metal.	Low temperature tests indicate no seizing.
Backup Holdown for core Assemblies	Seizing	Alloy 718 Instrument Posts react core assemblies.	Contact only if hydraulic balance is lost. Contact forces low.

4.2-446

Amend. 58
Nov. 1980

TABLE 4.2-64 (Continued)

<u>LOCATION</u>	<u>PROBLEM</u>	<u>DESIGN</u>	<u>COMMENT</u>
Core Restraint System and Removable Radial Shielding Core Assemblies	Seizing/ Self-Welding	Discriminator Post: Stainless base metal. Piston rings with hardface land, 0.010" radial gap.	No self-welding or seizing expected because of low temperature (800°F) and removal speed is low.
	Seizing/ Self-Welding	Load Pads: Stainless base metal. Chrome Carbide Hardcoat.	No self-welding or seizing expected due to material combinations.
58 Horizontal Baffle Access Port Plugs	Seizing/ Welding	Contact surfaces between the plug and its support are Haynes 273.	No self-welding or seizing expected because of low contact loads. Removal of plug occurs only at refueling temperature (400°F).

4.2-447

TABLE 4.2-65

CRBRP FUEL ASSEMBLY DEVELOPMENT PLANNING

AREA OF TECHNICAL UNCERTAINTY	TECHNICAL INFORMATION REQUIRED AND CATEGORY	REQUIRED EXPERIMENT OR ANALYSIS	STATUS	UTILIZATION OF RESULTS	
1. Cladding Integrity During Steady State Operation	Cladding Material Properties:	I			
	A. Irradiation Creep	DS	NICE Tests P-1 through P-9 to 1.4×10^{23}	Ongoing	Perf. Pred. for Tech. Release
			NICE Tests P-1 through P-9 to 2.4×10^{23}	Ongoing	FSAR Submittal
	B. Irradiation Swelling	DS	NICE Tests P-1 through P-9 to 1.4×10^{23}	Ongoing	Perf. Pred. for Tech. Release
			NICE Tests P-1 through P-9 to 2.4×10^{23}	Ongoing	FSAR Submittal
			Microstructural Effects and Swelling	Ongoing	FSAR Submittal
	C. Cumulative Damage Characteristics	DS	Assemblies X-221, X-222, and X-261 in EBR-II to 1.1×10^{23}	Ongoing	Perf. Pred. for Tech. Release
	D. Yield Stress	DS	Assemblies X-221, X-222, and X-261 in EBR-II to 1.1×10^{23}	Ongoing	Perf. Pred. for Tech. Release
	E. Creep-Rupture Characteristics	DS	Assemblies X-221, X-222, and X-261 in EBR-II to 1.1×10^{23}	Ongoing	Perf. Pred. for Tech. Release
	Integral Rod Testing in EBR-II (Run to Cladding Breach)	DV	NUMEC D, E PNL 5A, 5B, 10, 11 HEDL P-12A, 13, 14, 14A, 23A, 23B, 23C, WSA 3, 8 F9C, F9F, F11A	Complete	FSAR Submittal
Cladding Wastage	DS	See Item 4			
Fuel Rod Cladding Breach Criteria and Cladding Steady State Performance Code	DS	Development of FURFAN	Ongoing	Final Design Review	
		Comparison of FURFAN with Experiments	Ongoing	Perf. Pred. for Tech. Release	

TABLE 4.2-65 (Continued)
 CRBRP FUEL ASSEMBLY DEVELOPMENT PLANNING

AREA OF TECHNICAL UNCERTAINTY	TECHNICAL INFORMATION REQUIRED AND CATEGORY	REQUIRED EXPERIMENT OR ANALYSIS	STATUS	UTILIZATION OF RESULTS
2. Fuel Behavior During Steady State and Transient Operation	Cladding Transient Behavior	See Item 3		
	Run Beyond Cladding Breach	RGN See Item 2		
	Fuel-Cladding Interactions	DS See Item 2		
	Flow Induced Rod Vibrations	DS See Item 7		
	Irradiation Creep and Swelling	DS Analyze Data and Issue Topical	Ongoing	FSAR Submittal
	Cumulative Damage Function and Creep-Rupture Evaluations	DS Analyze Data	Ongoing	Perf. Pred. for Tech. Release
	Evaluation of Integral Rod Tests	DV Analyze Data and Issue Topical	Ongoing	FSAR Submittal
	Development of FURFAN Code	DS Update Code to Incorporate Most Recent Data	Complete	Final Design Review
	Performance of CRBRP Fuel Assembly	DS Cladding Steady State Analysis with FURFAN	Ongoing	Perf. Pred. for Tech. Release
			Complete	Final Design Review
			Ongoing	Perf. Pred for Tech. Release
	Fission Gas Release	DS EBR-II Experiments P-12, P-20 F1, P-23, and others with various burnups, powers, and fuel composition	Ongoing	FSAR Submittal
Fuel Swelling	DS EBR-II Experiments (See Integral Rod Tests Under Item 1)	Complete	Final Design Review	
Fuel Density	DV Topical Report Summarizing Previous Experience	Ongoing	FSAR Submittal	
Fuel Swelling	DS EBR-II Experiments (See Integral Rod Tests Under Item 1)			
Fuel Density	DV Topical Report Summarizing Previous Experience	Complete	PSAR Response	

4.2-449

51

Amend. 51
 Sept. 1979

TABLE 4.2-65 (Continued)

CRBRP FUEL ASSEMBLY DEVELOPMENT PLANNING

AREA OF TECHNICAL UNCERTAINTY	TECHNICAL INFORMATION REQUIRED AND CATEGORY	REQUIRED EXPERIMENT OR ANALYSIS	STATUS	UTILIZATION OF RESULTS
	Effect of Axial Blanket on Fuel Performance	DS		
	Fission Product Migration	DS		
	Fuel-Cladding Interactions (Steady State)	DS		
	Pu-U Segregation at High Burnup	DS		
	Development of LIFE (Steady State and Transient Fuel Performance Code)	DS	Ongoing	FSAR Submittal
	Fuel-Sodium Behavior During RBCB	RGN	Ongoing	FSAR Submittal
	Fuel-Cladding Behavior and Interactions During Transients	DS		
	Verify Fission Gas Release Model	DS	Ongoing	Perf. Pred. for Tech. Release
	Verify Fuel Swelling Model	DS	Ongoing	Perf. Pred. for Tech. Release
	Assessment of CRBRP RBCB Capabilities	RGN	Ongoing	FSAR Submittal
	Assessment of CRBRP Fuel Performance	DS	Complete Ongoing	Final Design Review FSAR Submittal

4.2-450

51

53

Amend. 53
Jan. 1980

TABLE 4.2-65 (Continued)
 CRBRP FUEL ASSEMBLY DEVELOPMENT PLANNING

AREA OF TECHNICAL UNCERTAINTY	TECHNICAL INFORMATION REQUIRED AND CATEGORY		REQUIRED EXPERIMENT OR ANALYSIS	STATUS	UTILIZATION OF RESULTS
3. Cladding Integrity During Transient Operation	Cladding Material Properties at Transient Temperatures and Strain Rates:				
	A. Creep Rupture Characteristics	DS	RCD Program Task A	In Planning	
	B. Cumulative Damage Characteristics	DS	RCD Program Task A	In Planning	
	Transient Rod Tests	DV	HOP, HUT, and HUC Tests in TREAT Reactor including PTO and FCTT Testing	Ongoing	FSAR Submittal
	Transient Performance of Failed Rods	RGN	HOP, HUT, and HUC Tests of Failed Rods in TREAT	In Planning	FSAR Submittal
	Fuel-Cladding Interactions	DS	See Transient Rod Tests (Above)		
	Transient Cladding Performance Code	DS	Develop Transient version of FURFAN	Ongoing	Perf. Pred for Tech. Release
			Comparison of FURFAN with In-pile and Out-of-Pile Experiments	Ongoing	FSAR Submittal
	Evaluation of Transient Rod Tests	DV	Analyze Data and Issue Topical	Ongoing	FSAR Submittal
High Temperature CDF and Creep-Rupture Evaluations	DS	Analyze Data and Issue Topical	Ongoing	FSAR Submittal	

TABLE 4.2-65 (Continued)
 CRBRP FUEL ASSEMBLY DEVELOPMENT PLANNING

AREA OF TECHNICAL UNCERTAINTY	TECHNICAL INFORMATION REQUIRED AND CATEGORY		REQUIRED EXPERIMENT OR ANALYSIS	STATUS	UTILIZATION OF RESULTS
4. Internal/ External Cladding Degradation	High Strain Rate Creep-Rupture Evaluation	DS	Analyze Data and Issue Topical	Ongoing	FSAR Submittal
	Assessment of Transient Performance of the CRBRP Cladding	DS	Cladding Analyses with Transient Version of FURFAN	Complete Ongoing	Final Design Review FSAR Submittal
	Fretting Wear	DS	Wire Wrap-Cladding Wear Test	Complete	Final Design Review
			Evaluation of EBR-II Experiment Results with a Similar Rod Bundle Porosity	Ongoing	FSAR Submittal
			Flow and Vibration Test In Water	Ongoing	Long Term Test Evaluation
	Sodium Corrosion	DS	Evaluation of EBR-II Experiments with Similar Cladding Temperatures	Ongoing	FSAR Submittal
			Evaluation of Out-of-Pile Data obtained with CRBRP Loop and Mass Transfer Characteristics	Ongoing	FSAR Submittal
	Fuel-Cladding Chemical Attack	DS	Evaluation of EBR-II Experiments with Similar Pellet Compositions, Burnups, and Power Histories	Ongoing	FSAR Submittal
Carbon and Nitrogen Depletion	DS	Evaluation of EBR-II Experiments with Similar Cladding Compositions, Power Ratings, and Temperatures but with a Variety of Lifetimes	Ongoing	FSAR Submittal	

4.2-452

51

TABLE 4.2-65 (Continued)
 CRBRP FUEL ASSEMBLY DEVELOPMENT PLANNING

AREA OF TECHNICAL UNCERTAINTY	TECHNICAL INFORMATION REQUIRED AND CATEGORY		REQUIRED EXPERIMENT OR ANALYSIS	STATUS	UTILIZATION OF RESULTS
5. Wire Wrap Integrity	Development of a Cladding Wastage Model	DS	Analyze Data and Issue Topical	Ongoing	FSAR Submittal
	Development of a Carbon/Nitrogen Depletion Model	DS	Analyze Data and Issue Topical	Ongoing	FSAR Submittal
	Wire Material Properties	DS	Use Cladding Material Properties (See Item 1)		
	Wire External Degradation	DS	Use Sodium Corrosion and Fretting Wear From Cladding (See Item 4)		
	Wire Wrap Performance Code	DS	Development of WRAPUP Code	Complete	Final Design Review
6. Fuel Assembly Thermal Behavior	Comparison of WRAPUP Predictions with Experimental Data			Ongoing	FSAR Submittal
	Performance of CRBRP Fuel Assembly Wire Wrap	DS	Wire Wrap Analysis of CRBRP Fuel Rods with WRAPUP	Complete	Final Design Review
	Power-to-Melt	DV	Correlate Code Predictions with P-19/P-20 Results	Complete	Final Design Review
	Gather Experimental Data for Other Lifetimes Than BOL				
	Hot Channel Uncertainty Factors	DS	Update Steady State and Transient Hot Channel Factors and Plant Conditions Uncertainties	Ongoing	Perf. Pred. for Tech. Release

4.2-453

53

51

Amend. 53
 Jan. 1980

TABLE 4.2-65 (Continued)

CRBRP FUEL ASSEMBLY DEVELOPMENT PLANNING

AREA OF
TECHNICAL
UNCERTAINTY

TECHNICAL INFORMATION REQUIRED
AND CATEGORY

REQUIRED EXPERIMENT OR ANALYSIS

STATUS

UTILIZATION OF RESULTS

Assembly Temperature Distribution

DS

Develop Rigorous Steady-State and Transient Subchannel Analysis Codes (COBRA IV)

Complete

Input to T&H Design

Ongoing

Perf. Pred. for Tech. Release

Experimental Characterization of Flow in Wire Wrap Bundles

Complete

Input to T&H Design

Large Rod Bundle Heat Transfer Test

Complete

FSAR Submittal

Rod Temperature Profile

DS

Develop Method of Calculations 3D Rod Temp. Profile (FATHOM-360 Codes)

Complete

Input to T&H Design

Assemblies Orificing

DS

Develop Criteria & Methodology for Orificing Core Assemblies (OCTOPUS and CATFISH Codes)

Complete

Input to T&H Design

Materials Properties and Behavior

DS

Characterize Thermal Property of Materials

Input to T&H Design

Perform Irradiation Tests

Reactor Operation

Analytical Modeling of Fuel Behavior (Fuel Rod Performance Code Development)

Input to T&H Design

Core Natural Circulation Capability Verification

DS

Whole Core Thermal Hydraulic Transient Analysis Code Development and Verification

Code Development Complete
Verif. Ongoing

Final Design
FSAR Submittal

EBR-II and FFTF Natural Circulation Testing

EBR-II Complete

Final Design

FFTF-FOTA Complete

Final Design

FFTF-BOTA Complete

FSAR Submittal

4.2-454

Amend. 71
Sept. 1982

TABLE 4.2-65 (Continued)
 CRBRP FUEL ASSEMBLY DEVELOPMENT PLANNING

AREA OF TECHNICAL UNCERTAINTY	TECHNICAL INFORMATION REQUIRED AND CATEGORY		REQUIRED EXPERIMENT OR ANALYSIS	STATUS	UTILIZATION OF RESULTS
7. Assembly Hydraulic Behavior	3-D Duct Temperature Profile	DS	Develop Analytical Code (TRITON) to Calculate Duct Temps. in CRBR Core Including Interassembly Heat Transfer	Ongoing	Final Design Review
	Rod T&H Performance Code	DS	Continue Development of Analytical Code for Fuel Rod T&H Design and Performance Under Steady State and Transient Conditions	Ongoing	Input to T&H Design
	Fuel Assembly and Rod T&H Design and Performance	DS	Perform T&H Design and Performance Evaluation of Fuel Assemblies	Complete	Final Design Review
	Pressure Drops Through The Following Components:				
	A. Inlet Nozzle	DV	F/A Inlet Nozzle Test in Water	Complete	Final Design Review
	B. Shield	DV	F/A Inlet Nozzle Test in Water	Complete	Final Design Review
	C. Rod Bundle	DV	F/A Flow and Vibration Test in Water	Complete	Long Term Test Evaluation
	D. Outlet Nozzle	DV	F/A Outlet Nozzle Test in Water	Complete	Final Design
	Data for Sizing the Orifice Plate Holes	DS	F/A Inlet Nozzle Test in Water	Ongoing	Final Design Verification
	Flow Induced Rod Vibrations	DS	F/A Flow and Vibration Test in Water	Complete	Long Term Test Evaluation
Leakage Flow Rates Past the Piston Rings	DV	F/A Inlet Nozzle Test in Water	Complete	Final Design Review Long Term Test Evaluation	

4.2-455

51

Amend. 51
 Sept. 1979

TABLE 4.2-65 (Continued)

CRBRP FUEL ASSEMBLY DEVELOPMENT PLANNING

AREA OF TECHNICAL UNCERTAINTY	TECHNICAL INFORMATION REQUIRED AND CATEGORY	REQUIRED EXPERIMENT OR ANALYSIS	STATUS	UTILIZATION OF RESULTS
	Flow Distribution In Rod Bundle During Transients and Low Flow Rates	DV Natural Circulation Sodium Heat Transfer Test	Complete	Transient Analysis
		COBRA Loss of Flow Event Transient Capability	Complete	Transient Analysis
		F/A Inlet Nozzle Test In Water	Complete	Transient Analysis
		F/A Flow and Vibration Test In Water	Complete	Transient Analysis
	Absence of Cavitation	DV Fuel Assembly Cavitation Tests	Ongoing	Final Design Verification
	Flow Induced Assembly Vibrations	DS F/A Outlet Nozzle Test In Water	Complete	Final Design Review
	Core Exit Instrumentation Uncertainties	DS Assembly Outlet Nozzle Instrumentation Test	Ongoing	Perf. Pred. for Tech. Release
	Size Orifice Plate Holes	DS Analyze Data	Ongoing	Perf. Pred. for Tech. Release
	Component ΔP Evaluation	DV Analyze Data and Issue Topical	Ongoing	Final Design Review
	Evaluation of Flow Induced Rod Vibrations	DS Analyze Data and Issue Topical	Complete	Long Term Test Evaluation
8. Rod Bundle Duct Interaction	Rod Bowing	DS Analyses of Rod Bow with Cladding Properties at Goal Exposure (See Item 1)	Ongoing	Perf. Pred. for Tech. Release
	Duct Bowing	DS Analyses of Duct Bowing with Duct Properties at Goal Exposure (See Item 9)	Ongoing	Perf. Pred. for Tech. Release
	Duct Dilation due to Irradiation Effects	DS Analyses of Duct Dilation	Complete	Final Design Review
	Rod-to-Rod Forces Caused by Bundle-Duct Differential Growth	DS Rod Bundle Compaction Test Analyses of Rod Bundle-Duct Interaction Forces	Complete Ongoing	Final Design Review Perf. Pred. for Tech. Release

TABLE 4.2-65 (Continued)
 CRBRP FUEL ASSEMBLY DEVELOPMENT PLANNING

AREA OF TECHNICAL UNCERTAINTY	TECHNICAL INFORMATION REQUIRED AND CATEGORY		REQUIRED EXPERIMENT OR ANALYSIS	STATUS	UTILIZATION OF RESULTS
9. Duct Integrity	Duct Material Properties: Irradiation Creep Irradiation Swelling Cumulative Damage Characteristics Fracture Toughness Creep-Rupture Characteristics Load Pad Strength Duct Bending Stiffness Evaluation of Duct Material Properties Steady State Duct Loading Duct Loading During Seismic Events Effect of Irradiation on Duct Loading and Property Change Stress Relaxation in Irradiated Material	DS DS DS DS DS DS DS DV DV DS DS	RCD Program Task B (See Item 1) RCD Program Tasks B and C (See Item 1) Assemblies X-195, X-229, X-230, X-231, and X-240 in EBR-II RCD Program Task A Assemblies X-195, X-229, X-230 Core Assembly Load Pad Strength and Duct Bending Stiffness Test Analyze Data and Issue Topical Core Restraint Analyses National Core Restraint Program Seismic Core Restraint Analyses EBR-II Duct Crushing Test Slit Tube Tests on Irradiated Fuel Rods Task B of RCD Program	Ongoing Ongoing Ongoing Complete Ongoing Ongoing Complete Complete	Perf. Pred. for Tech. Release Perf. Pred. for Tech. Release Perf. Pred. for Tech. Release Long Term Test Evaluation Final Design Review Final Design Review
10. Load Following	Cladding Ratchetting	RGN	TBD National Program on Steady State Reference Fuel Irradiation	In Planning	

DS - Design Support
 DV - Design Verification
 RGN - Go-No-Go Evaluation of Requirements

4.2-457

51

Amend. 51
 Sept. 1979

PRELIMINARY CLADDING FATIGUE ESTIMATE
Table 4.2-66

<u>Transient</u>	<u>ni</u>	<u>Ni</u>	<u>ni/Ni</u>
Scram and Restart	7 (with FCMI)	5,000 (with FCMI)	.0014
	13 (w/o FCMI)	200,000 (w/o FCMI)	.000065
Trip from Full Power*	14 (with FCMI)	5,000 (with FCMI)	.0028
	26 (w/o FCMI)	200,000 (w/o FCMI)	.00013
Reactivity Insertion**	5	>10 ⁶	~0

TOTAL 4.4×10^{-3}

- * Scram and restart included with each transient
- + No transient FCMI included

NOTE: This table based on preliminary first core duty cycle.

ni= number of applied cycles (in that strain range)

Ni= allowable number of cycles (in that strain range)

TABLE 4.2-67

DESIGN PARAMETERS FOR 61 PIN TESTS

SUBASSEMBLY	WIREWRAP DIAMETER in.	WIREWRAP PITCH in.	INITIAL POROSITY (mils/ring)	DESIGN FLOW VELOCITY (fps)	BEGINNING OF TEST		DUCT MATERIAL
					BOL POWER (kw/ft)	BULK COOLANT TEMP (°F)	
PNL-9,10,11 NUMEC-E,F	0.040	12	6.5	10-24	5-13	940	304 SS AN
P-13	0.042	6	3	15	13-14	984	316 20%CW
P-14	0.042	12	3	15	13-14	984	316 20%CW
P-14A	0.0427	12	1.5	8	7-8	1010	316 20%CW

4.2-459

Amend. 51
Sept. 1979

TABLE 4.2-68

REACTOR INTERVALS THERMAL STRIPING POTENTIALS AND STRIPING FACTORS

COMPONENT	LOCATION	MATERIAL	MAX. POTENTIAL FLUID ΔT	SOURCE	NORMALIZED STRIPING FACTOR	STRIPING TEST BASIS	MAXIMUM FLUID ΔT	MAXIMUM METAL ΔT	BASIS FOR ACCEPTABILITY
UIS	Instrumentation Post	1-718	291°F	1: F/A to B/A	.79	7-Assembly	230	222	Method #2
			343°F	1 above	.58	7-Assembly	199	-	Method #1
	Lower Shroud Tube	1-718	345°F	F/A to C/A	1	7-Assembly	345	270	Method #4
			170°F	Shroud Tube- Outlet Plenum	1	Analysis	170	-	Method #1
	Upper Shroud Tube	1-718	343°F	1 above	.41	7-Assembly	142	-	Method #1
	Lower Support Plate Liner	1-718	343°F	1 above	.41	IRFM	142	-	Method #1
	Skirt Liner	1-718	343°F	1 above	.41	IRFM	142	-	Method #1
	Skirt Ring Horizontal Liner	11-718	251	2: Radial Blanket Avg. to Peripheral F/A	.62	IRFM	156	-	Method #1
	Chimney Inlet	1-718	343	1 above	.45	IRFM	155	-	Method #1
	Chimney Outlet	1-718	343	2 above	.27	IRFM	93	-	Method #1
	IVTM Port Plug Liner	1-718	251	2 above	.49	IRFM	123	-	Method #1
	IVTM Port Plug Lower end	1-718	251	2 above	.49	IRFM	123	-	Method #1
	IVTM Port Plug Above 1-718	316SS	251	2 above	.24	IRFM	60	-	Method #1
	Seismic Keys Liner	316SS 1-718	251	2 above	.23	IRFM	58	-	Method #1
			251	2 above	.27	IRFM	68	-	Method #1
	Shear Web	316SS	251	2 above	.46	IRFM	115	88	Method #3
	Upper Support	316SS	343	1 above	.15	IRFM	51	-	Method #1

4.2-459a

Amend. 68
May 1982

TABLE 4.2-68 (Continued)

COMPONENT	LOCATION	MATERIAL	MAX. POTENTIAL FLUID ΔT	SOURCE	NORMALIZED STRIPING TEST BASIS	MAXIMUM FLUID ΔT	MAXIMUM METAL ΔT	BASIS FOR ACCEPTABILITY
	Upper Support Plate	31655	343	1 above	.15 IRFM	51	-	Method #1
Core Former Structure	Liners	1-718	326	F/A to Core Interstitial Flow	.61 IRFM & Interstitial Flow Test	200	- *	Method #1 *
Horizontal Baffle	Plate	316SS	145	Leakage to Outlet Plenum	.48 IRFM	70	-	Method #1
	FI&SA Nozzle	1-718	300	FI&SA to Outlet Plenum	.83 IRFM	248	192	Method #2

- Method #1 - Most conservative, all cycles are umbrellaed under the maximum fluid ΔT , and this fluid ΔT is compared to the allowable metal ΔT .
- Method #2 - All cycles are umbrellaed under the maximum metal surface ΔT , and this metal ΔT is compared to the allowable metal ΔT .
- Method #3 - The striping data peaks which are above the endurance strength ΔT are umbrellaed under increments of ΔT ranges, and the fatigue damage for these increments are determined and projected for the reactor life. This fatigue damage is added to the creep-fatigue for other transients, then compared to the damage envelope.
- Method #4 - A detailed finite element analysis (time history) of the component for its striping environment is performed.

*Evaluation In Process

TABLE 4.2-69

ALLOWABLE STRIPING METAL TEMPERATURE RANGE
FOR 304 AND 316 SS INCLUDING
MEAN STRAIN EFFECTS (< 1100°F).

ϵ mean (in/in)	$\Delta\epsilon$ (in/in)	Allowable Surface Temp. Range (°F)
no mean	.0014	84
-0002	.0013	78
-00045	.0012	72
-0009	.0011	66
-00165	.0010	60
-0025	.0009	54

Allowable Striping Metal Temperature Range for
304 and 316 SS Including Mean Strain Effects
(< 1100°F).

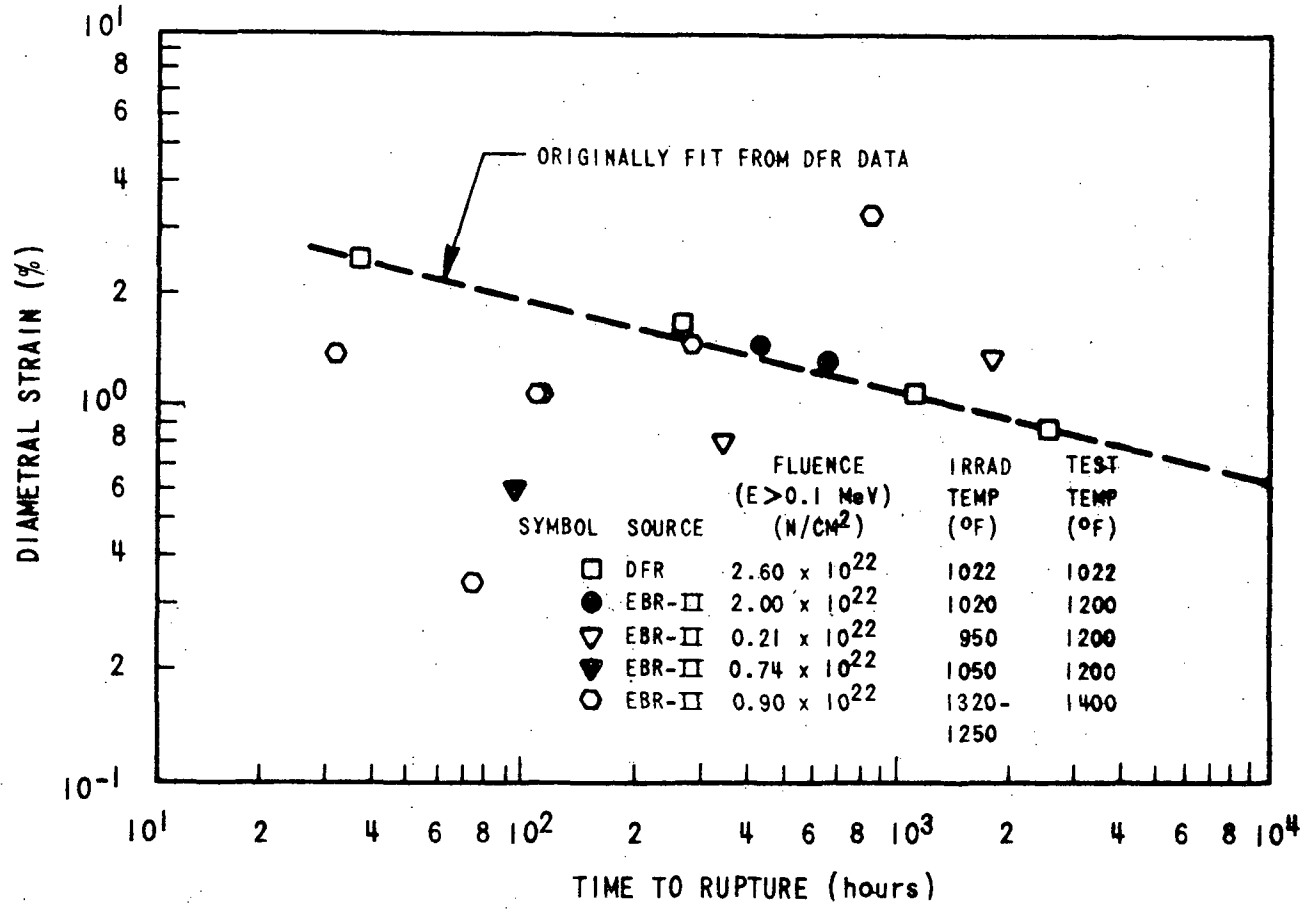


Figure 4.2-1. Creep-Rupture Data for 20% C.W. 316 Stainless Steel Tubes (Biaxial Data)

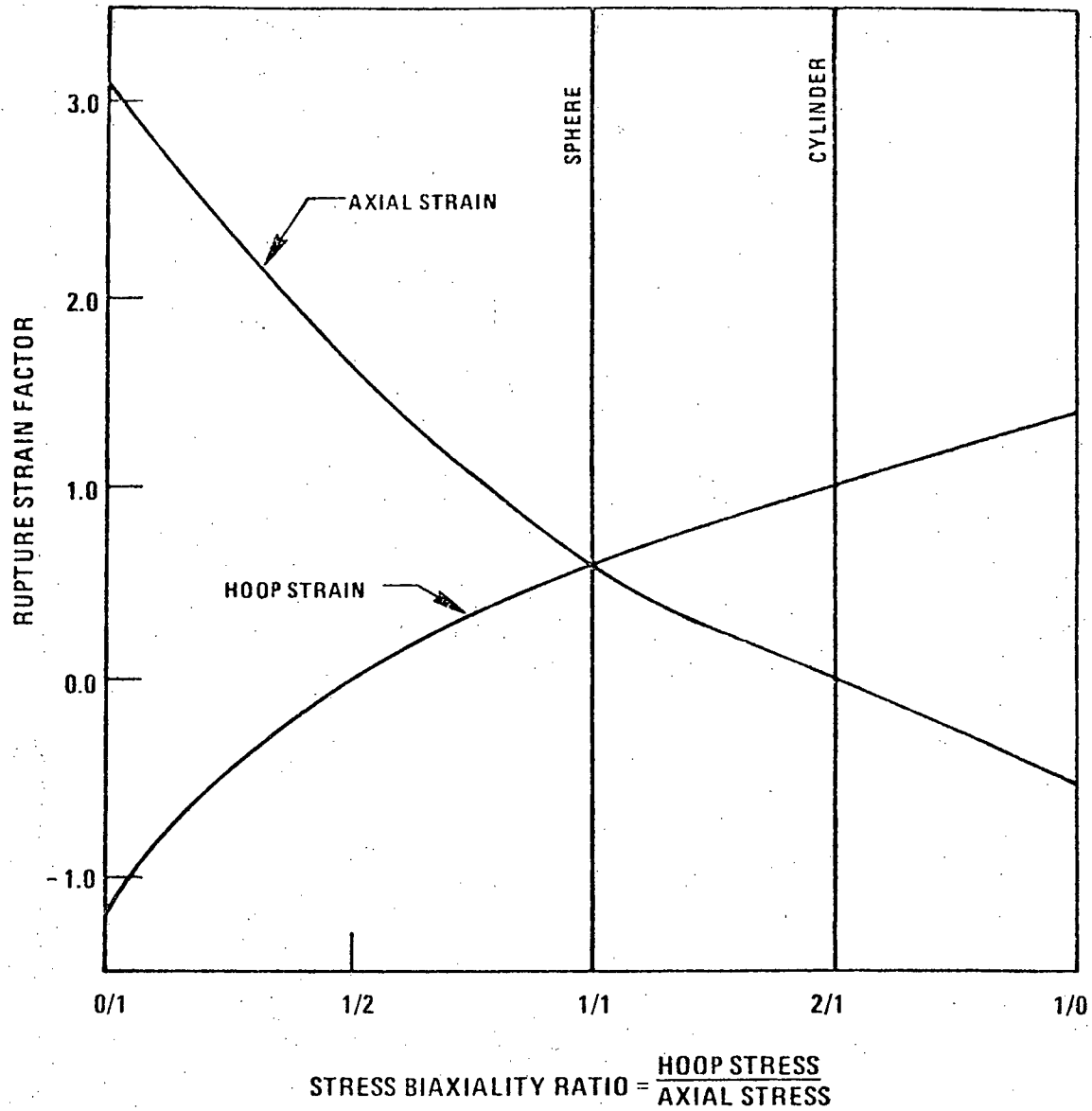


Figure 4.2-1A Stress Biaxiality Rupture Strain Factor

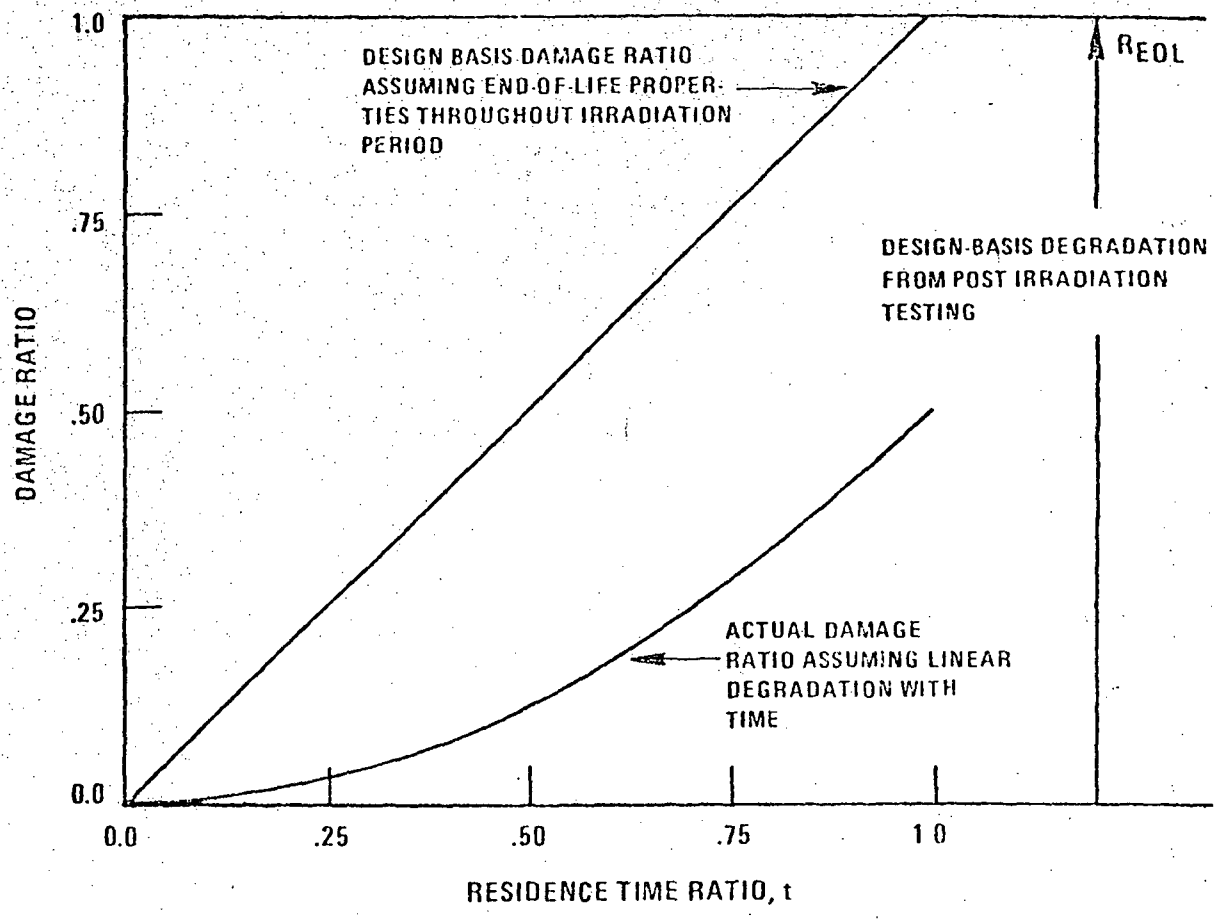


Figure 4.2-1B Effect Of Degradation On Damage Accumulation

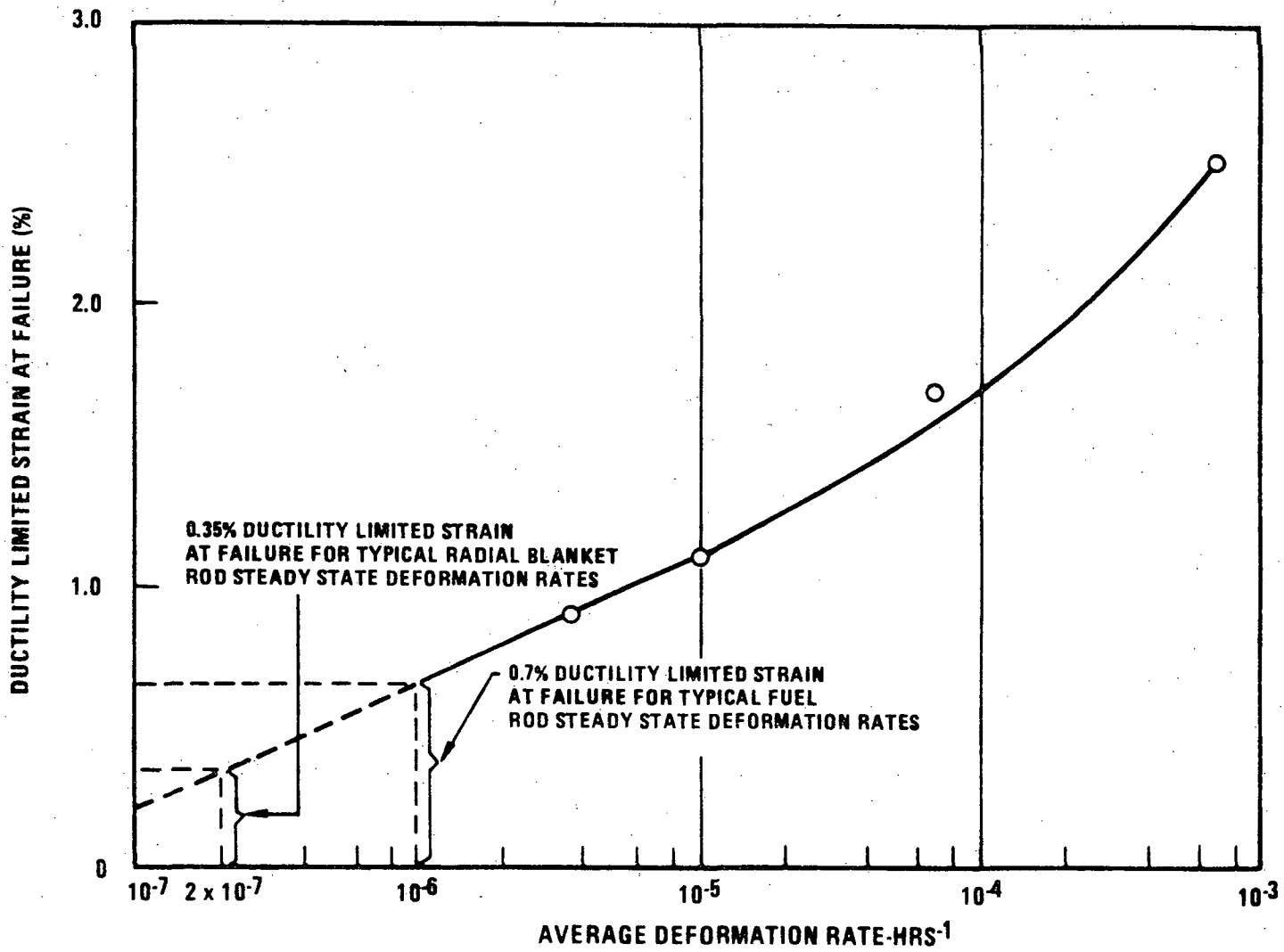


Figure 4.2-2. Creep-Rupture Data for 20% C.W. 316 SS Irradiated to 3×10^{22} nvt at $525 \pm 25^\circ\text{C}$

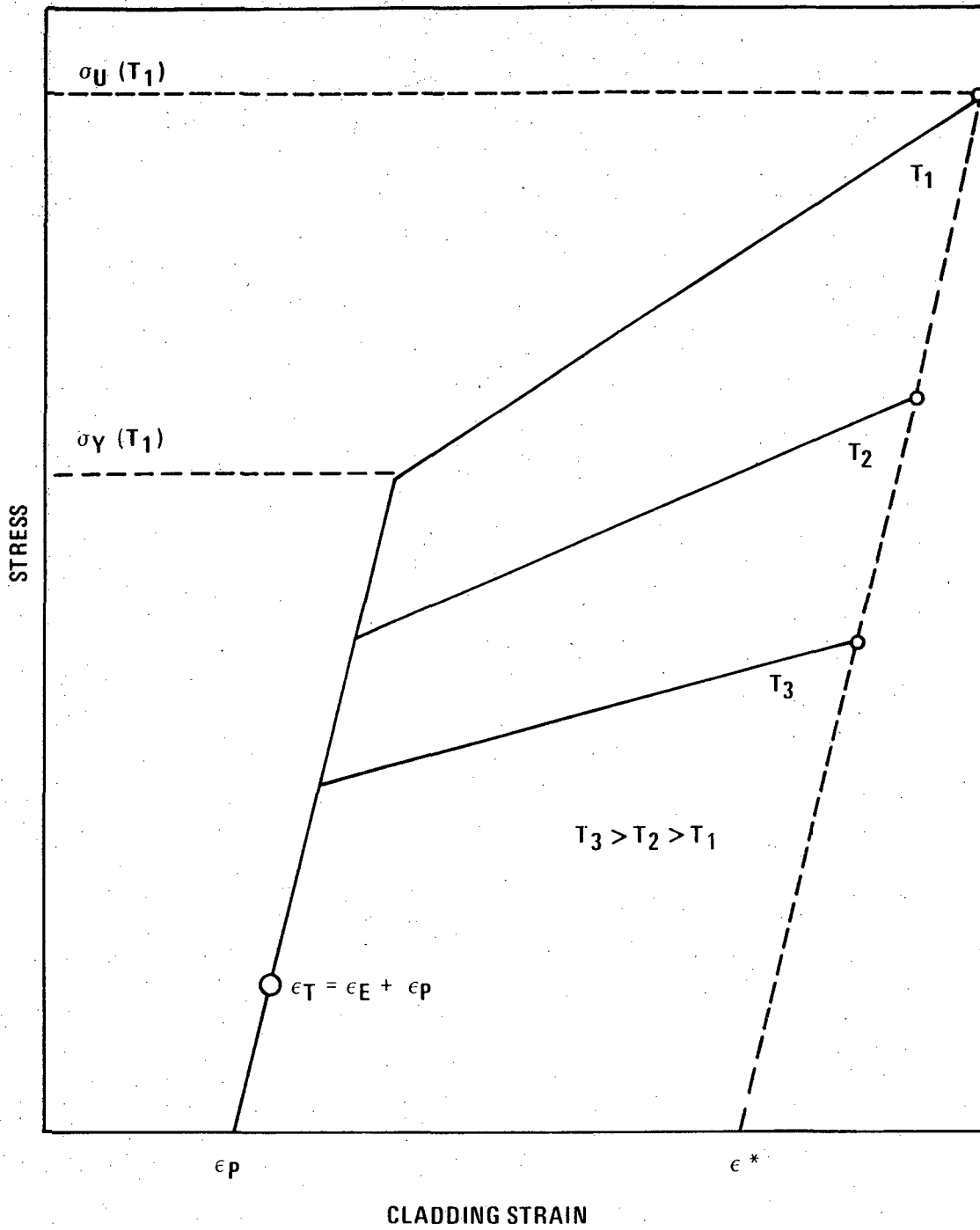


Figure 4.2-2A. Comparison of Assumed Values to Experimental Ultimate Stress for Dynamic Cladding Loading

6726-33

4.2-463a

Amend. 65
Feb. 1982

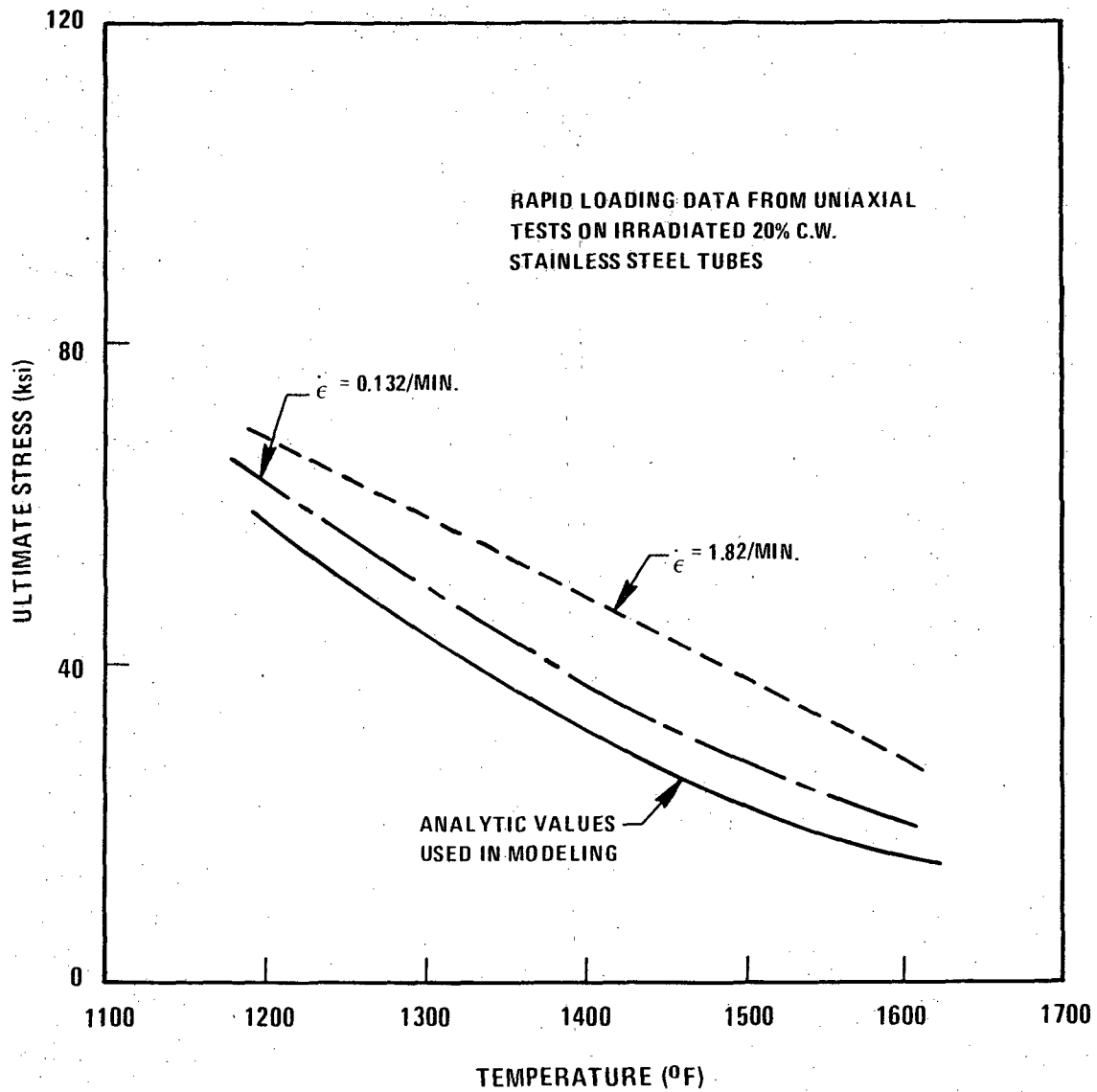


Figure 4.2-2B. Bilinear Stress - Strain Relationship for Cladding Strain Criterion

$$\text{FRACTIONAL VOLUME CHANGE} = \frac{\Delta V}{V_0} = (0.01) R \left[\phi t + \frac{1}{a} \left(\text{Ln} \left\{ \frac{1 + \exp [a(\tau - \phi t)]}{1 + \exp (a\tau)} \right\} \right) \right]$$

ϕt = NEUTRON FLUENCE IN UNITS OF 10^{22} n/cm² (E ≤ 0.1 MeV)

$$R(T) = \text{EXP} (0.0419 + 1.498 \Delta + 0.122 \Delta^2 - 0.332 \Delta^3 - 0.441 \Delta^4)$$

WHERE $\Delta = (T - 500)/100$ AND T IS THE TEMPERATURE IN °C

$$a = 2.0$$

$$\tau (\text{NOMINAL}) = 7.0$$

$$\tau_{\text{LOW}} = 5.0$$

$$\tau_{\text{HIGH}} = 9.0$$

UPPER BOUND: 130% OF PREDICTED R(T) VALUE

LOWER BOUND: 70% OF PREDICTED R(T) VALUE

Figure 4.2-3 Design Basis Stress Free Swelling Equation for 20%
C.W. Type 316 Stainless Steel

1764-1

A) RATE EQUATION FORM

$$1) \dot{\bar{\epsilon}}/\bar{\sigma} = \frac{A\phi}{\tau_{tr}} e^{-\phi t/\tau_{tr}} + \phi B(\phi t, T)$$

$$2) B(\phi t, T) = F(T) \cdot G(\phi t) + B_0$$

$$3) F(T) = \left\{ \frac{7.2 \times 10^{-25} \exp(-16,000/RT)}{1 + 2 \times 10^{19} \exp(-80,000/RT)} \right\}$$

$$4) G(\phi t) = [1 - e^{-\phi t/\Omega_c}]$$

B) INTEGRATED FORM (CONSTANT STRESS)

$$5) \bar{\epsilon}/\bar{\sigma} = A (1 - e^{-\phi t/\tau_{tr}}) + \phi t \bar{B}(\phi t, T)$$

$$6) \bar{B}(\phi t, T) = F(T) G'(\phi t) + B_0$$

$$7) G'(\phi t) = (1 - \frac{\Omega_c}{\phi t} [G(\phi t)])$$

WHERE $\bar{\epsilon}$, $\bar{\sigma}$ = EFFECTIVE STRAIN AND STRESS ($\bar{\epsilon}$ IS FRACTIONAL AND $\bar{\sigma}$ HAS UNITS OF PSI)

$\dot{\bar{\epsilon}}$ = EFFECTIVE STRAIN RATE (SEC⁻¹)

ϕ = NEUTRON FLUX, n/cm² SEC (E > 0.1 MeV)

ϕt = NEUTRON FLUENCE, n/cm² (E > 0.1 MeV)

$B_0 = 3 \times 10^{-30}$ psi⁻¹ n⁻¹ cm²

$\Omega_c = 0.9 \tau$ (SEE FIGURE 4.2-3 FOR τ VALUES)

$A = 8.4 \times 10^{-9}$ psi⁻¹ and $\tau_{tr} = 0.043 \times 10^{22}$ n/cm² (TORSIONAL OR COMPLEX MULTIAXIAL)

$A = 2.6 \times 10^{-8}$ psi⁻¹ and

$\tau_{tr} = 0.05 \times 10^{22}$ n/cm² (UNIAXIAL TENSION)

$A = 0$ and

$\tau_{tr} = \text{---}$ undefined (PRESSURIZED CLOSED END TUBE)

$R = 1.987$

CONFIDENCE LIMITS

±20% FOR $|\bar{\epsilon}| < 1\%$

±20% x $|\% \bar{\epsilon}|$ FOR $1\% < |\bar{\epsilon}| < 4\%$

±80% FOR $|\bar{\epsilon}| > 4\%$

Figure 4.2-4 Design Basis Stress Enhanced Swelling and Irradiation Creep for 20% C.W. Type 316 Stainless Steel

C) STRESS EFFECT ON SWELLING

$$\frac{\Delta \dot{V}}{V_0} = \left(\frac{\Delta \dot{V}}{V_0} \right)_0 [1 + P \sigma_{\text{HYD}}]$$

WHERE $\Delta \dot{V}/V_0$ = SWELLING RATE

$\left(\frac{\Delta \dot{V}}{V_0} \right)_0$ = STRESS-FREE SWELLING RATE

σ_{HYD} = HYDROSTATIC COMPONENT OF STRESS, PSI

$$P = 2 \pm 2 \times 10^{-5} \text{ psi}^{-1}$$

Figure 4.2-4 (cont.) Design Basis Stress Enhanced Swelling and Irradiation Creep for
20% C.W. Type 316 Stainless Steel

1764-3

Amend. 51

4.2-466

Sept. 1979

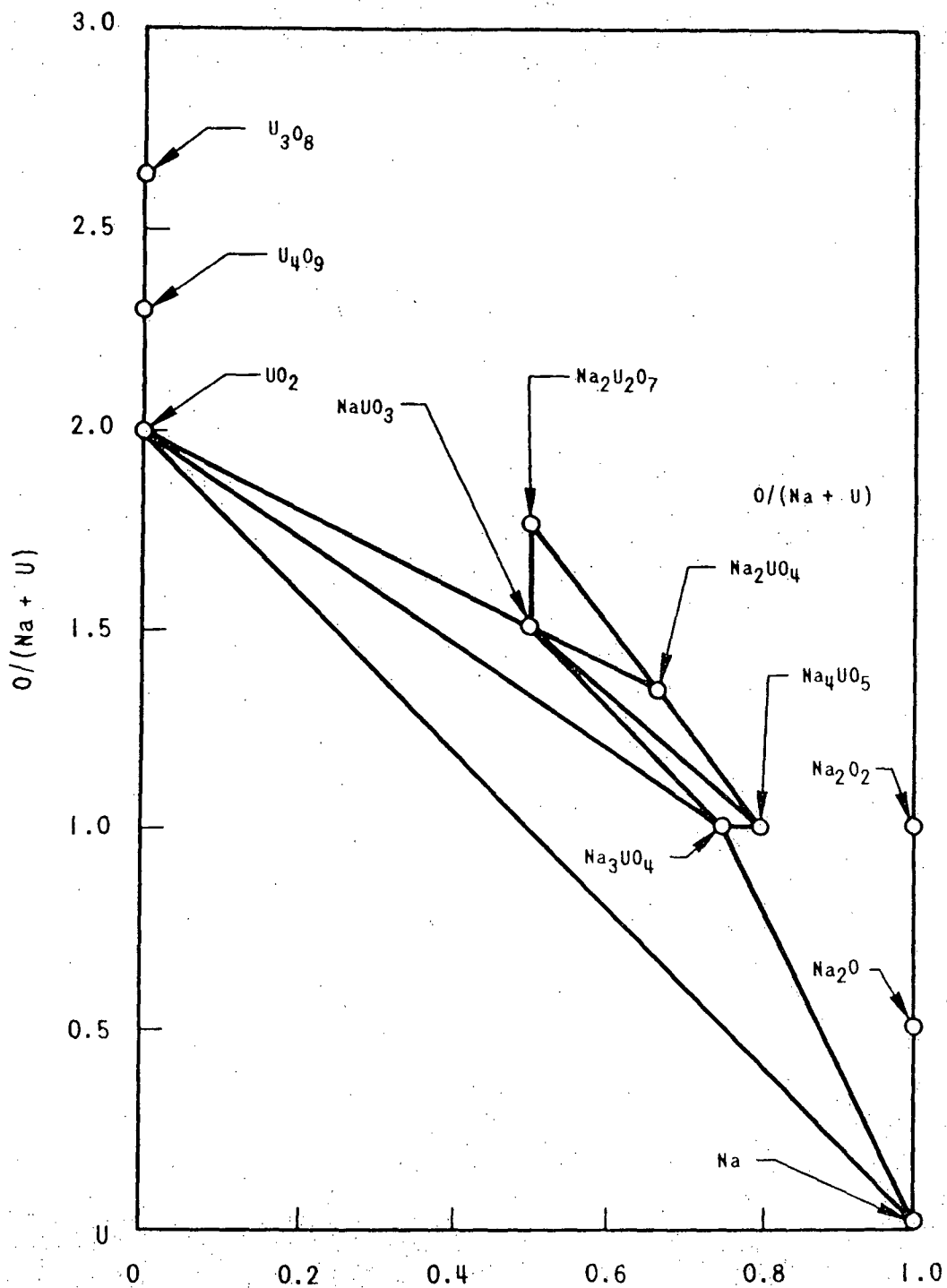


Figure 4.2-5. Isothermal Section of the Na-U-O Phase Diagram at About 800°C

6664-111

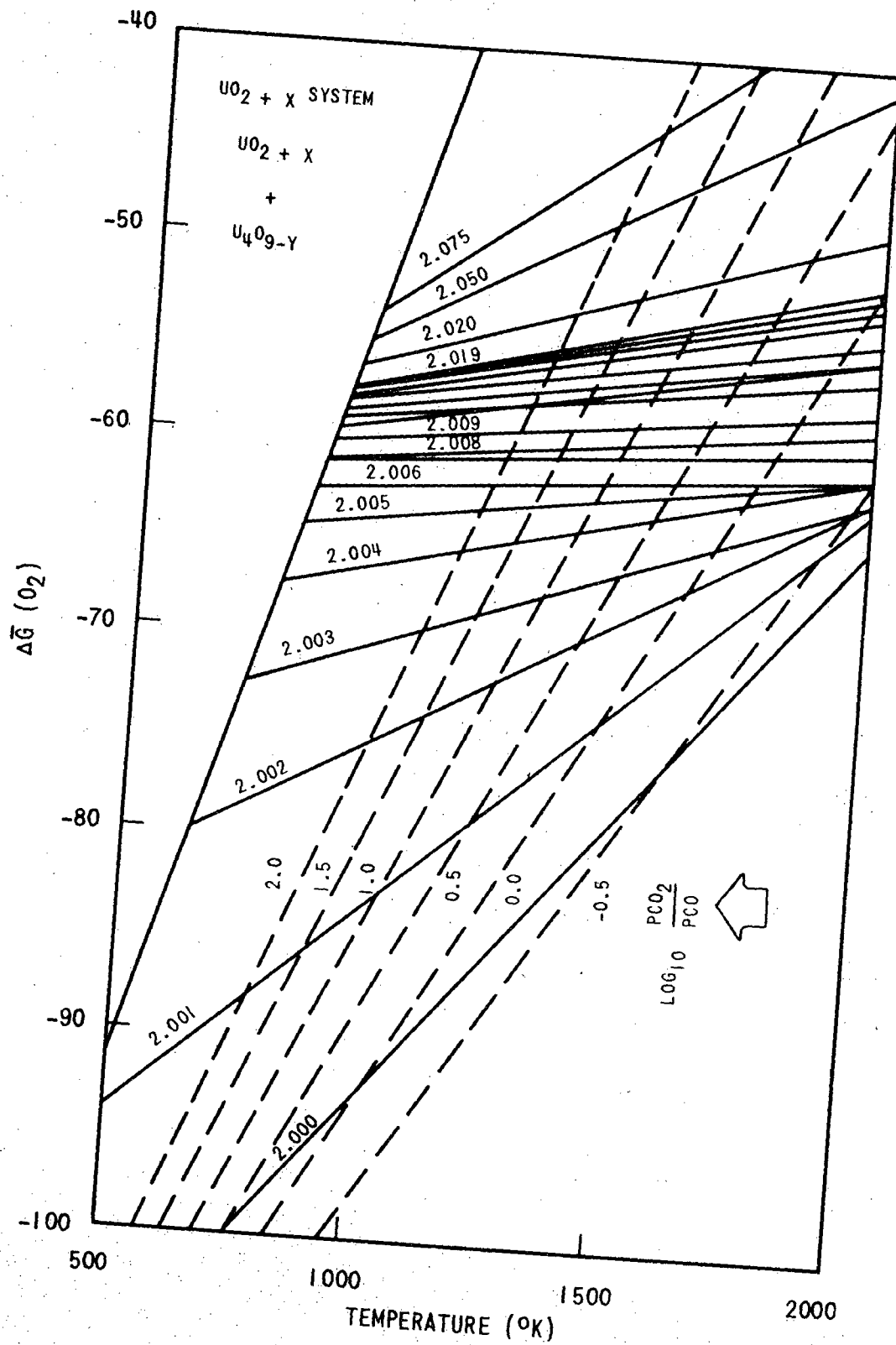


Figure 4.2-6. Oxygen Potentials for UO_{2+x} System

6664-112

4.2-468

Amend. 51
Sept. 1979

6664-113

4.2-469

Amend. 51
Sept. 1979

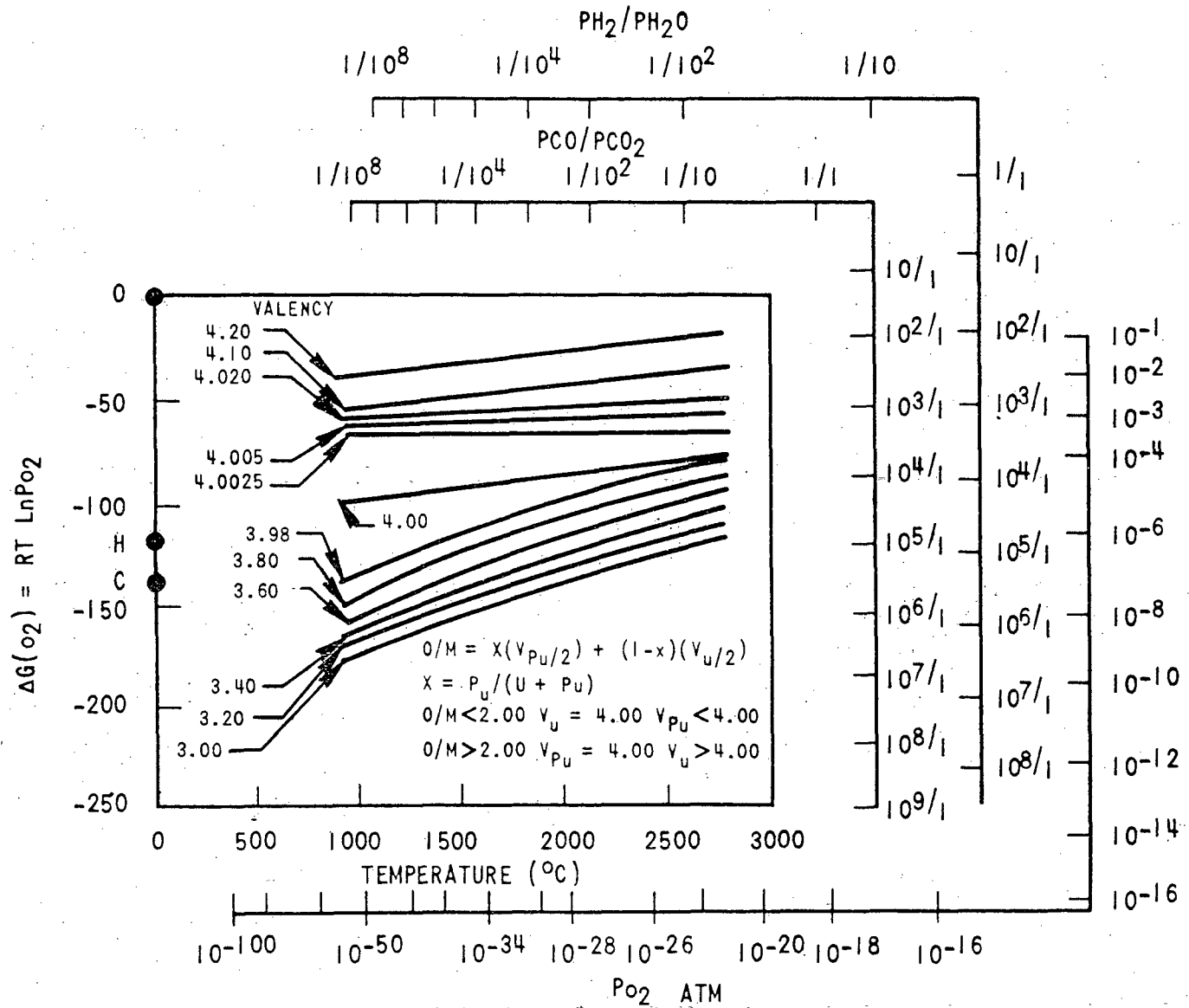


Figure 4.2-7. Oxygen Potentials for (U, Pu) $\text{O}_{2\pm x}$ as a Function of Metal Valence and Temperature

6664-114

4.2-470

Amend. 51
Sept. 1979

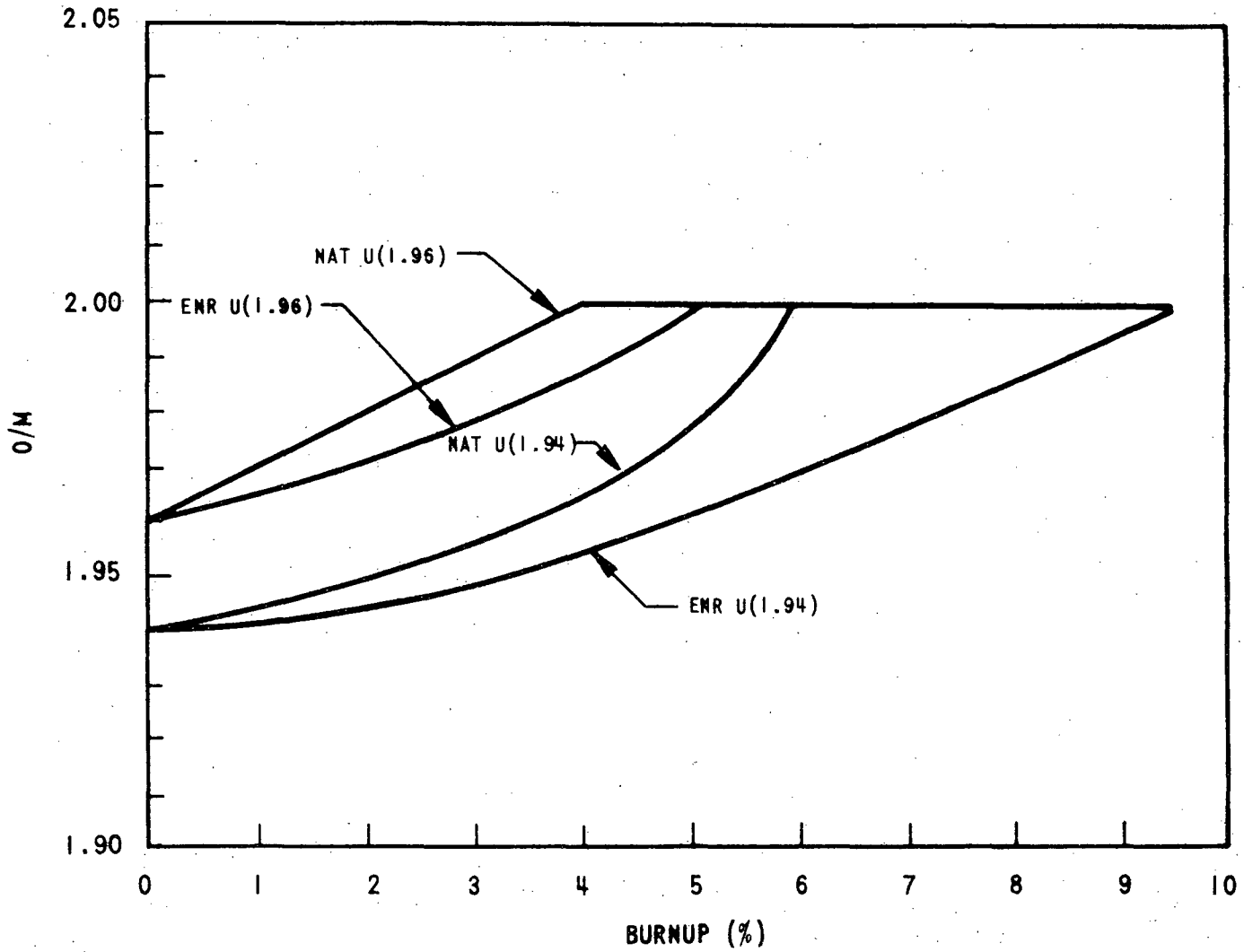


Figure 4.2-8. Variation of O/M With Burnup ($U_{0.75}Pu_{0.25}O_{2x}$)

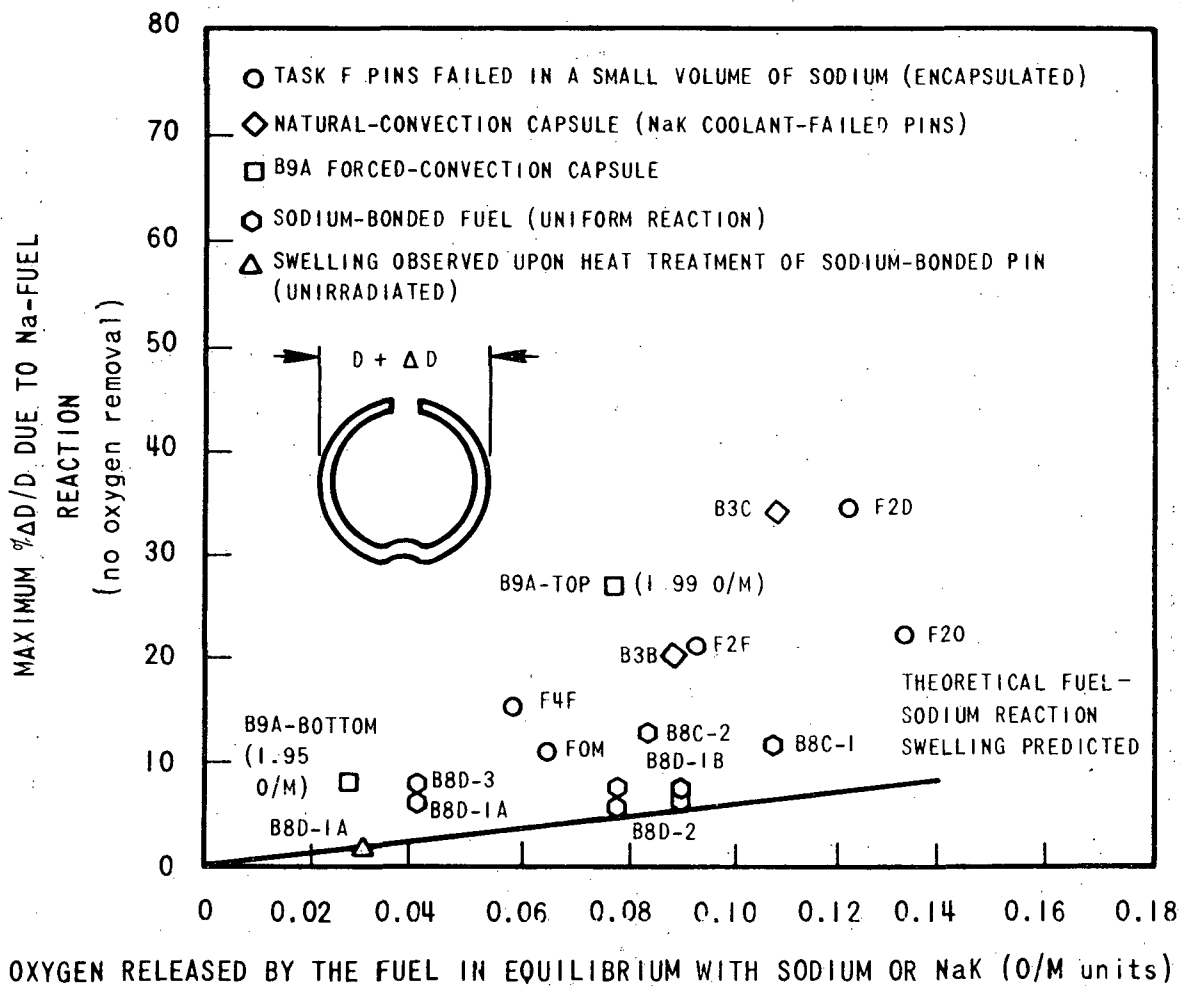


Figure 4.2-9 Maximum Swelling Observed as a Function of the Oxygen Available for Reaction. (Reference 5)

1764-4

7683-219

4.2-472

Amend. 51
Sept. 1979

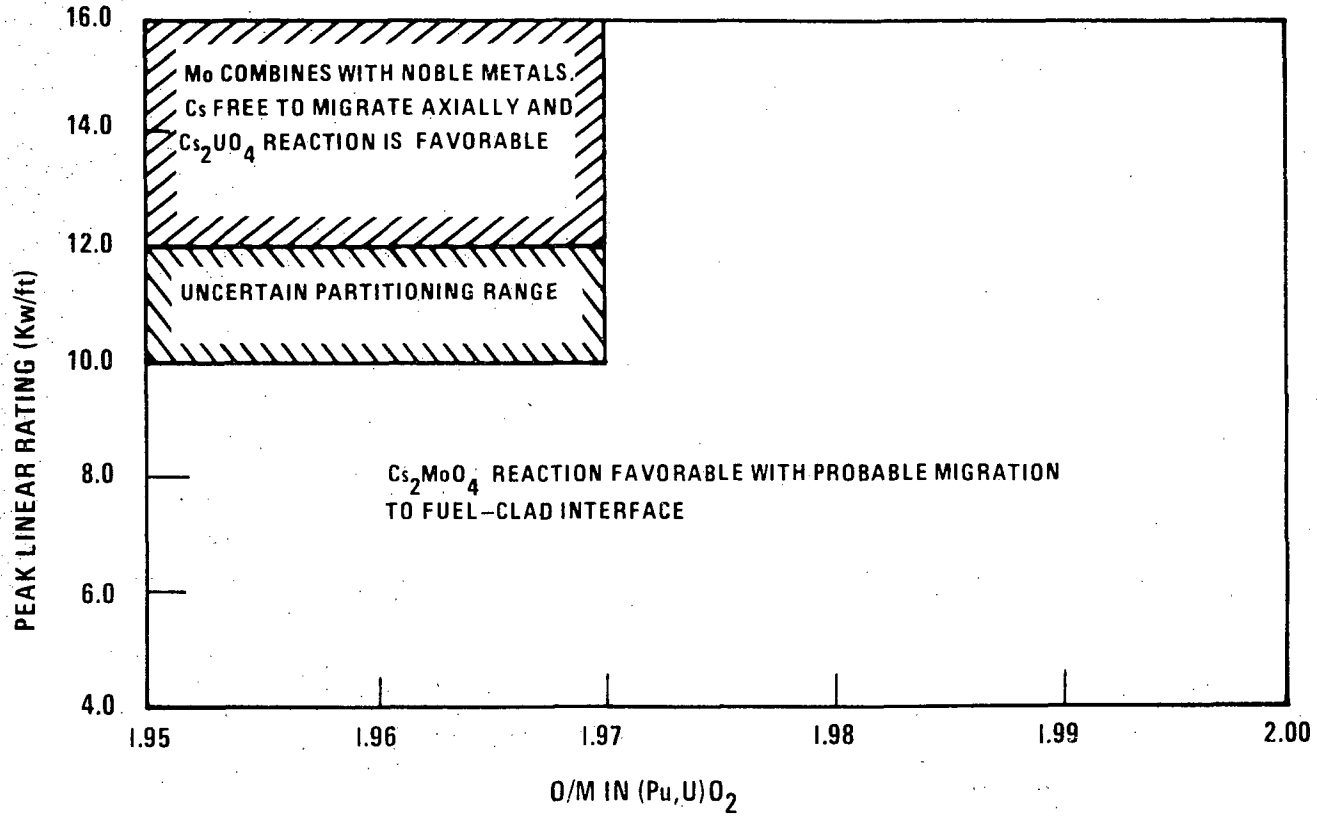


Figure 4.2-9A. Conditions Partitioning The CS₂UO₄ And CS₂MoO₄ Reactions In CRBRP

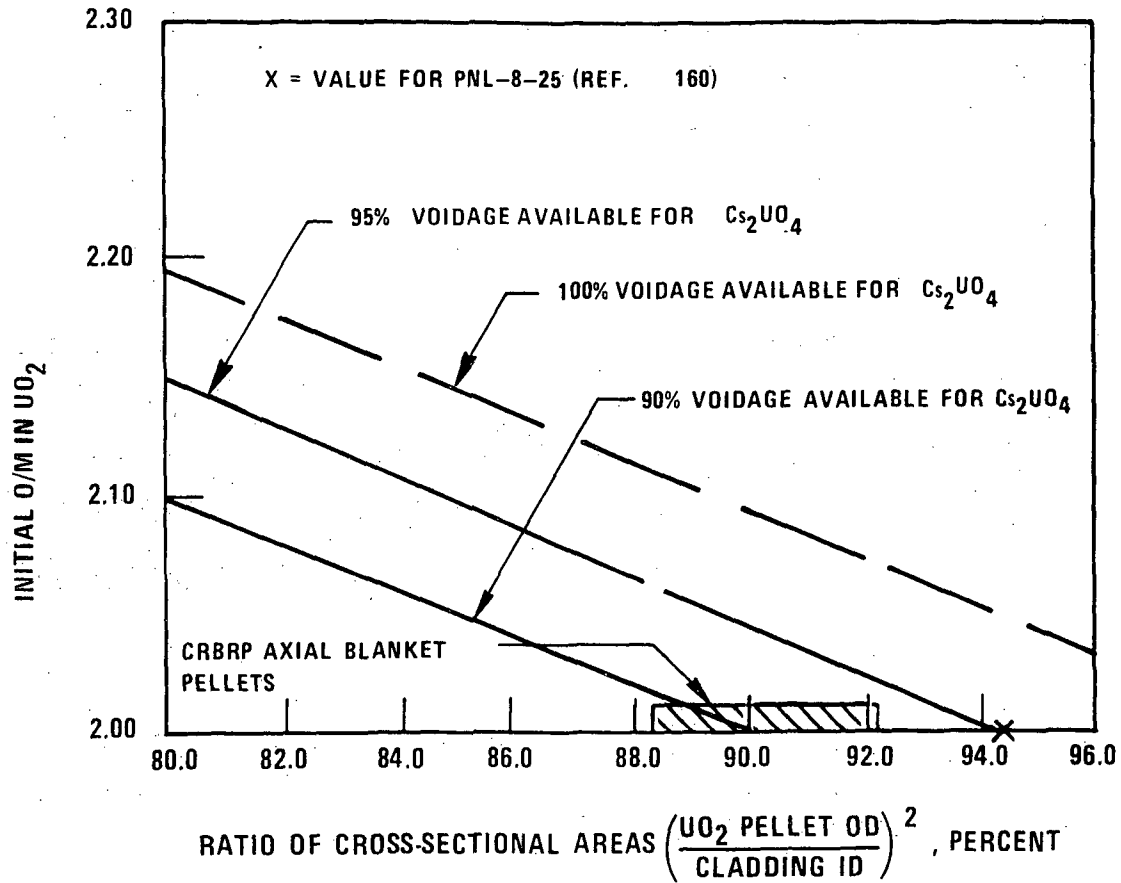
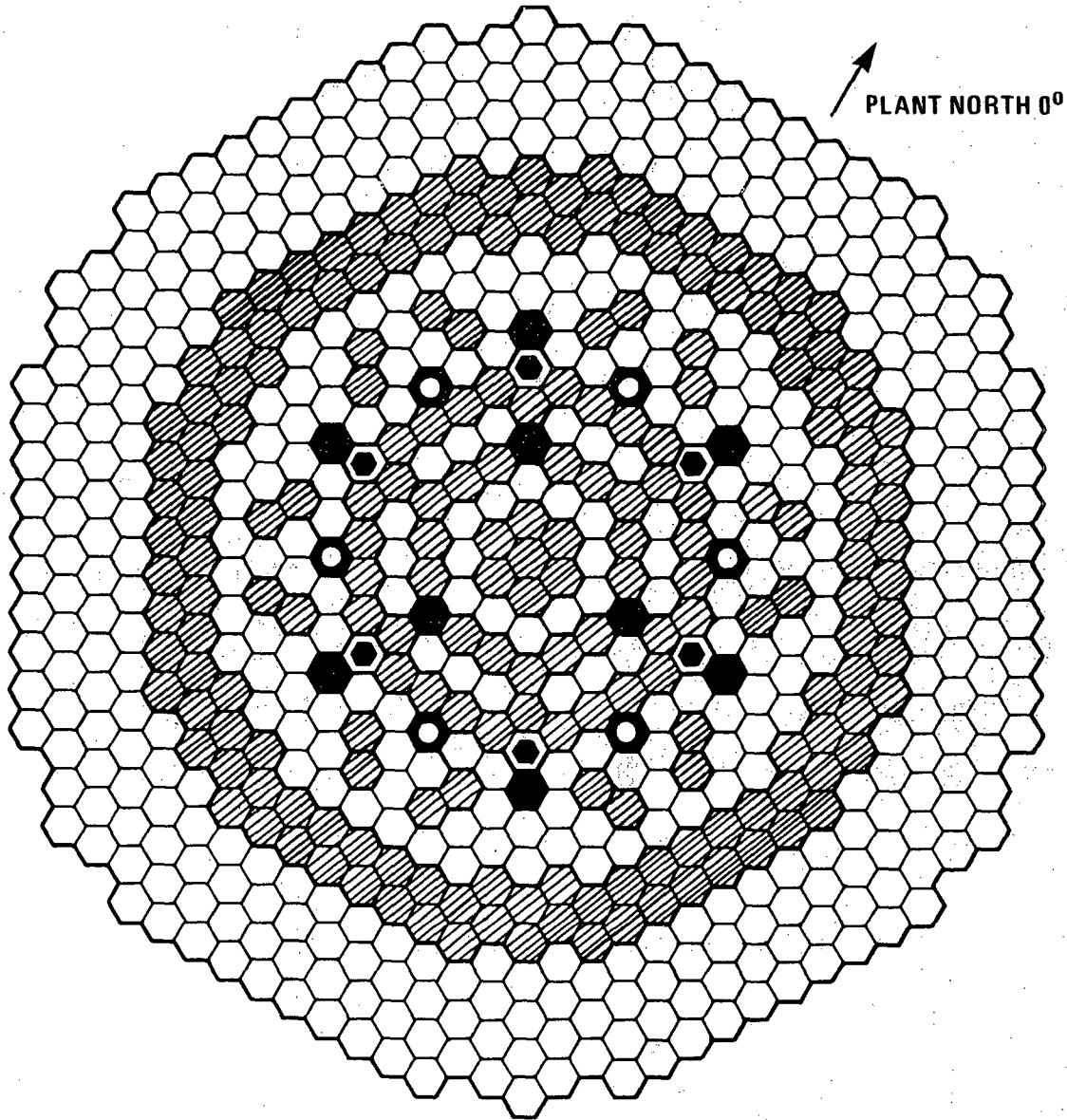


Figure 4.2-9B. As-Fabricated Smeared Density and O/M Ratio For UO_2 Pellets Required To Preclude Severe Mechanical Interaction With Cladding



- | | | | |
|---|-------------------------------|---|-------------------------------------|
|  | 156 FUEL ASSEMBLIES |  | 6 ALTERNATE FUEL BLANKET ASSEMBLIES |
|  | 76 INNER BLANKET ASSEMBLIES |  | 6 SECONDARY CONTROL ASSEMBLIES |
|  | 126 RADIAL BLANKET ASSEMBLIES |  | 9 PRIMARY CONTROL ASSEMBLIES |
| | | | 312 RADIAL SHIELD ASSEMBLIES |

FIGURE 4.2-10A. Core Layout

5894-8

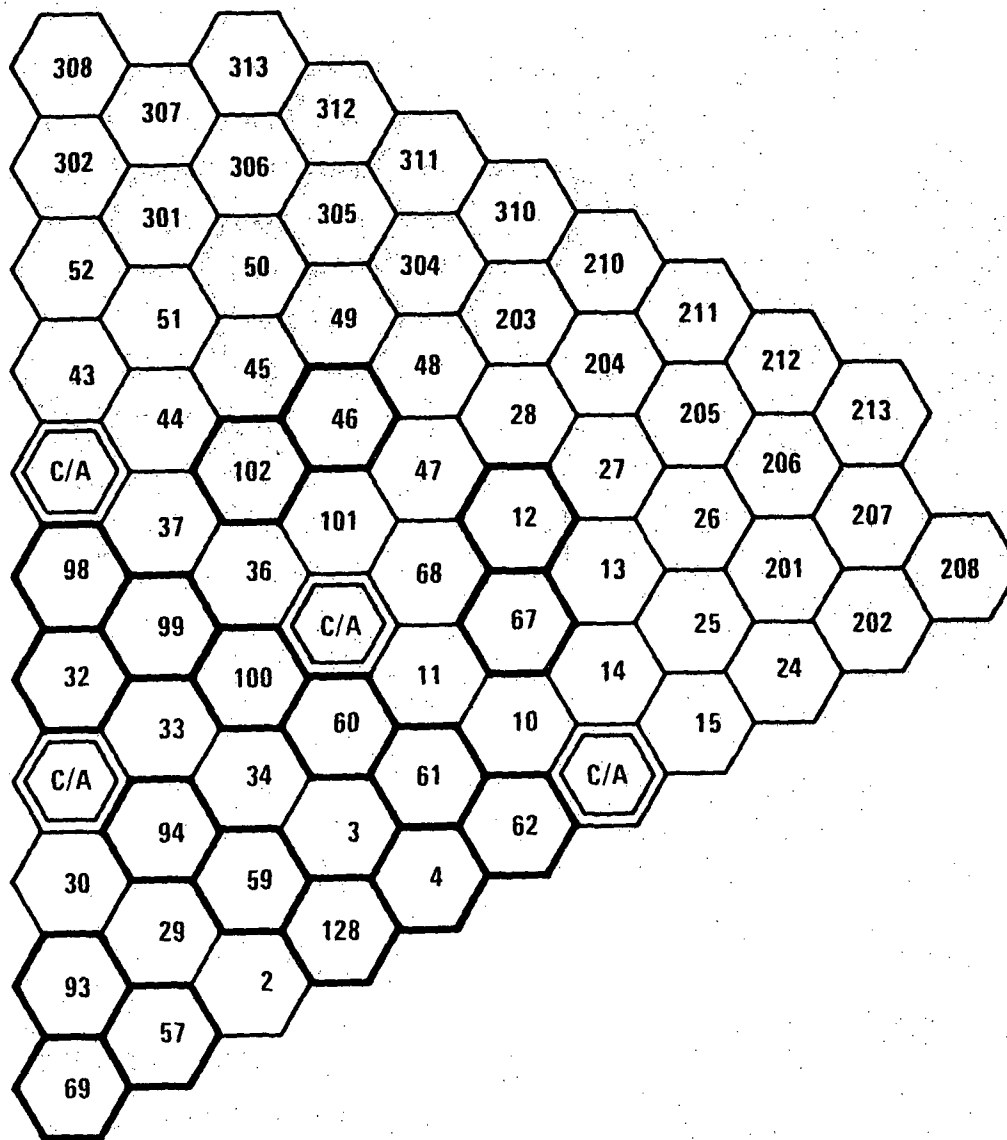


FIGURE 4.2-10B. Assembly Numbering Scheme

1764-6a

4.2-475

Amend. 64
Jan. 1982

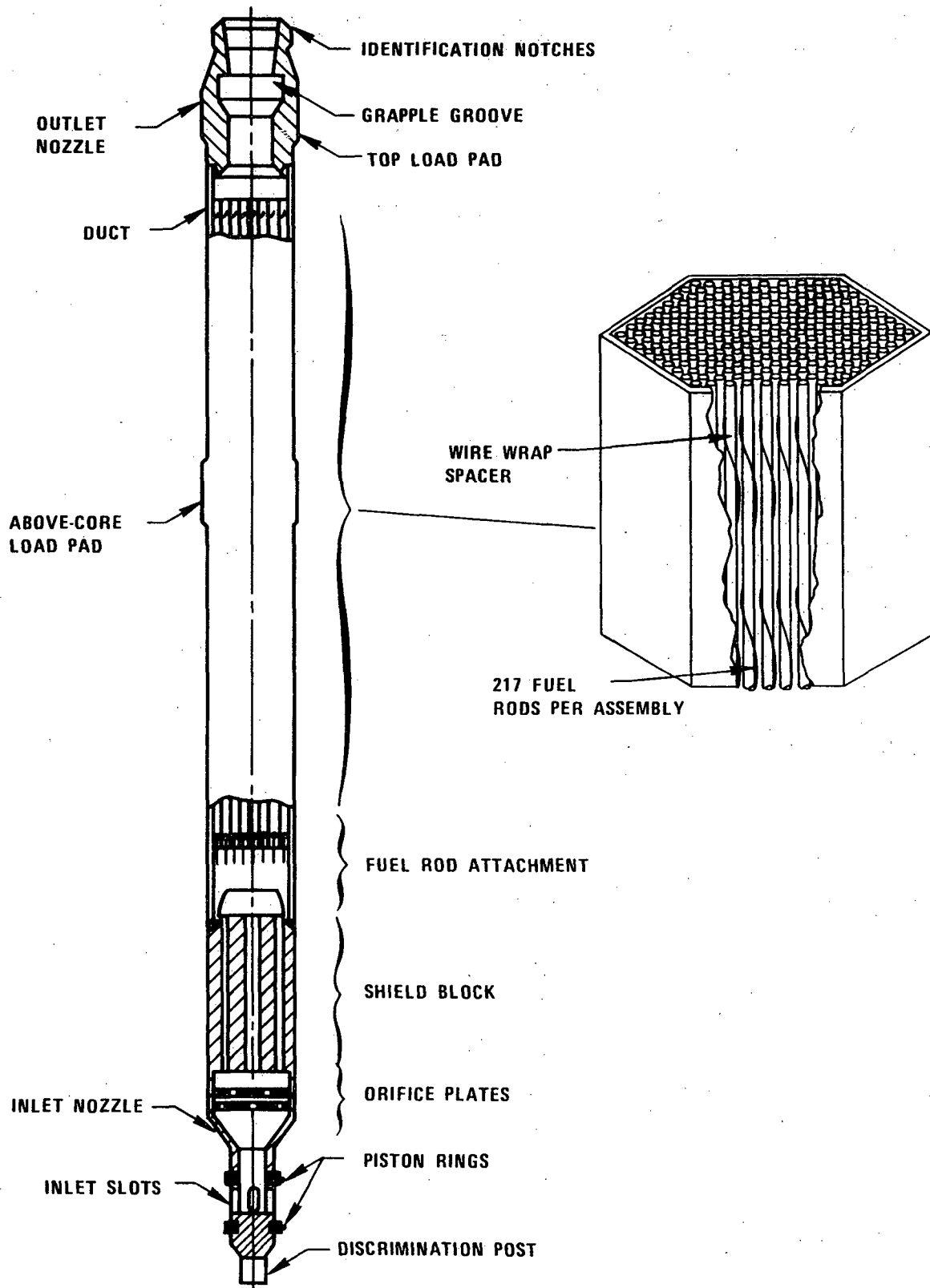


Figure 4.2-11 Fuel Assembly Schematic

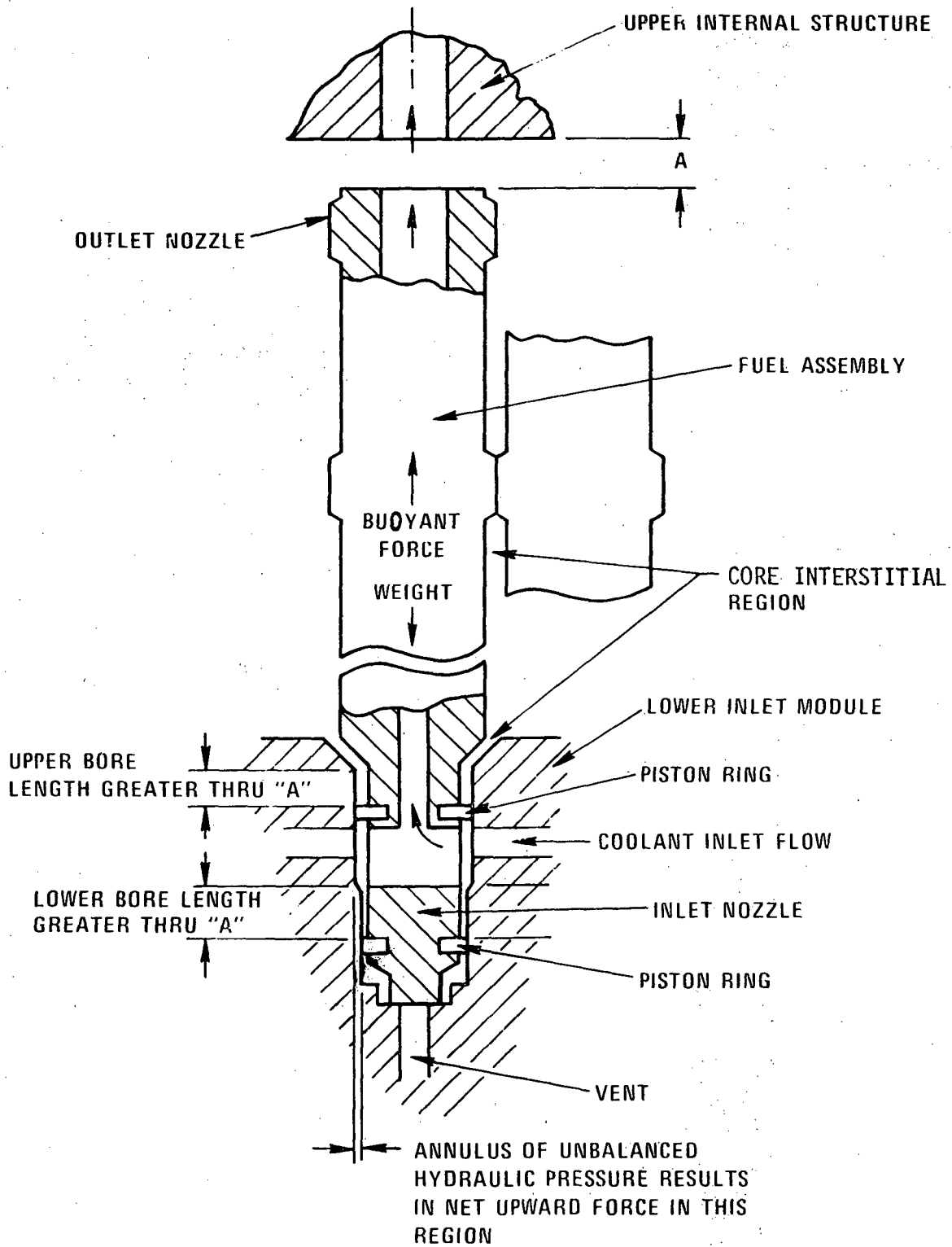


Figure 4.2-11A. Fuel Assembly Holddown System

7683-216

Amend. 51
Sept. 1979

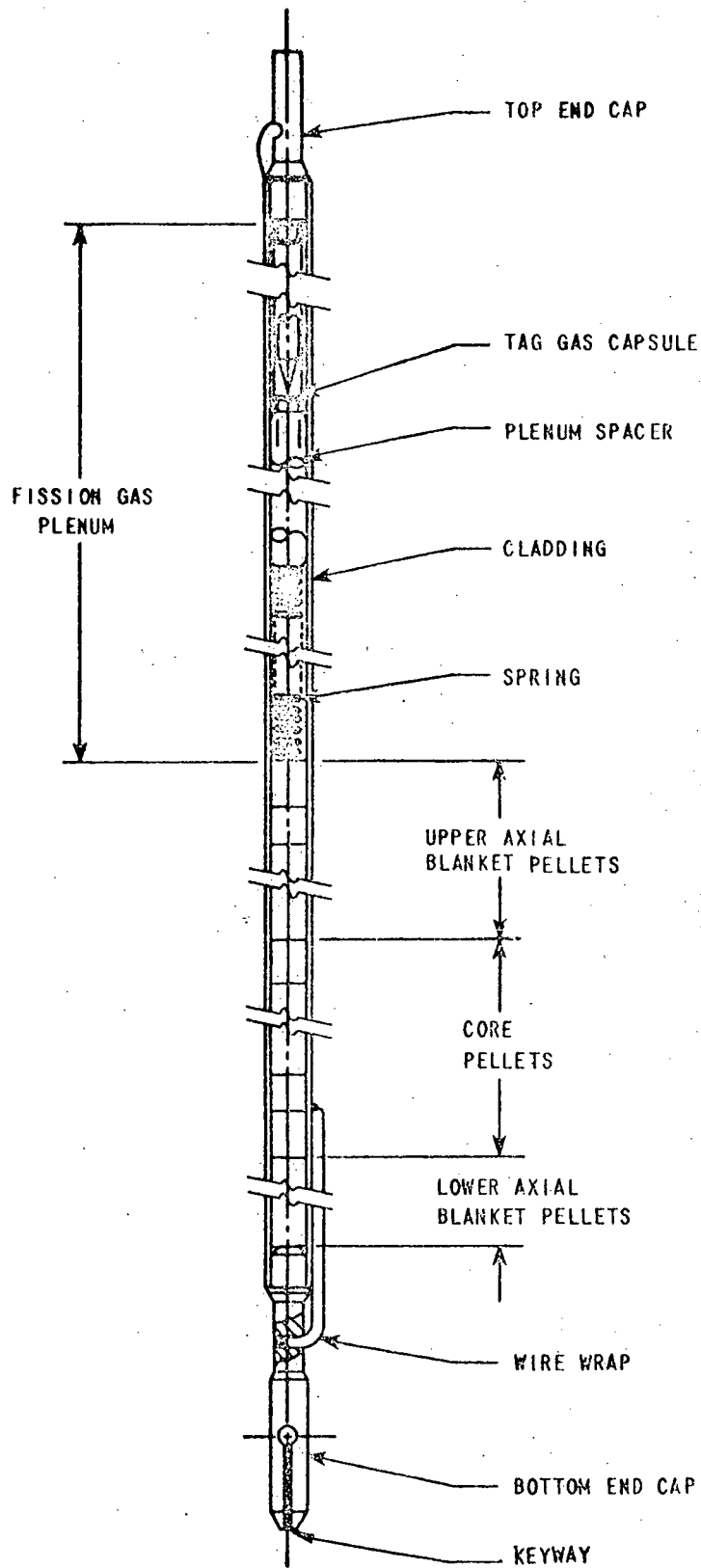


Figure 4.2-12. Fuel Rod Assembly

6664-44

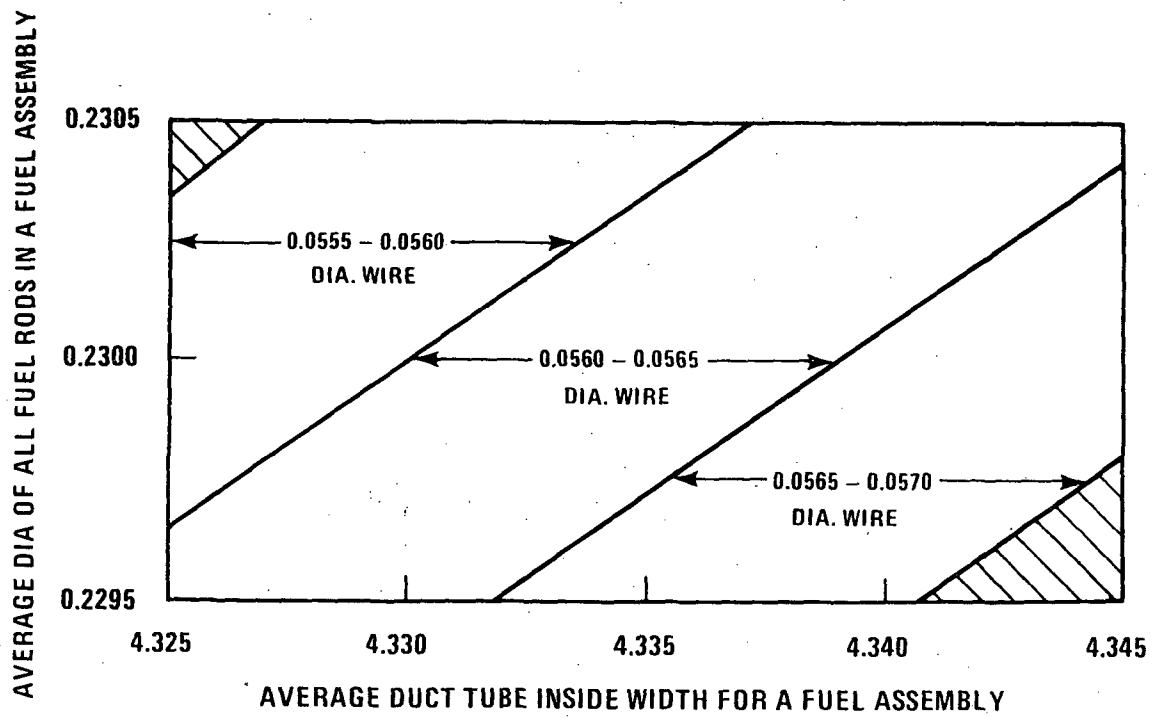


FIGURE 4.2-12A Determination Of Wire Wrap Diameter

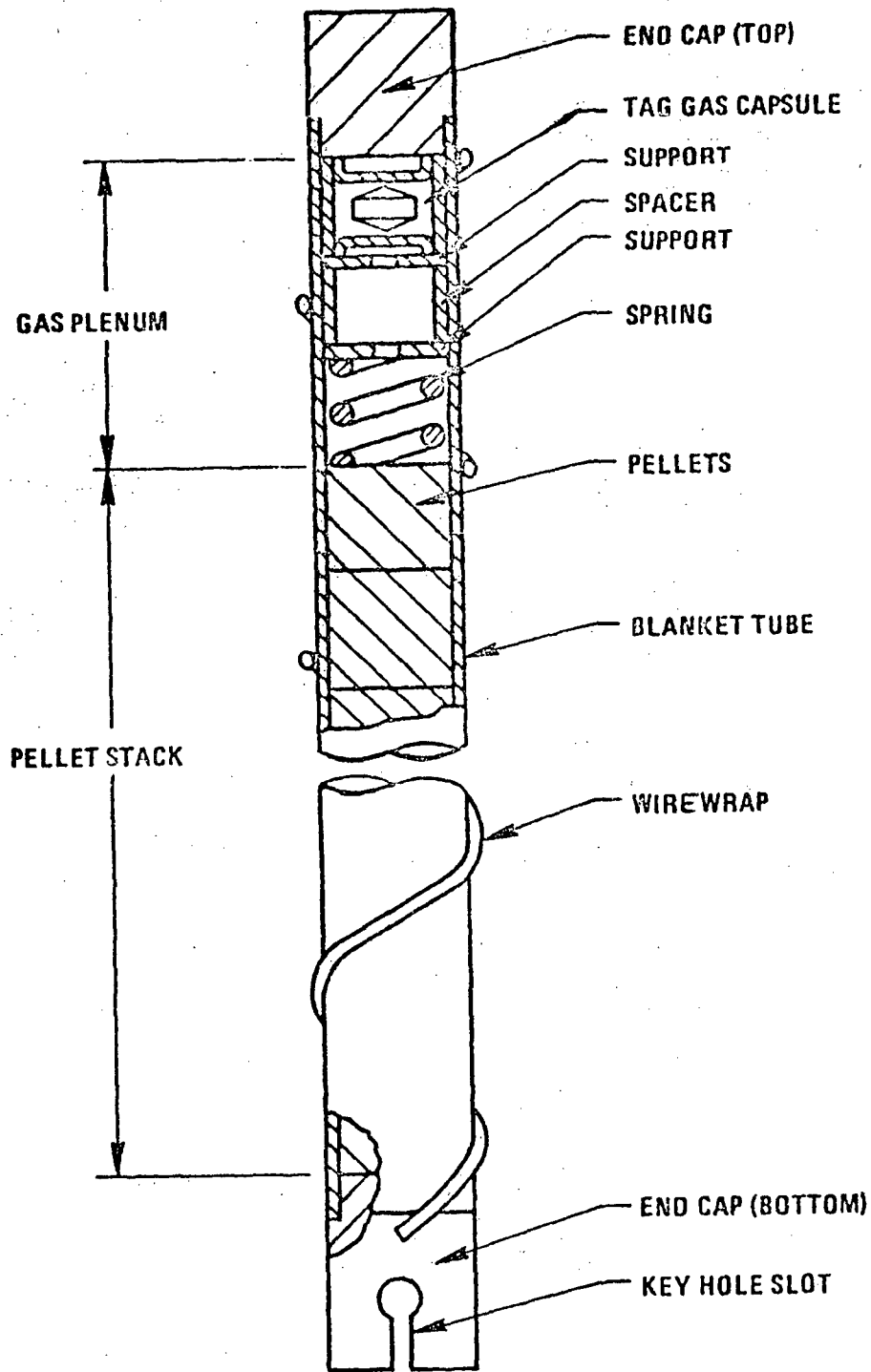


Figure 4.2-13. Blanket Rod Assembly Schematic

Amend. 51
Sept. 1979

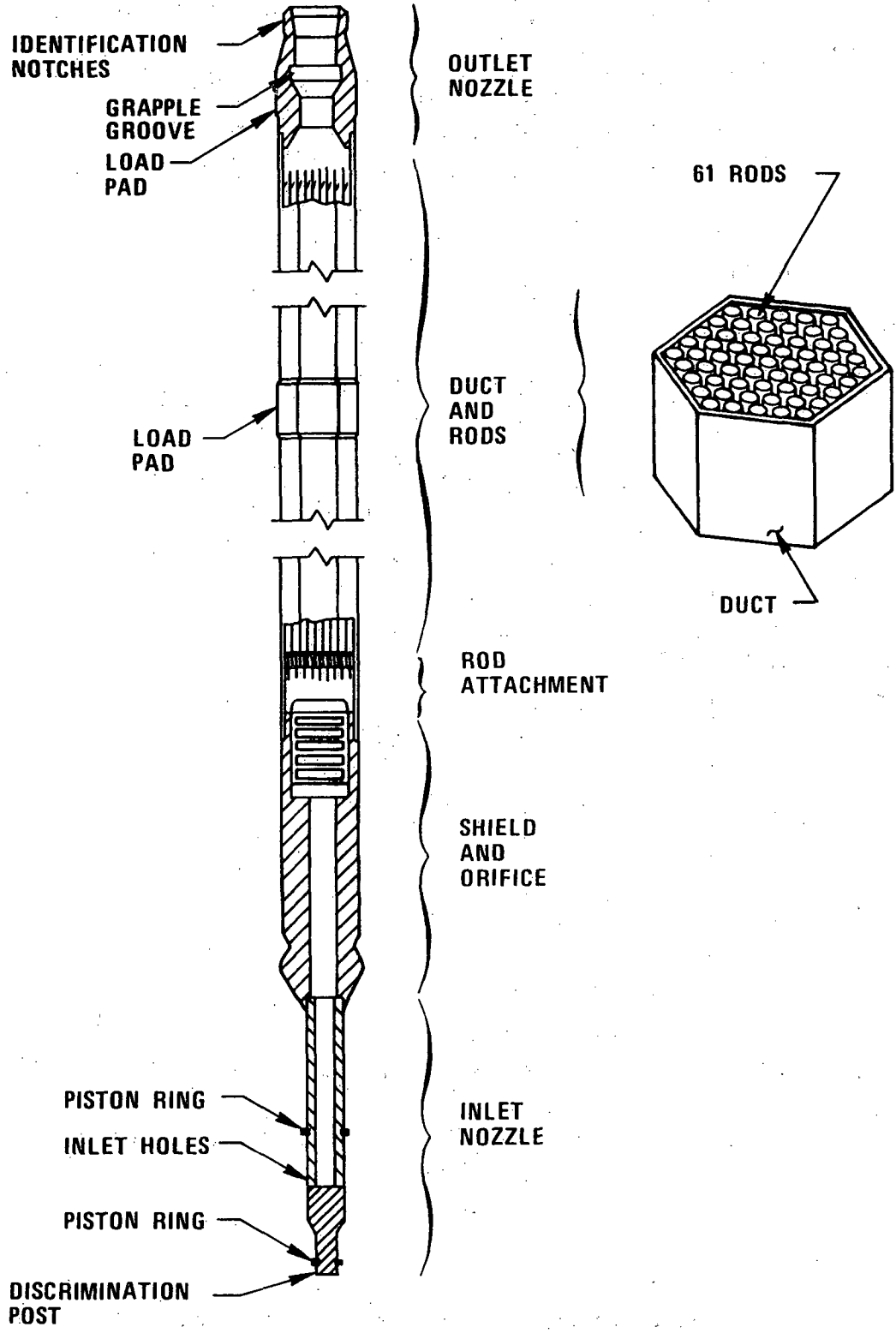


Figure 4.2-14 Radial Blanket Assembly Schematic

<u>BLANKET ASSEMBLY</u>	<u>FUEL AND BLANKET ASSEMBLY</u>	<u>FUEL ASSEMBLY</u>	<u>DIA. A</u>	<u>DIA. B</u>
1			0.875	---
2			1.236	---
	3		1.750	1.236
		4	1.514	0.875
		5	1.750	0.875
		6	1.956	1.514
		7	1.956	1.236
		8	1.956	0.875

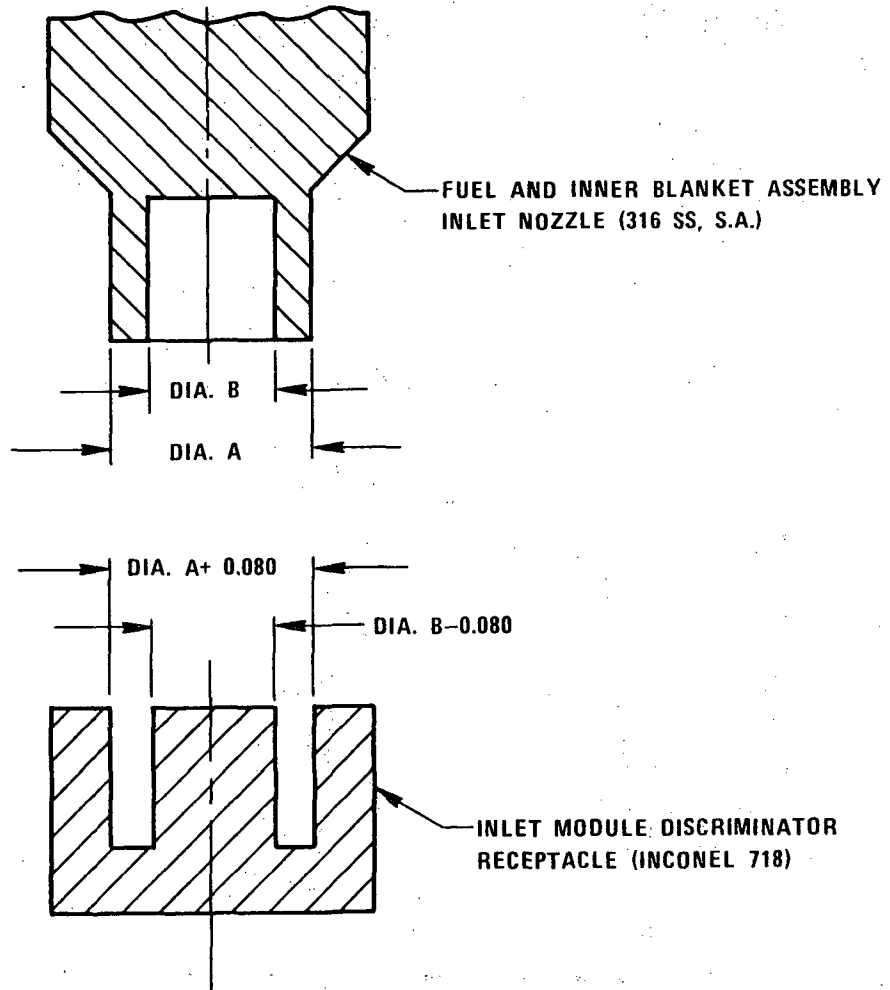


Figure 4.2-15 Fuel And Inner Blanket Assembly Discriminator Diameters

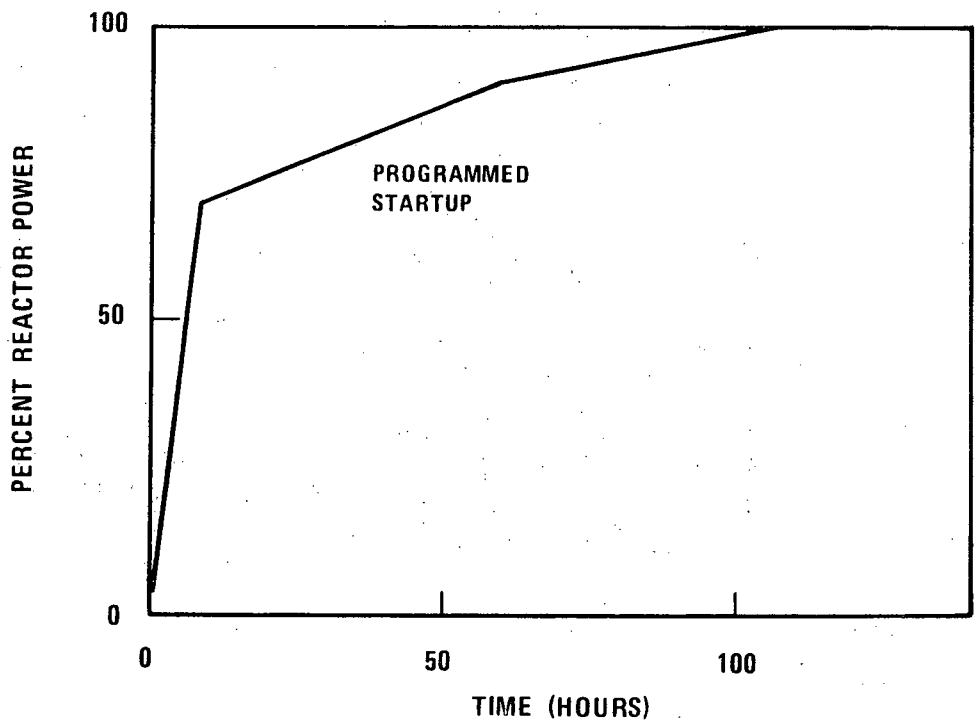
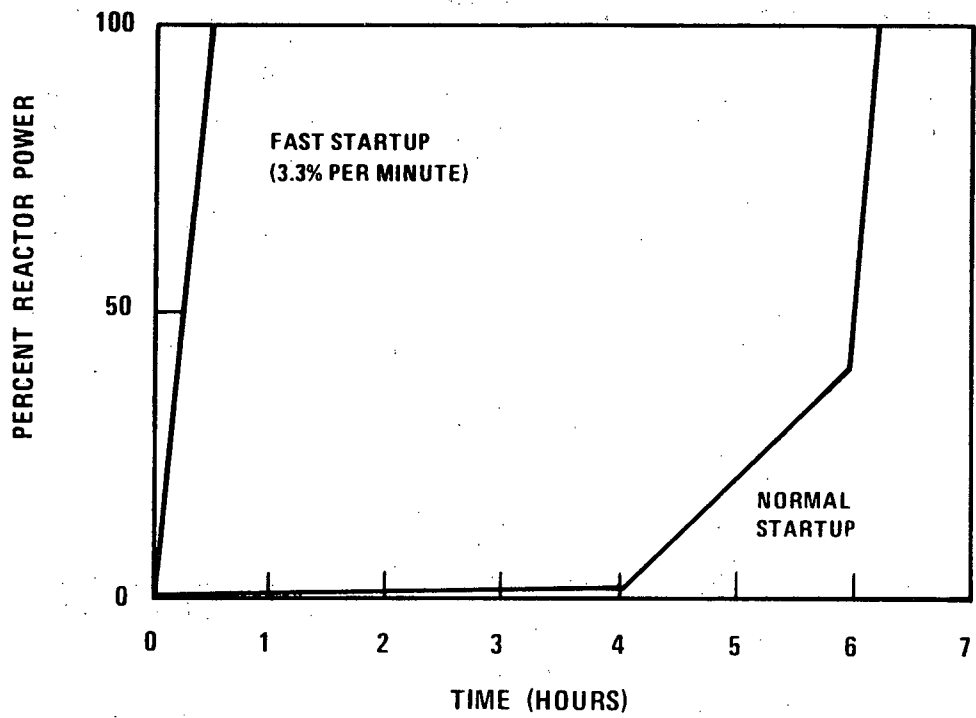


Figure 4.2-16 Startup Procedures

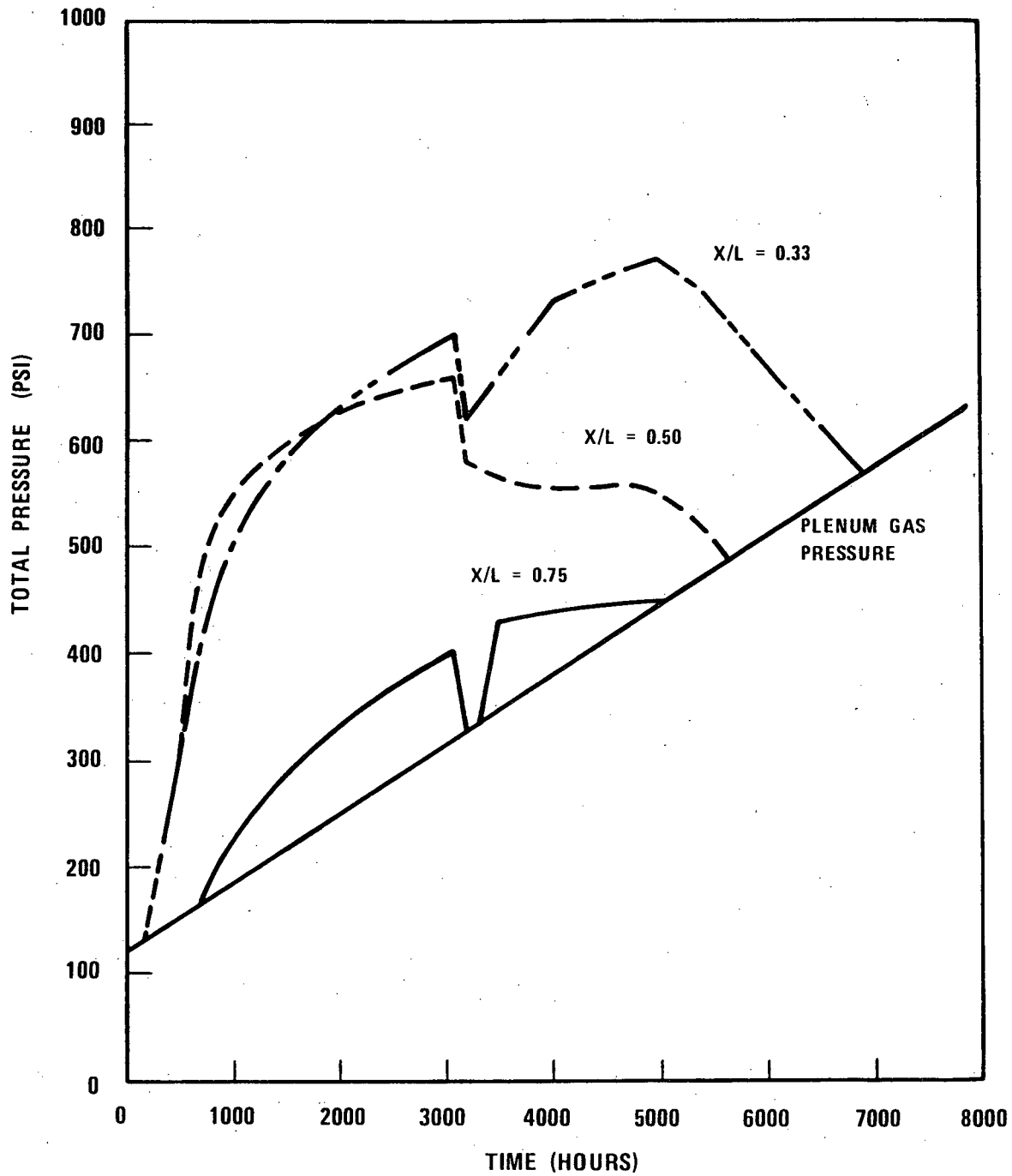


Figure 4.2-17A F/A 10 Hot Rod Total Cladding Design Pressure vs. Time, First Core

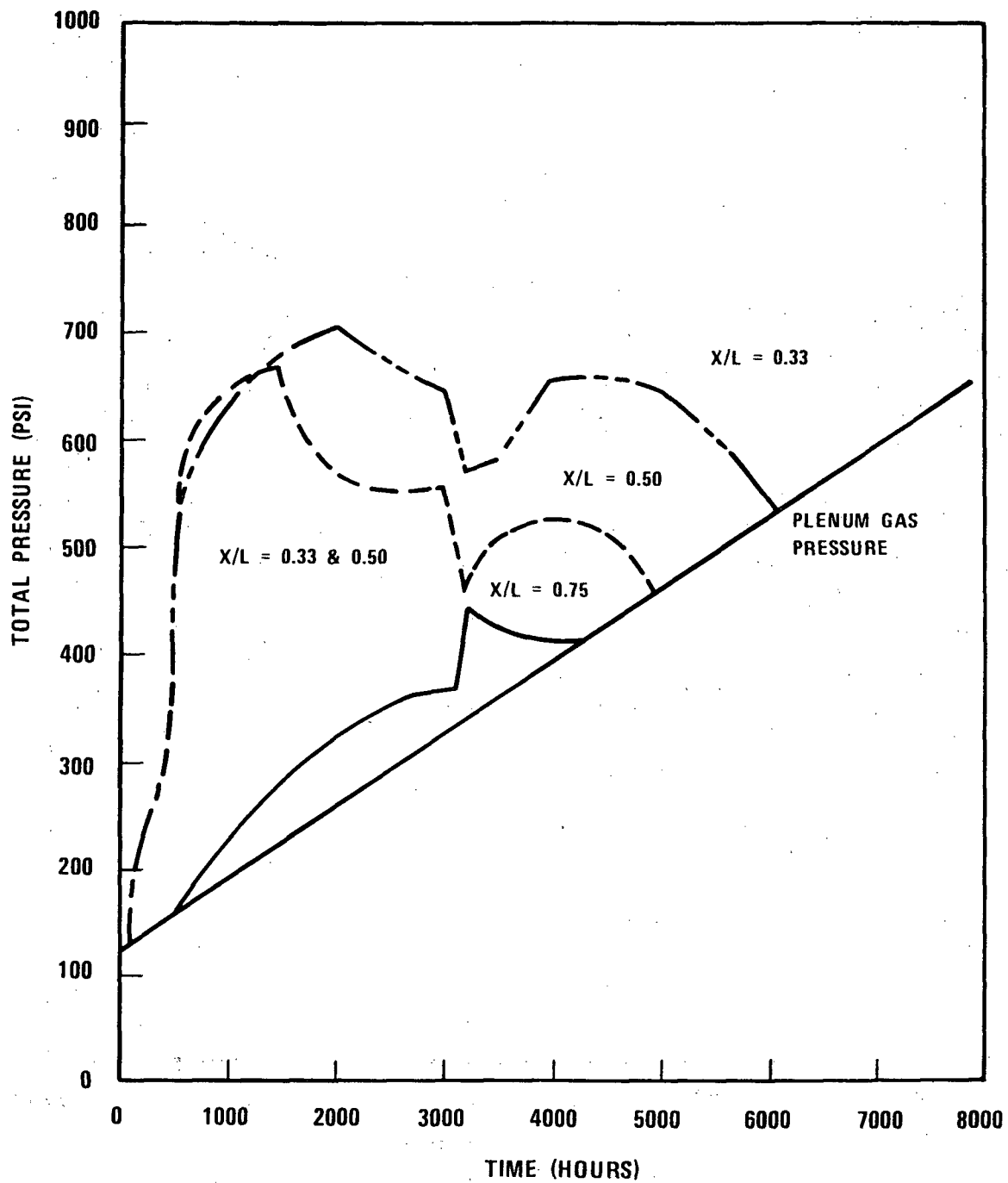


Figure 4.2-17B F/A 14 Hot Rod Total Cladding Design Pressure vs. Time, First Core

1764-13

4.2-486

Amend. 51
Sept. 1979

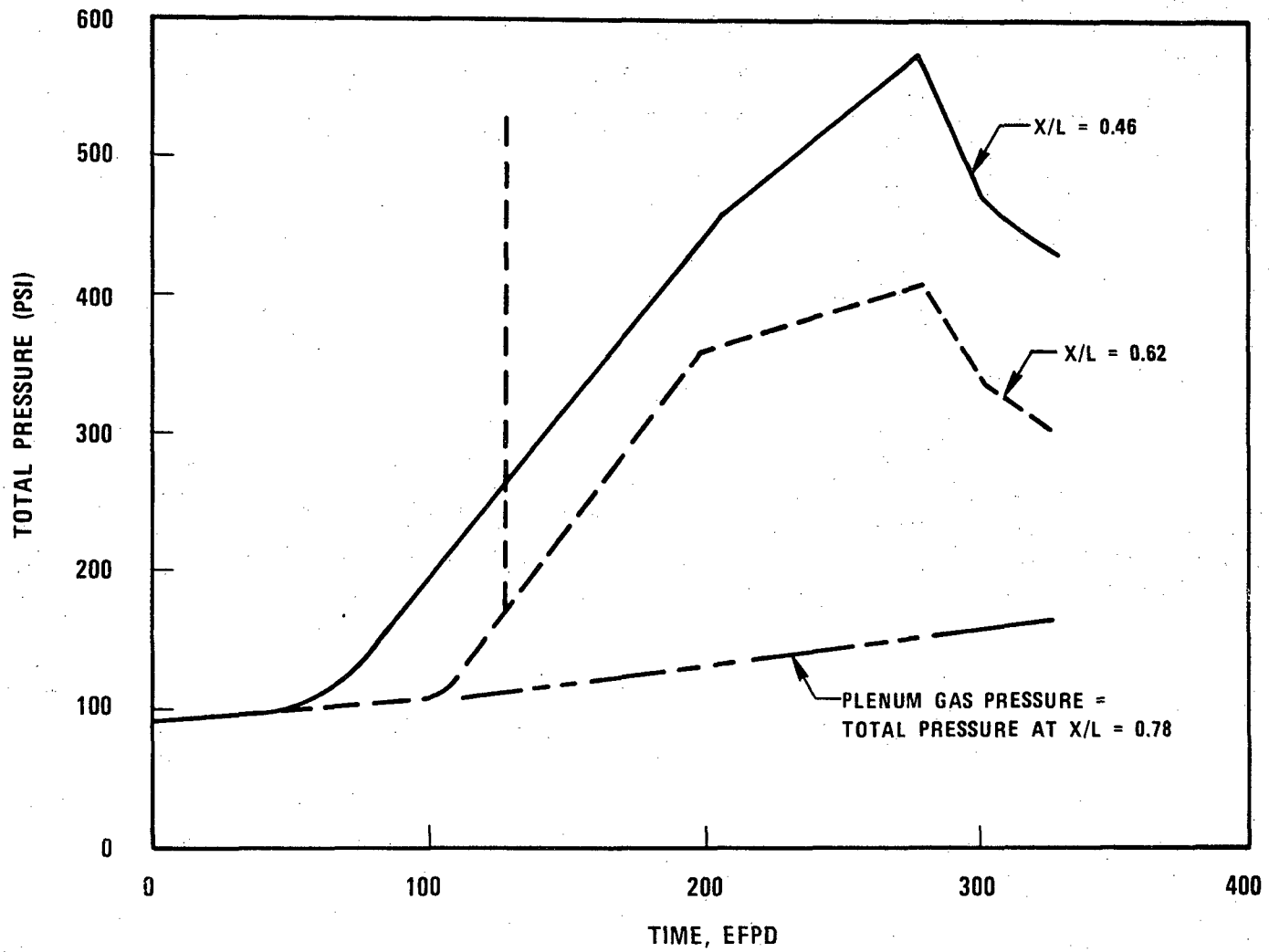


Figure 4.2-17C IB/A 67 Hot Rod Total Cladding Design Pressure

1764-14

4.2-487

Amend. 51
Sept. 1979

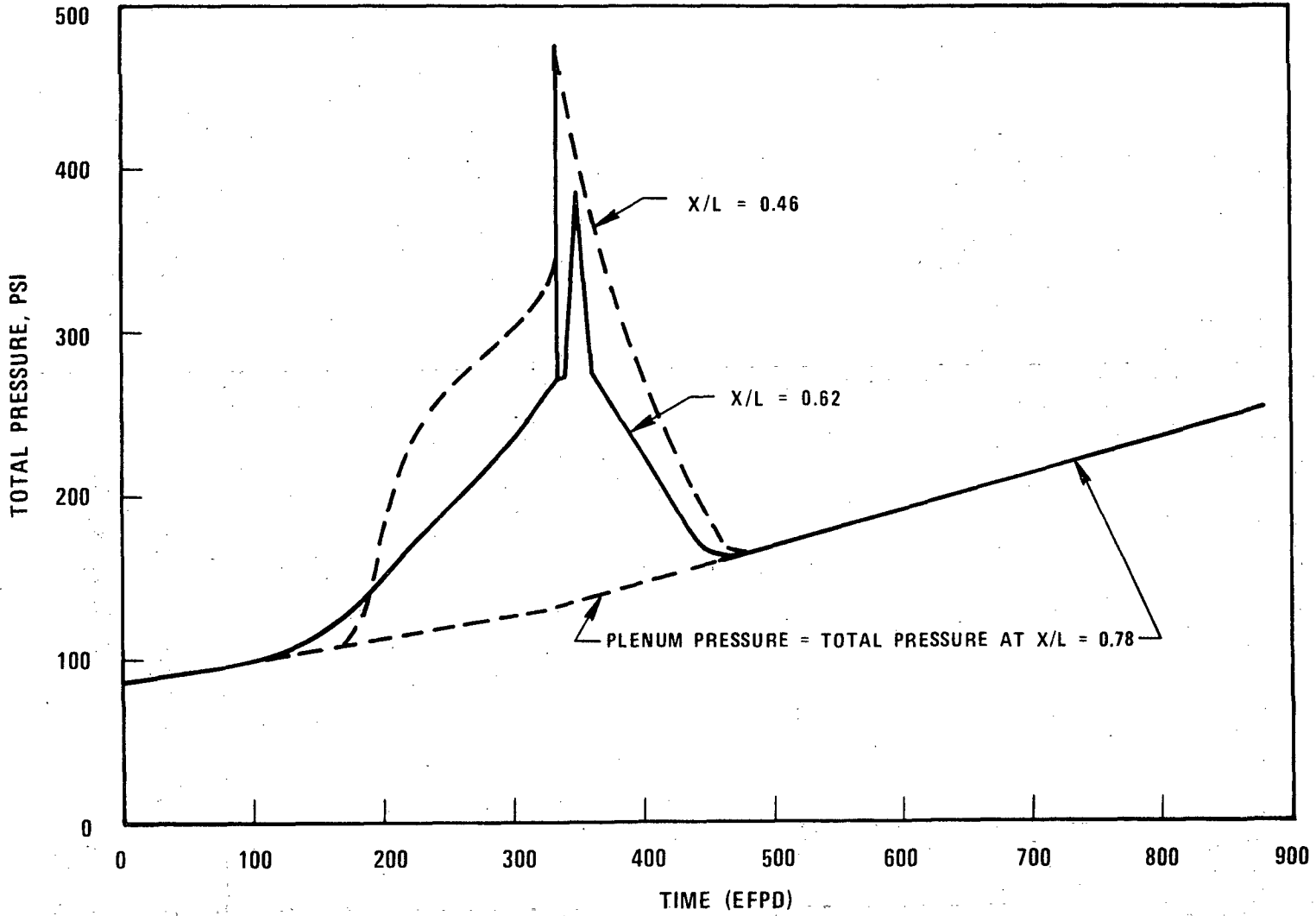


Figure 4.2-17D RB/A 201 Hot Rod Total Cladding Design Pressure

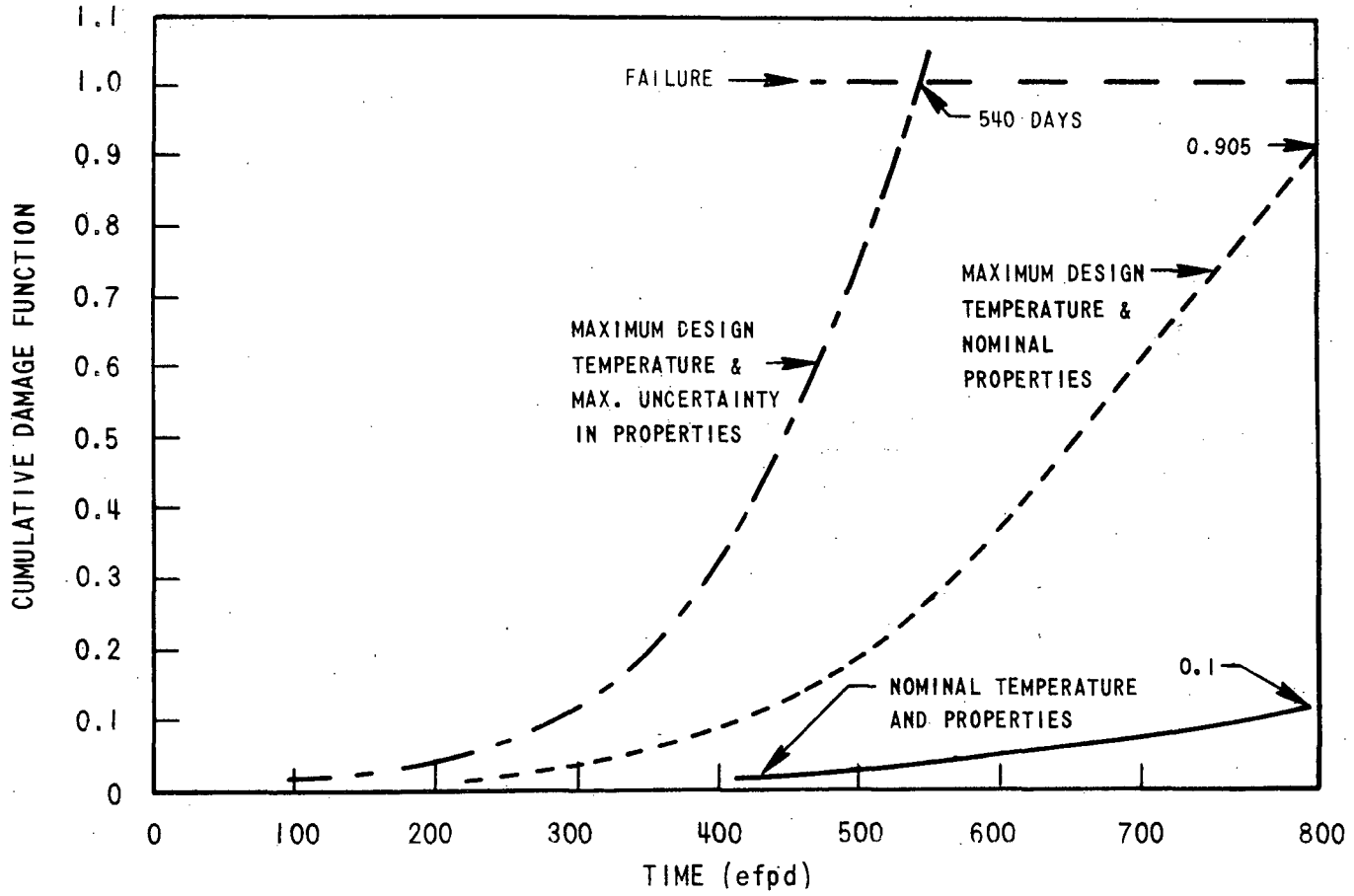


Figure 4.2-18 Cumulative Mechanical Damage Function Due to Steady State Operation Top of the Fuel Stack in Hot Pin in a Typical Fuel Rod

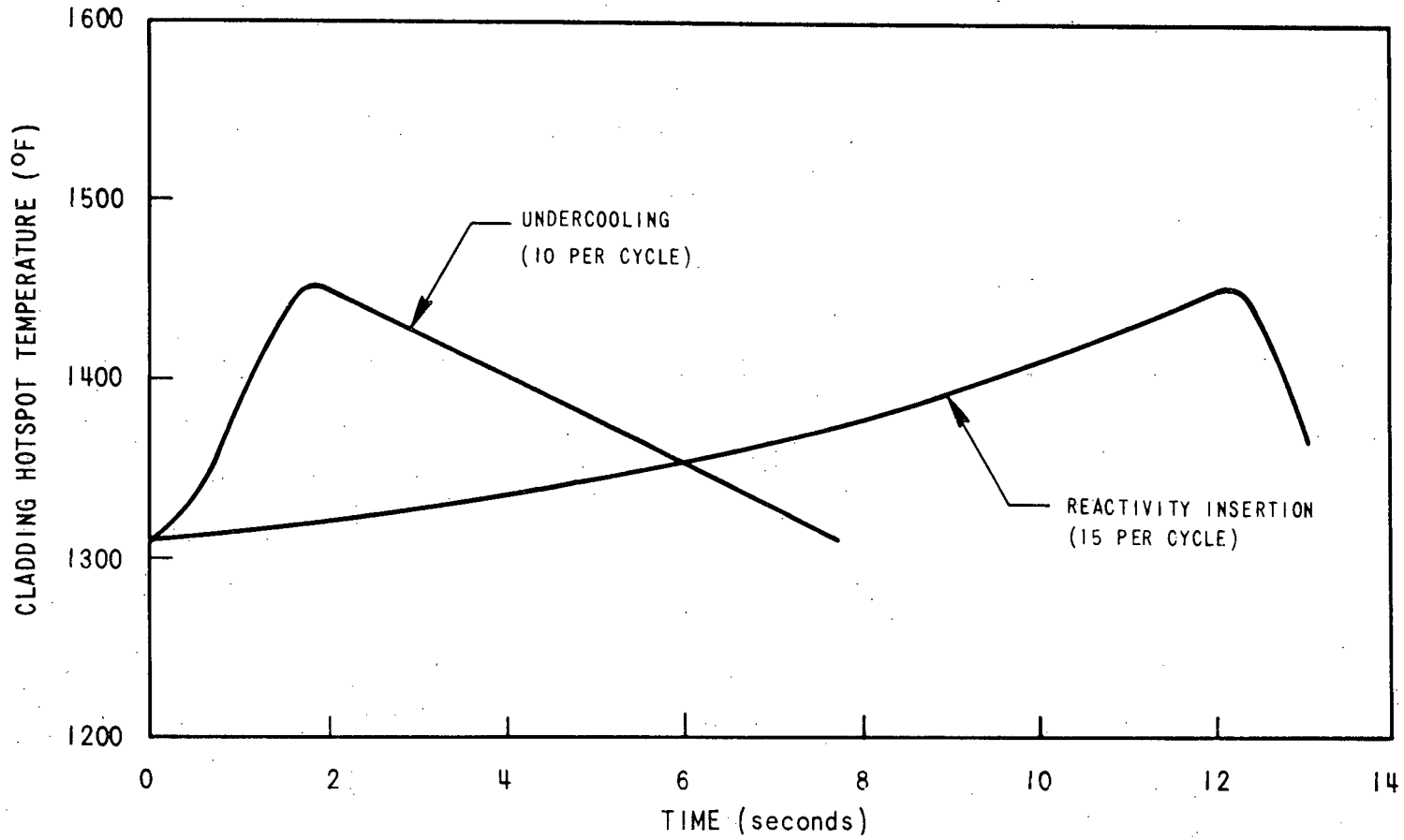


Figure 4.2-19 Umbrella Transients for Fuel Rod Cladding Upset Events for Example Calculation

1764-17

4.2-490

Amend. 51
Sept. 1979

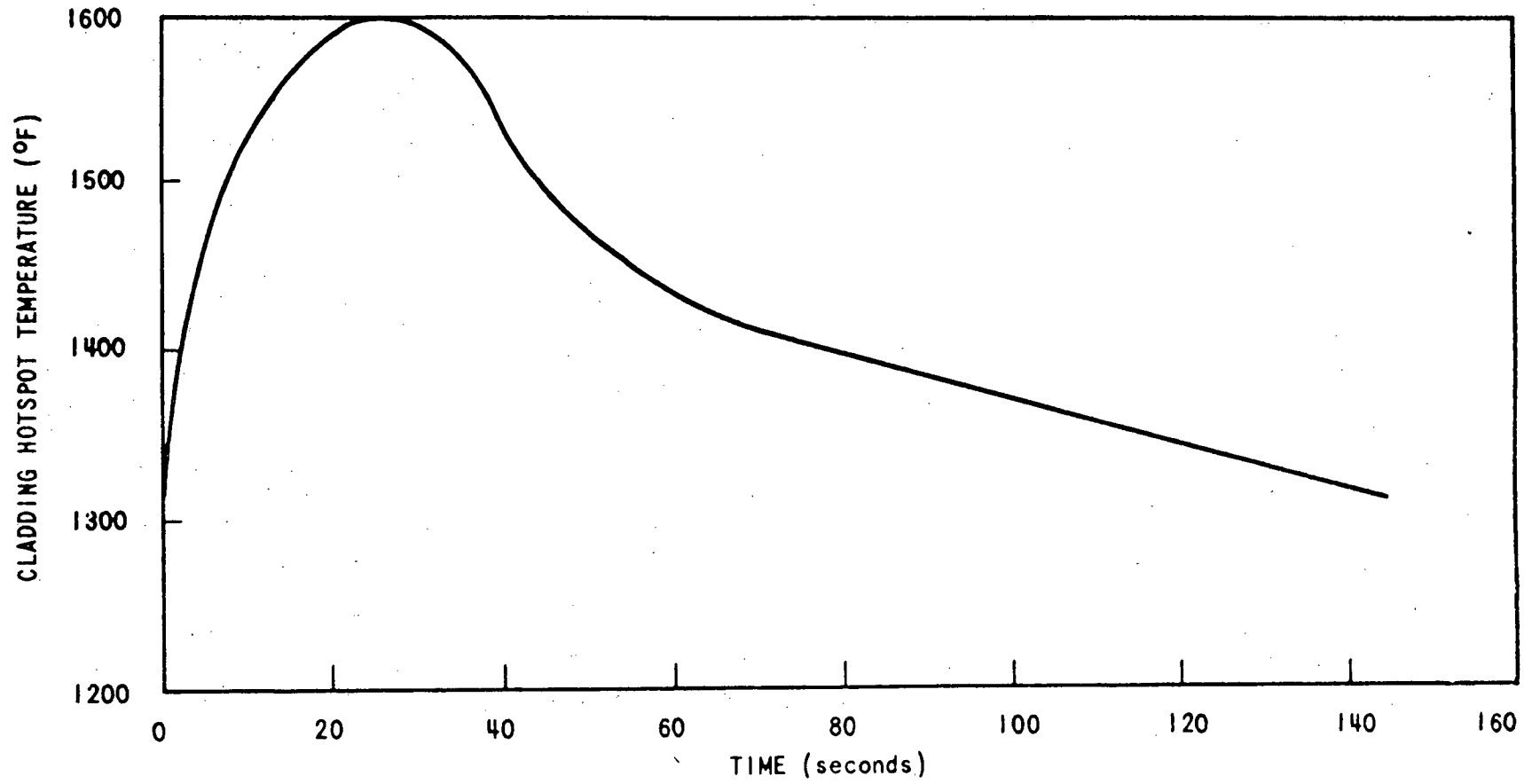


Figure 4.2-20 Umbrella Transient for Fuel Rod Cladding Emergency Event for Example Calculation

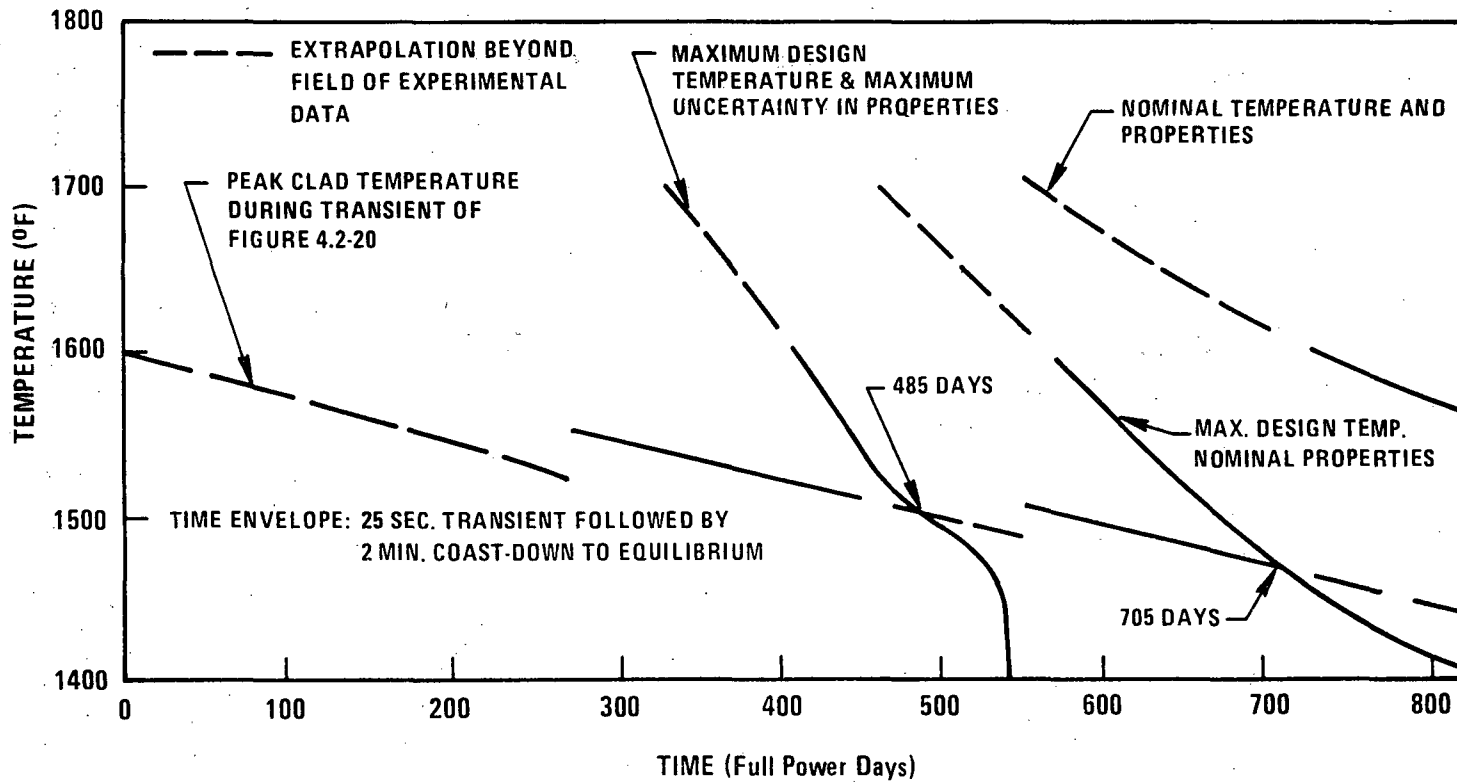


Figure 4.2-21 Loss of Flow Transient Limit Curve for Example Fuel Rod CDF Analysis Problem

1764-19

4.2-492

Amend. 51
Sept. 1979

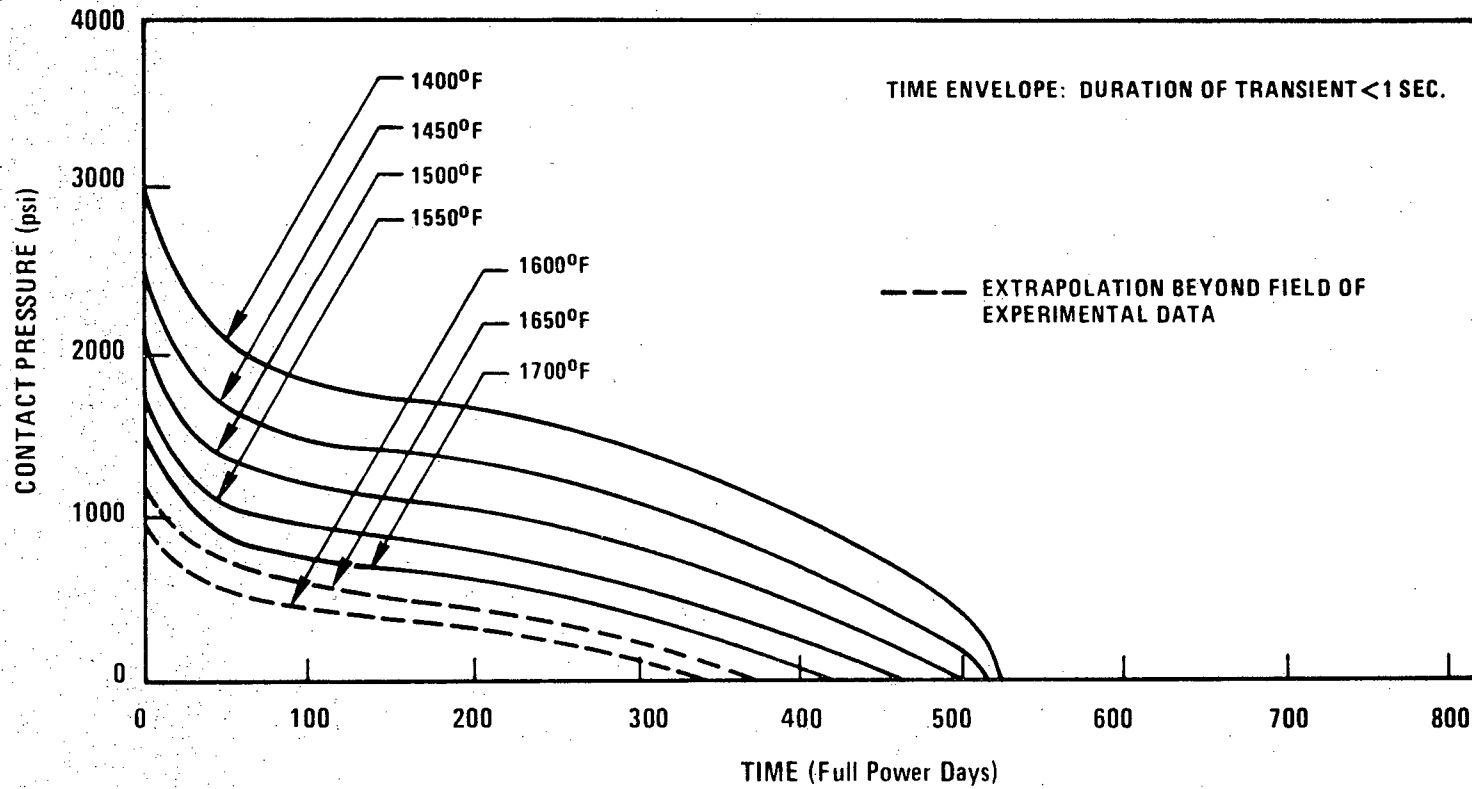


Figure 4.2-22 Transient Limit Curve for Fast Reactivity Insertion Emergency Events: Fuel Cladding Contact Pressure and Inner Wall Temperature to Cause Failure During Transient - Example Fuel Rod CDF Analysis Problem.

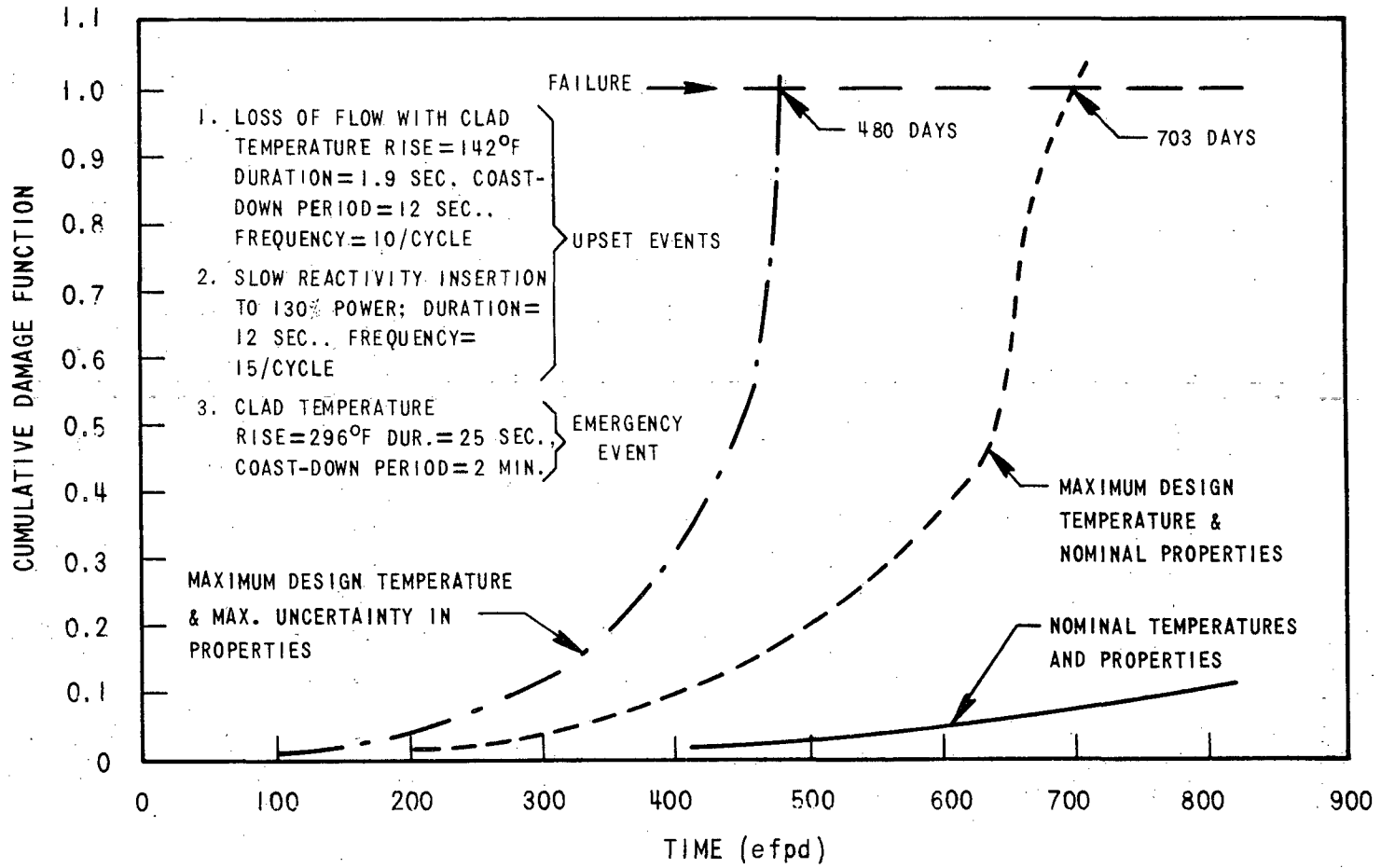


Figure 4.2-23 Cumulative Mechanical Damage Function Due to Steady State Operation, Upset Events and a Natural Circulation Emergency Event, Example Fuel Rod CDF Analysis Problem

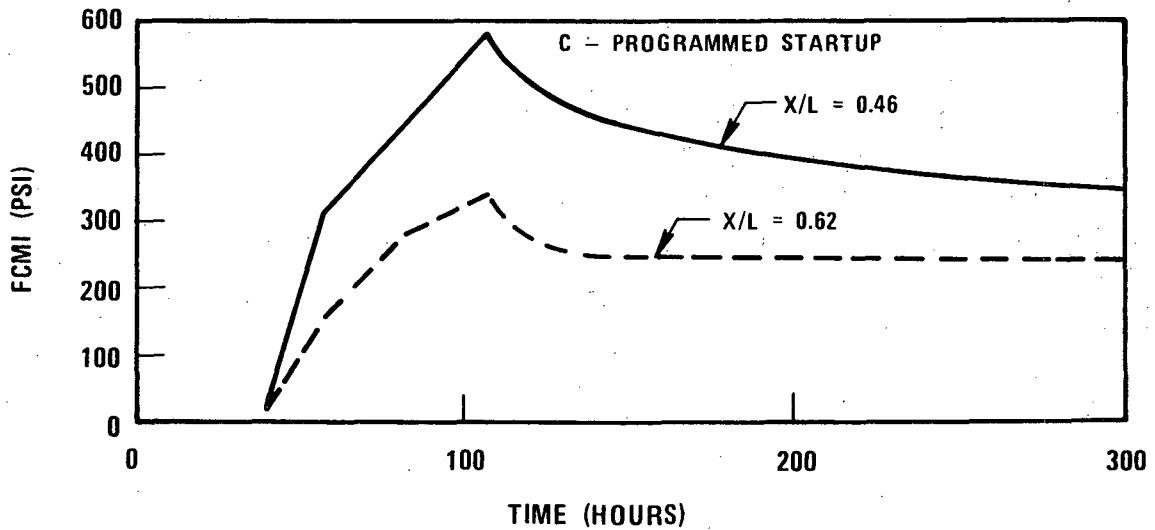
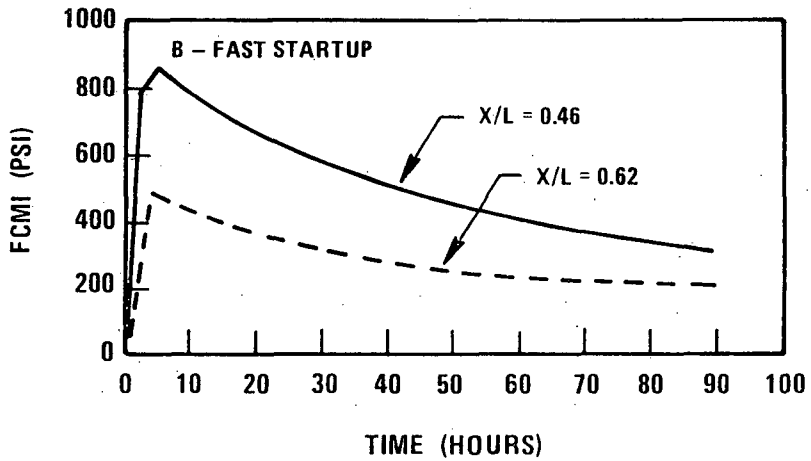
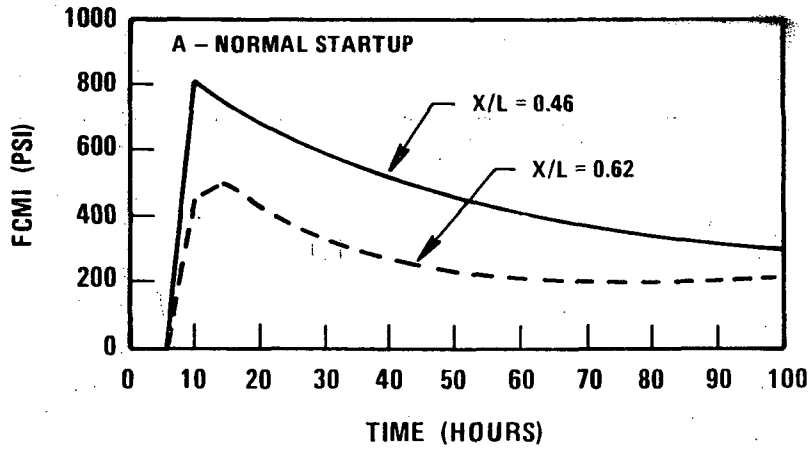


Figure 4.2-24 Comparison of FCMI for Various Startup Procedures

1764-22

4.2-495

Amend. 51
Sept. 1979

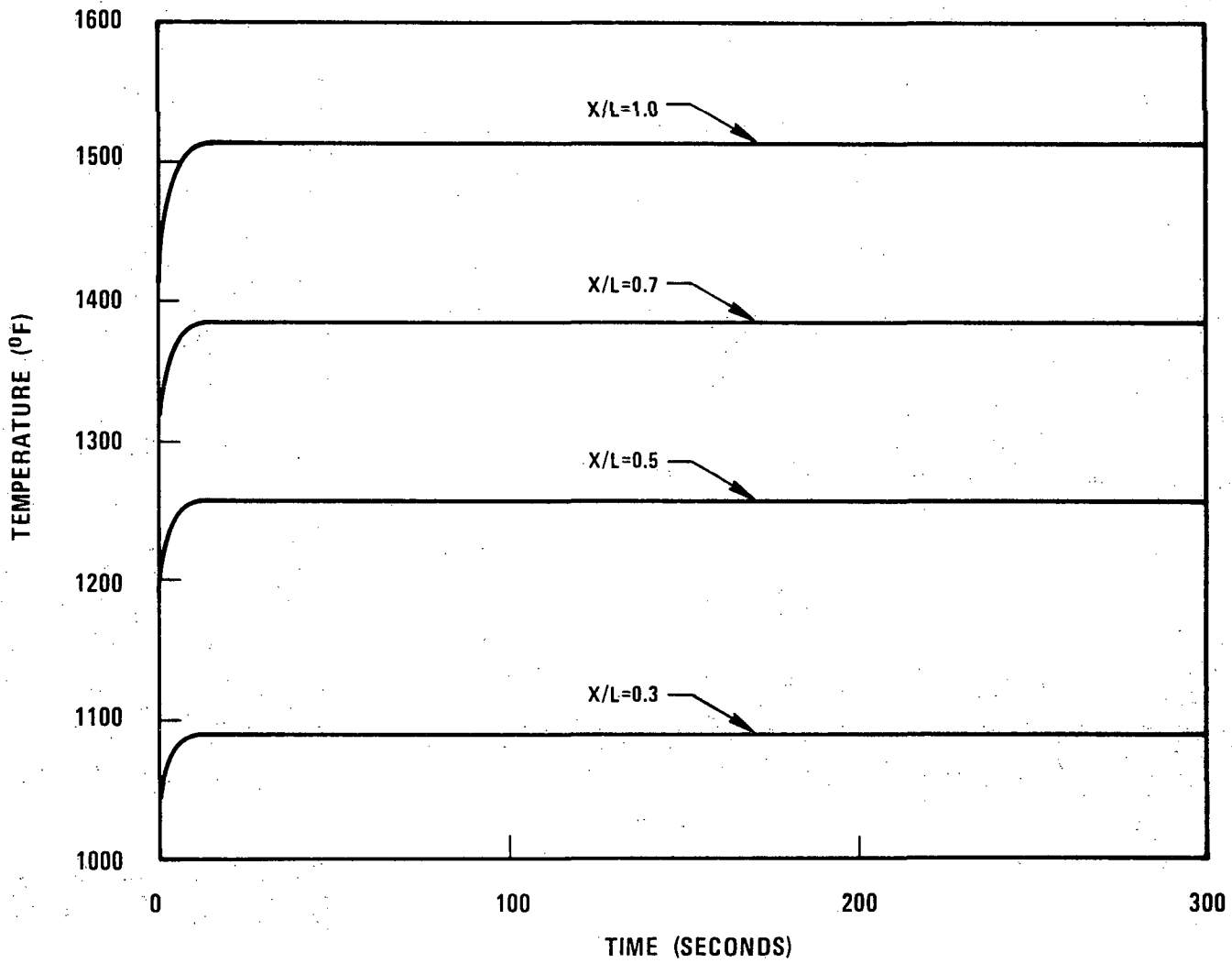


Figure 4.2-24E Enveloping Transient Fuel Rod Temperature Due to U-2b Event

1764-23

4.2-496

Amend. 51
Sept. 1979

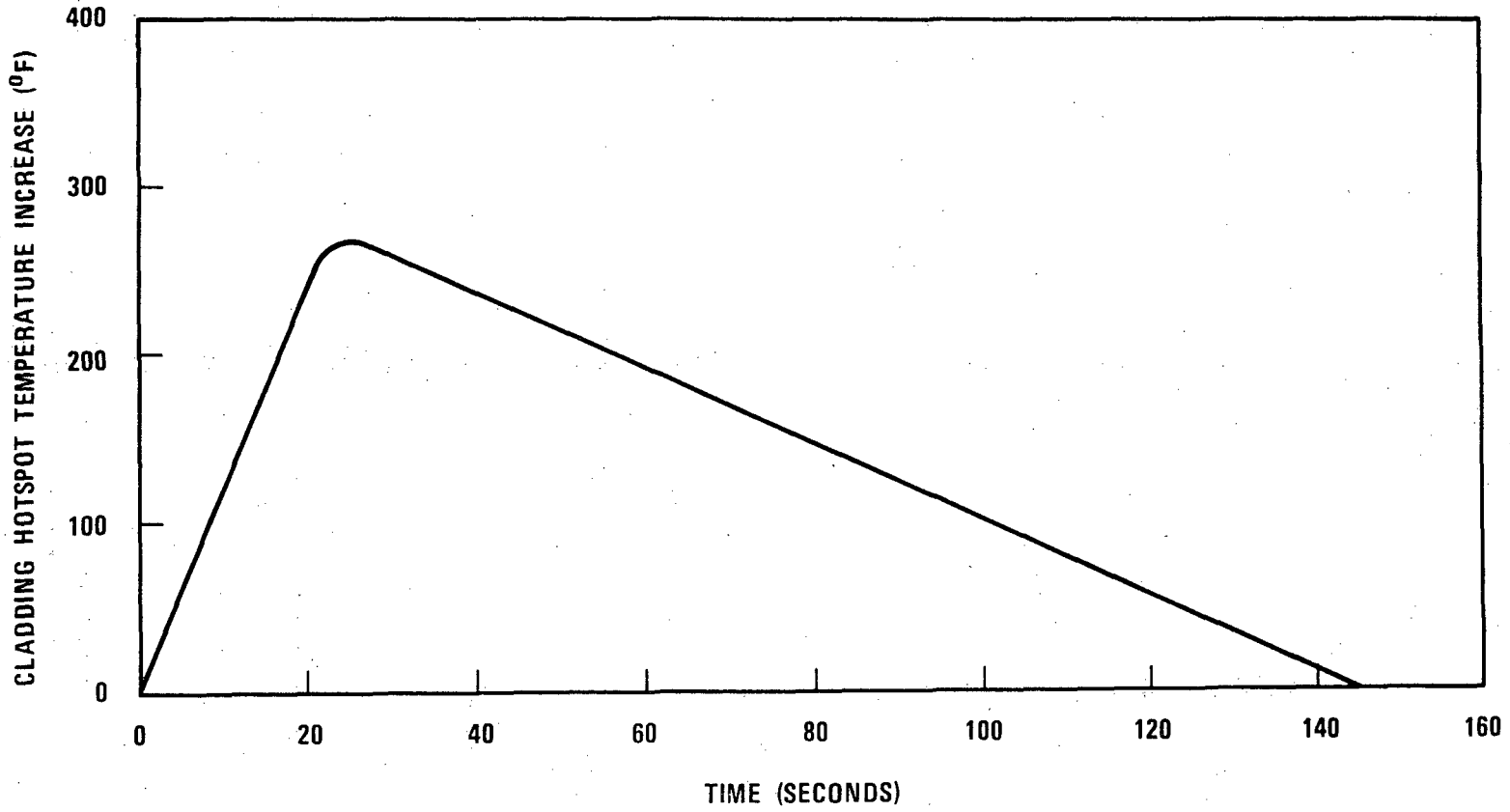


Figure 4.2-24F Fuel Rod Enveloping Emergency Undercooling Transient Temperature History

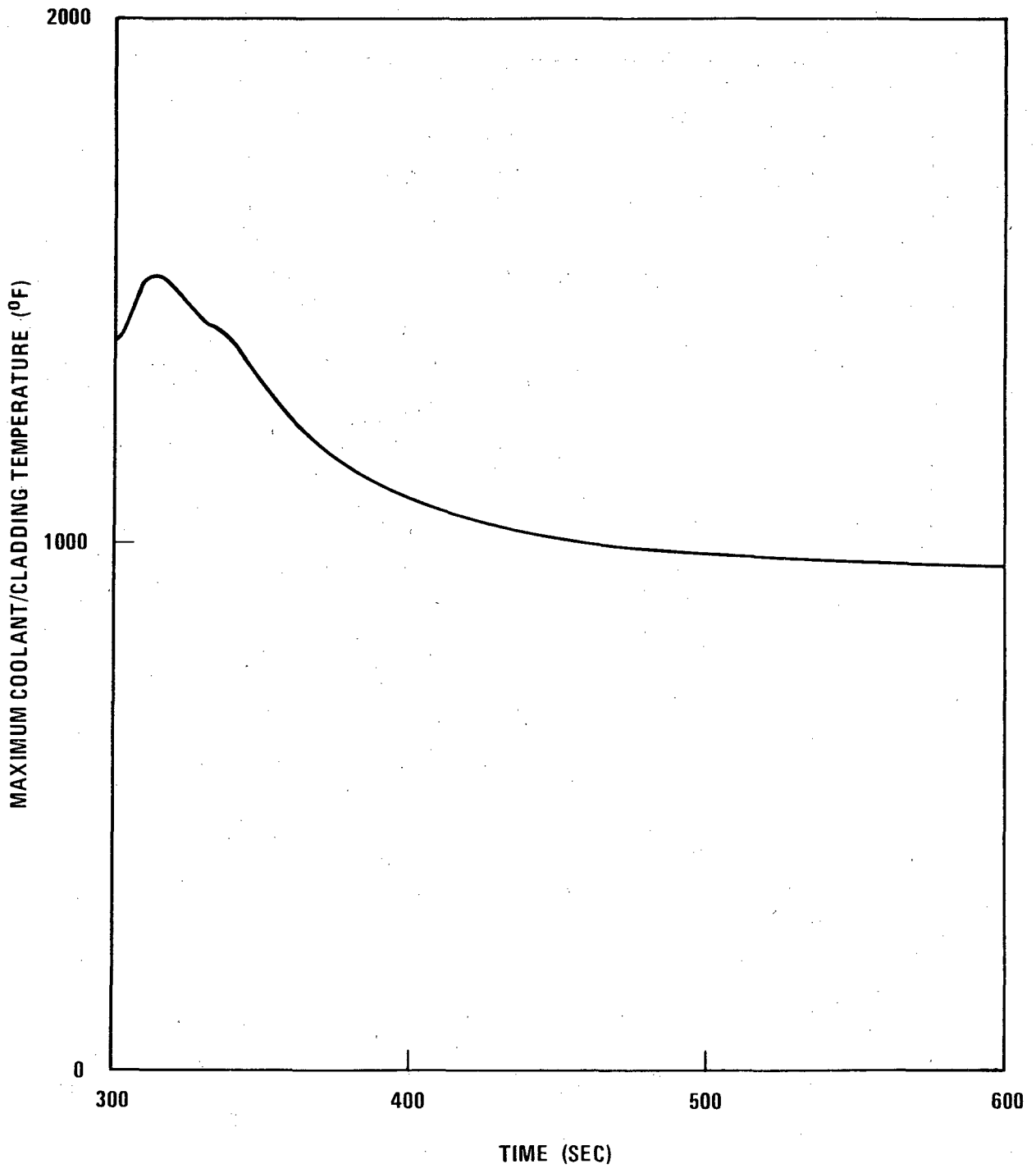


Figure 4.2-24G Variation of Maximum Cladding Temperatures of Inner Blanket Assembly for U-2b Transient

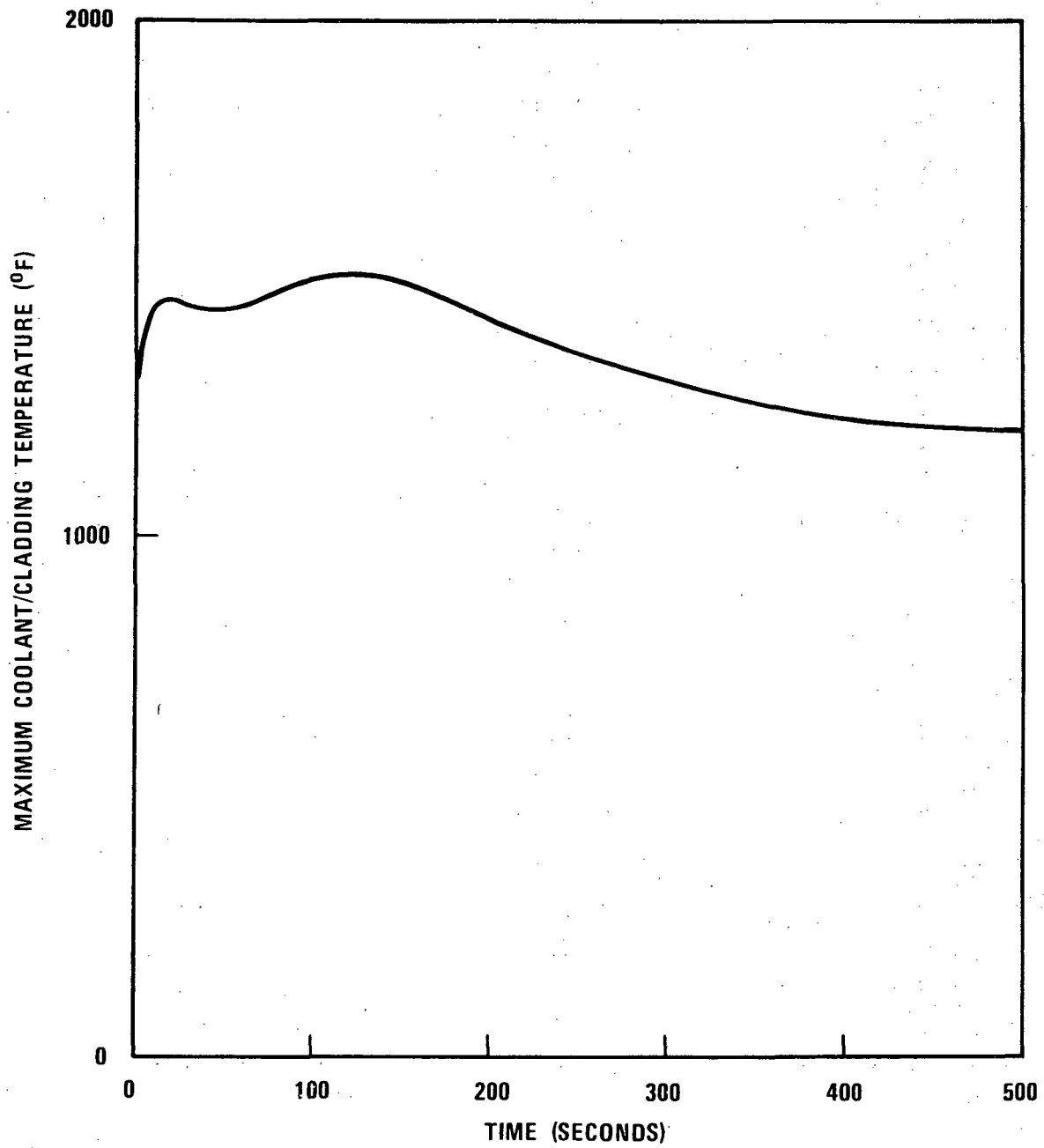


Figure 4.2-24H Variation of Maximum Cladding/Coolant Temperatures of Inner Blanket Assembly for E-16 Transient

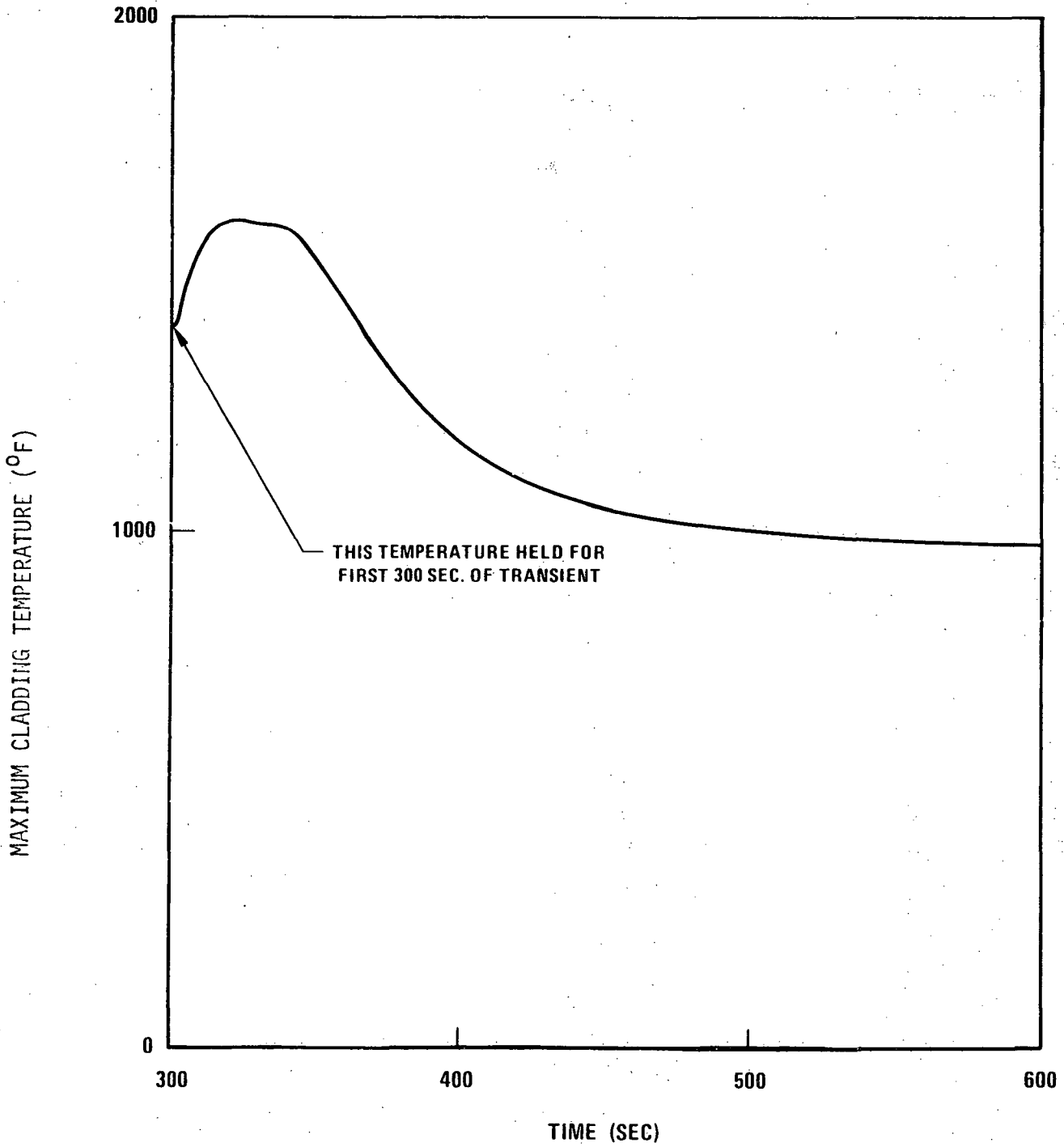


Figure 4.2-24I. Variation of Maximum Cladding Temperatures of Radial Blanket Assembly for U-2b Transient

1867-2

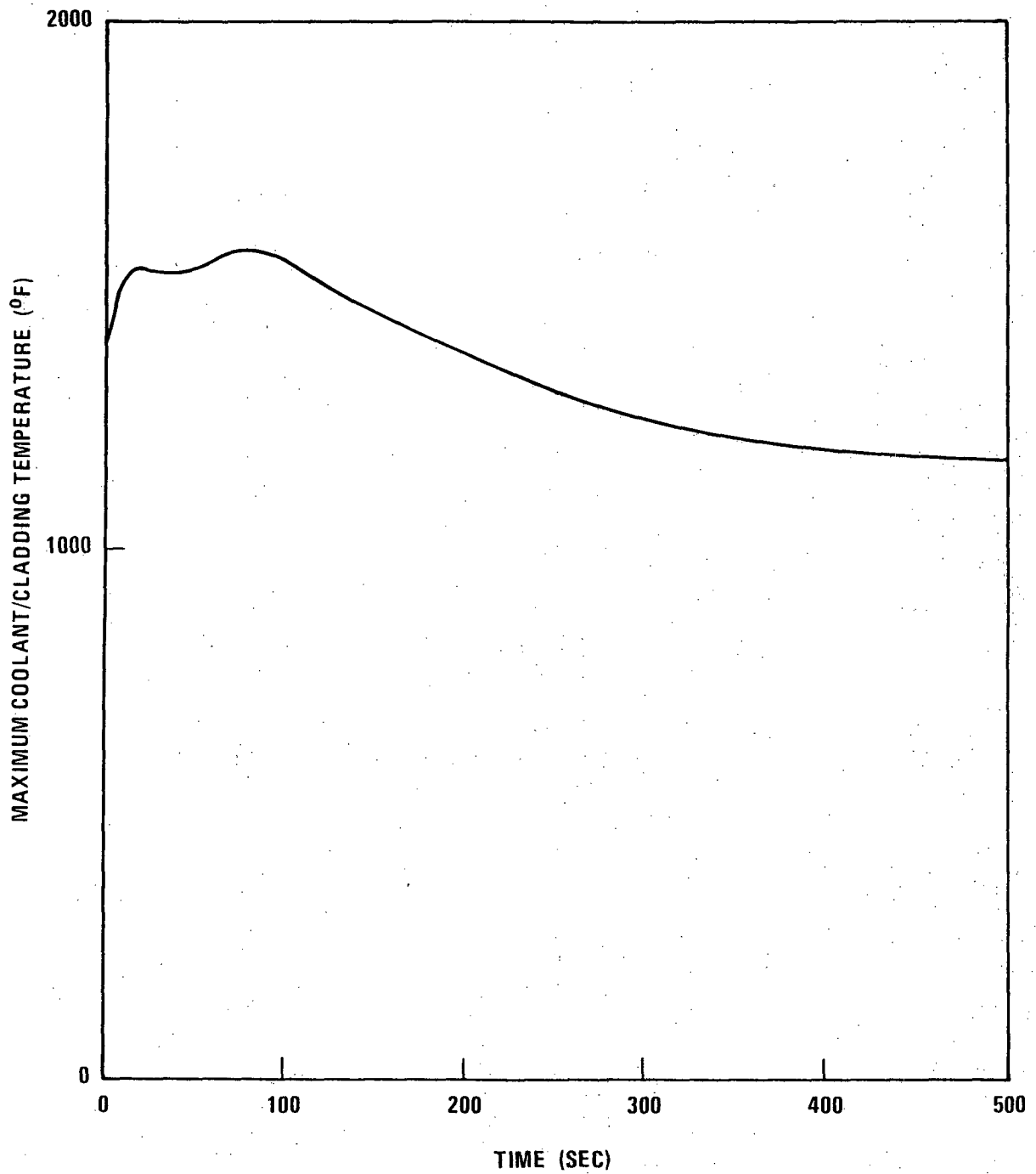


Figure 4.2-24J Variation of Maximum Cladding/Coolant Temperatures of Radial Blanket Assembly for E-16 Transient

FIGURE 4.2-26 DELETED

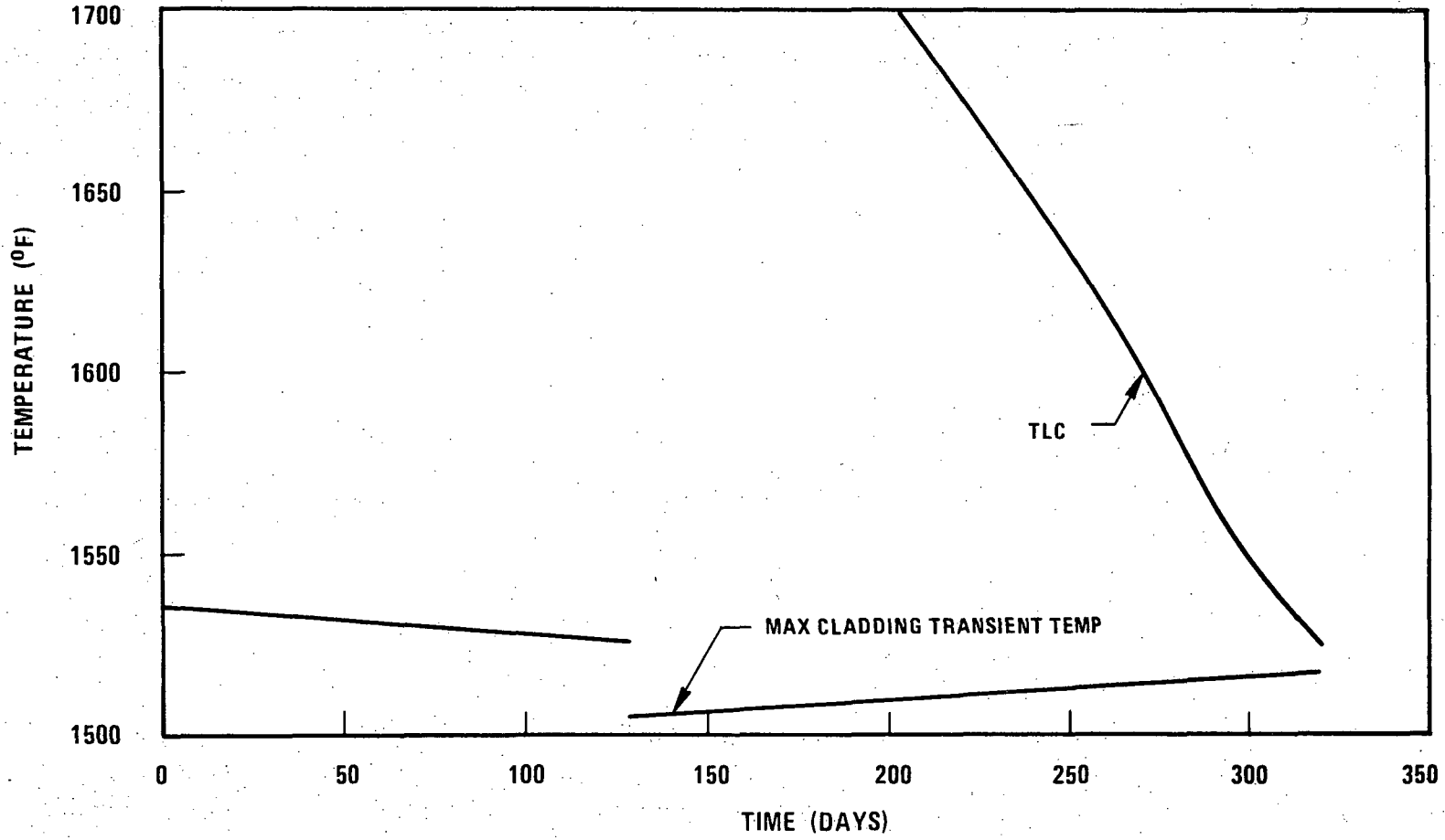


Figure 4.2-26A Transient Limit Curve for Fuel Assembly 14 Hot Rod, Hot Spot Location

1764-30

4.2-504

Amend. 51
Sept. 1979

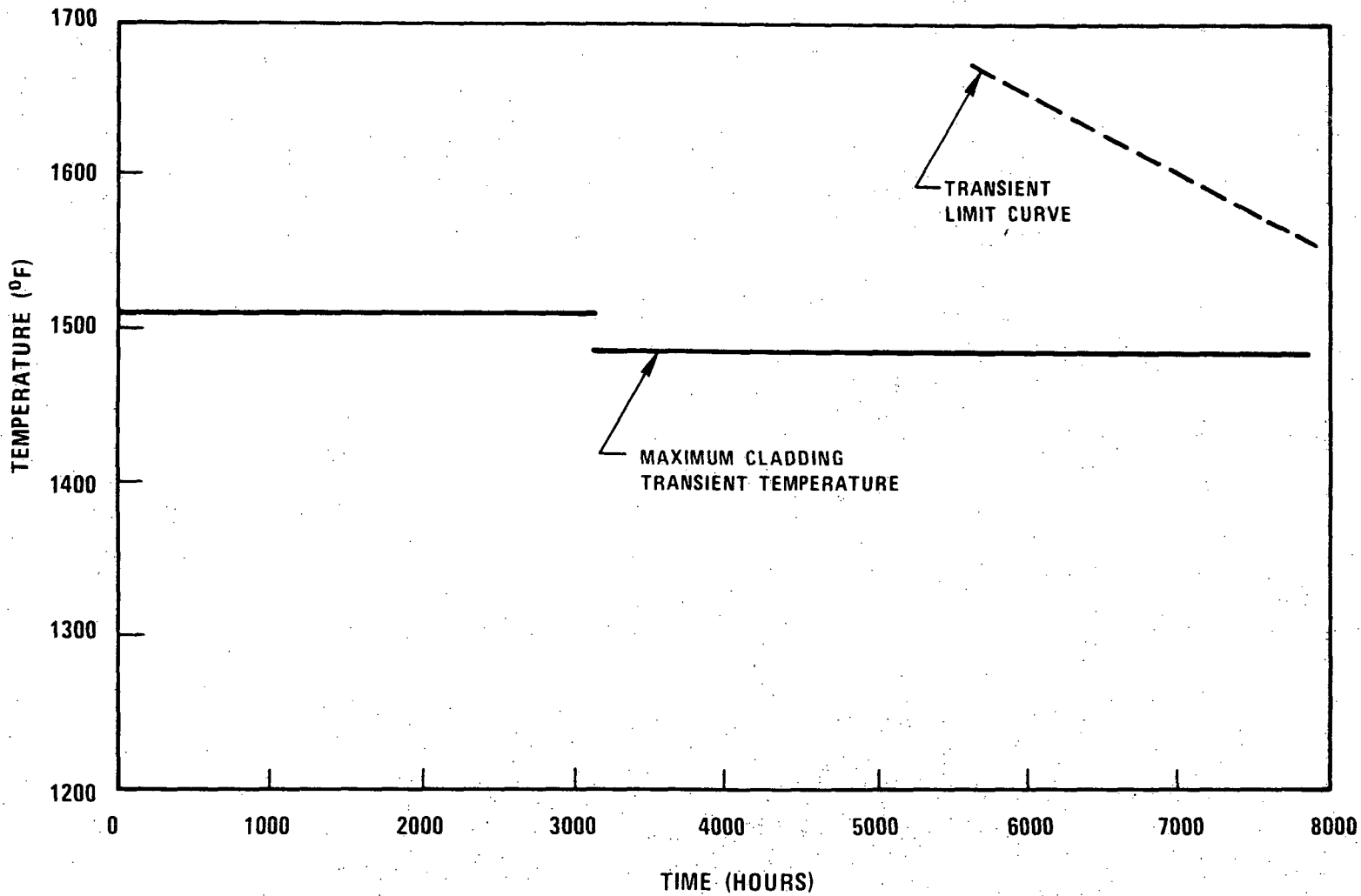


Figure 4.2-26B. Transient Limit Curve for F/A 14 Hot Rod X/L = 0.75

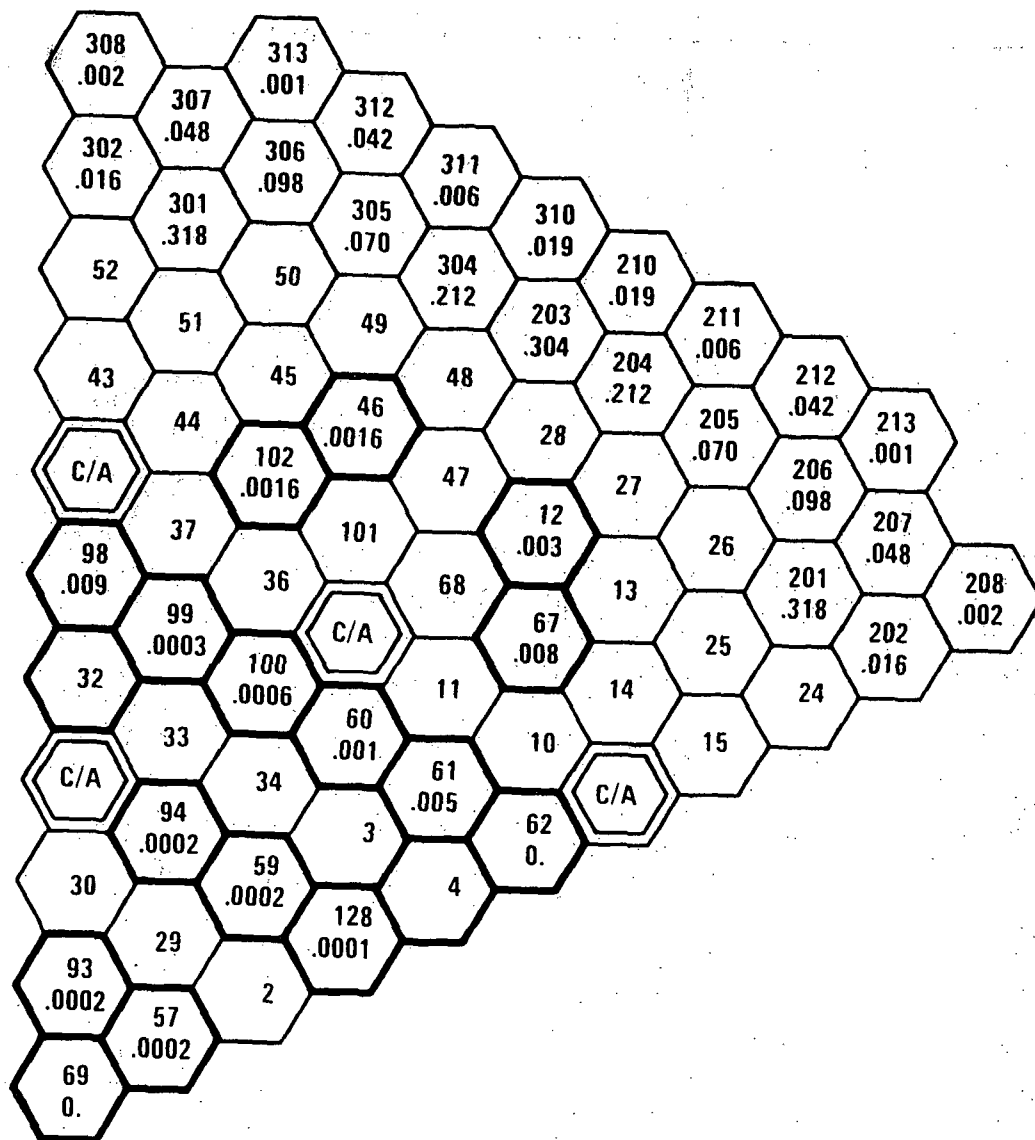


FIGURE 4.2-27. End-of-Life CDF at the Hot Spot of Each Blanket Assembly Hot Rod - Steady State Plenum Gas Pressure Loads Only

1764-31a